













Prof. Ir. A. S. Keverling Buisman

2 Nov. 1890 - 20 Febr. 1944

Prof.Ir. A.S. Keverling Buisman  
2 Nov. 1890 - 20 Febr. 1944

Engineering circles in the Netherlands learned with satisfaction of the decision, taken in 1936 at the First International Conference on Soil Mechanics at Cambridge, to hold the Second Conference in the Netherlands. At the time of meeting of the First Conference a general interest manifested itself in the Netherlands for soil mechanics. At the Technical University of Delft the Laboratory of Soil Mechanics, some years previously established, was in full development and already numerous practical problems came in from the field for consideration and advice. The foundation and the development of this laboratory are due in the first instance to the initiative and the devoted work of the late Prof.Ir. A.S. Keverling Buisman.

Those who have followed the pioneer work of Buisman with the greatest of appreciation, feel it their sad duty to commemorate his career and his merits on the occasion of this conference.

After having obtained his degree of civil engineer in 1912, Buisman entered the service of the Hollandsche Beton Maatschappij, where he found an extensive sphere of action both in this country and in the Netherlands East Indies. Already during this period his name became known by the publication of some papers, mainly on the subject of Applied Mechanics and in 1919 he was appointed professor of this subject in the Civil Engineering Department of the Technical University of Delft.

In his inaugural address "The science of applied mechanics and economical design" Buisman showed himself to be an engineer with a broad and practical vision. He qualified Applied Mechanics as the civil engineering science par excellence, stressing the part played by this science in the development of the constructive feeling of the civil engineer. For it does not suffice to calculate a once chosen construction in an economical manner. In the first place the general concept and the fundamental shape must be as favourable as possible. To achieve this, more than just knowledge and the application of formulae is required.

On their local, often water logged soils of poor bearing capacity the Dutch have successfully achieved the solution of problems of earth-works, foundations etc., the costs of which often constitute a considerable part of the total construction costs. More often here than elsewhere it is seen that the vast difference in soil conditions under structures that must fulfil similar requirements, may lead to totally different concepts, dependent on the locality where they are situated.

Is it any wonder that Buisman, true to this principles to further economical construction, understood that a more scientific investigation on the problems in the sphere of soil mechanics was urgently required?

The occasion that caused this study to be taken in hand effectively came when some failures of earth constructions occurred with serious consequences. The railway accident at Weesp in 1918 as a result of the failure of the embankment at the approach of the railway bridge over the Merwede Canal and the bursting of the dikes of the Zuiderzee in 1916, causing extensive flooding, lead in 1920 to the installation of a committee of inquiry into foundation soils, in which Buisman sat as a member. From now onward Buisman directed his efforts more and more towards the study of soil mechanics, efforts that were destined to yield such rich harvest for our country.

His practical experience had already convinced him that progress was only possible after a more exact insight had been acquired into the mechanical properties of the soil, the necessary basis on which the theory must be founded. His first preliminary tests in the field and on samples taken in the field were done in a rather primitive way. In later years he used to enjoy memories of hours at home, when, assisted by his family, he performed experiments in order to measure the angles of repose of slopes, shearing resistances etc.

The preparation in the Netherlands of large works each with their typical soil problems, in the solution of which Buisman was given an increasingly active part, soon gave rise to a general feeling that a scientific centre for the study of soil mechanics was indispensable.

The publication of Terzaghi's work in 1925 acted as a stimulant on Buisman to push his studies ahead and to persevere in his efforts for a speedy establishment of a well equipped laboratory. At first financed by Buisman's private means and later on aided by the Delft University Foundation the Laboratory of Soil Mechanics at the Technical University came into being in the years 1930 and 1931 on his initiative and at first under his direction. The need for this laboratory appeared to be such, that the number of inquiries showed a steady increase and soon the funds were augmented to such an extent that a healthy growth came within possible reach. It is the merit of Buisman, that he was the first to understand these possibilities and to promote the indicated development to the best of his capacities, thereby not losing sight of the fact that ultimately the laboratory should be the scientific centre for the Netherlands, where the new science should be vigorously furthered. He himself showed a lasting interest in the scientific section of the laboratory as evidenced by his many publications during that time.

About 1930 Buisman started to develop the cell apparatus, in which it was possible to effect any desired combination of the principal stresses, from neutral to critical.

By means of the "cone apparatus" Buisman tried to determine the shearing resistance of the soil sample by applying a load on the cone and by measuring the resulting depth of penetration into the sample.

Formulas, based on the relating studies of Prandtl for metals, showing the relationship between penetration depth and shearing resistance, were derived by him. For field investigation this apparatus was developed into the apparatus now known as the deepsounding apparatus, by means of which it became possible to estimate the point resistance of piles within fairly narrow limits. Some thousands of deep-soundings have since been made, both in this country and abroad.

Comparative observations, in the field as well as in the laboratory created in Buisman the conviction that the so called layer-thickness-effect for highly compressible soils of low permeability is not so great, at least for soil conditions in the Netherlands, as it would be according to the hydrodynamical consolidation theory of Terzaghi. He explained this by starting from the assumption of a "heterogeneous permeability" i.e. by assuming that the soil mass consists of systems of low permeability arranged alongside of systems with wide pores. On the time needed for the expulsion of moisture from these systems the thickness of the layer would play a less important part than in the case of "homogeneous permeability". Be it noted that the idea of physically adsorbed water was already present to his mind.

Another important contribution was the theory, formulated in cooperation with others, about the flow phenomena of the continuous capillary groundwater which, as demonstrated by experiments, follows the same laws as the "phreatic" water. As far as we know this is the first time that equilibrium computations by means of the so-called Swedish method of assumed curved surfaces of sliding, were performed, taking separately account of positive and negative water pressures.

Lastly, mention should be made of his studies on stress distributions in the soil, especially at earth retaining structures, where he took into account the relative deformations of soil, piles and sheet piling. An example of this is given in the article No. V b 4 adapted by Ir. T.K. Huizinga, Director of the Laboratory of Soil Mechanics at Delft.

In his book "Grondmechanica", published in 1940, Buisman gave an excellent survey of the position of modern soil mechanics.

In 1939 he departed for the Netherlands East Indies to give a course of lectures at the Technical University of Bandoeng. Prevented from returning by the occupation of the Netherlands by Germany, he made a virtue of necessity and prosecuted his studies vigorously. A new edition of his text-book, enlarged with typical local problems, was published there.

During the Japanese occupation of the Netherlands East Indies Buisman was interned in 1943. We were not to have the privilege of seeing him again: in the camp he contracted an illness, from which he did not recover and an active life, which still showed much promise, was broken off.

To his friends, colleagues and collaborators who had looked forward to renewed cooperation with Buisman, the consolation is given to remember that the work still proceeds in his spirit.

G.H. van Mourik Broekman.



**PROCEEDINGS OF THE SECOND  
INTERNATIONAL CONFERENCE**

**ON**

**SOIL MECHANICS AND  
FOUNDATION ENGINEERING**



**ROTTERDAM  
JUNE 21 TO 30 - 1948**

**VOLUME I**





#### PREFACE OF THE COMMITTEE ON ORGANISATION

When the exceptional success of the First International Conference on Soil Mechanics and Foundation Engineering had prompted the desire to hold similar Conferences at regular intervals, it was not long before the idea to hold the Second Conference in the Netherlands had received consideration. However, the Second World War prevented any such intention from materializing at the time originally foreseen.

Now that the moment has arrived to prosecute the once abandoned plane, the Netherlands Government and the Municipality of Rotterdam have invited the Permanent Committee of the International Conference on Soil Mechanics and Foundation Engineering to call the second Conference in the Netherlands. Although this is no longer the prosperous country of years gone by and although few countries emerged from the struggle more damaged and more plundered, it is the pride of government and nation to show how much their energy and resources are harnessed to the reconstruction of the devastation wrought by the war. In this context it is symbolic that Rotterdam, the town that was damaged most, has offered to be the seat of the Conference.

It is with these considerations in mind that the Committee on Organisation has assumed its task with great pleasure. It is glad that the preliminary announcements concerning the Conference have met with a wide response over the whole world, so much so, that the size of this Conference is likely to exceed the expectations which were founded on the experiences gained at Cambridge during the First Conference. It should be clear that this means a heavy strain on the available resources in a country, where three years ago no machines or supplies of any kind, no food nor the simplest daily requirement were to be had.

The Committee therefore invokes the clemency of the members of the Conference, should they not find everything up to the standard they would have expected on a similar occasion in pre-war days.

J.P. van Bruggen, president  
T.K. Huizinga, secretary  
E.C.W.A. Geuze

PREFACE BY THE EDITORIAL COMMITTEE

On the occasion of the publication of the first two volumes of papers for the Second International Conference on Soil Mechanics and Foundation Engineering, the Editorial Committee feels that a statement would be appreciated on the line taken for the composition of these Proceedings.

The great number of prospective contributions made the Committee's task to ensure timely distribution of the bound and printed copies of the Volumes difficult. On the 2<sup>nd</sup> of January of this year only 57 papers out of a total number of 480 promised, were received by the Committee. Although part of the preparatory work, especially the classification according to the subjects, had already been undertaken - based on the summaries previously received - the major part, viz. the preparation of the material for the printer, had to await the arrival of the complete papers. The delay in the forwarding of these papers has contributed to make the task of the Committee heavy.

In these circumstances, it has been found necessary to deviate from the initially set principles in two respects, viz:

- 1<sup>o</sup> While it has been tried to avoid undue splitting-up of sections and sub-sections over the various volumes, papers have been placed in order of their arrival more often than was foreseen.
- 2<sup>o</sup> The definition of the subjects of the various sub-sections had been based on the summaries received. A number of papers however have been submitted of which no previous summary had been sent. Therefore the classification does not necessarily cover all the papers as finally published.

Alterations in the author's text have been limited to the make-up and to obvious errors of typing and spelling.

The Committee apologizes for any errors, which may have occurred in the papers in the process of preparation for printing. It asks members to view these in the light of the difficulties outlined above.

N. Mannings, President  
G.A. Oosterholt, Secretary  
E.C.W.A. Geuze  
A.W. Koppejan

REVIEW OF SECTIONS AND SUB-SECTIONS

SECTION I: THEORIES, HYPOTHESES, CONSIDERATIONS  
OF A GENERAL CHARACTER

Sub-sections:

- a. general considerations
- b. geology and soil mechanics
- c. physical and physico-chemical properties of soils
- d. stress-strain relations; consolidation
- e. shearing strength and equilibrium of soils
- f. earth pressure
- g. stress distribution
- h. vibrations and mathematical problems
- i. miscellaneous

SECTION II: LABORATORY INVESTIGATIONS.

Sub-sections:

- a. general
- b. identification tests
- c. consolidation tests
- d. triaxial tests
- e. direct shear tests
- f. electro-osmosis
- g. miscellaneous

SECTION III: FIELD INVESTIGATIONS.

Sub-sections:

- a. boring and sampling
- b. measurements of special soil properties
- c. measurements of pressures and deformations
- d. vibrational research
- e. aerial photographing
- f. areal studies
- g. miscellaneous

SECTION IV: STABILITY AND DEFORMATIONS OF EARTH  
CONSTRUCTIONS.

Sub-sections:

- a. embankments of highways and railroads
- b. dams and levees
- c. excavations and slopes
- d. miscellaneous

SECTION V: EARTH PRESSURE; STABILITY AND DISPLACE-  
MENTS OF RETAINING CONSTRUCTIONS.

Sub-sections:

- a. earth pressure against rigid vertical walls
- b. earth pressure against flexible vertical walls
- c. earth pressure against underground constructions

S E C T I O N VI: FOUNDATION PRESSURE AND SETTLEMENTS OF BUILDINGS ON FOOTINGS AND RAFTS.

Sub-sections:

- a. measurements of settlements and comparison with theory
- b. measurements of stress distribution in the contact face
- c. influence of groundwater
- d. special problems in foundation engineering

S E C T I O N VII: PILE FOUNDATIONS, PILE LOADING TESTS.

Sub-sections:

- a. settlement and bearing capacity of piles
- b. horizontal pressures on pile foundations
- c. special problems

S E C T I O N VIII: PROBLEMS OF ROAD AND RUNWAY CONSTRUCTIONS.

Sub-sections:

- a. test sections
- b. methods of flexible pavement design
- c. methods of rigid pavement design
- d. design and construction of some roads and airfields
- e. investigations on failures, drainage and frost action
- f. miscellaneous

S E C T I O N IX: IMPROVEMENT OF THE MECHANICAL PROPERTIES OF SOIL.

Sub-sections:

- a. general considerations
- b. mechanical methods
- c. physico-chemical methods
- d. physical methods

S E C T I O N X: GROUNDWATER PROBLEMS.

Sub-sections:

- a. general groundwater investigations
- b. seepage problems of dams and levees

S E C T I O N XI: SUGGESTIONS FOR INTERNATIONAL COLLABORATION, EXCHANGE OF INFORMATIONS.

S E C T I O N XII: SUBJECTS OF A GENERAL CHARACTER.

Sub-sections:

- a. Classification of Soils
- b. Information on existing institutions and persons working in the sphere of Soil Mechanics and their sphere of action.  
(This information will be used to improve international collaboration).
- c. National exposition of the latest development and ideas in the sphere of Soil Mechanics, with a report of literature.

# SECTION I

## THEORIES, HYPOTHESES, CONSIDERATIONS OF A GENERAL CHARACTER

### SUB-SECTION I a

#### GENERAL CONSIDERATIONS

I a 1

#### EARLY HISTORY AND BIBLIOGRAPHY OF SOIL MECHANICS

JACOB FELD, Ph.D.

Consulting Engineer, New York, N. Y.

#### INTRODUCTION.

Both the art and the science of control and utilization of soil as a building material have their beginnings in prehistoric days. Some ten thousand years ago, Neolithic man built huge earth mounds to mark burial sites or for other commemorative, or possibly, useful, reasons. Mound building was continued by the early Greeks, the early Saxons, and even by the prehistoric American Indians, and is even now an important problem in soil mechanics as applied to embankments and earth dams. Near Silbury, England, Megolithic man built not only a huge mound but also a circular ditch to surround his stone erection project. Possibly pre-dating any of these earth-works were the pile foundations erected for supporting the shelters of Neolithic man along lake shores. Earth tunnelling dates back to at least 800 B.C. in the Persian underground galleries ("Kanats" or "karezes"), thousands of miles in total length to tap underground water and to artificially dewater the sub-soil. The art of this method of water production was brought to Egypt by Scylax about 500 B.C., in the irrigation of the El Khargeh oasis, and its use spread as a standard method from Baluchistan to Morocco.

Archeologic explorations indicate very little positive information of knowledge on the necessity for foundations under ancient structures. When structures settled too much, they were demolished and the rubble was used as a base for the succeeding structure. A critical examination made in 1931 by the writer of the walls of Jericho (four levels) as exposed in the excavations made there by Major Toulouk, indicated that a special layer of stones had been placed as a base for each succeeding wall. The lowest construction dates back to about 2400 B.C. Major Toulouk was quite convinced that he had solved the mystery of the Jericho wall failure when Joshua (1400 B.C.) took the city. The excavations showed the foundation tier of stones (for the wall of that period) displaced laterally to the outside and tipped forward, as if a trench had been dug along the bottom of the wall to undermine the base. A possible solution to an age old question, and an application of soil mechanics knowledge.

Ancient and mediaeval philosophers contributed to many sciences and there are references in the technical literature of the 17th and 18th centuries which gave credit to Galileo, Lambert, and others for basic ideas. The existing contributions in earth and soil studies, as an independent problem, date from the latter part of the 17th century. From the French military engineers, there came a succession of empirical and analytical analyses of earth pressures and earth slopes, necessary data for the design of fortifications.

During the same period, the English seem to have been more interested in the study of soil control and classification for application to agriculture. About the middle of the 18th century, contributions on lateral earth pressure begin to appear in Italian, Dutch and Swedish scientific publications, at first as applied to fortifications and later as a scientific problem attacked experimentally and analytically. Coulomb's essay in 1773 changed the entire method of approach to the problem of soil slopes and lateral earth pressure and was closely followed by many experimental attempts to prove and to disprove his theoretical results. Before the end of the 18th century, there appeared contributions in the French, Dutch, German, Italian and Russian scientific societies on Coulomb's theory and modifications of the formulae, chiefly simplifications to make the results of empirical value.

In the last quarter of the 18th century, Böhms "Magazin" must have been an important medium for the dissemination of new ideas, for it carried translations into German of almost all the contributions found in the printed transactions of the scientific societies in all the countries of Europe. Extensive summaries of earlier work are given by Brunings (1803, Dutch) and Mayniel (1808, French). The early part of the 19th century brings studies of other soil problems, such as shore erosion, pressures on the inside and outside of bins and cells, flow of soils from orifices, pile foundations and soil control by wood pile and by "sand pile" introduction, together with a continuous attack on the lateral earth pressure question.

The fifty earliest available references to soil mechanics contributions are listed in chronological order and a short discussion of the various contributions is given as an outline of the history in this subject, to record the origins of the study which is the subject of this Conference.

#### SOIL CLASSIFICATION AND IDENTIFICATION.

In a lengthy dissertation presented before the Royal Society of London on April 29, 1675, Evelyn states that the Ancients classified soils as: Creta, Argilla, Smetica, Tophacea, Pulla, Alba, Rufa, Columbia, Macra, Cariosa and Rubrica, and that Anathesius Kircher in his "De Arte Combinatoria" computed that there were 179,100,060 different sorts of earths, of which only 8 or 9 need be considered practically. Evelyn describes the methods of identification and the expected actions of soils found in the three different layers or horizons: (1) top layer or under-turf earth, (2) soil layer, which may be loam, clay, plastic figuline, or smetic, and (3) sub-soil layer,

which may be chalk, marle, fullers-earth, sandy, gravelly, stony, rock, shelly, coal or mineral. Each of the types is described and the suggestion presented that identification can be made by the use of the senses: smell, taste, touch and sight. Evelyn makes it clear that a composition of mixed soils does not exhibit the properties of all the constituent parts, since certain earths influence the soil behaviour far more than one would expect from the proportional content.

Lemaire (1737) revised the tables for fortification walls developed by Vauban by introducing the "tenacity" in the earth backing as helping the stability of the walls. Previous analysis had always been based on the assumption of a hypothetical solid earth.

Querlonde (1743) distinguishes between three types of soil backfill: vegetation soil, stiff earth and sand, having different natural slopes, namely 1:1, 3:2 and 1:2. Lorgna (1763) differentiates between various soil types, generally divided into four classes: various kinds of fresh earth, dried earth, sandy ground, and sands, which latter may be plain, mineral, river or sea sand. Rondelet (1767) divides all soil into earth and sand, and his monumental work influenced many later authors to disregard variations in different soils.

Chauvelot (1783) seems to be the first to attempt a soil classification by a numerical determination of physical properties: weight, friction and cohesion. When he presented his theory of lateral earth pressure determination before the Academy of Sciences in Paris (Jan. 22, 1783), in which he evaluates the pressure of any material where the weight, internal friction and cohesion are previously determined by experiment, that learned body declared that the problem of earth pressure was susceptible of a rigorous solution. It is strange that Coulomb's much more logical and complete solution of the problem was disregarded in this pronouncement.

Delanges (1788) studied the state of "semi-fluids", which he enumerated as sand, gravel, lead sparrow-shot, millet and similar materials. Mayniel (1808) in the practical applications of the theory to retaining wall design, tabulates values for the following soil types: soil fill, sand, gravel, rubbish fill and clay fill. Sir Humphrey Davy (1813), from the agricultural point of view, shows that all soils are mixtures of various types of earth, four types being most common: aluminous clay, siliceous sand, calcareous marle or chalky sand and magnesian. In 1818, an unknown author apparently much influenced by Davy, wrote in the "Treatise on Soils and Manures", on the subject of soil identification:

"In framing a system of definitions, a soil is to take a particular denomination from a particular kind of earth, not exactly in proportion as that earth may preponderate, or not, over others in forming the basis of the soil, but rather in proportion to the influence which a particular kind of earth, forming part of the sample, has." This statement is in close agreement with the most modern recommendations in soil classification and identification.

#### LATERAL EARTH PRESSURE THEORIES.

A large majority of early contributions deals with the subject of lateral earth pressure. In comparison, the first International Conference at Harvard included only three papers on the subject, showing that there is fair agreement on the solutions of this problem in soil mechanics. A "History of the De-

velopment of Lateral Earth Pressure Theories" was published by the author in the Brooklyn (N.Y.) Engineers' Club Proceedings, January 1928, and only a summary is included here.

Revetments for the fortification of cities and camps have been built from the earliest days, noteworthy examples being the masonry walls of the Romans erected to withstand the shock of catapult projectiles and to retain the earth fills. The walls of the mediaeval ages were copies from the Roman structures which outlived the empire. The earliest existing recorded rules for the design of revetments are those of Vauban, the great French military engineer, (1687). In his treatise on the fortification of fortresses he mentions the formulas which were used in constructing over 150 fortifications of various heights, using 4,000,000 cu. yds. of masonry. In all probability these rules are based upon older empirical rules coupled with "cut and try" experiment. Vauban assumed that his walls would rotate as units about the toe, the counterforts acting as integral parts of the wall. He realized that the counterforts decrease the acting earth pressure because of the frictional resistance along the sides as well as by a decrease of the exposed wall area. Audoy has shown that the typical Vauban revetment has a factor of safety of 4.70 for sliding and 3.80 for overturning, assuming ideal condition.

Bullet of the French Royal Academy of Architecture develops the earliest theory based upon the principles of Mechanics (1691). Starting with the assumption that all the retained earth above a  $45^\circ$  plane through the heel of the wall tends to slide as a solid mass upon this plane, he says that the weight of the wall must be to a weight of this wedge as the length of the plane of rupture is to the height of the wall.

Couplet (1726) published three excellent articles concerning the pressure of earth against revetments and the necessary resistance of revetments to withstand such pressure, containing the earliest synthetic earth pressure theories. In the first article he assumes a frictionless wall acted upon by a fill of an infinite number of small spherical grains. In 1727, he generalized to the case of a rough wall, the pressure now acting normal to the irregularities or grains in the back of the wall. Two cases are considered, where each grain rests on three or on four others; in each case the plane of rupture will pass through the toe of the wall. For, he says, if the portion of the wall below this plane is omitted, the material below the new wall, being in the natural state of equilibrium, will not move. The method is the same as in the first theory, except that the unbalanced force may now act obliquely. The general result is in the form of a cubic equation from the solution of which one obtains the required width of wall for rotational stability.

Belidor (1729), starting with Bullet's assumption of a  $45^\circ$  prism of rupture, investigates the action of the wedge by dividing it into parts by planes parallel to the plane of rupture. He summates the effects of the individual sections of earth in causing rotation about the toe, the earth pressure being the horizontal component, and deducted half of the resulting overturning moment as a loss due to the presence of friction. In any case of oblique wall or surcharged fill the wedge of rupture is the material contained between two  $45^\circ$  planes passed through the bottom and the top of the back of the wall.

Querlonde (1743), of the French Military

Engineers, refuses to accept the idea of a  $45^\circ$  wedge for all cases, but considers three types of soil - vegetation soil, stiff earth and sand. The earth pressure is horizontal, however, he says that the sum of the earth pressure and the frictional loss must equal the weight of the wedge. Also, the ratio of the pressure to the friction loss equals the ratio of the height of the plane of rupture to the horizontal width. This comes, he says, from the principle of the inclined plane.

Gadroy (1745), tried to prove Belidor's theory by experiment. Using a small model wall he found that failure occurred by rotational displacement; hence, he concludes that the lateral pressure must act at the top of the wall. He noticed that the first slip of sand did not include all the material above the plane of repose, but he missed the significance of this fact, although he went to the trouble of investigating the effect of the height of fill on the plane of rupture.

Numerous contributions, usually modifications of earlier theories appeared from 1745 to 1770. Louis de Cormontaigne (1750) advises a correction to Couplet's theory - his "every day practical method" was to take the lateral pressure as half the weight of a  $45^\circ$  prism of rupture. Lorgna (1755) assumes the lateral pressure to act at  $45^\circ$  and to be equal to the weight of the  $45^\circ$  prism of rupture times the sine of  $45^\circ$ . Kinsky (1763) follows the same reasoning to obtain the overturning moment, and Ypey (1765) bases his theory on a  $45^\circ$  plane of rupture passing through the toe of the wall.

Sallonyer (1767) of the French Department of Fortification resolves the weight of the prism of rupture, assumed to slide on the plane of repose, into two components, one of which acts parallel to this slope and is equal in magnitude to the weight of the wedge. This tangential force acts through the center of gravity, and is resolved into horizontal and vertical components at the back of the wall. The overturning moment is the algebraic sum of the moments of these two forces about the toe. The width of the wall is found by equating the moments causing and resisting overturning. Blaveau worked with Sallonyer and develops a similar theory. The lateral pressure has the same direction and point of application but its magnitude is the component of the weight of the wedge parallel to the plane of rupture. In calculating walls he disregards the vertical component of this pressure. A great advance was his generalization from the case of a  $45^\circ$  wedge to the wedge with an undetermined angle.

Rondelet in describing his earth pressure theory makes no mention of any previous author except Belidor. Rondelet decomposes the weight of the wedge into components parallel and perpendicular to the plane of slope. The tangential force acting through the center of gravity of the wedge is the earth pressure. Experimentally he deduced that the pressure is always caused by a wedge sliding on the plane of slope, which both for sand and earth is a  $45^\circ$  slope. At about the same time, according to Mayniel, the Department of Fortifications was using this theory with the reduction of the tangential component by the frictional resistance along the plane of slope. Other engineers were resolving the weight of the wedge into two components, one horizontal and the other normal to the plane of slope.

Trincano goes back to the assumption of a  $45^\circ$  wedge causing a horizontal pressure at  $2/3$  h, but says that its value is  $1/4$  of the weight of the wedge. The Italian engineers,

including d'Antony (1768), all assumed a  $45^\circ$  wedge of rupture. D'Antony made the same assumptions as in Trincano's theory and also recommended that the face of the wall be made parabolic in section since the pressure varies as the square of the depth. Another assumption in his theory was that the friction along the base of the wall aided the stability against overturning.

Up to 1773, all the attempts at the theoretic determination of the lateral pressure of granular materials began with the assumption of a definite plane of rupture, usually the plane of slope. Coulomb eliminated this assumption by deriving an expression for the pressure caused by a general wedge. Then letting the first derivative, with respect to the variable wedge angle, equal to zero, he obtained the value of the wedge angle corresponding to the maximum pressure. In this way he introduced the idea that a wall must be designed to withstand the maximum pressure; previous investigators had not considered the possibility that their methods might not picture the worst case.

Coulomb's essay on the application of the rules of maxima and minima to the statics of construction (1773) gives a remarkably complete analysis of the action of granular materials. He uses as his basis the laws of friction and cohesion for solid bodies which he assumed also hold for granular bodies:

- 1) The frictional resistance on any surface is equal to a constant, the coefficient of friction, times the normal pressure on that surface.
- 2) The cohesion resistance is equal to a constant times the area of the surface.

With but few exceptions, later writers have accepted these laws. Coulomb further assumes a plane surface of rupture for convenience of evaluation, and sliding of that wedge which will cause the maximum pressure. He gives no proof for this; later investigators have shown that these two assumptions are not consistent, for wedges bounded by curved surfaces of rupture may cause greater lateral pressures than Coulomb's wedge. The pressure exerted by this wedge is due to its weight and is decreased by the frictional and cohesive resistances along the plane of rupture. Disregarding friction along the wall, the pressure is horizontal. However, he states, if the wall is rough, there is frictional resistance, equal to the normal lateral pressure, times the coefficient of friction, which resistance must be subtracted from the weight of the wedge whenever there is motion between the wall and the fill.

To allow for cohesion, the true pressure equals the value obtained by disregarding cohesion less the pressure on the height of earth which is naturally self-sustaining. Nowhere in his discussion does he make mention of the angle of repose; his theory considers only the coefficient of friction inside the mass.

Woltmann (1790) translated Coulomb's theory into German and simplified the resulting equations by assuming that the tangent of the angle of repose was the coefficient of internal friction. Up to a very recent date this assumption has been included in practically every description of "Coulomb's theory." Prony (1797) simplified Coulomb's discussion by introducing trigonometric functions, and showed that, if the tangent of natural slope is the coefficient of friction, for the case of a vertical wall, the plane bounding the wedge maximum pressure bisects the angle between the wall and the natural slope. Since the coefficient of friction is a constant, the natural



slope and the plane of rupture are constant. Coulomb used the width of the wedge as the variable with respect to which he differentiated to obtain the condition for a maximum. Prony used the angle of the wedge, which is really the independent variable; the width of the wedge is a function of this angle and the height. Prony's method is the more general one for it may be used where the surface of rupture is not assumed as plane.

Mayniel (1808) extended the wedge theory to the case of a sloping wall, assuming the pressure as normal to the back, and taking into consideration the friction and cohesion along the plane of rupture and the friction along the back of the wall. He does not accept the assumption of the equality of the angles of friction and natural repose, though he mentions that Prony had made such an assumption. The mathematical work is very detailed and complicated, but as he says: "That is because of the general nature of the solution; we must take into account all the points of the problem." In summarizing previous theories he distinguishes between two types of friction in soils:

1) Perfect friction, as in sand, is caused by the interlocking of particles, acted upon by a continuous pressure, and is to be distinguished from cohesion which is a reunion of masses, like a glueing together.

2) Imperfect friction is the rubbing or rolling of particles over each other, due entirely to their own individual weights. Mayniel also gives a clear picture of how earth exerts a lateral pressure behind a wall: A certain part of the fill in the shape of a wedge with the apex at the heel of the wall slips down on a surface which is probably a plane; this material is not the entire volume which tends to slip, for later slips do occur if the wall slips or fails, but these do not concern the problem of the existing pressure.

Francois (1820) repeated Mayniel's work including in the discussion Woltmann's assumption. The total angle between the wall and the plane of rupture is taken as the variable. The effect of surcharges was studied by Navier (1813-1826) who also derived the most general formula for the lateral earth pressure acting normally to the wall. In the case of surcharge, he showed that the resultant must act at a point higher than  $1/3$  the height of the wall. Considering a bank of earth in equilibrium, the material above the plane of repose is prevented from sliding by the friction and cohesion along this plane. From this is evaluated an expression involving the tangent of the angle of natural repose in terms of the coefficient of friction and cohesion and the height. For small heights, he showed, the face of the earth bank may overhang and still be in equilibrium. When the cohesion is zero, the expression for the tangent of the angle of repose becomes the coefficient of friction, showing that Woltmann's assumption is only true when there is no cohesion.

Still tending towards a general solution, Audcy (1820) does not accept the assumptions of uniform density, friction and cohesion, but regards each as a general function of depth. Taking the pressure as normal to the wall, he derives a most complicated expression, which is of no use because of the lack of information of the factors involved. By accepting Coulomb's hypotheses the formula resolves into the result of Francois' theory.

But few advances in theory were made between 1820 and 1840; however, the experimental determination of the necessary facts upon which to base theory was begun. The work of

Huber Burnand (1828) on the physical characteristics of sand and Hagen's experiments showing the presence of a vertical component are most noteworthy, (1833). The latter also developed the theory of pressures in bins, based on the Coulomb wedge theory.

In spite of the considerable advances made in the wedge theories, many authors have reverted to the older ideas, very often appearing quite ignorant of the fact that the older theories had been modified. The French Department of Fortifications had not immediately accepted Coulomb's theory but used the method of de Montlong (1774). The plane of rupture was assumed to pass through the toe of the wall and, in equating moments, the material between the plane and a parallel plane through the heel was assumed to aid stability.

Chauvelot (1783) rejects all previous theories (he does not mention Coulomb's) because of the large number of assumptions required. Experiments showed that the natural slope of sand was  $39^{\circ} 21'$ , yet he recommends that a  $45^{\circ}$  wedge be assumed for all materials. The weight of the wedge is resolved into components; the lateral pressure is equal to the component acting normal to the wall less a correction for friction and cohesion in the fill and the point of application is at  $2/3 h$  from the base.

Gauthey (1785) obtained experimental data absolutely proving the existence of a wedge of maximum pressure, where the plane of rupture bisected the angle between the vertical wall and the plane of repose. However, he missed the significance of his results, advising the use of d'Antony's theory with the addition that  $1/3$  the weight of the wedge be subtracted to take into account the friction loss. He was a standard writer on engineering construction, see for example, his wonderful book on bridges. This may explain why his earth pressure theory was so widely accepted; as late as 1865, Curioni and de Benedict advised the use of Gauthey's formulas.

Delanges (1788) made some careful observations of the effect of the moisture content on the natural slope and density of soils, also experimentally determined the lateral pressure of various granular materials, but he applied his results to proving the older theories. Senguin (1792) edited the second edition of Bulet's "Traite", and inserts in a footnote his "newer" theory. The lateral pressure acts parallel to the plane of rupture and the wall is designed by the requirement that the resultant of the pressure and the weight of the wall pass through the toe. Goudriaan (1796) and Bruenings (1803) determine the effect of a  $45^{\circ}$  wedge; the latter also says that the surface of rupture may not be a plane but he assumes an average plane to derive a formula in the same way as the older methods. Similar disregard of the Coulomb contributions appeared regularly in the literature, even as late as 1911, the London "Architect and Contract Reporter" prints this statement in an unsigned article: "The earth pressure of loose earth is exactly the same as water pressure, being equal to the weight vertically above the area considered and the same in all directions."

#### EARTH PRESSURE EXPERIMENTAL WORK.

The earliest recorded experimental work is by Belidor, who states that as a result of experiment he was led to the conclusion that the prism of rupture of earth fills was on a slope of 1:1. Gadoy (1745), using a test wall 3 in. high, made to check Belidor's theory, concluded that the plane of rupture sloped at

2:3 and not at 1:1, even though the natural slope of the material was 1:1. Rondelet repeated these experiments with a test wall 17½ in. high, using both sand and natural soil as fill, and came to the conclusion that the plane of rupture did not coincide with the plane of natural slope. However, for simplicity, he suggests that a plane of rupture on a 1:1 slope be assumed for all materials.

D'Antony constructed a test box with one side hinged at the bottom and the top held by a cord which passed over a pulley and was balanced by weights hung in a pan. No reliable results were obtained from these tests. Gauthey using a box 30 in. high and 12 in. wide was the first to perform a complete set of earth pressure experiments. A bottom hinged gate with a cord tied at one-third the height and passing through the fill was counterbalanced by weights similar to the method of D'Antony. He then changed the wall to a gate made up of five parts, in a smaller bin, making each part 1-1/2 in. high and attaching two cords to each part. In this way he attempted to measure the pressure at each depth. In spite of the resistance of the imbedded cords, he did obtain an idea of the variation in pressure on the various slats, reporting that with a sand fill, the weights needed to balance the five slats were 1-1/2, 4, 6, 8 and 10 oz. To determine how much of the filling material in the bin was really responsible for the pressure against the test wall, he built a hinged sloping bottom in the bin and reported that the pressure against the vertical face was the same for the horizontal bottom and for a number of increasing slopes with the horizontal until he reached 67-1/2 deg. In this way he proved that the material below that plane had no effect on the pressure against the vertical wall.

Delanges, describes some experimental work on the shapes that semi-fluid materials will take and the vertical pressure in the small bins. In the lateral pressure experiments he used a small box with a hinged side 6 in. square, counter-balanced by two strings of silk, on which were hung equilibrium loadings. He points out very carefully that both the horizontal and the vertical pressures of semi-fluids contained in "vessels" is reduced below corresponding fluid pressures by the friction of the side walls.

The earliest large scale apparatus was built by Woltmann, a box 1.72 m long, 1.15 m high and 1.15 m wide. The front wall was hinged on the top and prevented from excessive rotation by an adjustable stop at about one-third of the height. Two methods were used to measure the overturning moment on the front wall. The first was by means of a string tied to the back of the wall at its middle point and connecting to balancing weights placed before backfilling, which were removed gradually after backfilling, until movement occurred. The second method was to counterbalance the wall by weighted crank arm beam attached rigidly to the wall. Materials tested included sand, gravel, soil and rye. The results obtained were approximately half of those given by the Coulomb formula.

The experiments conducted at Alexandria in 1805, at Piedmont in 1806 and at Juliers in 1806 and 1807, were started by Major of Engineers Laulanier, continued by Lieutenant Derche and were completed by Mayniel. The first apparatus built was a box 2 m wide, 1-1/2 m long and 1 m high. When filled with sand, the bottom hinged gate broke its hinges and fell with a "sharp detonation". However, the

experimenters had curiosity enough to measure the surface of rupture and found it to be practically a plane at an angle of 64°42' to the horizontal. The second apparatus built at Juliers, was 3 m long, 1½ m wide and 1½ m high. The box was of wood, but the gate was built much more substantially and also hinged at the bottom. At one-third the height an iron strut was hinged to the gate and pushed against the weights on a friction block. The resistance of the friction block was first made larger than the expected pressure and was reduced by adding weights in the pan helping to pull the block. Mayniel states, as a conclusion from the experiments, that Coulomb's theory is the only true and simple theory. The resultant pressure acts at one-third of the height and equals from 1/4 to 1/3 of the weight of the wedge of rupture when the fill is loose, and from 1/7 to 1/20 of the weight of the wedge of rupture when the fill is packed.

A very similar apparatus was used by Martony de Kossagh, 2.85 m long, 0.95 m wide and 1.90 m high. Pressures were also measured by a friction dynamometer. Of course this method prevented any measurement of a vertical component. The fill material was sand and also earth, and the results agreed fairly closely to those given by Coulomb's theory. A detailed report of all recorded experimental work was prepared by the author in 1923, and filed with the Engineering Societies Library in New York, and a summary was published in the Proceedings of the Highway Research Board, 1940.

#### PRESSURE ON BIN SIDES AND BOTTOM.

In addition to the military problem of fortification walls, the French Engineers spent considerable effort to solve the problem of bin storage, which had a practical application in the magazine silos. Moreau (1827) reported on the practical considerations of silo planning, above and below ground, and of square and circular sections. Both Moreau and Huber-Burnand knew that the base of a bin did not support the entire load above it. The latter proved it experimentally (1829), by weighing bottomless boxes filled with sand and with top soil, as they were lifted free of the supporting floor. Moreau and Niel (1835) experimented with a similar device, but with only part of the bin bottom detached, and showed how an arch formed over the opening and the pressure on the opening was independent of the height of the fill and of any surcharge placed thereon. In some cases, the surcharge loads actually decreased the pressure exerted on the bin bottom. Some of this experimental work was performed to determine the pressures at the bottom of the fills due to surcharge loads.

#### SOIL PHYSICS STUDIES.

Couplet (1726) pictured soil as a pile of spherical grains, arranged as tetrahedra, either one grain on three or one grain on four. Gauthey tried to check this picture experimentally, but found that soils did not fracture along a natural slope line, as did the piles of spheres. Gadroy (1745) studied the erosion of soil slopes and concluded that the windward side was more affected and the amount of erosion from wind and rain was smaller for soils with smaller natural slopes. That soil can stand vertically and even overhang seems to have been fairly well known, but Coulomb (1773) was the first to determine the height

of soil which can stand vertically as a function of the cohesion and internal friction. This formula he obtained by determining the height for which his general formula showed a zero value for the lateral earth pressure.

Delanges (1788) quotes two earlier authorities as having distinguished soils from solids or liquids: Galileo stated that semi-fluids in contradistinction to liquids "when heaped together maintain their condition; and when hollowed up to a certain mark, the cavity remains, without the surrounding parts flowing to fill it again; and when agitated and disturbed they quickly settle, as soon as the outside motion slackens." And further he finds cause "to be able to very reasonably argue that the smallest parts of water into which it seems to be resolved (since it has less consistency than the finest powders whatsoever, in fact it has no consistency) are very different from the smallest divisible quantities." Lambert (1772) on the other hand, claimed that restrained bodies of soil reacted more like liquids.

Delanges carefully measured the natural slope of several materials and noted that each had a definite slope, which was greater for rougher surfaced and for larger sized grains. He states that liquids assume a level surface because they consist of a minute smooth-surfaced spherical grains. Experimentally, in cylindrical and conical vessels, with loose bottoms, he proved that the bottom supported less than the total weight, of the contained materials, and correctly deduced that the reduction was caused by the friction along the sidewalls. When openings of various sizes were opened in the bottom of the vessels, the flow of the various granular materials seemed to be independent of the depth of the fill, and always ended with a conical cavity of fixed slope for each type of material. Then using glass cylinders and placing horizontal layers of grains stained different colors, he could watch the sequence of flow from the different depths and the relative velocities of motion. In similar experiments to measure the flow through horizontal openings, Delanges derives a result analogous to the flow of liquids through an orifice, modified by taking into account the fact that the particles arrive at the orifice "with a rate of speed much less than that which would be suitable for a free drop." This work was later repeated and expanded by Huber-Burnand (1829) with the same conclusions.

Woltmann (1802) studied the stability of slopes in canal excavations and derived a formula for determining such stability. Goudriaan (1810) developed the effect of different shaped waves on shore erosion and understood the mechanics of wave action and energy transmission from water to sand along the beaches. In 1796, he wrote on wood sheet-pile and other shore protection methods.

#### FOUNDATION AND PILE STUDIES.

Although the art of foundation construction must have been well established by 1772, it was Lambert who first made an attempt to rationalize the design of spread foundations as well as the use of piles. Some of his conclusions were based upon observation, and others on the results of experimental determination of settlements from static and falling models resting upon and "immersed" in sand.

An extensive research into the value of sand piles for consolidation and stiffening of miry soil, made necessary for the design of foundations at Bayonne, France, was report-

ed by Moreau (1827). Among the basic conclusions is found proof that soil can be consolidated to a much greater volume reduction by driving piles which are then withdrawn and replaced by "very friable stone reduced to powder," than by surface ramming. These sand pile foundations were test loaded, by load increments over long time periods, to a maximum of 66,000 lbs. on nine piles, 8 $\frac{1}{2}$  in. diameter and 4 $\frac{1}{2}$  ft. long, spaced about 16 in. on centers. Preference of sand piles over timber piles is also expressed because they act as wells into which the adjoining earth drains and therefore permits better consolidation.

In attempting to measure load distribution through soil by weighing the load carried on a loose panel in the bottom of bins, Moreau concludes: "Whatever may be the original pressures, when a portion of the bottom commences to give way, it is relieved of most of the weight upon it" and so "whatsoever may be the differences of resistance of the bed of the foundation, no part of this bed can yield without the pressure upon it decreasing or the neighbouring parts giving way at the same time and the settlement becoming uniform in sequence." Which is a simple and true description of what is now called "limit" design.

Neil (1835) experimentally determined the extent of load distribution through soils by noting how close to a load he could safely remove the soil slope. This information he applied to actual designs of foundations supported by layers of sand placed on soft clay and mire. Parallel loading tests on soil excavated in pits, with and without sand pads, were carried over 14 day periods. In a pit 4 ft. square and 9 ft. deep, a 4 ft. depth of sand reduced settlement values to almost one-third, the loading being 4000 lbs. per sq. ft. These methods of sand bases and sand piles to carry loads in alluvial silt soils were used at Bayonne, Marseilles and Paris, on a number of noteworthy projects in the first half of the 19th century and only recently have been recognized as proper methods.

Brünings in "Over de Zijdelingsche Drukking der Aarde", some 100 pages summarizing earlier work, (1803), ends with a very fitting quotation for this paper: "If these our good intentions shall be of service to any and favourably received, we have our end."

#### BIBLIOGRAPHY.

- 1) Evelyn, John: "Terra, a philosophical essay of Earth", 1679, London.
- 2) Vauban, Sebastian le Prestre: "Traité de la défense des places", 1687, Paris.  
1722, "New Method of Fortifications", London.
- 3) Bullet: "Traite d'Architecture pratique", 1691, (1792 ed. by Senguin), De la construction de Murs de Rempart et de Terrasse, p. 314 - 52.
- 4) Buchotte: 1716, see Mayniel, p. 64 - 6.
- 5) Couplet: "De la Pousse des Terres contre leurs Revestemens et la Force des Revestemens qu'on Leur Doit Opposer", 1726 - 8, Histoire de l'Académie Royale des Sciences, v. 28, p. 106 - 64; v. 29, p. 139 - 85; v. 30, p. 113 - 38.
- 6) Denzeldan: 1727, Mémoire de l'Acad. R. des Sci., v. 29, p. 200 - 60. Transl. in Eöhas Magazin, v. 12, p. 57 - 126.
- 7) Bellidor, Bernard Forest: "La Science des Ingénieurs", 1729, Paris (1813 ed. by Navier, p. 1 - 81).
- 8) Lemaire: 1737, see Mayniel, p. 67.

- 9) Querlonde: 1743, see Mayniel, p. 68 - 74.
- 10) Gdroy: 1745, see Mayniel, p. 3, 41 - 50.
- 11) de Cormontaigne, Louis: 1749, see Mayniel, p. 83.  
1809 ed. "Memorial pour la fortification permanente et passagère", Paris.
- 12) Muller, John: "Practical Part of Fortification", 1755, Stockholm. Transl. in Böhm Mag., v. 4, p. 145 - 62.
- 13) Stahlwerd: "Forelaesinger uti regulieri Fortification", 1755, Stockholm.  
Transl. in Böhm Mag., v. 4, p. 145-62.
- 14) Lorgna, Antonio: "Tentativo Fisico-Meccanico sulla resistenza de' Muri Contro la Spinta de Terreni", 1763, Gli Atti dell Accademia delle Scienze di Siena, v. 2, p. 155 - 75. Transl. in Böhm Mag., v. 4, p. 119 - 44.
- 15) Kinsky: "De Drukking der Aarde tegen Wal-muren", see Brünings. 1763, Transl. in Böhm Mag., v. 12, p. 127 - 60.
- 16) Ipey, N.: "Over de Profilen der Muren", 1765, Verhandelingen der Haarlemsche Maatschappij, v. 6, part 2, p. 516 - 42.
- 17) Sallouyer: 1767, see Mayniel, p. 85 - 6
- 18) Blaveau: 1767, see Mayniel, p. 87 - 90.
- 19) Rondelet, Jean Baptiste: "Traité théorétique et pratique de l'art de Bâtir", 1803, Paris, v. 3, p. 134 - 211.  
1767, see Mayniel, p. 9, 55 - 6.
- 20) Trincano: "Elements of Fortifications", 1768, see Mayniel, p. 89 - 91.
- 21) d'Antony, Papacini: 1768, see Mayniel, p. 4 50 - 2.
- 22) Lambert, Johann Heinrich: 1772, Nouveaux Mémoires de l'Acad. Royal des Sci., Berlin.
- 23) Coulomb, Charles August: "Essai sur une application des règles de maximis et minimis à quelques problèmes de statique relatifs à l'architecture"  
1773, Mémoire de mathématique et de physique présentée à l'Académie Royale des Sciences, Paris, v. 7, 1776.  
Transl. in Böhm Mag., v. 5, 1779.  
"Théorie des machines simples", 1821, Paris, p. 318-63.
- 24) de Montlong, Tersac: 1774, see Mayniel, p. 92 - 9.
- 25) Chauvelot: 1783, see Mayniel, p. 100 - 102.
- 26) Gauthey, Emiland Marie: "Oeuvres", publ. by Navier, 1809.  
1785, see Mayniel, p. 4 - 6, 53 - 4.
- 27) Delanges, Paolo: "Statica e macinica de semi-fluidi", 1788, Mémoire de matematica e fisica della Società Italiana, Verona, v. 4. Transl. in Brooklyn (N.Y.) Engineers Club Proceedings, by A.J. D'Atri, 1930, p. 9 - 51.
- 28) Woltmann, Reinhard: "Beiträge zur Hydraulische Architektur" 1794 - 9, v. 3 and 4.  
1802, "Beiträge zur Baukunst schiffbarer Kanäle".
- 29) Senguin: edited and revised Bullets: "Traité d'architecture", 1792.
- 30) Fuss, Nicholas: "Examen theoretique des Revetemens a dos Inclins et des Revetemens a assises inclinées", 1795 - 6, St. Petersburg Akademiya Scientiarum Nova Acta, v.13, series IV, p. 80 - 100.
- 31) Prony, de R.F.M.: "Poussée des Terres" 1797, Paris Societie Philomatique Bulletin, v. 1, p. 188 - 91.  
1802, "Reserches sur la Poussée des Terres".
- 32) Goudriaan, Adrianus Francois: "Over de Drukking der Aarde", 1796, Rotterdam Nieuwe Verhandelingen der Bataafsch Genootschap, deel X, p. 151 - 222, "Waterwerk-tuigen".  
1810, "Middelen ter beletting der Zandverstuiving", ibid, v. 5, p. 139 - 84.
- 33) Brünings, Conrad Lodewijk: "Zijdelingsche Drukking der Aarde", 1803, Rotterdam Nieuwe Verhandelingen, v. 3, p. 26 - 131.
- 34) Mayniel: "Traité expérimental, analytique et pratique de la poussée des Terres et des Murs de Revetement", 1808, D. Colas, Paris.
- 35) Stratico, Simone: 1810, Bologna Memoire dello R. Accademia delle Scienze, v. 2, pt.2, p. 261 -
- 36) Davy, Humphrey: "Elements of Agricultural Chemistry" 1813, London.
- 37) Practical Agriculturist: "Treatise on Soils and Manures", 1818, London.
- 38) Tredgold, Thomas: "On the Pressure of Earth against Revetments and Retaining Walls", 1818, London Philosophical Magazine, v. 51, p. 401 - 4.
- 39) Masetti, G.: 1819, Bologna Opuscoli Scientifici, v. 3, p. 341 - 357, 1823, ibid, v. 4, p. 9 - 11; "Sulla Spinta delle Terre".
- 40) Francois: "Recherches sur la Poussée des Terres" 1820, Memorial de l'Officier du Genie, No. 4, p. 156 - 251.
- 41) Audoy: "Notes sur la Poussée des Terres" 1820, Memorial de l'Officier du Genie, No. 4, p. 207 - 28.
- 42) Navier, C.L.M.H.: "Lecon sur l'Application de la Méchanique aux Constructions" 1826, Paris, p. 88 - 130. Transl. by Westphal, 1851; "Mechanik der Baukunst".
- 43) Moreau: "Notice sur une nouvelle manière de fonder en mauvais terrain" 1832, Memorial de l'Officier du Genie, No. 11, p. 11 - 40. Transl. by W.W. Curtis, 1886, Eng. News, p. 314-6, 340 - 2.
- 44) Moreau: "Mémoire sur l'emploi des Silos dans les Magasins aux vivres et les manutentions militaires" 1827, Memorial de l'Officier du Genie, No. 9, p. 7 - 74.
- 45) de Kőszegh: "Versuche über den Seitendruck der Erde" 1828, Vienna.
- 46) Huber-Burnand, and Prevost: "Sur l'Ecoulement et la Pression du Sable" 1829, Geneva Bibliothèque Universelle, Sciences et Arts, v. 40, p. 22 - 40.
- 47) de Lagorce, Mondot: "Dimensions à Donner aux Murs de Revetement" 1830, Journal Genie Civil, v. 7, p. 502 - 7.
- 48) Michaux: "Construction des Revetements avec voutés en décharge" 1832, Memorial de l'officier du Genie, No. 11, p. 344-78.
- 49) Hagen, G.H.L.: "Untersuchung über den Druck und die Reibung des Sandes" 1833, Annales der Physik und Chemie, v. 116, p. 17 - 48, 297 - 323.
- 50) Niel: "Mémoire sur l'emploi du Sable dans les Fondations en mauvais terrain" 1835, Memorial de l'Officier du Genie, No. 12, p. 760 - 84. Transl. by W.W. Curtis, Eng. News, 1888, p. 315, 340 - 7.



## SUB-SECTION 1 b

GEOLOGY AND SOIL MECHANICS1 b 1 ENGINEERING USES AND LIMITATIONS OF PEDOLOGY FOR REGIONAL EXPLORATION OF SOILS

HANS P. WINTERKORN

SUMMARY.

The field of pedologic science is defined and briefly described. It is indicated how the store of knowledge acquired and organized by this science can be of direct usefulness to the engineer engaged in regional soil exploration and in the engineering use of data obtained in such exploration. Specific reference is made to the methodique employed for this purpose by the State Highway Departments of Michigan and Missouri, respectively. Detailed description of the indicated use is found in the references given.

Pedology for the purpose of this paper is conceived in its widest sense as the science which concerns itself with:

1. Soil formation or the characterization of soil systems as functions of:
 

(a) climate	symbol: (cl)
(b) organisms	" (o)
(c) topography	" (r)
(d) parent material	" (p)
(e) time	" (t)
2. Classification of soil systems within the broad frame of climatic influences, but on the pragmatic basis of the soil type as a specific observable unit:
3. Mapping of Soil areas in accordance with a pragmatic classification, such as the U.S. Soil Survey system.

Of these three phases, the second and third are of most direct value to the soils engineer, because of their pragmatic basis. The first, because of its scientific complexity, is in a very unsettled condition, and a great diversity of opinion rules among the pedologists themselves, not only concerning the meaning of the phenomena involved, but even concerning the proper approach to the problem.

4) Because of this situation, the soil engineer may receive little direct help from the professional students of soil formation; on the other hand, he should be vitally interested in the problem itself because the same or closely related factors, which form soils, act on the surfaces of exposed structures or even throughout the entire structure as in pavement base-soil systems. For this reason the problems confronting the student of soil genesis will at least be formulated at this place.

The work of many scholars of different specific interests and leanings has resulted in the recognition that specific soil properties, as well as their integration to soil types, are functions of the above named five soil-forming factors which may vary independently of each other. Recognition of these factors leads to the next step, concerning the reason and mechanism of their functioning.

Joffe 5) differentiates between active and passive soil formers: the passive ones concerned with the mass and the source of the mass, the topography and the age, and the active ones supplying the energy that acts on the mass. The latter include the elements of the biosphere, atmosphere and, partly of the hydrosphere. Joffé's basic intention is good but the association of the respective factors is illogical.

To Vilensky and other Russian workers, soil-forming factors are synonymous with environment.

11). Glinke 3) employed the term "forces" in a transcendental sense, rather than in accordance with the physical meaning assigned to this term in the exact natural sciences. This, of course, is to be expected in pioneering work, but must give way to more exact formulations.

As a result, of the prevailing, somewhat confused situation, Jenny 4) one of the most astute and impartial scholars in this field, despairs of the possibility of a causal correlation between a particular soil-type and the independent soil forming factors, and contents himself with a purely functional correlation, expressing the relation of any or all properties (s) of a particular soil type to those factors as:

$$s = f (cl, o, r, p, t....)$$

Jenny's approach, though logically justified, is sterile at least as far as the engineer's problem is concerned. The engineer must be able to understand or at least to picture what is going on. Logical understanding or even picturing of any function of five independent variables is impossible, especially if the independent variables may range from the complexity of climate to the fundamental simplicity of time. The problem must be simplified until the phenomena can be pictured, even if a succession of pictures be necessary instead of but one. A more logical approach to the problem is as follows:

1. Renouncing the attempt of bringing the whole world of soils into one formula, and concentration instead on the formation of the most important soil types.
2. Reduction of the so-called soil-forming factors to something that can be visualized and expressed in terms of physics and chemistry.

Soil formation represents primarily a chain of chemical reactions. In chemical reaction one is interested in

1. Total energy involved in changing initial to final material.
2. Rate of reaction, as influenced by environmental factors, positive and negative catalysis, concentrations, etc.

The total energy change involved can be ascertained experimentally by means of calorimetric determination of the difference of the heat of solution of the parent material and the soil under consideration, respectively, in a suitable acid, in a similar way as the hydration rate of concrete is checked by determination of heats of solution.

Rates of reaction are influenced by temperature, concentration and catalysis. In

TABLE 1.

ITEMS GIVEN IN SOIL ENGINEERING DATA AND RECOMMENDATIONS  
IN THE FIELD MANUAL OF THE MICHIGAN STATE HIGHWAY DEPARTMENT

Soil Series Name :	
Characteristics	Brief Description of typical profile : 1.) adapted to winter grading :            yes or no 2.) normal depth to water table :        in feet 3.) subject to wind erosion                yes or no
	4.) recommended location of grade line with respect to natural ground: 5.) protection of slopes recommended: No or type 6.) estimated percent of boulders (rock excavation) 7.) stabilization of subgrade recommended for flexible surfaces: yes or no, or percent 8.) removal of topsoil recommended: yes or no, remarks. 9.) estimated lineal feet of frost heave excavation per 1000 feet of cut below natural ground elevation: 10.) estimated lineal feet of open joint sewer per 1000 feet of cut below natural ground elevation:
Treatment	11.) Source of borrow: yes or no, extent 12.) recommended method of restoring borrow pits where necessary. 13.) percent of shrinkage 14.) method of construction:
Resources	15.) sand-gravel material: yes or no 16.) source of suitable stabilizing material: yes, no, type 17.) possible source of gravel: yes, no 18.) source of topsoil: no, poor, fair, good, excellent.

dividing climate into its temperature and moisture components, we obtain the temperature and concentration factors influencing the reaction. The pattern of climate specially with respect to the moisture content of the soil, indicates whether the reaction rates are primarily determined by slow molecular and ionic diffusion processes (uniform moisture pattern) or by faster convection processes (non-uniform desiccation and flooding patterns). Topography by controlling amount of precipitation loss is important only as far as the relationship between macro- and micro-climate (i.e. temperature and moisture condition actually present in the system and not somewhere in the surrounding atmosphere 2)) is involved. If, as should be done, only the

micro-climate is taken into account, topography, as such, ceases to be an independent factor in our equation, except for its bearing on erosion.

For the picture as a whole, it is important that plants utilizing solar energy may, depending upon their type and by means of their root system, return elutriated materials to the reaction system. Thus, a dynamic equilibrium in the soil properties may be reached at a point where the potential chemical energy involved in further decomposition, equals that fraction of the solar energy utilized by the plants in counteracting natural depleting processes.

This picture, of course, gives only a general scheme, but it is thought to be suf-

TABLE 2.

ENGINEERING PROPERTIES SUGGESTED  
BY THE NAME OF CLARKSVILLE GRAVELLY LOAM 9)

General Characteristics	<p>(1) Consists of 3 horizons</p> <p>(2) Horizon No. 1 - gravelly silt loam - normally 5 to 8 inches in thickness.</p> <p>(3) Horizon No. 3 - gravelly silty clay - normally 20 to 30 inches in thickness.</p> <p>(4) Horizon No. 5 - gravelly clay - widely variably in thickness.</p> <p>(5) Pockets of very active stone-free red clay are common and are chiefly responsible for subgrade failures in the region.</p> <p>(6) Contains much clay with a lower liquid limit above 65 which is unsuitable for subgrade or for use in constructing high embankments.</p>
Slopes	<p>(7) Backslopes in horizons 1 and 3 will stand at 1 to 1.</p> <p>(8) To prevent backslope slides in deep cuts involving horizon 5 they should be laid back at 2 to 1.</p> <p>(9) Embankments of Clarksville, ordinarily lying on dolomite beds in an area of fairly rugged relief must be carefully drained to prevent slides if constructed on inclined surfaces.</p>
Compaction	<p>(10) Horizons 1 and 3 compact to high weights per cubic foot at low optimum moisture contents, No. 3 being the highest and most stable.</p> <p>(11) Horizon 5 compacts to a low weight per cubic foot at a high optimum moisture content. Standard compaction tests must be made in four lifts. Such material must be compacted in very thin layers in the fill and care must be exercised not to exceed the optimum moisture content.</p>
Foundation	<p>(12) Unless on inclined rock surfaces, if properly drained, the Clarksville gravelly silt loam provides form fill foundation.</p>

ficient to indicate a way for understanding and for scientific treatment of the dynamics of soil formation. As previously pointed out, understanding of these dynamics is of more direct importance to the engineer than to the general soil scientist.

PEDOLOGIC SYSTEM OF SOIL CLASSIFICATION.

Different methods of pedological classification have been employed in different countries. Because the U.S. have made the greatest qualitative and quantitative effort, and because it appears to be of greatest direct

usefulness to the engineer, the following treatment is restricted to the soil classification system of the U.S. Soil Survey 8). The basic physical unit of this system is the soil type. Marbut 6), 7) lists the following features as essential to the definition of a soil unit: number, color, texture, structure, thickness, chemical composition and relative arrangement of the horizons, and geology of the parent material.

The soil type always has at least 2 names: a SERIES NAME and a CLASS (texture) NAME. Example: Sassafraz Loam

TABLE 3

	Soil Categories 6)	
Category VI	Pedalfers (VI-I)	Pedocals (VI-2)
Category V	Soils from mechanically comminuted materials. Soils from siallitic decomposition products. Soils from allitic decomposition products.	Soils from mechanically comminuted materials.
Category IV	Tundra Podzols Gray-brown podzolic soils Red soils Yellow soils Prairie soils Lateritic soils Laterite soils	Chernozems Dark brown soils Brown soils Gray soils Pedocalic soils of Arctic and tropical regions.
Category III	Groups of mature but related soil series Swamp soils Glei soils Rendzinas Alluvial soils Immature soils on slopes Salty soils Alkali soils Peat soils	Groups of mature but related soils series Swamp soils Glei soils Rendzinas Alluvial soils Immature soils on slopes Salty soils Alkali soils Peat soils
Category II	Soil series	Soil series
Category I	Soil Units or types	Soil units or types.

THE SOIL SERIES:

All soils having identical properties with respect to the items listed below are classified in the same soil series.

- 1) Parent material: (a) solid rock - igneous, sedimentary, metamorphic.  
(b) loose rock - gravels, sands, clays.
- 2) Special features of parent materials, residual or transported by wind, water or ice.
- 3) Topographic position: rugged to depressed.
- 4) Natural drainage: excessive to poor.
- 5) Profile characteristics.

The different series usually carry geographic names indicating the location where they were first recognized and described.

THE SOIL CLASS (TEXTURE).

Considerable detail is employed in naming the various soil classes viz:

- |                      |                     |
|----------------------|---------------------|
| 1. Coarse sand       | 11. Fine sandy loam |
| 2. Sand              | 12. Very fine sandy |
| 3. Fine sand         | 13. Loam /loam      |
| 4. Very fine sand    | 14. Silt loam       |
| 5. Loamy coarse sand | 15. Sandy clay loam |

- |                         |                     |
|-------------------------|---------------------|
| 6. Loamy sand           | 16. Silty clay loam |
| 7. Loamy fine sand      | 17. Clay loam       |
| 8. Loamy very fine sand | 18. Sandy clay      |
| 9. Coarse Sandy loam    | 19. Silty clay      |
| 10. Sandy loam          | 20. Clay            |

If a soil contains considerable gravel, shale or stone the term gravelly, shaly or stony is added to designate the soil type.

It is obvious that the ability to recognize a soil in the field as belonging to a certain type and series, make available automatically a tremendous store of knowledge concerning the respective soil. It is of greatest practical importance that for such recognition in the field only few tools are required, and the most important of these are the five senses. On the other hand, this recognition is an art and can only be taught and learned in the field. "The engineer must learn his soils". 10)

The pedologic classification being of a qualitative rather than of a quantitative character, can, of course, not give all the data which the engineer likes to have, such as maximum density and optimum moisture content of compaction, susceptibility to different types of stabilization, required spacing of drainage tiles, etc. However, once these additional properties have been determined



for a certain soil type by engineering tests and (or) from experience, they continue to be of value for any future encounter with the respective soil type. Especially in soil stabilization, many phenomena which cannot be explained by the results of the standard engineering tests, can be correlated with, if not explained by the soil type.

A truly splendid example of engineering use and supplementation of the pedologic soil classification is presented by the Michigan State Highway Department 1). The Field Manual of Soil Engineering of this Department is the best available guide for practical application of pedology. Among other features, this manual contains descriptions in sufficient detail of the profile characteristics (with schematic presentation) of the 104 important soil series found in the State of Michigan. Also in a rather extensive table, for each of these 104 soils, 19 specific engineering items are listed under the respective headings given in Table 1.

The Michigan experience shows that the only limit in the practical use of the pedologic classification for highway and airport engineering is the capacity and willingness of the engineer to learn and use this method. Another pioneer in the use of the pedologic system of classification amalgamated with engineering experience and testing is the State Highway Department of Missouri 9). The Missouri way is presented in Table 2. More recently, the States of Indiana, North-Carolina, New York, New Jersey and others have entered actively into the utilization of pedological knowledge for highway construction purposes.

For most of the counties of the United States, soil survey maps are available. These serve for the first orientation of the soils engineer; however, since no general map can ever be made in all the detail necessary for construction purposes, the soil engineer must make his own detail map based on his ability to recognize soil types. Of course, the soil survey party will also take soil samples; but this samples will rather be taken whenever a variation in soil type is recognized. This helps to cut down considerably the number of samples which must be taken and tested per mile. For detailed description of soil survey procedure and reporting, reference is made to the respective soil manuals of Michigan and Missouri.

While pedologic knowledge is most useful in the exploration of highway and airport sites, Wooltorton 12) has shown that cracking of light buildings in Burma could be correlated with certain soil types. In Missouri, the same phenomenon was observed in rather drastic forms during the long drought in the Thirties on Buildings up to three and more stories high founded on Putnam soil. In a less drastic form opening and closing of cracks of a chapel at Concord, Mo; founded on the same soil, paralleling desiccation and wetting, has been observed and recorded for more than thirty years.

So far, utilization of pedology has been treated only with respect to the soil type and soil series. In the pedologic system, higher categories of classification exist. The higher the category, the less the number of actual properties which can be indicated by the place of the soil in the higher category. But, it so happens, that the indices employed for placement in the higher categories, such as salini-

ty, alkalinity, chemical composition of clay fraction, presence or absence of a lime accumulation zone, etc., are also general indices of the subceptibility of soils to different types of stabilization. It should be mentioned in this connection, that a one-million dollar airport concrete pavement is disintegrating at the present time for the sole reason that the engineer-in-charge neglected to utilize available pedologic knowledge with respect to a high sodium and magnesium sulfate content of the underlying soil. Because of this potential role of the higher categories of soil classification as warning signs and as guiding posts for country or continent wide planning the higher categories in the pedologic system are listed in Table 3.

#### CONCLUSIONS.

From the evidence presented in this paper and in the references given it is obvious that pedology in its three phases can be of great usefulness to the highway and airport engineer or in general to the engineer who deals with shallow foundations. This helpfulness may be (a) direct and immediate in reconnaissance and soil survey, and (b) indirect but no less important in country and continent wide planning for spotting potential trouble areas and for indicating most probable types of required soil treatment for economic highway and airport construction.

#### REFERENCES.

- 1) "Field Manual of Soil Engineering", Michigan State Highway Department, Lansing, Mich. 1946
- 2) Geiger, Rudolf: "Das Klima der bodennahen Luftschicht" Die Wissenschaft, 78, Braunschweig, Vieweg 1927
- 3) Glinka, K: "Die Typen der Bodenbildung, ihre Klassifikation und geographische Verbreitung", Gebr. Borntraeger, Berlin 1914.
- 4) Jenny, Hans: "Factors of Soil Formation". McGraw-Hill Book Co. Inc. New York and London, 1941.
- 5) Joffe, J.S. "Pedology", Rutgers University Press, New Brunswick, N.J.
- 6) Marbut, C.F. "The Contribution of Soil Surveys to Soil Science. Soc. Prom. Agr. Sci. Proc. 41, 116 - 142 (1920) 1921.
- 7) Marbut, C.F. "A scheme for soil classification. Proc. First Int. Congr. Soil Science, 4, 1-31, 1928.
- 8) Marbut, C.F. Soils of the United States, Atlas of American Agriculture, Part. III, Washington D. C. 1935.
- 9) Soils Manual, Division of Geology and Soils, Missouri State Highway Department, Jefferson City, Mo. 1941.
- 10) Stokstad, O. "Get Acquainted with your Soils". "Better Roads", July 1941, 15 - 17, 31.
- 11) Vilensky, D.G. "Concerning the principles of genetic soil classification. Contributions to the study of soils of Ukraina, 6: 129 - 151, Kharkov, U.S.S.R. 1927.
- 12) Wooltorton, D. "A preliminary investigation into the subject of foundations in the blackcotton" and "Kyatti" soils of the Mandalay district, Burma". Proc. Int. Conf. S.M. & F.E. III: 242-256, Harvard University, 1936.

## SUB-SECTION I c

### PHYSICAL AND PHYSICO-CHEMICAL PROPERTIES OF SOIL

I c 1

#### CONTRIBUTION TO THE THEORY OF SHRINKING

R. HAEFFELI and G. AMBERG

Laboratory for Hydraulic Research and Soil Mechanics  
of the Swiss Federal Institute of Technology, Zurich

#### I. INTRODUCTION.

After the theory of soil mechanics under the guidance of Terzaghi had conquered its own special territory of civil engineering 1), it has in recent years penetrated other branches with fruitful results. In addition to the science of snow and glacier mechanics, mention should be made here particularly of the testing of moulding sand and of work in connection with the clay industry, with whose problems our Institute had to occupy itself very closely during World War II 2) and 3).

Experience shows that the process of shrinking is of decisive importance for the quality of the products of the clay industry, particularly in the manufacture of bricks and tiles, since the undesired "structures" produced by the moulding process are later influenced to a considerable degree by the shrinking process. In order to investigate more closely the peculiar behaviour of the clay during shrinkage, exhaustive tests were carried out in our laboratory to the order of the Swiss Association of Brick and Tile Makers and Buhler Brothers Ltd., engineers, Uzwil. These tests dealt chiefly with three-dimensional shrinking. The test pieces used were principally cubes with sides 2 cm long and the corners cut off (Fig. 1). Four different kinds of clay, whose principal characteristics are shown comparatively in table 1, were used as material to be tested. The tests were carried out and evaluated with the collaboration of W. Eng, engineer. For valuable support and suggestions we have also to thank Dr. A. Stutz, director of the Brick and Tile Works Passavant-Iselin & Cie. A.-G., Allschwil, Basle.

by a group of curves in which the preparing-water content plays the part of parameter. The higher the preparing-water content - i.e. the water content present at the beginning of the compacting - the greater will be the water content remaining for a given compacting pressure, although the compacting is in itself more intense.

An analogous phenomenon may be noted also during the shrinking of clay. This is not surprising when consideration is taken of the relationship between the shrinking process on the one hand and the compacting under the action of external forces on the other hand. The shrinking process is indeed nothing else than a compacting taking place under the action of capillary pressure which increases in accordance with theoretical principles, instead of under the action of external mechanical forces.

As K. von Terzaghi and O.K. Fröhlich have already determined, two phases must be distinguished during the shrinking process 4: In the first phase the evaporating of the water takes place on the surface of the sample. Hand in hand with that, a reduction in size of the pores takes place, caused by a steady increase in capillary pressure, until finally the maximum is reached, which Terzaghi designates shrinking pressure. Here the second phase begins, in which the evaporating surface withdraws into the sample. The change in volume of the sample is comparatively small during this period; the capillary pressure remains approximately constant. Nothing definite can exactly be stated with regard to the actual magnitude of the shrinking pressure. On the other hand

TABLE 1

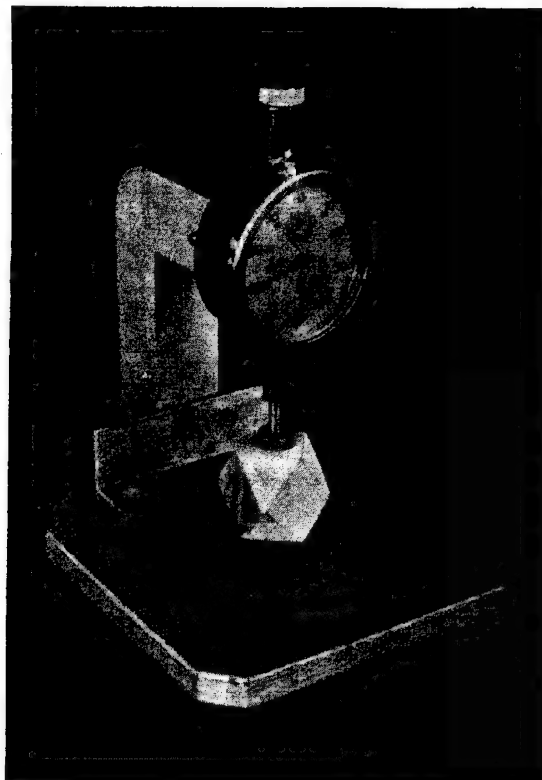
Characteristics of the material tested						
No. Laboratory	Limits of consistency			Coefficient of compressibility % (of 5)	Coefficient of permeability $\frac{\text{kg}^0}{\text{cm}^2 \cdot \text{sec}}$	Void ratio based on $\sigma = 1 \text{ kg/cm}^2$
	$\tau$ %	$a$ %	$p$ %			
1 1632	55,7	22,9	32,8	9,12	$2,0 \cdot 10^{-8}$	0,965
2 B <sub>1</sub>	76,6	34,7	41,9	6,53	$3,7 \cdot 10^{-8}$	1,27
3 1406	56,0	20,1	35,9	8,80	$6,1 \cdot 10^{-9}$	0,940
4 1407 (vacuum)	54,0	18,9	35,1	9,37	$7,0 \cdot 10^{-9}$	0,923

#### II. EXTERNAL CHARACTERISTICS OF THE SHRINKING PROCESS.

To-day, it is a known fact that the water content or the void ratio of a saturated, fine-grained loose sediment cannot be expressed as a simple function of the pressure. The dependance in question can only be illustrated

the equivalent compacting pressure (shrinking pressure equivalent) nevertheless allows the order of magnitude of the effective forces to be determined. By this is understood the compacting pressure which produces in the test sample in an oedometer the same water content as the shrinking process does. 5)

In Fig. 2 is illustrated on the one hand the

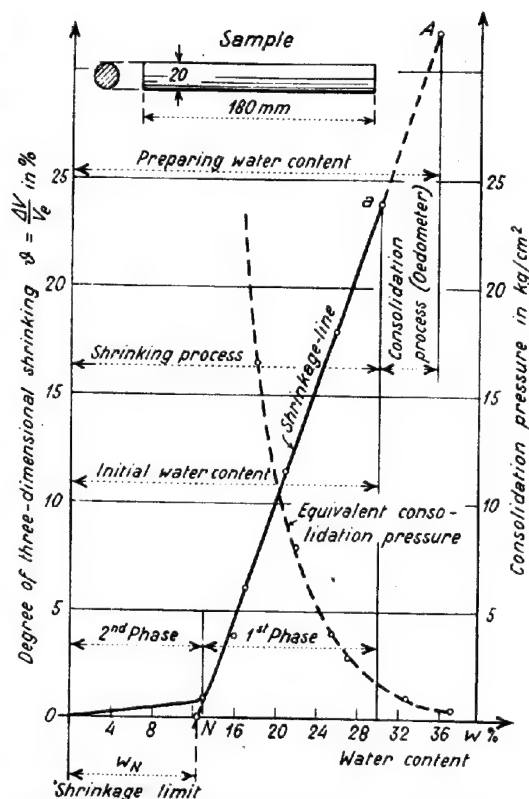


Shrinkage measuring.

FIG. 1

dependence of the degree of three-dimensional shrinking on the water content (curve 1), and on the other hand the relation between the water content and equivalent shrinking pressure (curve 2).

In the following considerations we must first of all make a clear distinction between two conceptions: the preparing water content  $w_A$  and the initial water content  $w_a$ . By the former we mean, as its name implies, the water content possessed by the sample immediately after it has been prepared, whilst the latter means the water content when the shrinking process begins. Quite exceptionally we shall have  $w_A = w_a$ . First of all we assume that, after the sample has been prepared, a compacting process is first performed in the oedometer until a certain consolidation has been reached. Secondly, after that the shrinking process starts and continues until the sample in the drying cupboard at  $105^\circ \text{C}$  no longer gives off any water. In this case the initial water content differs from the preparing-water content; in fact it is smaller. It has now been found that for a given clay the compacting, or the unit weight reached after completion of the shrinking process, depends only on the preparing water content. The higher the latter was chosen, the less was the final compacting, in other words, the dry unit weight of the respective test material was also less. From this the above-mentioned relationship between the compacting process in the oedometer on the one hand, and the shrinking process on the other hand, can be seen very clearly. Strictly speaking we have here fundamentally one single



Shrinkage-line. Three dimensional shrinking of a clay cylinder as a function of the water content. Clay No. 1632.

FIG. 2

process taking place in two different forms.

This particular behaviour of clay during the consolidating process can be explained by the fact that there is a quite definite texture corresponding to each preparing water content, and that during the consolidation a change certainly occurs in the texture in the sense of a compacting without the principle features of this texture being lost. A sudden alteration in the inner structure may only be caused by intense shaking or mechanical disturbance. This change is termed breakdown of structure.

### III. ANALYSIS OF THE SHRINKING PROCESS

#### (1st phase).

In the following theoretical investigation we deal only with the first phase of the shrinking process, which we presume to last until the straight line of shrinking shown in Fig. 2 and 3 intersects the axis of the abscissa at the point N. The corresponding section of the axis  $w_N$  is in the following termed the shrinkage limit.

First of all the relations between degree of shrinking and water content shall be determined. The fact that the sample remains saturated with water during the first phase of the shrinking process justifies us in putting the change in water content equal to the change in volume of the sample. Accordingly

the following holds good:

$$V = V_s + V_w = G_s \left( \frac{1}{\gamma_s} + \frac{W}{\gamma_w} \right) \quad (1)$$

$$dV = \frac{G_s}{\gamma_w} dw; \quad G_s = V_e \gamma_w \quad (2)$$

$$\frac{dV}{V_e} = d\psi = \frac{\gamma_e}{\gamma_w} dW = \text{tg} \alpha \cdot dW \quad (3)$$

Where  $V$  = volume of the sample

$V_s$  = volume of solids

$V_w$  = volume of water portion

$V_e$  = volume of dry sample (after the shrinking process)

$\gamma_e$  = unit weight of dry sample.

Neglecting the change in volume due to the second phase - the total extent of shrinking being considered as the result of the first phase, - the equation of the straight line of shrinking is obtained from equation 3) in the following form:

$$\psi = \frac{\Delta V}{V_e} = \frac{\gamma_e}{\gamma_w} (W - W_N); \quad \text{tg} \alpha = \frac{\gamma_e}{\gamma_w} \quad (4)$$

The inclination  $\text{tg} \alpha$  of the shrinkage-line is consequently identical with the unit weight ratio  $\frac{\gamma_e}{\gamma_w}$  (cf. Fig. 3). The relation between the three-dimensional shrinking and the linear degrees of shrinking ( $\partial x, \partial y, \partial z$ ) in the direction of the three axes in space is:

$$\psi = \partial_x + \partial_y + \partial_z + \partial_x \partial_y + \partial_x \partial_z + \partial_y \partial_z + \partial_x \partial_y \partial_z \quad (5)$$

Now if shrinkage tests are made with a given material with different preparing water contents and the results are plotted graphically, a corresponding number of shrinkage-lines with different inclinations and different shrinkage-limits will be obtained. Fig. 4 shows two such idealised shrinkage-lines with different preparing water contents. Between these two straight lines there are interesting relations which we formulate as follows. First of all the following holds good for three-dimensional shrinking:

$$\psi = \frac{V - V_e}{V_e} = \frac{V}{V_e} - 1 = (1 + W) \frac{\gamma_e}{\gamma_e'} - 1 \quad (6)$$

where  $\gamma_e'$  represents the unit weight of the material with water content  $w$ , whilst  $\gamma_e$  represents the unit weight of the dry material.

Solving equation (6) with respect to  $\gamma_e$ , we obtain:

$$\gamma_e = \frac{1 + \psi}{1 + W} \gamma_e' \quad (7)$$

The unit weights of the dry material in two parallel tests with different preparing water contents  $w_1$ , but with the same water content  $w$ , are therefore in the following relation to each other:

$$\frac{\gamma_{e1}}{\gamma_{e2}} = \frac{1 + \psi_1}{1 + \psi_2} \quad (\text{cf. Fig. 4}) \quad (8)$$

For the change of the shrinkage limit due to a change in the preparing water content, - which is also to be seen in Fig. 4, - the following relation can be obtained between the axis sections  $w_N$  and the corresponding unit weights of the dry material:

$$W_{N2} - W_{N1} = \frac{\gamma_w}{\gamma_{e2}} - \frac{\gamma_w}{\gamma_{e1}} \quad (9)$$

$$W_{N2} = W_{N1} + \frac{\psi_1 - \psi_2}{1 + \psi_2} \frac{\gamma_w}{\gamma_{e1}} \quad (10)$$

Since  $\gamma_{e1} > \gamma_{e2}$  and  $\psi_1 > \psi_2$ , then  $w_{N1} > w_{N2}$ . Since on the other hand  $w_{N2}$  belongs to the shrinkage test with the higher preparing water content, it is seen clearly from equations (9) and (10) that the shrinkage limit becomes greater with increasing preparing water content.

It is now necessary to determine the position of intersection S of the two shrinkage lines of the same material. First of all the ordinate of this point may easily be calculated as follows from equation (8) and Fig. 4:

$$\frac{1 + \psi_1}{1 + \psi_2} = \frac{\text{tg} \alpha_1}{\text{tg} \alpha_2} = \frac{D_1}{D_2} = \frac{-\psi_s + \psi_1}{-\psi_s + \psi_2}$$

$$\psi_s = -1 \quad (11)$$

Substituting this value in equation (4), the abscissa of the point S is finally obtained:

$$\psi_s = (W_s - W_N) \frac{\gamma_e}{\gamma_w} = -1 \quad (12)$$

$$W_s - W_N = \frac{\gamma_w}{\gamma_e}$$

or direct from Fig. 4) in another form:

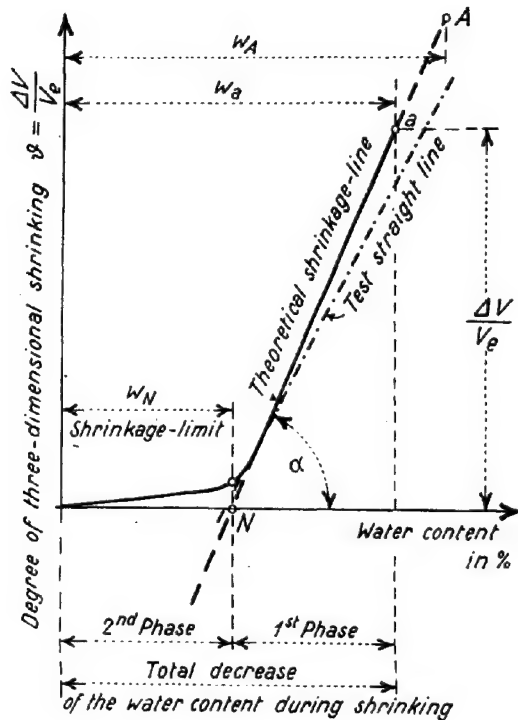
$$W_s = W_1 - (1 + \psi_1) \frac{\gamma_w}{\gamma_{e1}} \quad (13)$$

The final equations (11), (12) and (13) may be interpreted as follows:

From equations (12) and (13) it is evident that the abscissa  $w_s$  of the point S depends only on the elements of one single straight line. But this is only possible if all straight lines of shrinkage of one and the same material intersect at one common point S. Since  $w_s$  is normally less than  $\gamma_e$ ,  $w_s$  is as a rule negative. On the other hand, from equation (11) it is evident that the ordinate  $\psi_s$  of the point S has the same value for all materials, namely  $\psi_s = -1$ . Consequently the points S for all materials lie on a horizontal line at a distance  $\psi_s = -1$  below the origin A.

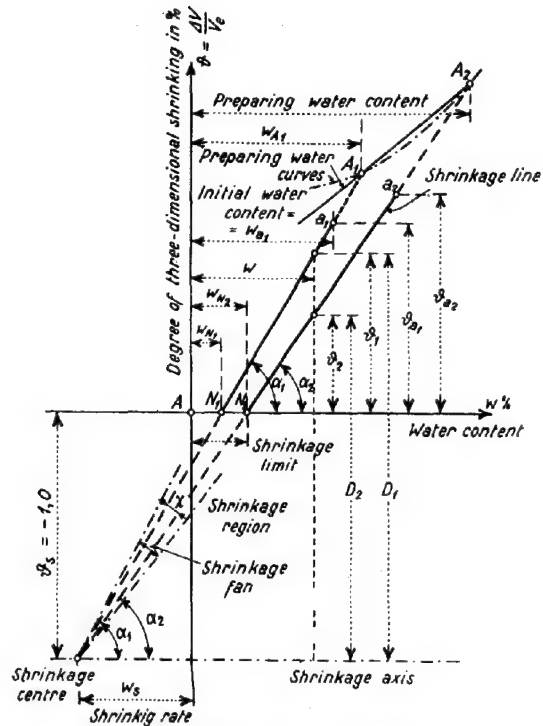
These results may be expressed in the following terms and definitions:

- 1) The point of intersection S of all shrinkage-lines for one and the same material is defined as the shrinking centre.
- 2) The shrinking centres of all materials lie on the horizontal line of the equation  $\psi_s = -1$ , which is defined as the shrinking axis.
- 3) The abscissa  $w_s$  of a given shrinking centre is termed the shrinking rate of the material in question. The behaviour of the loose sediment during the shrinking process in question is to a large extent characterised by this single magnitude.
- 4) The total of all physically possible straight lines of shrinking of one and the same material lies within the so-called shrinking fan, whose apex is the shrinking centre. With increasing preparing water content the shrinkage-lines rotate clockwise round the shrinking centre within the shrinking fan. Accordingly also the shrinkage limit  $w_N$  increases with increasing preparing water content.
- 5) The angle  $\chi$  of opening of the shrinking fan is termed the shrinking region. To determine it, at least two tests are required: A first test with as high a preparing water content as possible gives the shrinking-line with the greatest slope, and a second test



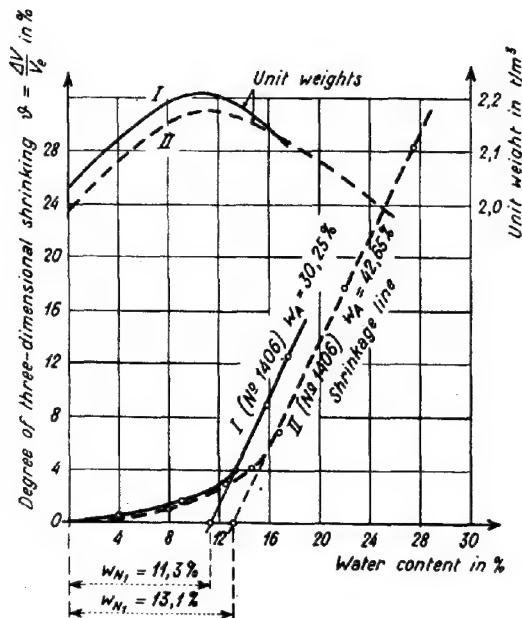
Shrinkage-line (diagrammatic)

FIG. 3



Degree of three-dimensional shrinking for different preparing water contents (diagrammatic).

FIG. 4



Results of two shrinkage tests with the same clay for different preparing water contents.

FIG. 5

with the minimum preparing water content gives the steepest straight line of shrinking.

6) The locus of all preparing water contents, i.e. the line connecting the points A, we define as the preparing water curve. For certain kinds of clay this line is practically straight within the shrinking fan, for other kinds it is bent. Theoretically it is for the moment not possible to make any more accurate statement with regard to the shape of this line.

The greater the possible variations of the material in question with respect to texture formation, the greater should be the shrinking region. The shrinking region will be caused to vary by additions which, as for instance electrolytes, affect the coagulation and consequently the structure formation to a great extent. It should further be noted that the formulae derived above are not confined to the shrinking operation, but hold good quite generally for any process of consolidation which corresponds to the assumptions made: Continuance of complete saturation with water during the whole process, and identity between the volume of water given up and the corresponding change in volume of the material.

#### IV. EXPERIMENTAL RESULTS.

In order to check the correctness of the theoretical assumptions, two samples of one and the same clay with different preparing and initial water contents were submitted to the shrinking process. The water content and also the corresponding degree of shrinkage, was then determined at different phases of the

shrinking process and plotted graphically (Fig. 5). From the measured unit weights  $\gamma_{e1}$  and  $\gamma_{e2}$  of the dry material, the total degree of shrinkage  $v_{a1}$  and  $v_{a2}$  and also the known initial water content  $w_{a1}$  and  $w_{a2}$ , the coefficients  $w_N$ ,  $w_S$  and  $v_S$  given in Fig. 2, were calculated on the basis of the equations derived in section 3; their significance can be seen from Fig. 5.

in reality withdraw to a certain extent into the interior of the sample during the first phase of the shrinking process; this was neglected in the theory also the assumed identity between the volume of water given off and the corresponding change in volume is not exactly realized. The measured shrinking centre moves somewhat more to the left in comparison with the calculated centre. But since a satis-

TABLE 2

Evaluation of the test results								
Clay	Test	$w_A$ %	$w_a$ %	$\gamma_e$ t/m <sup>3</sup>	$\theta_a$ %	$w_N$ %	$w_S$ %	$\theta_S$ %
		← measured →				← calculated →		
1406	I	30,25	17,55	2,023	12,6	11,3	- 38,0	- 100
1406	II	42,5	27,4	1,976	28,3	13,1	- 38,0	- 101

In conjunction with Fig. 5, these results lead to the following conclusions:

- The measured intermediate points of the same shrinkage curve actually lie on a straight line during the first phase of the shrinkage process. The existence of the shrinkage-line is thus proved experimentally.
- The slope of the straight line of shrinking II with higher preparing water content is somewhat less than that of the straight line of shrinking I, and this is in agreement with the theory.
- Test II with the higher preparing water content gives, in agreement with the theory, the lower unit weight  $\gamma_e$  of the dry material but the greater shrinkage limit  $w_N$ , than test I.
- The abscissa values  $w_S$  of the shrinkage centre S, as calculated independently for each separate degree of shrinking, are practically identical; as anticipated by theory.
- The values ( $v_S = -1 = 100\%$ ) of the ordinate of the shrinking centre, as calculated for each separate degree of shrinking, agree practically completely with the theoretical values.
- The curve of unit weights  $\gamma_e$  obtained when passing over from the first into the second phase of the process, becomes a maximum. This also agrees with our assumptions, since the weight-diminishing influence of the air makes itself perceptible in the second phase.

The experimental proof of the applicability of the theoretical laws has thus been demonstrated fundamentally. Complete accordance between theory and measurement could indeed not be reached. As a rule the slope of the measured shrinkage-lines was always somewhat less than the slope calculated theoretically from the unit weight of the dry material. This can be explained by the fact that the meniscus

factory accordance between theory and measuring has otherwise been determined, the theoretically accepted laws may be adopted as a basis for calculating the shrinking process in the region of the first phase. On the other hand, further explanation 6) and 7) is required for the behaviour of the linear degrees of shrinking, which depend to a very great extent on the orientation of the finest clay laminae and thus bring about the anisotropy of the consolidated material.

#### V. BIBLIOGRAPHY.

- K. v. Terzaghi: Erdbaumechanik auf bodenphysikalischer Grundlage. Wien 1935.
- R. Haefeli: Die Entwicklung und Probleme der Schnee- und Gletscherkunde in der Schweiz. Experientia. Vol. II/1 1946.
- A. v. Moos & R. Haefeli: Die Arbeiten der Erdbauabteilung der Versuchsanstalt für Wasserbau und Erdbau an der Eidg. Techn. Hochschule in Zürich.
- K. v. Terzaghi - O.K. Fröhlich: Theorie der Setzung von Tonschichten. Leipzig und Wien 1936.
- R. Haefeli: Mechanische Eigenschaften von Lockergesteinen. Schweizer Bauzeitung Bd. 111, Nr. 24 & 26, 1938.
- E. Gruner - R. Haefeli: Beitrag zur Untersuchung des physikalischen und statischen Verhaltens kohärenter Bodenarten. Schweizer Bauzeitung Bd. 103 Nr. 15 & 16, 1934.
- R. Haefeli: Erdbaumechanische Probleme im Lichte der Schneeforschung. Schweizer Bauzeitung Bd. 123 Nr. 2, 4 & 5 1944.



HEAT-FLOW TOWARDS THE FLOOR OF COLD STORES, SITUATED IN THE  
GROUND LEVEL, AND CALCULATION OF THE INSULATION OR THE  
HEATING SYSTEM TO PREVENT FROST PENETRATION IN THE GROUND

ROBERT F.X. RUCKLI, Dr. ès sc.techn. Ing.  
Inspecteur fédéral des travaux publics, Berne

### 1. PROBLEM.

The floor of cold stores has to be designed to prevent frost penetration in the ground and its effect, the ice segregation and the uplift of the superstructure. The protection of the basement against frost may be attained by insulation or heating of the floor. The usual methods of calculation assume the ground-temperature to be constant in a fixed depth below the basement (ground water level or 10 m). 1) and 6). Data obtained in England and Russia 2) and 8) from examination of cold stores, where frost heave damage has occurred show, that this assumption is not just. The writer proposes a method of calculation, which conforms more to nature and which demonstrates the distribution of the heat-flow from the subground over the area of cold stores.

### 2. COLD STORES WITH CIRCULAR AREAS.

#### a) Analogy with the Artesian well.

The groundwater-flow and the heat-flow are governed by the same differential equation. In case of the same formal boundary conditions, the solution of the hydro-dynamic problems may be transferred to the thermal problems.

Such an analogy exists between the Artesian well with a plane bottom lying in the sub-plane of the impermeable top layer and the circular cold store situated on the ground-level if the exterior heat conductivity between the open air and the open ground outside of the store is neglected.

The following are corresponding values:  
Fig. 1

well:	cold store:
hydrostatic pressure, H	initial ground temperature, $\vartheta_H$
piezometric level on the equi-potential-curve defined by b, h	temperature on the isothermal defined by b, $\vartheta$
lowered level during pumping, $h_r$	floor temperature in the cold room $\vartheta_I$
flowing-of f by pumping Q	loss of heat, $Q_w$
permeability, kp	heat-conductivity of the ground $\lambda_e$

$r_0$  radius

#### b) Calculation of the heat-flow to the basement of circular cold store.

The formula for the Artesian well, given by Forchheimer 4),

$$H-h = \frac{Q}{2\pi k_0 r_0} \arctg \frac{r_0}{b} \quad (1)$$

wherein b is the small axis of the rotation ellipsoid, may be applied in our case by changing the letters as indicated above 2a). Therefore

$$\vartheta_H - \vartheta = \frac{Q_w}{2\pi \lambda_e r_0} \arctg \frac{r_0}{b} \quad (2)$$

and for the whole difference of temperature

$$\left. \begin{aligned} \vartheta_H - \vartheta_I &= \frac{Q_w}{4\lambda_e r_0} \\ Q_w &= (\vartheta_H - \vartheta_I) 4\lambda_e r_0 \end{aligned} \right\} \quad (3)$$

eq.(3) in(2) substituted results in

$$\vartheta = \vartheta_H - \frac{2}{\pi} (\vartheta_H - \vartheta_I) \arctg \frac{r_0}{b} \quad (4)$$

We get the position b of the zero isothermal in the vertical axis by setting

$$\vartheta = 0$$

$$b_{\vartheta=0} = \frac{r_0}{\operatorname{tg} \frac{\pi \vartheta_H}{2(\vartheta_H - \vartheta_I)}} \quad (5)$$

In a meridional section the heat stream-lines are confocal hyperboles and the isothermals are confocal ellipses.

The heat-flow through the floor, rising from the ground at a point at the distance x from the middle of the cold store,  $x < r_0$  may be calculated by considering two neighbouring hyperboles, whose asymptotes have the inclination  $\beta$  and  $\beta + d\beta$  respectively fig. 2. Between these two stream-lines the heat-flow is constant owing to the condition of continuity. The heat, passing through the ring formed by rotation of the element dx round the vertical axis is

$$2\pi x dx \cdot q_x = 2\rho \cos \beta \cdot \pi \cdot \rho d\beta \cdot q_\rho$$

if  $q_\rho$  is the specific heat-flow at the great distance of  $\rho$  from the origin and  $q_x$  the heat-flow at the point x. At the distance  $\rho$  from the centre, the isothermal may be considered as a semi-sphere. Therefore we can write

$$q_\rho = \frac{Q_w}{2\rho^2\pi} \quad (7) \quad 2\rho^2\pi \text{ area of the semi-sphere}$$

eq. (7) substituted in eq. (6) produces

$$q_x = \frac{Q_w \cdot \cos \beta \cdot d\beta}{2\pi \cdot x \cdot dx} \quad (8)$$

On a hyperbole the following relations exist

$$\cos \beta = \frac{x}{r_0}$$

$$\beta = \arccos \frac{x}{r_0}$$

$$\frac{d\beta}{dx} = - \frac{1}{\sqrt{1 - \frac{x^2}{r_0^2}}} \cdot \frac{1}{r_0} \quad (9)$$

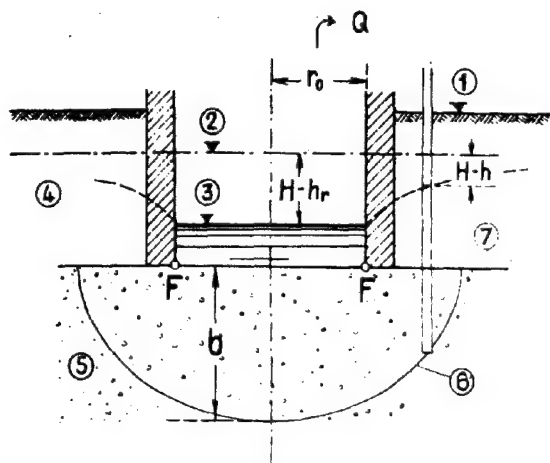
With this value the equation (7) becomes

$$q_x = \frac{Q_w}{2r_0^2\pi \sqrt{1 - \frac{x^2}{r_0^2}}} \quad (10)$$

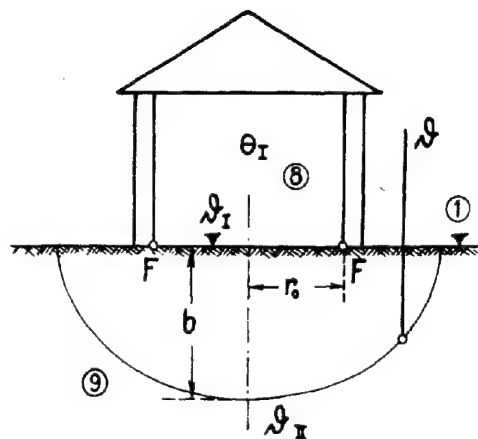
or

$$q_x = \frac{2\lambda_e (\vartheta_H - \vartheta_I)}{r_0 \pi \sqrt{1 - \frac{x^2}{r_0^2}}} \quad (10^a)$$

This is the repartition of the heat-flow over the area of the circular cold store.



Artesian Well



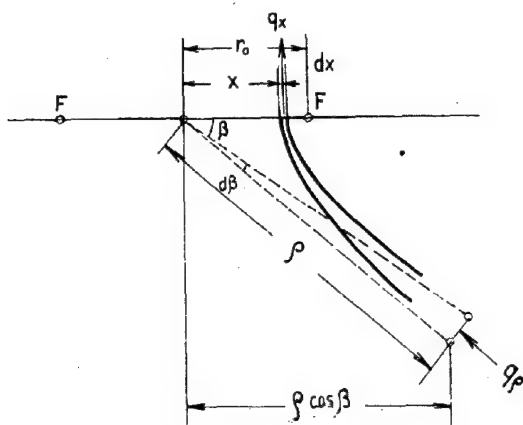
Circular Cold Store

Form of the equipotential faces for an Artesian well and form of the isotherms under a cold store, situated in the ground level.

- 1) ground level
- 2) hydrostatic pressure
- 3) lowered water level in the well
- 4) impermeable toplayer
- 5) ground-water stratum
- 6) equipotential faces, rotation ellipsoid
- 7) boundary face

- 8) cold room
- 9) isothermal, rotation ellipsoid
- Q: flowing off
- F: foci
- \theta: room temperature
- \vartheta\_I: floor temperature
- \vartheta: soil temperature in the cooling zone
- \vartheta\_{II}: undisturbed soil temperature

FIG. 1



Heat flow rising from the ground towards the basement of a cold store.

FIG. 2

#### c. Calculation of the insulation.

The insulation of the floor must be designed in a manner to keep the temperature under the basement at  $+0^\circ\text{C}$ . The heat-flow through the basement construction is governed by the equation (5)

$$q = \frac{\theta - \vartheta_o}{\frac{1}{\alpha_{fl}} + \frac{S_1}{\lambda_1} + \frac{S_2}{\lambda_2} + \frac{1}{k}} = \frac{\theta - \vartheta_o}{\frac{1}{k}} \quad (11)$$

wherein:

- \theta: air temperature of the cold room
- \vartheta\_o: temperature under the basement construction
- \alpha\_{fl}: surface emissivity or exterior conductivity of the floor (cal/cm<sup>2</sup> h°C)
- S\_1, S\_2: thickness of the insulation
- \lambda\_1, \lambda\_2: the respective heat conductibilities
- \frac{1}{k}: \frac{1}{\alpha\_{fl}} + \frac{S\_1}{\lambda\_1} + \frac{S\_2}{\lambda\_2} + \frac{1}{\lambda\_2} \quad (11a)
- \frac{1}{k}: resistance against heat transition
- k: ratio of heat transition

The resistance needed against heat transition  $\frac{1}{k}$  to keep the zero isothermal in the surface of the basement arises from the equation (11) and (10a);

$$\frac{1}{k} = \frac{\vartheta_o - \theta}{q_x} = \frac{\pi r_o (\vartheta_o - \theta)}{2 \lambda_e (\vartheta_{II} - \vartheta_o)} \sqrt{1 - \frac{x^2}{r_o^2}} \quad (12)$$

By  $\frac{1}{k}$  the thickness  $S_1$  of the insulation is determined if the thickness of  $S_1$  and  $S_2$  of the structural concrete slabs over and under the insulation and their respective conductivity.  $\lambda_1, \lambda_2$  and  $\alpha_{fl}$  are given.

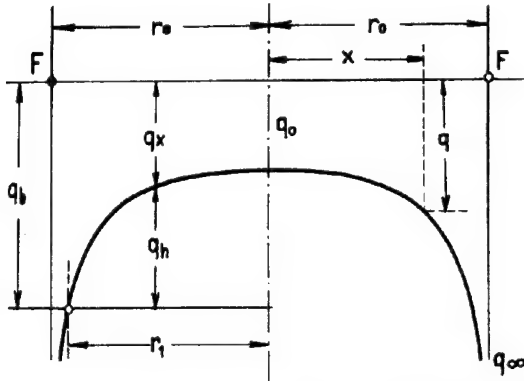
#### d. Calculation of the floor-heating to prevent the penetration of the zero isothermal into the ground.

Instead of a thick insulation it is possible to prevent the freezing of the subsoil by heating the surface of the basement construction as it was indicated by several authors 1), 2) and 6).

We stipulate, that the zero isothermal



remains on the subplane of the floor construction (no frost penetration). With a given construction of the floor and a fixed room temperature the heat  $q_b$  passing upwards through the floor is determined. If it is greater than the heat  $q_x$  rising from the subground, artificial heat  $q_h$  must be added, for: Fig. 3



Repartition of the heat flow  $q_x$  over the area of a circular cold store.

FIG. 3

$$q_h = q_b - q_x. \quad (13)$$

At a distance  $r < r_1$  from the centre of the cold room we find by the use of the equations (10a), (11) and (13)

$$q_h = k(\vartheta_o - \theta) - \frac{2\lambda_e(\vartheta_{II} - \vartheta_o)}{r_0 \pi \sqrt{1 - \frac{x^2}{r_0^2}}} \quad (14)$$

and the total heat which is to be added (15)

$$Q_{wh} = \int_0^{r_1} q_h dF = r_1^2 \pi k (\vartheta_o - \theta) - 4\lambda_e (\vartheta_{II} - \vartheta_o) \left[ r_0 - \sqrt{r_0^2 - r_1^2} \right]$$

$r_1$  is determined as follows.  $F_1$  is the circular area of the radius  $r_1$  to be heated artificially, in other words over which the heat-flow  $q_h$  is to be integrated; outside the circle  $r_1$ , the heat rising from the subground is great enough to prevent the penetration of the zero isothermal without addition of artificial heat.  $r_1$  is determined by the equation (12)

$$\frac{1}{k} = \frac{\pi(\vartheta_o - \theta)}{2\lambda_e(\vartheta_{II} - \vartheta_o)} \sqrt{r_0^2 - r_1^2} \quad \text{and} \quad r_1 = \sqrt{r_0^2 - \left( \frac{2\lambda_e(\vartheta_{II} - \vartheta_o)}{\pi k(\vartheta_o - \theta)} \right)^2} \quad (16)$$

#### Example:

With  $r_0 = 10 \text{ m}$      $\theta = -15^\circ$      $\vartheta_{II} = +10^\circ$   
 $S_i = 0,3 \text{ m}$   
 $\alpha_{II} = 6 \text{ kcal/m}^2\text{h}^\circ\text{C}$      $\lambda_i = 0,06 \text{ kcal/mh}^\circ\text{C}$   
 $\lambda_e = 1,5$     "    "

we find

$$r_1 = 9,45 \text{ m}$$

$$r_0 - \sqrt{r_0^2 - r_1^2} = 6,71 \text{ m}$$

$$Q_h = 412 \text{ kcal/h} \quad \text{or for electric heating}$$

$$E_h = 0,48 \text{ kW}$$

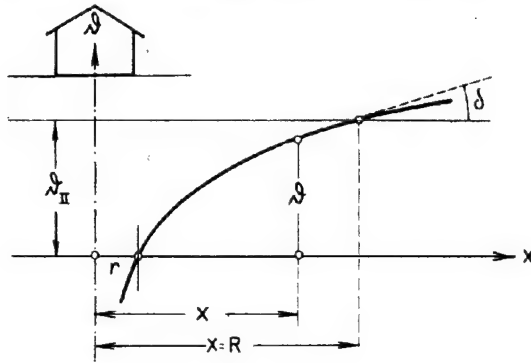
This example shows, that the consumption of energy is very small.

### 3. COLD STORES WITH INFINITELY LONG RECTANGULAR AREAS (TWO-DIMENSIONAL HEAT-FLOW.)

The solution found for the circular cold store can also be transferred to the cold store with an infinitely long rectangular area (two-dimensional heat-flow), if we take as the hydro-dynamic analogon the artesian ditch of the constant width  $2r$ , with a plane bottom lying in the subplane of the impermeable toplayer. Neglecting again the exterior heat conductivity between the open air and the ground surface outside the cold store, the heat stream-lines of the plane heat-flow are confocal hyperboles and the isotherms are confocal ellipses. By an analogous development as shown under 2 we find for the heat-flow to the surface of the floor of the infinitely long cold store per unit length 3)

$$\bar{q}_w = -\lambda_e (\vartheta_{II} - \vartheta_o) \frac{\pi}{2R} \quad (17)$$

The steady heat-flow is only possible if we assume, that at the distance  $R$  of the axis of the cold store, the soil temperature of the ground surface is not influenced by the cold store. Fig. 4. Theoretically  $R$  is infinitely



Temperature in the ground level beside an infinitely long cold store, plotted against the distance from the axis of the store.

FIG. 4

great; but for practical purposes it is allowed to assume, that for a great extent of  $R$  the influence of the cold store is negligible.  $R$  may be estimated with the assumption, that at the distance  $R$  the heat-flow  $q_{wk}$  is, owing to the cold store, only a part  $n$  of the geothermic heat  $q_w$ , rising from the earth because of the geothermic gradient  $G$ ;

$$q_{wk} = n q_w \quad n < 1 \quad \text{e.g. } \frac{1}{2}$$

By a short mathematical development we find

$$R = \frac{\vartheta_{II}}{n \cdot G \cdot \lambda_e} \quad (18)$$

in which

$$w + \ln w = \ln \frac{2\sqrt{\pi}}{nGr}$$

The repartition of the heat-flow from the subground to the basement is determined by the equation

$$q_x = \frac{\lambda_e (\bar{v}_H - \bar{v}_0)}{r \ln \frac{2R}{r} \sqrt{1 - \frac{x^2}{R^2}}} \quad (19)$$

and the insulation, needed to prevent the penetration of the zero isothermal in the subground

$$\frac{1}{k} = \frac{r(\bar{v}_0 - \theta)}{\lambda_2(\bar{v}_H - \bar{v}_0)} \cdot \ln \frac{2R}{r} \sqrt{1 - \frac{x^2}{R^2}} \quad (20)$$

If the penetration of the frostline is to be prevented by artificial heating, the heat to be added is at a point  $x$

$$q_{hx} = k(\bar{v}_0 - \theta) - \frac{\lambda_e (\bar{v}_H - \bar{v}_0)}{r \ln \frac{2R}{r} \sqrt{1 - \frac{x^2}{R^2}}} \quad (21)$$

and the heat per unit length of the cold store

$$\bar{q}_h = \int_0^{x_1} 2q_{hx} dx = 2k(\bar{v}_0 - \theta)x_1 - \frac{2\lambda_e (\bar{v}_H - \theta)}{\ln \frac{2R}{r}} \arcsin \frac{x_1}{r} \quad (22)$$

$$x_1 = \sqrt{r^2 - \left( \frac{\lambda_e (\bar{v}_H - \bar{v}_0)}{k(\bar{v}_0 - \theta) \ln \frac{2R}{r}} \right)^2} \quad (23)$$

Example:

$$r = 10 \text{ m} \quad \theta = -15^\circ \quad \bar{v}_H = 10^\circ \quad S_i = 0,3 \text{ m}$$

$$\lambda_i = 0,06 \text{ kcal/mh}^\circ\text{C}$$

$$\lambda_e = 1,5$$

$$\alpha_{fi} = 6 \text{ kcal/m}^2\text{h}^\circ\text{C}$$

$$\text{With } n = 0,5 \quad R = 185 \text{ m}$$

$$\ln \frac{2R}{r} = \ln 37 = 3,61$$

$$x_1 = 9,9 \text{ m}$$

and

$$\bar{q}_h = 45,6 \text{ kcal/m}^1\text{.h}$$

$$\bar{e}_h = 0,053 \text{ kW/m}^1$$

We compare the heat, needed for the circular cold store, and that needed for a part  $L$  of an infinitely long cold store of the same area and the same diameter.

$$r_0^2 \pi = 2rL \quad r_0 = r; L = \frac{r_0^2 \pi}{2}$$

$$\text{With } r_0 = 10 \text{ m} \quad L = 15,7 \text{ m}$$

Heat needed for the: -

- 1) circular cold store  
example 1, spatial  
heat-flow

$$E_1 = 0,48 \text{ kW}$$

- 2) infinitely long cold  
store, plane heat-  
flow part 15,7 m long  
 $L \cdot \bar{e} = 15,7 \cdot 0,053$

$$E_2 = 0,83 \text{ kW}$$

$$\frac{E_2}{E_1} = \frac{0,83}{0,48} = 1,73$$

Owing to the special heat-flow, the consumption of energy is smaller in the case of a circular cold store, than in a part of an infinitely long cold store of the same dia-

meter and area.

#### 4. MODEL TEST TO EXAMINE THE BOUNDARY CONDITIONS.

Fixing the boundary conditions two extreme assumptions concerning the exterior conductivity or surface emissivity ground-air ( $\alpha$ ) are possible:

- 1)  $\alpha = 0$ : No exterior heat conduction between the ground surface and the open air (outside the cold store).
- 2)  $\alpha = \infty$ : Outside the cold store the ground surface has the constant temperature of the air.

The results of a rough model test, made by the writer to examine the usefulness of the method developed above, are shown in fig. 5. Contrary to nature, the temperature difference between the store and the ground was for practicable reasons not produced by refrigeration but by heating the store. The ground was represented by dry sand and the circular store by an electric heated pot, filled with boiling water.

Fig. 5 shows that the assumption 1) ( $\alpha = 0$ ), which served as the basis of our theory, leads to a form and position of the isotherm under the basement, which is nearer reality than those of assumption 2) ( $\alpha = \infty$ ).

Neglecting  $\alpha$ , in other words, setting  $\alpha = 0$ , the calculated heat rising from the ground is a little too small; this fact guarantees a higher degree of security.

The heat rising from the subground is in the centre, which is the critical point, of the circular cold store

$$1) \text{ assumption } \alpha = 0: q_0 = \frac{2\lambda_e (\bar{v}_H - \bar{v}_0)}{r_0 \pi} \quad (24)$$

$$2) \text{ assumption } \alpha = \infty: q_0 = \frac{4\lambda_e (\bar{v}_H - \bar{v}_0)}{r_0 \pi} \quad (25)$$

The value of  $\alpha$  has no great influence on the calculated heat-flow. Fig. 6.

Equation (25) corresponds formally to the formula for the spatial groundwater-flow against a circular ice-lens, given by the writer in another paper of this collection 7).

#### SUMMARY.

For cold stores of circular and of rectangular infinitely long areas, situated on the ground surface, formulas are given to calculate the

repartition of the heat-flow from the subground to the basement of the store; the insulation, needed to prevent the frost penetration into the ground; the heating energy, needed to prevent the frost penetration into the ground for a given basement construction.

The results of a model test are reported to demonstrate that for the calculation of the heat-flow the surface emissivity of the ground outside the cold store can be neglected (setting  $\alpha = 0$ ).

This report represents an extract of the writer's book "Der Frost im Baugrund" (The Frost in the Sub-soil), which will probably be published in autumn 1948, by the firm "Springer, Vienna".

#### REFERENCES.

- 1) Cammerer, J.S.: Wärmeschutz mit elektrischer Hilfsheizung. Schweiz. Bauzeitung, 1937, Bd.109. Nr.3. S.34.



| c 3

PHYSICO-CHEMICAL PROPERTIES OF SOILS

HANS F. WINTERKORN  
Princeton University

SUMMARY.

The paper points out first the importance of structure and constitution of soils which govern the effectiveness of compositional factors. Next, the ordinary soil - engineering properties are shown to be derived from more fundamental surface and interfacial relationships between solid components and soil moisture. This leads to a demonstration of the importance of physico-chemical phenomena in all types of soil stabilization, and to the conclusion that knowledge of physico-chemical soil phenomena is a "sine qua non" for the engineer engaged in soil stabilization and a good tonic for the devotee of soil mechanics and foundation engineering in general.

The civil engineer dealing with soil is usually interested in its properties as a system and only rarely in the properties of the component particles. This is true not only for undisturbed but also for disturbed subgrade soil and base material. Except for cohesionless materials, disturbance by engineering use never breaks a cohesive soil system into its primary components.

The scientist, follows the "divide et impera" technique. He separates the material under consideration into fractions of like or similar properties, studying the characteristics of these fractions and even of the individual components. He proceeds from higher to lower levels of structure and arrives finally at the atomic and electronic levels. The engineer appreciates these divings to the lower levels of structure only if they result in bringing forth something useful on the working level.

The physical chemist, to be of real assistance to the engineer, must be a generalist as well as a specialist; he must understand that material properties are functions of the constitution as well as of the composition of the material; he must realize that, as a result of this constitution, the properties of a system may be more or may be less than the sum of the properties of the components. If the physical chemist is not sufficiently versatile to move freely, as necessity requires, from one level of structure to another, then he is, at best, a help-meet and, at worst, a seducer to the engineer. Possessing this versatility, this "ingenium", he can be truly an engineer and a teacher of engineers.

Physical chemistry offers fundamental explanations for observed soil-mechanical properties and indicates rational methods for improving soil properties (soil stabilization).

Soil systems are normally composed of solid, liquid and gaseous phases. The composition and character of these phases vary from soil to soil and within the same soil often from season to season. Of greatest importance to the engineer are the soil-water relationships. Since water can react only with the surface of the soil solids, the specific surface (surface/volume) of a soil is important. One percent of clay in a sand contributes more than ninety percent of the total internal surface. This illustrates the importance of the clay content; it is, however, not the whole story. Depending upon its chemical composition and environmental factors, clay is normally not in a dispersed but in an aggregated condition. Therefore, in most soils the calculated internal surface of clay is a potential not

an actual one, also, the soil mechanical "weight" of the clay depends on whether and to what extent it is present as a film around the coarser particles or as a filler in the pore spaces between the sand grains. The structural location, and, therefore, the role which a clay plays, depends on its own surface-chemical character as well as on that of the coarser material. On one hand, 1% of clay or other mineral cementing material may make the difference between a loose sand and a sandstone. On the other hand, if there exists no affinity between the clay and the coarse material, i.e. if the clay serves only as a pore filler, then we may incorporate into a sand, possessing a compacted density of 100 lb/cu ft as much as 30% of a clay (on the basis of the weight of the sand), which may double its volume by swelling in water, without appreciably affecting soil stability in moist condition. It is because of this situation that highway soil classifications consider as granular materials those which contain up to 35% of fines passing the No. 200 sieve. The actual role of clay in a soil may and normally does range between the two extremes indicated.

The phenomena resulting from the interaction of the mineral surfaces and water depend on the properties of the water as well as on those of the minerals. The properties of the water are as complex as those of the minerals. 1), 2), 3). In accordance with its molecular weight and in analogy with similar compounds ( $H_2S$ ,  $H_2S^+$ ,  $H_2T^+$ ), water should be a gas at normal temperatures, but it is a liquid; furthermore, x-ray examination of this liquid reveals properties normally associated with solids. This behavior is a consequence of the dipole nature and architecture of the water molecule. A dipole is a molecule in which the action center of the positive charges does not coincide with that of the negative. Some dipole molecules have only one pole sufficiently exposed to be reactive with other molecules or ions, while the other pole is sterically protected. In the water molecule, both poles are relatively accessible, which permits the molecule to freely associate itself with other molecules of its own kind or with other positively or negatively charged components of matter. The dipole character of water and the fact that soil minerals possess electrically charged surfaces, makes the whole field of soil-water relationships a branch of applied electrostatics 4), 5), 6).

Different soil minerals possess different electric surface structures. Because of the importance of the electric surface pattern for the understanding of mineral-water relation-

TABLE I  
Comparison of Consistency Properties of Clay  
Fraction and Whole Soil.  
Plasticity Index

Lab. Symbol	Soil Series and Texture	Mechanical Analysis %				determined clay <sup>2</sup> fraction	whole soil (a)	calculated whole soil		P.I. Ratios		% of organic matter in soil	colloid (extracted)	Liquid Limit (4) whole soil	(e) colloid
		sand	silt	clay	clay <sup>2</sup>			(b) <sup>3</sup>	(c) <sup>4</sup>	(a)/(b)	(a)/(c)				
P	Stephenville loamy sand	77	12	11	7.4	30.4	2.0	2.2	3.3	0.9	0.6	1.0	13.6	19.0	76
B	Zaneis sandy clay	67	11	22	12.5	36.2	4.1	4.5	3.0	0.9	0.5	1.4	10.9	22.1	84.6
E	Durant sandy loam	50	32	18	7.3	28.8	4.2	2.1	5.2	2.0	0.8	2.5	34.0	22.5	70.9
L	Peard loam	55	28	17	6.5	28.2	5.6	1.8	4.8	3.1	1.2	1.5	22.8	23.0	71.0
U	River Wash silty clayloam	39	41	20	10.8	49.9	11.7	5.4	10.0	2.2	1.2	1.3	12.2	31.8	92.0
M	Zaneis clay loam	45	30	25	21.8	33.4	13.7	7.3	8.4	1.9	1.6	1.8	8.2	32.1	80.0
N	Miller silty clay	33	27	40	34.2	40.9	26.1	14.0	16.4	1.9	1.6	2.0	5.7	45.0	82.8
V	Vernon clay	34	21	45	27.2	47.1	31.1	12.8	21.2	2.4	1.5	3.0	11.2	53.5	91.8

All the soils in the Table come from the State of Oklahoma; the colloidal fraction of these soils (except for soil M) were found by differential thermal analysis to consist of illite and organic matter; soil M appears to contain a small amount of kaolinite in addition to illite and organic matter. From the thermal analysis it appears also, that soils E, L, P, and N possess a similar type of organic matter differing from that of the other soils by a relatively higher range of combustion temperature.

- 1.) clay content from sedimentation curve
- 2.) -2- micron clay from exhaustive extraction (soil residue had P.I. = 0)
- 3.) P. I. of extracted clay X percentage of clay obtained by extraction
- 4.) P. I. of extracted clay X percentage of clay from sedimentation curve.

snips, the elucidation of clay crystal structure is of great value in theoretical soil physics. Hogentogler has shown that the plasticity index of mixtures of sand with diatoms, kaolin, and bentonite, respectively, equals the product of the clay mineral percentage and a proportionality constant. 7)

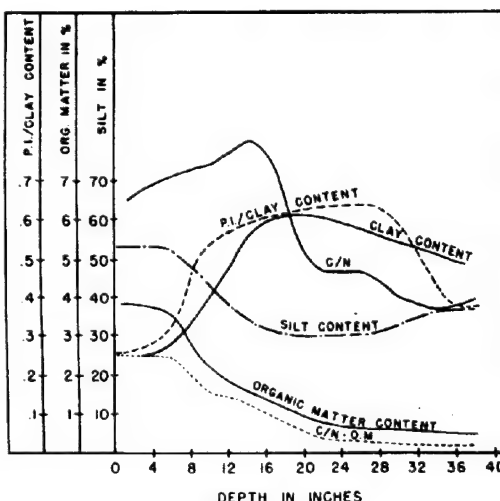
This relationship has been utilized also by clay mineralogists interested in foundry sands and ceramics. Some have even suggested that it is only necessary to know the amount and mineralogical character of the clay fraction in order to predict the behavior of a whole soil. This is unwarranted for a large number of reasons, only a few of which can be cited here.

The indicated relationship can exist only in artificial and structureless mixtures, but not in natural soils endowed with structure. Clay minerals in natural soils are not as clean as a scraped bone; rather, the mineral surface is normally in as close a relationship with adsorbed and syn-active organic matter as a bone in a living being is with cartilage and muscle tissue.

Opposite the indicated unwarranted simplification stands the complex reality as illustrated in Graph I and in Table I, respectively.

The tabulated data bring out an additional point, which is concerned with the problem of soil classification, and the discretion which must be employed in the practical use of any classification.

In the U.S. Engineers classification, organic silts and clays are separated from their inorganic counterparts by a line which



Factors influencing the plastic index

GRAPH 1

follows the equation:

$$P. I. = 0.73 (L. L. - 20)$$

If plotted, the data given in table I for the extracted colloids fall on the organic side

TABLE 2

Clay mineral - water relationships.(13)

Colloidal property	Type of H-colloid				
	Bentonite	Lufkin	Putnam	Susque- nanna	Cecil
Type of mineral	Montmoril- lonite	Montmoril- lonite Beidellite	Beidel- lite	Beidel- lite	Halloy- site
$SiO_2/R_2O_3$ ratio...	5.0	3.8	3.2	2.3	1.3
Exchange capacity m.e. per 100 g	95.0	82.0	65.0	47.0	13.0
Hygroscopicity, %, (30% $H_2SO_4$ )	21.5	20.1	18.1	15.5	6.1
Heat of wetting cal/g		15.0	13.8	11.7	5.9
Swelling, cc./gm	2.2	1.18	0.81	0.57	0.05
Swelling Exchange Capacity	2.44	1.44	1.24	1.21	0.41
Hygroscopicity Exchange capacity	6.22	0.24	0.28	0.33	0.47
Swelling Hygroscopicity	10.23	5.87	4.47	4.87	0.91

TABLE 3.

The Effect of Exchangeable Cations on the Properties of Colloidal Clays.

Colloidal system	Colloidal property	Nature of cation					
		H	Li	Na	K	Ca	Ba
Putnam	Hygroscopicity						
	(a)	18.13	17.13	16.53	12.75	17.37	16.29
	(b)	44.76	56.12	49.22	31.12	40.91	41.95
	Heat of Wetting cal/g	13.6	12.0	12.0	9.5	15.0	13.9
	Swelling cc/g	0.81	4.97	4.02	0.50	0.91	0.85
	Hydration (c) cc/g	5.20	5.25	5.25	4.07	5.20	5.20
	Dispersity (d)	37.4	60.1	62.2	56.3	4.9	24.4
Wyoming Bentonite	Swelling cc/g	2.20	10.77	11.08	8.55	2.50	2.50
	Hydration (c) cc/g	35.0	28.4	24.1	21.3	24.2	34.0
	Dispersity (d)	34.0	37.8	35.2	35.7	31.2	31.9

(a) %  $H_2O$  absorbed over 30% aqueous  $H_2SO_4$  solution;(b) %  $H_2O$  absorbed over 3.3% aqueous  $H_2SO_4$  solution;

(c) calculated from viscosity data by means of the Einstein equation.

(d) % particles smaller than 100 milli microns.

of the dividing line, while those for the whole soils fall on the inorganic side. Testing only the whole soils, there exists a serious danger that the organic matter in the soil be overlooked. For some applications, this may not be of great importance. For purposes of soil Stabilization, however, the "hidden" organic matter may make the difference between success or failure.

If the charge pattern on the surface of a solid soil constituent is ionic, it is matched by adsorbed ions of opposite charge. In the presence of water these adsorbed ions are partly dissociated into the surrounding water envelopes. These ions are exchangeable, i.e. they may be replaced by other ions.

If the mineral surface is predominantly negative, the counter-ions are positive or cations, and the soil possesses a cation-exchange capacity. Positively charged minerals possess an anion exchange capacity. If the electric field is of mixed character, then the system possesses both, cation and anion exchange capacity. Cation exchange capacity predominates in regions of temperate climate, anion exchange capacity predominates in soils developed under tropical weathering. The ion exchange capacity is usually expressed in milli-equivalents per 100 g of soil or clay. This exchange capacity is a property of any solid built up of ionic constituents; however, because clay contributes the largest relative amount of internal surface to a soil, practically all the exchange capacity of a normal soil is a function of the amount and type of its clay content.

With pure minerals, the exchange capacity can be related directly to the crystal structure. Minerals and especially their surfaces are rarely pure, however, in soils. For the same reason, the older characterization by means of the silica-sesquioxide ratio continues to be of practical importance in correlating clay-water relationships with chemical compositional factors. Furthermore, organic soil constituents contribute a large share of the exchange capacity of normal soils, and through this and other means influence soil-water relationships. Considering, also, the very close, almost symbiotic, physical relationship between organic and inorganic clay constituents existing in an actual soil, it becomes obvious, that exchange capacities of soils cannot be predicted from their mineralogical composition, but must be determined experimentally.

Table 2 illustrates relationships between water-affinity, base exchange capacity, silica-sesquioxide ratio, and type of clay mineral.

Table 3 illustrates the effect of the type of exchangeable ions on the water-affinity of Putnam clay and Wyoming bentonite.

Table 4 shows the effect of different exchange ions on whole Putnam soil.

Comparison of the data for Putnam clay in Table 3 and for the whole Putnam soil in Table 4 indicates clearly the modifying influence of the other soil fractions on the role played by the clay.

Materials added to soils for stabilization purposes will react physically or chemically with the surface of the soil solids. The type

TABLE 4. (14)

EFFECT OF EXCHANGE IONS ON ENGINEERING  
PROPERTIES OF PUTNAM SOIL

Ion	Nat	H	Na	K	Mg	Ca	Al
<u>TEST</u>							
Lower liquid limit ....	64.5	56.4	88	52.8	56.3	61.9	60.2
Lower plastic limit....	23.5	24.8	25.4	27.7	25.4	27.0	26.3
Plastic index.....	41.0	31.6	62.6	25.1	30.9	34.9	33.9
Volume change F.M.E....	56.0	52.4	68.6	40.1	68.9	63.8	51.7
Shrinkage limit.....	17.9	16.3	11.8	19.4	12.	12.4	16.4
Shrinkage ratio.....	1.91	1.94	2.08	1.80	2.01	2.00	1.95
Field moisture equivalent.....	47.2	43.3	44.8	41.7	46.7	44.3	42.9
Specific gravity.....	2.708	2.663	2.661	2.675	2.645	2.680	2.721
Hygroscopic moisture...	5.79	5.32	4.20	4.60	4.38	5.76	6.69
Vacuum moisture equivalent.....	57.1	54.3	Water logged	53.7	58.7	58.9	55.1
<u>Mechanical Analysis</u>							
Per cent passing No.40	100	100	100	100	100	100	100
Per cent passing No.60	99.6	99.8	99.4	100	99.8	99.8	99.8
Per cent passing No.200	98.1	98.7	97.5	98.5	98.5	98.5	98.3
Silt (.05-.005mm).....	39.0	46.0	33.0	48.0	45.0	47.0	49.0
Clay (.005 mm).....	54.0	48.0	61.0	44.0	49.0	45.0	44.0
Colloids (.001mm)....	33.0	26.0	48.0	21.0	25.0	22.0	23.0
<u>Proctor Compaction</u>							
Max. dry weight, lb/cuft	88.0	87.4	85	89.6	85.6	85.2	84.4
Optimum Moisture %	28.6	30.9	31.3	28.4	31.2	32.3	32.4
Void ratio.....	.915	.895	.951	.855	.924	.961	1.01

and extent of such reaction and of the degree of stabilization achieved depends upon the physical and chemical character of this surface as well as on the properties of the stabilizing agent. The susceptibility of soils to the different methods of stabilization is, therefore, influenced not only by physical factors such as gradation, but also, and sometimes dominantly, by surface-chemical factors; of the latter the clay mineral composition, the exchangeable ions, and the type and amounts of organic matter are of special importance. Space limitations prevent detailed treatment of the complex physico-chemical interactions between stabilizers and the surfaces of solid soil constituents; however, reference is made to the tables accompanying the paper on "Soil-Stabilization" (These Proceedings) and to publications cited in that paper.

Physico-chemical phenomena are important not only in the case of admixtures foreign to the soil, but also in granular stabilization. Well known is the setting up of a graded mixture of siliceous aggregate and lateritic clay, and of limestone aggregate and podsollic clay. Such cementation occurs whenever positively and negatively charged soil materials are mixed. This phenomenon is illustrated by the data in Table 5 which are concerned with dry strength and slaking resistance of Putnam and Cecil soils and their mixtures.

Some of the most important problems in soil engineering are related to the physical chemistry of soil organic matter and to microbial processes. The problem of living and dead organic matter in soil is quite complex because of the large number of different types of organic molecules and systems involved as well as because of structural interrelationships among these organic molecules and between the organic matter and the clay minerals. However, for most engineering purposes it is sufficient to know the total amount of organic matter and its relative distribution among the seven chemical groups shown in Table 6 for the Loess Pampeano top- and sub-soils (8). In these particular soils, the content in cellulose and hemicellulose is low and that in proteins and lignins high, showing an advanced state of decomposition of plant organic matter due to great bacterial activity, favored by the presence of mineral plant nutrients. Organic matter of the type and in the amount contained in the Loess Pampeano top soil is very favorable for any waterproofing stabilization, as long as further bacterial action is prevented (9,10).

Soils in which organic matter is accumulated under conditions of low bacterial activity, stymied by lack of mineral activators, contain a relatively large proportion of celluloses and hemicelluloses. This type of organic matter is almost always objectionable.



TABLE 5

Data on Tensile Strength and Slaking  
Resistance of Putnam and Cecil Soils  
and their combinations

P Putnam Soil

C Cecil Soil

Composition	Tensile Strength in lb/sq in.	Slaking time (2) in minutes
Putnam Soil	90	9
P <sub>9</sub> C <sub>1</sub>	167	8
P <sub>8</sub> C <sub>2</sub>	157	9
P <sub>7</sub> C <sub>3</sub>	147	20
P <sub>6</sub> C <sub>4</sub>	142	29
P <sub>5</sub> C <sub>5</sub>	140	17
P <sub>4</sub> C <sub>6</sub>	113	15
P <sub>3</sub> C <sub>7</sub>	107	19
P <sub>2</sub> C <sub>8</sub>	97	14
P <sub>1</sub> C <sub>9</sub>	82	11
Cecil Soil	47	13

- 1) Data represent averages of three determinations;
- 2) Method of Russian pedologists.

Inorganic stabilizers containing lime, may, if added to such soils, in amounts insufficient to kill the microbial organisms, result in their activation by the Ca-ion and, through a connected chain of events, may weaken rather than improve a subgrade soil. The general detrimental effect of organic matter on portland-cement products is too well known to require special emphasis. It should be emphasized, however, that knowledge of soil organic matter and of microbial phenomena not only assists in understanding the unpleasant consequences of their presence, but that this knowledge points out a way to a practical utilization of the organic matter, already contained in a soil, for coordinated action with other stabilizers. This is one of the principles on

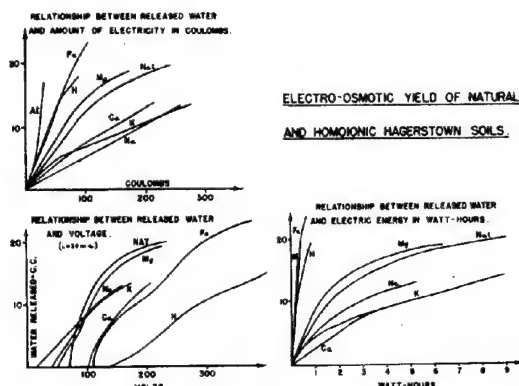
which the so-called natural method of soil-stabilization is based 11).

Within recent years, electro-osmosis has met with increasing use and interest on the part of the soil engineer. Theoretically pure electro-osmosis is an interfacial phenomenon and, consequently, depends on the physico-chemical characteristics of the interface. Electro-osmosis in normal soils is rendered impure by ionic conductance and transference; the latter, of course, also represent or depend on physico-chemical properties, such as base exchange capacity, type of exchangeable ions, degree of ionic dissociation and others 12). The effect of different exchange ions on electro-osmotic phenomena is shown in Graph 2.-

TABLE 6

Nature of the organic matter in loess pampeano soils

Constituent	% of total organic matter				
	Topsoil	Sub-soil	Top-soil	Sub-soil	Difference
Total organic matter.....	4.5	1.95			
Protein.....	47.00	42.75	1.615	0.833	0.782
Lignin.....	37.40	42.05	1.588	0.625	0.963
Celluloses.....	4.8	9.6	1.96	1.87	0.09
Hemicelluloses.....	5.8	10.4	0.261	0.202	0.059
Sugars, amino-acids, etc...	2.88	1.52	0.129	0.029	0.100
Wax, resins, alkaloids, etc.	0.89	2.11	0.040	0.041	
Wax, resin-like fatty substances.....	1.20	1.57	0.054	0.030	0.024



Electro-osmotic yield of natural and homoionic Hagerstown soils.

GRAPH 2

CONCLUSIONS

The facts and data presented in this paper and in the references cited should make clear the importance of physico-chemical phenomena in governing actual soil properties and in aiding or obstructing soil stabilizing measures. While there cannot exist intelligent soil stabilization without physico-chemical understanding, it does appear that the body of soil mechanics itself needs to absorb more and more physico-chemical principles and knowledge if it is to keep healthy; otherwise, it might degenerate into increasingly mathematical mental fictions, or return to its former status of a primitive art, unrelated to available scientific knowledge.

REFERENCES:

- 1) Tammann, G. The States of Aggregation(transl. by Robert F. Mehl). D. van Nostrand Co. New York, 1925.

- 2) Rae, I.R. Nature, 132, 480, 1933.
- 3) Winterkorn, Hans F. The Condition of water in porous systems. Soil Science, 56, 109-16, 1943.
- 4) Winterkorn, Hans F. and Bayer, L.D. Sorption of liquids by soil colloids. Soil Science, 38, 291-98, 1934.
- 5) Russel, E.W. The interaction of clay with water and organic liquids as measured by specific volume changes and its relation to the phenomena of crumb formation in soils. Phil. Trans. Royal Soc. London, 233A: 361 - 89, 1934.
- 6) Winterkorn, Hans F. Studies on the surface behaviour of bentonites and clays. Soil Science, 41, 25 - 32, 1936.
- 7) Hogentogler, C.A. Engineering Properties of Soil. (233) Mc Graw-Hill Book Co. New York and London, 1937.
- 8) Winterkorn, Hans F. and Eckert, George W. Consistency and physico-chemical data of a loess Pampeano-soil. Soil Science, 42, 73-82, 479-88, 1940.
- 9) Winterkorn, Hans F. and Eckert, George W. Physico-chemical factors of importance in bituminous soil stabilization. Report, Missouri State Highway Department 1939; Abstract: Proc. A. Asph. Pav. Techn. 11, 204-257, 1940.
- 10) Winterkorn, Hans F. Principios sobre moderna estabilización de suelos. Caminos. No. 70, Enero-Febrero 1947, Buenos Aires. Separate Printing by Comisión Permanente del Asfalto, B.A. 1947.
- 11) Winterkorn, Hans F. Soil Stabilization. U.S. Patent Application, Ser. No. 679859, 1946.
- 12) Winterkorn, Hans F. Escobar Jose L. and Gowda, K.R.S. Theoretical and practical aspects of electro-osmosis. Proc. Soil Science Soc. Am. 12, 1947.
- 13) Bayer L.D. and Winterkorn, Hans F. Sorption of liquids by soil colloids II. Surface behaviour in the hydration of clays. 40, 403 - 19, 1935.
- 14) Winterkorn, Hans F. and Moorman, Robert B.E. A Study of changes in physical properties of Putnam soil induced by ionic substitution. Proc. Highw. Res. B. 21, 415-34, 1941.

## SUB-SECTION I d

## STRESS-STRAINS RELATIONS; CONSOLIDATION

I d 1

## PROBLEMS OF SOIL SETTLEMENT

ir. T. EDELMAN

## I. HYDRODYNAMIC SETTLEMENT.

1) The settlement of homogeneous soil of which the voids are filled with water is ruled by the differential equation:  $\frac{\partial^2 w}{\partial x^2} = \frac{a}{k} \frac{\partial w}{\partial t}$

in which:

$w$  = the increment of pressure in the water, caused by the increment of load,  $x$  = the depth on which the named  $w$  appears,  $a$  = the coefficient of compressibility,  $k$  = the coefficient of permeability and  $T$  = the time passed since the increment of load is carried on.

In the formula the specific gravity of water = 1

By supposing:  $t = \frac{k}{a} T$ , the equation is simplified to  $\frac{\partial^2 w}{\partial x^2} = \frac{\partial w}{\partial t}$

2) For the case that a layer of soil, continuous till endless depth, of homogenous composition, is limited on the upper side by a horizontal flat plane and is loaded by an equal devided load  $p$ , which is stretched unlimited, the boundary conditions for this linear case can be defined as follows:

$w = p$  when  $t = 0$  at each value of  $x$ ;  
 $w = p$  when  $x = \infty$  at each value of  $t$ ;  
 $w = 0$  when  $x = 0$  at each value of  $t$ ,

except when  $t = 0$ .

The solution of the equation is formed by:  $w = f(u)$  in which  $u = \frac{x^2}{4t}$ . By introducing  $u$  the partial differential equation becomes the ordinary differential equation:

$$\frac{d^2 f}{du^2} = -2u \frac{df}{du} \quad \text{suppose} \quad \frac{df}{du} = f'$$

$$\text{then is } \frac{df'}{du} = -2uf'$$

$$\text{or } \frac{df'}{f'} = -2u du \quad \text{Then} \quad \frac{df}{du} = C_1 e^{-u^2}$$

$$\text{and } f = f(u) = w = C_1 \int e^{-u^2} du$$

Then substitution of  $u$  the boundary conditions can be taken together to two specimen:

$w = p$  when  $t = 0$  to:  $w = p$  when  $u = \infty$   
 $w = p$  when  $x = \infty$  to:  $w = p$  when  $u = 0$   
and  $w = 0$  when  $x = 0$ ; to:  $w = 0$  when  $u = 0$

The integral  $\int e^{-u^2} du$  cannot be expressed in elementary functions; tables exist for the definite integral:

$$\frac{2}{\sqrt{\pi}} \int_0^u e^{-u^2} du = E(u)$$

$E(u) = 1$  when  $u = \infty$  and  $E(u) = 0$  when  $u = 0$ . We can write:

$$\int e^{-u^2} du = \frac{1}{2} \sqrt{\pi} \{ E(u) + C_2 \} \quad \text{so}$$

$$w = C_1 \frac{1}{2} \sqrt{\pi} \{ E(u) + C_2 \}$$

The substitution of the boundary conditions gives:

$$C_1 = \frac{2}{\sqrt{\pi}} p \text{ and } C_2 = 0, \text{ so } w = p E(u)$$

It is preferred to expand the function  $E(u)$  in the form of a series:

$$\int e^{-u^2} du = \frac{1}{2} \sqrt{\pi} E(u) = u - \frac{1}{1!} \frac{u^3}{3} + \frac{1}{2!} \frac{u^5}{5} - \frac{1}{3!} \frac{u^7}{7} + \frac{1}{4!} \frac{u^9}{9} - \dots \text{a.s.o.}$$

The compression which a part of a soil-layer with thickness  $D$  undergoes, is:

$$Z_D = p \cdot a \cdot D - a \int_0^D w dx \quad \text{in which } x = 2u\sqrt{t}$$

$$dx = 2\sqrt{t} du$$

and for that reason

By performing the integration we get:

$Z_D = p \cdot a \cdot D (1 - A)$  in which:

$$A = \frac{2}{\sqrt{\pi}} \left\{ \frac{1}{2} u_0 - \frac{1}{1!} \frac{1}{3} \frac{1}{4} u_0^3 + \frac{1}{2!} \frac{1}{5} \frac{1}{6} u_0^5 - \frac{1}{3!} \frac{1}{7} \frac{1}{8} u_0^7 + \dots \right\}$$

$$\text{and } u_0 = \frac{D}{2\sqrt{t}} = \frac{1}{2} \cdot D \cdot \frac{1}{\sqrt{t}} \cdot \frac{1}{k} \quad \text{Suppose}$$

$$\alpha = \frac{1}{4} \frac{1}{u_0^2} \quad \text{then} \quad T = \alpha \cdot \frac{a}{k} \cdot D^2$$

When  $\alpha = 0 \quad 0.25 \quad 1 \quad 4 \quad 25 \quad \infty$   
 $A = 1.0 \quad 0.486 \quad 0.270 \quad 0.140 \quad 0.055 \quad 0.000$   
With the help of these values the time-settlement-curve can be designed (fig.1); it proves

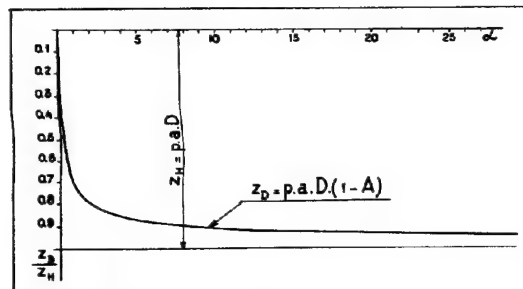


FIG. 1

to exist a final-value  $Z_h = p \cdot a \cdot D$ , which is reached after an endless time. The variation of the waterpressure at the depth is for a special time  $t$  represented by a dotted curve of fig. 2; these dotted curves are named "Isochrones".

3) A clay-layer, thickness  $D$ , on upper- and lower side bordered by a layer of large-

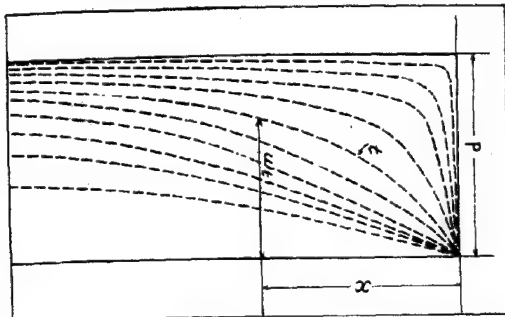


FIG. 2

grained sand (or by porous stone) will show isochrones of symmetric shape of which the maximum lies at  $x = \frac{1}{2} D$  and for which  $w = 0$  when  $x = 0$  and when  $x = D$  (fig. 3). The cal-

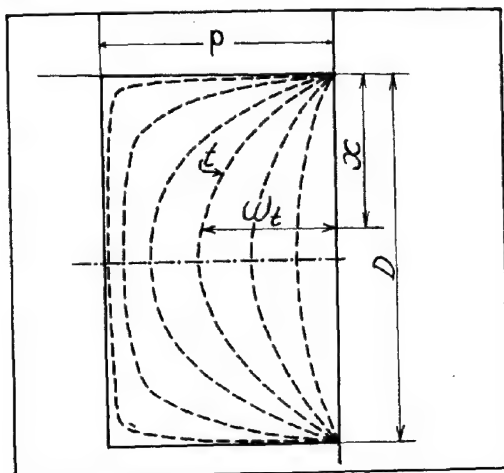


FIG. 3

ulation of  $w$  and therefore of  $x$  in this case can be connected with the preceding case, by the addition of two equal but removed, reflected images of the isochrones of fig. 2 and by subtracting off the function  $w_D$ , we got in this way. In fig. 4, in which this construction is carried out can be read:

$$w = w_x + w_{(D-x)} - w_D$$

The settlement amounts to:

$$Z_D = p \cdot a \cdot D - a \int_0^D w dx = p \cdot a \cdot D - a \left[ \int_0^D w_x dx + \int_0^D w_{(D-x)} dx - \int_0^D w_D dx \right]$$

From fig. 4 is further concluded:

$$\int_0^D w_x dx = \int_0^D w_{(D-x)} dx$$

$$\text{while too } \int_0^D w_x dx = p \cdot A \cdot D$$

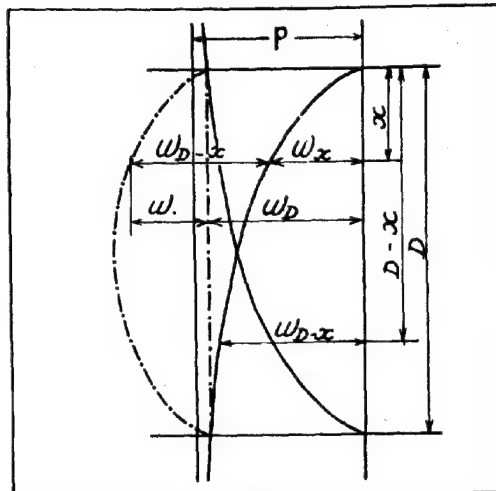


FIG. 4

It follows that  $Z_D = p \cdot a \cdot D (1-B)$  in which

$$B = \frac{2}{\sqrt{\pi}} \left\{ \frac{1}{2!} \frac{u_D^3}{3} - \frac{2}{3!} \frac{u_D^5}{5} + \frac{3}{4!} \frac{u_D^7}{7} - \frac{4}{5!} \frac{u_D^9}{9} + \dots \right\}$$

If  $\alpha = \frac{1}{4} \frac{1}{u_D^2}$  some values can be calculated :

When $\alpha =$	0	0.0625	0.25	0.56	1.-	4.-	$\infty$
is B =	1.-	0.190	0.118	0.047	0.022	0.003	0

With the help of these values the time - settlement-curve again can be plotted (fig.5).

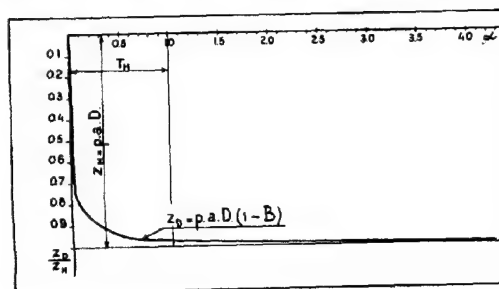


FIG. 5

For  $\alpha = 1$  the settlement is almost completed; the corresponding time-interval  $T_h = \frac{a}{k} \cdot D^2$  is called the "hydrodynamic period"

4) The formula  $Z_D = p \cdot a \cdot D (1-B)$  can be approximated by an orthogonal hyperbole:

$$Z_D = Z_r \left( F \frac{T}{T_h} + 1 \right)$$

in which  $Z_r$  is the remaining settlement on the time  $t$ ,  $Z_D$  is the eventual settlement,  $T_h$  is the hydrodynamic period and  $F$  is a constant. A value  $F = 30$  gives  $Z_r = 0.032 Z_D$  when  $t = T_h$

so that after the hydro-dynamic period the settlement would be finished for nearly 97%

5) Suppose  $D_u$  = the thickness to which a soil-layer of thickness  $D$  at the end can be compressed until there exist no more voids; then the voids-ratio  $n$ , defined as the volume of voids per unit volume equals  $\frac{D-D_u}{D}$  or

$$n = 1 - \frac{D_u}{D}$$

If the layer is hydro-dynamically compressed by an increment of load  $p$  from  $n_0$  till  $n_h$  then is

$$Z_r = \left( \frac{1}{1-n} - \frac{1}{1-n_h} \right) D_u \quad Z_D = \left( \frac{1}{1-n_0} - \frac{1}{1-n_h} \right) D_u$$

therefore the formula of the time-settlement curve changes in:

$$\frac{1-n}{n-n_h} \cdot \frac{n_0-n_h}{1-n_0} = F \frac{t}{T_h} + 1$$

6) Kinds of soil exist which show the settlement as may be expected from the mentioned theory. Such soils are defined as "singular soils", they show an ultimate settlement, while at the end of the hydrodynamic period by means of waterpressure-meters can be established that the increase of pressure in the water has disappeared.

## II. SECULAR SETTLEMENTS.

1) There too exist kinds of soil which will be named "composed soils" by which the settlement still continues during a long time after the pressure of the water is reduced to the original value. This "secular settlement" passes very slowly. It cannot be caused by the flow of the "free water" (the water, of which the pressure can be measured in a water-pressure-meter) because the influence hereof is charged already by the calculation of the hydrodynamic-settlement and because as is mentioned too, during the secular settlement there is no increase in pressure concluded in this free water. If a flow of fluid is responsible for this secular settlement this has to be a flow of a liquid with a great viscosity, by which the long duration of the secular settlement becomes acceptable.

Clay-investigations have laid to the opinion that water molecules in the presence of mineral particles of clay by these are aimed and electrically tied; near the mineral particles the density of the absorbed water seems to be so high and the molecules so hard movable that this water behaves as a very sticky fluid. By supposing that in composed soils there are micro-complexes between the bigger grains, composed of very little mineral-particles close one to another, then the voids of such a complex will be filled by sticky water. This tied water will show a stark retardation in flow by increase of load to the micro-complex; in consequence of this the micro-complex undergoes a stark retarded hydro-dynamic-settlement.

The addition of these micro-settlements delivers the secular-settlement of the soil. For the limited space we cannot go farther into the subject of the phenomena of different microstructures which are imaginable. No more we can go farther into the calculation of the settlements that follows from here. However it may be evident that the relation between the secular settlement and the time can be approximated by a similar formula as is distracted

for the hydro-dynamic settlement; approximately the secular time-settlement-curve can be represented by an orthogonal hyperbole.

2) In the following is considered the settlement of a layer of composed soil that, from the point of time of coming into existence, is influenced by a constant load  $p$ . Let the voids-ratio without load be  $n_K$  (characteristic voids-ratio); the load  $p$  carried on at the time  $t = 0$  makes the voids-ratio go down hydro-dynamically till  $n_m$  (virgin-voids-ratio). The settlement from  $n_K$  till  $n_m$  happens in a hydro-dynamic period  $T_h$ , which is neglected with respect to the geological period, in which the secular settlement takes place. Under influence of  $p$  the soil then becomes secularly compressed from  $n_m$  till  $n_s$ ; the secular voids-ratio, which represents the final situation to which the soil comes finally under the influence of  $p$ . This secular course from  $n_m$  till  $n_s$  may be represented by the formula

$$\frac{1-n}{n-n_s} \cdot \frac{n_m-n_s}{1-n_m} = G \frac{t}{T_s} + 1$$

completely analogic to the formula derived for the hydro-dynamic settlement. In the formula  $G$  is a constant,  $T_s$  = the secular period, while  $n_m$  and  $n_s$  may be taken as yet unknown functions of  $p$ . Plotting this formula as a straight line, by which  $t$  is plotted on linear scale, the  $n$ -scale becomes a projective scale, which is fixed by the alignment-equation:

$$R = \mu \cdot \frac{1-n}{n-n_s}$$

(in which  $\mu$  is the chosen length-unit) Of this projective scale the zero falls in  $n = 1$  (for  $n = 1$  when  $G = 0$ ) while the point  $n = n_s$  falls in the infinite (for  $n = n_s$  when  $R = \infty$ ). The scale is dependent on  $n_s$ , that is to say that to every  $n_s$ , and therefore to every load, belongs a separate  $n$ -scale. The plotting of different scales of various settlement-curves can be escaped in the way as is shown in fig. 6. Besides it is consider-

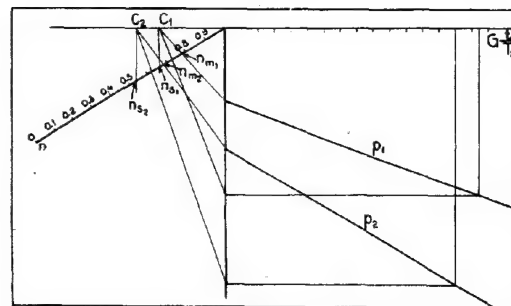


FIG. 6

ed that every projective-scale can be found by projecting from a fixed point a linear scale on a straight line, which cuts this scale. In fig. 6 consequently  $n$  is read on the inclined linear scale by using the projection-point  $C$ , that belongs to the concerning time-settlement-curve. Consequently every settlement-curve has its own reading-point  $C$ , that lays vertically above the corresponding  $n_s$  on the  $n$ -scale.

3) If at a fixed moment  $t_1$  the load  $p_1$  is increased till  $p_2$ , the soil will at first obtain a hydro-dynamic settlement from  $n_1$  till  $n_2$ , by which  $n_1$  is the voids-ratio that is reached at the moment  $t_1$  under influence of  $p_1$ , in consequence of the secular line for  $p_1$ . From the moment  $t_1$  the settlement will take place ( $t_1$  is to be neglected again) in consequence of the secular line for  $p_2$ , however in such a way that its point  $n_2$  falls in  $t_1$ . The original secular line for  $p_2$  thus moves parallel to its own over  $t_1$  in the direction of the time-axis. The projection-point  $C_2$  does not change by this movement; the part of the moved line between  $t = 0$  and  $t = t_1$  becomes fictive. The total course of settlement is given by the drawn line in fig. 7.

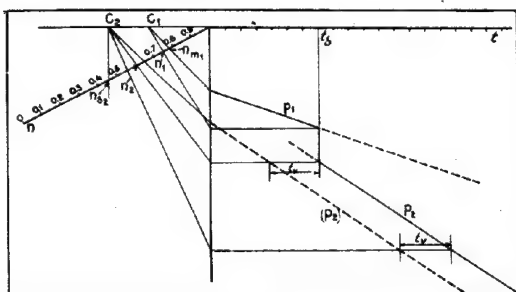


FIG. 7

4) As a projective scale is defined by three points, it is possible to appoint  $n_s$  by a fixed load if on three points of time is known the  $n$ , that the soil has obtained under this load. If at the points of time  $t_1$ ,  $t_2$  and  $t_3$  the respective observed voids-ratios are  $n_1$ ,  $n_2$  and  $n_3$ , the construction of  $n_s$  can take place in consequence of fig. 8. In this the

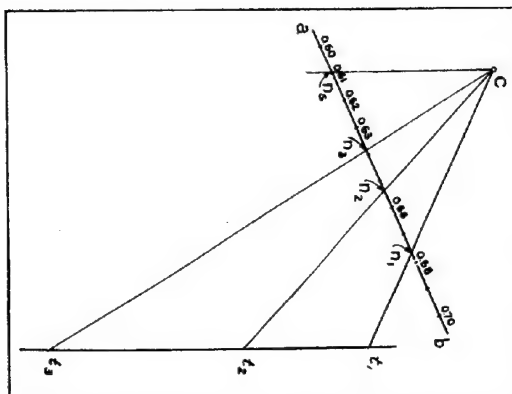


FIG. 8

distances  $t_3 - t_2$  and  $t_2 - t_1$  are in mutual good proportion but on arbitrary scale put on the vertical axis, while the point C in chosen arbitrarily. Then a linear scale is laid on the figure in this way, that its points  $n_1$ ,  $n_2$  and  $n_3$  fall on the lines  $Ct_1$ ,  $Ct_2$  and  $Ct_3$ ; the ultimate voids-ratio then vertically lays beneath C. The fixing of  $n_s$  is the more exactly as the timeperiods between  $t_1$ ,  $t_2$  and  $t_3$  are longer.

5) The results of some tests of undisturbed claysamples were checked; the results provisionally seem to show that between  $n_s$  and the load  $p$  exists the relation:

$$C n_s = \log \frac{M}{p + p_c}$$

in which C is a constant number, M is a modulus and  $p_c$  a (very little) pressure. In consequence, for the eventual settlement too the logarithmic relation according to the load-settlement-curve of Von Terzaghi seems to be true. It has been obvious to calculate C and M from the results of experiments.

It is not possible to calculate  $p_c$  with any exactness; because, when  $p = c$ ,  $n_s = n_k$  and therefore  $C n_k = \log \frac{M}{p_c}$ , it was difficult too to fix  $n_k$  with sufficient accuracy.

When  $n_g = 0$ ,  $\log \frac{M}{p + p_c} = 0$ , therefore  $M = p + p_c$ , or, because  $p_c$  is very small  $p = M$ . Consequently M can be imagined as the load, that is necessary to compress the soil ultimately to a solid stone.

6) As follows from the preceding pages it is possible to prophesy approximately the course of settlement of a ground layer, under influence of different load-increments.

It is not so simple to unravel the prehistory of a groundlayer. If the geological age of a layer is known and if the  $n_s$ -curve does not show an angle,  $n_m$  (fig. 7) can be obtained for the ground load. In this way the original thickness of the layer is approximated. If the relation between  $p$  and  $n_m$  was known, perhaps herefrom could be calculated  $n_m$  for the ground-load, and therefore the geological age of the layer.

If the  $n_s$ -curve shows a bob, these calculations become very unsafe. Truly it is possible to know the bigness of the load which formerly burdened the layer; nevertheless there is not yet found a method to fix the points of time at which this increment of load did begin or end. No more it has been possible to find out whether the layer formerly has been under the influence of a load that is smaller than the present. In general a bob in the load-settlement-curves troubles the prehistory considerably.

7) According to the method Buisman the secular-settlement is set out on a linear and the time on a logarithmic scale, if the zero of the log-scale falls at the time  $t = 1$  (day) the secular-time-settlement-curve becomes a straight line.

The maximum period over which this linear course has been found at a sample is about one year.

Plotting the formula  $\frac{1 - n}{n - n_s} \cdot \frac{n_m - n_s}{1 - n} = G \frac{t}{t_s} + 1$

in this way a curve comes into existence as shows fig. 9. Here out would be concluded that the straight line, as follows from the method Buisman, after some years bends and goes more steep, finally reaching a horizontal asymptote. By extra-polation, according to the method Buisman, over some decades so there could be foretold too small a settlement. Therefore it is important that settlements of constructions are observed over longer periods to ascertain how long for different soils and voids-ratios, is the time-period in which the linear course may safely be extrapolated.

8) During the hydro-dynamic-period the increment of the grain pressure increases grad-

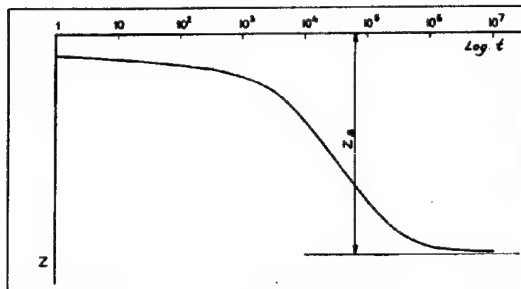


FIG. 9

usually from zero till maximum. The increment of the grain pressure is considered for the secular phenomena as the increment of load; so the

load which causes the secular settlement, increases during the hydro-dynamic-period gradually from zero till maximum. By this the secular-settlement is retarded and the secular-settlement curve deformed. During this period the total settlement then is not obtained by addition of the hydrodynamic and the undeformed secular-curve.

Incidentally may be point out the fact that constructing fig. 8 the moment  $t$  is to be chosen outside the area in which this deformation still has a noticeable influence.

The hydro-dynamic settlement shows a layer-thickness-effect ( $T_h$  is proportional to the square of the layer thickness) the secular-settlement does not show such an effect.

The deformation of the secular-curve during  $T_h$  therefore will be important longer in a layer than in a sample. Interpreting an observed settlement-curve of a layer this has to be considered; in general this curve is not directly comparable with the one, observed by the sample.

-O-O-O-O-O-O-

1 d 2

#### PRECISE DETERMINATION OF PRIMARY CONSOLIDATION

PROFESSOR A.H. MAYLOR, M.Sc., I.G. Doran, M.Sc. M.I.C.E.

#### SUMMARY.

In research on Secondary Consolidation of Clays the accurate determination of the end point of theoretical primary consolidation is essential. The accuracy of existing methods of determination is open to question. An improved method has therefore been developed. The paper commences by reviewing the existing methods of curve fitting. Using the new method the theoretical initial and final readings and the coefficient of consolidation can be determined. Examples of the application of the new curve fitting method are given and the accuracy of the results obtained is discussed.

In the analysis of settlement-time results obtained from the consolidation test it is necessary to fit the theoretical relation between percentage consolidation and time factor to the experimental readings. There are at present two methods of carrying out this curve fitting, due respectively to A. Casa-

grande and D.W. Taylor. 1)

The authors have found in general that these methods give results which are only rarely in agreement or correct. The errors, while not great, become of importance when amounts of secondary consolidation are being measured. Table I shows typical results from

TABLE I

Initial and Final Values of Primary Consolidation by various methods

Test	Material	Load tons/ft <sup>2</sup>	Initial Values			Final Values		
			Taylor	Casagrande	New Method	Taylor	Casagrande	New Method
C.14	Recent alluvium	0.285	1940	1940	1952	1151	1166	1161
C.2	Boulder clay	1.60	968	978	968	728	674	723
HC.1	Lias clay	4.00	1650	1648	1650	1360	1338	1332
C.12	Peat	1.50	2690	2710	2631	1485	1449	1449
C.24	Bentonite	0.80	1940	1938	1860	855	854	830



a number of tests on different compressible materials and the discrepancies are at once evident. The results obtained from the method developed by the authors are included in the Table.

It is now generally recognised that there are three phases in the consolidation of a clay sample - initial, primary and secondary consolidation. The phase known as primary consolidation follows classical Consolidation Theory exactly.

The Theory developed by Terzaghi (2) gives the relation between percentage consolidation  $U$ , and time factor  $T$ , as

$$U = 1 - \frac{8}{\pi^2} \sum_{n=0}^{\infty} \frac{1}{(2n+1)^2} e^{-\frac{(2n+1)^2 \pi^2 T}{4}} \quad (1)$$

Corresponding values of  $U$  and  $T$  given by this equation have been plotted in Figs. 1 and 2.

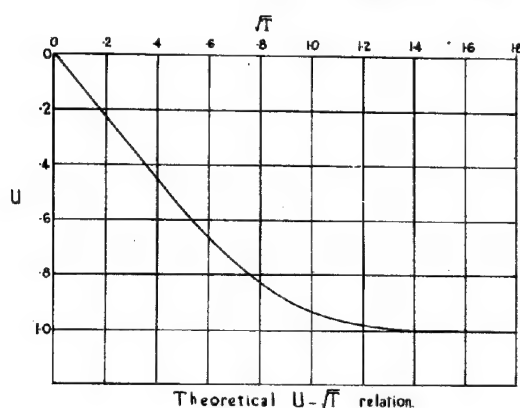


FIG. 1

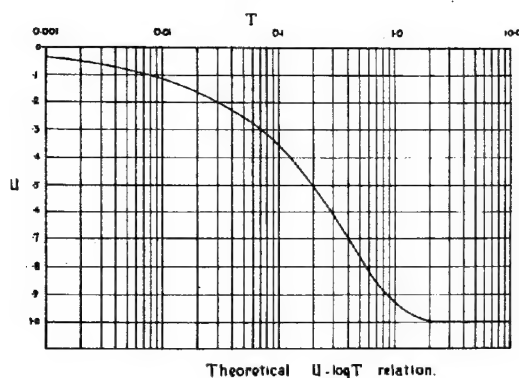


FIG. 2

In Fig. 1,  $U$  is plotted against  $\sqrt{T}$  and in Fig. 2 against  $\log T$ .

In order to fit the theoretical curve to the experimental results it is necessary to adjust the scales of the two axes.

$$\text{Now time factor } T = \frac{c_v t}{H^2}$$

$H$ , the half thickness of the sample, is known for any loading increment and hence it is necessary to determine  $c_v$ , the coefficient of consolidation.

$$U = \frac{\delta_1 - \delta}{\delta_1 - \delta_f} \quad (2)$$

Where  $\delta$  = experimental reading at any time  $t$

$\delta_i$  = theoretical initial dial reading (i.e. at  $t = 0$ )

$\delta_f$  = theoretical final dial reading (i.e. at  $t = \infty$ )

$\delta$  is given by the test readings and it is required to determine  $\delta_i$ ,  $\delta_f$  and  $c_v$ .

#### TAYLOR'S METHOD.

This curve fitting method makes use of a time curve in which dial readings are plotted against the square root of time. A typical test result is shown in Fig. 3. The similarity in shape between Figs. 1 and 3 is immediately

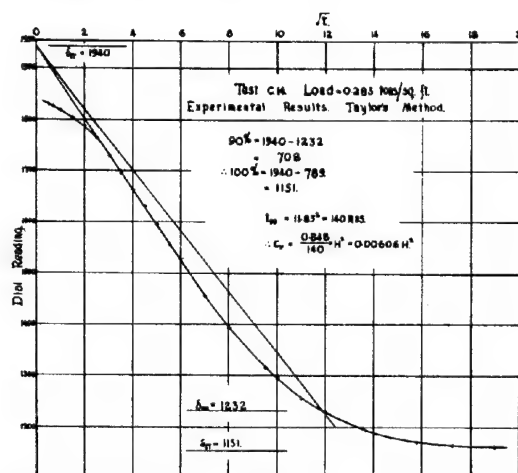


FIG. 3

evident. On the theoretical curve a straight line exists to beyond 50 per cent consolidation while at 90 per cent consolidation the abscissa is 1.154 times the abscissa of the straight line produced. The fitting method consists of drawing the straight line which best fits the first part of the curve and then a straight line which has abscissae 1.154 times those of the first line. The intersection of this line with the experimental curve is taken as 90 per cent consolidation. The intersection of the straight line with the dial reading axis gives the theoretical initial reading and hence the theoretical final reading can be calculated. The time value  $t_{90}$  of the 90 per cent consolidation point corresponds to the time factor at 90 per cent consolidation

$$T_{90} = \frac{c_v t_{90}}{H^2} = 0.848.$$

The coefficient of consolidation is therefore given by

$$c_v = \frac{0.848 H^2}{t_{90}}$$

#### CASAGRANDE'S METHOD.

Casagrande's method utilises a plot of dial readings against the logarithm of time. The results of Fig. 3 are plotted in Fig. 4 in this manner. A similarity in shape with Fig. 2 is again evident. The theoretical final reading is taken as the intersection of the tangent to the curve at the point of inflection with the final straight line produced backward. The theoretical initial reading is found from the fact that up to 50 per cent consolidation the  $U - T$  relation is approximately parabolic.



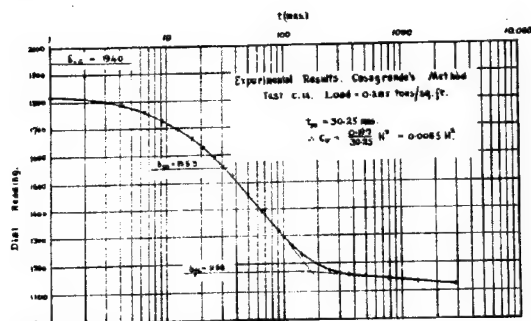


FIG. 4

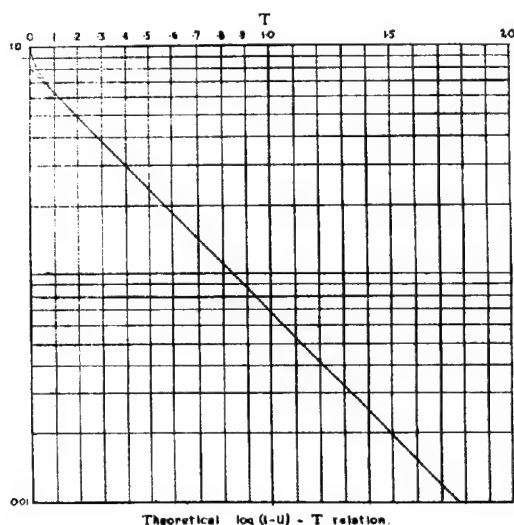


FIG. 5

It is obtained by marking off the differences in ordinates between any two points with times in the ratio 1 to 4, and laying off an equal distance above the upper point. Knowing the initial and final points the 50 per cent point can be located and the corresponding time value  $t_{50}$  noted.

$t_{50} = 0.197$  and hence the coefficient of consolidation is given by

$$C_v = \frac{0.197 H^2}{t_{50}}$$

For the results of Fig. 3 and 4, Taylor's final reading =  $\delta_{fr} = 1151$  and Casagrande's final reading =  $\delta_{fc} = 1166$ . The final reading after two days was 1122 so that at that time, the amount of secondary consolidation by Taylor's method was  $1151 - 1122 = 0.0029$  ins., and by Casagrande's method  $1166 - 1122 = 0.0044$  ins.

Due to the occurrence of initial consolidation in this test the initial part of the curve is not even approximately parabolic with the result that it is difficult to obtain a consistent initial reading by Casagrande's method. The coefficient of consolidation is from Taylor's method  $0.00606 H^2$  and from Casagrande's  $0.0065 H^2$ . Hence it may be stated that the final readings and the coefficients of consolidation obtained by the two methods differ widely. A weakness of Taylor's method lies in the fact that if an appreciable

amount of secondary consolidation has occurred at 90 per cent consolidation, then it will be in error.

#### NEW METHOD.

The new method of curve fitting is based on the fact that if equation 1 is plotted in the form logarithm of  $(1-U)$  against  $T$ , a straight line is obtained for all values of  $(1-U)$  less than 0.4. This is because the effect of the second and subsequent terms in the expansion for  $(1-U)$  may be neglected beyond this point. This is illustrated graphically in Fig. 5 where the straight line obtained by utilising the first term only (i.e.  $n = 0$ ) is compared with the correct theoretical curve.

Taking the first term of equation (1)

$$1-U = \frac{8}{\pi^2} e^{-\frac{\pi^2}{4} T}$$

$$\therefore \log(1-U) = \log \frac{8}{\pi^2} - \frac{\pi^2}{4} T$$

$$\text{Now } U = \frac{\delta_i - \delta}{\delta_i - \delta_f}$$

$$\therefore 1-U = \frac{\delta - \delta_f}{\delta_i - \delta_f}$$

Hence since  $t$  is proportional to  $T$ , if

$\log \left( \frac{\delta - \delta_f}{\delta_i - \delta_f} \right)$  is plotted against  $t$ , a straight

line should be obtained.

The effect of incorrect values of the initial and final reading on the shape of the curve can be investigated mathematically as follows.

Let  $\delta'_i$  = assumed incorrect initial reading

and  $\delta'_f$  = assumed incorrect final reading

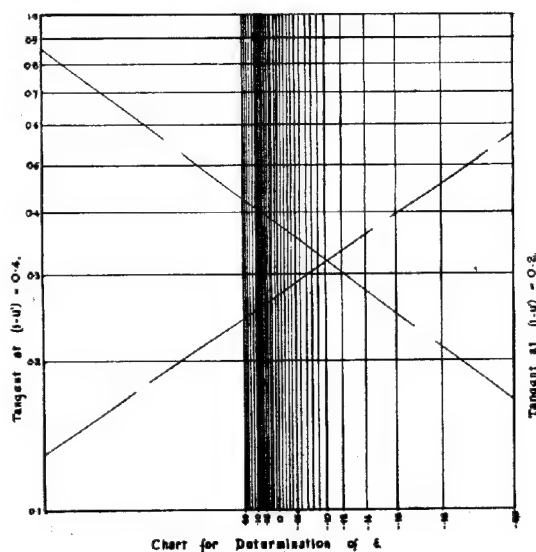


FIG. 6

$$\eta = \frac{\delta_i - \delta}{\delta_i - \delta_f} \quad \text{and} \quad \varepsilon = \frac{\delta_f' - \delta_f}{\delta_i' - \delta_f}$$

$$\therefore \delta_i' = \delta_i + \eta(\delta_i - \delta_f) \quad \text{and} \quad \delta_f' = \delta_f + \varepsilon(\delta_i - \delta_f)$$

Now the incorrect value of  $U' = \frac{\delta_i' - \delta}{\delta_i' - \delta_f'}$

$$\therefore \delta = \delta_i' - U'(\delta_i' - \delta_f')$$

$$= \delta_i - U(\delta_i - \delta_f) \quad \text{from equation (2)}$$

$$\therefore \delta_i - U(\delta_i - \delta_f) = \delta_i + \eta(\delta_i - \delta_f) - U'(\delta_i' - \delta_f')(1 + \eta - \varepsilon)$$

$$\therefore U + \eta = U'(1 + \eta - \varepsilon)$$

$$\therefore (1 - U')(1 + \eta - \varepsilon) = (1 - U) - \varepsilon \quad (3)$$

Let  $y = \log(1 - U)$  and  $y' = \log(1 - U')$

$$\therefore e^{y'}(1 + \eta - \varepsilon) = e^y - \varepsilon$$

$$\therefore e^{y'} \frac{dy'}{dt} (1 + \eta - \varepsilon) = e^y \frac{dy}{dt}$$

$$\therefore \frac{dy'}{dt} = \frac{dy}{dt} \left[ 1 + \frac{\varepsilon}{(1 + \eta - \varepsilon)e^{y'}} \right] \quad (4)$$

$$= \frac{dy}{dt} \left[ 1 + \frac{\varepsilon}{1 - U'} \right]$$

Hence the slope of the curve at any point is independent of  $\eta$ .  $\varepsilon$  cannot however be evaluated directly since  $\frac{dy}{dt}$  is unknown. If two points  $y'_1$  and  $y'_2$  are considered  $\frac{dy}{dt}$  may be eliminated and the error  $\varepsilon$  can be calculated from the equation

$$\frac{\left(\frac{dy'_1}{dt}\right)}{\left(\frac{dy'_2}{dt}\right)} = \frac{1 + \frac{\varepsilon}{1 - U'_1}}{1 + \frac{\varepsilon}{1 - U'_2}} \quad (5)$$

since  $\frac{dy}{dt}$  is constant.

Two widely separated points on the curve should be chosen e.g.  $(1 - U') = 0.4$  and  $0.2$ . It has already been explained that  $(1 - U') = 0.4$  represents the upper limit of straightness. Below  $(1 - U') = 0.2$  there may be vitiation of the results by the onset of secondary consolidation. Hence  $\varepsilon$  can be calculated from the ratio of the slopes of the tangents to the curve at these points.

Alternatively the calculation may be avoided and the value of  $\varepsilon$  read off directly by the construction of the nomogram in Fig. 6. In this, ordinates of the tangent at  $y' = 0.4$  corresponding to  $t = 0$  and some other convenient time are set off at the left hand side and the corresponding ordinates of the tangent at  $y' = 0.2$  are set off at the right hand side. The intersection of the diagonals drawn between these points then gives the value of  $\varepsilon$

on the bottom scale. The scale is graduated according to the equation

$$\alpha = \frac{0.4 + \varepsilon}{0.8 + 3\varepsilon}$$

where  $\alpha$  is the proportionate distance from the left hand side.  $\delta_f$  is then given by

$$\delta_f = \frac{\delta_i' - \varepsilon \delta_i}{1 - \varepsilon} = \frac{\delta_f' - \varepsilon \delta_i'}{1 - \varepsilon}$$

Using this value  $\log(1 - U')$ , which now contains only an error in  $\eta$ , can be calculated and replotted. The curve should now approximate to a straight line beyond  $(1 - U') = 0.4$ . If it is produced backwards the intercept on the  $y'$  axis is given by

$$\text{Intercept} = y' - \frac{dy'}{dt} t$$

$$= y' - \frac{dy'}{dt} t - \eta$$

$$= \log \frac{8}{\pi^2} - \eta$$

$$\therefore \eta = \log \frac{8}{\pi^2} - \text{Intercept}$$

This can be measured directly from the graph to a scale such that one cycle =  $\log_e 10 = 2.303$ .

Alternatively  $\eta$  can be obtained from Fig. 7 which represents the relation between  $\eta$  and intercept on the  $y'$  axis. This has been calculated using the relation

$$1 - U' = \frac{1 - U}{1 + \eta}$$

obtained from equation 3 by substituting  $\varepsilon = 0$

Having obtained  $\eta$ ,  $\delta_i = \frac{\delta_i' + \eta \delta_f'}{1 + \eta}$  can be calculated.

Having calculated the correct initial and final points and plotted the experimental results in the form  $\log(1 - U)$  against  $t$ , the time corresponding to a value of  $U = 0.8$  is measured. The coefficient of consolidation can then be obtained from the relation

$$c_v = \frac{T_{80} H^2}{t_{80}} = \frac{0.565 H^2}{t_{80}}$$

#### EXAMPLES BY NEW METHOD

The effect of incorrect initial and final readings is shown in Figs. 8 and 9. A set of results which follows Terzaghi's Theory exactly has been constructed from equation 1. They are given in columns 1, 2 and 3 of Table II. In Fig. 8, the results have been plotted using different assumed values for the final reading. As is shown by equation 4, if  $\delta_f$  is chosen too great a curve convex to the right is obtained, if  $\delta_f$  is too small a curve concave to the right is obtained, and only if  $\delta_f = \delta_f'$  does a straight line result. In Fig. 9, the results have been plotted assuming different initial values and it can be seen that a set of parallel straight lines is obtained. It should be noted that the correct final value can be determined by a process of trial and error, the assumed final value being adjusted until a straight line graph is obtain-

TABLE II

T	$\delta$	$\frac{\delta - \delta_f}{\delta_i - \delta_f}$	$\delta_i' = 190, \delta_f' = 90$		$\delta_i' = 190, \delta_f' = 99.3$		$\delta_i = 200, \delta_f = 99.9$	
			$\delta - \delta_f'$	$1 - u'$	$\delta - \delta_f'$	$1 - u'$	$\delta - \delta_f$	$1 - u$
0	200 <sup>+</sup>	1.00	100	1.00	90.7	1.000	100.1	1.000
0.008	190	0.90	100	1.00	90.7	1.000	90.1	0.900
0.017	185	0.85	95	0.95	85.7	0.945	85.1	0.850
0.031	180	0.80	90	0.90	80.7	0.890	80.1	0.800
0.049	175	0.75	85	0.85	75.7	0.835	75.1	0.750
0.072	170	0.70	80	0.80	70.7	0.780	70.1	0.700
0.097	165	0.65	75	0.75	65.7	0.724	65.1	0.650
0.126	160	0.60	70	0.70	60.7	0.670	60.1	0.600
0.159	155	0.55	65	0.65	55.7	0.614	55.1	0.550
0.195	150	0.50	60	0.60	50.7	0.559	50.1	0.500
0.238	145	0.45	55	0.55	45.7	0.504	45.1	0.451
0.287	140	0.40	50	0.50	40.7	0.449	40.1	0.401
0.342	135	0.35	45	0.45	35.7	0.394	35.1	0.351
0.405	130	0.30	40	0.40	30.7	0.338	30.1	0.301
0.475	125	0.25	35	0.35	25.7	0.284	25.1	0.251
0.565	120	0.20	30	0.30	20.7	0.228	20.1	0.201
0.684	115	0.15	25	0.25	15.7	0.173	15.1	0.151
0.848	110	0.10	20	0.20	10.7	0.118	10.1	0.101
1.000	106.9	0.069	16.9	0.169	7.6	0.084	7.0	0.070
1.127	105	0.05	15	0.15	5.7	0.0629	5.1	0.051
1.500	102	0.02	12	0.12	2.7	0.0298	2.1	0.021
$\infty$	100	0	10	0.10	0.7	0.0077	0.1	0.001

<sup>+</sup>This value is assumed to be 190 in Columns 4 and 5.

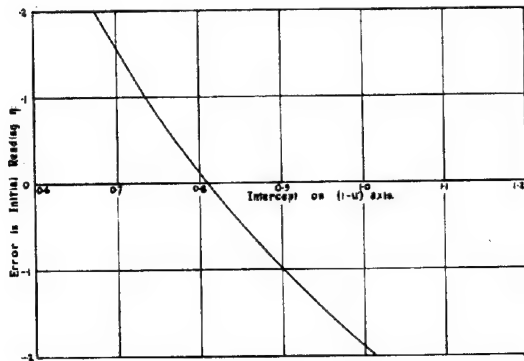
Chart for Determination of  $\eta$ 

FIG. 7

ed. The correct initial reading can then be scaled by the method described above.

The application of the method is illustrated by the results of Table II. Incorrect initial and final values have been assumed ( $\delta_i' = 190$  and  $\delta_f' = 90$ ) and  $\log(1-u')$  plotted against T in Fig. 10. Tangents have been drawn to the curve obtained at  $(1-u') = 0.2$  and  $0.4$ .

Let  $(1-u')_1'$  and  $(1-u')_2'$  be the intercepts of the tangents at T = 0 and T = 1.0. Then from the curve

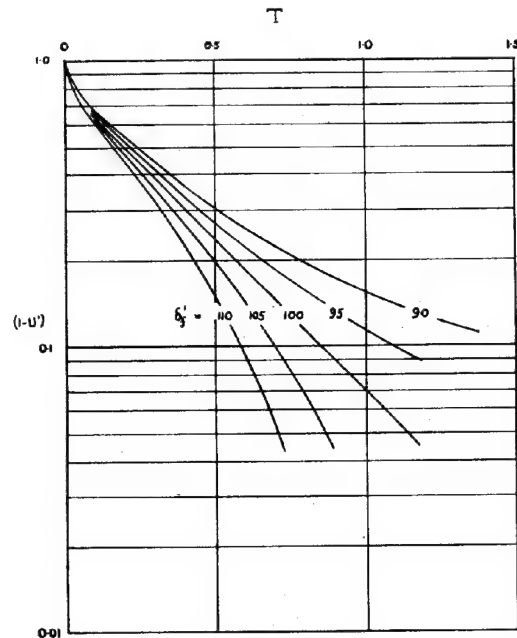
$$(1-u')_1' = 0.862 \text{ and } (1-u')_2' = 0.130$$

$$(1-u')_1 = 0.571 \text{ and } (1-u')_2 = 0.166$$

Referring to Fig. 6  $\epsilon = -0.103$

$$\therefore \delta_f = \frac{90 + 0.103 \times 190}{1.103} = 99.3$$

Using this value of  $\delta_f$ , a new set of values of  $(1-u')$  is calculated and plotted. It



Theoretical Curve. Effect of Incorrect Final Values.

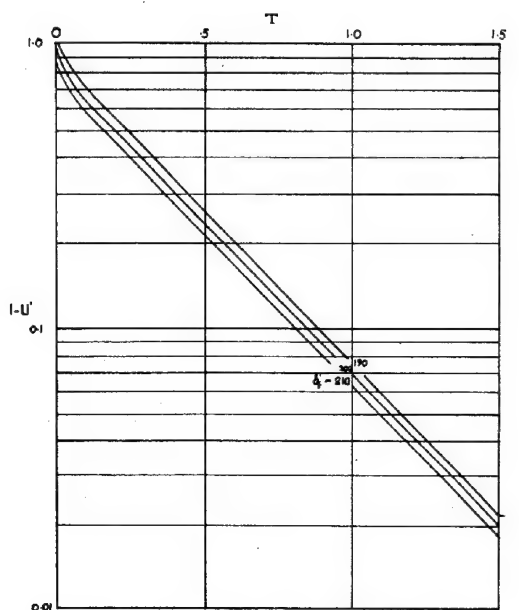
FIG. 8

is seen that the resulting curve is almost straight. Producing it backwards the intercept on the  $u'$  axis is found to be 0.899. Referring now to Fig. 7, this gives  $\eta = -0.099$  and therefore

$$\delta_i = \frac{190 - 0.099 \times 99.2}{1 - 0.099} = 200.0$$

TABLE III

Time (mns)	Dial Reading	$\delta_i = 1930, \delta_f = 1130$		$\delta_i = 1930, \delta_f = 1161$		$\delta_i = 1952$ $\delta_f = 1161$	
		$\partial - \partial_f$	$1 - U'$	$\partial - \partial_f$	$1 - U'$	$1 - U$	
0	(1930)	800	1.000	769	1.000	1.000	
$\frac{1}{2}$	1830	700	0.875	669	0.870	0.846	
$\frac{1}{4}$	1826	696	0.870	665	0.865	0.841	
1	1820	690	0.862	659	0.857	0.833	
$2\frac{1}{4}$	1805	675	0.844	644	0.838	0.815	
4	1788	658	0.822	627	0.816	0.793	
$6\frac{1}{4}$	1761	631	0.789	600	0.780	0.759	
9	1729	599	0.749	568	0.739	0.717	
$12\frac{1}{4}$	1695	565	0.706	534	0.695	0.675	
16	1661	531	0.664	500	0.650	0.632	
$20\frac{1}{4}$	1630	500	0.625	469	0.610	0.593	
25	1594	464	0.580	433	0.564	0.548	
$30\frac{1}{4}$	1555	425	0.531	394	0.512	0.498	
36	1528	398	0.498	367	0.477	0.464	
49	1454	324	0.405	293	0.381	0.370	
64	1392	262	0.327	231	0.300	0.292	
91	1313	183	0.229	152	0.198	0.192	
100	1293	163	0.204	132	0.171	0.167	
121	1255	125	0.156	94	0.122	0.119	
144	1228	98	0.1225	67	0.087	0.085	
250	1169	39	0.049	8	0.010	0.010	
300	1163	33	0.041	2	0.003	0.003	



Theoretical Curve. Effect of Incorrect Initial Values.

FIG. 9

It will be noted that there is an error of 0.7 in  $\delta_f$ . This is a second order effect due to the approximations made in the theory and the abnormally high value of  $\epsilon$  assumed. In practice there is no difficulty in selecting an assumed value for  $\delta_f$  which will be much less than 10 per cent in error. However if in any case greater accuracy is considered desirable there is no difficulty in carrying out a second approximation. To do this in the example under consideration it

will be noted that the error in  $\delta_f$  only caused a deviation from the straight at low values of  $1-U'$ . To rectify this new curve it is only necessary to draw the tangent at  $(1-U') = 0.2$  as the tangent at  $(1-U') = 0.4$  is indistinguishable from the straight line already drawn. The new intercepts are now

$$(1-U')_4^0 = 0.899 \quad \text{and} \quad (1-U')_4^{\infty} = 0.080$$

$$(1-U')_2^0 = 0.880 \quad \text{and} \quad (1-U')_2^{\infty} = 0.081$$

From Fig. 6  $\epsilon = -0.0055$

$$\therefore \delta_f = \frac{99.3 + 0.0055 \times 200}{1.0055} = 99.9$$

With the experimental results of Table III (Figs. 3 and 4), initial and final values of 1930 and 1130 respectively have been assumed. In this case the following results were obtained (Fig. 11)

$$(1-U')_4^0 = 0.817 \quad \text{and} \quad (1-U')_4^{\infty} = 0.196$$

$$(1-U')_2^0 = 0.724 \quad \text{and} \quad (1-U')_2^{\infty} = 0.204$$

Plotting on the nomogram (Fig. 6) or by calculation gives  $\epsilon = -0.041$ .

$$\text{whence} \quad \delta_f = \frac{1130 + 0.041 \times 1930}{1.041} = 1161$$

Plotting the rectified values of  $(1-U')$ , the intercept on the axis of the straight line produces is 0.834 which gives  $\eta = -0.028$

$$\text{then} \quad \delta_i = \frac{1930 - 0.028 \times 1161}{0.972} = 1952$$

Using these corrected figures  $\log(1-U)$  has been plotted against  $t$  in Fig. 11. To find the coefficient of consolidation, the time corresponding to  $U = 0.8$  is  $t_{80} = 88.5$  mns. and therefore

$$c_v = \frac{0.565 H^2}{t_{80}} = 0.00638 H^2$$

The close fit between the theoretical curve obtained using these values of  $\delta_i$ ,  $\delta_f$  and  $c_v$ , and the plot of the experimental results is shown in Fig. 12.

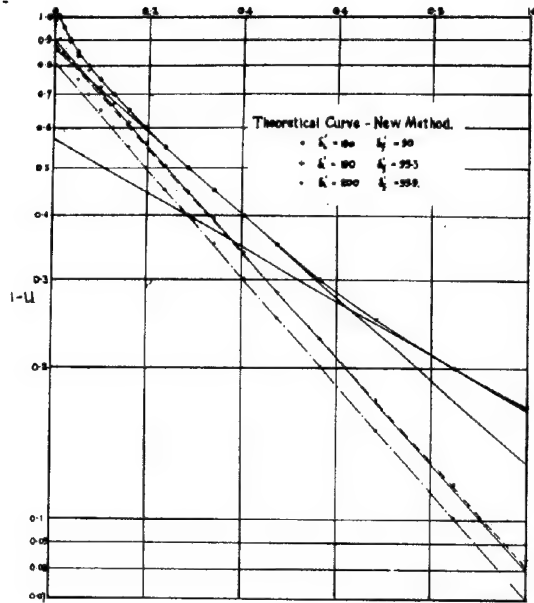


FIG. 10

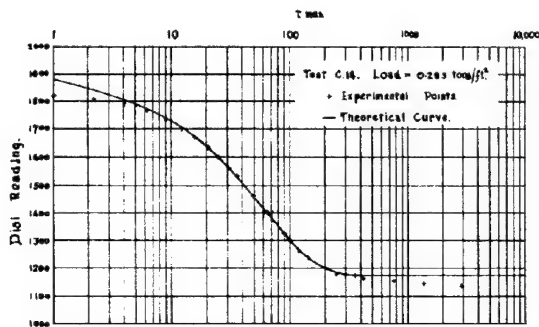


FIG. 12

#### COMPARISON OF METHODS.

In Casagrande's method the determination of the theoretical initial reading is vitiated by any Initial consolidation present. Taylor's method avoids this difficulty but is open to

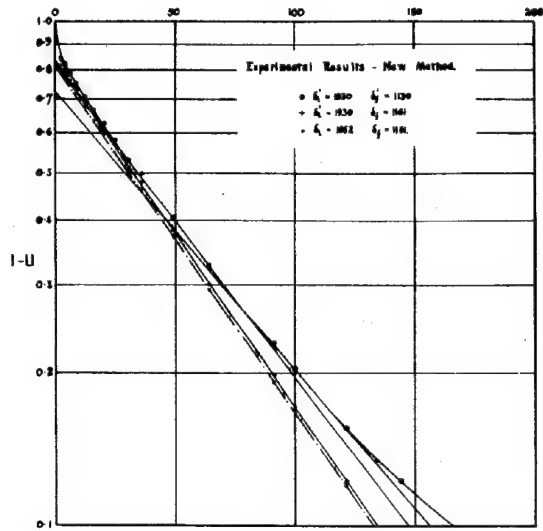


FIG. 11

the criticism that a parabolic relation can only be assumed for the early part of the curve. The new method fits a straight line to the range of readings  $U = 60\%$  to  $80\%$ , where there is every reason to believe that both Initial and Secondary consolidation are quite negligible.

The theoretical final reading of Casagrande is purely conventional as the slope of his curve at the point of inflection and the shape of the secondary consolidation curve (which is not always a straight line) cannot be related theoretically to the end point of Primary Consolidation. Taylor's determination assumes that Secondary consolidation has not commenced at all at  $U = 90\%$  and its accuracy depends on the accuracy of the single reading closest to this point. The new method would permit of Secondary consolidation commencing at  $U = 80\%$  and the final value is based on a range of readings.

#### REFERENCES.

- 1) Taylor. Research on Consolidation of Clays.
- 2) Terzaghi and Fröhlich. Theorie du Tassement des Couches Argileuses.

1 d 3

## THE MATHEMATICAL SOLUTION FOR THE EARLY STAGES OF CONSOLIDATION

E.N. FOX, Ph.D.

Department of Scientific and Industrial Research  
Building Research station

We consider the standard consolidation problem of a clay layer of thickness  $h$  with one impermeable face and one free drainage face, subjected to a pressure  $q_0$  uniform throughout the thickness applied at zero time. Using the further notation

$t$  = time  
 $z$  = distance from free drainage face  
 $w(z, t)$  = excess hydrostatic pressure  
 $c$  = coefficient of consolidation  
 $T = ct/h^2$   
 $\mu_v$  = coefficient of volume decrease  
 we have the well known Fourier solution.  $x$ ) (reference 1, page 105)

$$w(z, t) = \frac{4}{\pi} q_0 \sum_{m=1}^{\infty} \frac{1}{(2m-1)^2} e^{-(2m-1)^2 \pi^2 T / 4} \sin \frac{(2m-1)\pi z}{2h} \quad (1)$$

which leads to the corresponding form

$$\mu = 1 - \frac{8}{\pi^2} \sum_{m=1}^{\infty} \frac{1}{(2m-1)^2} e^{-(2m-1)^2 \pi^2 T / 4} \quad (2)$$

for the degree of consolidation  $\mu$ .

This solution for  $\mu$  is not very suitable for small values of  $T$ , when the series is slowly convergent, but it was early recognised that the initial form is parabolic and on an approximate theory, Fröhlich (reference 1, page 48) gives the relation

$$\mu = 2\sqrt{\frac{T}{3}} \quad , \quad 0 \leq T \leq \frac{1}{12} \quad (3)$$

for the early stages.

When this problem was first brought to the notice of the present writer in 1938, it was realised that the precise parabolic form of equation (1) for small  $T$  could be investigated by use of the operational calculus as applied by Jeffreys (reference 3, Chapter 5) to problems in the conduction of heat, which are analogous mathematically to those in the consolidation of clays.

Using this method (see for example, references 3) and 4) we can obtain in addition to the Fourier form (1) an alternative form of solution, namely

$$w(z, t) = q_0 - q_0 \sum_{n=0}^{\infty} (-1)^n \left[ 2 - \operatorname{erf} \left( \frac{2nh+Z}{2h\sqrt{T}} \right) - \operatorname{erf} \left( \frac{2nh+2h-Z}{2h\sqrt{T}} \right) \right] \quad (4)$$

where  $\operatorname{erf}$  denotes the error function defined by

$$\operatorname{erf} x = \frac{2}{\sqrt{\pi}} \int_0^x e^{-u^2} du \quad (5)$$

and tabulated, for example, in references 3 and 5.

From (4) we obtain, as an alternative to (2), the expression

$$\mu = 2\sqrt{\frac{T}{\pi}} - 4\sqrt{T} \sum_{n=1}^{\infty} (-1)^{n-1} \phi_1 \left( \frac{n}{\sqrt{T}} \right) \quad (6)$$

where  $\phi_1$ , as tabulated in reference 3,  $x_a$  is defined by

$$\phi_1(x) = \int_x^{\infty} (1 - \operatorname{erf} u) du \quad (7)$$

For small values of  $T$ , however, the series part of (6) is extremely small, indic-

ating that the parabolic relation  $\mu = 2\sqrt{\frac{T}{\pi}}$  (8)

holds in the early stages to a high degree of accuracy, as quoted by Cooling and Skempton (reference 5, page 388) from the author's work and later by Terzaghi (reference 2, page 284) with source unstated.

If we denote the error (to be subtracted) in using equation (8) by  $R$ , then from (6) we have

$$\mu = 2\sqrt{\frac{T}{\pi}} - R \quad (9)$$

$$\text{where } R = 4\sqrt{T} \sum_{n=1}^{\infty} (-1)^{n-1} \phi_1 \left( \frac{n}{\sqrt{T}} \right)$$

But since  $\operatorname{erf} x \leq 1$ , we see from (7) that  $\phi_1$  is a positive function which decreases as  $x$  increases. Hence in (9), the successive terms are alternately positive and negative and decreasing in absolute magnitude. Hence  $R$  will be positive and less than the sum of the positive terms, namely

$$R < 4\sqrt{T} \sum_{n=1}^{\infty} \phi_1 \left( \frac{n}{\sqrt{T}} \right) \quad (10)$$

Now from (5) and (7), it is easily shown by integration by parts that

$$\phi_1(x) = \frac{e^{-x^2}}{2\sqrt{\pi}x^2} - \frac{3x}{2\sqrt{\pi}} \int_x^{\infty} \frac{e^{-u^2} du}{u^4} < \frac{e^{-x^2}}{2\sqrt{\pi}x^2} \quad (11)$$

Hence from (10),

$$R < 4\sqrt{T} \sum_{n=1}^{\infty} \frac{T e^{-n^2/T}}{2\sqrt{\pi} n^2} \quad (12)$$

and if we replace the exponential factor in each term by its greatest value for  $n = 1$  and use the known relation

$$\sum_{n=1}^{\infty} \frac{1}{n^2} = \frac{\pi^2}{6} \quad (13)$$

we obtain the inequality

$$R < \frac{1}{4} \pi^{\frac{3}{2}} T^{\frac{3}{2}} e^{-\frac{1}{T}} \quad (14)$$

Using this equation we obtain the second column in Table 1 below, which indicates the extreme accuracy with which the parabolic form (8) represents the theoretical solution for small values of  $T$ .

Now we can write (2) in the form

$$\mu = 1 - \frac{8}{\pi^2} e^{-\pi^2 T / 4} - R_1 \quad (15)$$

Where  $R_1$  will be negligible for medium and large  $T$ . Using (13), it is in fact easily

x.) In reference 2, page 274, equation (I) is misquoted as applying when  $z$  is measured from the impermeable surface.

xa) It is also tabulated in reference 4 under the notation "ierfc  $x$ "

seen that

$$R_1 < \left(1 - \frac{8}{\pi^2}\right) e^{-\frac{8\pi^2 T}{4}} \quad (46)$$

which gives the third column of Table 1.

TABLE 1

T	R <	R <sub>1</sub> <
0.1	$2.0 \times 10^{-6}$	$2.1 \times 10^{-2}$
0.2	$8.4 \times 10^{-4}$	$2.2 \times 10^{-3}$
0.3	$8.2 \times 10^{-3}$	$2.4 \times 10^{-4}$

By virtue of this Table we can write

$$\left. \begin{aligned} \mu &= 2\sqrt{\frac{T}{\pi}} \quad , \quad 0 \leq T \leq 0.2 \\ \mu &= 1 - \frac{8}{\pi^2} e^{-\frac{8\pi^2 T}{4}} \quad , \quad T > 0.2 \end{aligned} \right\} \quad (47)$$

as a simple composite solution correct to errors of 0.002 or less in  $\mu$ . When  $T = 0.2$ ,  $\mu = 0.504$  and since the order of error is relatively unaffected by a small alteration of  $\mu$  or  $T$ , we can equally take  $\mu = 0.5$  as a convenient change-over point.

For less than 50 per cent consolidation, the parabolic form (8) is accurate to an absolute error of less than 0.001 (or a fractional error of less than 1/500th) in  $\mu$  and a plot of  $\mu$  against  $\sqrt{t}$  will be correspondingly linear. On this basis Cooling and Skempton (reference 5) have used (8) to estimate the coefficient of consolidation from the initial portion of experimental consolidation - root time curves.

It is perhaps worth noting that equation (8) corresponds to a total settlement

$$\rho = m_v q_0 h \mu = \frac{2}{\sqrt{\pi}} m_v q_0 \sqrt{ct} \quad (48)$$

-o-o-o-o-o-

which is independent of  $d$ , and is in fact the exact theoretical total settlement for a layer of infinite depth. The high accuracy of the parabolic form for a finite layer thus implies physically that for  $T \leq 0.2$ , i.e.  $t < h^2/5c$ , the layer behaves as one of infinite depth so far as total settlement is concerned. Conversely, we can say that to the same high accuracy for any given time, all layers of thickness  $h > 5\sqrt{ct}$  will have the same total settlement. The present note has been written to indicate the derivation of the parabolic form (8) and in particular to give numerical estimates of the error involved in its use. Apart from this, it may be noted that the operational calculus can equally be applied to other consolidation problems to give alternative forms of solution which together will generally enable the theoretical consolidation-time curve to be evaluated with small numerical effort.

#### ACKNOWLEDGMENT.

The work described in the paper was carried out at the Building Research Station of the Department of Scientific and Industrial Research, and the results are published by permission of the Director of Building Research.

#### REFERENCES.

- 1) K.v. Terzaghi and O.K. Fröhlich, (1936) "Theorie der Setzung von Tonschichten", Vienna, F. Deuticke.
- 2) K.v. Terzaghi, (1943) "Theoretical Soil Mechanics", New York, John Wiley and Sons.
- 3) H. Jeffreys, (1931) "Operational Methods in Mathematical Physics", Cambridge Tracts in Mathematics and Mathematical Physics, No.23.
- 4) H.S. Carslaw and J.C. Jaeger, (1947) "Conduction of Heat in Solids", Oxford, Clarendon Press.
- 5) L.F. Cooling and A.W. Skempton, (1941) "Some Experiments on the Consolidation of Clay", Journ.Inst.Civ.Eng. No.7, June, 1941.

1 d 4

#### ON THE COMPRESSIBILITY OF PRECONSOLIDATED SOIL-LAYERS

R. HAEFELI

Laboratory for Hydraulic Research and Soil Mechanics  
of the Swiss Federal Institute of Technology, Zurich

#### I. DEFINITION OF THE PROBLEM.

The formation of a proper judgement as to the possibility of consolidation of the subsoil is the main problem of settlement predictions, both qualitatively and quantitatively. It is therefore desirable to obtain a better idea of the essence of the compacting process, and an endeavour has been made to do this by means of a simple model, which may serve as extension to the model investigations carried out by von Terzaghi 1) 2). In addition to that, in the regions affected by the last ice-age, the difference between the soils once loaded by glaciers, i.e. preconsolidated ground, and the fresh deposits made after the ice age, with regard to their compressibility is particularly great. It is therefore necessary to form a clear idea of the influence of

the preconsolidation load on a soil. In connection with this, from the point of view of soil mechanics among the questions arising, the three following ones are of fundamental importance:

- 1) How does the magnitude of the preconsolidation load affect the compressibility of a loose sediment slowly relieved to a given pressure?
- 2) How does the magnitude of the relieved load affect the compressibility of a loose sediment for a given preconsolidation load?
- 3) What conclusions can be drawn from the replies to questions (1) and (2) with respect to the judgement of "undisturbed samples" and how consolidating tests must be arranged and evaluated in order to obtain a perfect basis for settlement analysis?

Before replying to these questions some fundamental conceptions have to be explained, and the results of certain series of investigations discussed.

## II. THEORETICAL CONSIDERATIONS.

If a saturated loose sediment, prevented from extending laterally, is subjected to a load increasing by steps (oedometer test), the specific settlement may be represented as a function of the natural logarithm of the pressure with sufficient accuracy by a straight line (straight line of settlement), of the form 3):

$$\Delta_i = \Delta_e \ln \lambda_i \quad (1)$$

where x):

$\Delta_i$  = primary specific settlement =  $\frac{h_i - h_f}{h_i}$   
(cf. Fig 1)

$\Delta_e$  = coefficient of compressibility

$\lambda_i$  = loading index =  $\frac{\sigma_i}{\sigma_1}$ , where  $\sigma_1 = 1 \text{ kg/cm}^2$ .

The coefficient of compressibility  $\Delta_e$  is consequently that specific settlement which the sample experiences by increasing the compacting pressure from  $\sigma = 1$  to  $\sigma = e = 2,72 \text{ kg/cm}^2$ . As is known, for a given material no definite relation exists between the specific settlement and the consolidating pressure, since a different settlement straight line is obtained for each initial water content. Therefore it holds good that, with increasing initial water content, also the inclination of the corresponding settlement straight line becomes greater until a certain limiting value is reached. This limiting value is obtained when the water content is chosen equal to the Atterberg flow limit. According to that, also  $\Delta_e$  is not to be regarded as a material constant, but as a constitutional magnitude whose value also increases with increasing initial water content.

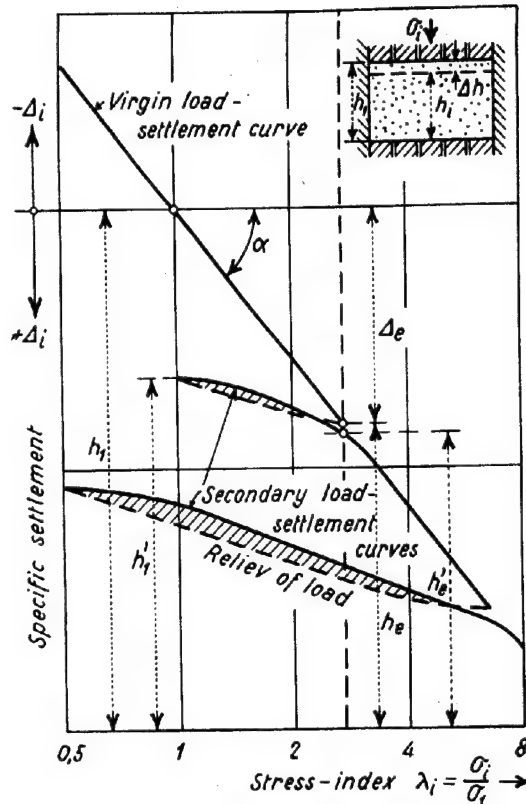
If the latter is chosen equal to the Atterberg flow limit, a maximum  $\Delta_e$  value is obtained, which is best suited for comparing the compressibility of different loose sediments 5).

If the behaviour of the plastic loose sediment is to be compared with that of elastic solid stone or other material, it will be found suitable to characterise the compressibility of the loose sediment by a magnitude corresponding to the modulus of elasticity, this magnitude being obtained as follows by drawing tangents to the settlement curve:

$$\frac{d\Delta_i}{d\lambda} = \Delta_e \frac{1}{\lambda_i} = \Delta_e \frac{\sigma_1}{\sigma_i} = \frac{\sigma_1}{\frac{\sigma_i}{\Delta_e}} = \frac{\sigma_1}{M_E} \quad (2)$$

$$M_E = \frac{\sigma_1}{\Delta_e}$$

This equation shows the well-known fact



Specific settlement as a function of stress (load-settlement curves)

FIG. 1

that the modulus of plasticity  $M_E$ , which is expressed in the same units as the modulus of elasticity  $E$ , is directly proportional to the compacting pressure  $\sigma_1$  and indirectly proportional to the coefficient of compressibility  $\Delta_e$  of the loose sediment in question. In order to compare the different kinds of soils on one common basis, we select as consolidating pressure  $\sigma_1 = 1 \text{ kg/cm}^2$  and form the corresponding modulus of plasticity:

$$M_E = \frac{\sigma_1}{\Delta_e} ; \sigma_1 = 1 \text{ kg/cm}^2 \quad (3)$$

The two coefficients  $\Delta_e$  and  $M_E$  of the different kinds of soil are in reciprocal relation to each other and vary approximately between the limits given in table 1:

TABEL 1

Type of soil	$\Delta_e$ in%	$M_E$ in $\text{kg/cm}^2$
Peat	10 - 30	10 - 3
Clay	5 - 15	20 - 7
Loam	2 - 10	50 - 10
Muddy sand	1 - 5	200 - 20
Sand	0,5 - 2	200 - 50
Gravel sand	0,4 - 1,5	250 - 70
Molasse marl	0,02 - 0,5	5000 - 200

x) This fundamental law was discovered in the Institute for Hydraulic Research in 1934 absolutely independent of the classic investigations of Terzaghi on the pressure void ratio diagram, thus confirming the latter 2) and 3)



If then a material compacted under any desired pressure  $\sigma_1 > e$ , with admission of wa is gradually relieved and then loaded again is known that the hysteresis loop illustrated in Fig. 1 is obtained, the rising branch of which is designated as swelling curve and the descending branch as reloading curve or curve of secondary setting, or consolidation. In manner analogous to the primary consolidation being characterised by the  $\Delta_e$ -value, the behaviour of the material when relieved and reloaded can be characterised by the following two magnitudes which may be calculated from the two branches of the hysteresis loop (cf. Fig. 1):

$$\Delta_e' = \frac{h_i' - h_e'}{h_i'} \quad \text{= secondary coefficient of compressibility} \quad (4)$$

$$\Delta_e'' = \frac{h_i'' - h_e''}{h_i''} \quad \text{= swelling coefficient.}$$

In order to standardise also this test, and thereby make it possible to compare the different materials, the consolidating and relieving pressures which bound the hysteresis loop were chosen by us not arbitrarily but uniformly, namely  $\sigma_1 = e$  and  $1 \text{ kg/cm}^2$  respectively. From this standard test also the modulus of plasticity can be derived for the relieved loading and the reloading. But since the law of the logarithmic straight lines for the two branches of the hysteresis loop is only partly complied with, to determine  $M_E'$  we use not the tangents to the corresponding curves but the chords between the points of the specific settlement  $\sigma_1$  and  $\sigma_1 = e \text{ kg/cm}^2$ . From this we have the corresponding moduli of plasticity:

$$M_E' = \frac{e-1}{\Delta_e'} \sigma_1 = \frac{1,72}{\Delta_e'} \sigma_1 \quad (5)$$

for reloading

$$M_E'' = \frac{e-1}{\Delta_e''} \sigma_1 = \frac{1,72}{\Delta_e''} \sigma_1 \quad \text{for relieving}$$

Since the  $\Delta_e'$  and  $\Delta_e''$  values are only a relatively small fraction of the  $\Delta_e$  values (about 1/3 to 1/10, depending on the kind of material), the  $M_E'$  and  $M_E''$  values become as a rule a multiple of the modulus of plasticity  $M_E$  of the primary consolidation. This accounts for the considerable influence of preconsolidation load on the magnitude of the settlement.

As an example, the coefficients of the plastic behaviour spoken of are brought together in table 2 for the loose sediment used in the following investigations:

separate grains are not directly in contact, the transmission of force from grain to grain takes place mainly through the film lying between them, this film corresponding to the molecularly combined water of the loose sediment. For this film there is a certain critical compressive stress  $\sigma_k$  (boundary loading) and when it is exceeded, the material yields laterally. If our system is loaded, the closest force-transmitting surfaces  $f$  must accordingly be formed in such a way that the boundary loading  $\sigma_k$  is just reached in them. If the external loading is increased, a fresh equilibrium can only be established by the grains moving together, thus giving rise to a corresponding increase in the contact surfaces  $f$  (compare Fig. 2, top). The volume of the plastic inter-

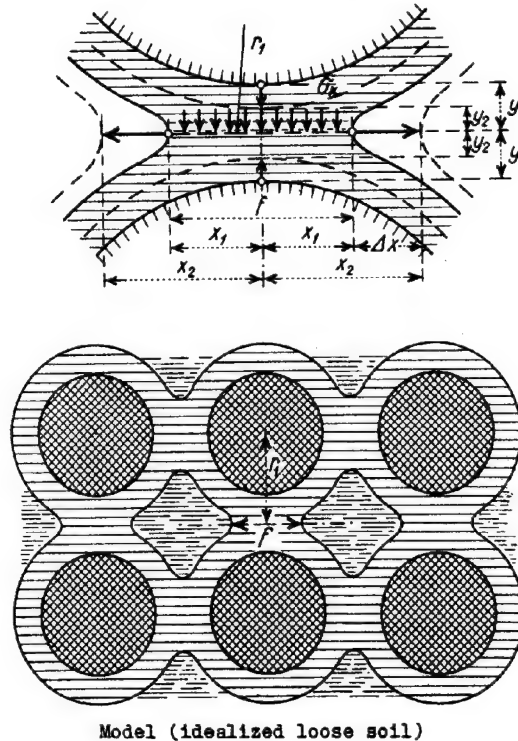


FIG. 2

TABLE 2  
Coefficients of compressibility and moduli of plasticity.

Material	$\Delta_e$ %	$\Delta_e'$ %	$\Delta_e''$ %	$M_{E1}$ $\text{kg/cm}^2$	$M_E'$ $\text{kg/cm}^2$	$M_E''$ $\text{kg/cm}^2$
Brick clay 1632	9,12	1,40	1,23	11	123	140
Loam No. 2101	5,08	0,52	0,38	20	331	453

After that an endeavour shall be made to explain the fundamental law of primary consolidation (equation 1) with the help of an imaginary model, without taking into consideration the influence of time which will be included later 4). This model consists of separate grains which, as shown in Fig. 2, are surrounded by a tough, plastic film. Since the

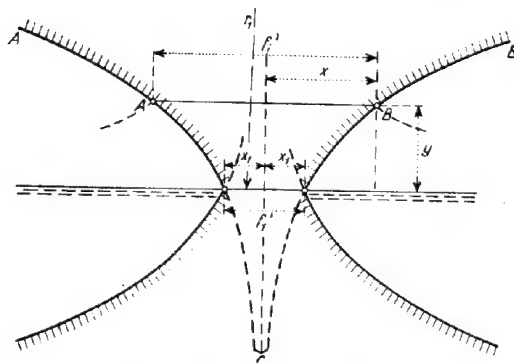
mediate substance then remains practically unchanged. Since the contact surface increases proportionally to the external pressure, the decrease in distance between two grains with the same increase in pressure will always be smaller the greater the consolidating pressure. Our model must therefore have a compressibility decreasing with the pressure, i.e. an in-

creasing modulus of plasticity, as is the case with loose sediment or with snow.

In order to pass over from purely qualitative considerations to analysis, we designate with  $f_i$  the sum of the contact surfaces per unit of surface for the consolidation pressure  $\sigma_i = 1 \text{ kg/cm}^2$ , and with  $f_i'$  the corresponding sum for  $\sigma_i' = \sigma_i$ . Then according to the above,  $f_i$  must be proportional to the compacting pressure, i.e.

$$\frac{f_i'}{f_i} = \frac{\sigma_i'}{\sigma_i} = \lambda_i \quad (6)$$

For the contact zone (meridian section) illustrated idealized in Fig. 3, the contact sur-



Contact zone of two separate particles of the model.

FIG. 3

face  $f_i'$  has been established under the compacting pressure  $\sigma_i$ , whilst half the distance between the centre points of the grains amounts to  $r_i$ . If the external pressure is increased, the two grains approach each other by the amount  $2y$ , whilst the contact surface of  $f_i'$  increases to  $f_i'$ . We assume that the ratio of  $f_i'$  to  $f_i$  increases with  $y$  according to an exponential function of the form:

$$\frac{f_i'}{f_i} = e^{\beta(\frac{y}{r_i})} = \lambda_i \quad (7)$$

For reasons of similarity it also follows:

$$\frac{y}{r_i} = \frac{\Delta h}{h_i} = \Delta_i \quad \text{and consequently:} \quad (8)$$

$$\frac{f_i'}{f_i} = e^{\beta \Delta_i} = \lambda_i \quad \text{according to equation 6.}$$

By taking logarithms, from equation(8) we obtain finally:

$$\left. \begin{aligned} \Delta_i &= \frac{1}{\beta} \ln \lambda_i \\ &= \Delta_e \ln \lambda_i \end{aligned} \right\} \beta = \frac{1}{\Delta_e} = M_{E_i} \quad \text{q.e.d.} \quad (9)$$

Equation(9) is identical with equation 1). The exponential function chosen for the ratio  $f_i' : f_i$  consequently leads to the known logarithmic law of primary settlement. The equation of the curves illustrated in Fig. 3 is accordingly as follows:

$$\frac{x}{x_i} = \sqrt{\frac{f_i}{f_i'}} = \sqrt{\frac{1}{e^{\beta(\frac{y}{r_i})}}} = \sqrt{\frac{1}{e^{\Delta_i}}} = \sqrt{e^{-\ln \lambda_i}} = \sqrt{\lambda_i} \quad (10)$$

If one had to deal not with plastic masses, but with the transmission of pressure between two solid bodies, whose form would correspond to the symmetrical solids of revolution according to Fig. 3 and whose compressive strength amounts to  $\sigma_k$ , the compressibility of the system would also have to be expressible by equation(1). The considered model may therefore be transmitted also to sand, whose behaviour - except of time effect - differs only slightly from that of loams and clays, although the solid bodies to a large extent are in direct contact with each other. On the other hand, if a metal point is constructed of the shape ABC and, as in the cone test, pressed under different loadings into a horizontally bounded material consisting of loam or clay with a given flow limit, penetration and pressure must also depend on each other as formulated in equation(1), only with the difference that, instead of  $\sigma$  the pressure P has to be substituted. Such penetrations will also occur when materials of mixed grains are pressed together (for instance moraine), and the pressure of sharp-sided grains is transmitted to fine clay laminas packed with liquid films.

### III. ARRANGEMENT AND RESULTS OF THE TESTS.

#### a) Test arrangement.

Corresponding to the questions 1) and 2) posed in the definition of the problem, two test groups were to be distinguished from the start, namely a group I with variable preconsolidation load (preloading) and constant relieving loading, and a group II in which on the contrary the preloading is kept constant but the relieving loading is varied. In the third test group (III) the preloading as well as the relieving loading was varied, and in such a way that the latter always amounted to one half of the former. These three groups of tests were further subdivided as shown in table 3:

TABLE 3

Summary of the conditions of the tests

Group	Designation	Material No.	Preconsolidation load $\sigma_r$ in kg/cm <sup>2</sup>	Relieving load $\sigma_u$ in kg/cm <sup>2</sup>
I	I a	1632	0,25-0,5-1-e-4-8-16	0,04
	I b	1632	4-6-10-12-14-16	1,00
II	II a	1632	$e = 2,72$	1,0-0,5-0,25-0,125-0,04
	II b	2101	16	8-4-1-0,5-0,25-0,04
III	III	2101	0,5-1-2-4-8-16	0,25-0,5-1-2-4-8

For the tests Ia, Ib and IIa the number of samples had to be the same as the number of loading combinations. Tests No. IIb and III on the other hand were carried out each on one sample by cyclic alteration of load in one single testing operation. The duration of one load increment amounted normally to 24 hours. The influence of the duration of loading was only

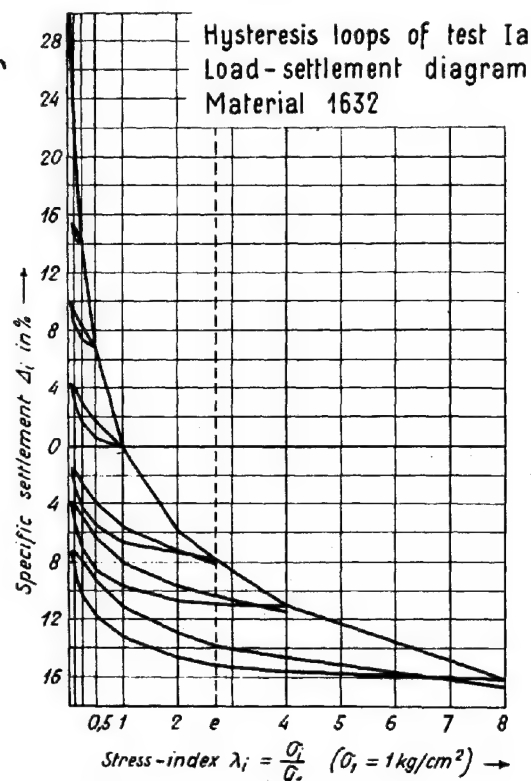
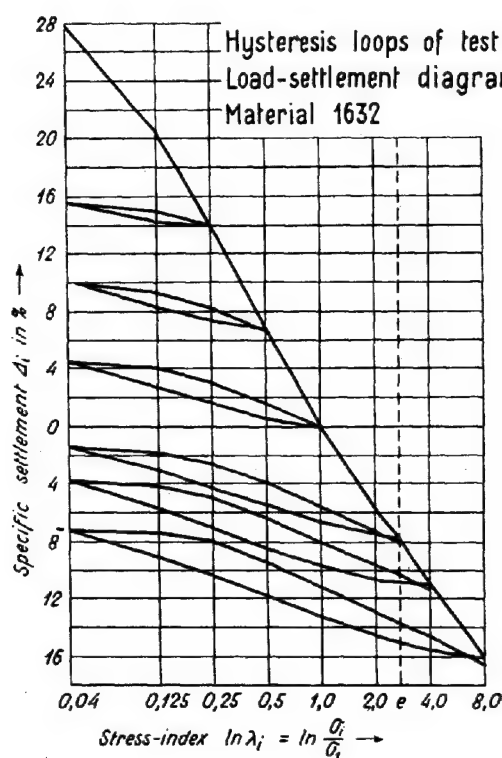
more closely investigated during test IIb.

The apparatus used was the oedometer known from publications, with a cross-sectional area of 25 cm<sup>2</sup> and taking samples 2 cm high.

6) The most important properties of the materials used for the tests are summarised in table 4.

TABLE 4  
Characteristics of the test materials.

Property	1632	2101
Flow limit (Ateerberg) $f$ in %	55,7	32,6
Plastic limit $a$ in %	22,9	17,9
Coefficient of plasticity $p = f - a$ in %	32,8	14,7
Coefficient of compression $\Delta_e$ in % (disturbed)	9,12	5,08
Coefficient of permeability $k_{10^0}$ cm/sec	$2,0 \cdot 10^{-8}$	$3,6 \cdot 10^{-8}$
Grain distribution,		
0 - 0,002	36,6	18,5
0,002 - 0,02	40,5	42,9
0,02 - 0,2	22,6	38,6
0,2 - 2,0	0,3	-
Lime content approx. in %	27,5	38,2



Hysteresis loops of test Ia

FIG. 4

## b) Test results.

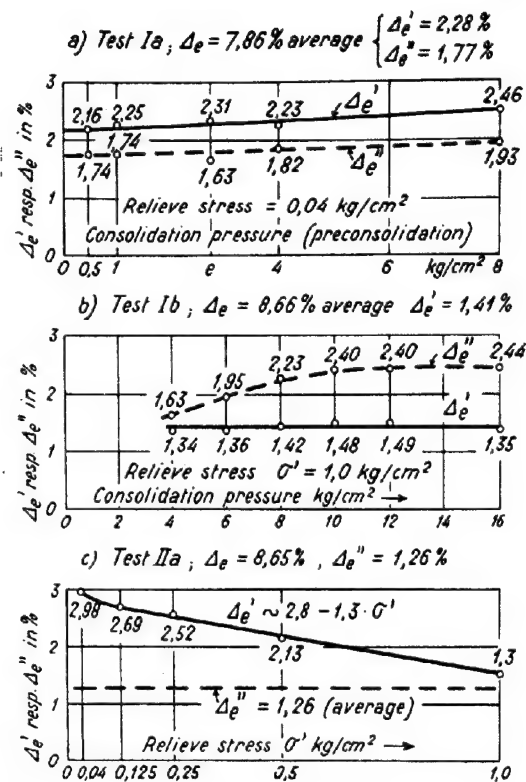
## Test group I.

For test Ia the curves of the primary compressing, of the relieving and of the reloading have been plotted in Fig. 4 and compared with each other to normal or semi-logarithmic scale. It should be noted that the swelling curves in the logarithmic scale lie closer to the straight lines than the secondary load settlement curve when reloading. The hysteresis loop therefore originates because, for obvious reasons, a departure from the straight line occurs at the beginning of the relieving as well as at the beginning of the reloading. The essential result of the tests consists in that the values  $\Delta_e'$  and  $\Delta_e''$  scarcely vary with preconsolidation load, i.e. they may be regarded as practically nearly independent of the height of preconsolidation load, as can clearly be seen from Fig. 5a. With higher preconsolidation loads and less relieving (test Ib), this constancy holds good only for the secondary coefficients of compression  $\Delta_e'$ , whilst the swelling coefficients exhibit an evident increase with increasing preloading (cf. Fig. 5b).

## Test group II.

According to fig. 5, test IIA, in which in contrast to test group I the preloading was kept constant at  $\sigma = 2,72 \text{ kg/cm}^2$  whilst the relieving on the other hand varied between 0,04 and 1 kg/cm<sup>2</sup>, gave exactly the polar reverse of the result obtained with test Ib: the  $\Delta_e'$  values showed an approximately linear increase as relieving proceeded, i.e. with increasing relieving stress. This is to be explained by the relieving favouring the regeneration of the original structure, due to the swelling process connected with the relieving. Therefore, the closer the relieving stress approaches the value 0, and the longer it is effective, the more is the compressibility with reloading. On the other hand, it is self-evident that the  $\Delta_e''$  values must be independent of the magnitude of the relieving.

With test IIB, in which the preloading was raised to 16 kg/cm<sup>2</sup>, fundamentally similar conditions as in test IIA resulted. For illustrating them the whole load cycle was plotted in Fig. 6, both to normal as well as to semilogarithmic scale. The logarithmic representation shows clearly that the hysteresis loops rapidly become broader with increasing relieving load or smaller relieving stress. Connected therewith we have the secondary settlement curves (reloading) becoming steeper the more intense the relieving; this has already been shown in test IIA. The comparison



Secondary coefficients of compressibility ( $\Delta_e'$ ) and swelling coefficients ( $\Delta_e''$ ) from tests Ia, Ib and IIA.

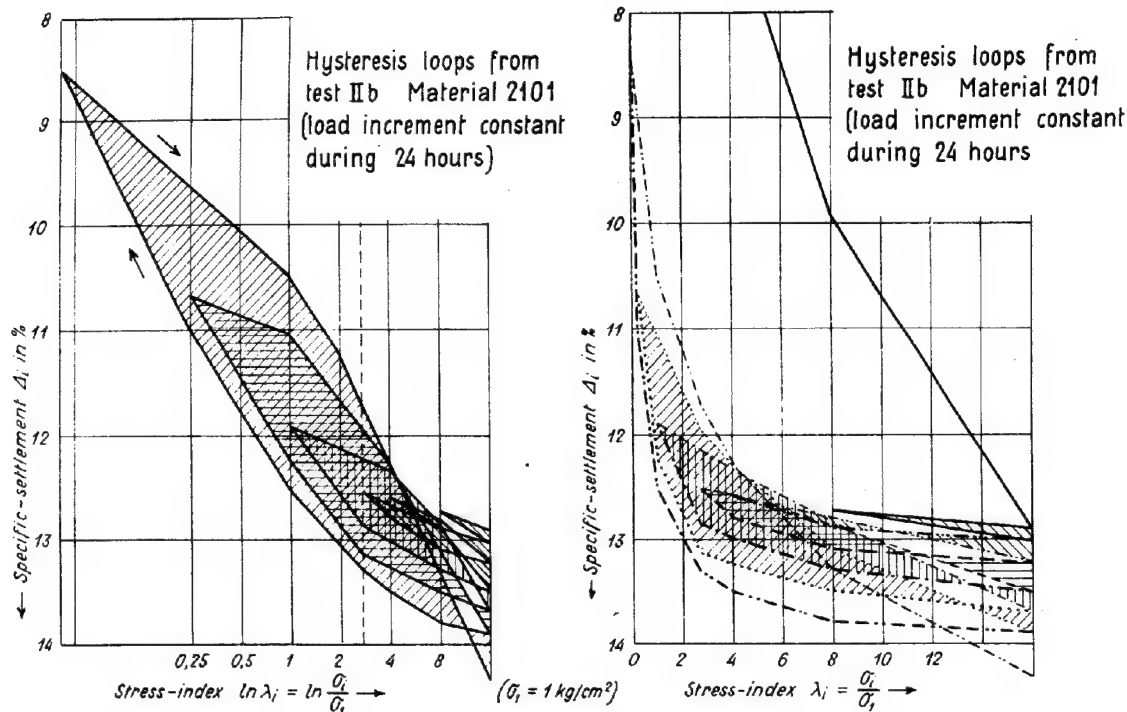
FIG. 5

of the two representations to normal and semi-logarithmic scales shows also that with slight relieving the secondary specific settlement is nearly proportional to the pressure, but with much relieving on the other hand proportional to the logarithm of the pressure. In order to recognise the dependence of the compressibility on the relieving stress - always with constant preloading - it is preferable to compare the  $M_E'$  values for the load range from 8 - 16 kg/cm<sup>2</sup> according to table 5.

TABLE 5

$M_E'$ -values for the loading range of 8-16 kg/cm<sup>2</sup> as a function of the relieving stress  $\sigma_u$  with constant preloading  $\sigma_1$   
(material 2101 ; test IIB)

$\sigma_u$ in kg/cm <sup>2</sup>	8	4	$\sigma = 2,72$	1	0,25	0,004
$M_E'(8-16) = \frac{16-8}{\Delta 16-\Delta 8}$	4450	1900	1310	950	-	775
$\Delta_e' \text{ in } \%$				0,27	0,95	1,31
$\Delta_e'' \text{ in } \%$				1,03	1,02	0,90
$M_E'(1-\sigma) = \frac{1,72}{\sigma} \text{ kg/cm}^2$				637	181	131



Hysteresis loops from test IIb.

FIG. 6

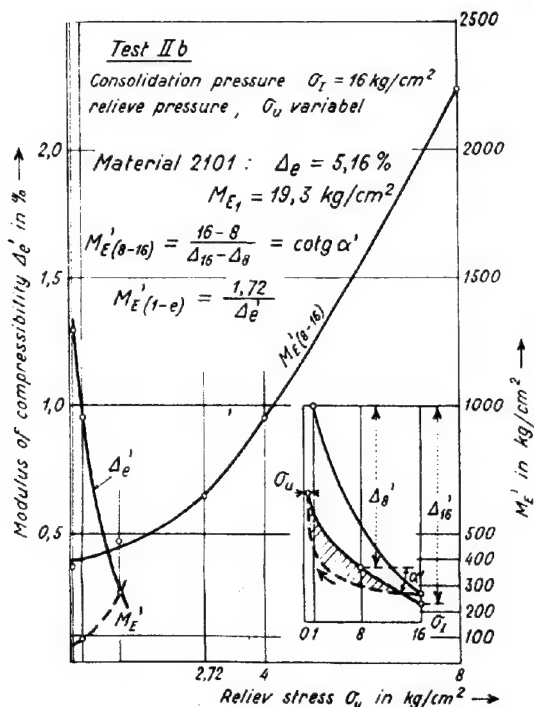


FIG. 7

In contrast to the standard test with  $M_{E1} = 20$  and  $M_{E1}' = 331 \text{ kg/cm}^2$ , the moduli of plasticity for the load increment of 8-16  $\text{kg/cm}^2$  fluctuate here, according to the degree of relieving, between 775 and 4450  $\text{kg/cm}^2$ . Very striking is the great increase in compressibility with increasing relieving, or diminishing of the relieving stress (Fig. 7).

The influence of the duration of the relieving time is seen particularly clearly on the other hand in Fig. 8, which illustrates the hysteresis loops for two parallel tests with relieving times of 24 hours and 5 minutes respectively per load increment. In order to show that the swelling process is in the first line decisive for all these occurrences, a analogical loading cycle was carried out with dry material powder for the purpose of comparison (Fig. 8). The corresponding moduli of plasticity gave the following values:

Saturated, load alteration every 24 hours  
 $M_E' = 575 \text{ kg/cm}^2$   
Saturated, load alteration every 5 minutes  
 $1430 \text{ kg/cm}^2$   
Dry powder, load alteration every 5 minutes  
 $3400 \text{ kg/cm}^2$

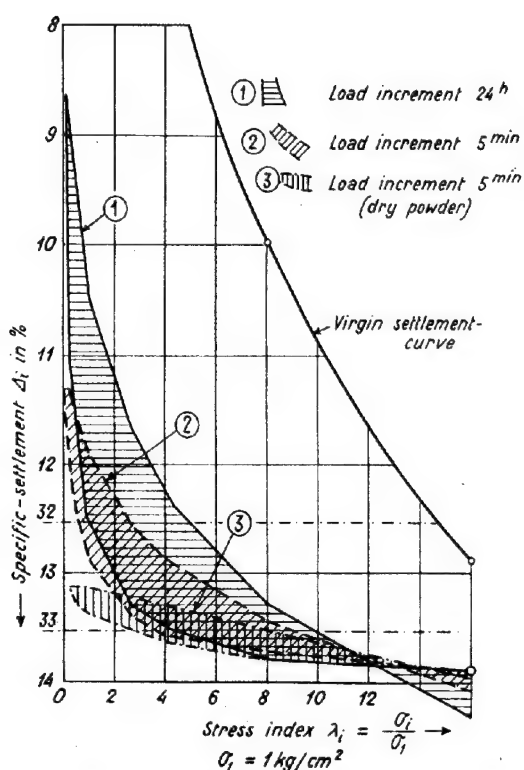
#### Test group III.

In test group III, in which the relieving stress  $\sigma_u$  was always the half of preconsolidation load  $\sigma_1$ , increase of the moduli  $M_E'$  and  $M_E''$  was approximately proportional to preconsolidation load  $\sigma_1$ , the moduli referring each time to the whole range of the relieving (table 6).

TABLE 6

Results of test III (Material 2101;  $\Delta e \sim 5.0\%$ ).

Preconsolidation load	kg/cm <sup>2</sup>	1,0	8,0	16,0
Relieving stress	"	0,5	4,0	8,0
$M_E' (\sigma_u - \sigma_z)$	"	114	840	1290
$M_E'' (\sigma_z - \sigma_u)$	"	177	1510	2600
$M_E = \frac{\sigma_z}{\Delta e}$	"	$\sim 20$	$\sim 160$	$\sim 320$



Dependence of the hysteresis loop on the duration of the test.

FIG. 8

From table 6 it can be seen that the secondary modulus of plasticity  $M_E'$  is here about 4 - 6 times greater than the primary one.

In carrying out and evaluating the tests, we are indebted to the engineers F. Germann and R. Ceberowicz for their collaboration.

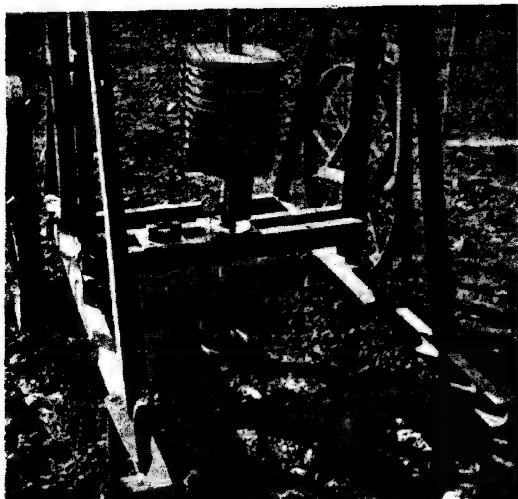
#### IV. CONCLUSIONS.

When investigating the compressibility of loose sediment it will be found preferable to start from the specific settlement. Through

the model described in section II, it becomes comprehensible that the specific settlement or the void ratio increases in proportion to the logarithm of the pressure. Based on the results of tests carried out up to the present, which refer for the moment only to the behaviour of two typical representatives of fine-grained loose sediment, the questions posed at the start may on the other hand be answered as follows:

- 1) The secondary coefficient of compression  $\Delta_e$  is, with constant relieving stress, practically independent of the height of preconsolidation load.
- 2) With a given preconsolidation load, the material is all the more compressible, or the  $\Delta_e$  value is all the greater, the more the material has been relieved before the reloading, or the more intense the swelling process was. The last-mentioned causes a partial regeneration of the original-structure.
- 3) The relieving due to the removal of the sample from the natural layer causes a disturbance which can hardly be avoided. The sample should be taken in such a way that the swelling process is absolutely prevented, and this gives new points of view for the further development of the samplers 7). Also the packing of the samples into the oedometer often entails disturbances. The results of the compression tests with so-called undisturbed soil samples must therefore be judged with very great care. Much more reliable are carefully conducted settlement tests on undisturbed layers of soil in order to determine the modulus of plasticity  $M_E'$ .

The result of field tests will preferably be checked by laboratory tests, the oedometer being used to determine the secondary coefficient of compression  $\Delta_e$  or the corresponding modulus of plasticity  $M_E'$ . The experience made by us up to the present shows that, with preconsolidated soils the two values  $M_E'$  and  $M_E''$  as a rule to a large extent agree with each other, which is to be attributed on the one hand to the slight dependence of the compressibility on the height of preconsolidation load, and on the other hand to the fact that in one method of testing as well as in the other, only a relatively slight relieving of the material takes place. The determining of  $M_E'$  is based on the accurate measurements of settlement by means of special appliances. Their adoption in a borehole makes it possible to test the subsoil with respect to its compressibility. Fig 9 shows an appliance designed by the Soil Mechanics Department with the collaboration of W. Schaad, engineer, for testing the subsoil when constructing the Kloten airport 8).



Light, movable settlement recorder, Kloten

FIG. 9

The connection between settlement and  $M_E$ -value is given by the following equation:

$$y = \frac{\sigma}{M_E^x} D \quad (11)$$

where  $D$  is the diameter of the circular-shaped loaded surface.

Equation(11) gives at the same time the relation between the modulus of plasticity, the coefficient of subgrade reaction  $C$  (ratio of soil pressure to settlement), and the diameter of the loaded surface, the following holding good:

$$M_E^x = \frac{\sigma}{y} D = C \cdot D \quad (12)$$

$C$  = coefficient of subgrade reaction

Finally, the methods illustrated here must be regarded as symptomatic for that new development of soil mechanics which is making efforts for further extension and increased adoption of field tests on undisturbed layers of soil, since the mere removing of the separate samples from the entirety of the soil entails a sensible disturbance in consequence of alterations in stressing. The coordination of field and laboratory tests leads to mutual extension and checking. This is the middle course which avoids the danger of oneness that may occur when one or other of the methods of testing is adopted exclusively.

#### BIBLIOGRAPHY

- 1) K. Terzaghi: Erdbaumechanik auf bodenphysikalischer Grundlage. Wien 1925.
- 2) K. Terzaghi - O.K. Fröhlich: Theorie der Setzung von Tonschichten. Leipzig und Wien 1936.
- 3) R. Haefeli: Mechanische Eigenschaften von Lockergesteinen. Schweiz. Bauzeitung, Bd.111, No. 24 and 26, 1938.
- 4) R. Haefeli - W. Schaad: Time effect in connection with consolidation tests. Second International Conference on Soil Mechanics. Rotterdam 1948.
- 5) R. Haefeli - G. Amberg: Contribution to the Theory of Shrinking. Second International Conference on Soil Mechanics. Rotterdam 1948.
- 6) E. Maag: Ueber die Verfestigung und Dichtung des Baugrundes (Injektionen). Hoch- und Tiefbau No. 23/24. Zürich 1938.
- 7) Committee on Sampling and Testing, Soil Mechanics and Foundations Division A.S.C.E.: The Present Status of the Art of Obtaining Undisturbed Samples of Soils.
- 8) F. German and W. Eng: Soil Mechanics Investigations for the Design of the Runways at the Kloten Airfield/Switzerland. Second International Conference on Soil Mechanics, Rotterdam 1948.
- 9) L. Bendel: Das Druckverformungsgesetz in der Erdbaumechanik. Schweiz. Bauzeitung Bd. 123 Nr. 4 22.Juli 1944.



## SUB-SECTION I e

### SHEARING STRENGTH AND EQUILIBRIUM OF SOILS

#### ON THE LAW OF FRICTION OF SAND

Takeo Mogami  
Prof., Tokyo University, Japan

I e 1

1. The law of friction of sand tells us that the shearing stress on the sliding surface is proportional to the normal stress on it, when the failure of the sand mass is going on. On the other hand, Mr. Reynolds 1) has pointed out that the characteristic property of sand concerning the motion of it is what he called "dilatancy", namely that the volumetric change in sand occurs when the shearing motion begins. Mr. Jenkin paid his serious attention to this property 2), and he performed careful experiments. He pointed out that the friction angle between sand layers varies as the compactness changes. He concluded that these facts show what is called "dilatancy". Mr. A. Casagrande 3) has also shown that the "critical density" is observed when the sand mass begins to fail. Mr. Casagrande's "critical density" may be closely related to Mr. Reynolds's dilatancy. We intend to investigate in detail the nature of failure of sand mass along these lines of ideas.

#### 2. EXPERIMENTAL FACTS.

a) We performed the so-called shearing tests with various kinds of sand. The apparatus is that described by Mr. N. Yamaguchi in the Proceedings of the international conference on soil mechanics and foundation engineering, held in June 1936, vol. II p. 42.

Our experiments were performed for the following kinds of sand; two kinds of sand used for the standard tests of cement mortar, in our country; the one finer, (0.3 mm in diameter), the other coarser (1.2 mm in diameter); a kind of river sand (larger than 2.38 mm 15.6%, 2.38 mm to 1.19 mm 30.15%, 1.19 mm to 0.59 mm 28.05%, 0.59 mm to 0.297 mm 16.70%, smaller than 0.297 mm 9.10%).

All kinds of sand are tested in dry and wet conditions.

#### b) Tests performed.

The shearing test of soil usually performed in our country is executed as follows. At first, the soil sample is placed in a shearing box of our apparatus and then applying a constant load vertically on the upper surface of the sample, then the middle box is pushed laterally, the soil sample is sheared off at the boundary planes which separate the middle box from neighbouring upper and lower boxes. There are many defaults about this method of test in case of sand; then the new method which is effected by the same equipment is proposed. This method is verified to be very satisfactory by experiments. But the most important point is that the mechanism of motion of sand may be investigated closely by this method of experiment. A new method, we proposed, is as follows. No load is applied vertically on the upper surface of the soil sample at first, shearing off the soil sample as above stated. At the same time, the heaving up motion of the upper cover plate is measured. As the shearing motion advances the

upper cover plate is heaved up by sand, this shows the property "dilatancy". Some results obtained are illustrated in the figures 1 to fig. 3 and fig. 5.

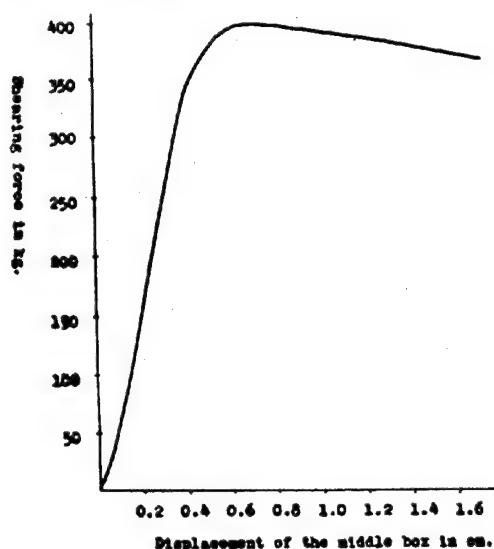


FIG.1

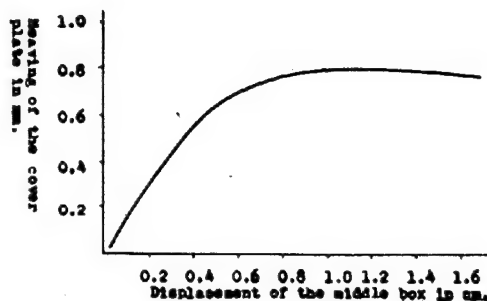


FIG.2

#### c) The motion of sand.

The motion of sand near the shearing plane is observed closely and the conclusions as described below are obtained. In the first stage of the shearing motion, the sand layer near the shearing plane is made to be loose, in this stage the motion is similar to that of viscous liquid and this layer of motion has a finite breadth and the cover plate on the upper surface is heaved up by sand continuously. But when the second stage which we call it as steady state of motion is reached, the motion becomes stationary and the



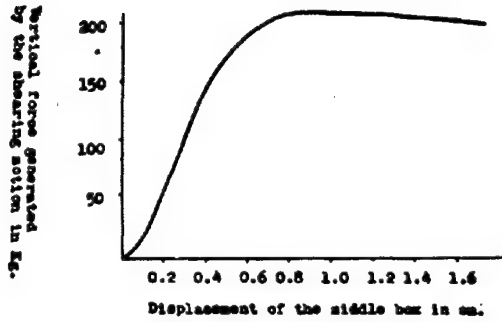


FIG. 3

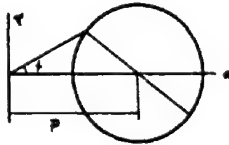


FIG. 4

heaving up motion of the cover plate and the generation of the vertical force will stop. And the shearing force becomes constant. In the first stage the angle of internal friction calculated by the following formula, namely  $\tan \theta = \tau/n$

where

$\tau = S/2A$  : The shearing stress,  
 $S$  : The shearing force,  
 $A$  : The sectional area of the shearing box,  
 $n = N/A$  : The vertical normal stress,  
 $N$  : The developed vertical force due to shearing motion,

is not constant, and in the steady state it attains a constant value, approximately equal to the angle of repose of the sand tested or in some cases, after reaching a minimum, it increases a little.

This shows that the Coulomb's law of friction does not hold when the state of motion of sand is not steady. But it holds in the steady state of motion of sand. When the steady state of motion is reached the region of motion is confined in a very thin layer and then it may be concluded that the sliding surface is found in the steady state in place of sliding layer.

### 3. THEORETICAL CONSIDERATIONS.

a) As the relations between stresses and strain velocities of the sand in motion, we assumed the following formula.

$$\left. \begin{aligned} \sigma_x &= -p + 2mp \frac{\partial u}{\partial x}, \quad \sigma_y = -p + 2mp \frac{\partial v}{\partial y}, \\ \sigma_z &= -p + 2mp \frac{\partial w}{\partial z}, \quad \tau_{yz} = mp \left( \frac{\partial w}{\partial y} + \frac{\partial v}{\partial z} \right), \\ \tau_{zx} &= mp \left( \frac{\partial u}{\partial z} + \frac{\partial w}{\partial x} \right), \quad \tau_{xy} = mp \left( \frac{\partial v}{\partial x} + \frac{\partial u}{\partial y} \right). \end{aligned} \right\} (2)$$

, where  $u, v, w$  are the velocity components

and  $p$  is the mean pressure, namely

$$-p = \frac{1}{3} (\sigma_x + \sigma_y + \sigma_z). \quad (3)$$

and  $m$  is a constant.

In the above relations, if we consider  $u, v, w$  as the displacement components, these formulae are the same as those due to Boussinesq in his theory of the pulverulent masses. When the motion is not steady, the above mentioned formula are considered as to be a rough approximation, because the rate of the volume dilatation is not zero.

The validity of these relations would be inferred from the results which are stated in the followings.

b) The principle of minimum rate of energy loss.

When the motion of sand is steady it may be verified that the possible manner of motion is determined from the principle above stated. The time rate of the loss of energy in the sand in motion is formulated from the relations (2) as follows.

$$\begin{aligned} \frac{dI}{dt} &= \int \left[ \sigma_x \frac{\partial u}{\partial x} + \sigma_y \frac{\partial v}{\partial y} + \sigma_z \frac{\partial w}{\partial z} + \tau_{yz} \left( \frac{\partial w}{\partial y} + \frac{\partial v}{\partial z} \right) + \right. \\ &\quad \left. + \tau_{zx} \left( \frac{\partial u}{\partial z} + \frac{\partial w}{\partial x} \right) + \tau_{xy} \left( \frac{\partial v}{\partial x} + \frac{\partial u}{\partial y} \right) \right] dV \\ \frac{dI}{dt} &= - \int \left[ \left( -p + 2mp \frac{\partial u}{\partial x} \right) \frac{\partial u}{\partial x} + \left( -p + 2mp \frac{\partial v}{\partial y} \right) \frac{\partial v}{\partial y} + \right. \\ &\quad \left. + \left( -p + 2mp \frac{\partial w}{\partial z} \right) \frac{\partial w}{\partial z} + mp \left( \frac{\partial w}{\partial y} + \frac{\partial v}{\partial z} \right)^2 + \right. \\ &\quad \left. + mp \left( \frac{\partial u}{\partial z} + \frac{\partial w}{\partial x} \right)^2 + mp \left( \frac{\partial v}{\partial x} + \frac{\partial u}{\partial y} \right)^2 \right] dV. \end{aligned} \quad (4)$$

Taking the variation of this equation we have

$$\begin{aligned} \delta \frac{dI}{dt} &= - \int \delta p \left[ \left( -1 + 2mp \frac{\partial u}{\partial x} \right) \frac{\partial u}{\partial x} + \dots + \right. \\ &\quad \left. + m \left( \frac{\partial w}{\partial y} + \frac{\partial v}{\partial z} \right)^2 + \dots \right] dV - \\ &\quad - \int \left[ \left\{ \frac{\partial p}{\partial x} - 4m \frac{\partial}{\partial x} \left( p \frac{\partial u}{\partial x} \right) - 2m \frac{\partial}{\partial y} \left\{ p \left( \frac{\partial v}{\partial x} + \frac{\partial u}{\partial y} \right) \right\} - \right. \right. \\ &\quad \left. \left. - 2m \frac{\partial}{\partial z} \left\{ p \left( \frac{\partial u}{\partial z} + \frac{\partial w}{\partial x} \right) \right\} \right\} \delta u + \right. \\ &\quad \left. + \left\{ \frac{\partial p}{\partial y} - 4m \frac{\partial}{\partial y} \left( p \frac{\partial v}{\partial y} \right) - 2m \frac{\partial}{\partial z} \left\{ p \left( \frac{\partial w}{\partial y} + \frac{\partial v}{\partial z} \right) \right\} - \right. \right. \\ &\quad \left. \left. - 2m \frac{\partial}{\partial x} \left\{ p \left( \frac{\partial v}{\partial x} + \frac{\partial u}{\partial y} \right) \right\} \right\} \delta v + \left\{ \frac{\partial p}{\partial z} - 4m \frac{\partial}{\partial z} \left( p \frac{\partial w}{\partial z} \right) - \right. \right. \\ &\quad \left. \left. - 2m \frac{\partial}{\partial x} \left\{ p \left( \frac{\partial u}{\partial z} + \frac{\partial w}{\partial x} \right) \right\} - 2m \frac{\partial}{\partial y} \left\{ p \left( \frac{\partial w}{\partial y} + \frac{\partial v}{\partial z} \right) \right\} \right\} \delta w \right] dV \end{aligned} \quad (5)$$

From the equation (2) and (3) we can obtain

$$\begin{aligned} \delta \left( \frac{\partial u}{\partial x} + \frac{\partial v}{\partial y} + \frac{\partial w}{\partial z} \right) &= 0 \\ \text{Then we get } \int p \delta \left( \frac{\partial u}{\partial x} + \frac{\partial v}{\partial y} + \frac{\partial w}{\partial z} \right) dV &= \\ = - \int \left( \frac{\partial p}{\partial x} \delta u + \frac{\partial p}{\partial y} \delta v + \frac{\partial p}{\partial z} \delta w \right) dV. \end{aligned} \quad (6)$$

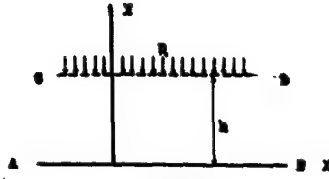


FIG. 5

If the body force has the potential  $\Omega$   
(The components of the body force are  
 $X, Y, Z$ )

$$\left. \begin{aligned} & - \int \rho (X \delta u + Y \delta v + Z \delta w) dV = \\ & = \int \rho \left( \frac{\delta \Omega}{\delta x} \delta u + \frac{\delta \Omega}{\delta y} \delta v + \frac{\delta \Omega}{\delta z} \delta w \right) dV = \\ & = - \int \rho \Omega \delta \left( \frac{\delta u}{\delta x} + \frac{\delta v}{\delta y} + \frac{\delta w}{\delta z} \right) dV = 0 \end{aligned} \right\} (7)$$

If we combine the formula (5), (6) and (7) we get

$$\begin{aligned} \delta \frac{dI}{dt} = & - \int \rho p \left[ \left( -1 + 2mp \frac{\delta u}{\delta x} \right) \frac{\delta u}{\delta x} + \dots + \right. \\ & + m \left( \frac{\delta w}{\delta y} + \frac{\delta v}{\delta z} \right)^2 + \dots \left. \right] dV + 2 \int \left[ \left\{ -\frac{\delta p}{\delta x} + 2m \frac{\delta}{\delta x} \left( p \frac{\delta u}{\delta x} \right) + \right. \right. \\ & + m \frac{\delta}{\delta y} \left\{ p \left( \frac{\delta v}{\delta x} + \frac{\delta u}{\delta y} \right) \right\} + m \frac{\delta}{\delta z} \left\{ p \left( \frac{\delta u}{\delta z} + \frac{\delta w}{\delta x} \right) \right\} + \rho X \right\} \delta u + \\ & + \left\{ -\frac{\delta p}{\delta y} + 2m \frac{\delta}{\delta y} \left( p \frac{\delta v}{\delta y} \right) + m \frac{\delta}{\delta z} \left\{ p \left( \frac{\delta w}{\delta y} + \frac{\delta v}{\delta z} \right) \right\} + \right. \\ & + m \frac{\delta}{\delta x} \left\{ p \left( \frac{\delta v}{\delta x} + \frac{\delta u}{\delta y} \right) \right\} + \rho Y \right\} \delta v + \\ & + \left\{ -\frac{\delta p}{\delta z} + 2m \frac{\delta}{\delta z} \left( p \frac{\delta w}{\delta z} \right) + m \frac{\delta}{\delta x} \left\{ p \left( \frac{\delta u}{\delta z} + \frac{\delta w}{\delta x} \right) \right\} + \right. \\ & + m \frac{\delta}{\delta y} \left\{ p \left( \frac{\delta w}{\delta y} + \frac{\delta v}{\delta z} \right) \right\} + \rho Z \left. \right\} \delta w \left. \right] dV. \end{aligned} \quad (8)$$

If we put this variation to be zero, remembering that

$$p = \lim_{\Delta \rightarrow 0} k \left( \frac{\delta u}{\delta x} + \frac{\delta v}{\delta y} + \frac{\delta w}{\delta z} \right) \quad (9)$$

where  $\Delta = \frac{\delta u}{\delta x} + \frac{\delta v}{\delta y} + \frac{\delta w}{\delta z}$ ,  $k$  - a constant,

we can obtain the equations of motion of sand in the steady state, namely when the acceleration terms in equations are zero.

In these equations, if we consider the formulae (2) we have the well known equations of motion in case of the steady state, i. e.,

$$\left. \begin{aligned} & \frac{\delta \sigma_x}{\delta x} + \frac{\delta \tau_{xy}}{\delta y} + \frac{\delta \tau_{xz}}{\delta z} + \rho X = 0 \\ & \frac{\delta \tau_{yx}}{\delta x} + \frac{\delta \sigma_y}{\delta y} + \frac{\delta \tau_{yz}}{\delta z} + \rho Y = 0 \\ & \frac{\delta \tau_{zx}}{\delta x} + \frac{\delta \tau_{zy}}{\delta y} + \frac{\delta \sigma_z}{\delta z} + \rho Z = 0 \end{aligned} \right\} (10)$$

c) The law of friction and the above theorem.  
When the motion is considered as 2-dimen-

sional and we can assume that,

$$\tau_{yz} = 0, \tau_{zx} = 0, \delta w / \delta z = 0$$

the variation of the time rate of the energy loss in a moving layer of sand is written as follows.

$$\frac{dI}{dt} = -m \int p \left\{ 2 \left( \frac{\delta u}{\delta x} \right)^2 + 2 \left( \frac{\delta v}{\delta y} \right)^2 + \left( \frac{\delta v}{\delta x} + \frac{\delta u}{\delta y} \right)^2 \right\} dV. \quad (10)$$

In case of 2-dimension, the formulae (2) becomes very simple and we get

$$\left. \begin{aligned} p &= \frac{\sigma_x + \sigma_y}{2} \\ 2mp \frac{\delta u}{\delta x} &= -2mp \frac{\delta v}{\delta y} = \frac{\sigma_y - \sigma_x}{2} \\ mp \left( \frac{\delta v}{\delta x} + \frac{\delta u}{\delta y} \right) &= \tau_{xy} \end{aligned} \right\} (11)$$

Then we can transform the equation of the time rate of energy loss as follows (reference may be made to Mohr's circle, figure 4)

$$\frac{dI}{dt} = -\frac{1}{m} \int p \sin^2 \psi dV. \quad (12)$$

From the formula (9) we can say  $\delta p = 0$  then applying this formula to the elementary volume of sand mass, we can conclude, that if the motion of sand is steady the angle between stress and the normal to the surface which the stress acts is minimum, say,  $\phi$ .

If the real angle between stress and the normal is larger than  $\phi$  the motion is not steady and if it is less than  $\phi$ , the motion of sand cannot occur.

This conclusion is not other than the Coulomb's law of friction.

d) Formation of the sliding surface in sand.  
We assume the motion as 2-dimensional and we take the axes  $X$  and  $Y$  as shown in the fig. 5.

And we consider that the sand layer between  $y = 0$  and  $y = h$  is moving from left to right and the sand masses which lies in the region  $y < 0$  and  $y > h$ , are in motion as a whole.

In this case we can put

$$\left. \begin{aligned} \sigma_x &= -p, \sigma_y = -p + 2mp \frac{\delta v}{\delta y}, \sigma_z = -p \\ \tau_{yz} &= 0, \tau_{zx} = 0, \tau_{xy} = mp \frac{\delta u}{\delta y} \end{aligned} \right\} (13)$$

and then the equations of motion of sand mass is as follows,

$$\left. \begin{aligned} \frac{\delta \tau_{xy}}{\delta y} &= 0 \\ \frac{\delta \sigma_y}{\delta y} - \rho &= 0 \end{aligned} \right\} \text{namely } \left. \begin{aligned} \frac{d}{dy} \left( p \frac{\delta u}{\delta y} \right) &= 0 \\ \frac{dp}{dy} + \rho &= 0 \end{aligned} \right\} (14)$$

$$\text{and } \frac{dv}{dy} = 0 \quad (15)$$

Solving above fundamental equations of steady motion of sand between  $y = 0$  and  $y = h$  under

the boundary conditions  $\left. \begin{array}{l} \text{at } y = 0 \quad u = u_0 \\ \text{at } y = h \quad u = u_1 \end{array} \right\} \tau_{xy}/\sigma_y = \tan \phi_0 \quad (16)$

$$\left. \begin{array}{l} \text{at } y = 0 \quad u = u_0 \\ \text{at } y = h \quad u = u_1 \end{array} \right\} \tau_{xy}/\sigma_y = \tan \phi_1 \quad (17)$$

, where  $\phi_0$  and  $\phi_1$  are the angles of friction at  $y = 0$  and  $y = h$  respectively, we can get the following results,

$$-p = -q(h-y) - p_0 \quad (18)$$

$$h = \frac{p_0}{q} \left( \frac{\tan \phi_1}{\tan \phi_0} - 1 \right) \quad (19)$$

From the equation (18) we can conclude that the pressure distribution in the moving sand layer is hydrostatic and the equation (19) tells us that if the friction angle at  $y = 0$  is less than that at  $y = h$  we get  $h > 0$  and in the reverse case we have  $h < 0$ .

And if these angles are equal we have  $h = 0$ .

Then we can say that if the angle of friction at  $y = 0$  is larger than the angle of friction at  $y = h$  the steady motion of sand in a layer of finite breadth cannot occur and if both angles are equal with each other the breadth of the layer of the sand in motion reduces to zero.

Of course, the theoretical calculation is for the steady motion of sand, but we may consider that its results are approximately true when the motion is not steady.

Then from these theoretical considerations and the facts obtained from experiments we can conclude the following results.

When the layer is put in motion by the shearing action of the lower sand mass, the layer between AB and CD in the figure 5 expands (dilatancy). The nearer the sand mass lies to AB the more it expands.

Then the effective friction angle of sand near CD is larger than that for the neighbourhood of AB. In this stage the moving portion is approximately confined by CD and AB. As the layer between AB and CD expands the frictional angle in this layer may become more and more uniform and then breadth of the moving layer of sand becomes thinner.

At last the expansion reaches to its maximum then this layer reduces to a very thin sheet, the sliding surface may be formed in this way. From these considerations we expect that the effective angle of friction of sand decreases from a larger value to a smaller constant, namely the angle of repose of the sand tested.

The results of experiments verify this expectation as shown in the figure 6. In this figure the angle  $\theta$  is calculated

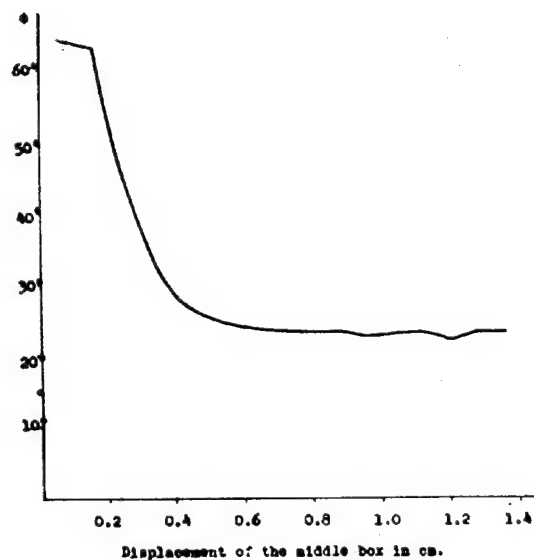


FIG. 6

by the following formula,

$$\tan \theta = \tau/\sigma = S/2N$$

, where

$S$  : the shearing force applied,

$N$  : the vertical force generated.

In case of some kind of sand, after decreasing the angle calculated as above from the date of experiments to a minimum then it increases a little. This phenomena may be interpreted as follows.

In this case the layer becomes too loose when the state  $\theta = \theta_{\min}$  is reached, then it must contract a little.

#### BIBLIOGRAPHY.

- 1) O. Reynolds: The Dilatancy of Media Composed of Rigid Particles in Contact. Phil. Mag. December, 1885.
- 2) C.F. Jenkin: The Pressure exerted by Granular Material: an Application of the Principles of Dilatancy, Proc. Royal Society, Vol. 131, 1931. p. 54.
- 3) A. Casagrande: Characteristics of Cohesionless Soils Affecting the Stability of Slopes and Earth Fills. Journ. Boston Soc. C. E., Vol. 23, 1936.

## DETERMINATION OF THE BEARING POWER OF CLAY FOUNDATION

TAKAO MOGAMI

Prof., Tokyo University, Japan

## SUMMARY AND CONCLUSIONS.

Assuming the clay soil as visco-elastic material, the author deduced the relation between the loading intensity and the amount of the sinking of the bearing plate on the soil. Using the data of the bearing tests due to Mr. Housel, the elastic and viscous constants are plotted against the amount of the sinking of the plate.

These curves explain the variations of the mechanical characteristics during the test, and these suggest the clear method of the determination of the bearing power of the clay foundation.

The method of the determination of the bearing power of the clay foundation was investigated fully by Mr. Housel in 1929 and in 1933. His method is based on the fact which he found, that the intensities of the pressure on the bearing plate of various size are related linearly with the periphery-area ratio, namely

$$p = mx + n \quad (1)$$

where

$p$ : the intensity of the pressure,

$x$ : the periphery-area ratio, the ratio of the periphery of the plate to the area of it.

The above relation exists at every stage of the bearing test. The  $m$  and  $n$  vary with the amount of the sinking of the plate, and from these values Mr. Housel derived so-called physical characteristic coefficient numbers  $K_1$ ,  $K_2$ .

These coefficients  $K_1$ ,  $K_2$  are regarded to be related with the physical properties of soil under consideration, and by these facts the manner of variation of these numbers tells us the bearing power of the clay foundation. This is the opinion of Mr. Housel.

But his and Mr. Williams theory about this is somewhat ambiguous, i.e. it contains some uncertain coefficients and the essential characteristic numbers of the soil are not included.

The author intended to clarify this point. The soil under consideration is assumed to have the visco-elastic properties, namely the soil is characterized by the viscous and elastic coefficients by the following relation,

stress = (a constant)  $\times$  strain + (a constant)  $\times$  strain velocity.

Assuming the surface of the ground is the plane  $z = 0$ , the positive direction of  $z$ -axis to tend to the interior of the ground, and taking the cylindrical coordinates, the relations between stresses and strains may be as follows,

$$\left. \begin{aligned} \bar{r}r &= -p + 2k \frac{\partial u}{\partial r}, \quad \bar{r}\theta = 0 \\ \bar{\theta}\theta &= -p + 2k \frac{u}{r}, \quad \bar{\theta}z = 0, \quad k = \mu + \nu \frac{\partial}{\partial t} \\ \bar{z}z &= -p + 2k \frac{\partial w}{\partial z}, \quad \bar{r}z = k \left( \frac{\partial u}{\partial z} + \frac{\partial w}{\partial r} \right) \end{aligned} \right\} (2)$$

where  $u$ ,  $w$  are displacements to the directions of the axes  $r$  and  $z$  and  $t$  is used to indicate time,  $p$  is the mean pressure,  $\mu$ ,  $\nu$  are coefficients of elasticity and viscosity respectively.

To derive above relations the author assumed the soil is incompressible. This property is always verified by the plastic flow

of the metal, but in this case the condensation of soil under the bearing plate is obviously observed and then this assumption is only approximate.

The constancy of the elastic- and viscous coefficients are also approximate, the elastic constant varies with the condensation and the viscous coefficient also varies with the moisture content remarkably as Mr. Ishimoto and Mr. Iida have shown.

Assuming above relations to be true, the fundamental equations of the visco-elastic soil are as follows,

$$\left. \begin{aligned} \frac{\partial u}{\partial r} + \frac{u}{r} + \frac{\partial w}{\partial z} &= 0 \\ -\frac{\partial p}{\partial r} + k \left( \frac{\partial^2 u}{\partial r^2} + \frac{1}{r} \frac{\partial u}{\partial r} - \frac{u}{r^2} + \frac{\partial^2 u}{\partial z^2} \right) &= \rho \frac{\partial^2 u}{\partial t^2} \\ -\frac{\partial p}{\partial z} + k \left( \frac{\partial^2 w}{\partial r^2} + \frac{1}{r} \frac{\partial w}{\partial r} + \frac{\partial^2 w}{\partial z^2} \right) &= \rho \frac{\partial^2 w}{\partial t^2} \end{aligned} \right\} (3)$$

When the loading velocity is small, right hand member of the last two equations may be neglected.

The intensity of the vertical stress under the bearing plate is rather uniform, when the soil is clayey. When the confinement of soil under the bearing plate at the periphery is complete the distribution of vertical pressure is increasing to the periphery of the plate but the soil is clayey the plastic flow of the soil at the boundary of the plate may lower the magnitude of this stress and the vertical stress under the plate may be considered to be uniform.

Consequently, the distribution of the vertical pressure under the plate is assumed to be uniform and to be increasing linearly with the time. The case when the plate holds its surface horizontal constantly is treated analogously, and these results are referred later.

Solving above fundamental equations under the boundary conditions, when  $z = 0$ ,  $\bar{z}z = -(P_0 + P_1 t)$ , when  $r < a$ ,  $\bar{r}z = 0$ , when  $r > a$

we obtain

$$(w)_{z=0} = \frac{a}{2\mu} \left( p_0 + p_1 t - \frac{\nu}{\mu} p_1 \right) \int_0^\infty \frac{J_0(\alpha r) J_1(\alpha a)}{\alpha} d\alpha \quad (4)$$

where  $J_0$ ,  $J_1$  denote Bessel's functions of zero and 1 order respectively.

Under the boundary conditions, when  $z = 0$ ,  $\bar{z}z = 0$  when  $r > a$ ,  $\bar{r}z = 0$ , when  $r < a$

we obtain

$$(\bar{z}z)_{z=0} = -\frac{4\mu}{\pi} \left( W_0 + W_1 t + \frac{\nu}{\mu} W_1 \right) \frac{1}{\sqrt{a^2 - r^2}} \quad \left. \begin{array}{l} r < a \\ r > a \end{array} \right\} (5)$$

$$= 0$$

The condition that  $\bar{r}z = 0$  when  $z = 0$ , is checked by the fact that the influence of the shearing stress over the surface to the vertical deformation of the surface of soil does not exist.

In the above equation the numerical value of the term under the integral sign is a function of  $r/a$ , and equals to the value between 0.6369 and 1 then in the following discussions we take it as 1. From the equation (4), we get

$$p_0 + p_1 t = \frac{2\mu}{a} (w)_{z=0} + \frac{\nu}{\mu} p_1 \quad (6)$$

in the present case, the periphery-area ratio of the bearing plate is  $2/a$  and then we obtain the formula

$$p = p_0 + p_1 t = mx + n$$

, where  $m = \mu(w)_{z=0}$ ,  $n = \nu/(\mu p_1)$  (7)

This is the same equation as Mr. Housel's. The approximate character of the assumptions above mentioned, the results obtained are expected to be also approximate, but we intend to use these results to examine the characters of the clay foundation. By the help of the equations (7), and using the data obtained by Mr. Housel, we get the viscous and elastic coefficients of soil during the bearing tests.

The coefficient of viscosity thus obtained are related to the sinking of the bearing plate as shown in the figures 2, 4. The

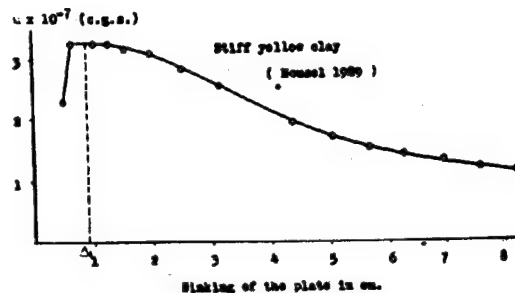


FIG. 3

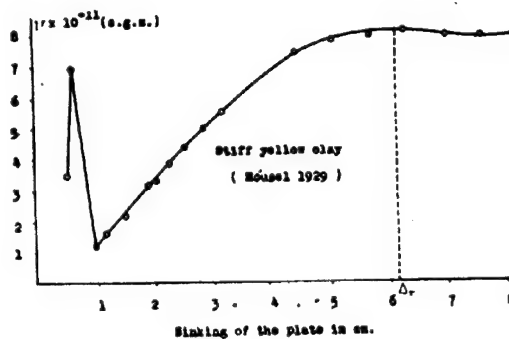


FIG. 4

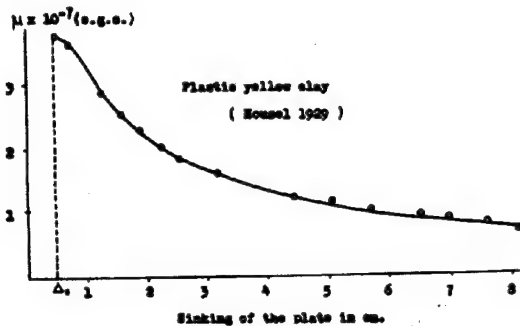


FIG. 1

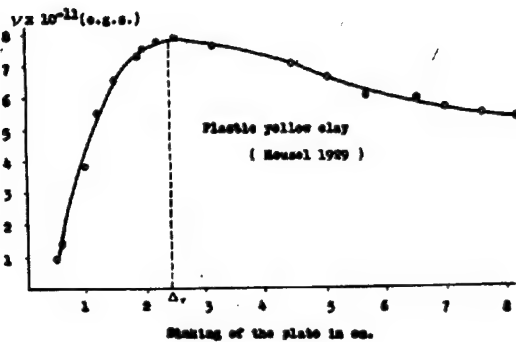


FIG. 2

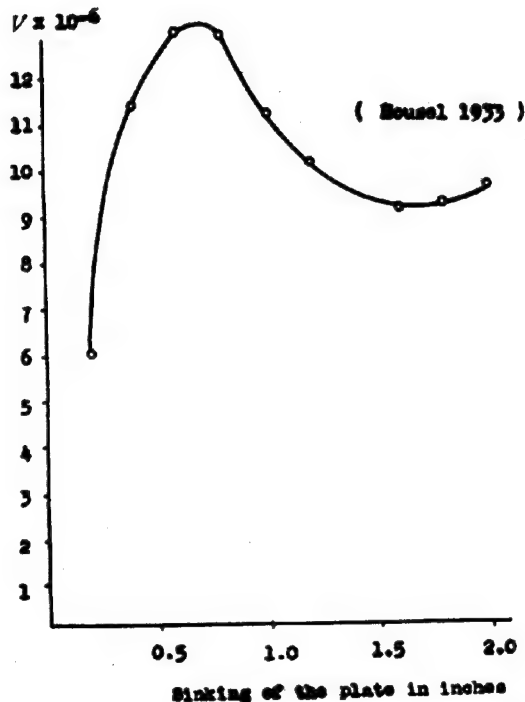


FIG. 5

coefficient of elasticity also varies with the amount of sinking as described in the figures 1, 3.

These curves show that the coefficients by which the mechanical properties of soil under considerations are characterised vary during the bearing test.

We assumed that these coefficients are constant, then these facts are to be interpreted as follows, i.e. the average values of these coefficients if these are constant from the beginning of the test to the instant under consideration, vary with the amount of the sinking of the plate.

From these curves we conclude that the resistance of the soil by elastic properties is considerable when the test was begun but shortly this resistance falls down when the sinking of the plate attained some value, say  $\Delta_z$  and then it decreases slowly.

Contrary to this, the resistance of soil by viscous properties increases steadily and attains its maximum when the sinking of the plate is, say,  $\Delta_v$ . When the soil is not stiff the viscous resistance decreases when the sinking of the plate passes  $\Delta_v$ .

The stiffness of the soil is characterised by the value of  $\Delta_z$  and  $\Delta_v$ . The stiffer

soil has larger  $\Delta_z$ ,  $\Delta_v$  and  $\Delta_v - \Delta_z$ . From the above considerations we may take the value of  $\Delta_z$  or  $\Delta_v$  as the critical amount of sinking, as the case may be.

If we compare these values with that obtained by Mr. Housel from the consideration that the amount of sinking of the plate is critical when  $K_2$  attains its maximum, we conclude that his value is approximately equal to our  $\Delta_v$ .

Figure 5 shows the results calculated from the data of the test performed by Mr. Housel in 1933, for the foundation consisting of two layers of soil. The curve shows that the resistance of the lower layer is growing after the upper layer loses its power of resisting.

#### BIBLIOGRAPHY

- 1) W.S. Housel: A practical method of the selection of foundations Univ. Mich. Eng. Research Bull. October 1929.  
W.S. Housel: Bearing power of clay is determinable. Eng. News-Record, Vol. 110, 1933.
- 2) M. Ishimoto and K. Iida: Bulletin Geotechnical Committee Gov. Railways of Japan No. 5 1938.

-0-0-0-0-0-0-

| e 3

#### THE STABILITY OF SLOPES ACTED UPON BY PARALLEL SEEPAGE

R. HAEFELI

Laboratory for Hydraulic Research and Soil Mechanics of  
the Swiss Federal Institute of Technology, Zurich.

#### I. INTRODUCTION.

The stability and conditions of inclination of natural and built-up slopes are influenced in a definite manner by the conditions of flow of the water in the pores. Then we have to deal either with steady percolating flow or with the known unsteady hydrodynamic tension phenomena of the pore water. In close connection with this stand above all the slipping phenomena taking place in different phases on hill-sides saturated with water.

Fig. 1 illustrates diagrammatically the two first phases of such a slipping phenomenon. It has been assumed that a source of water on the slope at A has first of all caused a slipping of the steep slope between A and B on a shell-shaped sliding surface. The material fallen down causes a sudden loading on the adjoining zone of slope downwards C - D. Under the action of this load a region of pore water subjected to compressive stressing starts in loam soil which has a very small permeability. A seepage, directed towards the free slope C - E on the valley side, exists in parallel with the gradual expanding of the pore water, and in the neighbourhood of the slope may be regarded approximately as parallel flow. The flow pressures thereby occurring cause a disturbance in the equilibrium of the lower parts of the slope

in the form of a fresh sliding as second phase of a process which, by a repetition of such sliding phenomena, progresses downwards step by step and may attain formidable proportions, depending on morphological and geological conditions. The sequence of slips ends in the form of wave peaks, and sagging zones as wave troughs, gives that greatly cut relief which is characteristic of hill-sides that are in danger of sliding and creeping.

In contrast to the above case of a movement of pore water directed outwards and disturbing the equilibrium, is the case of an percolating flow directed inwards, which acts not as a disturbing factor, but as a stabilising factor on the equilibrium of the slope in question. If, for instance in an earth dam as sketched in Fig. 2, the percolation gradient along a stream line is increased by the damming of the water, this causes an increased lift in the zone of the dam freshly submerged, and with this a relieving of the slope is connected.

Closer investigation of the conditions of stability of a slope with seepage shows that the problem may be regarded as purely static and without separation between solid and liquid phases. In the first place the question of the hydraulic gradient  $i$  along a normal to the surface of the slope comes into consider-



which is practically identical with the angle of the slope.

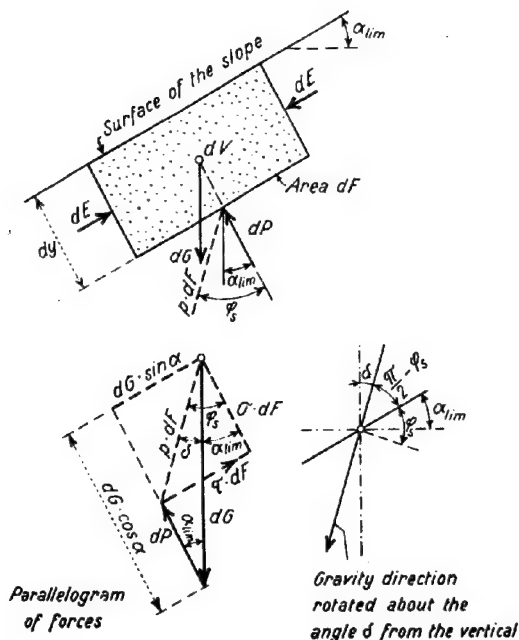
With regard to the pressure conditions in the pore water, the only assumption holding good is that the lines of uniform water pressure (equi-pressure lines), which are not identical with the known lines of uniform potential or piezometer conditions (equi-potential lines) must run parallel to the surface of the slope. This condition is only fulfilled with parallel flows when the surface of the slope is free. If the slope lies under water, as for instance in Fig. 2, the following theory is not applicable. On the other hand the assumption made regarding the run of the lines of uniform water pressure with free surface of slope is as a rule fulfilled even in the case of bent parallel flow (Fig. 7a).

For solving the present problem we first of all consider the equilibrium of a prismatic element coinciding with the surface of the slope, the element consisting of solid and liquid phases and being completely saturated (Fig. 3).

The base  $dF$  of the mentioned element  $dV$  forms a possible sliding surface running parallel to the surface of the slope, and is at the same time a surface of uniform water pressure. In the limiting case of equilibrium, the resulting tension  $p$  on the surface  $dF$  makes with the normals to the surface the angle  $\varphi_s$ , i.e. the following hold good:

$$\frac{\tau}{\sigma} = \operatorname{tg} \varphi_s \alpha_{\text{lim}} + \delta = \varphi_s \quad (1)$$

The following forces act on the element  $dV$ : Its own weight  $dG$ , the symmetrical lateral forces  $dE$  which mutually cancel each other, and the lift  $dP$ . From the partial forces  $dG$  and  $dP$  the tensions  $\sigma$  and  $\tau$  acting on the surface



Considerations of equilibrium of a prismatic element.

FIG. 3

$dF$  can be calculated as follows:

Weight :  $dG = \gamma_e \cdot dV$

Lift :  $dP = dp \cdot dF = \frac{dp}{d\eta} \cdot dV \quad (2)$

According to Fig. 2 the pressure gradient  $\frac{dp}{d\eta}$  is determined first of all for any desired angle  $\alpha < \alpha_{\text{lim}}$

$$\left. \begin{aligned} \frac{dp}{d\eta} &= du \cos \alpha + dv \sin \alpha \cdot \operatorname{tg} i \\ \frac{dp}{du} &= (\cos \alpha + \sin \alpha \operatorname{tg} i) \gamma_w \end{aligned} \right\} \quad (3)$$

Substituting equation (3) in equation (2) we have:

$$dP = (\cos \alpha + \sin \alpha \operatorname{tg} i) \gamma_w \cdot dV \quad (4)$$

By introducing this value of  $dP$  into the equilibrium conditions (2), the tensions  $\tau$  and  $\sigma$  are obtained, whose quotient in the limiting case according to equation (1) gives the limiting angle  $\alpha_{\text{lim}}$  which was sought.

$$\sigma dF = dG \cos \alpha - dP (\gamma_e' \cos \alpha - \cos \alpha \gamma_w -$$

$$\sin \alpha \operatorname{tg} i \gamma_w) dV$$

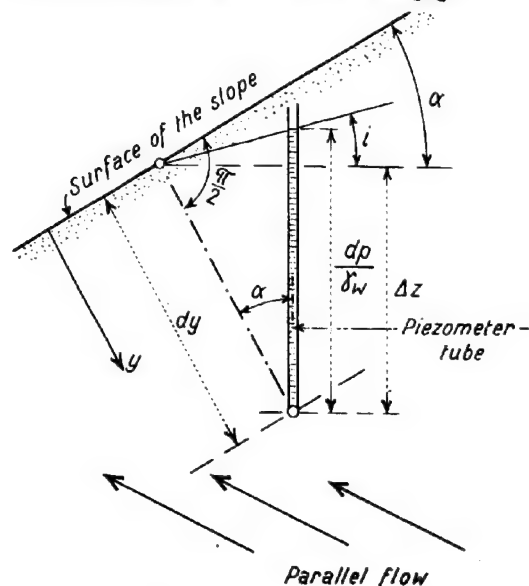
$$\sigma dF = [\cos \alpha (\gamma_e' - \gamma_w) - \sin \alpha \operatorname{tg} i \gamma_w] dV \quad (5)$$

$$\tau dF = \gamma_e' \sin \alpha dV \quad (6)$$

$$\frac{\tau_{\text{lim}}}{\sigma} = \left(1 - \frac{\gamma_w}{\gamma_e'}\right) \operatorname{ctg} \alpha_{\text{lim}} - \frac{\gamma_w}{\gamma_e'} \operatorname{tg} i = \operatorname{ctg} \varphi_s \quad (6a)$$

$$\operatorname{tg} \alpha_{\text{lim}} = \frac{\gamma_e' - \gamma_w}{\gamma_e' \operatorname{ctg} \varphi_s + \gamma_w \operatorname{tg} i} \quad (7)$$

The coefficient factor  $\lambda$  serves as a measure for the influence of the seepage on



Definition of the decisive hydraulic gradient  $\operatorname{tg} i$ .

FIG. 4



the angle of inclination of the slope in the limiting position of equilibrium:

$$\zeta = \frac{\operatorname{tg} \alpha_{\text{lim}}}{\operatorname{tg} \varphi_s} = \frac{\gamma_e' - \gamma_w}{\gamma_e' + \gamma_w \operatorname{tg} i \operatorname{tg} \varphi_s} = \frac{\frac{\gamma_e'}{\gamma_w} - 1}{\frac{\gamma_e'}{\gamma_w} + \operatorname{tg} i \operatorname{tg} \varphi_s}$$

$$\zeta = \frac{\lambda' - 1}{\lambda' + u}; \lambda' = \frac{\gamma_e'}{\gamma_w} \quad u = \operatorname{tg} i \operatorname{tg} \varphi_s \quad (8)$$

This equation shows that, with a given material which is characterized by its unit weight at saturation ( $\gamma_e'$ ) and its angle to the apparent internal friction  $\varphi_s$ , the limiting angle  $\alpha_{\text{lim}}$  of the slope with seepage depends solely and alone on the hydraulic gradient  $i$  along a normal to the slope. Amongst others the following special cases are of interest (Fig. 4):

- a) The limiting angle of the slope with seepage reaches a right angle, i.e.

$$\alpha = \frac{\pi}{2} \text{ and } \zeta = \infty$$

$$\text{Condition: } u = -\lambda'; \operatorname{tg} i = -\frac{\gamma_e'}{\gamma_w} \operatorname{ctg} \varphi_s$$

- b) The limiting angle  $\alpha_{\text{lim}}$  of the slope with seepage is equal to that of the slope without seepage, i.e.

$$\alpha_{\text{lim}} = \varphi_s; \zeta = 1$$

$$\text{Condition: } u = -1; \operatorname{tg} i = -\operatorname{ctg} \varphi_s; i = \varphi_s - \frac{\pi}{2}$$

In this case the slope has seepage vertically from above.

- c) The flow is parallel to the surface of the slope. Consequently there cannot be any flow gradient at right angles to the slope, i.e.  $i$  becomes = 0 and thereby  $u = 0$ . Equation (8) then passes over into the condition derived at another place (4).

$$\zeta = \frac{\lambda' - 1}{\lambda'} = \frac{\gamma_e' - \gamma_w}{\gamma_e'} = \frac{\gamma_e''}{\gamma_w} \quad (9)$$

- d) With a gradual increasing of the hydraulic gradient  $i$  (Fig. 4), the limiting angles  $\alpha_{\text{lim}}$  become theoretically always smaller until finally the horizontal is reached ( $\alpha_{\text{lim}} = 0$  for  $i = \infty$ ). This extrapolation, however, does not hold good whenever the gradient  $i$  is exceeded at which hydraulic rupture of the soil occurs. If the gradient  $i$  is increased beyond this critical value, it is no longer the danger of slipping but the danger of soil rupture which is decisive for stability. Equation (8) then becomes of no importance. In order to find the position of transition from the region in which sliding conditions hold good to that of the usual soil rupture condition, we calculate the respective limiting angles  $\alpha_k$  by introducing as first approximation in equation (8) the critical gradient

$$i_k = \frac{\gamma_e''}{\gamma_w} \text{ for material without cohesion.}$$

$$\zeta_k \approx \frac{\gamma_e''}{\gamma_e' + \gamma_w} = \frac{1}{\frac{\gamma_e''}{\gamma_e'} + \operatorname{tg} \varphi_s} \quad (10)$$

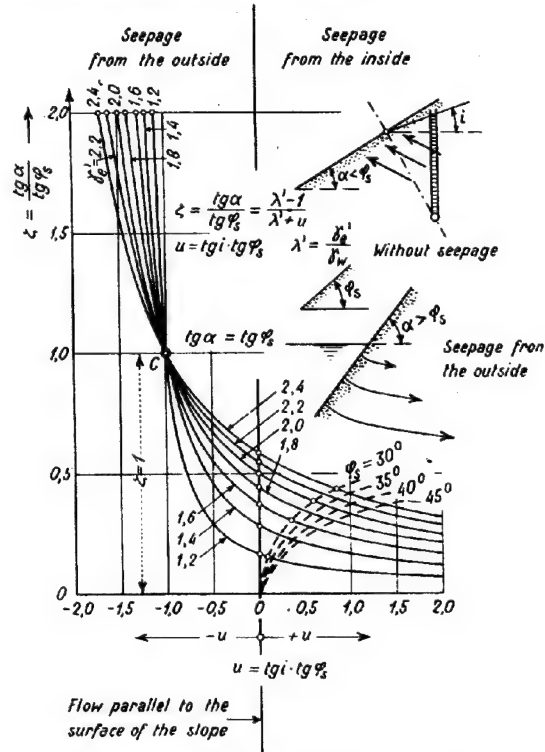
where  $\gamma_e''$  means the specific gravity under water, i.e.  $\gamma_e'' = \gamma_e' - \gamma_w$ .

From equation (10) it also follows:

$$\operatorname{tg} \alpha_k \approx \zeta_k \operatorname{tg} \varphi_s = \frac{1}{1 + \frac{\gamma_e''}{\gamma_e'} \operatorname{ctg} \varphi_s} \quad (11)$$

Since the deriving of the critical gradient

for soil rupture is with reference to a flow directed vertically from below to above, whilst the normal to the slope in which the gradient  $i$  is measured deviates from the vertical by the angle  $\alpha_k$ , equations (10) and (11) hold good only approximately. In addition they can only be adopted for material without cohesion, since we have taken the tensile strength of the material = 0 when deriving the critical gradient  $i_k$  (5).



Ratio  $\zeta$  of the natural stability of the slope with and without seepage in function of the decisive hydraulic gradient  $\operatorname{tg} i$ .

FIG. 5

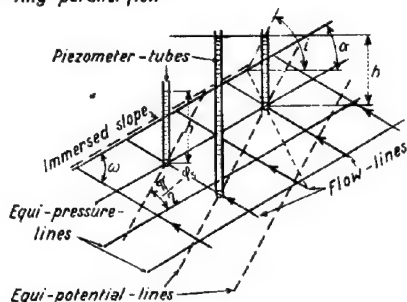
In Fig. 5 the coefficient factors  $\zeta$  are represented as parameter as a function of the gradient  $i$  for different unit weights  $\gamma_e'$ . This group of curves shows that seepage from within requires a considerable reduction of the limiting angle  $\alpha_{\text{lim}}$  with respect to the angle  $\varphi_s$  of the natural slope. As transition between seepage from within to percolation from the outside, the case  $u = 0$  or  $i = 0$  appears, for which the flow is directed parallel to the surface of the slope. From the point  $u = 0$  the  $\zeta$  curves lie steeply to the common point of intersection C, which is given by the ordinate  $\zeta = 1$  and the abscissa  $u = -1$ . In this case the seepage - which takes place here from the outside - has no influence on the stability on the slope ( $\alpha_{\text{lim}} = \varphi_s$ ). After closer consideration it is found that we are dealing here with a percolation of the material in the vertical direction from above to below. To the left of C the curves approach their corresponding vertical asymptotes in a steep rise, the position of the asymptotes being given by the abscissa sections  $u = -\lambda'$ .

The corresponding limiting angle amounts to  $\alpha_{lim} = \frac{\pi}{2}$  which corresponds to a vertical slope. At the righthand side of the diagram the validity of the group of curves is limited by the region of validity of the soil rupture condition, whose extent also depends on  $\psi_s$ . As an example the limiting lines for  $\psi_s = 30^\circ, 35^\circ, 40^\circ$  and  $45^\circ$  have been plotted in chain-dotted lines. Beyond these limiting lines the gradient  $i$  cannot be increased, even with a horizontal material surface, without the occurrence of rupture of the ground.

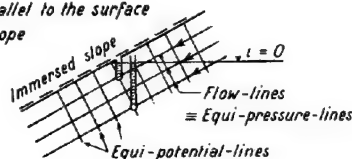
### III. CONCLUSIONS.

As can be seen clearly from the above theory, in determining the stability of a slope saturated with water, the velocity of flow plays no part; it depends exclusively on the pressure ratio in the pore water, or on the run of the lines of uniform water pressure (equi-pressure lines) which are not to be confused with the lines of uniform potential (equi-potential lines). Of course this holds good only under the supposition that no fine particles are swept away by the percolation process

#### a) Any parallel flow



#### b) Flow parallel to the surface of the slope



#### c) Flow rectangular to the surface of the immersed slope

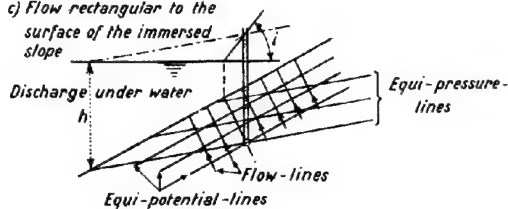


FIG. 6

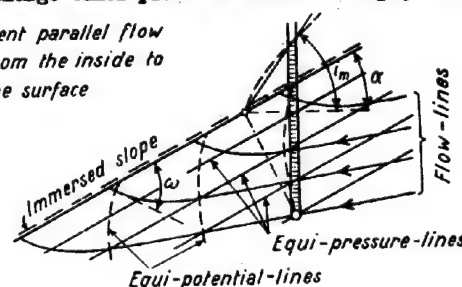
or are chemically dissolved.

In the case of little-pervious fine-grained slopes percolation can very often be scarcely perceived, the evaporation on the surface of the slope being sufficient to remove the issuing water; this is very frequently the case in dams. Although in this case the velocities of flow are practically = 0, the slope in question is nevertheless subjected to unfavourable conditions of stability for the material through which the flow occurs, since it just depends on the run of the equi-pressure lines which, like the

flow picture, are known to be independent of the coefficient of permeability and thereby of the speed of percolation.

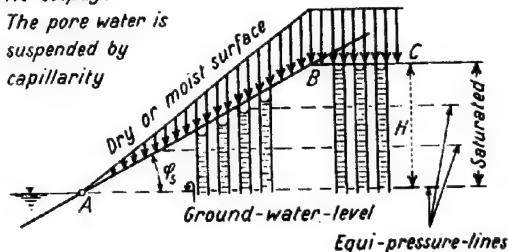
In order to make clear the difference between the equi-pressure and the equi-potential lines, three different cases of parallel flow are illustrated in Fig. 6. Fig. 6a shows a flow from inside directed at an angle  $\omega$  to the slope, where the equi-pressure lines, which here run parallel to the surface of the slope, enclose with the equi-potential lines the angle  $(\frac{\pi}{2} - \omega)$ . Fig. 6b shows a flow parallel to the surface of the slope, where the flow and equi-pressure lines coincide, whilst the equi-potential lines are at right angles to the slope. In these two cases a) and b) the surface of the slope will be slightly flooded over. Case c) shows a parallel flow at right angles to the slope and directed outwards, as is normally observed below the surface of the water. Here the equi-potential lines are parallel to the slope, but the equi-pressure lines on the other hand are directed obliquely to it. Our theory is therefore not applicable in this case. Only if the discharge takes place on the free slope, with-

#### a) Bent parallel flow from the inside to the surface



#### b) No seepage

The pore water is suspended by capillarity



#### c) Vertical seepage of a slope

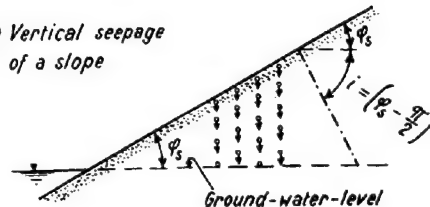


FIG. 7

out being submerged, so that the slope is only slightly flooded over, the lines of uniform potential and uniform pressure will also in case c) be identical and parallel to the surface of the slope and thereby fulfil the assumptions of the theory.

Three further cases of practical importance are illustrated in Fig. 7. Fig. 7a shows a bent parallel flow issuing on the slope at an acute angle  $\omega$ , whilst in Fig. 7b the circumstances are indicated which arise under the influence of capillary forces with no

flow and horizontal ground-water level. The fact is important that the equi-pressure lines in this case run horizontally, so that the lifting forces, which are also effective in the closed capillary region, remain vertical. The equilibrium of such a slope may therefore be investigated in the usual manner with bent sliding surfaces. The weights of the solid and liquid phases may then be inserted in the calculation either separately, by introducing the capillary forces as an external loading; or such a separation is not adopted, the unit weight  $\gamma_s$  of the saturated material above water being introduced into the calculation, a proceeding which is much simpler. If the water evaporates on the surface of the slope, a certain percolating movement directed upwards takes place in consequence of the capillary rise above the groundwater level. No change is thereby made in the external static conditions of the slope, since the frictional forces that occur neutralise each other mutually as action and reaction in the interior of the static system. As polar opposite of the capillary rise of the water, the case of vertical parallel flow from above to below is illustrated in Fig. 7c; this may occur for instance with rain of with the melting of snow. The vertical percolation of the slope is here characterised by the pressure of the pore water at all points, and therefore also along a normal to the slope, being everywhere equal to atmospheric pressure, i.e.  $i = \varphi_s - \frac{1}{2}$  and  $u = -1$ .

This case thus corresponds to the point of intersection C in Fig. 5, for which, in accordance with what has been said already, the limiting angle  $\alpha_{lim}$  becomes identical with  $\varphi_s$ .

The above comparisons show that in general the slight flooding of the surface of the slope has an unfavourable influence on its stability. Account must be taken of this fact especially when slopes are being drained. Certainly, even if there is no flooding, seepage flow directed down the slope may occur within the closed capillary region, and this has an adverse effect on the equilibrium, but it will take place as a rule with a very small gradient  $i$ . On the other hand, it may frequently be observed that the evaporating surface withdraws into the interior of the slope and an evaporating crust is formed through drying, and this acts as a stabiliser. Also the latest attempts to improve the stability of slopes with seepage by adopting electro-osmotic methods 7) should be noted in this connection.

If it is desired to investigate the conditions of equilibrium of a slope with an angle of inclination  $\alpha$  and parallel seepage, this slope being in a stable condition, two different methods may be adopted with a given gradient  $i$ : Either the limiting inclination  $\text{tg} \alpha_{lim}$  is calculated according to equation (7) and the degree of safety  $N$  is found in the form:

$$N = \frac{\text{tg} \alpha_{lim}}{\text{tg} \alpha} \quad (12)$$

or the angle  $\delta$  is calculated, which is included by the parallel directed resultants of own weight and lift with the verticals (cf. Fig. 3). This angle  $\delta$  therefore gives particularly valuable conclusions, since the influence of the parallel flow on the equilibrium of the slope may be regarded as a field of

gravity rotated about the angle and somewhat reduced in intensity. The criterion for the equilibrium of the slope is then:

$$\alpha \leq \varphi_s - \delta \quad (13)$$

(cf. Fig. 13)

The angle  $\delta$  is easily calculated from equation (6') by substituting the sum of the angles  $\alpha + \delta$  for  $\varphi_s$ ; then we obtain:

$$\text{tg} \delta = \frac{1 + \text{tg} \alpha \text{tg} \alpha}{\frac{\gamma_s}{\gamma_w} \text{tg} \alpha + \frac{\gamma_w}{\gamma_s} \text{ctg} \alpha - \text{tg} i} \quad (14)$$

From this equation the rapid increase of  $\delta$  with increasing gradient  $i$  can be clearly seen.

Finally it should once again be pointed out that the above theory, derived in the first place for cohesionless material, is only applicable to a coherent material if the cohesion increases from 0 at the surface of the slope proportionally to the depth, so that the  $\alpha$ -line of the shear diagram remains valid at all points of the slope, corresponding to a constant angle  $\varphi_s$  of the apparent internal friction. Such cohesion conditions may for instance arise with the compacting of fresh sediment under its own weight, also the modulus of plasticity then increasing in proportion to the depth 5) and 6). If on the other hand a loose sediment of another kind of cohesion conditions - for instance with constant cohesion - as considered the stability of the slope with seepage may be examined only with the help of known methods by adopting bent sliding surfaces.

#### BIBLIOGRAPHY.

- 1) W. Bernatzik: Grenzneigung von Sandböschung--en bei gleichzeitiger Grundwasserströmung. Die Bautechnik Nr. 55, 1940.  
W. Bernatzik: Baugrund und Physik. Zürich 1947.
- 2) E. Meyer-Peter, H. Favre und R. Müller: Beitrag zur Berechnung der Standsicherheit von Erddämmen. Schweiz. Bauzeitung, Bd. 108, Nr. 4, 1936.
- 3) R. Müller: Die Anwendung von Strömungsbildern zur Berechnung durchsickerter Erdschüttungen. Strasse und Verkehr, 1938.
- 4) R. Haefeli: Zur Mechanik aussergewöhnlicher Gletscherschwankungen. Schweiz. Bauleitung Bd. 115, Nr. 16, 1940.
- 5) R. Haefeli: Erdbaumechanische Probleme im Lichte der Schneeforschung. Schweiz. Bauzeitung Bd. 123, Nr. 2, 4 und 5, Januar 1944.
- 6) R. Haefeli, Ch. Schaerer: Der Triaxialapparat, ein Instrument der Boden- und Eis-mechanik zur Prüfung von Verformungs- und Bruchzuständen. Schweiz. Bauzeitung, Bd. 128, Nr. 5, 6 und 7, 1946.
- 7) W. Schaad und R. Haefeli: Die Anwendung der Elektrizität zur Entwässerung und Verbesserung feinkörniger Bodenarten. Strasse und Verkehr, Bd. 32, 1946. - Elektrokinetische Erscheinungen und ihre Anwendung in der Bodenmechanik. Schweiz. Bauzeitung, 65. Jahrgang, Nr. 16-18, 1947.

| e 4

LIMITATION OF THE VALIDITY OF APPLICATION OF THE FORMULAS  
FROM PRANDTL-BUISMAN AND FROM ANDERSEN FOR THE ULTIMATE  
BEARING CAPACITY OF THE SOIL UNDERNEATH FOOTINGS.

E. DE BEER and M. WALLAYS -Ghent (Belgium)

The formula of Prandtl gives the value of the ultimate bearing capacity of an incompressible material with a cohesion  $c$  and an angle of friction  $\phi$ , not subjected to gravity and loaded at its surface. The surface of failure has the shape of a logarithmic spiral situated between two straight lines (fig. 1). Buisman

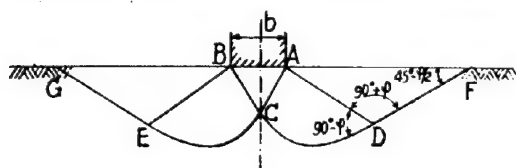


FIG. 1

first completed the formula of Prandtl for the case of an uniform overload  $p_0$  on the surface of the material beside the loaded area. The existence of such an overload doesn't alter the shape of the surface of failure.

Going further, and with the purpose to take into account the own weight  $\gamma$  of the material, Buisman assumed that, even if the material is subjected to gravity, the shape of the surface of failure is not altered; thus it becomes easy to find an expression for the part of the ultimate bearing capacity produced by the own weight of the soil located above the surface of failure.

With the assumption that the most dangerous surface of sliding is a logarithmic spiral with two straight extensions, Prandtl-Buisman found for the ultimate bearing capacity  $d_g$  the following expression:

$$d_g = V_b p_0 + V_c c + V_\gamma \gamma b \quad (1)$$

where

$d_g$  = the ultimate bearing capacity ( $t/m^2$ )

$p_0$  = the overload existing beside the footing ( $t/m^2$ )

$c$  = the cohesion ( $t/m^2$ )

$\gamma$  = that part of the volume-weight of the soil, which is to be taken into account for the computation of the effective stresses.

$b$  = the width of the footing.

$V_b$ ,  $V_c$  and  $V_\gamma$  = three functions of the angle of friction  $\phi$

$$V_b = e^{n\gamma\phi} \lg^2 \left( \frac{\pi}{4} + \frac{\phi}{2} \right) \quad (2)$$

$$V_c = e^{n\gamma\phi} \frac{2\cos\phi}{1-\sin\phi} (e^{n\gamma\phi} - 1) \cot\phi \quad (3)$$

For  $V_\gamma$  the following analytical expression was found by Prof. Raas:

$$V_\gamma = \frac{1}{8} \left[ \frac{1 + \lg^2 \left( \frac{\pi}{4} + \frac{\phi}{2} \right)}{1 + 9\lg^2 \phi} \left\{ \left[ 3\lg\phi \lg \left( \frac{\pi}{4} + \frac{\phi}{2} \right) - 1 \right] e^{n\gamma\phi} + \right. \right. \\ \left. \left. + 3\lg\phi + \lg \left( \frac{\pi}{4} + \frac{\phi}{2} \right) \right\} + 2e^{n\gamma\phi} \lg^2 \left( \frac{\pi}{4} + \frac{\phi}{2} \right) + \right. \\ \left. - 2\lg \left( \frac{\pi}{4} + \frac{\phi}{2} \right) \right] \quad (4)$$

When the foundation is established at a

depth  $h$  underneath the surface of the soil, the phreatic level being located at the surface of soil or at a great depth underneath the foundation level, one gets

$$p_0 = \gamma h \quad (5)$$

thus

$$d_g = V_b \gamma h + V_c c + V_\gamma \gamma b \quad (6)$$

The formula (6) is the expression of the

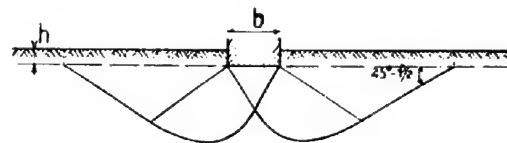


FIG. 2

ultimate bearing capacity for the case of fig. 2. The only arbitrary assumptions are that the material is incompressible and that the most dangerous surface of sliding is a logarithmic spiral with 2 straight extensions.

On the other hand prof. Andersen of the University of Minnesota established an analytical expression for the ultimate bearing capacity of a material  $c, \phi, \gamma$ , underneath a footing with a breadth  $b$  established at a depth  $h$ , starting from the arbitrary assumption that the most dangerous surface of sliding is composed by two circles with radius  $r$  and  $r + h$  (fig. 3).

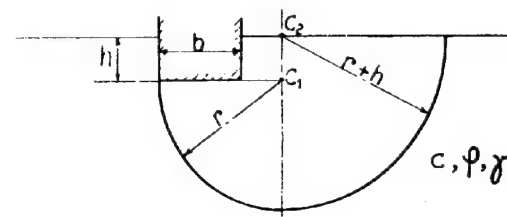


FIG. 3

The radius  $r$  of the most dangerous circular surface, and the value of the ultimate bearing capacity corresponding to circular surfaces  $d'_g$ , are given by the following system of equations:

$$\left. \begin{aligned} 2r^2 \lg\phi + r \left[ (2\lg\phi + 1)h + \frac{\pi c}{\gamma} \right] + \frac{2\lg\phi + 1}{2} h^2 + \\ + \frac{\pi c}{2\gamma} h = \frac{bd'_g}{4\gamma} \left( 2 - \frac{\pi}{2} \lg\phi \right) \end{aligned} \right\} \quad (7)$$

$$\left. \begin{aligned} \frac{2\gamma}{3} \left[ r^3 (2\lg\phi - 1) + (r+h)^3 (2\lg\phi + 1) \right] + \\ + \pi c [r^2 + (r+h)^2] = bd'_g \left[ r \left( 2 - \frac{\pi}{2} \lg\phi \right) - b \right] \end{aligned} \right\} \quad (8)$$

The formulas of Prandtl-Buisman, as well



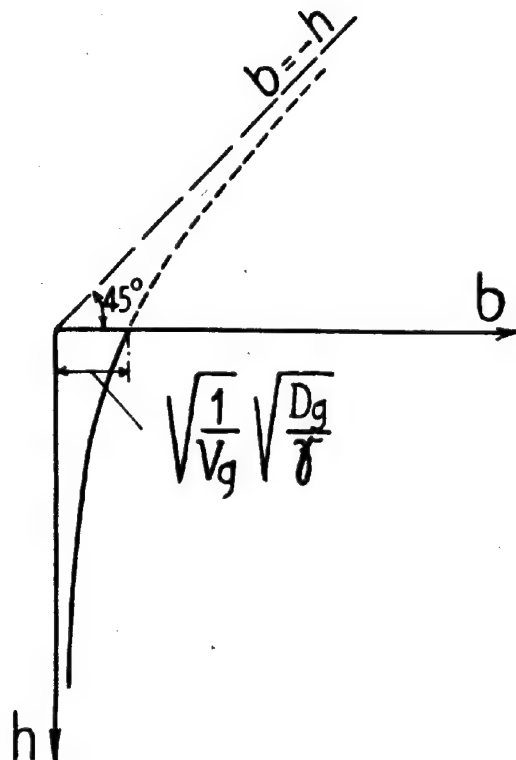


FIG. 5

meter  $D_g/\gamma$ , so that the value of  $D_g/\gamma$  corresponding to an arbitrary line of the net can instantaneously be found. On the other hand, putting  $D_g = b d_g$  (13), the equation (6) gives:

$$\frac{D_g}{\gamma} = V_b b h + V_g b^2 \quad (14)$$

For each value of  $D_g/\gamma$ , the equation (14) represents an hyperbola, with the asymptotes  $b = 0$  and  $b = -h$  (see fig. 5). The hyperbolas cut the axis of the  $b$ 's at the points

$$b = \sqrt{\frac{1}{V_g} \frac{D_g}{\gamma}} \quad (15)$$

With the relation (15) it is possible to draw, next to the scale of the  $b$ 's, a scale of the parameter  $D_g/\gamma$ ; thus the value of  $D_g/\gamma$  corresponding to a given hyperbola of the net, can be found. The values of  $V_g$  and  $\sqrt{V_g}$  are given in the table 1.

Let us now determine the locus of the points  $(b, h)$ , for which the formulas of Andersen (11) and of Buisman (14) give the same value of the ultimate bearing capacity  $D_g = D'_g$ .

Eliminating  $D_g = D'_g$  between the equations (11) and (14) one gets:

$$n_1 b^7 + n_2 b^6 h + n_3 b^5 h^2 + n_4 b^4 h^3 + n_5 b^3 h^4 + n_6 b^2 h^5 + n_7 b h^6 + n_8 h^7 = 0 \quad (16)$$

where  $n_1, n_2, \dots, n_7$  = seven functions of the angle  $\phi$ .

The equation (16) is homogeneous and of the 7th degree. It can be composed in the equation of real or imaginary straight lines going through the origin ( $b = 0, h = 0$ ). In the first quadrant there is but one real straight line. The equation (16) can be written:

$$n_1 + n_2 \frac{h}{b} + n_3 \left(\frac{h}{b}\right)^2 + n_4 \left(\frac{h}{b}\right)^3 + n_5 \left(\frac{h}{b}\right)^4 + n_6 \left(\frac{h}{b}\right)^5 + n_7 \left(\frac{h}{b}\right)^6 = 0 \quad (17)$$

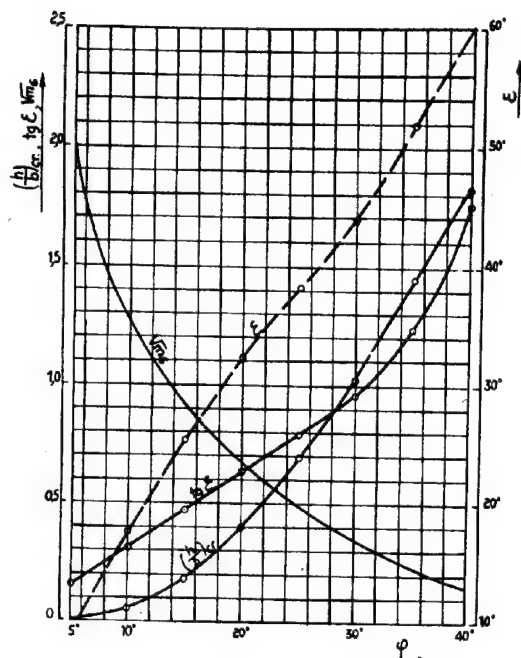


FIG. 6

The values of the coefficients  $n_1$  till  $n_7$  are given in function of  $\phi$  in the table I. The equation (17) has been solved by trying; in this way the values  $h/b$  given in the table I were found.

Finally in a diagram  $b, h$ , the zones of applicability of the formulas of Andersen and of Buisman are separated by a straight line going through the origin. For small foundation depths  $h$ , combined with large footing widths  $b$ , the formula of Andersen gives smaller values and therefore is determining; on the contrary for high values of the ratios  $h/b$  the formula of Prandtl-Buisman must be retained.

The critical values of the ratio  $h/b$  are given in the table I, and also in the diagram of fig. 6. These critical values increasing with the angle  $\phi$ , it means that the range of applicability of the formula of Buisman becomes narrower when the value of the angle  $\phi$  is increasing. With the data of the table I it will be possible to verify rapidly in each real case in what zone it is located and what formula has to be applied.

For practical purposes it is sufficiently correct to assimilate the curves of Andersen

$D_g/\gamma = \text{cte}$  to straight lines. These straight lines are determined by the point ( $h_0 = 0, b_0 = \sqrt{1/V_g} \sqrt{D_g/\gamma}$ ) and by their angle  $\epsilon$  (fig. 4). The value of the angle  $\epsilon$  can easily be found from the consideration that the curve of Andersen cuts the straight line  $h/b = (h/b)_{\text{crit}}$  in the point  $b_1, h_1$  where  $D_g = D'_g$ . This point is defined by

$$\left. \begin{aligned} \frac{h_1}{b_1} &= \left(\frac{h}{b}\right)_{\text{crit}} \\ \frac{D'_g}{\gamma} &= V_b h_1 b_1 + V_g b_1^2 \end{aligned} \right\} \quad (18)$$



$$h_1 = \frac{\sqrt{\frac{D_g}{\gamma}}}{\sqrt{V_b \left(\frac{b}{h}\right)_{crit} + V_g \left(\frac{b}{h}\right)_{crit}^2}} \quad (19)$$

$$b_1 = \frac{\left(\frac{b}{h}\right)_{crit} \sqrt{\frac{D_g}{\gamma}}}{\sqrt{V_b \left(\frac{b}{h}\right)_{crit} + V_g \left(\frac{b}{h}\right)_{crit}^2}} \quad (20)$$

Fig. 4 gives  $\text{tg } \varepsilon = \frac{h_1}{b_0 - b_1} \quad (21)$

The equations (12) (19) (20) and (21) give:

$$\text{tg } \varepsilon = \frac{1}{\sqrt{m_0} \sqrt{V_b \left(\frac{b}{h}\right)_{crit} + V_g \left(\frac{b}{h}\right)_{crit}^2 - \left(\frac{b}{h}\right)_{crit}}} \quad (22)$$

The values of  $\text{tg } \varepsilon$  are given in function of  $\phi$  in the table I and in the fig. 6.

For the cases  $\phi = 20^\circ$ ,  $25^\circ$  and  $30^\circ$ , the fig. 7, 8 and 9 give the straight laws of Andersen  $D_g/\gamma_t = c^t$  and the hyperbolas of Buisman  $D_g/\gamma = c^t$ , and also the straight separation between the respective zones of applicability.

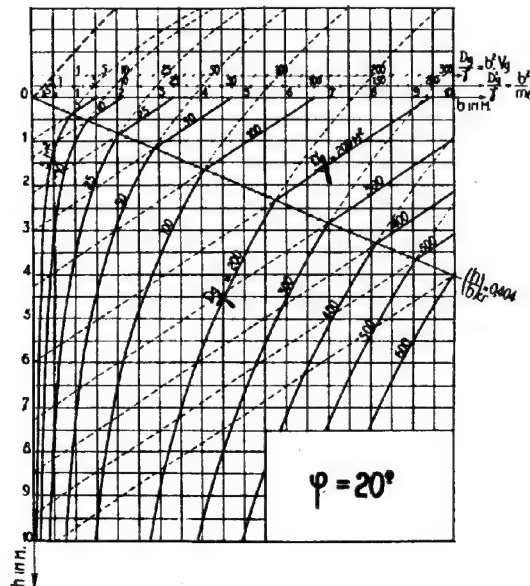


FIG. 7

The use of the fig. 7, 8 and 9 is direct, and doesn't need any other explanation.

It is worthwhile to note that the straight lines  $D_g/\gamma_t = c^t$  intersect the hyperbolas  $D_g/\gamma = c^t$  under a certain angle; this would correspond to an abrupt change in the law of variation of the ultimate bearing capacity. As this capacity is a physical phenomena such an abrupt change is excluded. Thus the indicated combination of the formulas of Andersen and Buisman is itself but an approximation of the problem.

The circular shape adopted by Andersen for the surface of failure is only strictly valid for very small values of  $h/b$ ; on the other hand the surface of rupture consisting of a logarithmic

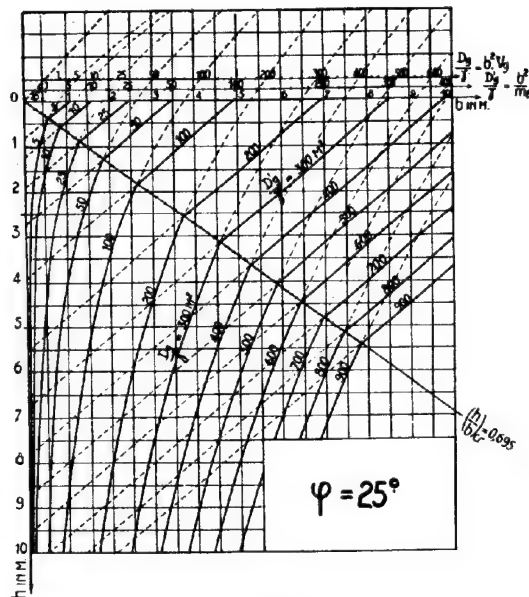


FIG. 8

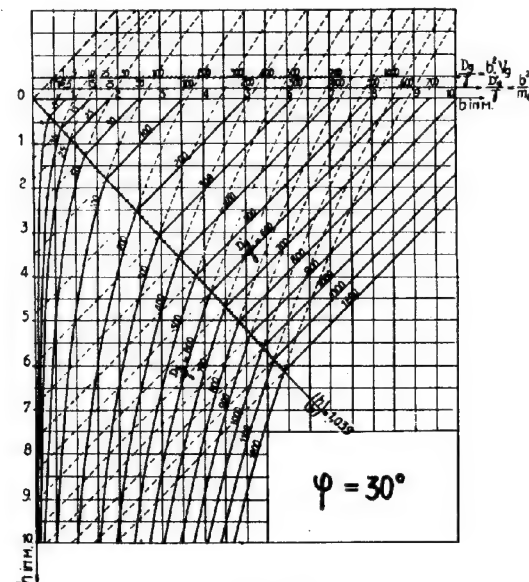


FIG. 9

mic spiral with two straight extensions, is only valid for very high values of  $h/b$ ; for values of  $h/b$  approaching the critical value, the surfaces of failure must have a more complicated shape, intermediate between that of circular surfaces and that of the spiral surfaces; the shape of the surface changing gradually, there will be a smooth junction between the two laws  $D_g/\gamma_t = c^t$  and  $D_g/\gamma = c^t$  in the neighbourhood of the critical line. This junction is necessarily located beyond the point A (fig. 10), and will have the shape of the dotted line. In the neighbourhood of the critical line the formulas of Andersen and of

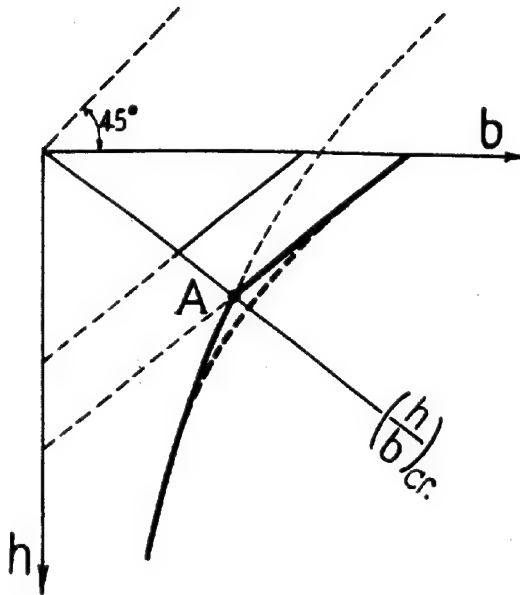


FIG. 10

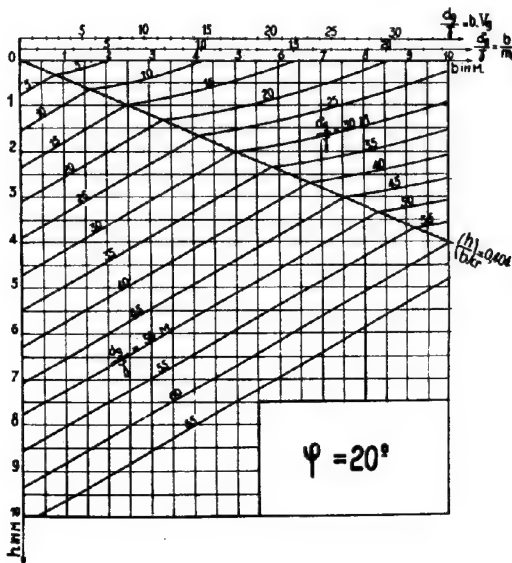


FIG. 11

Buisman both will give too small values; thus it is indicated to take this into account by the choice of the factors of safety.

#### REMARKS.

- 1) Instead of considering the ultimate bearing capacities per linear meter  $D_g$  and  $D'_g$  (t/m), the ultimate bearing capacities per unit of area  $d_g$  and  $d'_g$  (t/m<sup>2</sup>) can also be used.

Then the equation (9) is maintained, but this equation doesn't represent straight lines, but more complicated curves.

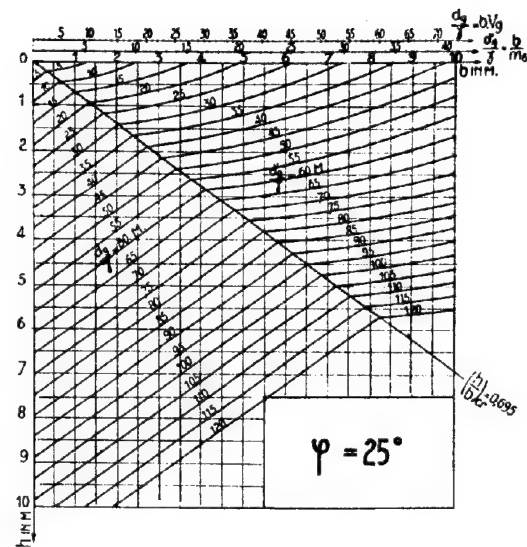


FIG. 12

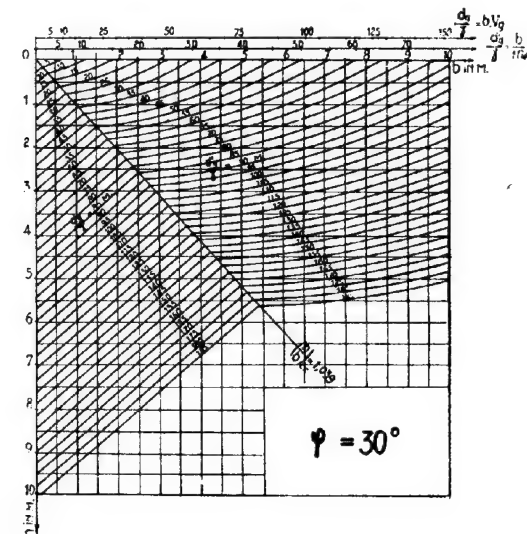


FIG. 13

The equation (6) becomes  $d_g = V_b \gamma h \cdot V_g \gamma b$  (23)

In the diagram  $b, h$  the equation (23) represents a net of parallel straight lines.

The elimination of the parameters  $d_g/\gamma = d'_g/\gamma$  between the equations (9) and (23), gives again the equation of a straight line.

The advantage to consider the parameter  $d_g/\gamma$  (t/m<sup>2</sup>) instead of  $D_g/\gamma$  (t/m) consists in the fact that the formula of Buisman is now represented by a straight line, what is easier when the problems to solve are frequently located in the range of applicability of this formula. For this reason the fig. 11, 12 and 13 represent the diagrams  $h$  in function of  $b$  for the parameters  $d_g/\gamma$ . Apart from that these diagrams are identical to those of the fig. 7, 8 and 9.

- 2) When the value of  $h/b$  becomes very large, then the problem is no longer one concerning



a direct foundation, but one of a deep foundation (piles, foundation-pits). For these latter problems neither of the considered formulas is

applicable, but direct information can be obtained from the results of deep penetration tests in situ.

-o-o-o-o-o-o-

le 5

# IMPROVEMENT OF THE METHOD OF CALCULATION OF THE EQUILIBRIUM ALONG SLIDING CIRCLES.

H. Raedschelders - Ghent ( Belgium ).

## INTRODUCTION.

In controlling the equilibrium of slopes, one has to consider two possible failures. The first is in relation to a failure of the base and can be examined by the theory of the bearing capacity of the soil. The second, called slope failure, will occur when the shearing resistance of the earth along a certain surface is not large enough to make an equilibrium with the own weight of the slope and the waterpressure acting upon it.

We will consider the possibility of a slope failure in case of a well-defined toe-circle and we will propose a method for the determination of the factor of safety of that given slope in case of an homogeneous soil mass.

The shearing resistance of the earth is determined by the equation

$$\tau = c + \sigma \tan \varphi.$$

Often the control of equilibrium along sliding circles is limited to the verification of the equation of the moments about the centre of rotation. The method becomes very simple in case of an angle of internal friction  $\varphi = 0$ . Then we have the equation (fig. 1)

$$W \cdot l_w = c_0 \cdot l_0 \cdot R.$$

where:

$W$  = weight of the body of earth in tons per unit of length of the slope.

$l_w$  = lever arm of the weight  $W$  with reference to the centre  $O$  of the toe circle in meter.

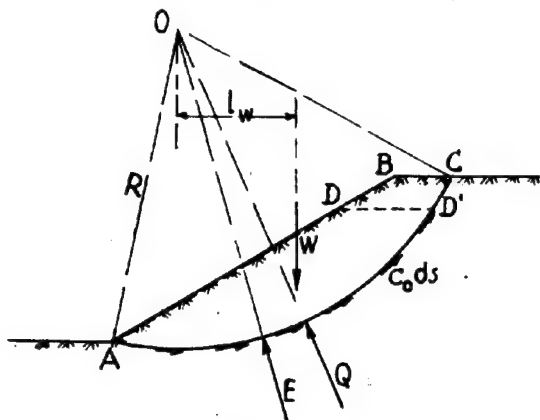


FIG. 1

$c_0$  = cohesion in  $t/m^2$  required to have an equilibrium.

$l_0$  = length of the sliding surface in meter.

$R$  = radius of the sliding circle in meter. On the fig. 1 are also shown the quantities  $Q$  and  $E$ .

$Q$  = resultant of the normal effective stresses (in tons)

$E$  = resultant of the waterpressures on the sliding circle.

The dotted line  $ADD'$  represents the hydrostatic pressure line above the sliding circle.

The factor of safety can then be found by the comparison of the required cohesion with the existing cohesion  $c_e$  of the soil. The latter has to be determined by means of laboratory-tests on undisturbed samples.

The factor of safety can be written :

$$s = \frac{c_e}{c_0}$$

The control of the equilibrium of rotation is insufficient, because each state of equilibrium is controlled by three conditions: the equilibrium of translation along two mutual perpendicular directions (for instance a vertical and an horizontal direction) and the equilibrium of rotation.

In the different methods of controlling the stability of slopes, one or two of the 3 conditions of equilibrium are often overlooked. For instance in the method consisting of cutting the sliding mass into slices by means of pseudo-sliding surface, often only the polygon of forces is drawn, thus taking only into account the conditions of translation. To take notice of the condition of rotation, it is necessary to draw also the pressure line, thus taking into account the value, the direction and the point of application of all forces involved. Fig. 2 shows an example of this method.

The control by means of slices, even when complete, still presents a few inaccuracies : 1) one admits that the effective soil reactions  $K_1 \dots$  on the pseudo-sliding surfaces between the different slices are parallel to the tangent on the sliding circle and that the points of application of these forces are located in the middle third of the height. Thus the point of application is not exactly known and a more or less arbitrary assumption can be made on its account.

2) The reaction  $Q$  is assumed to be a tangent of the  $R \sin \varphi$  circle. This is only true for an elementary part of the surface but not for a certain length : this inaccuracy can be

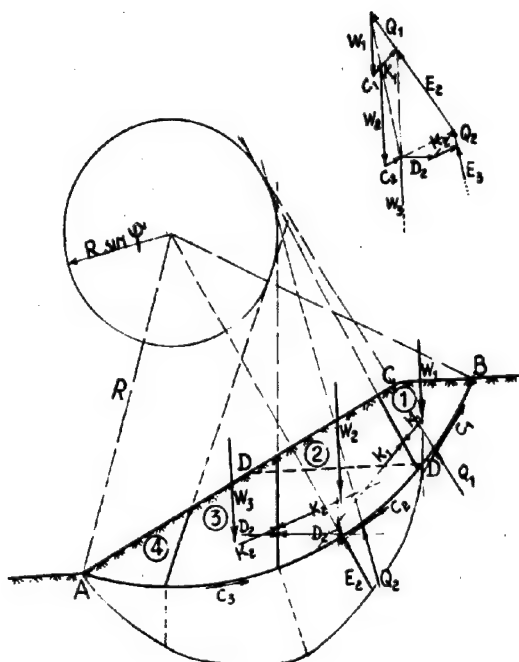


FIG. 2

neglected when a sufficient number of slices is considered.

- 3) The method takes much more time than the control of the moments.
- 4) The factor of safety  $s$  has to be taken on the two elements of the shearing resistance  $\tau$ . For each considered sliding circle one has to repeat the total calculations and drawings for several values of  $s$  and this with new values of  $C$  and  $\varphi$  given by the relations  $c' = \frac{c_e}{s}$  and  $\varphi' = \arctg \frac{[\tau g \varphi]}{s}$ .

One has to make at least two or three trials for each surface.

#### THEORY OF THE NEW METHOD.

In case of an homogeneous soil mass we will suggest a more rapid method, nevertheless taking into account the three conditions of equilibrium.

The simplified method consists in the consideration of only one slice.

The advantage of the method lies in the rapidity of the examination of the equilibrium along a sliding circle without neglecting some important points on theoretical view.

On the same time there are no longer difficulties with the reactions between the different slices, because they are no longer to be considered.

On the other hand the resultant of all the reactions  $Q$  is no longer a tangent of the  $R \sin \varphi$ -circle, but it can be proved that the error is on the side of safety.

We will now consider all the forces acting on the sliding mass of earth :

- 1) The weight of the earth located above the arc is  $W$  tons per unit of length of the slope. This force is acting along a vertical line through the centre of gravity of the area of the slice.

- 2) The resultant of the cohesive forces can no longer be approached by multiplying the cohesion per unit of length of the sliding surface by the length of the surface of the sliding circle. In case of a constant cohesion on the whole surface of sliding, the fig. 3

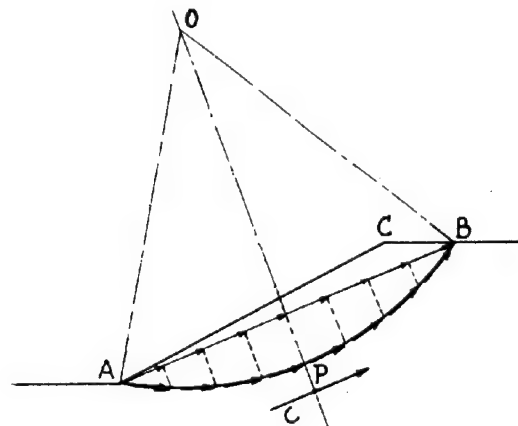


FIG. 3

shows that the resultant can be determined by the equation

$$C = c_0 \cdot \text{chord AB.}$$

The direction is that of the chord AB and the point of application can easily be found by the method of moments about the centre O. By that way we find :

$$OP = R \cdot \frac{\text{arc AB}}{\text{chord AB}}$$

For the method of slices this correction had not to be made because for each slice of a limited length the

factor  $\frac{\text{arc AB}}{\text{chord AB}}$  is nearly equal to 1.

- 3) The waterpressure  $E$  can be computed by means of a flow net, which values make it possible to determine the waterpressure in each point of the sliding surface. This is an exact method for a permeable soil-mass. For cuts in a clay stratum it is safe to consider in each point of the sliding surface an hydrostatic waterpressure corresponding to the surface of the slope and the free water-table existing before the cut was digged, the adaptation of the groundwater to the new situation being very slow.

All these elementary forces are directed to the center of the sliding circle.  $E$  can be found graphically by composing all the elementary forces. By this way we know the resultant in value and direction. The point of application follows from the fact that  $E$  has to go through the centre of the circle.

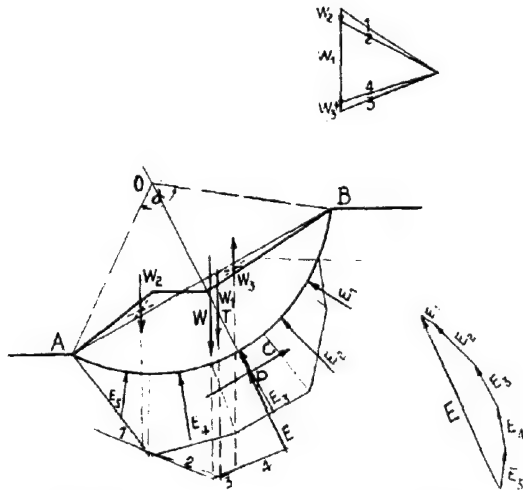
- 4) The resultant  $Q$  can be found by means of the polygone of forces which must be closed with it.

Since the factor of safety will be applied on the two elements of the shearing resistance, one has to do a little "trial and error" work to find that factor. But now the trials are very quick and without any serious calculation.

By means of comparison it will be possible to estimate the importance of the error introduced by the fact that the resultant  $Q$  is not exactly to the  $R \sin \varphi$ -circle.

# PRACTICAL APPLICATION OF THE NEW METHOD.

1) Computation of the weight  $W$  of the sliding earth mass. Since we consider a slope with a width of 1 meter, we must only determine the slice in  $m^2$  and multiply it with the unit weight  $\gamma$ . In all cases the considered surface of the slice can be represented by a sum of a circle-segment and one or more triangles with a positive or negative value (fig. 4). The



surface also in value and direction. The point of application follows from the fact that this resultant has to go through the centre O of the sliding surface.

4) Now we make a graphical composition of all the previous determined forces :  
We draw first W known in value, direction and point of application as indicated under 1). We

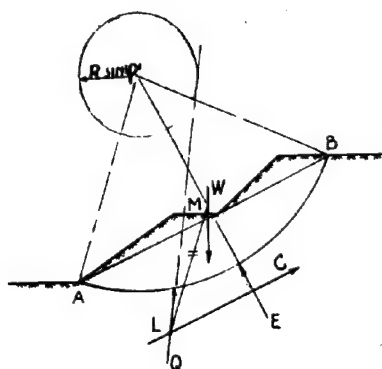


FIG. 7

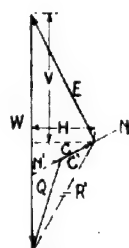


FIG. 7 b

#### Computations

$$S_1 = \frac{\pi R^2 d}{360} - \frac{AC \cdot R \cos \psi}{2}$$

$$= \frac{3.14 \times 0.1 \times 0.8}{360} - \frac{12.5 \times 0.1 \times 0.725}{2} = 21.5 \text{ m}^2$$

$$S_2 = \frac{12.5 \times 0.8}{2} = 6.25 \text{ m}^2$$

$$W_1 = 43.0 \text{ t}$$

$$W_2 = 12.5 \text{ t}$$

$$C = C_0 + AC = 0.3 \times 12.5 = 3.75 \text{ t}$$

$$OM = 3.9 \text{ m}$$

$$OZ = \frac{AC^2}{12.5} = \frac{0.8^2}{12.5} = 7.6 \text{ m}$$

$$H = bR \left[ \sin \psi_1 \sin \psi_2 \right] + \frac{\pi R^2}{2} \left[ \cos 2\psi_1 - \cos 2\psi_2 \right]$$

$$= \frac{\pi R^2}{2} \left[ \left( \frac{\psi_1}{2} - \frac{\psi_2}{2} \right) + \left( \sin 2\psi_1 - \sin 2\psi_2 \right) \right]$$

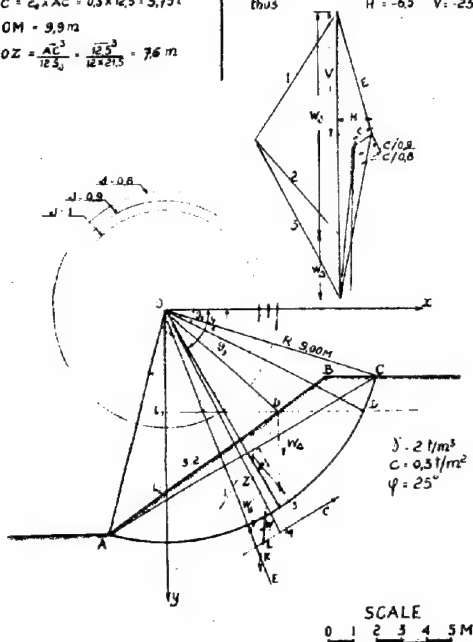
$$V = -bR \left[ \cos \psi_1 - \cos \psi_2 \right] - \frac{\pi R^2}{2} \left[ \frac{\psi_1}{2} - \frac{\psi_2}{2} \right] - \left( \sin 2\psi_1 - \sin 2\psi_2 \right)$$

$$+ \frac{\pi R^2}{4} \left[ \cos 2\psi_1 - \cos 2\psi_2 \right]$$

$$\text{for the line } DD' \quad H_1 = -4.7 \quad V_1 = -7.4$$

$$\text{for the line } AD \quad H_2 = -1.8 \quad V_2 = -16.3$$

$$\text{thus} \quad H = -6.5 \quad V = -23.7$$



Example of proposed method

FIG. 8 a

compute the value, direction and point of application of E as explained under 3). We know the direction of C, and also its point of application, because these two quantities are independent of the unknown required cohesion  $c_0$ .

On the other hand composing the two known forces W and E, as done in fig. 7b we get the force R. The working line of R goes through the point of intersection M (fig. 7) of the forces W and E. This line cuts the working line of C in the point L. The unknown force Q must go through this point L. Farther this same force is assumed to be tangent to the circle  $R \sin \psi$ .

Now we adopt an arbitrary value for the safety coefficient s, and obtain then easily

$$c_0 = \frac{C_0}{s}$$

From that, one gets  $C' = c_0 \cdot \text{chord } AB$ , which is put on the line  $HN'$  of fig. 7b. Now we try to close the polygon with a direction of Q given by a tangent on the circle  $R \sin \psi$  through the point C (fig. 7), the angle  $\psi'$  being given by the equation

$$\psi' = \text{arc.tg} \left[ -\frac{\text{tg} \psi}{s} \right]$$

$\sin \psi'$  can be found immediately by the graphs of fig. 6. Generally the diagram of fig. 7b will not close, because the value of s has been arbitrarily adopted. But with a few try-

#### Computations

$$W_1 = \frac{2.6 \times 0.3}{2} = 0.39 \quad 3.89 \times 2 = 7.8 \text{ t}$$

$$W_2 = \frac{2.6 \times 2.7}{2} = 3.51 \quad 7.88 \times 2 = 15.76 \text{ t}$$

$$W_3 = \frac{3.0 \times 1.85}{2} = 2.78 \quad 3.0 \times 2 = 6.0 \text{ t}$$

$$W_4 = \frac{3.8 \times 0.8}{2} = 1.52 \quad 5.91 \times 2 = 11.82 \text{ t}$$

$$E_1 = \frac{1.7 \times 2}{2} = 1.7 \text{ t} \quad C_1 = \frac{2.6 \times 0.3}{360} \times 2 \times 25^\circ = 1.32 \text{ t}$$

$$E_2 = \frac{2.6 \times 2.3}{2} = 6.4 \text{ t} \quad C_2 = 25^\circ = 1.38 \text{ t}$$

$$E_3 = \frac{3.6 \times 1.5}{2} = 4.2 \text{ t} \quad C_3 = 22^\circ = 1.32 \text{ t}$$

$$E_4 = \frac{5.4 \times 0.3}{2} = 0.81 \text{ t} \quad C_4 = 21^\circ = 1.26 \text{ t}$$

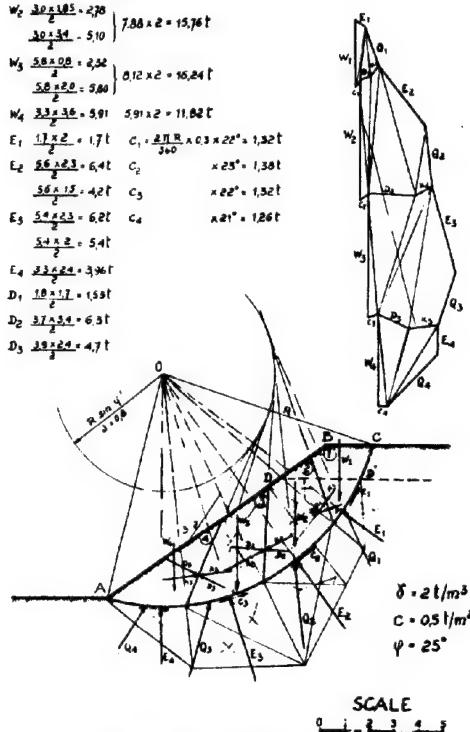
$$E_5 = \frac{5.4 \times 2}{2} = 5.4 \text{ t}$$

$$E_6 = \frac{2.3 \times 2.4}{2} = 2.76 \text{ t}$$

$$D_1 = \frac{1.8 \times 1.7}{2} = 1.53 \text{ t}$$

$$D_2 = \frac{3.7 \times 3.4}{2} = 6.3 \text{ t}$$

$$D_3 = \frac{2.8 \times 2.4}{2} = 4.7 \text{ t}$$



Example of method of slices

FIG. 8 b

ings one finds rapidly the value of  $s$  closing the diagram and thus corresponding to the real margin of safety.

#### EXAMPLE.

Figures 8 a and b give an example of all the computations and drawings necessary for

the determination of the factor of safety for a determined sliding-circle. We find  $s = 0.8$ .

The same examination has been done with the method of slices, also giving  $s = 0.8$ .

The method of slices asked 2 hours, for one trial. The complete determination by three trials asked 5 hours.

The proposed method gives the real value of the coefficient of safety within 1½ hour.

-o-o-o-o-o-o-

## I e 6

### THE $\phi = 0$ ANALYSIS OF STABILITY AND ITS THEORETICAL BASIS.

A. W. Skempton M.Sc., A.M.I.C.E., F.G.S.  
University Reader in Soil Mechanics and  
Assistant Professor at Imperial College,  
University of London.

#### I. INTRODUCTION.

It is known that saturated clays when tested under conditions of no water content change behave, with respect to the applied stresses at failure, as purely cohesive materials with an angle of shearing resistance  $\phi$  equal to zero. This experimental observation is the basis for a method of stability analysis which is now becoming widely used and which is known as the  $\phi = 0$  analysis of stability.

Experience is showing that the analysis is reliable in practice; leading to correct estimates of bearing capacity of clay soils and of earth pressure, and giving satisfactory results for the factor of safety of clay slopes. Yet there are important limitations to the range of application of the  $\phi = 0$  analysis and to the soils in which it can be applied. These limitations must be fully appreciated in the application of the method to practical problems.

#### II. EXPERIMENTAL EVIDENCE OF $\phi = 0$ .

In 1915 Langtry Bell carried out a series of shear box tests on various cohesive soils in which a restricted opportunity for water content change under the normal pressure was allowed. These tests showed that, at least for the softer clays, the angle of shearing resistance  $\phi$  was small.

Bell also presented equations for active and passive earth pressure in cohesive soils and for their bearing capacity. He did not, however, conclude that  $\phi$  should be taken as zero for clay soils in the analysis of these problems.

So far as the author is aware this assumption was first made explicitly by Fellenius in 1922 in connection with the stability of clay slopes, when he put forward the equation shown in Fig. 5 (a). Later, in 1927, Fellenius dealt with the problem more fully and, in particular, he derived the concept of the stability number  $c/\gamma H$  which of great significance in earth pressure and slope stability in clays.

But at this time little was known of the

shear properties of clays and there was insufficient evidence for the acceptance of an analysis based on the  $\phi = 0$  assumption. The problem was, in fact, not placed on a firm experimental basis until 1932 when Terzaghi published the tests results shown in Fig. 1. These demonstrated that when a saturated clay is tested in the triaxial apparatus, under conditions of no water content change (the so-called "immediate" or "quick" triaxial test), the angle of shearing resistance is zero; although the angle of shearing resistance obtained in a test where the clay is allowed to consolidate under the applied stress is very considerably greater than zero.

Subsequent work has confirmed this result (see, for example, Jurgenson 1934a, Golder and Skempton 1948), and it follows that in saturated clays, tested under conditions of no water content change, the criterion of failure may be expressed in the form

$$\sigma_1 - \sigma_3 = 2c \quad (1)$$

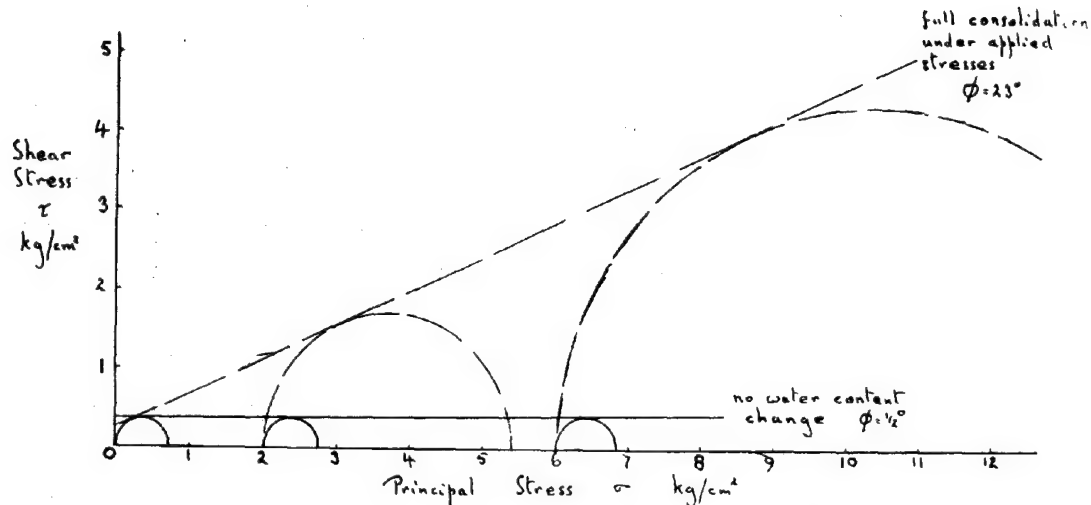
where  $\sigma_1$  and  $\sigma_3$  are the major and minor applied principal stresses at failure and  $c$  is the "cohesion" or shear strength of the clay at the particular water content of the test.

An analysis of stability can therefore be based upon equation (1) and will lead to correct results with respect to the applied stresses at failure, provided the basic conditions implicit in this equation are complied with.

It should be noted that  $(\sigma_1 - \sigma_3)$  is the compression strength of the clay and therefore  $c = \frac{1}{2}$  compression strength (2) This result provides a ready means of determining the cohesion of a clay sample, since the compression strength can easily be measured.

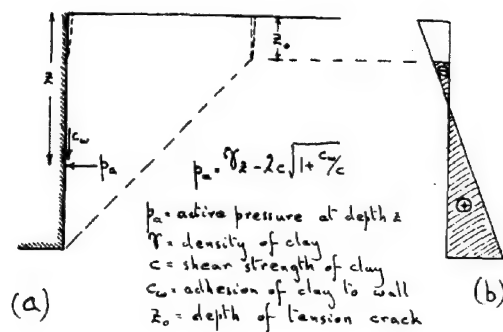
#### III. THE $\phi = 0$ ANALYSIS OF STABILITY.

Based upon equation (1) the  $\phi = 0$  analysis has been developed for the calculation of active and passive pressure and bearing capacity of clays and the calculation of factors of safety in clay slopes. The methods are summarised in the following paragraphs:



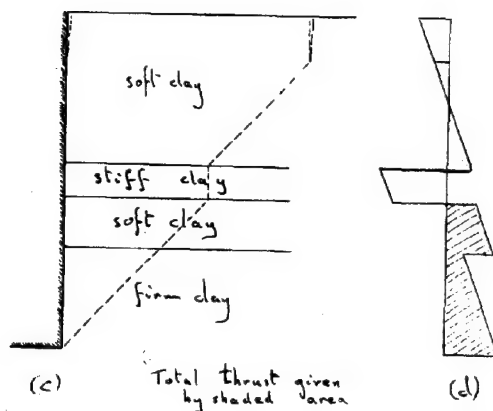
Triaxial Tests on Clay, showing  $\phi = 0$  (approx.) with no Water Content Change. (Terzaghi 1932)

FIG. 1



(a)

(b)



(c)

Total thrust given by shaded area

(d)

Application of  $\phi = 0$  Analysis to Calculation of Active Earth Pressure in Clays.

FIG. 2

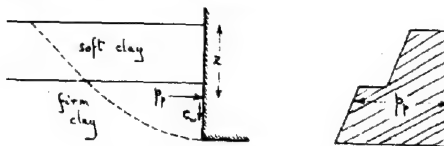
- 1) Active earth pressure (Fig. 2). For a vertical wall with horizontal backing

$$P_a = \gamma z - 2c \sqrt{1 + c_w/c} \quad (3)$$

This gives a pressure distribution with depth as shown in Fig. 2(b). With a tension crack of depth  $z_0$ , the total thrust on the wall is equal to the algebraic sum of the shaded area. With variable strata a diagram such as that shown in Fig. 2(d) is obtained. The total thrust is again equal to the algebraic sum of the shaded areas.

The distribution of the total thrust depends on the mode of yield of the wall.

- 2) Passive earth pressure (Fig. 3)



$$p_p = \gamma z + 2c \quad (c_w = 0) \\ = \gamma z + 2.4c \quad (c_w = \frac{1}{2}c) \\ = \gamma z + 2.6c \quad (c_w = c)$$

$p_p$  = passive pressure at a depth  $z$   
Other symbols as in Fig. 2

Application of  $\phi = 0$  Analysis to Calculation of Passive Pressure in Clays.

FIG. 3

$$P_p = \gamma z + 2c \quad (c_w = 0) \quad (4) \\ = \gamma z + 2.4c \quad (c_w = \frac{1}{2}c) \\ = \gamma z + 2.6c \quad (c_w = c)$$

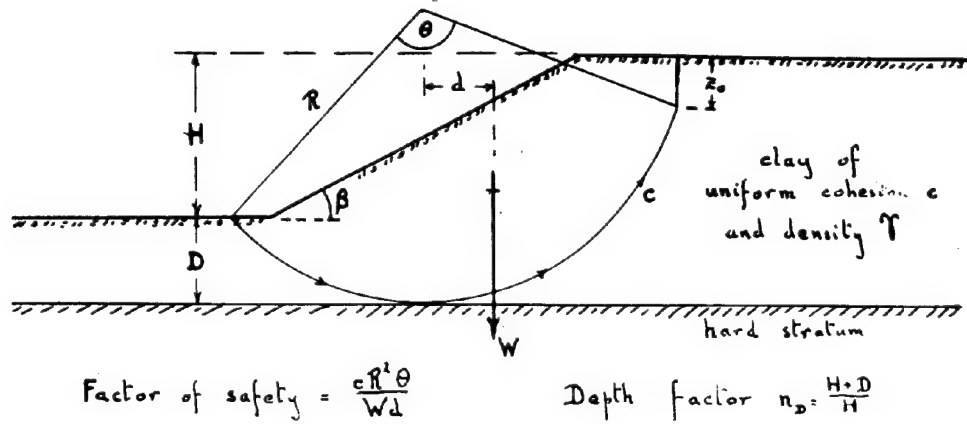
the coefficients of  $c$  have been derived by Packahaw (1946) from the modified wedge theory given by Terzaghi (1943).

- 3) Bearing capacity of shallow foundations (Fig. 4)

$$q_u = \gamma z + (2 + \pi) c \quad \text{strip footings} \quad (5)$$

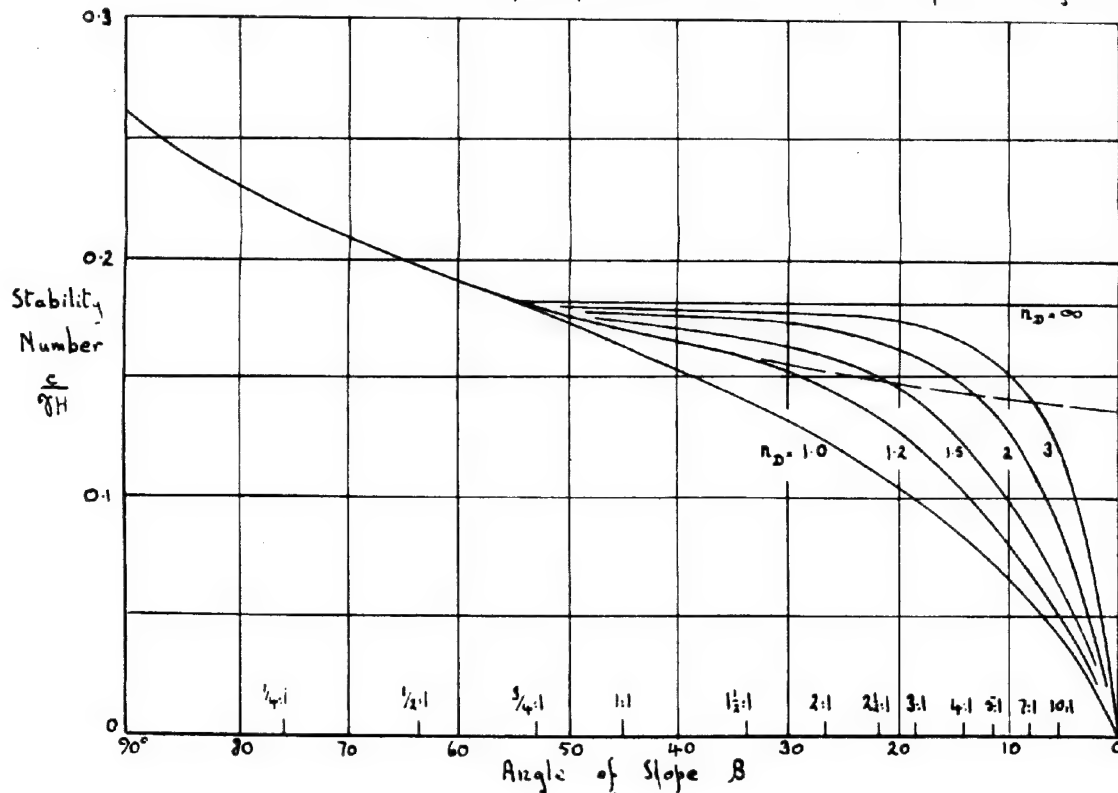
$$q_u = \gamma z + 6.7c \quad \text{square footings} \quad (6)$$

The strip footings equation was introduced by



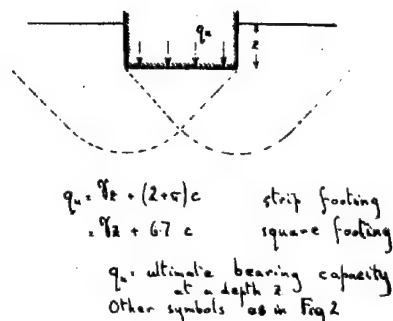
(b) Stability Number Chart

Allow for tension crack by appropriate reduction in  $c$   
 Use dotted line if slip circle is constrained to pass through toe



$\phi = 0$  Analysis in Slopes of Uniform Clay.  
 (Fellenius 1927 and Taylor 1937)

FIG.5



Application of  $\phi = 0$  Analysis to Calculation of Ultimate Bearing Capacity in Clays.

FIG. 4

Jurgenson (1934 b) from a theoretical analysis by Prandtl (1920). The square footing equation is based upon experimental work by Golder (1941) and Terzaghi (1942) and a field investigation by Skempton (1942). With variable strata an average value of  $c$  in a depth equal to the width of the footing can generally be taken.

An alternative approach is to calculate the shear stresses  $(\sigma_1 - \sigma_2)/2$  in the ground beneath the foundation and ensure that at no point is the stress in excess of the cohesion of the clay (Cooling 1942).

4) Stability of slopes (Figs. 5 and 6)

For homogeneous clays the problem has been solved by Taylor (1937), Fig. 5, following the original work of Fellenius. For variable strata the procedure is to analyse a chosen slip circle, as shown in Fig. 6, and then re-

peat with other circles until a minimum factor of safety has been established.

#### IV. LIMITATIONS OF THE $\phi = 0$ ANALYSIS.

The foregoing methods of analysis have been applied with success in practical problems. (see Skempton and Golder 1948 for a summary of ten field examples). It must, however, be realised (a) that the analyses are based on the assumption that the soil behaves as if  $\phi = 0$  and (b) and there are three important limitations to this assumption. These limitations are:

1) For fully saturated clays the angle of shearing resistance is zero only when there is no water content change under the applied stresses. The rate of consolidation of clays is so small that, in most cases, the change in water content during construction is negligible. Therefore the  $\phi = 0$  analysis applies, from this point of view, almost exactly to the conditions obtaining immediately after construction. Thus the bearing capacity of a foundation when the structure is completed, the stability of a dock wall after dredging in front of the wall has been carried out, or the stability of a cutting after excavation is completed, are all given correctly by the  $\phi = 0$  analysis.

But with time water content changes will take place under the changed stress-conditions, and the shear strength of the clay will progressively alter from that used in the analysis. In the case of a foundation the change will be due to consolidation and the  $\phi = 0$  analysis is therefore conservative in that it gives the lower limit of bearing capacity. In some problems it is justifiable to allow for the increase in strength during construction (see, for example, Bishop 1948). In the case of dock walls and cuttings, however, the

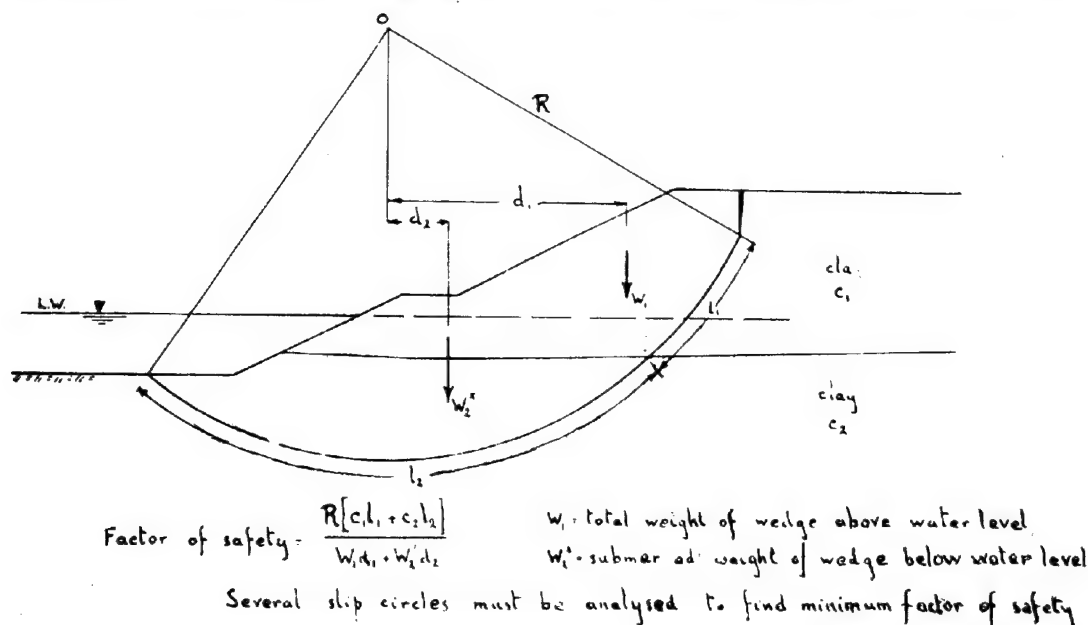


FIG. 6



general tendency may sometimes be a reduction in strength, and this possibility must be carefully considered in design.

The special case of stiff-fissured clays, where the changes in strength with time are great, is considered in another paper by the author (Skempton 1948 b).

2) Even in fully saturated clays, tested under conditions of no water content change, the true angle of internal friction  $\phi_f$  of the clay is not zero. Although the clay, at any particular water content, behaves with respect to the applied stresses at failure as if it were a purely cohesive material (when tested under these conditions) its behaviour is at all times controlled by the true cohesion and true angle of internal friction and the effective stresses. As shown by Terzaghi (1936) the presence of the true internal friction is apparent from the observation that the shear planes in a compression test specimen are inclined to the horizontal at angles greater than  $45^\circ$ , ( $45^\circ$  corresponding to the case of true non-frictional materials). The inclination  $\alpha$  is in fact theoretically equal to  $(45^\circ + \frac{1}{2}\phi_f)$  for all tests including those where no water content change take place and the angle of shearing resistance is zero.

In tests on individual undisturbed samples it is often difficult to obtain consistent values of  $\alpha$  owing to lack of homogeneity. The author has, however, examined a number of cases where reasonably consistent results have been obtained and it appears that a significant correlation exists between  $\phi_f$  and porosity (Skempton 1948a). In Fig. 7 the results for saturated clays are given (x). These soils without exception, were found to have a zero angle of shearing resistance although as will be seen, the shear planes were in all cases inclined at angles greater than  $45^\circ$ .

It therefore follows that whereas the applied stresses at failure are given correctly by the  $\phi = 0$  analysis, according to equation (1), the shear surface is controlled by the

true angle of friction  $\phi_f$ : an angle which is greater than zero. Thus the  $\phi = 0$  analysis will not, in general, lead to a correct prediction of the actual shear surface, nor will the analysis, theoretically, give a correct factor of safety if the values of  $c$  are applied to an observed shear surface. In practice the errors arising from this latter point may often, though not always, be small. 3) Clays which are not fully saturated do not give an angle of shearing resistance equal to zero when tested under conditions of no overall water content change. Thus in many problems associated with earth dams, embankments and compacted bases and sub-grades the  $\phi = 0$  analysis will not apply. In addition it appears that some silts, even when fully saturated, show an angle of shearing resistance in the immediate triaxial test greater than zero (Golder and Skempton 1948). For these soils also the  $\phi = 0$  analysis does not apply.

#### V. PRACTICAL EXAMPLES.

Three practical examples will be taken as illustrative of the above points.

1) Sau Brink Cut. (Skempton 1945). Here the actual shear surface was determined with reasonable accuracy, and the shear strengths of the strata were measured as one-half the unconfined compression strength. Using the  $\phi = 0$  analysis the factor of safety was found to be 1.0, which is correct. But the slip surface corresponding to this factor of safety lays definitely behind the actual slip surface. This is analogous to the fact that the  $45^\circ$  plane in a compression test is flatter than the actual shear plane. Moreover the factor of safety as calculated on the actual slip surface was 1.30

x.) Lack of homogeneity is largely eliminated in remoulded clays and their  $\phi_f$  porosity relation is therefore also given in Fig. 7. It is clear that a definite correlation exists for these samples.

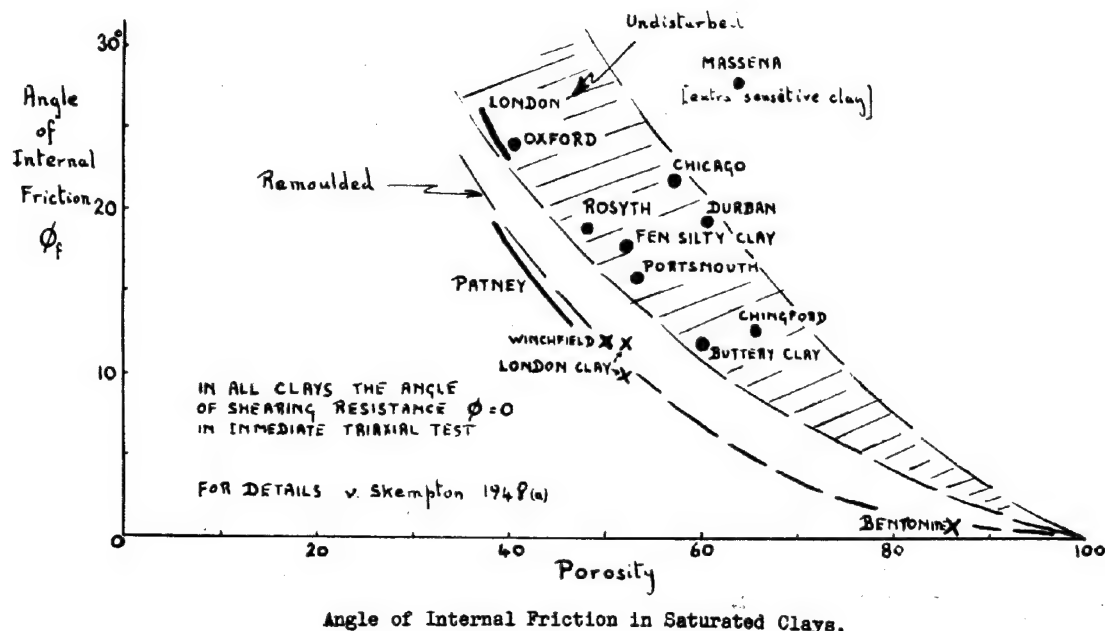


FIG. 7

In triaxial compression tests carried out with no water content change  $\phi$  was zero. Yet the shear planes were inclined at angles of more than  $45^\circ$  without exception.

2) Chicago Subway. (Peck 1942). Here the earth pressure as calculated on the  $\phi = 0$  analysis agreed well with the observed loads in the struts. The conclusion drawn by Peck was that the clay had an "angle of internal friction" equal to zero. In the author's opinion the correct conclusion is that during the few weeks of observation no appreciable water content change could take place and the essential basis for the  $\phi = 0$  assumptions in saturated clays was therefore complied with. Nevertheless the clay would almost certainly have a true angle of friction  $\phi_f$  in excess of zero. The strut load observations could not possibly supply any evidence on this point. But the author would be surprised if the shear planes in the compression tests were inclined at  $45^\circ$ , or if any more elaborate analysis such as that developed by Hvorslev (1937) would show that  $\phi_f = 0$  for this clay.

3) Wynne-Edwards' Critical Height Tests. In these tests, which are described by Skempton and Golder (1948), it was found that the critical height of a vertical bank of remoulded London Clay was 8 ft. This result is in reasonable agreement with the height calculated on the  $\phi = 0$  analysis using the measured values of  $c$  and  $\gamma$  for the clay and the observed depth of tension crack. Yet the slip plane, which was well defined in each of the three tests, was inclined at  $51^\circ$ , and not at  $45^\circ$ . Moreover the value of  $\phi_f$ , deduced from the relation  $\alpha = 45^\circ + \frac{1}{2}\phi_f$  is  $12^\circ$  and this is in close agreement with the values of  $\phi_f$  found from the inclination of the shear planes in compression specimens of remoulded clay at the particular porosity (52 percent), of the clay used in the critical height tests, see Fig. 7.

## VI. CONCLUSIONS.

1) When tested with no water content change a saturated clay behaves with respect to the applied stresses at failure as if it were a purely cohesive material with an angle of shearing resistance  $\phi$  equal to zero.

Consequently an analysis of stability based on this result will give correct results for earth pressure, bearing capacity, or the factor of safety of a clay slope for the period when water content changes are negligible. This will often be the case for the conditions at the completion of construction.

2) With increasing time after construction water content changes may occur which lead to different strengths in the clay from those assumed in the  $\phi = 0$  analysis. These should be allowed for as far as possible in the design. The special case of stiff-fissured clays is an extreme example of this effect.

3) The fact that the  $\phi = 0$  analysis leads to a correct evaluation of stability under conditions of no water content change does not in any way prove that the clay has a true angle of internal friction  $\phi$  equal to zero. On the contrary there is evidence that most clays exhibit an angle of internal friction definitely in excess of zero. This leads to the conclusion that, in so far as the position of the shear surface is controlled in part by the angle of internal friction (friction being a directional porosity and not merely a coefficient representing increase in shear strength under increasing pressure), the  $\phi = 0$  analysis will

lead to an incorrect placing of the shear surface. It is also concluded that a  $\phi = 0$  analysis based on the actual shear surface will, at least theoretically, lead to an incorrect estimate of the forces and of stability.

The correct estimate of stability will be obtained from a  $\phi = 0$  analysis using the shear surface compatible with the  $\phi = 0$  assumption, even though this surface is itself not coincident with the true slip surface.

4) The  $\phi = 0$  analysis cannot be applied to partially saturated clays, nor to those silts which show an angle of shearing resistance greater than zero in the immediate triaxial test.

5) It may be possible to evolve an analysis which overcomes the difficulties expressed in conclusions (3) above. Meanwhile, provided its limitations are appreciated, the  $\phi = 0$  analysis is a method of great value in civil engineering design.

## REFERENCES.

- BISHOP, A.W. 1948. "Some factors involved in the Design of a Large Earth Dam in the Thames Valley".  
2nd Int. Conf. Soil Mechanics.
- BELL, A.L. 1915. "The Lateral Pressure and Resistance of Clay and the Supporting Power of Clay Foundations".  
Min. Proc. Inst. C.E. Vol. 149. p. 233
- COOLING, L.F. 1942. "Soil Mechanics and Site Explorations". Journ. Inst. C.E. Vol. 18 p. 37.
- PELLENIUS, W. 1922. Statens Järnvägars Geotekniska Kommission, Stockholm.
- PELLENIUS, W. 1922. "Erdstatistische Berechnungen" W. Ernst. Berlin.
- GOLDER, H.Q. 1941. "The Ultimate Bearing Pressure of Rectangular Footings".  
Journ. Inst. C.E. Vol. 17. p. 161.
- GOLDER, H.Q. and SKEMPTON A.W. 1948. "The Angle of Shearing Resistance in Cohesive Soils for Tests at Constant Water Content".  
2nd Int. Conf. Soil Mechanics.
- HVORSLEV, M.J. 1937. "Über die Festigkeitseigenschaften gestörter bindiger Boden".  
Ingeniörvidenskabelige Skrifter. A. No. 45. Copenhagen
- JURGENSEN, L. 1934 (a) "The Shearing Resistance of Soils".  
Journ. Boston Soc. C.E. Vol. 21. p. 242
- JURGENSEN, L. 1934 (b) "The Application of Theories of Elasticity and Plasticity to Foundation Problems".  
Journ. Boston Soc. C.E. Vol. 21. p. 206.
- PACKSHAW, S. 1946. "Earth Pressure and Earth Resistance". Journ. Inst. C.E. Vol. 25 p. 233
- PECK, R.B. 1942. "Earth Pressure Measurements in Open Cuts, Chicago Subway".  
Proc. Am. Soc. C.E. Vol. 68. p. 900
- PRANDTL, L. 1920. "Über die Härte plastischer Körper". Nachr. Königl. Gesell. Wiss. Göttingen. Berlin.
- SKEMPTON, A.W. 1942. "An Investigation of the bearing Capacity of a Soft Clay Soil".  
Journ. Inst. C.E. Vol. 18. p. 307.
- SKEMPTON, A.W. 1945. "A slip in the West Bank of the Eau Brink Cut".  
Journ. Inst. C.E. Vol. 24. p. 267.
- SKEMPTON, A.W. 1948. (a) "A study of the Immediate Triaxial Test on Cohesive Soils".  
2nd Int. Conf. Soil Mechanics.
- SKEMPTON, A.W. 1948 (b) "The Rate of Softening in Stiff-Fissured Clays, with Special Reference to London Clay".  
2nd Int. Conf. Soil Mechanics.
- SKEMPTON, A.W. and H.Q. Golder, 1948. "Practical Examples of the  $\phi = 0$  Analysis of Sta-

- bility of Clays".  
 2nd Int. Conf. Soil Mechanics.  
 TAYLOR, D.W. 1937. "Stability of Earth Slopes".  
 Journ. Boston Soc. C.E. Vol. 24, p. 197.  
 TERZAGHI, K. 1932. "Tragfähigkeit der Flach-  
 grundungen".  
 Int. Assoc. Br. Struct. Eng.

- p. 559 Paris  
 TERZAGHI, K. 1942. Discussion of paper by A.W.  
 Skempton (1942).  
 Journ. Inst. C.E. Vol. 18 p. 572.  
 TERZAGHI, K. 1943. "Theoretical Soil Mechanics"  
 John Wiley, New York.

-o-o-o-o-o-o-

le 7

# A SIMPLIFIED METHOD FOR COMPUTING THE BEARING CAPACITY OF THE SOIL SUPPORTING FOOTINGS OR PIERS

L. MARIVOET  
 Ghent ( Belgium ).

## INTRODUCTION.

In engineering practice, it is often useful to dispose of a simplified method for estimating rapidly the bearing capacity of the soil beneath footings or piers.

By this estimation two main conditions are to be taken in consideration: firstly the foundation load will be limited in such a way that shear failure and loss of stability of the soil cannot occur, and secondly the foundation must be designed to distribute the load so that dangerous settlements of the superstructure are prevented.

The ultimate value of the bearing capacity of the soil and the magnitude of the settlements depend not only on the mechanical properties of the soil, but also on the size of the loaded area, its shape, and its location with reference to the surface of the soil. It is evident that settlements are dependent on the allowed unit load.

In order to reduce the time required to solve both problems of stability and deformation of the soil, for some practical cases of loading conditions, diagrams are presented, which greatly simplify the use of formulas.

## BASIC FORMULAS.

### 1) The bearing capacity of the soil.

In accordance with the investigations of Prandtl and Buismann, M. De Beer obtained a general formula for the ultimate bearing capacity of the soil supporting a continuous and centric loaded footing with a width  $b$ . In that formula, it is assumed that the shearing resistance  $s$  of the soil is determined by the equations:

$$s = c + p_b \cdot \operatorname{tg} \varphi + (\sigma - p_b) \operatorname{tg} \varphi', \text{ when } \sigma > p_b, (1)$$

$$s = c + \sigma \cdot \operatorname{tg} \varphi', \text{ when } \sigma > p_b, (2)$$

wherein:

- $c$  = the cohesion
- $\varphi$  = the angle of internal friction
- $\varphi'$  = the "apparent" angle of friction
- $\sigma$  = the effective normal stress
- $p_b$  = the effective normal stress beside the base of the footing.

For cohesionless soils ( $c = 0$ ), M. De Beer obtains for the ultimate bearing capacity  $d_r$ , the following formula:

$$d_r = V''_b \cdot p_b + V'_g \cdot \gamma_k \cdot b \quad (3)$$

in which:

- $b$  = the width of the footing.
- $\gamma_k$  = the unit weight of the earth below the footing, in correlation with effective normal stress.

$V''_b$  and  $V'_g$  = factors which depend on  $\varphi$  and  $\varphi'$

$$V'_g = \left[ e^{\pi \operatorname{tg} \varphi'} \cdot \operatorname{tg} \left( \frac{\pi}{4} + \frac{\varphi'}{2} \right) - 1 \right] \frac{\operatorname{tg} \varphi}{\operatorname{tg} \varphi'} - 1 \quad (4)$$

An analytic expression of the factor  $V'_g$ , whose values depend only on  $\varphi'$ , has been elaborated by Prof. Raess. Some values of  $V'_g$ , obtained by means of this expression, are contained in table I. Corresponding values of  $V''_b$ , given by (4) for the case  $\varphi = 30^\circ$ , are also indicated.

TABLE I.

$\varphi'$	$V''_b$	$V'_g$	$\varphi'$	$V''_b$	$V'_g$
$50^\circ$	4,7	0,2476	$20^\circ$	9,6	3,4522
$10^\circ$	5,8	0,7233	$25^\circ$	13,0	7,1634
$15^\circ$	7,3	1,6413	$30^\circ$	18,2	15,190

### 2) The settlements.

The final settlement  $Z$  of a rigid footing may be computed from the Terzaghi formula:

$$Z = \int_0^h \frac{dh}{C} \cdot 2,3 \cdot \log \frac{\sigma_0 + i \cdot \Delta p}{\sigma_0} \quad (5)$$

wherein:

- $C$  = coefficient of compressibility
- $dh$  = thickness of an elementary layer
- $\sigma_0$  = original effective stress upon the layer  $dh$ , located at a depth  $z$  below the base of the footing.
- $\Delta p$  = increase of the effective stress at the level of the base.
- $i$  = influence value of the surcharge  $\Delta p$ , on the vertical normal stress at a depth  $z$ .
- $\sigma_0 + i \cdot \Delta p$  = final effective vertical stress upon the layer  $dh$  (depth  $z$ ). At the level of the base ( $z = 0$ ), where the influence value  $i = 1$ , and the original effective

vertical stress  $\sigma_0 = p_0$ , acts a unit load:

$$p = (\sigma_0 + 1 \cdot \Delta p)_0 = p_0 + \Delta p.$$

#### INFLUENCE VALUE $i$ DUE TO A SURFACE LOAD $\Delta p$ .

The vertical normal stress increase  $d\sigma_z$  at an arbitrary point A, located at a depth  $z$  below an elementary surface  $dS$  of a loaded area  $S$ , which carries a load  $\Delta p$ , can be obtained by the Boussinesq-Buisman formula:

$$d\sigma_z = \frac{2 dS}{\pi z^3} \cdot \cos^3 \theta \cdot \Delta p, \quad (6)$$

wherein  $\theta$  is the angle between the vertical axis through the point A and the vector (A,  $dS$ ).

The influence value  $i$  for the point A is obtained by integration of the expression (6) over the whole loaded area  $S$ :

$$\sigma_z = \iint_S d\sigma_z = \iint_S \frac{2 dS}{\pi z^3} \cdot \cos^3 \theta \cdot \Delta p = i \cdot \Delta p \quad (7)$$

It has been proved (Voitus van Hamme, Delft) that for some particular points of a continuous, a rectangular, a square or a circular footing, the settlements computed in using the formula (3), are practically independent of the law of distribution of the contact pressure over the base of the footing. In these particular points the settlements may then be computed in the assumption that the distribution of the contact pressure is uniform. Further by absolute rigidity of the footing, the settlements will be uniform and equal to these calculated for the particular points. The location of these points is indicated in figure 1. (points P). The following

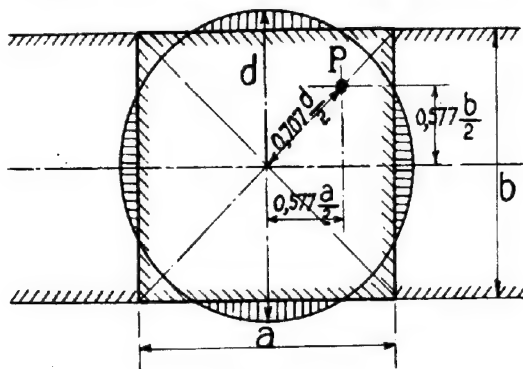


FIG. 1

TABLE II

Influence values  $i$ .

continuous footing width $b$		square footing side $a$		circular footing diameter $d$	
depth $\frac{z}{b}$	$i$	depth $\frac{z}{a}$	$i$	depth $\frac{z}{d}$	$i$
0	1,00	0	1,00	0	1,00
0,2	0,95	0,2	0,90	0,2	0,87
0,4	0,82	0,4	0,67	0,4	0,64
0,6	0,70	0,6	0,52	0,6	0,48
0,8	0,62	0,8	0,40	0,8	0,37
1,0	0,56	1,0	0,33	1,0	0,28
1,2	0,50	1,2	0,26	1,2	0,23
1,4	0,45	1,4	0,21	1,4	0,19
1,6	0,41	1,6	0,18	1,6	0,16
1,8	0,37	1,8	0,15	1,8	0,13
2,0	0,35	2,0	0,13	2,0	0,12

table (table II) contains the calculated influence values  $i$ , at different depths of the vertical axis passing through the point P of a continuous, a square and a circular footing. The depths are expressed by the ratio of the ordinate  $z$  to the width of the footing.

#### THE CHARACTERISTICS OF THE SOIL.

##### Location of the water level and unit weight of the soil.

The effective pressure  $p_0$  at the level of the base of the footing or the effective pressure  $\sigma_0$  at an arbitrary depth below the base depend on the location of the groundwater level and the unit weight of the soil.

In the following investigations it is arbitrary assumed that the water level corresponds with the foundation level. Further it is supposed that the pressure in the water is hydrostatic.

As unit weights of the soil, we admit:

- soil above the water level :  $\gamma = 1,6 \text{ t/m}^3$
- soil below the water level :  $\gamma_n = 2,0 \text{ t/m}^3$ .

Taking in account the hydrostatic pressure in the pore-water, the unit weight  $\gamma_k$  to introduce in the formula (3) is:

$$\gamma_k = (2,0 - 1,0) \text{ t/m}^3 \text{ or } 1 \text{ t/m}^3 \quad (8)$$

Hence, if the surface of the ground is horizontal and does not carry any surcharge, we obtain:

$$\text{- effective pressure } p_0 : \quad p_0 = 1,6 h \quad (h \text{ in m., } p_0 \text{ in t/m}^2) \quad (9)$$

wherein  $h$  is the depth of the base below the surface of the ground.

- effective pressure  $\sigma_0$  :

$$\sigma_0 = 1,6 h + 1 z \quad (h \text{ and } z \text{ in m., } \sigma_0 \text{ in t/m}^2) \quad (10)$$

in which  $z$  is the depth below the level of the base.

##### THE SHEARING RESISTANCE OF THE SOIL.

It is assumed that the shearing resistance  $s$  of the soil located below the base of the footing can be expressed by the formulas (1) and (2). Assuming furthermore that the soil is cohesionless ( $c = 0$ ), and has an angle of internal friction  $\varphi = 30^\circ$  for a normal stress smaller than  $p_0$ , the shearing resistance  $s$  of the idealized soil we will introduce in our calculations, can be represented by figure 2. The shearing resistance of the soil located

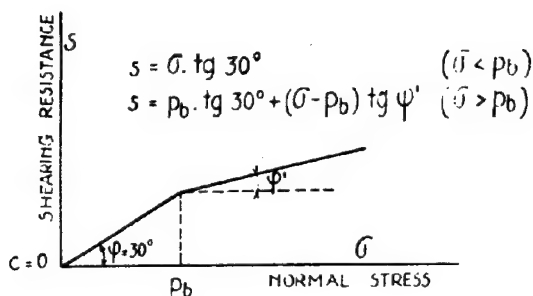


FIG. 2

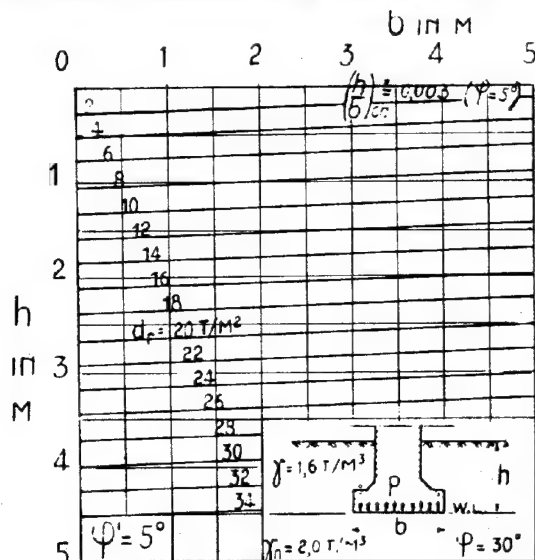
above the level of the base of the footing is neglected. An approximate value of  $\varphi'$  can be obtained from triaxial compression tests or derived from deepsounding results. The following table contains some limits of  $\varphi'$  found for different soil types:

TABLE III.

Soil type	$\varphi'$
soft alluvium	$5^\circ - 10^\circ$
firm tertiary clay	$10^\circ - 15^\circ$
loam, or clayey sand	$15^\circ - 25^\circ$
loose sand	$25^\circ - 30^\circ$
compact sand	$> 30^\circ$

#### THE COMPRESSIBILITY OF THE SOIL.

In computing the settlements of a soil stratum which is subjected to a foundation load, it is generally assumed that the soil is homogeneous, isotropic and perfectly elastic. Furthermore we select a foundation material whose deformation characteristics correspond to a



Lines of equal bearing capacity for continuous footings.

FIG. 3

given coefficient of compressibility, namely  $C = 100$ . The coefficient of compressibility of the real soil has to be determined by consolidation tests or can be derived from deepsounding results. Some values of  $C$  obtained for some soil types are given in the table IV.

TABLE IV.

soil type	$C$
peat	5 - 10
clay	10 - 20
sandy clay, loam	20 - 50
sand (according to the compacity)	5 - 500

#### BEARING CAPACITY DIAGRAMS.

Combining the equations (3), (8) and (9), we get:

$$d_r = 1.6 V''_b \cdot h + V'_g \cdot b \quad (11)$$

This equation shows that the bearing capacity  $d_r$  is a linear function of the depth  $h$  below surface and the width  $b$  of the footing.

In the figures 3 to 8, where  $b$  is plotted against  $h$  for various angles  $\varphi'$ , the expression (11) is represented by a net of straight lines of equal bearing capacity.

#### SETTLEMENT GRAPHS.

In integrating graphically the equation (5), in which  $C = 100$ , settlements have been computed for various widths of the footing and various depths below surface. Different values of the unit load  $p$  were taken in consideration namely  $p = 5 - 10 - 15 - 20 \text{ t/m}^2$ . These operations have been repeated for a continuous long strip, for a square and for a circular loaded area. The influence values  $i$  of the table II were used. In addition to this, it will be said that the integration of the expression

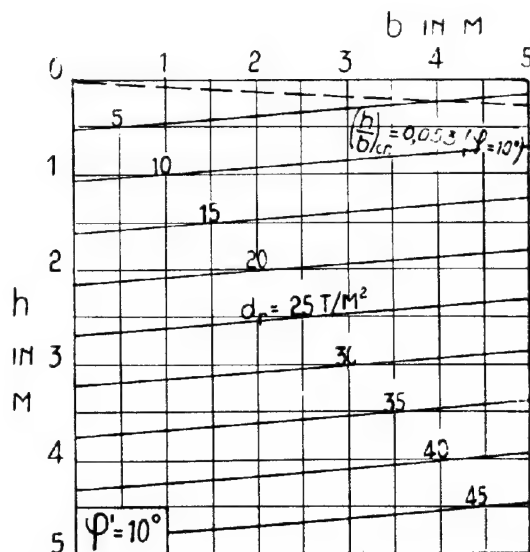


FIG. 4

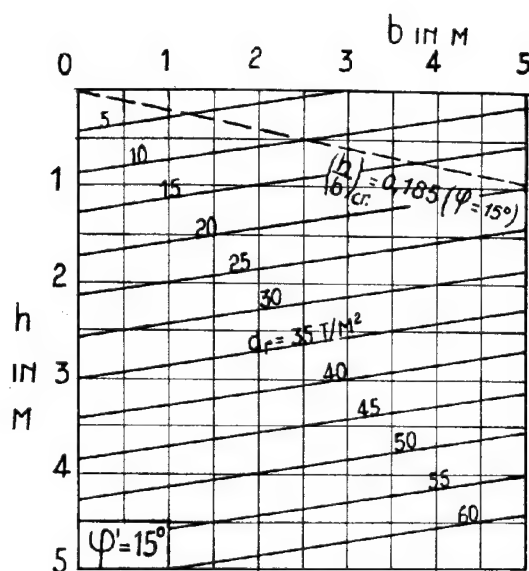


FIG. 5

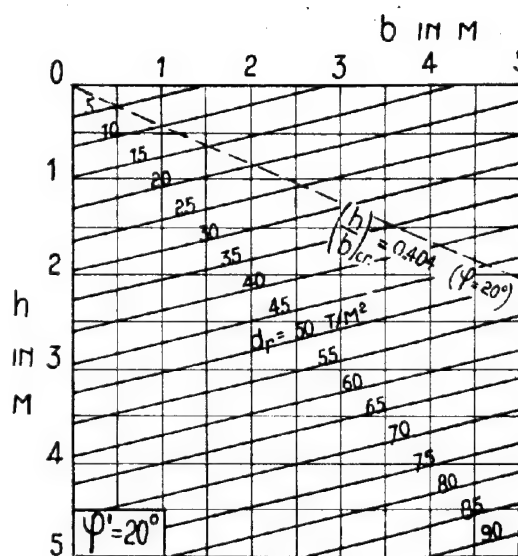


FIG. 6

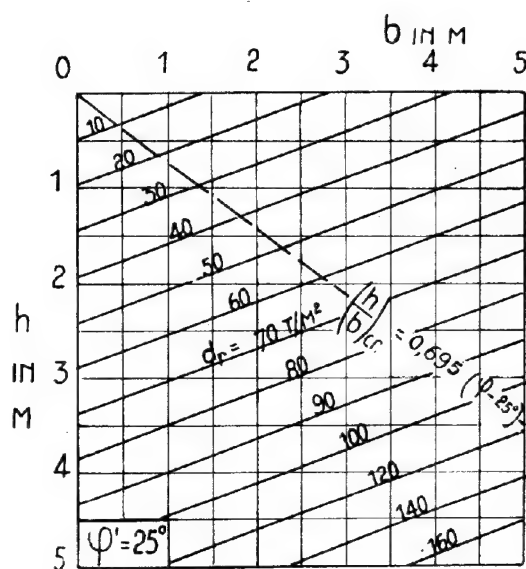


FIG. 7

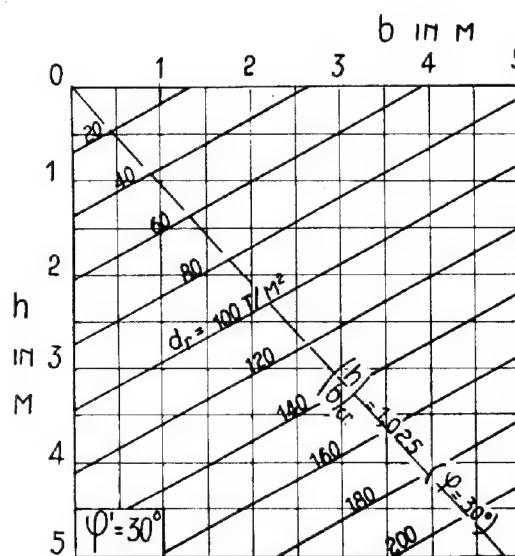


FIG. 8

Lines of equal bearing capacity for continuous footings.

(5) was limited to a depth equal to two times the smallest plan dimension of the loaded area. The results of these computations (about 200 in number) have permitted to draw the graphs of figures 9 to 20, in which the width  $b$  is plotted against the depth  $h$ , and curves of equal settlement are represented.

It may be seen in figures 9, 13 and 17,

that the curves of equal settlement approach an horizontal asymptote with an ordinate  $h_c = \frac{5}{1.6} = 3.125$  m. At this critical depth, the weight of the soil balances the unit load  $p = 5 \text{ t/m}^2$  of the footing. For values of  $h$  greater than  $h_c$ , the underlying strata will have a tendency to swell.

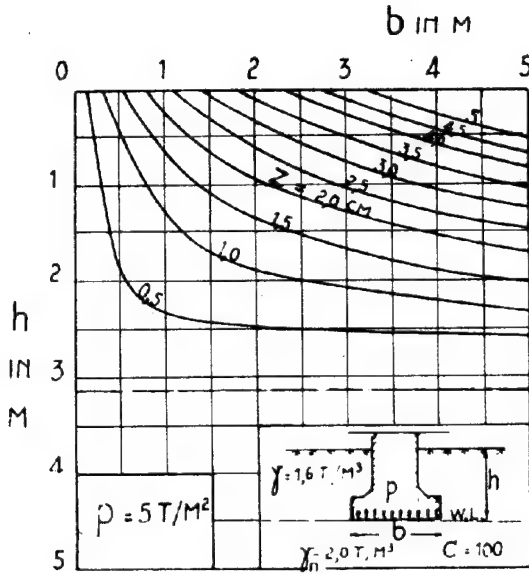
Continuous footing.

FIG. 9

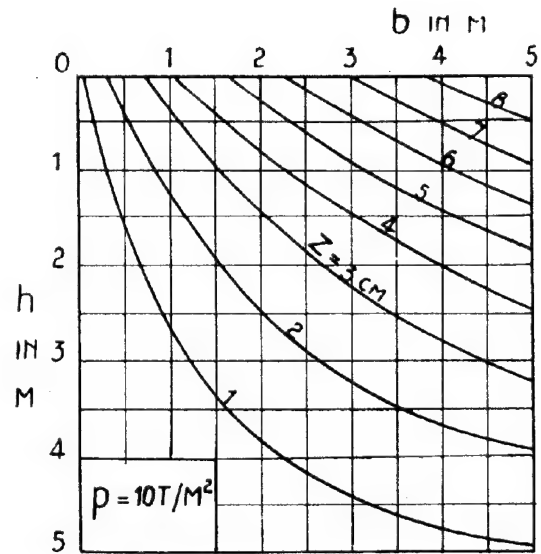


FIG. 10

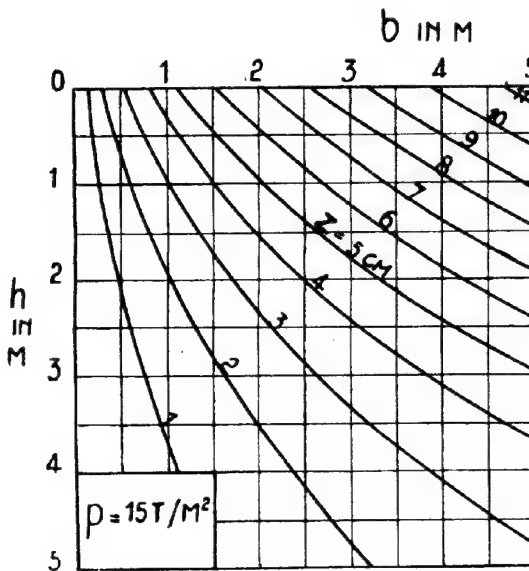


FIG. 11

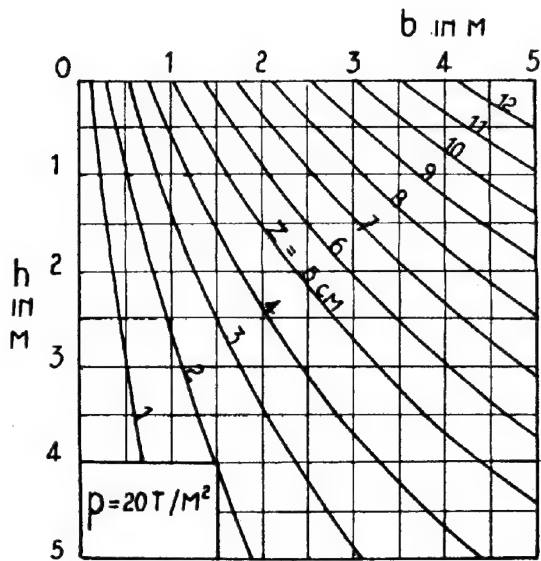


FIG. 12

Curves of equal settlement for different values of unit load.

SIMPLIFIED METHODS FOR ESTIMATING BEARING CAPACITY AND SETTLEMENTS.

1) Where the soil characteristics and the loading conditions correspond to the assumptions introduced by elaborating our diagrams, the use of them, for example for design of footings,

presents no more difficulties. Even interpolation can be easily effected for intermediary values of  $q'$  or  $p$ .

2) Equation (11) and figures 3 to 8 refer to continuous footings. Practically the equation (11) and the corresponding graphs are also applicable to rectangular footings whose



Square footing.

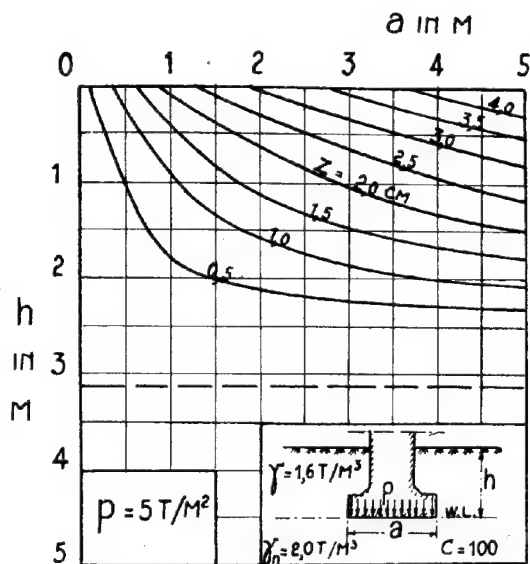


FIG.13

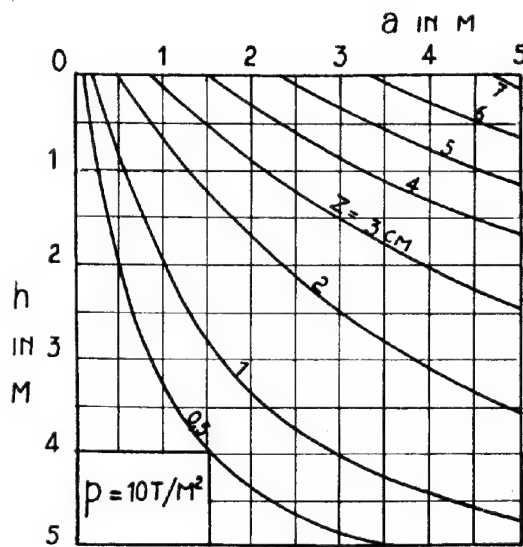


FIG.14

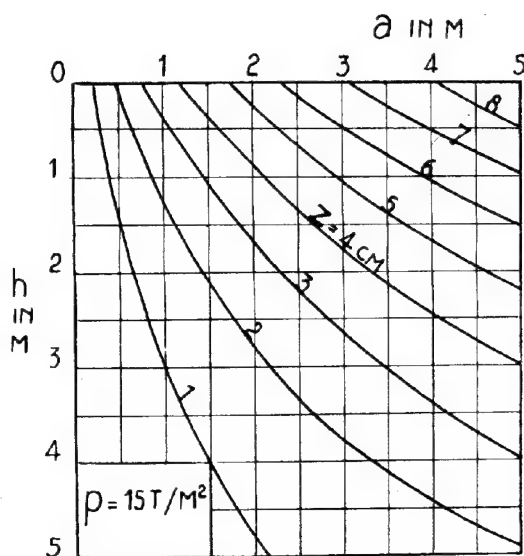


FIG.15

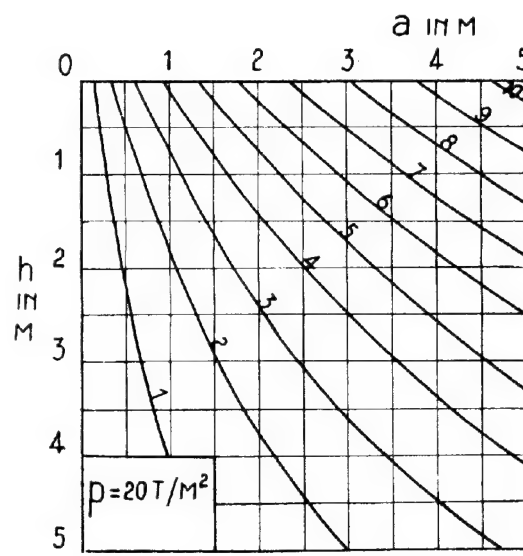


FIG.16

Curves of equal settlement for different values of unit load.

lengths are large compared to their widths. Laboratory experiments made in Delft have shown that, for a loaded area whose width is equal to its length, such as a square or a circular area, the bearing pressure is about 30 per cent greater than for a strip load. On the basis of this experience, the diagrams may

be used for a square or a circular footing; it is only necessary to multiply the indicated values of  $d_r$  by the coefficient 1.3. 3) The formula (11) has been obtained for a centric loaded strip. By eccentric loading, and if the eccentricity is small, the use of the formula, (11) may give sufficient results,



## Circular footing.

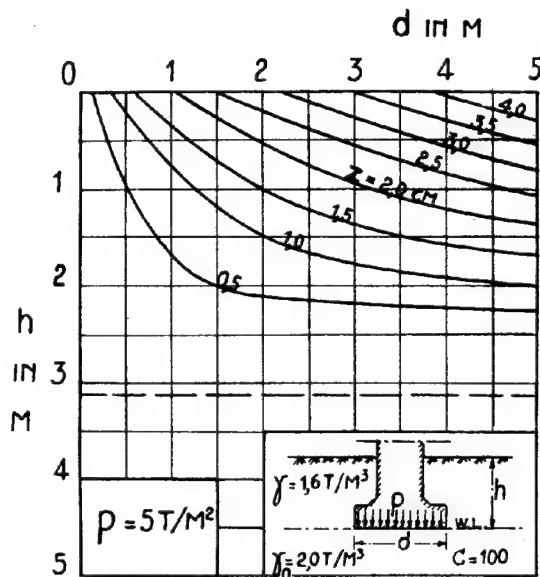


FIG. 17

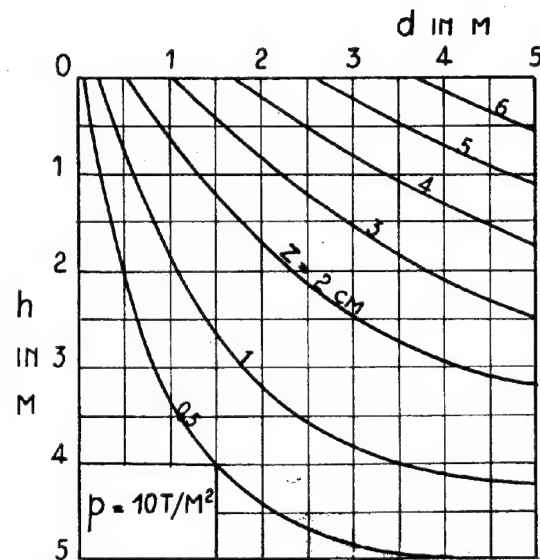


FIG. 18

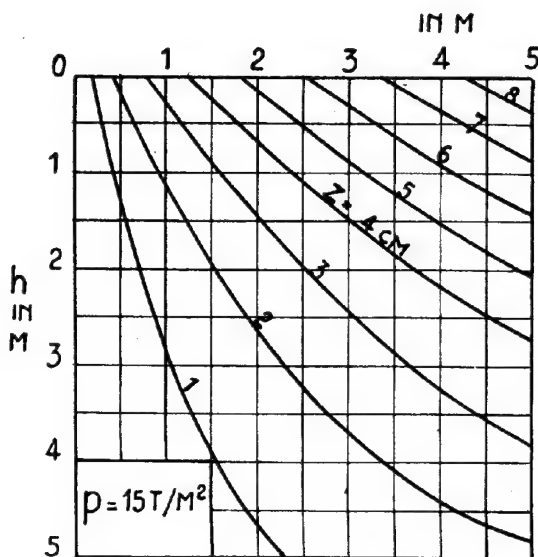


FIG. 19

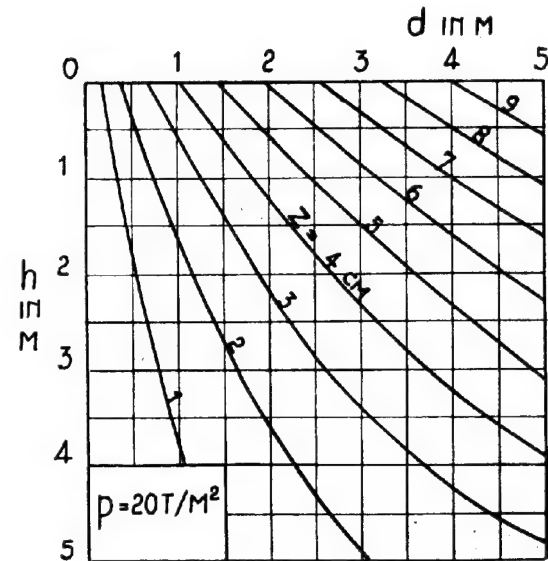
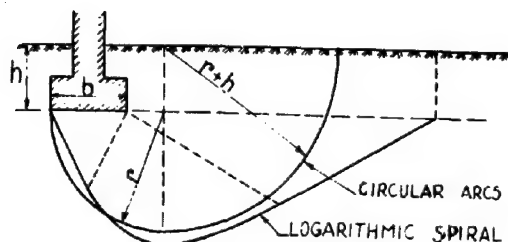


FIG. 20

Curves of equal settlement for different values of unit load.

when the width  $b$  is substituted by two times the complementary eccentricity  $2u$ .  
 4) The developed formula of the bearing capacity assumes that the surface of failure consists of a logarithmic spiral tangent to two straight lines (Prandtl's theory).  
 M. Andersen (Minnesota) has developed

formulas in which it was assumed that the surface of rupture can be approximated by circular arcs, as shown in figure 18. In comparing the two methods, for a cohesionless soil in which  $\phi = \phi'$ , Mr. De Beer has found that the method of circular arcs gives smaller values than the Prandtl method, when the width of the



Prandtl and Andersen Methods.

FIG. 21

footing is great compared to the depth of foundation (shallow foundation). Fig 21. On the contrary, the Prandtl-method leads to more safe results when dealing with deep foundations. Mr. De Beer has shown elsewhere that the applicability of both methods can be limited by a critical value of the ratio of the depth to the width of the footing. Since this value depends only on the angle of internal friction, the zones of applicability of both methods may be separated by the straight lines shown in figures 3 to 8 (dotted lines). Above these critical lines, the curves of equal bearing capacity may give exaggerated values of  $d_r$ .

On the other hand, in the developed formula, the shearing resistance of the soil located above the level of the base of the footings has been disregarded. However on the safe side, when dealing with deep foundations, such simplification is not justified, because the resulting error may be excessive.

Now the diagrams developed for the bearing capacities, give ultimate values, at which rupture will occur. If they are applied to design of footings, regardless the problem of settlement, suitable factors of safety should be used. When dealing with deep footings or piers, a factor of safety,  $s = 2$  or less, may be allowed. When the load of the construction is transmitted by means of shallow foundations, a factor of safety of  $s = 4$  or more may be necessary.

5) The bearing capacity diagrams have been computed in the assumption that the surface of the ground beside the foundation is horizontal and not surcharged. When the surface of the ground carries a uniformly distributed surcharge  $q$  per unit of area, the graphs can be used by introducing an equivalent depth of foundation  $h_r$ , by means of the following equations:

$$\begin{aligned} p_b &= q + 1,6 h = 1,6 h_r \\ h_r &= h + \frac{q}{1,6} \end{aligned} \quad (12)$$

6) A similar method can be used when the real

the water level.

$\gamma'_k$  = the real unit weight of the soil below the base of the foundation, reduced by the unit weight of water.

$q$  = a uniform surcharge.

$h_r, b_r$  = equivalent depth and width of foundation which lead to an equal bearing capacity in an unsaturated soil with characteristics:

$$\gamma = 1,6 \text{ t/m}^3, \gamma'_k = 1 \text{ t/m}^3.$$

The ultimate bearing value may then be computed, by replacing  $h$  and  $b$ , with  $h_r$  and  $b_r$ :

$$p_b = q + \gamma'_k h = 1,6 h_r \quad (13)$$

$$\gamma'_k \cdot b = (2,0 - 1,0) b_r \quad (14)$$

7) If the groundwater level does not correspond with the level of the base, but is located only at a depth  $h_n < h$  below the surface of the ground, we can introduce the equivalent depth  $h_r$ :

$$p_b = 1,6 h_n + (2,0 - 1,0) (h - h_n) = 1,6 h_r \quad (15)$$

If the water level is far below the level of the base of the footing, an equivalent width  $b_r$  is given by:

$$1,6 b = (2,0 - 1,0) b_r \quad (16)$$

8) The use of the formula (11) is justified when in the proximity of the foundations, the surface of the ground has not to be modified by excavation or cutting works. In construction of buildings, it is often necessary to found the footing near a deep cut needed to provide basement room, for example for cellars. If  $h$  represents the depth of the foundation with reference to an horizontal section through the bottom of the cut, the method based on the equation (11) could be used. Nevertheless for small values of  $\varphi'$  and small values of  $h$ , this method can lead to very unfavorable results, because the preconsolidation under the original natural pressure was disregarded. In order to take in account the effect of the preconsolidation, Mr. de Beer presents in this case the following bearing capacity formula:

$$d_r = p_{b,0} \left[ X(\varphi, \varphi') \left( \frac{p_b}{p_{b,0}} \right)^{\frac{1}{1+\varphi}} - \frac{1+\varphi}{1+\varphi'} + 1 \right] + \gamma'_k \cdot b \quad (17)$$

wherein:

$p_{b,0}$  = the original effective vertical pressure at the level of the foundation, before the cut was opened, and which corresponds to the weight of the earth below the surface of the ground (height  $h_0$ ).

$p_b$  = the actual effective pressure beside the base of the foundation, and which is exerted by the earth located below the bottom of the cut (height  $h$ ).

$X(\varphi, \varphi')$  = a function of  $\varphi$  and  $\varphi'$ . Some values of  $X(\varphi, \varphi')$ , when  $\varphi = 30^\circ$ , are given in table V.

TABLE V

$\varphi'$	$X(\varphi, \varphi')$	$\varphi'$	$X(\varphi, \varphi')$
$5^\circ$	17,9	$20^\circ$	17,6
$10^\circ$	14,0	$25^\circ$	22,9
$15^\circ$	14,6	$30^\circ$	31,8

unit weights of the soil are not the same as those introduced in the elaboration of the diagrams.  
Let:  $\gamma'_k$  = the real unit weight of the soil above

In order to obtain a convenient solution of the equation (15), we introduce an equivalent depth  $h_r$  of foundation, by means of the following equations:

$$V_{\text{f}}'' \cdot 1,6 h_f = \left[ X(\varphi, \varphi') \operatorname{tg} \varphi \left( \frac{P_{\text{b}}}{P_{\text{b},0}} \right)^{\frac{\operatorname{tg} \varphi}{1-\operatorname{tg} \varphi}} - \frac{\operatorname{tg} \varphi}{1-\operatorname{tg} \varphi} + 1 \right] \cdot P_{\text{b},0} \quad (18)$$

$$K = \frac{X(\varphi, \varphi') \operatorname{tg} \varphi \left( \frac{P_{\text{b}}}{P_{\text{b},0}} \right)^{\frac{\operatorname{tg} \varphi}{1-\operatorname{tg} \varphi}} - \frac{\operatorname{tg} \varphi}{1-\operatorname{tg} \varphi} + 1}{V_{\text{f}}''} \quad (19)$$

$$1,6 h_f = K \cdot P_{\text{b},0} = K \cdot 1,6 h_0 \quad (20)$$

$$h_f = K \cdot h_0$$

The factor  $K$  has been computed for different values of the ratio  $\frac{P_{\text{b}}}{P_{\text{b},0}}$  or  $\frac{h}{h_0}$ , and different values of  $\varphi'$ . Values of  $K$  for  $\varphi = 30^\circ$  are given in table VI.

TABLE VI

$h/h_0$	$\varphi'$					
	$5^\circ$	$10^\circ$	$15^\circ$	$20^\circ$	$25^\circ$	$30^\circ$
1,0	1,000	1,000	1,000	1,000	1,000	1,000
0,8	0,928	0,905	0,875	0,850	0,825	0,800
0,6	0,838	0,798	0,756	0,707	0,656	0,600
0,4	0,718	0,662	0,598	0,533	0,469	0,400
0,2	0,528	0,462	0,390	0,322	0,259	0,200

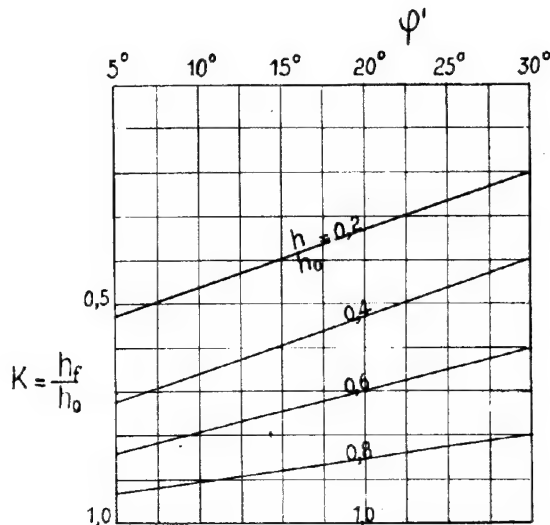


FIG. 22

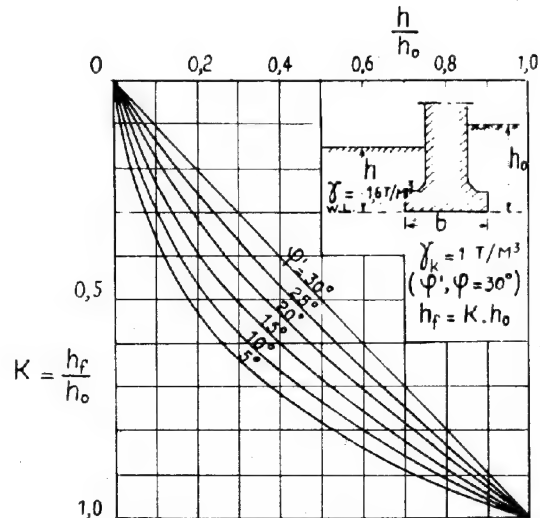


FIG. 23

For rapid interpolation, the values of the table VI may be plotted, in figures 22 and 23.

To obtain directly by the usual procedure, (diagrams 3 to 8) the bearing capacity  $d_r$  of the footing near a cut, it is now only necessary to select the tabular or the graphical value of the ratio  $K$ , and to calculate the equivalent depth of foundation  $h_f$ , by means of the equation (20).

9) The settlement graphs represented by figures 9 to 20, are constructed for a given degree of compressibility of the soil, namely  $C = 100$ . Since, in accordance to the basic formula, (5),

the value of the final settlement  $Z$ , depends on the opposite value of the coefficient of compressibility  $C$ , the probable settlement for the real soil will be obtained by multiplying the values of the graphs by the ratio  $\frac{100}{C}$ , in which  $C$  is the real coefficient of compressibility.

If the load conditions are not the same as those introduced in the basic graphs, a graphical interpolation can lead to a sufficient accurate solution of the problem.

If the soil characteristics, as unit weight and water level, differ from the assumed ones, in the most cases the graphs give an upper limit for the real settlement. In introducing equivalent values for the width or the depth

of the footings, as was done for the use of the bearing capacity diagrams, useful and sufficient approximate information on the settlement problem may rapidly be obtained.

10) Even, when the compressibility of the soil has not been previously determined, the diagrams may give useful indication in order to avoid differential settlement. For instance in the case of an approximately homogeneous soil, it will be possible to choose judiciously the size and the depth of the different footings of the construction, in such a way that the final settlements of the various parts of the construction will be as uniform as possible.

Prof. Dr. J. JAKY

To characterize the state of failure in Soil Mechanics Coulomb's equation of stability:  $t = n \operatorname{tg} \phi + C$  is made use of. This law has been proved experimentally partly only, because in the range of tension, the envelope curve characterising failure differs greatly from the straight line determined by the above mentioned equation (Fig. 1.a.) In the following an attempt is made to deduce the exact law of failure. It is assumed that Mohr's stress circles have an envelope, but this is generally a curve, its coordinates  $t$  and  $n$  are functions of angle  $\varepsilon$  (Fig. 1.b.).

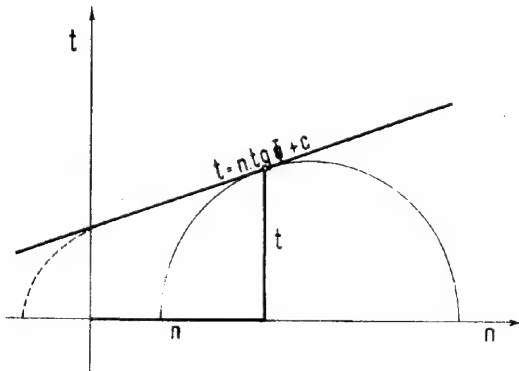


FIG. 1a

## I. AUXILIARY THESIS.

From stresses  $t$  and  $n$  acting on the sliding surface inclined at angle  $\alpha$  and from conditions of the envelope curve, i.e.  $\operatorname{tg}(2\alpha - \varepsilon) = \frac{\sigma_y - \sigma_x}{2\tau}$  equations of the conjugate stresses can be deduced, i.e.

$$\left. \begin{aligned} \sigma_y &= n + 2t \frac{\sin \alpha \cos(\alpha - \varepsilon)}{\cos \varepsilon} \\ \sigma_x &= n - 2t \frac{\sin(\alpha - \varepsilon) \cos \alpha}{\cos \varepsilon} \\ \tau &= t \frac{\cos(2\alpha - \varepsilon)}{\cos \varepsilon} \end{aligned} \right\} \quad (1)$$

That is, all stresses are combined functions of angles  $\varepsilon$  and  $\alpha$ .

In a shearing test, according to arrangement on Fig. 2. after compression of the soil, angle  $\alpha$  is equal to zero, the sliding surface becomes horizontal, therefore, substituting in equation (1)  $\alpha = 0$ , we obtain

$$\left. \begin{aligned} \sigma_y &= n \\ \sigma_x &= n + 2t \operatorname{tg} \varepsilon \\ \tau &= t \end{aligned} \right\} \quad (2)$$

all stresses are functions of  $\varepsilon$  only.

## II. AUXILIARY THESIS.

The soil sample is under arbitrary stress and its weight per unit volume varies either under an external load or under its own weight,

therefore  $\gamma$  is not constant but generally:  $\alpha = \alpha(x, y)$ . Since  $\gamma$  is function of stresses  $\sigma_y$ ,  $\sigma_x$  and  $\tau$  and the latter are functions of  $\varepsilon$  only,  $\gamma = f(\varepsilon)$  (3) because either  $\alpha$  is constant or  $\alpha = f(\varepsilon)$ , hence all stresses are functions of  $\varepsilon$  only.

The conditions of equilibrium of the elementary prism can be expressed by Cauchy's equations:

$$\left. \begin{aligned} \frac{d\sigma_y}{d\varepsilon} \frac{\partial \varepsilon}{\partial y} + \frac{d\tau}{d\varepsilon} \frac{\partial \varepsilon}{\partial x} &= \gamma(\varepsilon) \\ \frac{d\sigma_x}{d\varepsilon} \frac{\partial \varepsilon}{\partial x} + \frac{d\tau}{d\varepsilon} \frac{\partial \varepsilon}{\partial y} &= 0 \end{aligned} \right\} \quad (4)$$

From Eq. (4) we obtain  $\frac{\partial \varepsilon}{\partial x}$  and  $\frac{\partial \varepsilon}{\partial y}$

$$\left. \begin{aligned} \frac{\partial \varepsilon}{\partial y} &= \gamma \frac{\frac{d\sigma_y}{d\varepsilon} \frac{d\sigma_x}{d\varepsilon} - \left(\frac{d\tau}{d\varepsilon}\right)^2}{\frac{d\sigma_x}{d\varepsilon} \frac{d\sigma_y}{d\varepsilon} - \left(\frac{d\tau}{d\varepsilon}\right)^2} = \gamma f(\varepsilon) \\ \frac{\partial \varepsilon}{\partial x} &= -\gamma \frac{\frac{d\sigma_x}{d\varepsilon} \frac{d\sigma_y}{d\varepsilon} - \left(\frac{d\tau}{d\varepsilon}\right)^2}{\frac{d\sigma_x}{d\varepsilon} \frac{d\sigma_y}{d\varepsilon} - \left(\frac{d\tau}{d\varepsilon}\right)^2} = -\gamma f(\varepsilon) \end{aligned} \right\} \quad (5)$$

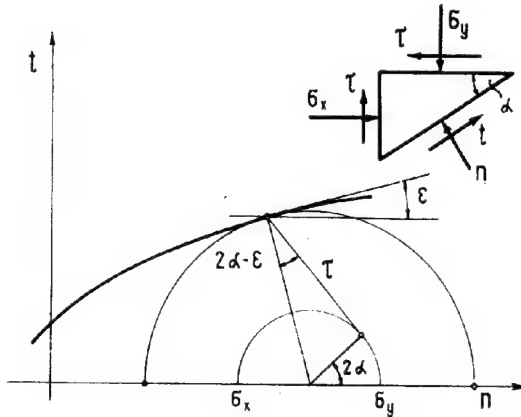


FIG. 1b

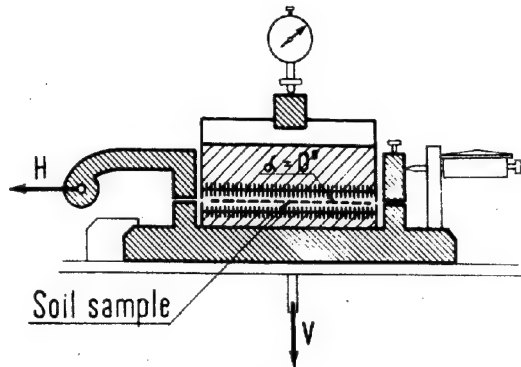


FIG. 2

Generally, the denominator cannot be zero or it would follow that  $\gamma = 0$ , which is possible only in the case of the weightless mass.

Differentiating the first equation under (4) with respect to  $x$ , the second with respect to  $y$  and equating  $\frac{\partial \varepsilon}{\partial x \partial y}$  to  $\frac{\partial \varepsilon}{\partial y \partial x}$  we obtain:

$$\frac{d\gamma}{d\varepsilon} \frac{\partial \varepsilon}{\partial x} f_1 + \gamma f_1' \frac{\partial \varepsilon}{\partial x} = -\frac{d\gamma}{d\varepsilon} \frac{\partial \varepsilon}{\partial y} f_1 - \gamma f_1' \frac{\partial \varepsilon}{\partial y}$$

substituting  $\frac{\partial \varepsilon}{\partial y}$  and  $\frac{\partial \varepsilon}{\partial x}$  from Eq.(5)

$$-\frac{d\gamma}{d\varepsilon} f_1 \gamma f_1' - \gamma^2 f_1' f_1' = -\frac{d\gamma}{d\varepsilon} \gamma f_1 f_1' - \gamma^2 f_1' f_1'$$

hence  $\frac{f_1'}{f_2} = \frac{f_1'}{f_1}$

that is  $f_1 = k f_2$

substituting from Eq. (4)

$$\left. \begin{aligned} \frac{d\tau}{d\varepsilon} &= k_1 \frac{d\sigma_x}{d\varepsilon} \\ \tau &= k_1 \sigma_x + k_2 \end{aligned} \right\} \quad (6a)$$

that is, the shearing stress ( $\tau$ ) at an arbitrary point in the interior of the body is a linear function of the normal stress  $\sigma_x$ . This law, as the basic law of the state of stress of a body possessing weight is satisfied as long as stresses are functions of  $\varepsilon$  only.

Substituting  $\tau$  and its differential-quotient with respect to  $\varepsilon$  in the second equation under (4) we obtain:

$$\frac{d\sigma_x}{d\varepsilon} \left( \frac{d\varepsilon}{dx} + k_1 \frac{\partial \varepsilon}{\partial y} \right) = 0 \quad (7)$$

$$\text{either 1.) } \frac{d\sigma_x}{d\varepsilon} = 0 \quad \text{thus } \sigma_x = C_1 \quad (8)$$

$$\text{or 2.) } \frac{\partial \varepsilon}{\partial x} + k_1 \frac{\partial \varepsilon}{\partial y} = 0$$

This equation is satisfied, if

$$\varepsilon = f(k_1 x - y) \quad (9)$$

ad 1.) If  $\sigma_x = C_1$  it follows after Eq.(6.a):

$$\tau = C_2$$

In this case Mohr's stress circles have a point in common and have no envelope curve (Fig. 3.). Therefore, this case lies outside of the conception of the envelope and is thus impossible.

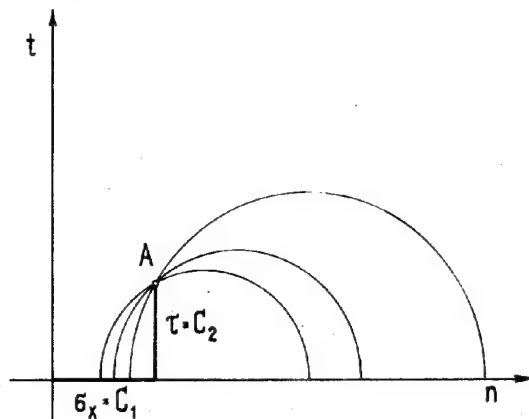


FIG.3

ad 2.) Eq.(9) yields the required function  $\varepsilon = f(x, y)$ . There is an infinite number of possible solutions, for instance

$$\varepsilon = C_1 (k_1 x - y)$$

$$\varepsilon = \frac{C_1}{k_1 x - y} \quad \text{etc.}$$

a.) Stress conditions in the shearing test.

In the shearing test, the sample has such small dimensions that its own weight can be neglected in comparison with the external load, thus  $\gamma = 0$ . The system of equations (4) holds, if:

$$1) \quad \frac{\partial \varepsilon}{\partial x} = 0, \quad \frac{\partial \varepsilon}{\partial y} = 0 \quad \text{that is} \\ \varepsilon = \text{constant}$$

it means, that the envelope is a straight line. This is Coulomb's solution:  $t = n \tan \phi + C$ . or 2.) if the main determinant of the equation system:

$$\begin{vmatrix} \frac{d\sigma_y}{d\varepsilon} & \frac{d\tau}{d\varepsilon} \\ \frac{d\tau}{d\varepsilon} & \frac{d\sigma_x}{d\varepsilon} \end{vmatrix} = 0$$

$$\text{that is} \quad \frac{d\sigma_x}{d\varepsilon} \frac{d\sigma_y}{d\varepsilon} = \left( \frac{d\tau}{d\varepsilon} \right)^2 \quad (11)$$

Substituting the values of Eq.(2) in the preceding equations and considering that along the envelope curve:  $\frac{dt}{d\varepsilon} = \frac{dn}{d\varepsilon} \tan \phi$  we get after reductions:

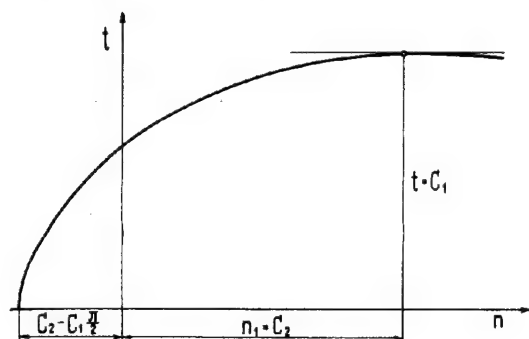


FIG.4 a

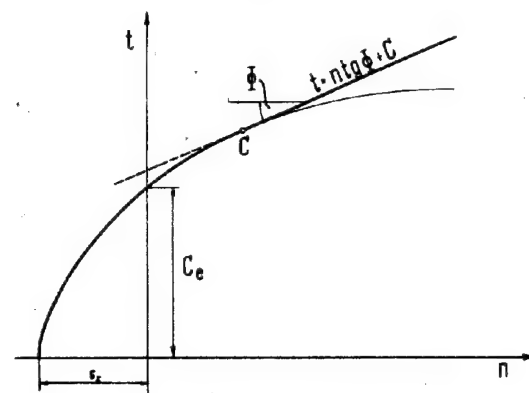


FIG.4 b

$$\frac{dt}{d\varepsilon} + 2t \operatorname{tg} \varepsilon = 0 \quad (12)$$

Solving this differential equation we obtain

$$\left. \begin{aligned} t &= C_1 \cos^2 \varepsilon \\ n &= C_2 - C_1 (\varepsilon + \sin \varepsilon \cos \varepsilon) \end{aligned} \right\} \quad (13)$$

respectively.

These are the equations of the envelope curve with parameter  $\varepsilon$ . We plotted same in Fig. 4.a.

This is a novel and as yet unknown law of failure, valid mainly in the range of tension, the curve of which is joined tangentially at angle  $\phi$  by Coulomb's boundary straight line. (Fig. 4.b.)

Computing angle  $\phi$  from the compression-shearing test and the tensile strength ( $\sigma_z$ ) from the tension test, we obtain the characteristics of the combined envelope curve (Fig. 4.a.):  $C_2 - C_1 \frac{\pi}{2} = -\sigma_z$

In the point of contact  $\underline{C} : \varepsilon = \phi$  substituting (13) in Eq. (10)

$$C_1 \cos^2 \phi = [C_2 - C_1 (\phi + \sin \phi \cos \phi)] \operatorname{tg} \phi + C$$

The constants  $C_1$  and  $C_2$  may be determined and the envelope curve will be known in the range of tension too.

Indeed, the envelope curve intersects the  $t$ -axis below the Coulomb line, thus, the effective cohesion ( $C_e$ ) will be smaller than obtained from the straight line ( $C_c$ ). This fact was suggested long ago by researchers, because the Coulomb line gave cohesion values unsuitable to explain stability conditions and slope failures. Fig. 5. shows a combined envelope curve obtained by tests on clay.

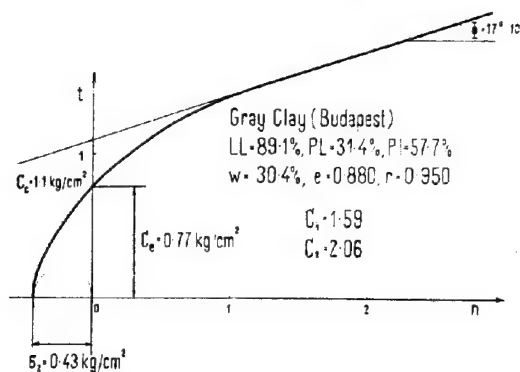


FIG. 5

b.) Law of shearing in mass possessing weight.

Let the law of shearing in a heavy earth mass be investigated. There exists in this case the relationship (6.a), substituting values of  $\sigma_x$  and  $\tau$  from (1) and equating  $k_1 \operatorname{tg} \psi$  we obtain

$$t \frac{\cos(2\alpha - \varepsilon)}{\cos \varepsilon} = \operatorname{tg} \psi \left( n - 2t \frac{\sin(\alpha - \varepsilon) \cos \alpha}{\cos \varepsilon} \right) + k_2$$

After reductions:

$$t \frac{\cos(2\alpha - \varepsilon - \psi) - \sin \varepsilon \sin \psi}{\cos \varepsilon \sin \psi} = n + k_2 \cot \psi \quad (14)$$

If  $\alpha = f(\varepsilon)$  is given, Eq. (14) may be integrated and the stresses  $t$  and  $n$  will be known, thus the state characterised by stresses  $\sigma_x, \sigma_y$  and  $\tau$  and also the sliding surfaces will be cleared up.

I. E.g. let the simple case of  $\alpha = \varepsilon$  be considered.

It means, that the vertical lines are sliding surfaces, too, because - according to Mohr's theorem - the angle between the sliding surfaces is  $(90^\circ - \varepsilon)$  thus, if  $\alpha = \varepsilon$  the angle of inclination of the other sliding surface  $\alpha_1 = 90^\circ - \varepsilon + \varepsilon = 90^\circ$  (15)

In this case from Eq. (14)

$$t \cot \psi = n + k_2 \cot \psi$$

thus

$$t = n \operatorname{tg} \psi + k_2$$

We obtain Coulomb's law, that is  $\varepsilon = \alpha = \psi$ , whence, the sliding surfaces are planes inclined at  $\psi$  on the one hand and vertical planes on the other hand. That is, Coulomb's law is valid for the heavy earth mass, too, but in this case, the sliding surfaces are planes inclined at  $\alpha = \psi$

Moreover, Coulomb's linear law of failure holds also in the case of other (plane of curved) sliding surfaces. Since  $\varepsilon = \phi$ , this time Eq. (4) cannot be used, stresses  $\sigma_x, \sigma_y$  and  $\tau$  being functions of the angle of the sliding surface and not of angle  $\varepsilon$

II. Let now  $\alpha = 45^\circ + \frac{\psi}{2}$ , then after Eq. (1) (16)

and from Eq. (4)

$$t \frac{1 - \sin \varepsilon}{\cos \varepsilon} = n + k_2 \cot \psi$$

Differentiating with respect to  $\varepsilon$  and substituting the relationship

$$\frac{dn}{d\varepsilon} = \frac{dt}{d\varepsilon} \cot \varepsilon$$

we obtain

$$\frac{dt}{d\varepsilon} + t \operatorname{tg} \varepsilon = 0$$

whence

$$t = C_1 \cos \varepsilon$$

and

$$n = C_2 - C_1 \sin \varepsilon$$

That means, the body is in a homogeneous state of stress (Fig. 6.) i.e.  $\sigma_y = C_1 + C_2$   
 $\sigma_x = C_2 - C_1$  (17)

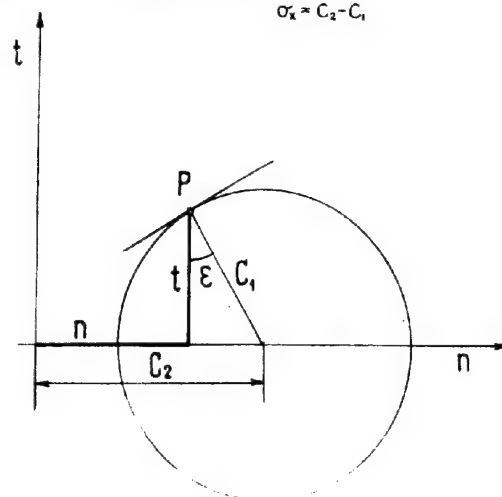


FIG. 6

If all stresses are constant, it follows from Cauchy's law of equilibrium:  $\gamma = 0$ , therefore the case of  $\alpha = 45^\circ$  does not refer to the heavy earth mass, and must be excluded.

It would lead far to deal in detail with a given problem, therefore only the way, how to solve it is shown now.

- 1) If  $\alpha = f(\epsilon)$  is given or assumed relation Eq. (14) leads to a homogeneous linear equation of first degree, from which we obtain  $t = F(\epsilon)$  and by integrating  $n = G(\epsilon)$  respectively and using these relationships, all stresses as functions of  $\epsilon$  may be determined from Eq. (1).
- 2) Assuming now on basis of Eq. (9) function  $\epsilon = f(x, y)$ , the stresses, as the functions of coordinates  $(x, y)$  will be known as well and determining from the first equation under (4) function  $\gamma = \gamma(\epsilon) = \gamma(x, y)$ , we have in every point the value of the weight per unit volume and in connection with it, the value of the void ratio and finally, on basis of  $\alpha = f(\epsilon) = g(x, y)$  the geometry of the sliding surfaces is

established.

#### CONCLUSIONS

In order to examine conditions of equilibrium of earth masses with respect to the failure, Coulomb's linear law has as yet used. This is a very primitive law, since we proved that the form of the function giving the stresses acting on the sliding surfaces,  $t = f(n)$  is greatly affected by the shape of the sliding surfaces produced by the movement of the earth masses and by the variation of  $\gamma$  that is of the void ratio, briefly, it is determined by the manner of movement. As soon as we know these, the stress conditions can be computed.

#### ACKNOWLEDGEMENT

The author wishes to express his gratitude to A. Kézdi for preparing the figures and completing the manuscript.

-0-0-0-0-0-0-

le9

#### STATE OF STRESS IN GREAT DEPTH

Prof. Dr. JOZSEF JAKY

The author wishes to deal in this paper with two states of stress, namely with the law of compression and shearing due to great pressures. Laboratory tests used to be extended up to the pressure  $p \approx 10 \text{ kg/cm}^2$  and the results of numerous tests are summarized in the following empirical laws:

- 1) The compression is well characterized by Prof. Terzaghi's law:

$$e = e_0 - c_1 \ln \left( \frac{p + p_c}{p_c} \right) \quad (1)$$

that is, the void ratio  $e$  depends on the logarithm of the  $p$  - pressure.

- 2) The shearing test proves Coulomb's assumption that is on the surface of shear:

$$t = n \tan \phi + c \quad (2)$$

The question is whether the above equations are also valid in the range of great pressures. An effort is made to give an answer partly by experiments partly by theoretical considerations. The tests were made on dry sand only, but the results obtained may be generalized for cohesive soils, too.

The grain distribution curve of the sand used in the experiments is shown on Fig. 1, the effective grain size:  $D = 0.2 \text{ mm}$ . Its void ratio is  $e_{\text{min}} = 0.568$  in dense state and  $e_{\text{max}} = 0.985$  in loose state, its specific gravity  $s = 2.66 \text{ g/cm}^3$ .

#### a) Compression.

The compression test carried out in an oedometer after Casagrande, dimensions of the soil sample were as follows: diameter  $\phi 45 \text{ mm}$ , height  $18 \text{ mm}$ . The water content of the sand was  $w = 5.8 \%$ . The pressure raised in uniformly graduated steps up to  $p = 200 \text{ kg/cm}^2$ . The function  $p = f(e)$  is plotted on semi and double logarithmic scale (Fig. 2). It may be stated, that the curve follows the logarithmic law to  $p_1 = 4.0 \text{ kg/cm}^2$  only, from there it obeys a power parabolic law, that is, the more general law of compression:

$$e = e_0 - c_1 p^m \quad (3)$$

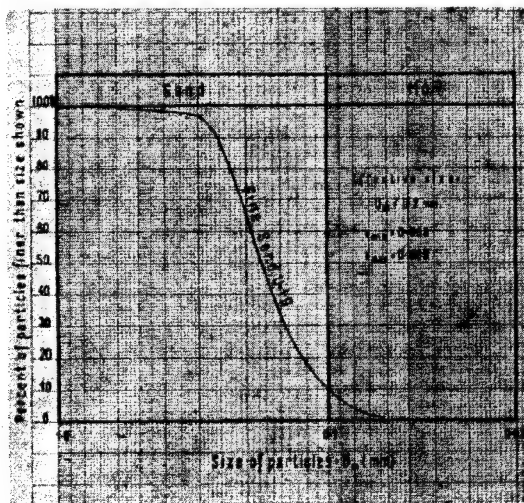


FIG.1

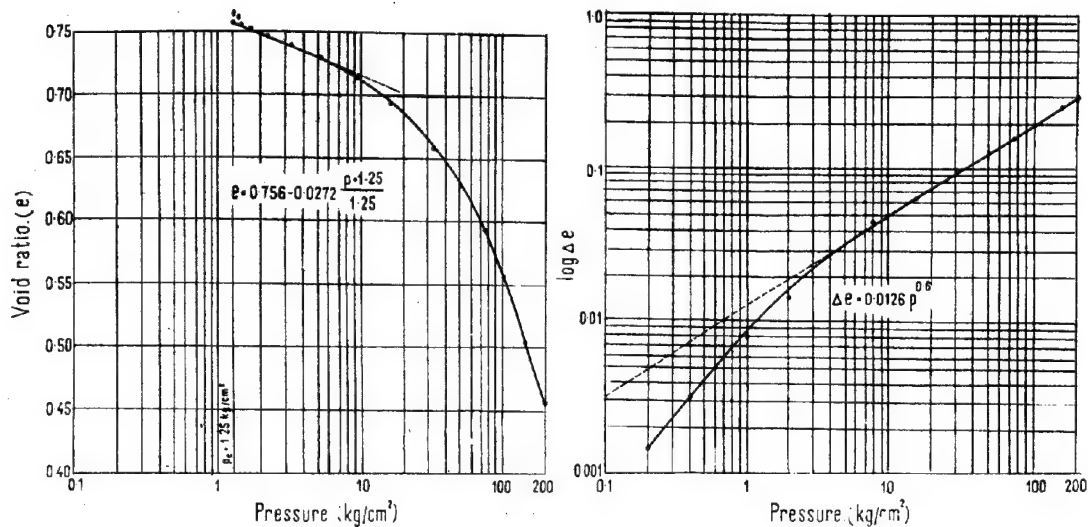


FIG. 2

In the case of our experiment:

$$e = 0.756 - 0.0126 p^{0.6}$$

Result: the law of compression of soil between pressures  $p = 0 - p_1$  is expressed by Terzaghi's logarithmic law, above pressure  $p_1$  the power parabolic law.

#### b) Geostatic pressure.

In a semi-infinite solid bounded by a horizontal line, as a result of  $\tau = 0$  the horizontal and vertical lines are trajectories of principal stresses, the principal stresses are functions of  $y$  only. From the equilibrium of the elementary prism:

$$\frac{d\sigma_y}{dU} = \gamma \quad (4)$$

wherein  $\gamma$  specific weight is not a constant, the density increases with increasing depth.

(Fig. 3) In the case of dry soil:

$$\gamma = \frac{s}{1+e} \quad (5)$$

Substituting the value of  $s$  from Eq.(1) or (3)

a)  $\sigma_y < p_1$

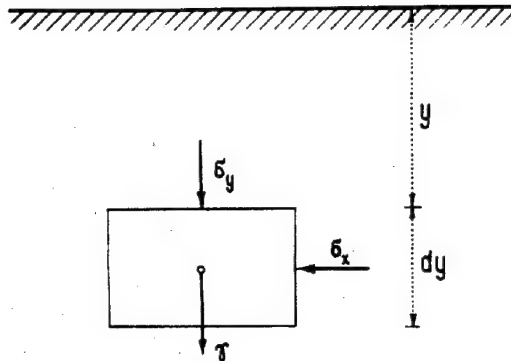


FIG. 3

$$\frac{d\sigma_y}{dU} = \frac{s}{(1+e_0) - c_1 \ln(\frac{\sigma_y + p_c}{p_c})} = \frac{s}{A - c_1 \ln(\sigma_y + p_c)}$$

Using the abbreviation  $A = 1 + e_0 + c_1 \ln p_c$  integrating and considering that if  $y = 0$ ,  $\sigma_y = 0$

$$U = \frac{A}{s} \sigma_y - \frac{c_1}{s} (\ln \sigma_y - 1) \quad (6)$$

That is the geostatic pressure is not linear with depth as has been computed generally up to the present.

1) If  $\sigma_y > p_1$  the power parabolic relation must be used, i.e.

$$\frac{d\sigma_y}{dU} = \frac{s}{1 + e_0 - c_1 \sigma_y^m}$$

whence

$$U = \frac{\sigma_y}{\gamma_0} - \frac{c_1}{s(m+1)} \sigma_y^{m+1} \quad (7)$$

wherein  $\gamma_0 = \frac{s}{1+e_0}$  in the original state, the specific weight on the surface.

The curves according to Eq. (6) and (7) are plotted on Fig. 4. The curves coincide in the upper part in such a way, that their distinction is not possible, therefore, the power parabolic law may be accepted in both sections.

The geostatic pressure computed from constant  $\gamma_0$  is a straight line plotted against the depth and gives values 10 % smaller than the correct formula. The curve reveals the real situation up to  $y = 1300$  m depth.

c) Specific weight varying with the depth.  $s$   
The specific weight of the dry sand  $\gamma_0 = 1.5$  t/m<sup>3</sup> substituting  $e = e_0 - c_1 \sigma_y^m$  we obtain:  $1 + e$

$$\gamma = \frac{s}{(1+e_0) - c_1 \sigma_y^m} \approx \gamma_0 \left( 1 + \frac{c_1}{1+e_0} \sigma_y^m \right) \quad (8)$$

that is, the specific weight increases with the power of pressure its variation with depth is shown on Fig. 4. The specific weight of the soil on the surface  $\gamma_0 = 1.5$  t/m<sup>3</sup> increases up to  $\gamma = 1.8$  t/m<sup>3</sup> in a depth of  $y = 1200$  m.



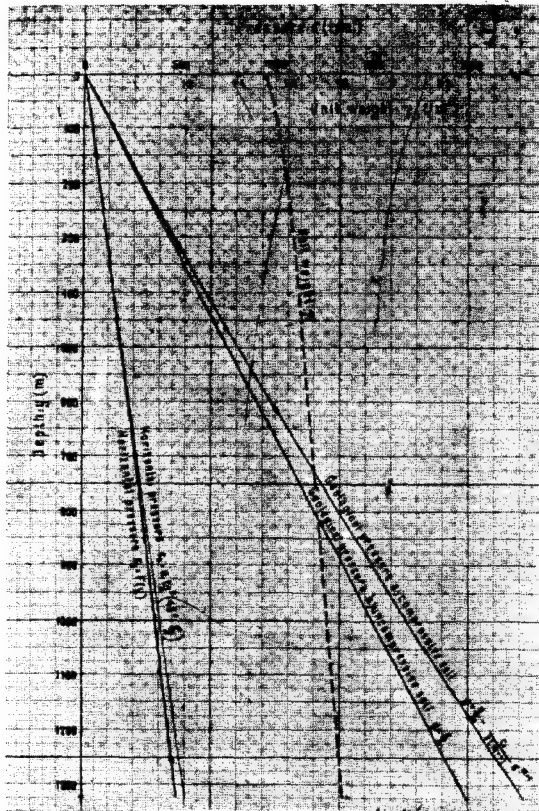


FIG. 4

## d) Law of shearing.

Shearing tests under great pressures were carried out by the Geotechnical Committee Gov. Railways of Japan 1). It was proved that the law of shearing is better characterized by the power parabolic relationship  $t = A n^m$  than by Coulomb's assumptions. This fact was suggested by the author in 1934 plotting one test of the M.I.T. to double logarithmic scale 2), 3) (Fig. 5). The straight lines prove between wide limits  $n = 0.01 - 10 \text{ kg/cm}^2$  the validity of the power parabolic law.

We examine theoretically in the following the law of friction of compressive soils. Assume a nonlinear relationship between  $t$  and  $n$ , which is characterized by some curve (Fig. 6). The cohesion belonging to compression pressure  $n$  is the value  $(t - n \operatorname{tg} \epsilon)$  measured at  $n = 0$ . Based on the preceding facts it may be assumed, that cohesion increases with increasing  $n$  pressures according to a power parabolic law, that is

$$t - n \operatorname{tg} \epsilon = c n^m \quad (9)$$

or substituting  $\operatorname{tg} \epsilon = \frac{dt}{dn}$  :  $t - \frac{dt}{dn} n = c n^m$

whence the demanded law:

$$t = k n + \frac{c}{1-m} n^m \quad (10)$$

$k$  = constant of integration.

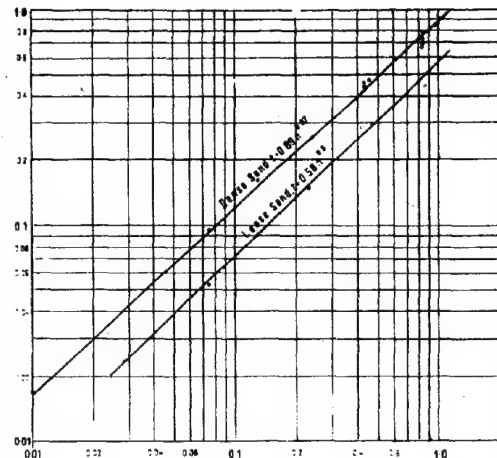


FIG. 5

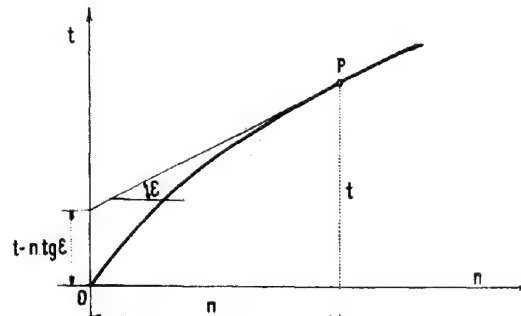


FIG. 6

Since

$$\operatorname{tg} \epsilon = \frac{dt}{dn} = k + \frac{cm}{1-m} n^{m-1} \quad (11)$$

it may be seen that

$$1. \text{ if } m < 1 \quad \operatorname{tg} \epsilon = k + \frac{cm}{1-m} n^{m-1}$$

the curve is a power parabola, its tangent at the origin is vertical, its asymptote has slope  $k = \operatorname{tg} \phi_0$  (Fig. 7) curve 1.

$$2. \text{ if } m > 1 \quad \operatorname{tg} \epsilon = k - \frac{cm}{m-1} n^{m-1}$$

the slope of the tangent at the origin:  $k = \operatorname{tg} \phi_0$

The curve has a horizontal tangent at  $n_0^{m-1} =$

$k \cdot \frac{m-1}{cm}$  with increasing  $n$  values  $\epsilon$  becomes

negative and the curve intersects the  $n$  axis, that is  $t = 0$  (fig. 7) curve 2. Which is physically nonsense, so the curve is valid up to point B only, the law of friction is expressed by the continuation of curve 1.

3. if  $m = 1$ ;  $\epsilon = \text{constant}$ , we obtain Coulomb's law of friction:  $t = n (\operatorname{tg} \epsilon + c) = n \operatorname{tg} \phi$

All three curve shapes may occur in accordance with the compactness of granular material. Test results carried out with sand by various  $e_0$  initial void ratios are shown on

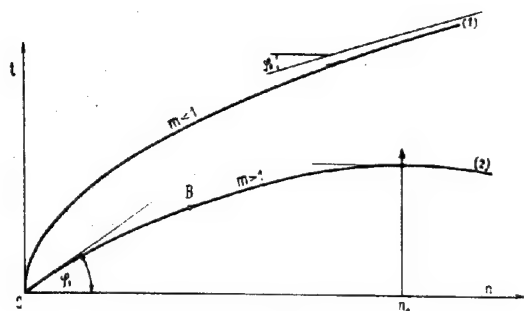


FIG. 7

Fig 8. If  $n > 2 \text{ kg/cm}^2$  the relationship between  $t$  and  $n$  is expressed by the power parabolic law:

$$\begin{aligned} e_0 = 0.85 & \quad t = 0.478 n^{1.14} \\ e_0 = 0.76 & \quad t = 0.54 n^{1.1} \\ e_0 = 0.67 & \quad t = 0.74 n \\ e_0 = 0.56 & \quad t = 0.906 n^{0.93} \end{aligned}$$

The exponent  $n \approx 1$ , so Coulomb's law is a practically acceptable approximation.

The importance of the first term of Eq. (10) could not be stated as well as required, because the construction of our shearing apparatus did not allow to produce reliable normal stress under  $n = 1 \text{ kg/cm}^2$ . The law of shearing by small stresses remains to be investigated.

The tests were carried out by Assist. E. Szilvgyi, besides him, H. Hjj willingly participated in preparing the figures and the manuscript.

#### REFERENCES:

1) Bulletin Geotechnical Committee Gov. Rail-

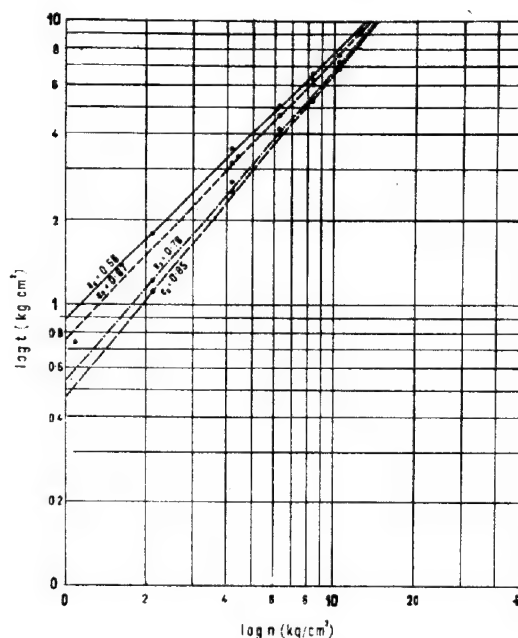


FIG. 8

ways of Japan. No. 4. 1936 Tokyo.

- 2) Jky, J.: The classical Earth Pressure Theory. Intern. Congress for Applied Mech. IV. Cambridge, 1934.
- 3) Karl v. Terzaghi: Festigkeitseigenschaften der Schuttungen Sedimente und Gels. Handbuch der physik. und techn. Mechanik Bd. IV.2.

-0-0-0-0-0-0-

I e 10

### A FUNDAMENTAL THEORY OF PLASTIC DEFORMATION AND BREAKAGE OF SOIL

KANO HOSHINO

Japan

#### I. PLASTIC DEFORMATION AND BREAKAGE OF SOIL MASS.

Under the action of external forces, a soil mass underwent a gradually increasing deformation and finally reaches to a breaking point, which appears only when tensile or shearing stresses are working. On the other hand, by compaction it becomes more solid and dense, increasing the difficulty of deformation and affording a higher breaking strength. We must deal with soil masses as plastic materials with narrow or no range of elasticity. Researches on the plastic deformation

have been in lower stage, remaining a vast room for future developments and we can find no proper theory applicable to the soil mechanics.

In this paper, author presents a hypothetical theory of plastic deformation and breakage of soil mass based on a assumption that the deformation and breakage have close relations to the volume of strain energy stored in the soil mass.

A series of results including those of elastic theory as a special case were obtained under the conditions that the elastic relations between stresses and strains can exist only when the stresses change in infinite-

simal small amounts and that the both coefficients have a linear proportion to the strain energy which increases under compressive stresses, but decreases under tensile or shearing stresses.

New rigorous formulae of strain energy and both coefficients were derived as functions of mean normal and mean shearing stresses. Also the fundamental equations between stresses and strains beyond the elastic limit and a condition of breakage obtained. Applying these relations to some fundamental cases of such stress conditions as pure shear, simple normal stress, and equal stresses in two- or three- dimensional problems, the stress-strain relations and the values of stresses and strains at breakage were determined.

Those relations and values can explain properly the well known tendencies of experimental results and can solve some important problems in the strength of materials.

Finally the envelopes of Mohr's circles were determined under such stress conditions as plane stresses, plane strains, and triaxial symmetrical stresses.

## II. CONDITIONS ASSUMED AND FUNDAMENTAL RELATIONS OBTAINED.

As the elastic theory is reasonable when the change of stress remains in a small amount, we can express the relations between stresses and strains at a point in a soil mass exerted by external forces as follows.

$$\begin{aligned} d\epsilon_1 &= \{d\sigma_1 - \nu(d\sigma_2 + d\sigma_3)\} / E \\ d\epsilon_2 &= \{d\sigma_2 - \nu(d\sigma_1 + d\sigma_3)\} / E \\ d\epsilon_3 &= \{d\sigma_3 - \nu(d\sigma_1 + d\sigma_2)\} / E \end{aligned} \quad (1)$$

where  $\sigma_1, \sigma_2, \sigma_3$  = three principal stresses

$\epsilon_1, \epsilon_2, \epsilon_3$  = three principal strains.

$E$  = modulus of elasticity.

$\nu$  = Poisson's ratio.

Using the designations

$$G = \frac{3E}{4(1+\nu)} \quad V = \frac{E}{1-2\nu} \quad (2)$$

we can transform (1) into

$$\begin{aligned} d\epsilon_1 &= (d\tau_1 - d\tau_2)/2G + (d\sigma_1 + d\sigma_2 + d\sigma_3)/3V \\ d\epsilon_2 &= (d\tau_2 - d\tau_1)/2G + (d\sigma_1 + d\sigma_2 + d\sigma_3)/3V \\ d\epsilon_3 &= (d\tau_3 - d\tau_1)/2G + (d\sigma_1 + d\sigma_2 + d\sigma_3)/3V \end{aligned} \quad (3)$$

where  $\tau_1, \tau_2, \tau_3$  = three principal shearing stresses, namely

$$\tau_1 = (\sigma_1 - \sigma_2)/2, \quad \tau_2 = (\sigma_2 - \sigma_3)/2, \quad \tau_3 = (\sigma_3 - \sigma_1)/2$$

The change of strain energy due to these small changes of stresses can be determined by

$$dX = dX_G + dX_V \quad (4)$$

where  $dX_G = \frac{3d(\tau_1^2)}{G}$   $dX_V = \frac{3d(\sigma_1^2)}{V}$  in which

$$\tau_m = \sqrt{\frac{\tau_1^2 + \tau_2^2 + \tau_3^2}{3}} \quad \sigma_m = \frac{\sigma_1 + \sigma_2 + \sigma_3}{3} \quad (5)$$

$\tau_m$  and  $\sigma_m$  are to be called the mean shearing stress and the mean normal stress respectively. From the equations (3) and (4), we can know that each principal strain and the strain energy can be divided into two parts, one due to the change in form by shearing stresses, the other due to the change in volume by normal stresses.

If both coefficients  $G$  and  $V$  are taken as constants in the case of elasticity, we obtain the strain energy from (4) expressed by

$$X = X_G + X_V = \frac{3\tau_m^2}{G} + \frac{3\sigma_m^2}{V} \quad (6)$$

Let  $\tau_m = 0$  in (6), we get  $X = \frac{3\sigma_m^2}{V}$  (7)

The strain energy changes, as well known, in proportion to the square of the mean normal stress when no shearing stress is existing.

Author assumed that both coefficients  $G$  and  $V$  have no constant values, but vary in linear proportion to the strain energy stored in the soil mass. Then taking  $g$  and  $v$  as constants, we have

$$G = gX, \quad V = vX \quad (8)$$

Assuming that the strain energy can be stored only by compressive stresses but consumed by tensile and shearing stresses, and taking a compressive stress as positive and a tensile one as negative, we can express the change of strain energy in the soil mass by

$$dX = dX_V - dX_G \quad (9)$$

in which

$$dX_V = \frac{3d(\sigma_m^2)}{V} \quad dX_G = \frac{3d(\tau_m^2)}{G}$$

By integration of (9) introducing (8), we have

$$X = \sqrt{3(\sigma_m^2/v - \tau_m^2/g)}$$

Let  $V = V_0$  when  $\tau_m = 0$  and  $\sigma_m = \sigma_0$  as initial condition and taking  $G = \mu^2 V$ , we get

$$v = \frac{(V_0/\sigma_0)^2}{3} \quad g = \mu^2 v - \mu^2 \frac{(V_0/\sigma_0)^2}{3} \quad (10)$$

Hence we can express the strain energy by

$$X = \frac{3\sigma_0}{V_0} \sqrt{\sigma_m^2 - (\tau_m/\mu)^2} \quad (11)$$

Let  $\tau_m = 0$  in (11), we have

$$X = \frac{3\sigma_0\sigma_m}{V_0} \quad (12)$$

We know from (12) that the strain energy is proportional to the mean normal stress in this plastic theory, but not to the square of it in the case of elastic theory. Those expressions of strain energy by (11) and (12) may be more natural and rigorous than those in elastic theory.

Putting (10) and (11) in (8), we can express the both coefficients as functions of mean normal and mean shearing stresses:

$$\begin{aligned} V &= \frac{V_0}{\sigma_0} \sqrt{\sigma_m^2 - (\tau_m/\mu)^2} \\ G &= \mu^2 V - \mu^2 \frac{V_0}{\sigma_0} \sqrt{\sigma_m^2 - (\tau_m/\mu)^2} \end{aligned} \quad (13)$$

The three principal strains in this case can be expressed by (3) introducing the values of  $V$  and  $G$  from (13) as follows.

$$d\epsilon = d(\tau - \tau_0)/2\mu^2 V + d(\sigma_1 + \sigma_2 + \sigma_3)/3V$$

$$d\epsilon = d(\tau - \tau_0)/2\mu^2 V + d(\sigma_1 + \sigma_2 + \sigma_3)/3V$$

$$d\epsilon = d(\tau - \tau_0)/2\mu^2 V + d(\sigma_1 + \sigma_2 + \sigma_3)/3V \quad (14)$$

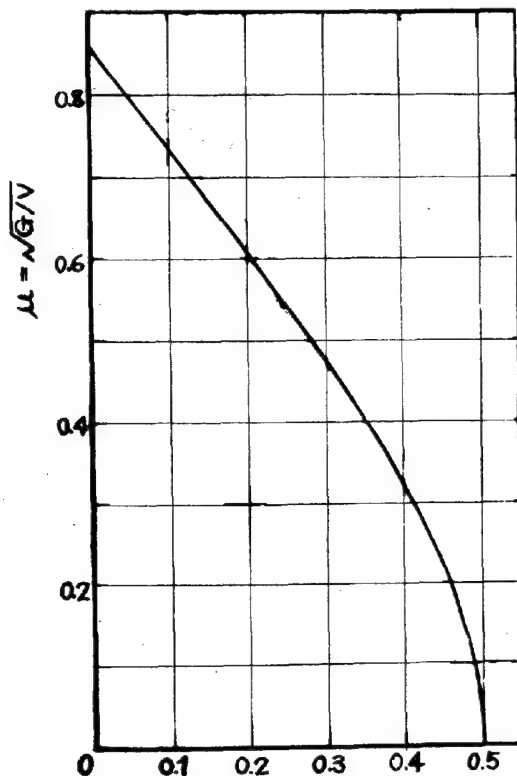
The following relations are derived referring to (2)

$$\mu = \frac{\sqrt{G}}{V} = \frac{\sqrt{3(1-2\nu)}}{4(1+\nu)}$$

$$E = \frac{6VG}{3V+2G} = \frac{6\mu^2}{3+2\mu^2} V$$

$$\text{or } \nu = \frac{3V-4G}{2(3V+2G)} = \frac{3-4\mu^2}{2(3+2\mu^2)} \quad (15)$$

From (15) we know that  $\mu$  is a constant which represents a ratio of a resistance in form change due to the shearing stresses to that in volume change due to the normal stresses and its value changes from zero to  $\sqrt{3}/2$  (0.866) with the value of Poisson's ratio (Fig.1).



Relation between the new constant  $\mu$  and Poisson's ratio  $\nu$ .

FIG.1

At the breakage of a soil mass, the strain energy reduces to zero.

Then taking  $I=0$  in (11), we obtain the following relation as a condition of breakage

$$\tau_m = \mu \sigma_m \quad (16)$$

From (16) we know that  $\mu$  is also a ratio of mean shearing stress to the mean normal stress which is to be held at the breaking point.

Under some fundamental conditions of stress or strain, we can easily determine the stress-strain relations from the integration of (14) and the stresses and strains at breakage from (16).

### III. STRESS-STRAIN RELATIONS AND THE VALUES OF STRESSES AND STRAINS AT BREAKAGE UNDER SOME FUNDAMENTAL CONDITIONS OF STRESS OR STRAIN.

It may be assumed that a soil body has a bulk modulus  $V_0$ , holding its shape under a hydrostatic pressure  $\sigma_0$  as an initial condition.

The following cases were studied.

- A. Two-dimensional problems (plane stresses or plane strains).
  1. Pure shear.
  2. Simple normal stress in plane strains.
  3. Equal normal stresses in plane stresses.
  4. Equal normal stresses in plane strains.
- B. Three-dimensional problems.
  1. Pure shear.
  2. Simple normal stress.
  3. Consolidation with no permission of lateral flow.
  4. Equal normal stresses (hydrostatic pressure).

- A. Two-dimensional problems.

1. Pure shear.

Denote the stress and the strain by external forces only by the letters  $\bar{\sigma}$  and  $\bar{\epsilon}$

Let  $\sigma_1 = \sigma_0 + \bar{\sigma}$ ,  $\sigma_2 = \sigma_0$ , and  $\sigma_3 = \sigma_0 - \bar{\sigma}$ , then we

get from (5)  $\sigma_m = (\sigma_1 + \sigma_2 + \sigma_3)/3 = \sigma_0$

$$\text{and } \tau_1 = \frac{\sigma_1 - \sigma_2}{2} = \frac{\bar{\sigma}}{2}, \tau_2 = \frac{\sigma_2 - \sigma_3}{2} = \frac{\bar{\sigma}}{2}, \tau_3 = \frac{\sigma_3 - \sigma_1}{2} = -\frac{\bar{\sigma}}{2}$$

$$\text{hence } \tau_m = \frac{\tau_1^2 + \tau_2^2 + \tau_3^2}{3} = \bar{\sigma}^2/2$$

Putting these values in (13), we get

$$V - \frac{V_0}{\sigma_0} \sqrt{\sigma_m^2 - (\tau_m/\mu)^2} = V_0 \sqrt{1 - \frac{(\bar{\sigma}/\sigma_0)^2}{2\mu^2}}$$

hence from (14)

$$d\epsilon = d\epsilon_1 = -d\epsilon_2 = \frac{d\tau_1 - d\tau_2}{2\mu^2 V} = \frac{3}{4\mu^2 V_0} \frac{d\bar{\sigma}}{\sqrt{1 - \frac{(\bar{\sigma}/\sigma_0)^2}{2\mu^2}}}$$

$$d\epsilon_3 = 0$$

Integrating and taking  $\bar{\epsilon}=0$  when  $\bar{\sigma}=0$ , we get the stress-strain relation expressed by

$$\bar{\epsilon} \frac{V_0}{\sigma_0} = \frac{3}{2\sqrt{2}\mu} \sin^{-1} \left( \frac{1}{\sqrt{2}\mu} \cdot \frac{\bar{\sigma}}{\sigma_0} \right) \quad (17)$$

If the change of stress remains in a small amount, the above relation becomes

$$\Delta \bar{\epsilon} = \frac{3}{4\mu^2} \cdot \frac{\Delta \bar{\sigma}}{V_0} \quad (18)$$

The coefficient of tangent at the zero point of stress-strain curve is equal to

$$k = \frac{\Delta \bar{\sigma}}{\Delta \bar{\epsilon}} = \frac{4\mu^2}{3} V_0 \quad (19)$$

At the breakage of soil mass, the stress and strain can be obtained putting the values of  $\sigma_m$  and  $\tau_m$  in (16) as follows.



$$\begin{aligned} \mu^2 < \frac{3}{8} : \bar{\epsilon} \frac{V}{\sigma_1} &= \frac{3\sqrt{3}}{\sqrt{3-8\mu^2}} \left[ \ln \left( \sqrt{1 + \frac{6}{3+8\mu^2} \cdot \frac{\bar{\sigma}_1}{\sigma_1} + \frac{3(3-8\mu^2)}{(3+8\mu^2)^2} \left( \frac{\bar{\sigma}_1}{\sigma_1} \right)^2} \right) \right. \\ &\quad \left. + \frac{\sqrt{3(3-8\mu^2)}}{3+8\mu^2} \cdot \frac{\bar{\sigma}_1}{\sigma_1} + \frac{\sqrt{3}}{\sqrt{3-8\mu^2}} \right] - \ln \left( 1 + \frac{\sqrt{3}}{\sqrt{3-8\mu^2}} \right) \\ \mu^2 = \frac{3}{8} : \bar{\epsilon} \frac{V}{\sigma_1} &= 3 \left( \sqrt{1 + \frac{\bar{\sigma}_1}{\sigma_1}} - 1 \right) \\ \mu^2 > \frac{3}{8} : \bar{\epsilon} \frac{V}{\sigma_1} &= \frac{3\sqrt{3}}{\sqrt{8\mu^2-3}} \left[ \sin^{-1} \frac{\sqrt{3}}{2\sqrt{2}\mu} + \right. \\ &\quad \left. - \sin^{-1} \left\{ \frac{\sqrt{3}}{2\sqrt{2}\mu} - \frac{\sqrt{3}(8\mu^2-3)}{2\sqrt{2}\mu(3+8\mu^2)} \cdot \frac{\bar{\sigma}_1}{\sigma_1} \right\} \right] \end{aligned} \quad (38)$$

At the breakage

$$\begin{aligned} \mu^2 > \frac{3}{8} : \frac{\bar{\sigma}_1}{\sigma_1} &= \frac{8\mu^2+3}{\sqrt{3}(2\sqrt{2}\mu-\sqrt{3})} \\ \bar{\epsilon} \frac{V}{\sigma_1} &= \frac{3\sqrt{3}}{\sqrt{8\mu^2-3}} \cdot \left[ \sin^{-1} \frac{\sqrt{3}}{2\sqrt{2}\mu} \pm \frac{\pi}{2} \right] \end{aligned} \quad (39)$$

4. Equal stresses (hydrostatic pressure).

Let  $\sigma_1 = \sigma_2 = \sigma_3 = \sigma + \bar{\sigma}$  we get

$$\bar{\epsilon} \frac{V}{\sigma_1} = \ln \left( 1 + \frac{\bar{\sigma}}{\sigma_1} \right) \quad (40)$$

$$\Delta \bar{\epsilon} = \Delta \frac{\bar{\sigma}}{V}, \quad K = V_0 \quad (41)$$

At the breakage  $\frac{\bar{\sigma}}{\sigma_1} = -1, \quad \bar{\epsilon} \frac{V}{\sigma_1} = -\infty \quad (42)$

The stress-strain curves are shown in Fig. 2(a), (b), and (c) for the case of  $\mu = 0.3, 0.5$ , and  $0.7$  (or  $\nu = 0.415, 0.286$ , and  $0.131$ ). The effects of  $\mu$  on the values of the initial coefficient of tangent  $k$  and on the values of stress  $\bar{\sigma}$  or strain  $\bar{\epsilon}$  at the breakage are shown in Figs. 3 and 4(a), (b).

It is a well known fact that the brittle materials with lower Poisson's ratio have higher ratios of shearing and compressive strengths to tensile strength, and on the contrary, the ductile materials with higher Poisson's ratio have lower ratios of those strengths. We can know that the new theory shows similar tendencies, if the correspondences of the lower values of Poisson's ratio to the higher values of the new constant  $\mu$  are taken into consideration.

#### IV. ENVELOPES OF MOHR'S CIRCLES.

We can determine the envelopes of Mohr's circles from the condition of breakage under such stress conditions as plane stresses, plane strains, and triaxial symmetrical stresses. Mohr's circle may be expressed by

$$F = \bar{\sigma}^2 - (\bar{\sigma} + \bar{\sigma}_1) \bar{\sigma} + \bar{\sigma}_1 \bar{\sigma}_2 - \bar{\tau}^2 = 0 \quad (43)$$

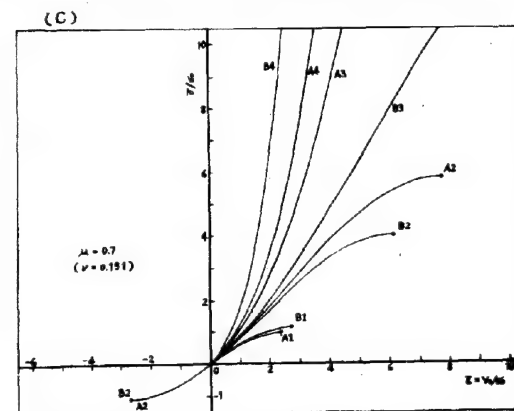
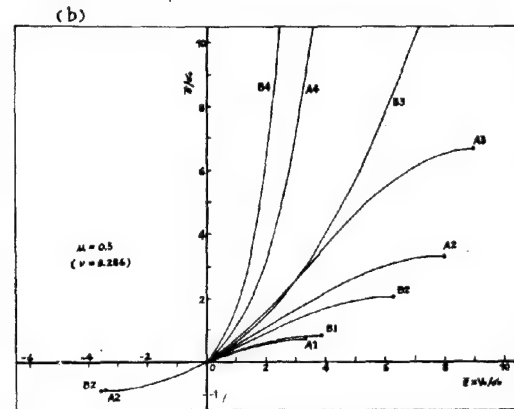
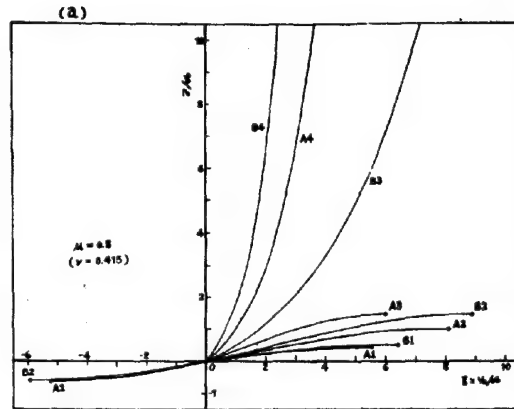
where  $\bar{\sigma}$  normal stress,  $\bar{\tau}$  tangential stress.

The envelope of  $F$  can be determined from the result of its partial differentiation by  $\bar{\sigma}_1$  or by  $\bar{\sigma}_2 + \bar{\sigma}_3$ , putting in  $F$  a relation between  $\bar{\sigma}_1$  and  $\bar{\sigma}_2$  obtained from the condition of breakage.

##### 1. Plane stresses.

In the case of plane stresses,

$$\sigma_3 = \sigma_4 = \sigma_5 = 0, \quad \sigma_1 = \sigma_2 + \bar{\sigma}_1$$



Stress-strain curves.

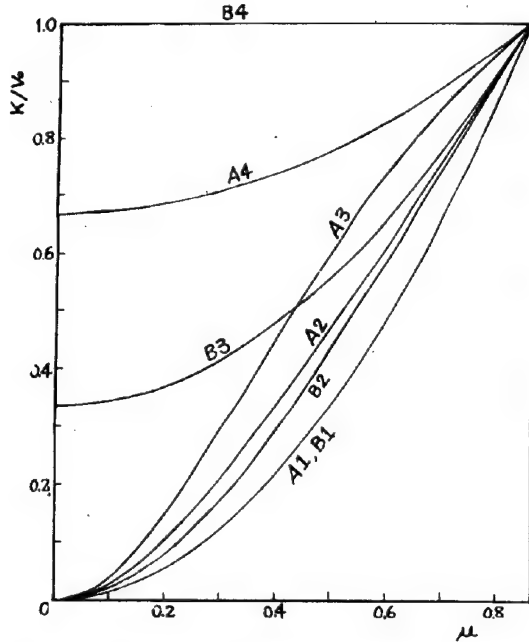
FIG. 2

Then 
$$\sigma_m = \sigma_1 + \frac{\bar{\sigma}_1 + \bar{\sigma}_2}{3}$$

$$\tau_m = \frac{\sqrt{(\bar{\sigma}_1 + \bar{\sigma}_2)^2 - 3\bar{\sigma}_1\bar{\sigma}_2}}{\sqrt{6}}$$

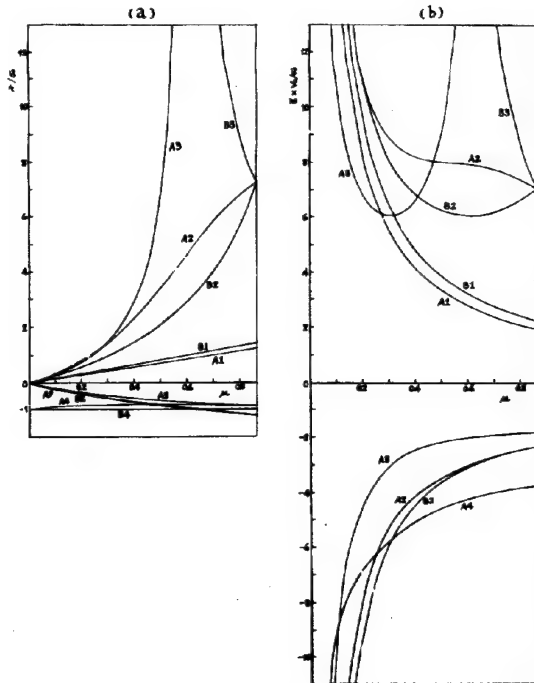
hence putting these values in the condition of breakage  $\tau_m = \mu \sigma_m$  we get

$$\bar{\sigma}_1 \bar{\sigma}_2 = \frac{3-2\mu^2}{9} (\bar{\sigma}_1 + \bar{\sigma}_2)^2 - \frac{4\mu^2}{3} (\bar{\sigma}_1 + \bar{\sigma}_2) \sigma_1 - 2\mu^2 \sigma_1^2$$



Effects of  $\mu$  on the initial coefficient of tangent  $k$ .

FIG.3



Effects of  $\mu$  on the stresses and strains at breakage.

FIG.4

Putting this value in  $F$  and differentiating it partially by  $\bar{\sigma}_1 + \bar{\sigma}_2$ , we have  $\frac{3(3\bar{\sigma} + 4\mu^2\sigma_1)}{\bar{\sigma}_1 + \bar{\sigma}_2} = \frac{2(3-2\mu^2)}{2(3-2\mu^2)}$

Substituting this relation in  $F$ , we obtain the equation of its envelope expressed by

$$\tau^2 = \frac{-(3-8\mu^2)\bar{\sigma}^2 + 24\mu^2\bar{\sigma}\sigma_1 + 24\mu^4\sigma_1^2}{4(3-2\mu^2)} \quad (44)$$

In this case, we obtain

ellipses when  $\mu^2 < \frac{3}{8}$  a parabola when  $\mu^2 = \frac{3}{8}$ ,

hyperbolas and if  $\sigma_1 = 0$ , straight lines when  $\mu^2 > \frac{3}{8}$

## 2. Plane strains.

In the case of plane strains,  $d\epsilon_3 = 0$  Then

$$\bar{\sigma}_1 = \frac{3-4\mu^2}{2(3+2\mu^2)} \cdot (\bar{\sigma}_1 + \bar{\sigma}_2)$$

$$\sigma_2 = \sigma_1 + \frac{2(3+2\mu^2)}{2(3+2\mu^2)} \cdot (\bar{\sigma}_1 + \bar{\sigma}_2)$$

$$\tau_m = \sqrt{\frac{9+12\mu^2+16\mu^4}{8(3+2\mu^2)} \cdot (\bar{\sigma}_1 + \bar{\sigma}_2)^2 - \frac{\bar{\sigma}_1\bar{\sigma}_2}{2}}$$

Similarly as before, from the condition of breakage, we get

$$\bar{\sigma}_1\bar{\sigma}_2 = \frac{9-6\mu^2+16\mu^4}{4(3+2\mu^2)} \cdot (\bar{\sigma}_1 + \bar{\sigma}_2)^2 - \frac{6\mu^2}{3+2\mu^2} \cdot \sigma_1(\bar{\sigma}_1 + \bar{\sigma}_2) - 2\mu^4\sigma_1^2$$

Putting this value in  $F$  and differentiating it partially by  $\bar{\sigma}_1 + \bar{\sigma}_2$ , we get

$$\bar{\sigma}_1 + \bar{\sigma}_2 = \frac{2(3+2\mu^2)^2}{9-6\mu^2+16\mu^4} \cdot \left( \bar{\sigma} + \frac{6\mu^2}{3+2\mu^2} \cdot \sigma_1 \right)$$

Hence the equation of envelope is expressed by

$$\tau^2 = \frac{2\mu^2}{9-6\mu^2+16\mu^4} \left[ 3(3-2\mu^2)\bar{\sigma}^2 + 6(3+2\mu^2)\sigma_1\bar{\sigma} + (9+12\mu^2+16\mu^4)\sigma_1^2 \right] \quad (45)$$

In this case, we obtain hyperbolas and if  $\sigma_1 = 0$ , straight lines.

## 3. Triaxial symmetrical stresses.

In the case of triaxial symmetrical stresses,  $\sigma_1 = \sigma_2 = \bar{\sigma}_1$   $\sigma_3 = \sigma_1 + \bar{\sigma}_2$

Then

$$\sigma_1 = \sigma_1 + (\bar{\sigma}_1 + 2\bar{\sigma}_2)/3$$

$$\tau_m = \tau(\bar{\sigma}_1 - \bar{\sigma}_2)/\delta$$

From the condition of breakage, we get

$$\bar{\sigma}_1 = \frac{1}{(\pm 3 - \sqrt{6}\mu)} [3\sqrt{6}\mu\sigma_1 + (\pm 3 \pm \sqrt{6}\mu)\bar{\sigma}_2]$$

Putting this value in  $F$  and differentiating it partially by  $\bar{\sigma}_2$ , we get

$$\bar{\sigma}_2 = \frac{(\pm 6 + \sqrt{6}\mu)\bar{\sigma} - 3\sqrt{6}\mu\sigma_1}{(\pm 6 + 4\sqrt{6}\mu)}$$

$$\bar{\sigma}_1 = \frac{(\pm 6 + \sqrt{6}\mu)\bar{\sigma} + 3\sqrt{6}\mu\sigma_1}{(\pm 6 - 2\sqrt{6}\mu)}$$

Hence the equation of envelope is expressed by

$$\tau = \frac{\pm 3\sqrt{6}\mu}{\sqrt{2}(\pm 3 - \sqrt{6}\mu)(\pm 3 + 2\sqrt{6}\mu)} \cdot (\bar{\sigma} + \sigma_1) \quad (46)$$

In this case, we obtain straight lines and we can determine the values of cohesion and of coefficient of internal friction as follows.

$$C = \frac{3\sqrt{3}\mu}{\sqrt{2(\pm 3 - \sqrt{6}\mu)(\pm 3 + 2\sqrt{6}\mu)}} \cdot \sigma_1$$

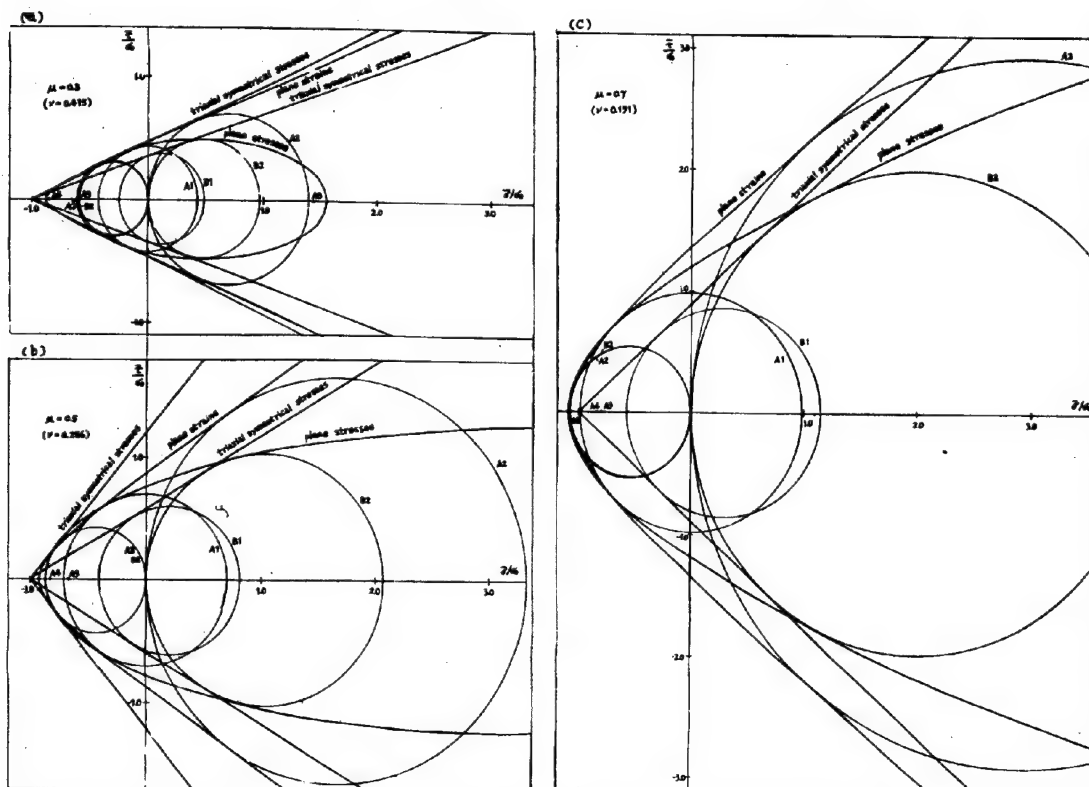
$$\tan \varphi = \frac{3\sqrt{3}\mu}{\sqrt{2(\pm 3 - \sqrt{6}\mu)(\pm 3 + 2\sqrt{6}\mu)}} \quad (47)$$

The envelopes are shown in Fig. 5 (a), (b),

where  $\sigma_1, \tau_1$  = constants given by the initial condition.

$\sigma_m, \tau_m$  = mean normal and mean shearing stress  
 $\mu$  = a constant ratio determined by Poisson's ratio referred to (15),

$$\mu = \sqrt{\frac{3(1-2\nu)}{4(1+\nu)}}$$



Envelopes of Mohr's circles.

FIG. 5

and (c) for the case of  $\mu = 0.3, 0.5$ , and  $0.7$  (or  $\nu = 0.415, 0.286$ , and  $0.171$ ).

#### V. SUMMARY.

##### 1. Assumptions are:

- The equations of elastic deformations can be applied only when the changes of stresses remain in small amounts.
- The two coefficients existing between stress and strain (one of form change by shearing stresses, the other of volume change by normal stresses) are both in proportion to the strain energy stored in a soil mass.
- The strain energy in a soil mass may be stored by compressive stresses, but consumed by tensile or shearing stresses.

##### 2. The fundamental relations obtained from the above assumptions are:

- The strain energy can be expressed by (11):

$$X = 3 \frac{\sigma_1}{V_1} \cdot \sqrt{\sigma_1^2 - \left(\frac{\tau_1}{\mu}\right)^2}$$

We can know that in this new theory the strain energy in a soil mass is proportional to the mean normal stress when no shearing stress appears, which is more natural and rigorous relation than that proportional to the square of it in the elastic theory.

- Both coefficients can be expressed by (13) as functions of the mean normal and mean shearing stresses and there exists a proportionality between them:

$$V = \frac{V_1}{\sigma_1} \cdot \sqrt{\sigma_1^2 - \left(\frac{\tau_1}{\mu}\right)^2}$$

$$G = \mu^2 V = \mu^2 \frac{V_1}{\sigma_1} \cdot \sqrt{\sigma_1^2 - \left(\frac{\tau_1}{\mu}\right)^2}$$

- Introducing the values of  $G$  and  $V$  in (3), we can determine the fundamental equations expressed by (14), which represent the relations between stresses and strains in a plastic material.

- At the breakage of a soil mass, under a condition that the strain energy reduces to zero, we obtain a condition of breakage



expressed by (16):  $\tau = \mu \sigma$

from which we can derive the stresses and strains at breakage under some fundamental conditions of stresses or strains.

3. Under some fundamental conditions of stresses or strains, such as pure shear, simple normal stress and equal normal stresses etc. in two- and three-dimensional problems, the stress-strain relations were determined and the obtained results showed:

- They can express quite well the tendencies of the well known experimental results.
- Elasticity can be applied to the new theory as its special case when the changes of stresses in a soil mass remain in small amounts compared with the initially existed stress  $\sigma_0$ .
- The effects of the new constant  $\mu$  or Poisson's ratio  $\nu$  on the deformations under different loading conditions can be clearly

explained.

d. The stresses and strains at breakage in the case of pure shear, simple normal stress or equal stresses can be determined. We can know the effects of a new constant  $\mu$  on the stresses or strains at breakage, the tendencies of which coincide with those of the well known experimental results.

The relations between the breaking strengths under different loading conditions, such as simple compression or tension test, shear test and triaxial loading test can be explained.

4. Under such stress conditions as plane stresses, plane strains, and triaxial symmetrical stresses, the envelopes of Mohr's circles were determined. They are not always straight lines, but are ellipses, parabolas, or hyperbolas in accordance with the values of  $\mu$  under the different stress conditions.

-o-o-o-o-o-o-

## 1 e 11

### ON THE BEARING CAPACITY OF PILES

Prof. Dr. József. JAKY

The bearing capacity of piles consists of two parts: point resistance and skin friction. It is an old problem of Science of Foundations to compute both numerically. The point resistance is essentially the bearing capacity of a shallow pier founded at very great depth, the skin friction is produced by earth pressure acting on the surface of the pile. Several attempts have been made to compute theoretically the bearing capacity of piles 1), 2), but no one is used generally, because they give too low values in view of point resistance, considerably lower than gained by pile load tests.

The aim of this paper is to find a formula giving point resistance and skin friction value in accordance with the reality. It is intended to deal with the bearing capacity of individual piles only.

Sliding surfaces in cohesive soil at instant of failure beneath the base of footings in depth  $h$  are - according to theory of Prandtl-Gaquot - composed of planes and logarithmic spirals (Fig. 1). If the base lies at depth  $h$ , sliding is on both sides hindered by load  $p_1 = h\gamma$  and the pressure producing failure 3):

$$p_0 = (h\gamma + c \cot \phi) \operatorname{tg}^2 \left( 45^\circ + \frac{\phi}{2} \right) e^{\pi \operatorname{tg} \phi} - c \cot \phi \quad (1)$$

Point resistance beneath the pile with cross section  $A$ :

$$P_1 = A \left[ (h\gamma + c \cot \phi) \operatorname{tg}^2 \left( 45^\circ + \frac{\phi}{2} \right) e^{\pi \operatorname{tg} \phi} - c \cot \phi \right] \quad (1a)$$

On the surface of the pile in state of rest earth pressure at rest is acting, its value for cohesive soil:

$$E_0 = \frac{h^2 \gamma}{2} k_0 - h k_1 \quad (2)$$

wherein  $k_0$  and  $k_1$  are coefficients of earth pressure at rest 4).

Let the perimeter of the pile be equal to  $U$ , the coefficient of skin friction  $\operatorname{tg} \delta$ , the bearing capacity produced by skin friction:

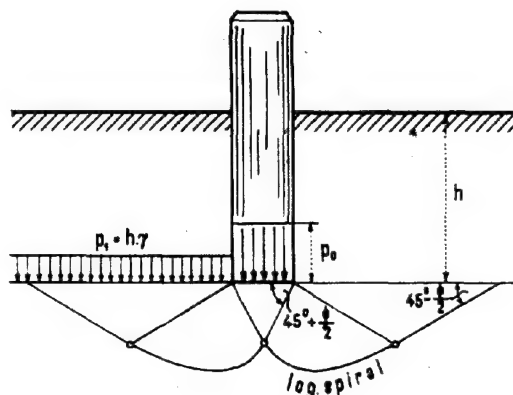


FIG. 1

$$P_2 = U \operatorname{tg} \delta \left( \frac{h^2 \gamma}{2} k_0 - h k_1 \right)$$

and the total bearing capacity:

$$P = A \left[ (h\gamma + c \cot \phi) \operatorname{tg}^2 \left( 45^\circ + \frac{\phi}{2} \right) e^{\pi \operatorname{tg} \phi} - c \cot \phi \right] + U \operatorname{tg} \delta \left( \frac{h^2 \gamma}{2} k_0 - h k_1 \right) \quad (3)$$

Eq. (3) is plotted on Fig. 2. taking angle of friction  $\phi = 35^\circ$  for sand,  $\phi = 10^\circ$  for clay, pile lengths up to  $h = 10$  m. In the same figure are plotted results obtained from Dörr's formula:

$$P = A h \gamma \operatorname{tg}^2 \left( 45^\circ + \frac{\phi}{2} \right) + U \frac{h^2 \gamma}{2} \operatorname{tg} \delta (1 + \operatorname{tg}^2 \phi) \quad (4)$$

From this comparison it may be stated that Dörr's formula

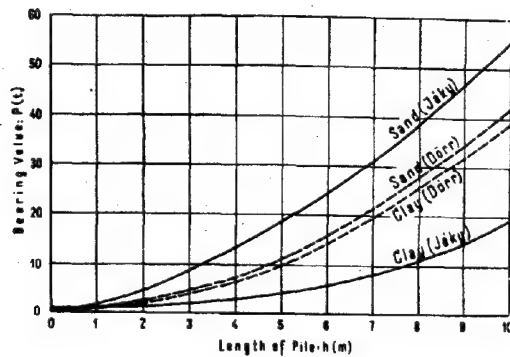


FIG. 2

1) generally gives too low bearing capacities,  
2) bearing capacities in sand or clay scarcely differ but this fact contradicts practical observation. The shortcoming of Derr's formula originates from computing erroneously the point resistance (first term in Eq. (4)) and from determining the pressure of the soil on the skin by means of the theory of the passive earth pressure (second term) although the smaller earth pressure at rest would have to be considered.

Although results given by Eq. 3. are closer to reality, they give still lower values than observed by load tests. This fact may be explained as follows:

The point of the pile is on all sides surrounded with soil, therefore, there is no obstacle whatever to the sliding surface being developed right up the surface of the pile as shown on Fig. 3.

This state of stress has been investigated by the author as early as in 1945 - generalizing Prandtl's theory and neglecting the weight of soil:  $\gamma = 0$ . He named this combined state of stress as "cleft-resistance" and deduced its value to be

$$p_2 = c \cot \phi \left[ \operatorname{tg}^2 \left( 45^\circ + \frac{\phi}{2} \right) e^{2\pi \operatorname{tg} \phi} - 1 \right] \quad (5)$$

This value exceeds importantly Prandtl's resistance to punching ("Schneidefestigkeit") characterized by Eq. (1) and gives for large angles of internal friction many times as much as Eq. (1).  $p_2$  values for different angles of internal friction are shown on Table I.

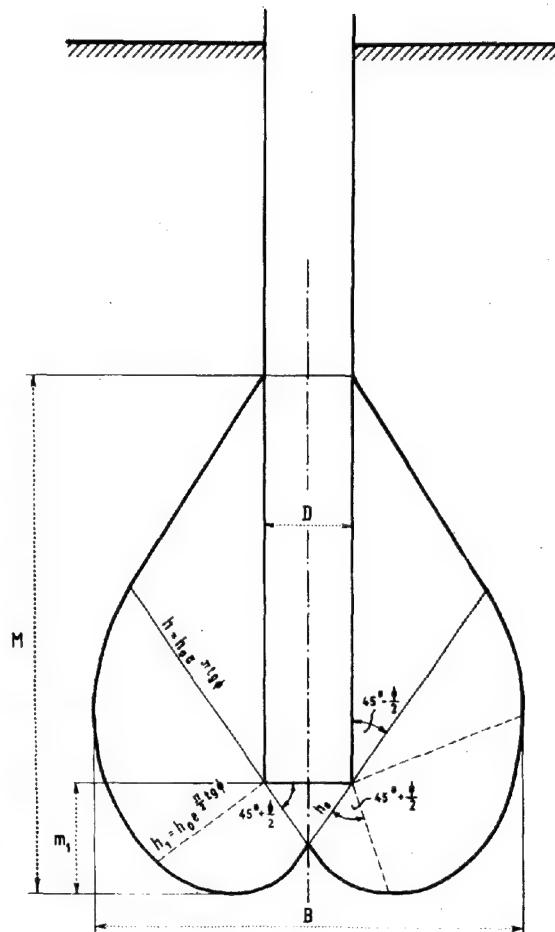


FIG. 3

TABLE I

Angle of internal friction	0°	10°	20°	25°	30°	35°	40°	45°
Coefficient k	0	18.6	52.6	97.0	194.0	423.0	1063	3122

The value of point resistance for cross-section A:

$$P_2 = A c \cot \phi \left[ \operatorname{tg}^2 \left( 45^\circ + \frac{\phi}{2} \right) e^{2\pi \operatorname{tg} \phi} - 1 \right] \quad (5a)$$

The dimensions of the bearing bulb developed around the point of the pile may be easily determined, the most important of them are:

$$m_1 = \frac{D}{2} \frac{\cos \phi}{\cos \left( 45^\circ + \frac{\phi}{2} \right)} e^{\left( \frac{\pi}{2} + \frac{\phi}{2} \right) \operatorname{tg} \phi} \quad (6)$$

$$M = D \left[ \operatorname{tg} \left( 45^\circ + \frac{\phi}{2} \right) e^{\pi \operatorname{tg} \phi} + \frac{1}{2} \frac{\cos \phi}{\cos \left( 45^\circ + \frac{\phi}{2} \right)} e^{\left( \frac{\pi}{2} + \frac{\phi}{2} \right) \operatorname{tg} \phi} \right] \quad (7)$$

$$B = D \left[ 1 + \frac{\cos \phi}{\cos \left( 45^\circ + \frac{\phi}{2} \right)} e^{\left( \frac{\pi}{2} + \frac{\phi}{2} \right) \operatorname{tg} \phi} \right] \quad (8)$$

The quite different shape of bulbs developed in sand ( $\phi = 35^\circ$ ) and clay ( $\phi = 10^\circ$ ) is shown on Fig. 4. There is a mass of bulb in sand ~ 25 times as large as in clay and that is roughly the relation between the bearing capacities, too.

The depth to which the pile has to be driven in order to develop a complete bearing bulb is:

$$h_1 \geq M - m_1 = D \operatorname{tg} \left( 45^\circ + \frac{\phi}{2} \right) e^{\pi \operatorname{tg} \phi} \quad (9)$$

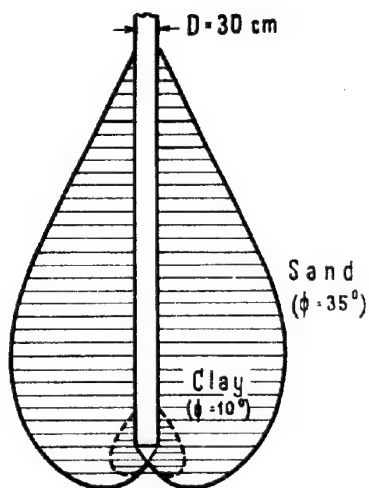


FIG. 4

condition satisfied by short piles too, because, for instance:  $D \cdot \tan\left(45^\circ + \frac{\phi}{2}\right) e^{\pi \tan \phi} = 5.20 \text{ m}$ .  $\phi = 35^\circ$  and  $D = 30 \text{ cm}$  that is the bearing bulb is developed in the case of individual piles by lengths:  $h > 5 \text{ m}$

which is valid up to the moment when  $P_2 > P_1$ , i.e.:

$$A c \cot \phi \left[ \tan^2 \left( 45^\circ + \frac{\phi}{2} \right) e^{2\pi \tan \phi} - 1 \right] \geq$$

$$\geq A \left[ (h\gamma + c \cot \phi) \tan^2 \left( 45^\circ + \frac{\phi}{2} \right) e^{\pi \tan \phi} - c \cot \phi \right]$$

whence the other boundary depth:

$$h_2 \leq \frac{c}{\gamma} \cot \phi (e^{\pi \tan \phi} - 1) \quad (10)$$

For instance:  $\phi = 35^\circ$  and  $c = 2 \text{ t/m}^2$ ,  $\gamma = 2 \text{ t/m}^3$

$$h_2 = 11.50 \text{ m.}$$

Result: by pile length between limits characterized by Eq. (9) and (10) the point resistance does not depend on the depth and is a constant given by Eq. (5 a), if  $h > h_2$  point resistance increases with increasing depth, its value is given by Eq. (1 a). So piling is economical beyond  $h > h_1$  only, on the other hand, it is superfluous to drive piles deeper than  $h = h_1$ , supposing homogeneous soil strata.

Numerical example.

a) Physical properties of soft clay:  $\phi = 10^\circ$ ,  $c = 3 \text{ t/m}^2$ ,  $\gamma = 2 \text{ t/m}^3$ ; diameter of pile:  $D = 30 \text{ cm}$ .

The limit depths:  $h = 0.62 \text{ m}$ ,  $h = 6.30 \text{ m}$ . Point resistance of a pile  $h = 5.0 \text{ m}$  long:

$$P_2 = 4.0 \text{ t}$$

b) Dense sand soil:  $\phi = 35^\circ$ . Dense sand has a certain cohesion, according to test results:

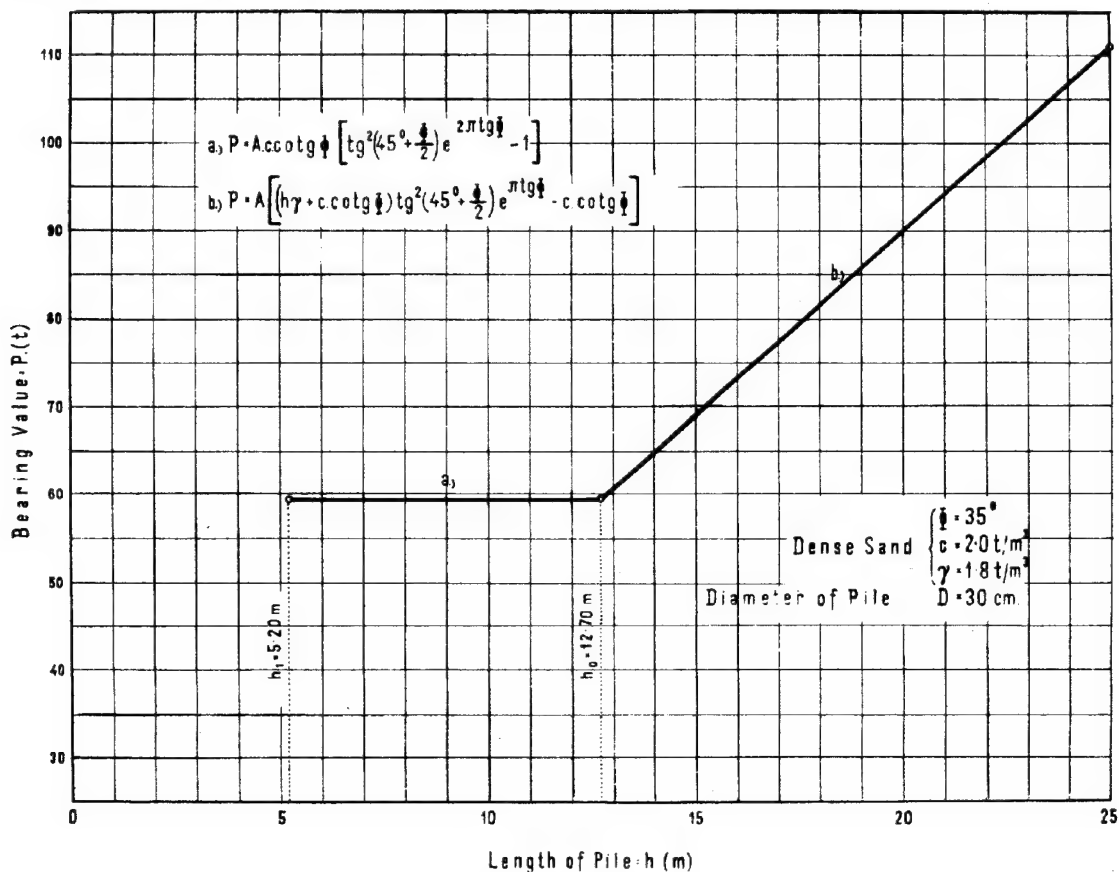


FIG. 5

$c = 0.1 - 0.2 \text{ kg/cm}^2$   
 Taking  $c = 2 \text{ t/m}^2$ ,  $\gamma = 1.8 \text{ t/m}^3$ , the depths  $h_1$  and  $h_2$  ( $D = 30 \text{ cm}$ ):  $h_1 = 5.20 \text{ m}$ ,  $h_2 = 12.70 \text{ m}$ .  
 If  $h = 10.0 \text{ m}$ , from Eq. (5 a):  $P_2 = 62 \text{ t}$ .

Taking a safety factor  $n = 3$ , the allowable point resistance:  $P_1 = 20 \text{ t}$  which remains constant up to  $h_2 = 12.70 \text{ m}$ , beyond that the point resistance increases linearly as shown on Fig. 5.

The width of the bulb:  $B = 3.72 \text{ m}$ , thus, the distance of the piles must be  $B = 3.72 \text{ m}$ , otherwise the sliding surfaces intersect each other and the surfaces of shear would be insufficient.

In the case of pile group the angle between the surfaces of sliding joined symmetrically is to be examined and - based on that - the new state of stress revealed. Without dealing with this question, it may be stated that the bearing capacity of the pile placed in a

group where the distance between them:  $d < B$  will be considerably smaller and the question may be justified whether the piling with small distances be economical.

The author express his thanks to A. Kézdi and E. Szilvgyi for helping and willing assistance in preparing the figures.

#### LITERATURE.

- 1) H. Dörr: Die Tragfähigkeit der Pfähle. Berlin, 1922.
- 2) W. Schenck: Zur Frage der Tragfähigkeit von Rammpfählen. Berlin, 1939.
- 3) Erdbaukurs der E.T.H. 1938. Zürich.
- 4) N. Gersevanoff: Improved Methods of Consolidation Test .... Proceedings of the Int. Conference on Soil Mechanics. Cambridge, Mass. 1936. Vol. I.
- 5) Jáky, J.: Összetett nyomó feszültségi állapotok. Technika, Budapest, 1945. 246. füzet.

-0-0-0-0-0-0-

## SUB-SECTION I f

### EARTH PRESSURE

#### PRESSURE IN SILOS

Prof. Dr. J. JÁKY

The so-called classical theory 1) to compute pressures exerted by granular material stored in silos is erroneous from the point of view of Statics, because it supposes the angle of friction between the wall and the granular material to be a constant. Since the conditions of equilibrium are expressed for an elementary slice having infinitely small height but finite width, stresses  $\sigma_x$ ,  $\sigma_y$  and  $\tau$  acting in an arbitrary point of the mass and their distribution cannot be determined, from which it follows that the obtained formulae are not in accordance with the dimensions of the silo. The aim of this paper is to give an approximate solution which is correct from point of view of Statics and takes the influence of dimensions - diameter of silo - on pressure correctly into account. The variation of pressures during storing time is not dealt with, nor are pressure problems of emptying and filling treated. 2)

#### I. BASIC ASSUMPTIONS.

The problem of pressure in silos is essentially that of earth pressure of cohesionless materials, which might be solved by means of the classical earth pressure theory if we could make a plausible assumption on the shape of the surface of sliding. For want of it, the solution is obtained by making use of empirical curves gained by measurements in silos. 3)

Considering a silo of  $2b$  width, bounded by parallel vertical walls it is certain that a wall of  $AC = y_0$  height represents that limit down to which the classical earth pressure is

acting, (Fig. 1) since the surfaces of slid-

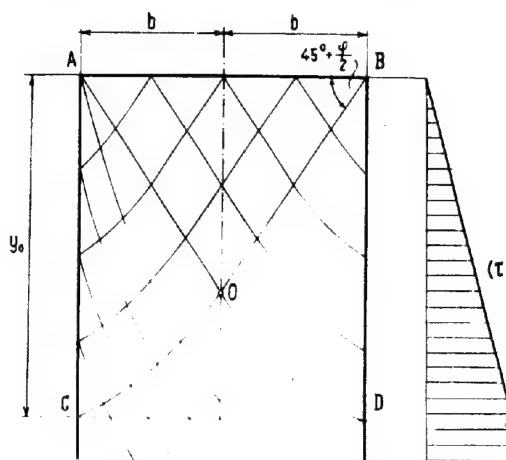


FIG. 1

ing (planes + curves) still run out to superficies AB free from external load, the so-called silo effect is produced solely in depths  $y > y_0$ .

Assuming approximately the surfaces of sliding joining to AO as logarithmic spirals, the depth  $y_0$  may be computed as

$$j_0 = \frac{b \tan(45^\circ - \frac{\phi}{2})}{\sin(45^\circ - \frac{\phi}{2})} \quad (1)$$

Between the angles  $\phi = 25-30^\circ$  its value is obtained for  $j_0 = (2.4 - 2.7) b$ , but this is an approximate value only, an accurate one will be furnished later.

According to the classical earth pressure theory the stresses including  $\tau$  acting along the wall are linear with depth  $y$ , that is in the range of  $y \leq y_0$  the diagram of  $(\tau)$  becomes a triangle.

The normal stresses acting on the elementary prism are  $\sigma_1$  and  $\sigma_2$ , the shearing stress  $\tau_1$  from the condition of equilibrium of the vertical forces (Fig. 2) we obtain

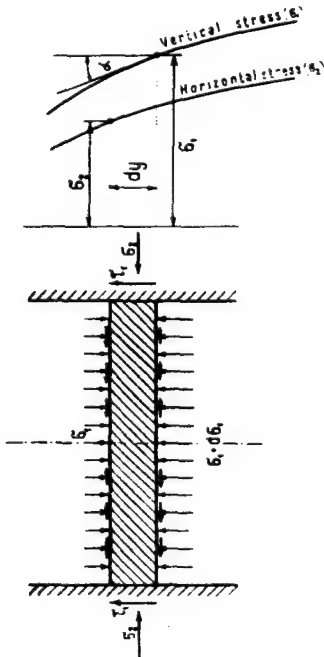


FIG. 2

$$A d\sigma_1 + \tau_1 P dy = d\sigma_2 A$$

wherein  $A$  = cross sectional area,  $P$  = perimeter

$$\text{Hence} \quad \frac{d\sigma_1}{dy} + \tau_1 \frac{P}{A} = \gamma \quad (2)$$

If the law of  $\sigma_1$  is known from empirical curves, that is  $\tau_1 \propto \frac{d\sigma_1}{dy}$  may be measured off the stress diagram:  $\tau_1 = (\gamma - \tau_1 \alpha) \frac{A}{P}$  (3)

Introducing this value into equation  $\lambda = \frac{\tau_1}{\sigma_2}$  we obtain the value of wall friction:

$$\lambda = (\gamma - \tau_1 \alpha) \frac{A}{P} \cdot \frac{1}{\sigma_2} \quad (4)$$

Also the coefficient of earth pressure at rest may be computed:  $k = \frac{\sigma_2}{\sigma_1}$  (5)

Fig. 3 shows the revision of Jamieson's 4) and Pleissner's 5) tests selected from some silo tests. The stored material is in both cases wheat in a grain bin depth  $h = 20$  and  $15$  m and the cross section  $A = 3.66 \times 4.12$  m in the first case and  $A = 1.57 \times 1.57$  m in the second. Both of them were wainscoted.

1) It is evident from Fig. 3 that curve  $(\tau)$

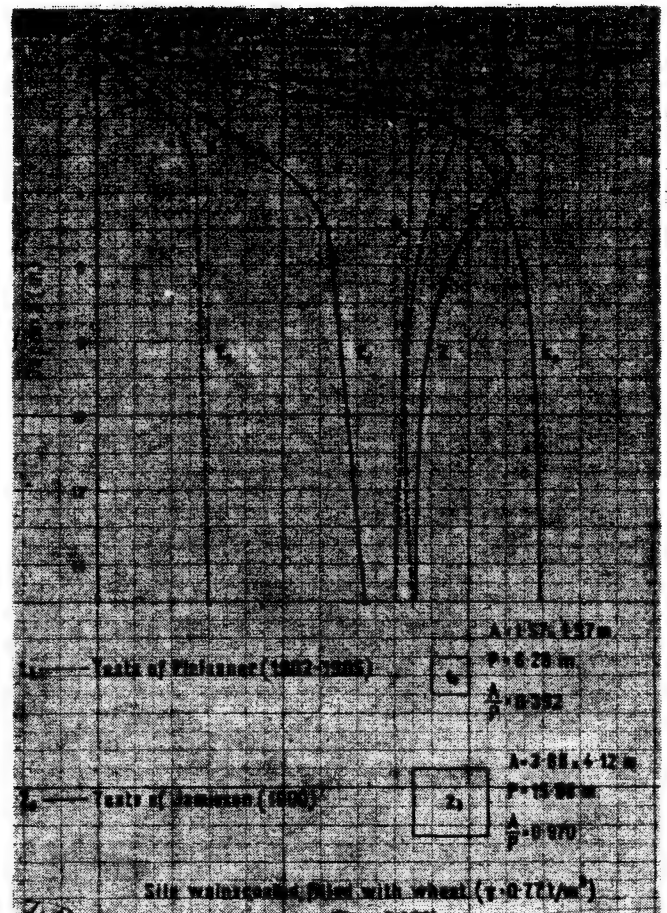


FIG. 3

consists of two sections, the upper (I) is a slanting straight line, the section (II) a nearly vertical curve.

2) It may be stated that the coefficient of earth pressure at rest considered along the wall is variable, but it remains approximately constant in the second section, its value depends on the width of the bin, therefore it is not only a physical, but also a geometrical function.

3) Wall friction increases in small depths approximately linearly and after reaching a maximum, asymptotically tends to a constant value. It generally shows the shape of shearing strain curve of dense granular materials (Fig. 4) and is the same if we put

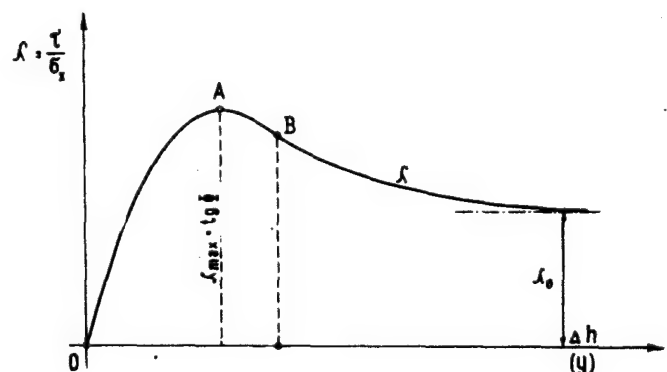


FIG. 4

y instead of deformation  $\Delta h$ . This is reasonable because deformation  $\Delta y = y \frac{\Delta e}{1+e}$  due to settling is proportional to  $y \cdot \frac{1}{1+e}$ .

The maximal value of wall friction as plotted on Fig. 3 is produced in the first section and this is evidently the angle of internal friction of the granular material, because it is a well known phenomenon emptying the silos that the material adheres to the wall: sliding occurs first in the interior of the granular material, wall friction starts to act later.

4) In the lower part wall friction  $\lambda_0$  is constant and does not depend on pressure.

## II. EQUILIBRIUM OF THE ELEMENTARY PRISM.

### 1) Examination of the upper section.

To construct a suitable  $\tau$  function let us consider that in the symmetry axis  $x = 0$  and in height  $y = 0$ ,  $\tau$  must be zero, besides that, according to test results,  $\tau$  increases with  $y$  linearly, therefore the simplest form for  $\tau$  is:

$$\tau = \alpha y \quad (5)$$

Substituting into Cauchy's equations of equilibrium:

$$\left. \begin{aligned} \frac{\partial \sigma_y}{\partial y} + \frac{\partial \tau}{\partial x} &= \gamma \\ \frac{\partial \sigma_x}{\partial x} + \frac{\partial \tau}{\partial y} &= 0 \end{aligned} \right\} \quad (6)$$

wherein the specific weight  $\gamma$  of the granular material is considered as constant, the compression caused by the proper weight of the mass being insignificant and  $\gamma$  practically remains invariable.

Solving the differential equations we get

$$\sigma_y = \gamma y - \frac{\alpha}{2} y^2 \quad (7)$$

that is  $\sigma_y$  is uniformly distributed in the horizontal cross section.  $\sigma_x = F(y) - \frac{\alpha}{2} x^2$  (8)

In the axis  $x = 0$  and  $\sigma_x = F(y)$ ; since there is a pure compression in this vertical line, the state of stress is characterized by the pressure at rest and its law being  $\sigma_x = k_0 \sigma_y$  therefore

$$F(y) = k_0 \left( \gamma y - \frac{\alpha}{2} y^2 \right) \quad (9)$$

and so

$$\sigma_x = k_0 \gamma y - \frac{\alpha k_0}{2} y^2 - \frac{\alpha}{2} x^2 \quad (10)$$

With respect to Eq. (7) and (10) both stresses  $\sigma_y$  and  $\sigma_x$  follow a parabolic law and the coefficient of pressure at rest along the wall:

$$k_b = \left( \frac{\sigma_x}{\sigma_y} \right)_{x=b} = \frac{k_0 \gamma y - \frac{\alpha k_0}{2} y^2 - \frac{\alpha}{2} b^2}{\gamma y - \frac{\alpha}{2} y^2} = k_0 - \frac{\frac{\alpha}{2} b^2}{\gamma y - \frac{\alpha}{2} y^2} \quad (11)$$

is not a constant but increases with depth as shown on Fig. 3.

### 2) Law of wall friction.

The  $(\lambda)$  diagrams given on Fig. 3. consist of a parabolic and a vertical portion. Assuming now, that the shape of the  $(\lambda)$  diagram is as shown on Fig. 5., that is the curve has in point  $(y = y_0)$   $F$  a vertical tangent,  $\lambda = \lambda_0$  is equal to wall friction. This assumption is reasonable, because the shearing - resistance curve of loose granular material is like that; the bellshaped form of  $(\lambda)$  curve as shown on Fig. 3 is due to non-uniform distribution of  $\sigma_y$  in the horizontal cross section.

In the upper portion the coefficient of wall friction

$$\lambda = \frac{\tau}{\sigma_x} = \frac{\alpha y}{k_0 \gamma y - \frac{\alpha k_0}{2} y^2 - \frac{\alpha}{2} b^2} \quad (12)$$

its differentialquotient with respect to  $y$ :

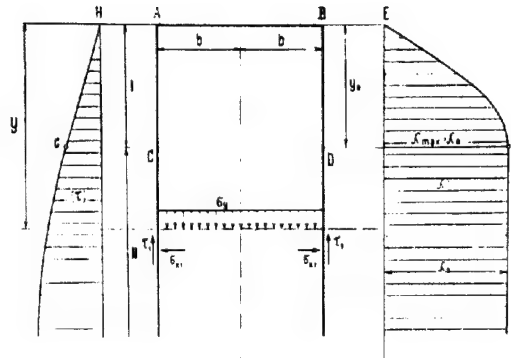


FIG. 5

$$\frac{d\lambda}{dy} = \frac{\alpha b}{k_0 \gamma y - \frac{\alpha k_0}{2} y^2 - \frac{\alpha}{2} b^2} \quad (13)$$

In point  $F$  where  $\lambda = \max \frac{d\lambda}{dy} = 0$ , i.e.

$$y_0 = \frac{b}{\sqrt{k_0}} \quad (14)$$

If the coefficient of friction is at this point  $\lambda = \lambda_0$ , substituting the value under Eq. (14) in Eq. (12) we obtain

$$\alpha = \lambda_0 \frac{k_0 \gamma}{b(1 + \sqrt{k_0} \lambda_0)}$$

The coefficient of stress  $\tau$  depends not only on the physical properties of the granular material, but also on the distance of silo walls.

### 3) State of stress in the lower section.

This section is characterized by a constant wall friction coefficient (Fig. 5). Assuming now, in accordance to the upper section that the vertical stress  $\sigma_y$  is uniformly distributed over the cross section:

$$\sigma_y = f(y) \quad (16)$$

From the first equation under (6)

$$f'(y) = \gamma - \frac{\partial \tau}{\partial x}$$

that is  $\tau = (\gamma - f')x + F(y)$

Since  $x = 0$  is a symmetry axis along which  $\tau = 0$ ,  $F(y) = 0$  and we obtain:

$$\tau = (\gamma - f')x \quad (17)$$

The shearing stress is distributed linearly over the horizontal cross section; on the wall:  $\tau = (\gamma - f')b$

The horizontal normal stress from second equation under (6):

$$\sigma_x = f'' \frac{x^2}{2} + G(y) \quad (18)$$

In the symmetry axis we have pure compression, therefore:

$$\sigma_{x=0} = G(y) = k_0 \sigma_y = k_0 f(y) \quad \sigma_x = k_0 f + f'' \frac{x^2}{2} \quad (19)$$

Laws of stress in the upper and lower sections join each other with mathematical precision, because it follows from comparing Eq. (5) and (7) that at the boundary  $y = y_0$  the shearing stress is linear with respect to  $x$  and according to Eq. (8) and (18)  $\sigma_x$  consists of two terms, one constant, the other proportional to  $x^2$ .

### 4) Differential equation of solution.

Along the wall:

$$\lambda_0 = \frac{\tau}{\sigma_x} = \frac{(\gamma - f')b}{k_0 f + f'' \frac{x^2}{2}} \quad (20)$$

from which:

$$f'' \frac{b^2}{2} + f' \frac{b}{\lambda_0} + k_0 f = \frac{b\gamma}{\lambda_0} \quad (21)$$

this is the fundamental equation of the silo problem.

To solve the non-homogeneous differential equation of second order let us take

$$k_0 f - \frac{b\gamma}{\lambda_0} = z \quad \text{and we obtain} \quad z'' + \frac{2}{b\lambda_0} z' + 2 \frac{k_0}{b^2} z = 0 \quad (22)$$

characteristic equation of the latter is

$$\xi^2 + \frac{2}{b\lambda_0} \xi + 2 \frac{k_0}{b^2} = 0$$

the roots of which:

$$\left. \begin{aligned} \xi_1 &= -\frac{1}{b\lambda_0} \left( 1 + \sqrt{1 - 2k_0 \lambda_0^2} \right) \\ \xi_2 &= -\frac{1}{b\lambda_0} \left( 1 - \sqrt{1 - 2k_0 \lambda_0^2} \right) \end{aligned} \right\} \quad (22a)$$

Using symbols

$$\left. \begin{aligned} \frac{1}{\lambda_0} \left( 1 + \sqrt{1 - 2k_0 \lambda_0^2} \right) &= \mu_1 \\ \frac{1}{\lambda_0} \left( 1 - \sqrt{1 - 2k_0 \lambda_0^2} \right) &= \mu_2 \end{aligned} \right\} \quad (22b)$$

the solution of Eq. (22):

$$z = C_1 e^{-\frac{\mu_1}{b} x} + C_2 e^{-\frac{\mu_2}{b} x} \quad (23)$$

$$\sigma_{ij} = \frac{C_1}{k_0} e^{-\frac{\mu_1}{b} x} + \frac{C_2}{k_0} e^{-\frac{\mu_2}{b} x} + \frac{b\gamma}{\lambda_0 k_0}$$

respectively.

$$\tau = \left( \gamma + \frac{C_1 \mu_1}{k_0 b} e^{-\frac{\mu_1}{b} x} + \frac{C_2 \mu_2}{k_0 b} e^{-\frac{\mu_2}{b} x} \right) x \quad (24)$$

$$\sigma_x = \left( C_1 e^{-\frac{\mu_1}{b} x} + C_2 e^{-\frac{\mu_2}{b} x} \right) + \frac{x^2}{2} \left( \frac{C_1 \mu_1^2}{k_0 b^2} e^{-\frac{\mu_1}{b} x} + \frac{C_2 \mu_2^2}{k_0 b^2} e^{-\frac{\mu_2}{b} x} \right) + \frac{b\gamma}{\lambda_0} \quad (25)$$

The above equations give the stresses in any point of the mass in the silo. To proportion the silo-walls we are interested only in stresses acting along the wall. We obtain these by substituting  $x = b$  into Eq. 23 - 25. At the same time we pass from plane to spacial state of stress by substituting

$$\frac{1}{b} = \frac{P}{A} \quad (26)$$

$$\left. \begin{aligned} \sigma_{ij} &= \frac{C_1}{k_0} e^{-\frac{P}{A} \mu_1 y} + \frac{C_2}{k_0} e^{-\frac{P}{A} \mu_2 y} + \frac{A}{P} \frac{\gamma}{\lambda_0 k_0} \\ \sigma_x &= C_1 \left( 1 + \frac{\mu_1^2}{2k_0} \right) e^{-\frac{P}{A} \mu_1 y} + C_2 \left( 1 + \frac{\mu_2^2}{2k_0} \right) e^{-\frac{P}{A} \mu_2 y} + \frac{A\gamma}{P k_0} \\ \tau_i &= \frac{A}{P} \gamma + \frac{C_1}{k_0} \mu_1 e^{-\frac{P}{A} \mu_1 y} + \frac{C_2}{k_0} \mu_2 e^{-\frac{P}{A} \mu_2 y} \end{aligned} \right\} \quad (27)$$

The formulae are valid in the second section that is in depths  $y > y_0$  for an arbitrary silo having symmetry axis.

It pertains to complete solution to determine the constants  $C_1$  and  $C_2$ . Two necessary equations hereto are furnished by the coincidence without break of the stresses in depth  $y = y_0$ . On the surface CD the values of  $\sigma_{ij}$  according to Eq. (7) and (23) are the

$$\text{same, therefore } \sigma_{ij0} = \frac{1}{2} \gamma y_0 - \frac{C_1}{k_0} e^{-\frac{\mu_1}{b} y_0} - \frac{C_2}{k_0} e^{-\frac{\mu_2}{b} y_0} + \frac{b\gamma}{\lambda_0 k_0} \quad (28)$$

so  $\sigma_x$  and  $\tau$  will be the same, too.

Junction without break requires the coincidence of tangents  $\left( \frac{d\sigma_{ij}}{dy} \right)_{y=y_0}$

$$\text{that is } -\frac{C_1 \mu_1}{k_0 b} e^{-\frac{\mu_1}{b} y_0} - \frac{C_2 \mu_2}{k_0 b} e^{-\frac{\mu_2}{b} y_0} = \gamma - 2\mu_0 \quad (29)$$

From Eq. (28) and (29) we obtain

$$\left. \begin{aligned} C_1 &= k_0 \frac{b(\lambda_0 \gamma - \mu_2)(\mu_2 y_0 - \frac{1}{2} \mu_0^2 - \frac{b\gamma}{\lambda_0 k_0}) e^{-\frac{\mu_1}{b} y_0}}{\mu_1 - \mu_2} \\ C_2 &= k_0 \frac{\mu_1(\mu_0 y_0 - \frac{1}{2} \mu_0^2 - \frac{b\gamma}{\lambda_0 k_0}) - b(\lambda_0 \gamma - \mu_2) e^{-\frac{\mu_2}{b} y_0}}{\mu_1 - \mu_2} \end{aligned} \right\} \quad (30)$$

$$\text{wherein: } b = \frac{A}{P}$$

### III. PHYSICAL PROPERTIES OF GRANULAR MATERIALS.

We sum up below the test results carried out in the Laboratory for Soil Mechanics Technical University Budapest by Assist. E. Szilvgyi. He determined the angle of wall friction of various agricultural products by means of Casagrande's shearing apparatus and of natural slope 6). The following column of the table gives the values of the coefficient of earth pressure at rest, computed by the author's formula 7)

$$k_0 = 1 - \sin \phi \quad (31)$$

Coefficients of wall friction are determined in the same way putting in brick, concrete and wood filling. It is to be mentioned that the angle of wall friction is always smaller than the angle of internal friction. The last column gives specific weight.

#### NUMERICAL EXAMPLE.

$$\begin{aligned} \text{Jamieson's test. } A &= 3.66 \times 4.12 = 15.1 \text{ m}^2 \\ P &= 2(3.66 + 4.12) = 15.6 \text{ m} \\ A/P &\approx 1.0 \text{ m} \end{aligned}$$

The angle of internal friction of wheat:

$$\begin{aligned} \phi &= 27^\circ \quad k_0 = 1 - \sin 27^\circ = 0.55, \quad \gamma = 0.78 \text{ t/m}^3, \\ \text{the coefficient of wall friction in silo wainscoted with boards } \lambda_0 &= 0.44, \text{ the boundary depth: } \mu_0 = \frac{b}{\sqrt{k_0}} = \frac{1.00}{\sqrt{0.55}} = 1.35 \text{ m} \end{aligned}$$

From Eq. (15):

$$a = 0.44 \frac{0.55 \times 0.78}{1.0(1 + 0.44\sqrt{0.55})} = 0.142 \text{ t/m}^4$$

Pressures in section I. from Eq. (7) and (10):

$$\sigma_{ij} \text{ t/m}^2 = 0.78 y - 0.071 y^2$$

$$\sigma_x \text{ t/m}^2 = 0.43 y - 0.039 y^2 - 0.071$$

In section II. from Eq. (30) the constants and the equations of pressures along the

$$\text{wall: } C_1 = -2.12 \quad C_2 = -1.69$$

$$\sigma_{ij} \text{ t/m}^2 = -3.88 e^{-4.42 y} - 3.09 e^{-0.24 y} + 3.16$$

$$\sigma_x \text{ t/m}^2 = -37.9 e^{-4.42 y} - 1.77 e^{-0.24 y} + 1.725$$



Kind of material	Angle of internal friction $\phi$ determined by		$k_0$ $1 - \sin \phi$	Angle of wall friction $\phi$ on			Specific weight $t/m^3$
	shearing test	natural slope		concrete	brick	wood	
Wheat	30°30'	27°10'	0.493-0.544	28° 0'	26°20'	24°40'	0.75 - 0.85
Rye	29° 0'	24°30'	0.516-0.585	25°10'	26°30'	24°40'	0.72 - 0.82
Barley	32°30'	30°55'	0.463-0.487	28°40'	26°30'	25°40'	0.69 - 0.74
Oats	33° 0'	29°30'	0.455-0.508	28° 0'	27°50'	25°40'	0.48 - 0.56
Corn	36° 0'	31°40'	0.412-0.475	27°50'	27°50'	25°05'	0.70 - 0.78
Bean	33°20'	26°30'	0.450-0.544	27°50'	26°30'	24°45'	0.83 - 0.88
Pea	33°50'	30°20'	0.443-0.495	26°40'	26°40'	24°10'	0.70 - 0.80

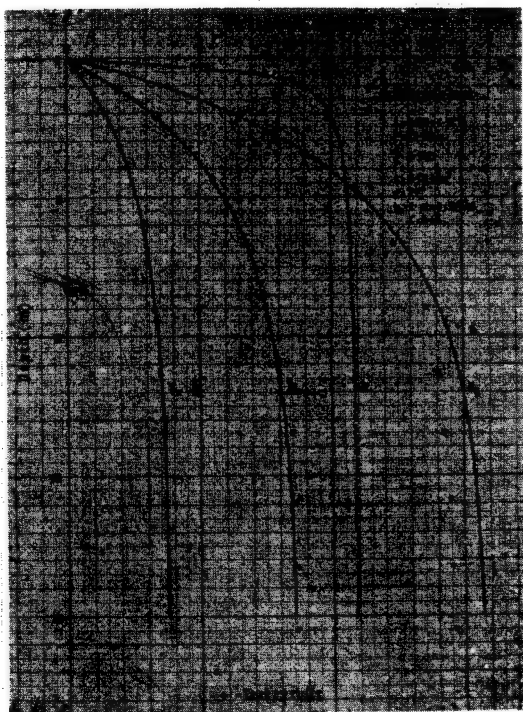


FIG. 6

$$p, t/m^2 = -16.7e^{-4.42h} - 0.724e^{-0.24h} + 0.76$$

We plotted the curves representing pres-

ures along the wall in Fig. 6. Points indicated with small circles give the tests results, the coincidence is very good. It is to be mentioned, that the difference of 7% in the values of  $\sigma_1$  is due to the fact, that the distribution of  $\sigma_1$  on the cross section is not uniform, it is smaller along the wall than in the middle.

In practical calculations the first term in Eq. (27) can be neglected with respect to the second, because it is approximately equal to zero.

The author wishes to express his thanks to A. Kézdi and E. SzilvÁgyi for working out the numerical example and for the arrangement of the manuscript.

#### LITERATURE.

- 1) Janssen, H.A.: Versuche über Getreidedruck in Silozellen. Zeitschrift des Vereins deutscher Ingenieure 1895. S. 1045.
- 2) Reimbert, M.: Recherches nouvelles sur les efforts exercés par les matières pulvérulantes ensilées sur les parois des silos. Circulaire, Série I. No. 11. Institut technique du bâtiment et des travaux publics. Paris, le 10 Mai 1943.
- 3) Lufft, E.: Druckverhältnisse in Silozellen. Berlin, 1920.
- 4) Jamieson: Grain pressures in deep bins. Engineering News, 1904 pp. 236.
- 5) Pleissner, J.: Versuche zur Ermittlung der Boden- und Seitenwanddrucke in Getreidesilos. Zeitschrift des Vereins deutscher Ingenieure, 1906, S. 97.
- 6) SzilvÁgyi, I.: Angle of Internal and Wall Friction of Agricultural Products. /Hungarian/ Magyar Mérnök és Építész Egylet Közönye 1944. 358 o.
- 7) Jáky, J.: The Coefficient of Earth Pressure at Rest. /Hungarian/ Magyar Mérnök és Építész Egylet Közönye 1944. 355. o.



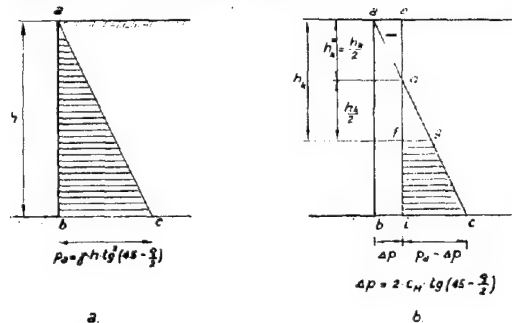
## CALCULATION OF SHEET PILE WALLS IN COHESIVE SOIL

Dr.sc.techn. **HART F. KOLLERUNNER**, Civil Engineer  
Zurich

## I. INTRODUCTION.

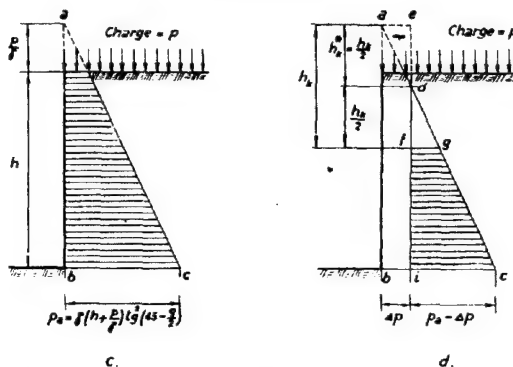
In practice the sheet pile walls are mostly calculated by the method of Krey 1) (linear distribution of stresses) or by the parabolic-method built up by O. Mohr on basis of tests executed by Engels. 2)

For the calculation of sheet pile walls in cohesive soil the cohesion is considered according to Jacoby 3) in such a way that the surface of the earth (fig. 1) for the active



Distribution of the active earth pressure without and with cohesion.

FIG.1 ab



Distribution of the active earth pressure with charge p without and with cohesion.

FIG.1 cd

earth pressure is reduced by  $h_k^* = h_k/2$

With the average value of the cohesion

$$C_m = \frac{\gamma h_k}{4} \operatorname{tg} \left( 45^\circ - \frac{\rho}{2} \right) \quad (1)$$

we receive

$$h_k^* = \frac{4 C_m}{\gamma} \operatorname{tg} \left( 45^\circ + \frac{\rho}{2} \right) \quad (2)$$

Hereby is the meaning of:

$\gamma$  : unit weight of the soil  
 $\rho$  : angle of internal friction

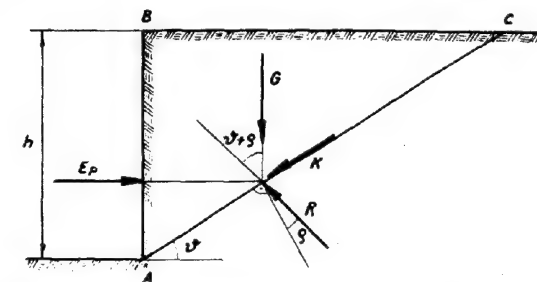
Deducting from the classical triangle of earth pressure of fig. 1 a the earth pressure reduced by the cohesion (rectangle with

the width  $\Delta p$  and the height  $h$ ), whereby

$$\Delta p = 2 C_m \operatorname{tg} \left( 45^\circ - \frac{\rho}{2} \right) \quad (3)$$

we receive fig. 1 b. In the triangle ade of fig. 1 b a negative earth pressure is produced (tension), which can only be taken up as long as there is a possibility of adherence between the soil and the sheet piles. As this is not the case with steel sheet piles the cleft will enlarge itself continually until the entire superior earth pressure will be equal to Zero, i.e. that the soil is standing free to the depth  $h_k^*$ . If we reckon on the basis of the earth pressure triangle dci instead of the trapezoid of earth pressure fgci we have to take into account a bigger active earth pressure. By reducing the surface of the earth by  $h_k^*$  according to fig. 1 we obtain therefore an additional security.

For the passive earth pressure Jacoby is increasing the earth surface by the same value  $h_k^*$ . This hypothesis seems to be quite convincing at the first look, but it must be pointed out that for bigger angles and exacter calculations it cannot be adopted. 4) According to fig. 2 and fig. 3 we obtain:



Passive earth pressure  $E_p$  on vertical wall with smooth surface. Friction and cohesion.

FIG.2

$$\Delta E_p = k \frac{\sin(90^\circ + \rho)}{\sin(90^\circ - (\beta + \rho))} = k \frac{\cos \rho}{\cos(\beta + \rho)} \\ = \frac{C_m h}{\cos(90^\circ - \beta)} \cdot \frac{\cos \rho}{\cos(\beta + \rho)} \quad (4)$$

$$\Delta p_p = \frac{\Delta E_p}{h} = \frac{C_m}{\sin \beta} \cdot \frac{\cos \rho}{\cos(\beta + \rho)} \quad (5)$$

The angle for the most dangerous surface of sliding on passive earth pressure is:

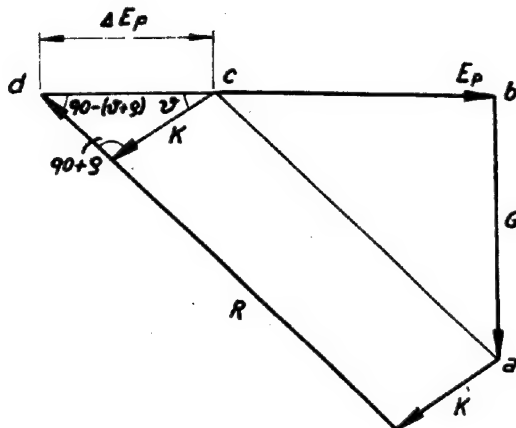
$$\beta = 45^\circ - \frac{\rho}{2} \quad (6)$$

Therefore equation (5) is converted into:

$$\Delta p_p = \frac{C_m}{\sin(45^\circ - \rho/2)} \cdot \frac{\cos \rho}{\cos(45^\circ + \rho/2)} \quad (7)$$

and after trigonometrical transformations

$$\Delta p_p = 2 C_m \operatorname{tg} \left( 45^\circ + \frac{\rho}{2} \right) \quad (8)$$



Force polygon  $G - K - R - E_p$   
 $cb = E_p$  (without cohesion)  
 $db = E_p$  (with cohesion)

FIG. 3

Calculating  $P_k = \Delta p_p$  according to Jacoby we get

$$P_k = \gamma h_k^2 \lambda_p = \gamma h_k^2 \tan^2 \left( 45^\circ + \frac{\rho}{2} \right) \quad (9)$$

with equation (1) follows:

$$P_k = 2C_M \tan^2 \left( 45^\circ + \frac{\rho}{2} \right) = \Delta p_p \tan^2 \left( 45^\circ + \frac{\rho}{2} \right) \quad (10)$$

i.e. the cohesion determined by Jacoby on the earth surface, is the effective cohesion multiplied with  $\tan^2(45^\circ + \rho/2)$

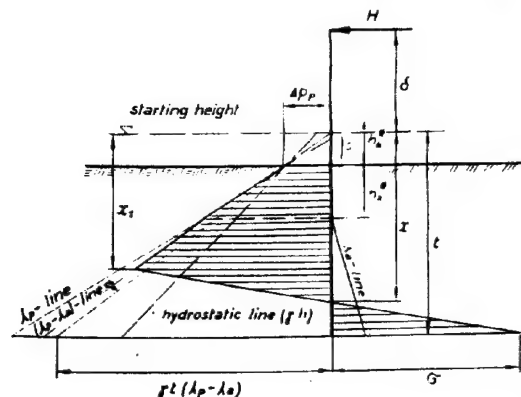
## II. LINEAR STRESS DISTRIBUTION.

### a. Self-supporting sheet pile wall.

The earth resistance on the earth surface is starting according to fig. 4 with the ordinate  $\Delta p_p$  (equation (8)) in front of the sheet piles.

$$\text{With } \Delta p_p = \gamma s (\lambda_p - \lambda_a) \quad (11)$$

we receive the starting height  $s$  above the effective earth surface in front of the sheet



Self supporting sheet pile wall in cohesive soil, charged by a singular force H.

FIG. 4

pile wall

$$s = \frac{2C_M \tan^2(45^\circ + \rho/2)}{\gamma(\lambda_p - \lambda_a)} \quad (12)$$

or, after introduction of the value  $h_k^* = h_k/2$  and equation (1)

$$s = \frac{h_k^*}{\lambda_p - \lambda_a} \quad (13)$$

The values  $x_1$ ,  $x$  and  $\sigma$  of fig. 4 result from the equilibrium conditions to:

$$x_1 = \frac{k(4t+6\delta) + 2s^2(t-s)}{t^2 - 2k - s^2} \quad (14)$$

$$x = \frac{k(4t+6\delta) + 2s^2(t-s)}{2tx_1 - x_1^2 - 2k - s^2} \quad (15)$$

$$\sigma = \gamma(\lambda_p - \lambda_a) \left[ \frac{x_1 x - 2k - s^2}{t - x} \right] \quad (16)$$

Hereby are:

$$k = \frac{H}{\gamma(\lambda_p - \lambda_a)b}$$

$$\lambda_p = \tan^2 \left( 45^\circ + \frac{\rho}{2} \right)$$

$$\lambda_a = \tan^2 \left( 45^\circ - \frac{\rho}{2} \right)$$

$b$  = width of the sheet pile wall

$\Delta p_p$  can be found graphically in such a way that we draw through the point of intersection of the sheet pile wall and the earth surface which we consider increased by  $h_k^*$  the hydrostatical pressure line  $\gamma h$  (pressure line with  $\lambda = 1$ , i.e.  $\rho = 0$ ), and bring this line with the real earth surface to intersection. According to fig. 4 we receive:

$$\Delta p_p = \gamma h_k^* \quad (17)$$

as well as:  $\Delta p_p = \gamma s (\lambda_p - \lambda_a)$

or

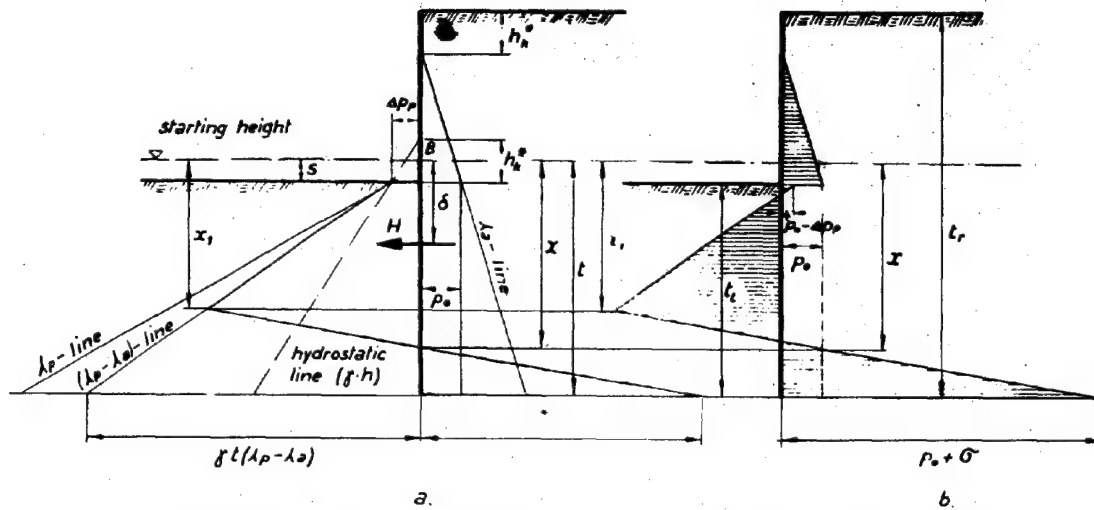
$$s = \frac{h_k^*}{\lambda_p - \lambda_a} \quad \text{i.e. equation (13)}$$

The bounds of the pressure figure are starting with the ordinate  $\Delta p_p$  according to equation (8) in the height of the effective earth surface (fig. 4) firstly according to the line of the biggest possible passive earth pressure ( $\lambda_p$  - line) to the depth  $h_k^*$  beneath the earth surface. Due to the fact that from this point the active earth pressure is reigning on the right hand side of the wall, the line underneath  $h_k^*$  will be steeper, i.e. parallel with the  $(\lambda_p - \lambda_a)$  - line up to depth  $x_1$  beneath the starting height  $s$ .

The further development is the same as for cohesionless soil and is the result of considerations due to equilibrium conditions.

If the sheet pile wall is charged with active earth pressure, the calculation follows according to fig. 5. The starting height  $s$  must be introduced according to equation (12).

In that case the above mentioned graphical determination of  $\Delta p_p$  is only valid when  $c_M$  at the left and right hand side of the sheet pile wall will be considered as equal. Of course,  $c_M$  beneath the bottom of the foundation trench (left hand side of the sheet pile wall, fig. 5) is often considerably bigger than  $c_M$  at the right hand side of the wall (reckoned from the original earth surface). When the average value of the cohesion from the original earth surface to the foot



a Active and passive earth pressure. b Summation of the pressures.  
Self supporting sheet pile wall in cohesive soil,  
charged by earth pressure.

FIG. 5

of the sheet pile wall is introduced, we receive an additional security, because  $\Delta p_p$  is taken into account smaller than in reality.

According to fig. 5 b there must be:

$$\sigma + p_0 \leq \gamma t \lambda_p + \Delta p_p - \gamma (t_r - h_k^*) \lambda_a \quad (18)$$

#### b. Simple propped sheet pile wall.

The cohesion is considered in the same way as mentioned above, i.e. for the active earth pressure we decrease the earth surface by  $h_k^*$  and introduce the cohesion value  $\Delta p_p$  for the passive earth pressure according to equation (8), or construct  $\Delta p_p$  graphically as shown above.

The sheet pile wall being charged with active earth pressure, we receive according to fig.

5a the minimal ramming depth  $t_{min}$  from the condition

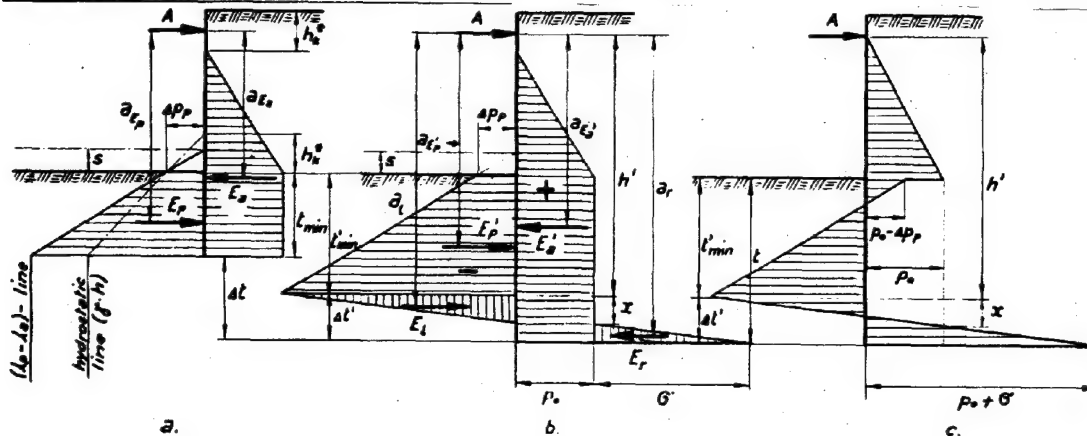
$$E a_{E_a} = E_p a_{E_p} \quad (19)$$

Increasing the ramming depth by  $\Delta t$ ,  $E_a$  is growing to  $E'_a$  and the minimal ramming depth  $t_{min}$  up to  $t'_{min}$ . Up to this depth the stress distribution is considered as to be increasing in linear line. The position of point zero (fig. 6b) will be found from the relation:

$$E'_a a_{E'_a} = E_p a_{E_p} \quad (20)$$

The summation of the pressure figures is shown in fig. 6 c. The condition of safety for a sheet pile wall being rammed down deeper than the supposed minimal ramming depth  $t_{min}$  is always fulfilled.

The influence of the cohesion results in the following:



$$\Delta t' = \Delta t - (t'_{min} - t_{min})$$

FIG. 6



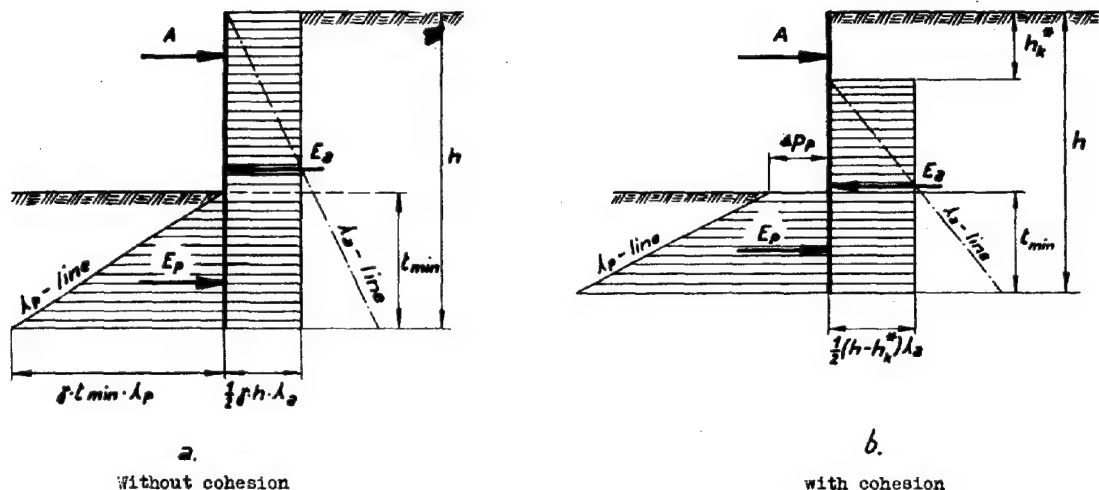


FIG.10

- 2) H. Engels: Zur berechnung der Bohlwerke. Zentralblatt der Bauverwaltung, 1903, Nr. 44, S. 273, Nr. 103, S. 649.
- 3) E. Jacoby: Grundsätzliches über die Berechnung von Spundwänden. Bautechnik, 1941, Nr. 8, S. 88. (Berichtigung S. 256).
- 4) C. F. Kollbrunner: Fundation und Konsolidation, Band II. Schweizer Druck- und Verlags-haus, Zürich, 1948.
- 5) F. Kötter: Die Entwicklung der Lehre vom Erddruck. Jahresbericht der deutschen mathem. Ver. 1891-92, S. 128.
- 6) H. Reissner: Theorie des Erddruckes. Enzyklopädie der mathematischen Wissenschaften, Bd. IV 2, II, S. 387. Teubner, Leipzig, 1907-1914.
- 7) K. v. Terzaghi: Distribution of the lateral pressure of sand on the timbering of cuts.

- Proceedings of the Intern. Conf. on Soil Mechanics and Found. Eng. Harvard University, Cambridge, Mass. Vol. I, p. 211, 1936.
- 8) A. Spilker: Mitteilung über die Messung der Kräfte in einer Baugrubenaussteifung. Bautechnik, 1937, Heft 1, S. 16.
- 9) J. Ohde: Zur Theorie des Erddruckes unter besonderer Berücksichtigung der Erddruckverteilung. Bautechnik, 1938, Heft 10/11, S. 150.
- 10) G. Klenner: Versuche über die Verteilung des Erddruckes über die Wände ausgesteifter Baugruben. Bautechnik, 1941, Heft 29, S. 316.
- 11) H. Lehmann: Die Verteilung des Erdangriffes an einer oben drehbar gelagerten Wand. Bautechnik, 1942, Heft 31/32, S. 273.
- 12) H. Dörr: Erddruck auf die Wände ausgesteifter Baugruben. Bautechnik, 1942, Heft 6, S. 54.

-o-o-o-o-o-o-

## SUB-SECTION I 9

### STRESS DISTRIBUTION.

I 91

#### APPROXIMATIVE CALCULATIONS OF THE STRESS-DISTRIBUTIONS DUE TO CONCENTRATED VERTICAL LOADS

IR. G.A. OOSTERHOLT

Technical University, Delft, Holland

In the Netherlands, Prof. dr. ir. F.K.Th. van Iterson was the first author, who tried to study this problem by means of approximative calculations 1). He computed the stress distribution, arising in a homogeneous isotropic material, if a smooth semi-sphere is pressed into it (fig. 1). If  $i$  denotes the vertical settlement of the sphere, the radial displacement of a point, located on the sphere in the direction  $\theta$ , will amount to  $i \cdot \cos \theta$ . Supposing

that the radial stress  $\rho_\theta$  spreads linear in the material, the radial displacement of the point considered will also be proportional to  $\rho_\theta$ . In consequence of this, the stress distribution can be written,

$$\rho_\theta = \rho_{\max} \cos \theta \quad (1)$$

which is the same as Bousinesq's equation.

Further

$$\rho_{\max} = \frac{3}{2} \frac{P}{\pi r_0^2} \cos \theta \quad (2)$$

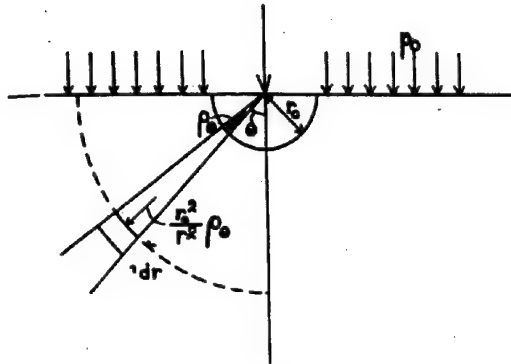


FIG. 1

A few years later on, Prof. Ir. A. S. Keverling Buisman studied the same problem, for materials with a modulus of elasticity, which increases in linear proportion to the depth. If  $\gamma$  denotes the unit weight of the soil and  $C$  the constant from Terzaghi's law, the modulus of elasticity may be expressed by  $\gamma r \cos \theta$ .  $C$  provided that the increase of the stresses due to the vertical load is very small. The total compression in the direction  $\theta$  then amounts to

$$\int_{r_0}^{\infty} p_e \left( \frac{r_0}{r} \right)^2 \frac{dr}{\gamma r \cos \theta} = \frac{p_e}{2 \gamma C \cos \theta}$$

As this is equal again to  $i \cos \theta$ , he found

$$p_e = 2 \gamma C i \cos^2 \theta \quad (3)$$

$$p_{\max} = 2 \cdot \frac{P}{\pi r_0^2} \quad (4)$$

Comparing these new formulae with (1) and (2), Prof. Buisman stated, that the latter might apply to some special cases, for instance if the capillary tensions are so high, that the increase of the effective normal stresses due to the weight of the soil, as well as to the load, may be neglected. On the contrary (3) and (4) should apply to a mass of soil without any capillary tensions, provided that the loads are very small.

The author has now tried to compute the stress distribution, if the loads are greater. The same method of calculation has been followed, but the increase of the modulus of elasticity when the sphere is pressed into the earth, has been taken into account. The computations are based again on the assumption, that the stress trajectories are straight lines through the centre of the sphere (3). The stress  $p_e$ , acting in the direction  $\theta$  (fig. 1) at the contact surface between the sphere and the soil, then expands in such a manner, that the stress

amounts to  $\frac{r_0}{r^2} p_e$  at a distance  $r$  from the centre of the sphere. There the original vertical stress was  $p_0 + \gamma r \cos \theta$  if  $p_0$  denotes the load per unit of area and  $\gamma$  the unit weight of the soil. Assuming, that Terzaghi's law may be applied at an inclined direction, the compression of the element plotted in fig. 1 amounts to

$$\frac{dr}{C} \ln \frac{p_0 + \gamma r \cos \theta + p_e \cdot r_0^2 / r^2}{p_0 + \gamma r \cos \theta}$$

and the total compression of all elements in the same direction can be written

$$\int_{r_0}^{\infty} \frac{dr}{C} \ln \left\{ 1 + \frac{p_e r_0^2}{r^2 (p_0 + \gamma r \cos \theta)} \right\}$$

If  $i$  denotes again the settlement of the sphere, the integral will be equal to  $i \cos \theta$ . Thus the general equation for the problem is found to be

$$C i \cos \theta = \int_{r_0}^{\infty} \ln \left\{ 1 + \frac{p_e r_0^2}{r^2 (p_0 + \gamma r \cos \theta)} \right\} dr \quad (5)$$

The integration will be worked out for two different cases. In the first place  $p_0$  is assumed to be zero, which is true for a load at the surface of the earth. If we substitute

$$a^3 = \frac{r_0^2 p_e}{\gamma \cos \theta}$$

the integral can be reduced to

$$C i \cos \theta = r \ln \left( 1 + \frac{a^3}{r^3} \right) \Big|_{r_0}^{\infty} + \int_{r_0}^{\infty} \frac{3 a^3 dr}{r^3 + a^3}$$

By splitting into fractions we then obtain

$$C i \cos \theta = r \ln \left( 1 + \frac{a^3}{r^3} \right) - \frac{a}{2} \ln \frac{r^2 - ar + a^2}{(r+a)^2} + a \sqrt{3} \operatorname{tg} \cotg \frac{-2r+a}{a\sqrt{3}} \Big|_{r_0}^{\infty}$$

Substituting  $\frac{r-a}{a} = \psi$  the formula can be written

$$\frac{C i}{r_0} \cos \theta = \frac{\pi \sqrt{3}}{\psi} - \ln \left( 1 + \frac{1}{\psi^3} \right) + \frac{1}{2\psi} \ln \frac{\psi^2 - \psi + 1}{(\psi+1)^2} - \frac{\sqrt{3}}{\psi} \operatorname{tg} \cotg \frac{1-2\psi}{\sqrt{3}} = f(\psi) \quad (6)$$

$$\text{while } \psi^3 = \frac{r_0 \gamma \cos \theta}{p_e} \quad (7)$$

The function  $f(\psi)$  has been plotted in fig. 2. If  $r_0$ ,  $\gamma$ , and  $C$  are known and a value of  $i$  has been chosen, the relation between  $\theta$  and  $p_e$  can be computed.

For point loads  $P$  the formula becomes more simple. Multiplying (6) with  $\psi$

$$\frac{C i \psi}{r_0} \cos \theta = \psi f(\psi)$$

and substituting  $\psi \rightarrow 0$  we find:

$$\frac{C i \gamma^{1/3}}{p_e r_0^{2/3}} \cos^{4/3} \theta = \lim_{\psi \rightarrow 0} \psi f(\psi) = \frac{2\pi}{\sqrt{3}}$$

Writing in the well known way

$$P = \int p_e \cos \theta dF$$

we find the relation between  $i$  and  $p_e$  and  $P$  for point loads at the surface of the earth:

$$i = \frac{3.57}{C} \sqrt[3]{\frac{P}{\gamma}} \quad (8)$$

$$p_e = \frac{3P}{\pi r^2} \cos^4 \theta \quad (9)$$

In the second place we assume  $p_0$  to be much greater than  $\gamma r \cos \theta$  in the vicinity of the sphere; generally this will approximately be true for deep footings, like pilepoints. Equation (5) then is reduced to:

$$C i \cos \theta = \int_{r_0}^{\infty} \left( 1 + \frac{p_e r_0^2}{r^2 p_0} \right) dr$$

In an analogous way as before, we can write the solution as follows:

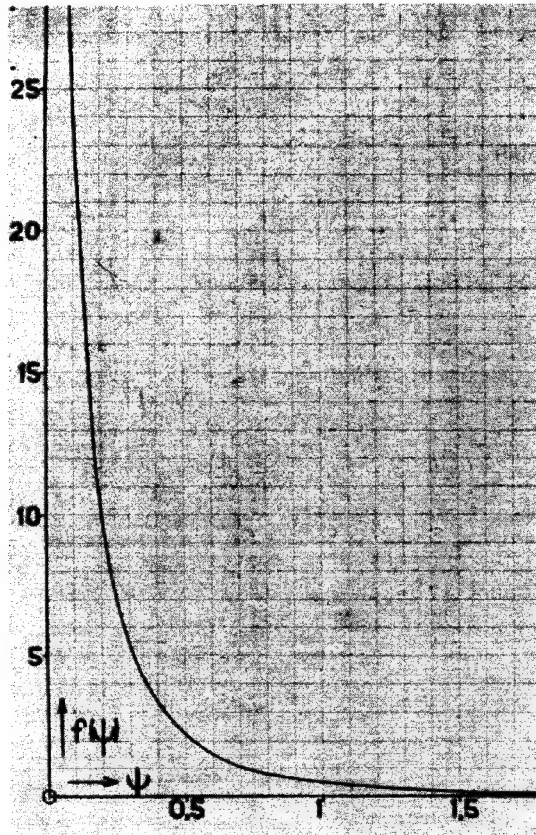


FIG. 2

$$\frac{C_i}{r_0} \cos \theta = \frac{\pi}{\varphi} - \ln \left( 1 + \frac{1}{\varphi^2} \right) - \frac{2}{\varphi} \operatorname{tg} \varphi = f(\varphi) \quad (10)$$

$$\varphi = \sqrt{\frac{P_0}{P_e}} \quad (11)$$

The function  $f(\varphi)$  has been drawn in fig. 3. For point loads we now can derive the following equations:

$$P_e = \frac{2P}{\pi r^2} \cos^2 \theta \quad (12)$$

and

$$i = \frac{1}{C} \sqrt{\frac{2\pi P}{P_0}} \quad (13)$$

If the new formulae for point loads are compared with those of the mentioned authors, it is striking, that the concentration factors are higher. For a constant modulus of elasticity (Boussinesq, Van Iterson) the concentration factor amounts to  $3/2$ ; in the corresponding case of a soil with a constant vertical stress  $P_0$  (form. 12) we now found 2. Calculating some stress distributions by the aid of (10) and (11), it turned out, that the concentration factor decreases with increasing values of  $\varphi$  and for  $\varphi \rightarrow \infty$  the formula becomes identical with Boussinesq's equation  $\varphi \rightarrow \infty$  means that  $P_e \rightarrow 0$ , so  $E = C \cdot P_0 = \text{a constant}$ .

When the resistance against compression increases with the depth, the difference is yet more striking; Prof. Buisman found

$$P_e = \frac{2P}{\pi r^2} \cos^2 \theta$$

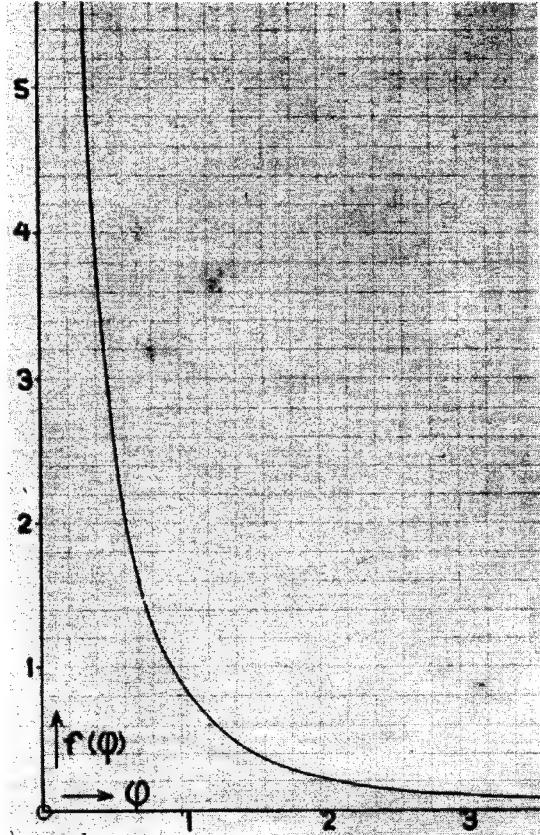


FIG. 3

while for point loads now was found

$$P_e = \frac{3P}{\pi r^2} \cos^4 \theta$$

Calculating  $P_e$  according to (6) and (7) it turns out, that the concentration factor decreases with increasing values of  $\psi$  and for  $\psi \rightarrow \infty$  the formula is identical again with prof. Buisman's formula  $\psi \rightarrow \infty$  corresponds also with

$$P_e \rightarrow 0 \text{ so } E = C \gamma r \cos \theta$$

It was well known from several experiments that the concentration factors could be considerably greater than indicated by Boussinesq's formula; different causes have been sought to explain this (Fröhlich, Buisman). Results of all tests of loads at the surface of soil, made by several investigators, were controlled by Fröhlich (4); he found semi-empirically, that a formula, identical with (6), was in the best harmony with these tests. Obviously the main cause of the great stress concentration therefore seems to be the fact, that the modulus of elasticity increases, when the load is brought upon the soil; other factors however, as mentioned by Buisman and Fröhlich, will also have influence.

The author is well conscious, that the calculations are a simplified scheme of reality. As long as the laws, governing the deformations of soils, are not known better however, it is necessary to seek the best approximation of the problem. The object of the above, therefore, was only to complete a train of thought,



that was ended half-way and to obtain by this a better harmony with reality.

#### REFERENCES.

1) De Ingenieur 1928 No.38/39.

- 2) De Ingenieur 1932 No.37; Grondmechanica p. 180.  
 3) Fröhlich, O.K. Druckverteilung im Baugrunde. 1934 9.  
 4) Fröhlich, op cit., p. 128.

-o-o-o-o-o-o-

192

#### ON THE DEPTH OF FOUNDATION

F. SZELĄGOWSKI

Polytechnical School, Warsaw

Among many conditions required of a new building the most important one is its stability against loading.

Stability of a building will not change, if the position of its foundation does not change.

It follows that the construction of a foundation should prove stable against any rotary movement, against any horizontal slipping, and finally against differential (varying) settlement, which might occur due to the upward pressure of the soil underneath the foundation.

The object of these lines is to set forth such a theory for depth of foundations which will make impossible the above mentioned movements.

In this connection it is necessary to say that an upward movement of the soil from underneath the foundation would be prevented when the pressure on the foundation bed of earth caused by the load of the foundation does not change the state of the extreme equilibrium of the soil determined by the equations:

$$t_{nt} = t_{nn} \operatorname{tg} \varphi \quad (1)$$

in the case of loose earths, and

$$t_{nt} = t_{nn} \operatorname{tg} \varphi + C \quad (2)$$

in the case of firm cohesive soil.

The first one is known as Rankine's formula of earth pressure, whereas the second one as Coulomb's formula.

Both of them when expressed in functions of stresses  $N_1$ ,  $N_2$  and  $T$  have the following form:

$$\sqrt{(N_1 - N_2)^2 + 4T^2} - (N_1 + N_2) \sin \varphi = 0 \quad (3)$$

in the case of loose earths, and

$$\sqrt{(N_1 - N_2)^2 + 4T^2} - (N_1 + N_2) \sin \varphi = 2C \cos \varphi \quad (4)$$

in the case of firm cohesive soil, where  $\varphi$  means the angle of friction, whereas  $C$  means the force of adhesion per square unit.

Rankine and Pauker were the first to initiate the study of the subject.

Rankine in the basis of the theory of equilibrium of cohesionless soil, and Pauker on the basis of equilibrium of retaining walls have both come independently from one another to the same results. In fact Rankine determined the smallest depth of a foundation by the formula:

$$h = H \frac{(1 - \sin \varphi)^2}{(1 + \sin \varphi)}$$

$$\text{whereas Pauker: } h = H \operatorname{tg}^4 \left( 45^\circ - \frac{\varphi}{2} \right)$$

where  $H$  means the height of a column of earth exerting pressure on the base corresponding to the pressure of the extreme equilibrium of loose earth.

It is known that

$$\frac{1 - \sin \varphi}{1 + \sin \varphi} = \frac{\operatorname{tg} (45^\circ - \frac{\varphi}{2})}{\operatorname{tg} (45^\circ + \frac{\varphi}{2})} = \operatorname{tg}^2 \left( 45^\circ - \frac{\varphi}{2} \right)$$

hence

$$h = H \frac{(1 - \sin \varphi)^2}{(1 + \sin \varphi)} = H \operatorname{tg}^4 \left( 45^\circ - \frac{\varphi}{2} \right) \quad (5)$$

where  $\varphi$  in both these formulae means the same angle of friction, commonly known as the angle of natural sliding of the soil.

Neither Rankine's nor Pauker's deductions which served as the starting point to formula (5) are correct from the theoretical point of view as both these authors assume in the vertical plane BC (fig. 1) a sudden turn at

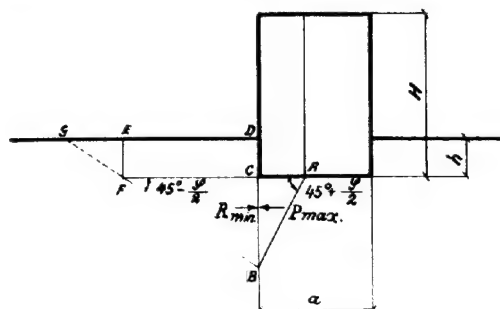


FIG. 1

an equal angle in the Lamé's ellipse of stresses. They assume as well the surfaces of sliding being planes which from an angle of  $45^\circ + \frac{1}{2}\varphi$  towards the level change their position to  $45^\circ - \frac{1}{2}\varphi$  in a non continuous way. Moreover the stresses of friction have not been taken into account.

In spite of these drawbacks formula (5) due to its simple form grew very popular in the technical literature and, as it always happens, all the drawbacks have been compensated by a factor of safety, the value of which has been lately reduced from 1.75 to 1.5. In



order to improve the matter Jankowski derived from the above the following formula:

$$h = \frac{H}{2} \frac{\left( \frac{45^\circ - \varphi}{2} \right)^2}{\left( \frac{45^\circ + \varphi}{2} \right)} \quad (6)$$

Although the results of this formula were confirmed by the experiments of Kurdiumow, nevertheless the assumption of the surfaces of sliding of the upward pushed soil as planes still did not correspond to the real facts. From the experiments of Kurdiumow it was evident that the movement of the particles of the upward pushed soil proceeds on continuous curves beginning right at the bottom of the foundation (fig. 2).

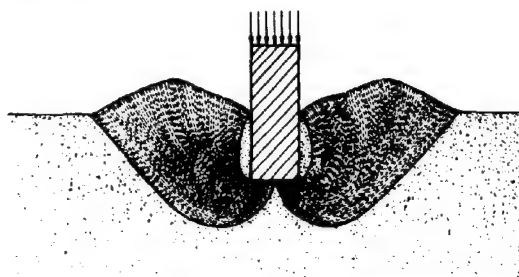


FIG. 2

Betzecki's formula 1) has a similar drawback. He has determined the necessary depth of a foundation (for loose earth) by the following formula:

$$h = H \frac{\left( \frac{45^\circ - \varphi}{2} \right)^2}{2 \frac{a}{\tan \left( \frac{45^\circ + \varphi}{2} \right)} \left[ 1 - \frac{\left( \frac{45^\circ - \varphi}{2} \right)^2}{\left( \frac{45^\circ + \varphi}{2} \right)^2} \right]} \quad (7)$$

where  $a$  means half the width of a foundation (fig. 3).

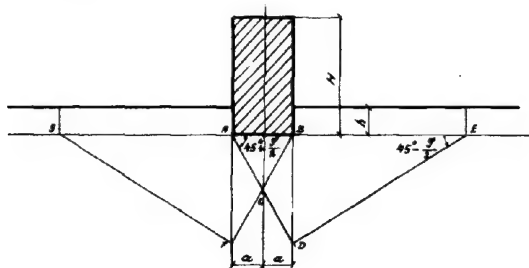


FIG. 3

In connection with the above it must be mentioned that in his reasoning Betzecki assumed the possibility of a formation of a wedge causing the upward push of clods of soil with quadrangular profiles BCDE and ACFG. Apart from this it should be noted that Betzecki when giving his formula (7) has taken in account only the state of loading on the surfaces of sliding AC and BC, appearing in the extreme equilibrium of soil.

However, in the above reasoning the possibility of there being a wedge ABC of  $90^\circ - \varphi$  at the top, which should force its way into the soil together with the foundation according to the experimental observations of Kurdiumow, has not been taken into account at all. The sliding of the soil, as already mentioned, takes place right at the middle of the foundation footing while the soil is being

pushed off both sides.

The first attempt of approaching the real state of things was done by Caquot 2) who has given an equation in the following form:

$$h = \frac{H}{\tan^2 \left( \frac{45^\circ + \varphi}{2} \right) e^{\pi \tan \varphi}} \quad (8)$$

in the case of loose earths, and

$$h = \frac{H - \frac{C}{\gamma \tan \varphi} \left[ \tan^2 \left( \frac{45^\circ + \varphi}{2} \right) e^{\pi \tan \varphi} - 1 \right]}{\tan^2 \left( \frac{45^\circ + \varphi}{2} \right) e^{\pi \tan \varphi}} \quad (9)$$

in the case of firm cohesive soil, where  $\gamma$  means the specific weight of earth.

Caquot in his reasoning in accordance with the previous work of Boussinesq and Résal considered a continuous joining of the surfaces of sliding inclined at an angle of  $45^\circ + \frac{\varphi}{2}$  towards the level with the surfaces of sliding inclined at an angle of  $45^\circ - \frac{\varphi}{2}$  by means of a logarithmical spiral (fig. 4).

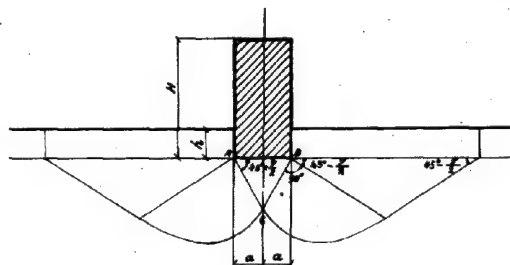


FIG. 4

In connection with the above assumption there arises a question whether the surfaces of sliding of the pushed off soil will have taken that configuration at all.

The answer to this question, judging by the results of experiments, is a negative one, as the experimental observations show that the surfaces of sliding change their configuration with the depth. Moreover the wedge of the top angle  $90^\circ - \varphi$ , which should force its way into the soil does not exist either.

Finally the last one who tried to determine the necessary depth of a foundation was Ritter whose formula based on the pushing off soil particles from underneath the foundation was given in the following form: 3)

$$h = \frac{2H - a \left[ \tan^5 \left( \frac{45^\circ + \varphi}{2} \right) - \tan \left( \frac{45^\circ + \varphi}{2} \right) \right]}{2 \tan^4 \left( \frac{45^\circ + \varphi}{2} \right)} \quad (10)$$

in the case of loose earth, and

$$h = \frac{2H - a \left[ \tan^5 \left( \frac{45^\circ + \varphi}{2} \right) - \tan \left( \frac{45^\circ + \varphi}{2} \right) \right] - \frac{2C}{\gamma \tan \varphi} \left[ \tan^4 \left( \frac{45^\circ + \varphi}{2} \right) - 1 \right]}{2 \tan^4 \left( \frac{45^\circ + \varphi}{2} \right)} \quad (11)$$

in the case of firm cohesive soil.

In his considerations Ritter assumed, as Betzecki and Caquot did before, the possibility of a formation of a wedge (fig. 5) causing the pushing off clods of soil having certain curved surfaces the shape of which was not exactly determined by him. This was due to the fact to the deduction of formulae (10) and (11). Ritter's starting point was

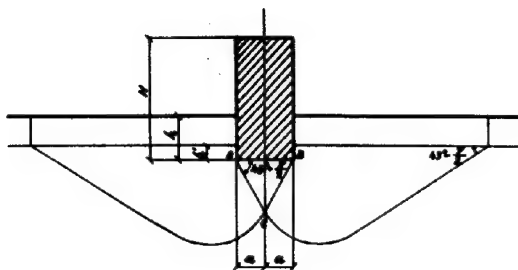


FIG. 5

the relation determining the values of principal stresses in the form independent of the sliding surfaces of the pushed off soil.

Analysing the above formulas (7) and (10), and taking into consideration the existence of the below quoted connection:

$$\operatorname{tg}(45^\circ + \frac{\varphi}{2}) = \frac{1}{\operatorname{tg}(45^\circ - \frac{\varphi}{2})}$$

it must be stated that Ritter's formula (10) is identical with that of Betzecki (7). So here again both these authors, Betzecki and Ritter, starting from different points independently from one another arrive, as it can be seen, to identical formulas.

The above quoted formulas, as it can be observed, are to a certain extent, based on assumptions incompatible with experiments which did clearly explain a complex process of the phenomenon of the thrust of soil from underneath the foundation.

Moreover on the basis of these experiments it was possible to come to a conclusion that just before the formation of the surfaces of sliding, i.e. before the thrust of soil from underneath the foundation there took place a strong condensation of the soil beneath the foundation. It could also be deduced that the parts of soil directly adhering to the side surfaces of the foundation did not come into the area of sliding, i.e. they were not included in the bulk of clods of soil pushed off (fig. 2).

Seeing the non defined configuration of the surfaces of sliding of the soil pushed off and the sheer impossibility of basing thereupon any exact calculation of the necessary depth of a foundation, it will be to the point to make the above mentioned on the basis of the pertaining results of the elasticity theory taking simultaneously into account Rankine's or Coulomb's condition.

This way was adopted by Pigeaud, 4) who using Boussinesq's definition of the stress distribution under the influence of intense pressure, did obtain an equation the whole of the question, however, without final deduction of respecting formulas concerning the calculation of the necessary depth of a foundation in the case of loose or firm earths.

That's why in this article having reference to Michell's formulas defining the stresses in continuous sphere under uniform load spread over a sector  $2\alpha$  long, the respective formulas are arrived at in quite a simple way.

Michell's formulas for the load shown on fig. 6 have the following form:

$$N_1 = \frac{p}{\pi} \left( \operatorname{arctg} \frac{\alpha-x}{y} + \operatorname{arctg} \frac{\alpha+x}{y} \right) + \frac{2py\alpha(x^2-y^2-\alpha^2)}{[(y^2+x^2-\alpha^2)^2+4\alpha^2y^2]\pi}$$

$$N_2 = \frac{p}{\pi} \left( \operatorname{arctg} \frac{\alpha-x}{y} + \operatorname{arctg} \frac{\alpha+x}{y} \right) + \frac{2py\alpha(x^2-y^2-\alpha^2)}{[(y^2+x^2-\alpha^2)^2+4\alpha^2y^2]\pi}$$

$$T = \frac{4\alpha y^2 p}{\pi[(y^2+x^2-\alpha^2)^2+4\alpha^2y^2]}$$

Taking into account the above values in formulas

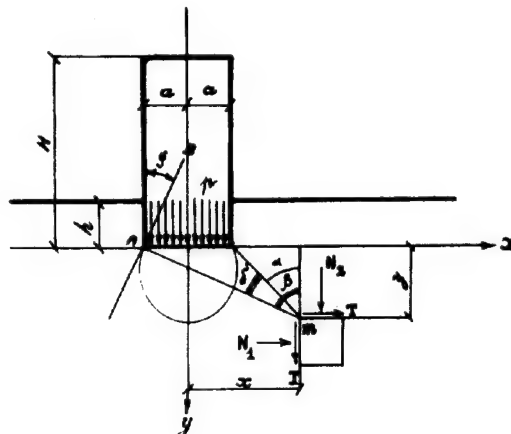


FIG. 6

(3) and (4) and then to simplify the calculation introducing the angles  $\alpha$ ,  $\beta$ , and  $\delta = \beta - \alpha$ , we shall obtain as the result the Rankine's and Coulomb's conditions in very simple form

$$\frac{2p}{\pi} (\sin \delta - \delta \sin \varphi) = 0 \quad (12)$$

$$\frac{p}{\pi \cos \varphi} (\sin \delta - \delta \sin \varphi) = C \quad (13)$$

On the other hand it must be noted that Rankine's and Coulomb's conditions represent the maximum shear stresses.

Thus the extreme value of angle  $\delta$  can be determined from the equation which will result of differentiating of equation (12) and (13). Thus when differentiating we arrive at:

$$\cos \delta - \sin \varphi = 0$$

The value of angle

$$\delta = \frac{\pi}{2} - \varphi \quad (14)$$

solves, as it can be seen, the above equation. The geometrical place of points where the maximum shear stresses occur is the circumference of a circle to which the straight line AB inclined at an angle  $\varphi$  is tangent.

The specific weight of earth in its turn should be taken into account.

In connection with the above it must be stated that for a certain point the corresponding stresses will have the following values:

$$N_1 = N_2 = \gamma y$$

and

$$T = 0$$

Thus Rankine's and Coulomb's conditions because of

$$N_1 - N_2 - T = 0,$$

and

$$N_1 + N_2 = 2\gamma y$$

will have one symbol more  $-2\gamma y \sin \varphi$

Finally should the position of the foundation footing be at a given depth  $-b$ , reason-

ing analogous to the above should be made.

Thus considering the above results in Rankine's and Coulomb's conditions, we will finally obtain these equations in the following form:

$$\frac{2(p-\gamma h)}{\pi} \left[ \sin\left(\frac{\pi}{2}-\varphi\right) - \left(\frac{\pi}{2}-\varphi\right) \sin\varphi \right] - 2\gamma(h+\eta) \sin\varphi = 0 \quad (15)$$

$$\frac{1}{\cos\varphi} \left[ \frac{(p-\gamma h)}{2} \left[ \sin\left(\frac{\pi}{2}-\varphi\right) - \left(\frac{\pi}{2}-\varphi\right) \sin\varphi \right] - \gamma(h+\eta) \sin\varphi \right] = C \quad (16)$$

It will be noticed that a maximum  $-h-$  will be obtained when  $\eta = 0$  in the expressions (15) and (16).

If we introduce here the notation  $p = \gamma H$ , then after suitable transformation the necessary depth of a foundation can finally be expressed by the following formula:

$$h = H \frac{1 - (\sqrt[3]{2} - \varphi) \tan\varphi}{1 + (\sqrt[3]{2} + \varphi) \tan\varphi} \quad (17)$$

in the case of loose earths, and

$$h = \frac{H[1 - (\sqrt[3]{2} - \varphi) \tan\varphi] - \pi C}{1 + (\sqrt[3]{2} + \varphi) \tan\varphi} \quad (18)$$

in the case of firm, cohesive soil. Moreover on the basis of the equations (15) and (16) pressures at the  $-h-$  depth (at the moment of the extreme equilibrium of the earth) could be defined:

$$p = \gamma h \frac{1 + (\sqrt[3]{2} + \varphi) \tan\varphi}{1 - (\sqrt[3]{2} - \varphi) \tan\varphi}$$

in the case of loose earths,

$$p = \frac{\gamma h[1 + (\sqrt[3]{2} + \varphi) \tan\varphi] + \pi C}{1 - (\sqrt[3]{2} - \varphi) \tan\varphi}$$

in the case of cohesive soil.

For practical purposes the formulae (17) and (18) defining the necessary depth of a foundation should be applied with the 1.25 factor of safety against a possible existence of the extreme equilibrium of the soil.

The question of the necessary depth of a foundation with a not uniformly spread load will be treated somewhat further (fig. 7).

In the case under discussion only active earth pressure is taken into account as exerting influence on those side parts of the foundation block which due to a certain rotation exert the corresponding pressure on the ground. The passive earth pressure is better not to be taken into account at all, as it appears only when caused by a previous condensation of soil under the influence of relatively considerable movement of the foundation block, which is altogether inadmissible in buildings.

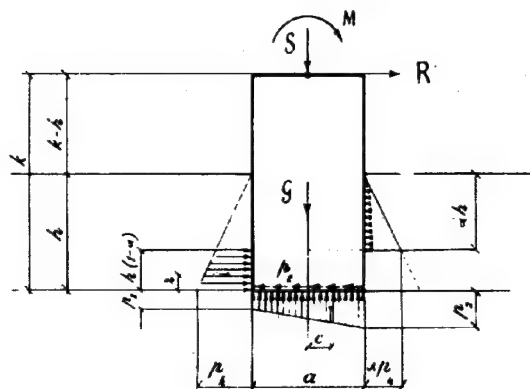


FIG. 7

That's why friction on the surfaces of the foundation block which in certain kinds of soil takes place only during the movement of the foundation is not taken into consideration. Moreover this friction is often diminished by the application of slightly inclined side surfaces of the foundation block and by loosening the adhering parts of soil.

To define the value of pressure on the foundation base, the equilibrium of the foundation block as a solid body must be born in mind, when writing three principal equations of equilibrium, i.e.:

$$\frac{P_1 + P_2}{2} a = P \quad (19)$$

$$\frac{P_1(1+\alpha)}{2} h(1-\alpha) + \frac{\alpha P_1}{2} \alpha h + \frac{\mu(P_1 + P_2)}{2} a = R \quad (20)$$

$$\frac{P_1(1+\alpha)}{2} h(1-\alpha)(k-z) - \frac{\alpha P_1}{2} \alpha h(k-h + \frac{2\alpha h}{3}) - \frac{\mu(P_1 + P_2)}{2} \alpha k + \frac{P_1 + P_2}{2} a e = M \quad (21)$$

where

$P = S + G$ ,  
and  $\mu$  coefficient of friction between the foundation block and the soil.

Taking into consideration in equations (19), (20) and (21) relative distances of centres of gravity

$$e = \frac{a}{6} \cdot \frac{P_2 - P_1}{P_2 + P_1},$$

$$z = \frac{h}{3} \cdot \frac{(1-\alpha)(1+2\alpha)}{1+\alpha}$$

we obtain from the solution of these equations the pressure values  $P_1$ ,  $P_2$  in the form of the following formulae:

$$P_1 = \frac{P}{a} \cdot \frac{6}{\alpha^2} \left\{ M + \mu P k + \frac{P_1 h}{2} \left[ \alpha^2 \left( k-h + \frac{2\alpha h}{3} \right) - (1-\alpha^2)(k-z) \right] \right\} \quad (22)$$

$$P_2 = \frac{P}{a} \cdot \frac{6}{\alpha^2} \left\{ M + \mu P k + \frac{P_1 h}{2} \left[ \alpha^2 \left( k-h + \frac{2\alpha h}{3} \right) - (1-\alpha^2)(k-z) \right] \right\} \quad (23)$$

and besides

$$\alpha = \sqrt{\frac{1 - R - \mu P}{2 + \frac{R - \mu P}{P_1 h}}}$$

Finally the value of pressure on the foundation base should be defined in the case shown on fig. 8.

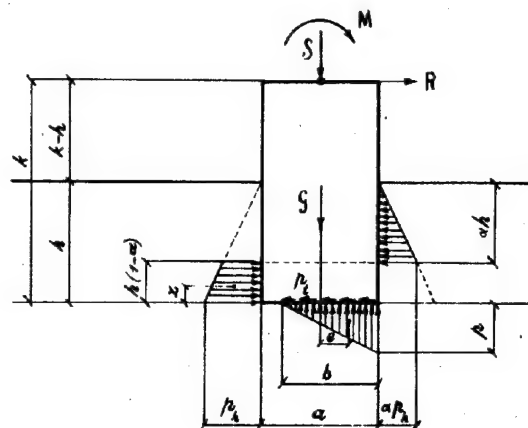


FIG. 8

Here the equilibrium equations will take the following form:

$$\frac{pb}{2} = P, \quad (24)$$

$$\frac{P_h(1+\alpha)}{2}h(1-\alpha) + \frac{\alpha P_h}{2}\alpha h + \frac{\mu pb}{2} = R \quad (25)$$

and

$$\frac{P_h(1+\alpha)}{2}h(1-\alpha)(k-z) - \frac{\alpha P_h}{2}\alpha h(k-h + \frac{2\alpha h}{3}) - \frac{\mu pb}{2}k + \frac{pb}{2}e = M$$

where

$$P = S + G.$$

In the case under consideration it will be

$$e = \frac{a}{2} - \frac{b}{3},$$

where the distance  $-z-$ , as well as the  $\alpha$  will be defined on the basis of the above mentioned formulas.

From the solution of the equations (24), (25) and (26) we will obtain

$$P = \frac{2P^2}{3 \left\{ \frac{P_h h}{2} \left[ (1-\alpha^2)(k-z) - \alpha^2 \left( k-h + \frac{2\alpha h}{3} \right) \right] - P \left( \mu k - \frac{\alpha}{2} \right) - M \right\}} \quad (27) \text{ and}$$

$$b = \frac{3}{P} \left\{ \frac{P_h h}{2} \left[ (1-\alpha^2)(k-z) - \alpha^2 \left( k-h + \frac{2\alpha h}{3} \right) \right] - P \left( \mu k - \frac{\alpha}{2} \right) - M \right\}$$

Thus when determining the necessary foundation depth exerting non uniform pressure on the soil, one may practically speaking, apply formula (17) or (18) (taking into account the safety factor 1.25), in which formulas the height of the column of earth  $H$  should be taken for the maximum pressure on the soil. This pressure is determined by the formula (23) or (27).

#### REFERENCES.

- 1) S. Betzecki. "Statyka ciat sypkich i scian podporowych." 1914.
- 2) A. Caquot. "Equilibre des massifs à frottement interne." Paris 1934.
- 3) M. Ritter. "Grenz Zustände des Gleichgewichtes in Erd- und Schüttmassen." Intern. Ver. für Brück. und Hoch. Zweiter Kongress. Berlin 1936.
- 4) G. Pigeaud. "Résistance des matériaux et élasticité." Paris 1934.

-0-0-0-0-0-0-

193

#### COMPUTATION OF BEAMS RESTING ON SOIL.

E. DE REER - Ghent (Belgium)

#### INTRODUCTION

The computation of beams resting on soil is generally made by considering the soil as a perfectly elastic material, defined by a modulus of soil reaction  $K$  (kg/cm<sup>3</sup>). Doing so, the soil is supposed to be a perfect liquid with a specific weight  $K$ , or an infinity of independent springs.

The method of the modulus of soil reaction has first been introduced in railway-construction, to define the settlement of the sleepers resting on the ballast.

The same method is currently used in the U.S.A. to determine the thickness required for concrete pavements of airfields. The modulus of soil reaction is defined by means of a loading test on a slab of 30" diameter which nearly corresponds to the contact area of the tires of large planes.

When it is necessary to compute beams with arbitrary contact areas and subjected to arbitrary loads, the problem is to find which value can yet be attributed to the figures obtained by the method of the modulus of soil reaction, this method being based on assumptions which differ largely from the real properties of the soil. Another problem is how, for arbitrary contact areas, arbitrary dimensions and arbitrary loads, the modulus of soil reaction can be deducted from real, directly measurable soil properties.

The question of the exactitude of the method of the modulus of soil reaction has already interested many technicians. For instance Wieghardt and Schiel believed to have found a more exact solution by assuming the soil to be a perfect liquid with non negligible superficial tensions. On the other hand Borowicka gave the exact solution for a cir-

cular slab resting on a material with a constant modulus of elasticity.

#### GENERAL SOLUTION.

One can try to base the computation of beams resting on soil on the real properties of the soil itself. Consider a beam with an arbitrary stiffness, subjected to arbitrary forces, and resting on a soil with an arbitrary compressibility (fig. 1). Under the effect of the forces, the beam and the soil will deflect. These deflections are a priori unknown, but it is known that the deformations of the beam and the soil are to concord in each point of contact. Thus the reactions soil-beam must be so distributed that in each point this condition is fulfilled. Beside the usual equations of the equilibrium of forces, one disposes of an infinity of relations expressing for each point of contact the equality of the deformations of the soil and of the beam.

Theoretically the problem thus is solved. Practically one can proceed as follows: one adopts arbitrarily a distribution of the reactions soil-beam, but which satisfies the normal equation of equilibrium. For this solicitation the deformations  $s_p$  of the beam and  $s_t$  of the soil are computed, on the base of the real properties of deformability of the latter. As the law of distribution has been arbitrarily adopted, the values of  $s_p$  will generally be different from those of  $s_t$ . Then a new law of distribution can be chosen, to obtain values  $s'_p$  and  $s'_t$ , which better agree, and by successive approximations each desired degree of exactitude can be obtained.

For laterally confined soils the deformability is expressed by the law of compress-

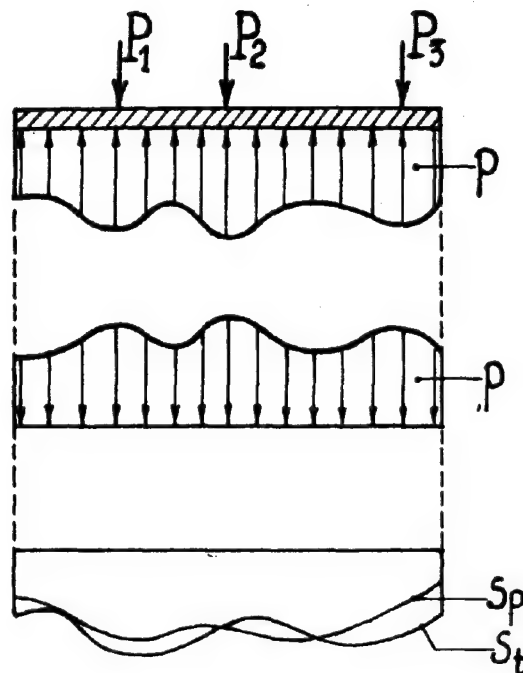


FIG. 1

ibility of Terzaghi. The foundation beams are generally located at a sufficient depth underneath the soil surface; on the other hand, as long as the effective loads are but a fraction of the ultimate bearing capacity of the soil underneath the beam, the settlements of the latter produced by lateral displacements of the soil particles are small in comparison with those produced by the compression without lateral displacement.

A simple derivation of the formula of Terzaghi indicates that, if the lateral displacements are prevented, the modulus of elasticity  $E_s$  of the soil can be expressed by:

$$E_s = C\sigma_k \quad (1)$$

where  $E_s$  - the modulus of elasticity ( $\text{kg/cm}^2$ )  
 $C$  - the constant of compressibility, which can be determined by consolidation tests  
 $\sigma_k$  - the effective stress at the considered point and on the considered plane ( $\text{kg/cm}^2$ ).

The law (1) indicates that, according to the nature and the history of the soil, it is possible to have a material with a constant modulus of elasticity, or a material that is heterogeneous and/or anisotropic in relation with its compressibility.

If, in view of the simplicity, the tangential reactions soil-beam are neglected, the increase of the stresses in the soil produced by the arbitrarily chosen law of sollocation can be easily computed on the base of the law of Boussinesq or any other similar law. For this purpose the diagrams of Newmark are very useful.

#### APPLICATION TO RECTANGULAR BEAMS SUBJECTED TO CENTRAL LOADS.

The described general solution has been systematically used for the computation of

rectangular beams with an arbitrary length  $l$  and a width  $b$ , subjected to a central load  $P$  and resting on a soil with a constant modulus of elasticity  $E_s$ . Assuming that the unknown distribution of the reactions soil-beam is a parabola of the 2nd degree, one relation of deformability is sufficient. It is obtained by expressing that the maximum deflection of the beam has to be equal to the difference in settlement of the centre and the borders. An example of calculation is given on fig. 2. It appears that the deformed surfaces of the soil  $S_o$  and of the beam  $P_o$  only concord at the centre and at the borders; thus the parabolic distribution of the 2nd degree is only a first approach to the problem.

By defining the law of distribution by the formula

$$p = A\left(\frac{x}{l}\right)^4 + B\left(\frac{x}{l}\right)^2 + C - D \ln\left(\frac{P_o}{P_{o,\infty}} - \frac{2x}{l}\right) \quad (2)$$

it is possible, by a judicious choice of 3 parameters, to obtain practically the exact distribution.

In the formula (2) are:

- $p$  - the reaction soil-beam in the point with abscissa  $x$
- $x$  - the abscissa of the considered point, the origin being at the centre  $C$  of the beam.
- $l$  - the length of the beam.
- $P_o$  - the reaction at the centre.
- $P_{o,\infty}$  - the reaction at the centre under the same beam and the same load, the stiffness of the beam being supposed infinite.

$A, B, C, D$  - coefficients having the dimension of a stress.

As it is necessary to know  $P_{o,\infty}$ , the formula (2) must first be applied to the case of the beam, supposed to have an infinite stiffness.

The fig. 3 represents an application of the formula (2).

Although the parabolic distribution of the second degree is not an exact one, the values of the moment at the centre given by this distribution differ only very little from the moments corresponding to the distribution of the formula (2).

The case of rectangular beams resting on soils with a modulus of elasticity linearly increasing with depth has also been considered. One gets practically the same conclusions as for a soil with a constant modulus of elasticity.

#### COMPARISON OF THE RESULTS OBTAINED BY THE METHOD OF SUCCESSIVE APPROXIMATIONS WITH THOSE OBTAINED BY THE METHOD OF THE MODULUS OF SOIL REACTION.

The modulus of soil reaction  $K$  being no physical constant for a given soil, it is finally necessary to define this quantity.

In cases of a soil with a constant modulus of elasticity  $K$  is defined by:

$$K = \frac{4}{3} \frac{E_s}{\sqrt[3]{b^3 l}} \quad (3)$$

In case of a soil with a variable modulus of elasticity,  $K$  is defined by

$$K = \frac{P_m}{\Delta_o} \quad (4)$$

where  $P_m$  - mean value of the reactions soil-beam.

$\Delta_o$  - the settlement of the beam, supposed to be of infinite stiffness.

This settlement is computed on the

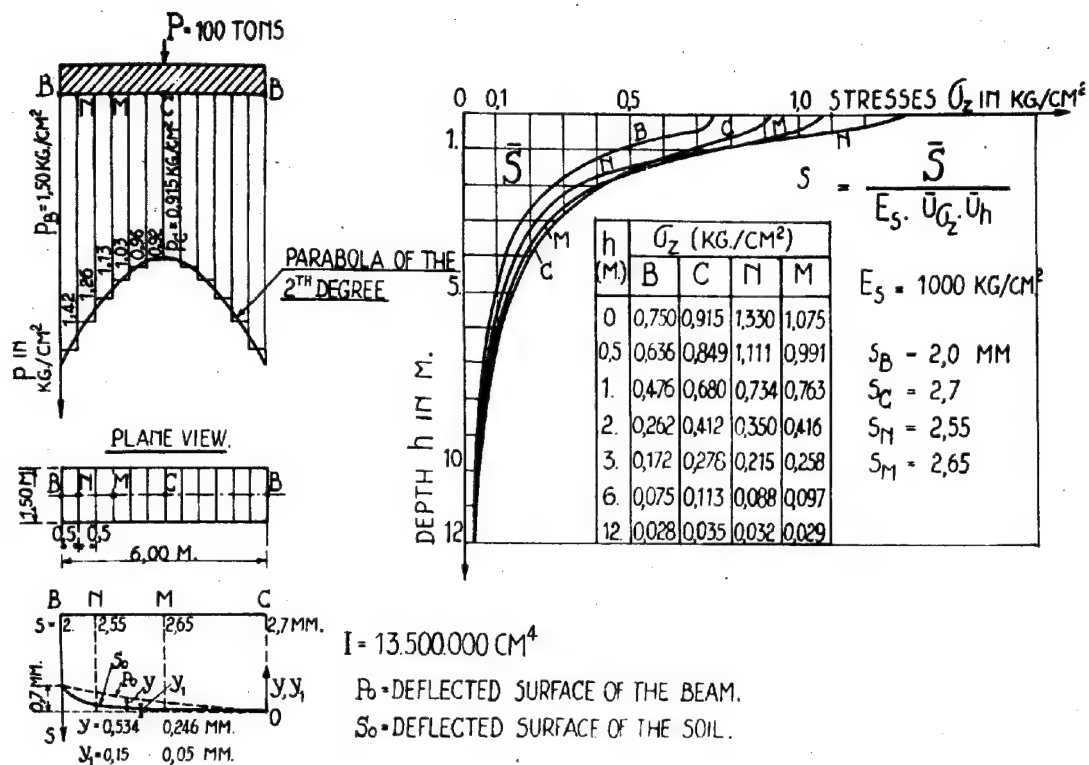


FIG. 2

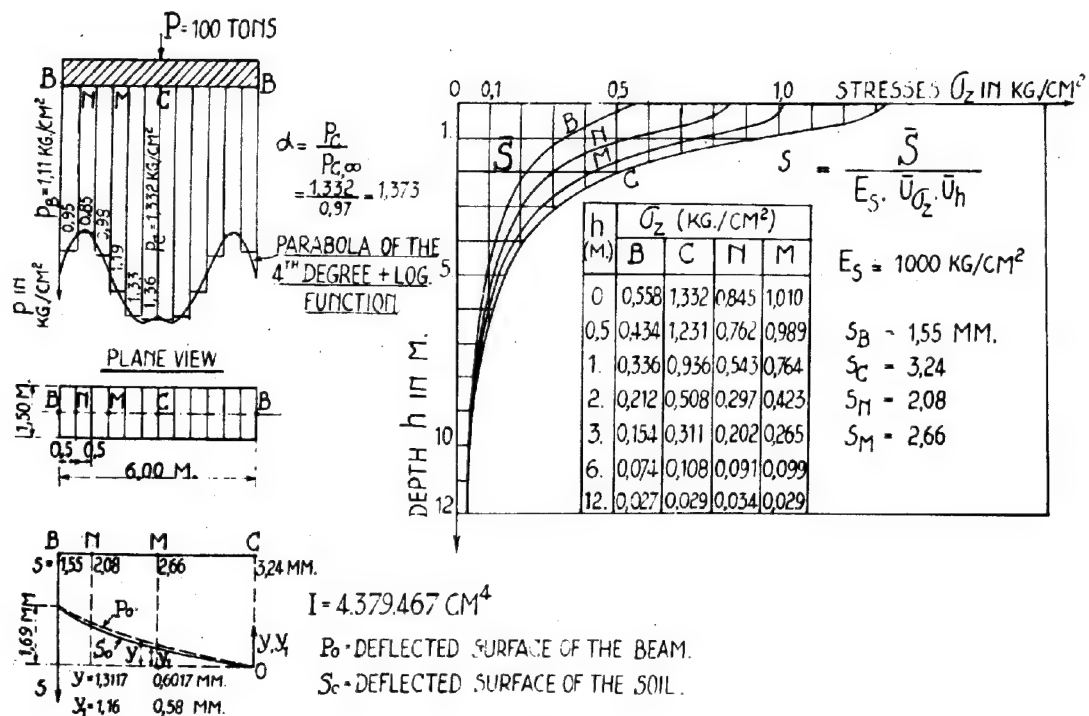


FIG. 3

base of the real properties of compressibility of the soil.

The value of  $K$  having been defined, it is now possible to utilize the method of the modulus of soil reaction to compute the moment at the centre.

Comparing the values obtained for the moment at the centre by the method  $K$  with those obtained with the formula (2) or with the parabolic distribution of the 2nd degree, it is found that for a high stiffness  $I$  the method  $K$  gives for the moment  $M_C$  values smaller than the exact ones, while for very low stiffnesses  $I$  it is the contrary. Thus for high stiffnesses the application of the method  $K$  can furnish values which are too low and thus could become dangerous.

The negative divergence being maximum for  $I = \infty$ , fig. 4 gives in case  $E_s = c^2$ , the values

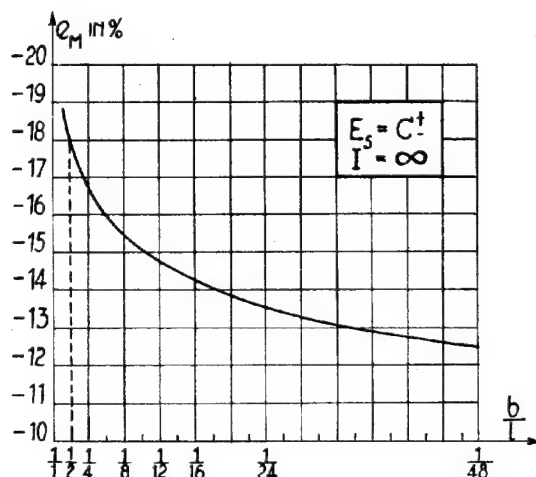


FIG. 4

of the divergence  $e_M$  in function of the ratio  $l/b$  for  $I = \infty$ . The divergence becomes larger, when the ratio  $l/b$  decreases, thus when the shape of the beam approaches that of a square slab. Since only "beams" were considered, for which the length is much larger than the width, the curve on fig. 4 is limited to values  $l/b > 2$ .

For these values, the maximum negative divergence between the moment at the centre given by the method  $K$  and the one obtained by the parabolic method is smaller than 18 %.

In case of a beam subjected to an axial single load and resting on a soil with a constant  $E_s$ , a safe value of the moment at the centre can easily be found. Indeed, it is sufficient to compute the mean value of the modulus of soil reaction by means of the formula (3). One applies the method  $K$  to obtain  $M'_C$ .

For the ratio  $l/b$  of the given beam, the fig. 4 gives the value of  $e_M$ . Finally  $M_C$  is computed by the formula

$$M_C = M'_C \frac{100}{100 + e'_M} \quad (5)$$

The value  $M_C$  so computed will be larger than the real moment, whatever the value of the moment of inertia  $I$  and of the ratio  $l/b$  will be.

Another way, which is a little less rapid, but gives a more exact value, is to assume that the reactions soil-beam are distributed according to a parabola of the 2nd degree, and to apply the general method.

In case of a soil with a variable modulus of elasticity, the computations show that the maximum value of the negative divergence between the moment at the centre given by the method  $K$  and the exact moment is smaller than 30 %; the negative divergence attains its maximum value, when the stiffness of the beam is infinite. For every small stiffnesses the method  $K$  gives safe values. A more exact value for the moment at the centre can again be obtained by assuming the law of distribution of reactions soil-beam to be a parabola of the second degree.

Finally for rectangular beams, subjected to a single central load, the moment at the centre obtained by applying the method of the modulus of soil reaction - this latter being defined by the formulas (3) or (4) - is never more than 30 % smaller than the exact value. Since the safety factors adopted for the computation of the dimensions of a beam are at least 2, it follows that, by using the method of the modulus of soil reaction for the considered case, dangerous errors in the choice of the dimensions of the beam are excluded.

For the rest it is worthwhile to note that this conclusion is not longer valid, when it is necessary to compute the moments and the shear forces in an arbitrary section.



Prof. K. HRUBAN

Technical University, Brno (Czechoslovakia).

**SUMMARY.**

In some cases, it may be appropriate to use the theory of a heterogeneous semi-infinite solid for the purpose of deriving settlement estimates from observations on full-size structures. Solutions for different load distributions are given.

In general, the compressibility of soil masses below foundations is variable from spot to spot. In most cases, it decreases in vertical direction downwards. The phenomena observed under loads distributed over a limited portion of the surface of sand deposits lead to the conclusion that in such cases variations of the compressibility in horizontal direction are also bound to occur. For the purpose of stress computations, we simplify the actual state of things and represent the foundation soil by a semi-infinite elastic body. On two conditions, this working assumption may lead to suitable results:

i/ The configuration of the foundation soil is such that there are no important irregularities in the degree of consolidation of individual strata and that the rock surface is not, or but slightly, inclined.

ii/ The intensity of loading does not exceed a certain limit so that it is reasonably possible to admit the law of proportionality between unit deformations and stresses produced in single elements of the mass.

In many cases of foundation practice both these conditions are satisfied with a sufficient approximation. They definitely are not fulfilled, however, with laboratory experiments either on sand fillings confined in rigid vessels or on earth accumulations placed on a concrete floor. The type of heterogeneity of such artificial models is obviously essentially different from that of an unlimited soil mass which has been consolidated by the pressures of its upper layers, the compressibility of its elements being dependent upon the intensity of the principal stresses acting on them.

If the foundation soil can be considered as corresponding to both the conditions mentioned above, it will be possible to derive the constants characterizing its behaviour from the settlement measurements on full-size structures and to forecast, consequently, the expected settlement of a proposed structure from the data gained by the observation of the existing ones. In such investigations, however, it has proved inappropriate to neglect the influence of the variations of the compressibility of the soil mass. Thus, in the following, we propose to analyse the deformation of an elastic semi-infinite solid with a modulus of elasticity which depends upon the position of the mass element in the body and which can be represented by a continuous function of the coordinates. We shall confine our considerations to those cases only in which it is possible to express the resulting deformation of the solid by simple closed relations suitable for use in foundation practice.

**1. FORCE APPLIED AT A POINT.**

Let a force  $P$  acting along the  $Z$ -axis of the system of spherical coordinates  $R, \varphi, \psi$ , (Fig. 1) be applied to the point  $O$  of the boundary plane  $Z = 0$ .

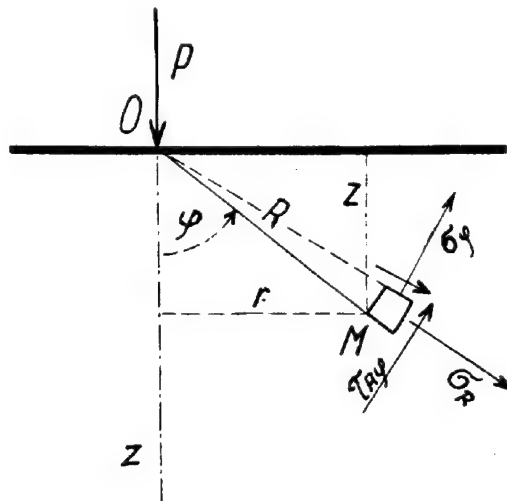


FIG. 1

We shall use the following notations:

$u, v, w$  components of displacements,  
 $\epsilon_R, \epsilon_\varphi, \epsilon_\psi$  unit elongations,  
 $\gamma_{R\varphi}, \gamma_{R\psi}, \gamma_{\varphi\psi}$  shearing strain components,  
 $\sigma_R, \sigma_\varphi, \sigma_\psi$  normal components of stress,  
 $\tau_{R\varphi}, \tau_{R\psi}, \tau_{\varphi\psi}$  shearing-stress components.  
 The axis of  $z$  being that of symmetry, it may be written

$$w=0, \gamma_{R\psi}=\gamma_{\varphi\psi}=0,$$

$$\epsilon_R = \frac{\partial u}{\partial R}, \quad \epsilon_\varphi = \frac{1}{R} \left( u + \frac{\partial v}{\partial \varphi} \right), \quad \epsilon_\psi = \frac{1}{R} \left( u + v \cot \varphi \right), \quad (1)$$

$$\gamma_{R\varphi} = \frac{\partial v}{\partial R} + \frac{1}{R} \left( \frac{\partial u}{\partial \varphi} - v \right),$$

$$\epsilon_R = \frac{1}{E} \left( \sigma_R - \frac{\sigma_\varphi + \sigma_\psi}{m} \right), \quad \epsilon_\varphi = \frac{1}{E} \left( \sigma_\varphi - \frac{\sigma_R + \sigma_\psi}{m} \right), \quad \tau_{R\varphi} = \frac{mE}{2(m+1)} \gamma_{R\varphi} \quad (2)$$

Herein  $m$  is the reciprocal of Poisson's ratio, which is assumed to be constant throughout the body, and  $E=f(R, \varphi)$  is the variable modulus of elasticity.

Adding the differential equations of equilibrium to the expressions (1) and (2), the conditions of compatibility may be derived in terms of strain or stress components.

If the compressibility of the material decreases with the depth  $z$ , the modulus of elasticity may be expressed by the equation  $E=Cz^n$  where  $C$  is constant and  $n \neq 0$  is a positive number.

It may be shown 1) that the displacements are

in this case

$$u = \frac{n+3}{n+1} \frac{P \cos \varphi}{2\pi C R^{n+1}}, \quad v = -\frac{n+3}{(n+1)(n+2)} \frac{P \sin \varphi}{2\pi C R^{n+2}}, \quad (3)$$

under the condition that  $m = n+2$ . (4)  
The stress distribution is a simple radial one, the principal stress amounting to

$$\sigma_r = -\frac{n+3}{2\pi} \frac{P \cos^{n+1} \varphi}{R^2} \quad (5)$$

and all other stress components being nil.

#### Possible value of $n$ .

Tests and observations have shown, that the settlement of circular areas under equal load per square unit increases with their radius, but not in direct proportion to it. Excluding very small areas, the relation between the settlement and the radius of the loaded circle can be represented by a curve of parabolic type. Accordingly, the settlement of an individual footing or of a single pile is always smaller than the settlement of an entire group of such units.

If our semi-infinite body shall be an appropriate representation of the foundation soil, we have to choose for  $n$  such a number that the deformation of the solid corresponds with these observations.

From the second of Eqs. (3) we conclude that the deflections of the points of the boundary plane are

$$\xi = \frac{P}{K r^{n+1}}$$

$r$  being the distance of the point in consideration from the point of the application of the force  $P$ , and  $K$  constant.

Let us compute the deflection  $\xi_c$  of the centre of a loaded circular area with the radius  $a$ , if the intensity of a uniform loading is  $p$ . We obtain

$$dP = 2\pi r dr p, \quad \xi_c = \int_0^a \frac{p 2\pi r dr}{K r^{n+1}} = \frac{2\pi p}{K} \int_0^a \frac{dr}{r^n},$$

As the deflection is in no case infinitely large, the exponent  $n$  must be smaller than 1.

For  $n = 0$ , we should have  $\xi_c = \frac{2\pi p}{K} a$ ; the deflection

would increase in direct proportion to the radius. This is, however, not in accordance with observations. Therefore, it must be  $0 < n < 1$  (6)

In this case  $\xi_c = \frac{2\pi p}{K(1-n)} a^{1-n}$

This is actually a relation of a parabolic type. The number  $n$  being greater than 0 and smaller than 1, the reciprocal of Poisson's ratio lies, according to Eq. (4), between 2 and 3, which also is applicable to soils.

Let us consider more closely the case when  $n$  has the middle value, i.e.  $n = \frac{1}{2}$ . That means  $E = C\sqrt{z}$  the modulus of elasticity increasing in direct proportion to the square root of the depth below the surface of the semi-infinite solid and  $m = 2.5$ . Eqs. (3) yield the displacements

$$u = \frac{7P \cos \varphi}{6\pi C \sqrt{R^3}}, \quad v = -\frac{7P \sin \varphi}{15\pi C \sqrt{R^3}} \quad (7)$$

It may easily be verified that this is the exact solution of the problem. Substituting into Eqs. (1) and (2), we find that there is only one component of stress different from zero, i.e.  $\sigma_r = -\frac{7P}{4\pi R^2} \sqrt{\cos^2 \varphi}$ , (8)

which satisfies the only remaining condition

of equilibrium

$$2\sigma_r + R \frac{\partial \sigma_r}{\partial R} = 0$$

It is also, in fact,

$$P = 2\pi R^2 \int_0^{\pi/2} \sigma_r \sin \varphi \cos \varphi d\varphi$$

which is necessary because of statical equivalency.

#### 2. PLANE DEFORMATION.

Using the notations indicated in Fig. 2, the expression for the unit strain components are

$$\epsilon_r = \frac{\partial u}{\partial r}, \quad \epsilon_s = \frac{1}{r} \left( u + \frac{\partial v}{\partial \varphi} \right), \quad \gamma_{rs} = \frac{\partial v}{\partial r} + \frac{1}{r} \left( \frac{\partial u}{\partial \varphi} - v \right). \quad (9)$$

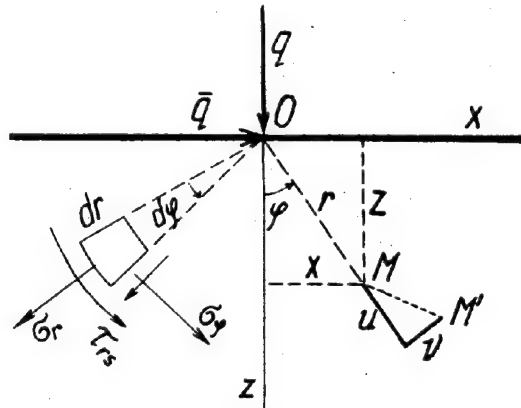


FIG. 2

The relations connecting stress and strain components may be written down as follows:

$$\sigma_r = \frac{mE}{m+1} \left( \frac{m-1}{m-2} \epsilon_r + \frac{\epsilon_s}{m-2} \right), \quad \sigma_s = \frac{mE}{m+1} \left( \frac{m-1}{m-2} \epsilon_s + \frac{\epsilon_r}{m-2} \right), \quad (10)$$

$$\tau_{rs} = \frac{mE}{2(m+1)} \gamma_{rs}.$$

Let us consider the case of  $E = C\sqrt{z}$ ,  $m = 2.5$

i) If pressures of intensity  $q$  per unit length, acting perpendicularly to the surface plane, are distributed uniformly over the  $y$ -axis as shown in Fig. 2, the exact solution is given by the following equations:

$$u = 1.1685 \frac{q \cos \varphi}{C \sqrt{r}}, \quad v = -0.7790 \frac{q \sin \varphi}{C \sqrt{r}}, \quad \sigma_r = 0.6955 \frac{q \cos^2 \varphi}{r} \quad (11)$$

which may be easily verified.

Herein, the coefficients are expressed by ratios of Gamma-functions which have been calculated to four decimal places, so that

$$\frac{42\Gamma(\frac{7}{4})}{25\Gamma(\frac{5}{4})\Gamma(\frac{3}{4})} = 1.1685, \text{ etc.}$$

ii) If loads of intensity  $\bar{q}$  per unit length, distributed uniformly over the  $y$ -axis, are applied in the surface plane in the direction of  $x$  (Fig. 2), we find the following solution:

$$u = 1.7527 \frac{\bar{q} \sin \varphi}{C \sqrt{r}}, \quad v = 1.1685 \frac{\bar{q} \cos \varphi}{C \sqrt{r}},$$

$$\sigma_r = -10.433 \frac{\bar{q}}{r} \sin \varphi \sqrt{\cos \varphi}, \quad (12)$$

where it was taken

$$\frac{42}{25} \frac{\Gamma(\frac{3}{2})}{\Gamma(\frac{1}{2})} = \frac{21\Gamma(\frac{3}{2})}{20\sqrt{2}\pi} = 17527 \text{ etc.}$$

The normal stress components in rectangular coordinates  $x, z$ ,

$$\sigma_x = -10433 \frac{\bar{q}}{z} \sin\varphi \sqrt{\cos\varphi}, \quad \sigma_z = -10433 \frac{\bar{q}}{x} \sin\varphi \sqrt{\cos\varphi}$$

may be represented by curves of the form shown in Fig. 3.

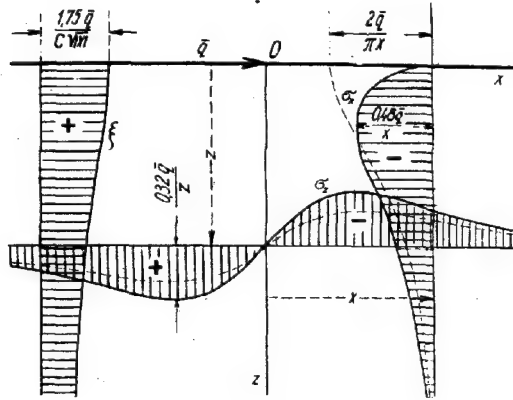


FIG. 3

The horizontal displacements

$$\xi = u \sin\varphi + v \cos\varphi = \frac{17527}{C\sqrt{k}} \left( \sin^2\varphi + \frac{2}{3} \cos^2\varphi \right) \sqrt{|\sin\varphi|}$$

at the points of a straight line  $x = \text{const.}$  are shown in the same figure, where the dotted curves represent corresponding stresses in a homogeneous body. Horizontal displacements in points of a homogeneous solid become logarithmically infinite, if the condition shall be satisfied that they vanish in infinite distances from the boundary plane.

The interesting point brought out by the results shown in Fig. 3 is the remarkable difference in the intensity of horizontal stresses close to the boundary plane. In a homogeneous body, the most intensive tensile stresses are produced in the surface plane. This may be possible only in extremely cohesive materials such as rocks, but not in sandy layers or in clays; the shearing strength of similar types of compressible soils is not sufficient to support the shearing stress originated by the difference between both the extreme principal stresses.

We know, however, that retaining walls and similar structures do transmit considerable horizontal forces into their foundations. Hence, we arrive again at the conclusion that the stress distribution in soil must be different from that occurring in a homogeneous body. It follows, that the theory of an elastic solid with a constant modulus of elasticity, if applied to foundation soils, cannot give satisfactory results.

Some authors suggest, therefore, the law  $E = Cz$ . This gives, however, infinite deflection even under a distributed load, as we have shown above.

It seems that the results of computations will approach the statistically most probable state of stress and strain in a regularly stratified foundation soil below a normal foot-

ing, when they are derived from the theory of a semi-infinite elastic solid the modulus  $E$  of which increases in proportion to the square root of the depth beneath the footing.

Eqs. (7), (8), (11) and (12) may serve as the basis for such investigations. Some results are given in the following.

### 3. INCLINED FORCES.

Solutions may be expressed by superposing the effects due to the horizontal and the vertical component of the inclined load. If those components are  $q_1$  and  $q_2 = 3q_1$  respectively, the principal radial stress is

$$\sigma_r = -\frac{06955}{r} \left( \frac{3}{2} q_1 \sin\varphi + q_2 \cos\varphi \right) \sqrt{\cos\varphi}.$$

This may be represented by a curve such as shown in Fig. 4.

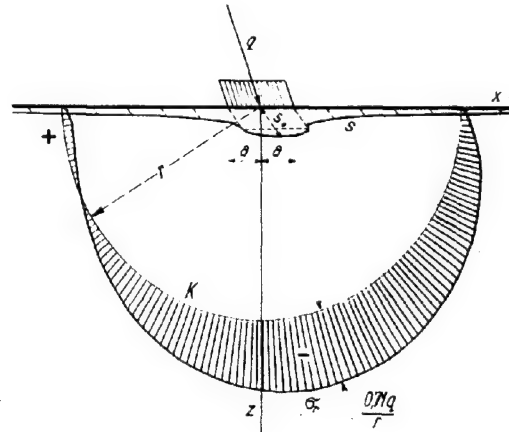


FIG. 4

### 4. STRIP LOADING.

Let the width of strip be  $2a$  (Fig. 5).

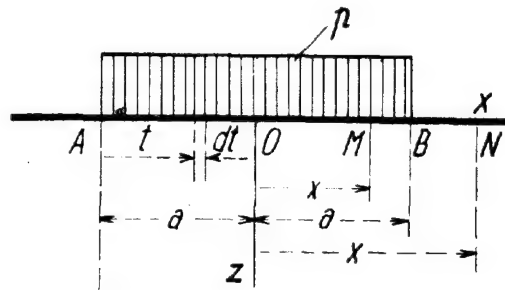


FIG. 5

1) Forces of intensity  $p$  per unit square acting normally inwards produce at the point A the deflection

$$\xi_A = \frac{0.779p}{C} \int_0^{2a} \frac{dt}{\sqrt{t}} = \frac{1558p}{C} \sqrt{2a}.$$

The displacement of any point M under the loading is the sum of the deflections caused by both the strips AM and MB:

$$\xi_M = \frac{1558p}{C} \left( \sqrt{a+x} + \sqrt{a-x} \right), \quad -a < x < a.$$

Under the middle line of the strip, we obtain

$$\zeta_0 = \frac{1558p}{C} 2\sqrt{a},$$

which is larger by 41 per cent than the deflection under the borders of the strip.

At any point  $N$  outside the loaded area, there is

$$\zeta_N = \frac{1558p}{C} (\sqrt{|x|+a} - \sqrt{|x|-a}), |x| > a.$$

In the boundary plane, there are no displacements in the  $x$ -direction.

ii) Horizontal forces of intensity  $\bar{p}$  distributed uniformly over the same strip, produce at points of the boundary plane displacements only in the  $x$ -direction. These are as follows:

$$\xi_M = \frac{3505\bar{p}}{C} (\sqrt{a+x} + \sqrt{a-x}), -a < x < a.$$

$$\xi_N = \frac{3505\bar{p}}{C} (\sqrt{|x|+a} - \sqrt{|x|-a}), |x| > a.$$

iii) Superposing the effects of both the horizontal and the vertical component of an inclined pressure, the settlement of the boundary may be represented by the curve  $s$  shown in Fig. 4 for the case  $p=3\bar{p}$ . All points of the boundary move in the same direction which is, however, not parallel to the direction of acting forces. This phenomenon is due to the type of heterogeneity expressed by the law  $E=C\sqrt{z}$ . The greatest displacement is that of the middle line of the strip:

$$s = \frac{1558p}{C} 2\sqrt{a} \sqrt{1 + \frac{3}{4}} = \frac{3.995p\sqrt{a}}{C}.$$

According to the preceding results, a horizontal load produces at a point of the boundary a displacement  $\xi$  which is 2.25 times greater than the deflection  $\zeta$  caused by a vertical load of the same intensity. In fact, remarkable horizontal movements of bridge abutments have been observed in many cases.

The methods of the consolidation theory offer no possibility of estimating the horizontal component of settlement which is, however, very important in bridge construction.

##### 5. LOAD DISTRIBUTED UNIFORMLY OVER A CIRCULAR AREA.

Let the radius of the loaded area be  $a$  and the intensity of the load be  $p$  per square unit. The elemental load distributed over a circle with the radius  $r$  is  $dP = p 2\pi r dr$ .

According to Eqs. (7) and (8), this load produces in a point of the  $z$ -axis the vertical displacement

$$d\zeta = du \cos \varphi - dv \sin \varphi = \frac{pr}{C(\sqrt{z}+r)} \left( \frac{7}{3} \cos^2 \varphi + \frac{14}{15} \sin^2 \varphi \right) dr,$$

the vertical stress component

$$d\sigma_z = d\sigma_r \cos^2 \varphi - \frac{7pr}{2(\sqrt{z}+r)} \cos^2 \varphi dr$$

and the horizontal stress component

$$d\sigma_r = -d\sigma_z \sin^2 \varphi = -\frac{7pr}{2(\sqrt{z}+r)} \sin^2 \varphi \cos^2 \varphi dr.$$

Integrating from  $r=0$  to  $r=a$ , we obtain

i) the vertical displacements of the points in the  $z$ -axis

$$\zeta = \frac{14p\sqrt{z}}{15C} \left( 2\sqrt{\frac{z}{a}} - 1 - \sqrt{\frac{z}{a^3}} \right) \cdot s = \sqrt{a+z};$$

ii) the stress components at the same points

$$\sigma_z = -p \left[ 1 - \left( \frac{z}{s} \right)^{\frac{3}{2}} \right], \quad \sigma_r = -\frac{p}{6} \left[ 4 + 3 \left( \frac{z}{s} \right)^{\frac{3}{2}} - 7 \left( \frac{z}{s} \right)^{\frac{5}{2}} \right].$$

In the middle of the loaded area, there is

$$\zeta_0 = \frac{28p\sqrt{a}}{15C}, \quad \sigma_z = -p, \quad \sigma_r = -\frac{2}{3}p.$$

At a point situated on the  $z$ -axis at a depth  $z=4a$  below the surface, there is

$$\zeta_{(z=4a)} = \zeta_0 \left( \sqrt{17} - 1 - \frac{8}{\sqrt{17}} \right) = 0.075 \zeta_0, \quad \sigma_z = -0.100p, \quad \sigma_r = -0.009p$$

Thus, 0.925 of the magnitude of the deflection  $\zeta_0$  is due to the compression of the upper mass layer, the thickness of which equals double the diameter of the loaded circle. Not more than about a thirteenth of the deflection is due to the deformation of deeper parts of the solid.

When, however, the shape of the loaded portion of the surface is a rectangular one, the part of the deflection originating in the compression of the surface layer depends on the proportion of both the sides of the rectangle. The longer the rectangle is, the more the deeper parts of the body are affected. In the case of an infinitely long strip, at last, only about 0.63 of the settlement is caused by the compression of the material located within the depth equal to double the width of the strip.

This may be one of the sources of error in settlement estimating, as often only a relatively shallow bulb of pressure is taken into consideration.

##### Conclusion.

Observations and theoretical investigations indicate that a suitable representation of a regularly stratified foundation soil may be obtained by thinking of it as a semi-infinite solid with a variable modulus of elasticity. The assumption  $E=C\sqrt{z}$  yields infinite values of settlement even under a distributed load, whereas the results of the investigation of a solid with  $E=C\sqrt{z}$  are in reasonable agreement with observed phenomena. As they can be represented by simple closed formulae, they may be of use for foundation practice.

##### REFERENCE:

- 1) K. Hruban, The Semi-infinite Solid with Variable Modulus of Elasticity. Bulletin international de l'Académie tchèque des Sciences, XLVI, (1944), No. 13. In this paper, several other solutions are derived.

Prof. K. HRUBAN,  
Technical University, Brno (Czechoslovakia).

## SUMMARY.

Settlement computations based on consolidation tests on undisturbed soil samples give results which are sometimes essentially different from observed values. The principal causes of such shortcomings are discussed with regard to the deformation laws of soil samples established by triaxial compression tests. The decisive influence of horizontal pressures in natural deposits on the settlement of buildings is demonstrated.

It is generally known that the observed value of settlement may be largely different from that calculated on the results of consolidation tests on undisturbed samples. Considering for instance the data published by L. Casagrande 1), we find, that from 10 cases in which it is possible to compare the measured settlement with the estimated one, in three cases only the difference was smaller than 50 per cent of the observed value. In a further three cases, the difference was between 200 and 400 per cent and in two cases, it was greater than 600 per cent. The ratio of the computed to the observed settlement was between 0.7 and 7.5. Many other cases of similar errors in forecasts are known 2).

What are the causes of such important discrepancies? Some are indicated in the paper dealing with the heterogeneous semi-infinite solid. Here, I shall try to show the principal sources of error.

1) In general, soil consists of mineral grains, water with dissolved gases, and air. Freyssinet denotes such materials as pseudosolid. Deformation laws of pseudosolid bodies differ essentially from those of solids. The theory of strain of a similar mass was developed by Boussinesq, 3), who showed that the deformation of its element depends essentially on the ratio of the principal stresses acting on it.

This rule holds for all types of compressible soils and has been verified by adequate evidence in triaxial compression apparatuses. Its effect may be demonstrated on the following example.

Let us consider an element of soil which is submitted in its natural location to a vertical pressure of  $\sigma_v = 0.4 \text{ kg/cm}^2$ . We want to find its unit vertical compression, produced by a foundation load which causes an increase of  $\Delta\sigma_v = 0.2 \text{ kg/cm}^2$  of the vertical pressure, connected with a negligible small increase of horizontal stress.

Following the practice of the consolidation tests, we take this soil element out of its bed as a part of an undisturbed sample, put it in an oedometer, produce the initial pressure  $0.4 \text{ kg/cm}^2$ , increase it by  $0.2 \text{ kg/cm}^2$  and find that its unit compression grows e.g. 4), from  $0.00217$  (measured when  $\sigma_v = 0.4 \text{ kg/cm}^2$ ) to  $0.01250$  (measured when  $\sigma_v = 0.6 \text{ kg/cm}^2$ ).

Hence, the unit vertical compression produced by the increase  $\Delta\sigma_v = 0.2 \text{ kg/cm}^2$  in the apparatus is  $s_v = 0.01250 - 0.00217 = 0.01033$ .

Will the compression of the soil element in its natural location be the same? It might be so only in that case when the initial ho-

izontal pressures, acting on the element in the bed, were the same as the horizontal pressures which we produced in the apparatus by applying the vertical pressure  $\sigma_v$ . These pressures were about

$$\sigma_h = \frac{\sigma_v}{m-1}$$

where  $m$  denotes the reciprocal of Poisson's ratio, the horizontal strain of the sample having been prevented by the rigid wall of the apparatus.

Our natural foundation soil, however, has had its history. For ages, it had been submitted to the pressure of icebergs or of upper deposits, which later were carried away by the action of water or of man. It is supporting the weight of neighbouring structures and, eventually, the pressure of near hills. The actual horizontal pressures, acting on the considered element in its natural bed, may have a value within the limits

$$\sigma_h' = \frac{\sigma_v}{n}$$

and  $\sigma_h' = n\sigma_v$ , where  $n$  is determined by the shearing strength and the cohesion of the soil. The value of this pressure in a bed of sand may be, for instance,  $\sigma_h' = 0.25 \sigma_v$  until  $4 \sigma_v$ , whereas in the consolidation apparatus it is  $\sigma_h' = \text{about } 0.5 \sigma_v$ .

Let us assume that it was established that the actual horizontal pressures acting in the layer in all directions equal  $\sigma_v$ . This means that our element is submitted initially to the pressure  $0.4 \text{ kg/cm}^2$  in all directions.

We can appreciate the compression caused by an increase of  $\Delta\sigma_v = 0.2 \text{ kg/cm}^2$  of the vertical pressure in the considered point of the soil mass, if we put the undisturbed sample in a triaxial compression apparatus, submit it to a hydrostatic pressure of  $0.4 \text{ kg/cm}^2$ , increase afterwards the vertical stress by  $0.2 \text{ kg/cm}^2$  and measure the deformation produced by this increase. In this way it will be found a unit compression of only, e.g.,

$$\varepsilon_v = 0.00119 \quad 4)$$

That means: the compression of this soil element in its natural location will be in this

case  $\frac{0.01033}{0.00119} = 8.7$  times smaller than that established by the consolidation test.

Thus, an estimate based only on oedometer tests precludes the possibility of giving reliable information on the absolute amount of settlement, as the natural state of stress

cannot be reproduced in an apparatus where horizontal pressures are neither controlled nor measured. Nevertheless, the value of such tests for indicating the time rate of settlement and for throwing light upon the laws of the consolidation process of recent deposits is undeniable.

2) Another source of error is the supposition that the compression caused by an increase of  $\sigma_z$  of the vertical pressure can be determined without regard to the simultaneous increase of stress in perpendicular directions. That is impossible even for homogeneous solid materials.

According to the basic equation

$$s_z = \frac{1}{E} \left( \sigma_z - \frac{\sigma_x + \sigma_y}{m} \right)$$

the unit compression  $s_z$  in vertical direction depends upon all the three normal components of stress. If, for instance  $m = 3$  and

$\sigma_x = \sigma_y = 0$ , there is  $s_z = \frac{\sigma_z}{E}$ . If, however,  $\sigma_x = \sigma_y = \frac{m}{2} \sigma_z$ , there is no vertical compression at all.

The same increase  $\sigma_z$  of the vertical pressure can thus produce any value of the compression  $s_z$ , according to what is the simultaneous increase  $\sigma_x$  and  $\sigma_y$  of the other two normal components of stress. In the consolidation apparatus, we apply a pressure  $\sigma_z$  accompanied

automatically by  $\sigma_x = \sigma_y = \frac{\sigma_z}{m-1}$ . The compression resulting from this axially symmetrical

deformation is  $s_z = \left[ 1 - \frac{2}{(m-1)m} \right] \frac{\sigma_z}{E}$

As the horizontal components of stress produced by a foundation load differ essentially from the test value  $\frac{\sigma_z}{m-1}$ , the compression  $s_z$  measured in the oedometer does not even approximately equal the real compression  $s_z$  of the soil element in its natural location. Usually, the value  $\sigma_x - s_z'$  is negative in places immediately under the footing where horizontal pressures exceed  $\frac{\sigma_z}{m-1}$ , and positive in deeper parts of the earth mass.

#### CONCLUSION.

Those methods of settlement computations, which disregard the very important effect of horizontal pressures on the compressibility of soil elements, are bound to give unreliable results. They fail in all cases when horizontal stresses in a natural soil layer differ from those produced in the apparatus in which samples are tested. The fault may amount to several times the value of the real settlement, so that such forecast may lead to utterly erroneous conclusions.

#### REFERENCES.

- 1) Intern. Assoc. for Bridge and Structural Engineering, Second Congress, Preliminary Publication, p.1542.
- 2) Prof. Terzaghi mentioned some in the discussion at the Internat. Conference, Cambridge, 1936 / Proceedings, vol. III, p.85/.
- 3) Essai théorique sur l'équilibre des massifs pulvérulents, Bruxelles, 1876.
- 4) The numerical values are taken from the results carried out by W. Bernatzik, s. Wasserwirtschaft u. Technik, 1935, p.185. The soil samples were a fine sand with a voids-ratio of 0.7.

THE MEAN ELASTIC SETTLEMENT OF  
A UNIFORMLY LOADED AREA AT A DEPTH BELOW THE GROUND SURFACE

E.N. FOX, Ph.D.  
Building Research Station

INTRODUCTION.

An estimate of the elastic settlement of a rectangular surface footing can be obtained by using the classical solution of Boussinesq for a point load on the surface of a semi-infinite elastic solid. This is well-known and numerical results are quoted, for example, by Timoshenko (reference 1, page 338).

In 1936 Mindlin (reference 2) published an extension of Boussinesq's theory to the more general case of forces applied within a semi-infinite elastic medium. This suggested that estimates of the elastic settlement of sunk footings could be obtained by following the same procedure as for a surface footing and the necessary analysis and calculations were carried out at the Building Research Station prior to the recent war. As these have proved to be of some practical use and similar results have not, so far as is known, been published in the meantime, the present note gives the results of calculation together with a brief account of the analysis which is relatively straightforward.

ANALYSIS.

We consider a semi-infinite elastic medium with horizontal surface taken as  $z = 0$  and we measure  $z$  downwards into the medium. In the horizontal plane ( $z = c$ ) at a depth  $c$  below the surface we assume a vertical load to be uniformly distributed with intensity  $q$  per unit area over the rectangle  $x = 0$  to  $a$ ,  $y = 0$  to  $b$ . We seek an expression for the mean deflection of the loaded area, since this may be expected to be relatively insensitive to the error in assuming a "flexible" footing as opposed to the practical case of a footing of finite rigidity. In support of this procedure we may note the known result (reference 1, page 339) for a circular surface footing, that the theoretical settlement when completely rigid is only about  $7\frac{1}{2}$  per cent smaller than the corresponding average settlement due to the same total load uniformly distributed under the footing.

Mindlin's analysis applies directly to an element of load  $q \, dx_0 \, dy_0$  acting at the point  $(x_0, y_0, c)$  and the resulting vertical displacement  $w$  at any point  $(x, y, z)$  may be written in the form

$$w = \frac{(1+\nu)}{8\pi E(1-\nu)} \left\{ \frac{a_1}{R_1} + \frac{a_2}{R_2} + \frac{a_3}{R_1^3} + \frac{a_4}{R_2^3} + \frac{a_5}{R_1^3} \right\} q \, dx_0 \, dy_0$$

where  $E$  denotes Young's Modulus,  $\nu$  is Poisson's ratio and

$$R_1^2 = (x - x_0)^2 + (y - y_0)^2 + (z - c)^2$$

$$R_2^2 = (x - x_0)^2 + (y - y_0)^2 + (z + c)^2$$

$$\left. \begin{aligned} a_1 &= 3 - 4\nu \\ a_2 &= 5 - 12\nu + 8\nu^2 \\ a_3 &= (z - c)^2 \\ a_4 &= (3 - 4\nu)(z + c)^2 - 2cz \\ a_5 &= 6cz(z + c)^2 \end{aligned} \right\} \quad (3)$$

To obtain the deflection at any point  $(x, y, z)$  of the loaded rectangle we have now to integrate (1) for  $x_0$  from 0 to  $a$  and  $y_0$  from 0 to  $b$  and then put  $z = c$ . First we note that the contribution of the third term in (1) then becomes zero. Thus

$$\int_0^a \int_0^b \frac{a_3}{R_1^3} \, dy_0 \, dx_0 = (z - c) \int_0^a \int_0^b \frac{(z - c)}{R_1^3} \, dy_0 \, dx_0 = (z - c)\Omega$$

where  $\Omega$  is the solid angle subtended at the point  $(x, y, z)$  by the loaded rectangle. For a point on the loaded area  $\Omega = 2\pi$  and (4) will vanish since  $z = c$ . Secondly, to obtain the mean deflection of the loaded area we have to integrate further with respect to  $x$  and  $y$  over the rectangle. The result of both sets of integration leads to the following expression for the mean settlement  $\bar{w}_c$  of the loaded area,

$$\bar{w}_c = \frac{q}{a \cdot b} \left\{ b_1 J_1 + b_2 J_2 + b_4 J_4 + b_5 J_5 \right\} \quad (5)$$

where

$$b_n = \frac{(1+\nu)}{8\pi E(1-\nu)} (\partial_n) z = c, \quad n = 1, 2, 4, 5 \quad (6)$$

whilst  $J_1, J_2, J_4, J_5$  are quadruple integrals. These do not, however, require to be integrated separately since if we regard  $J_2$  as the basic integral defined by

$$J_2 = \int_0^a \int_0^b \int_0^a \int_0^b \frac{du_0}{[(x-x_0)^2 + (y-y_0)^2 + 4c^2]^{\frac{3}{2}}} \, du_0 \quad (7)$$

then  $J_1, J_4$  and  $J_5$  can be easily derived from the relations

$$\left. \begin{aligned} J_1 &= (J_2)_c = 0 \\ J_4 &= -\frac{1}{4c} \frac{\partial J_2}{\partial c} \\ J_5 &= -\frac{1}{12c} \frac{\partial J_4}{\partial c} \end{aligned} \right\} \quad (8)$$

We require therefore first to evaluate  $J_2$  from (7) which can be immediately reduced to a double integral by using the following



lemma,

$$\int_0^a dx \int_0^b du \int_0^a dx_0 \int_0^b f(x-x_0, u-u_0) du_0 = \\ = 4 \int_0^a d\zeta \int_0^b (a-\zeta)(b-\eta) f(\zeta, \eta) d\eta \quad (9)$$

which holds under fairly general conditions for any function  $f$  which is even in both arguments. (The quadruple integral will be zero if  $f$  is odd in either argument.) This lemma is proved at the end of the paper.

If we use (9) to simplify (7), the resulting double integral for  $J_2$  is easily evaluated algebraically by standard methods and thence  $J_1$ ,  $J_4$  and  $J_5$  can be obtained without difficulty by using (8).

The final result for  $\bar{w}_c$  can be expressed in the following form

$$\bar{w}_c = \frac{q(1+\nu)}{4\pi E(1-\nu)} \sum_{s=1}^5 \beta_s Y_s \quad (10)$$

where

$$\left. \begin{aligned} \beta_1 &= 3-4\nu \\ \beta_2 &= 5-12\nu+8\nu^2 \\ \beta_3 &= -4\nu(1-2\nu) \\ \beta_4 &= -1+4\nu-8\nu^2 \\ \text{and } \beta_5 &= -4(1-2\nu)^2 \end{aligned} \right\} \quad (11)$$

$$\left. \begin{aligned} Y_1 &= a \log \frac{r_4+b}{a} + b \log \frac{r_4+a}{b} - \left\{ \frac{r_4^3 - a^3 - b^3}{3ab} \right\} \\ Y_2 &= a \log \frac{r_3+b}{r_1} + b \log \frac{r_3+a}{r_2} - \\ &\quad \left\{ \frac{r_3^3 - r_2^3 - r_1^3 + r^3}{3ab} \right\} \\ Y_3 &= \frac{r^2}{a} \log \left\{ \frac{(b+r_2)r_1}{(b+r_3)r} \right\} + \frac{r^2}{b} \log \left\{ \frac{(a+r_1)r_2}{(a+r_3)r} \right\} \\ Y_4 &= \frac{r^2(r_1+r_2-r_3-r)}{ab} \\ Y_5 &= r \tan^{-1} \left( \frac{ab}{rr_3} \right) \end{aligned} \right\} \quad (12)$$

whilst

$$\left. \begin{aligned} r &= 2c \\ r_1^2 &= a^2 + r^2 \\ r_2^2 &= b^2 + r^2 \\ r_3^2 &= a^2 + b^2 + r^2 \\ r_4^2 &= a^2 + b^2 \end{aligned} \right\} \quad (13)$$

If we put  $r = 2c = 0$  in this solution we obtain the mean settlement  $\bar{w}_0$  under a surface footing in the form

$$\bar{w}_0 = \frac{2q(1-\nu^2)}{\pi E} Y_1 \quad (14)$$

This may be written in the form used by Timoshenko (reference 1, page 338), namely

$$\bar{w}_0 = m \frac{(1-\nu^2)}{E} q \sqrt{ab} \quad (15)$$

where the coefficient  $m$  is given in our notation by

$$m = \frac{2}{\pi} \frac{Y_1}{\sqrt{ab}} \quad (16)$$

and is a function only of the ratio  $a/b$ .

For the other extreme case of a very deep footing,  $c \rightarrow \infty$  and we find for the mean deflection

$$\bar{w}_\infty = \frac{q(1+\nu)(3-4\nu)}{4\pi E(1-\nu)} Y_1 \quad (17)$$

Thus the ratio of the settlements of a very deep footing and a surface footing is given from (14) and (17) by

$$\frac{\bar{w}_\infty}{\bar{w}_0} = \frac{3-4\nu}{8(1-\nu)^2} \quad (18)$$

which depends only on Poisson's ratio  $\nu$  and increases steadily from  $3/8$  to  $1/2$  as  $\nu$  increases from 0 to  $1/2$ .

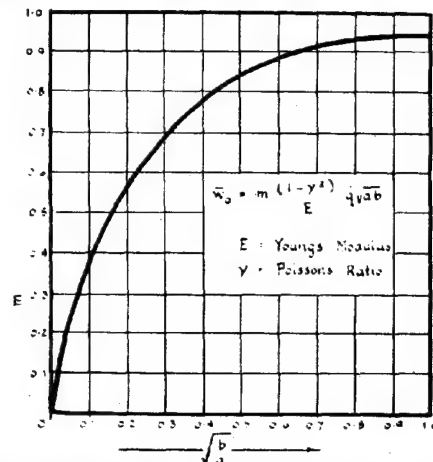
Finally, from (10) and (14), the ratio of the mean settlement of a footing at depth  $c$  to that of a surface footing is given by

$$\frac{\bar{w}_c}{\bar{w}_0} = \frac{\sum_{s=1}^5 \beta_s Y_s}{(\beta_1 + \beta_2) Y_1} \quad (19)$$

#### NUMERICAL RESULTS.

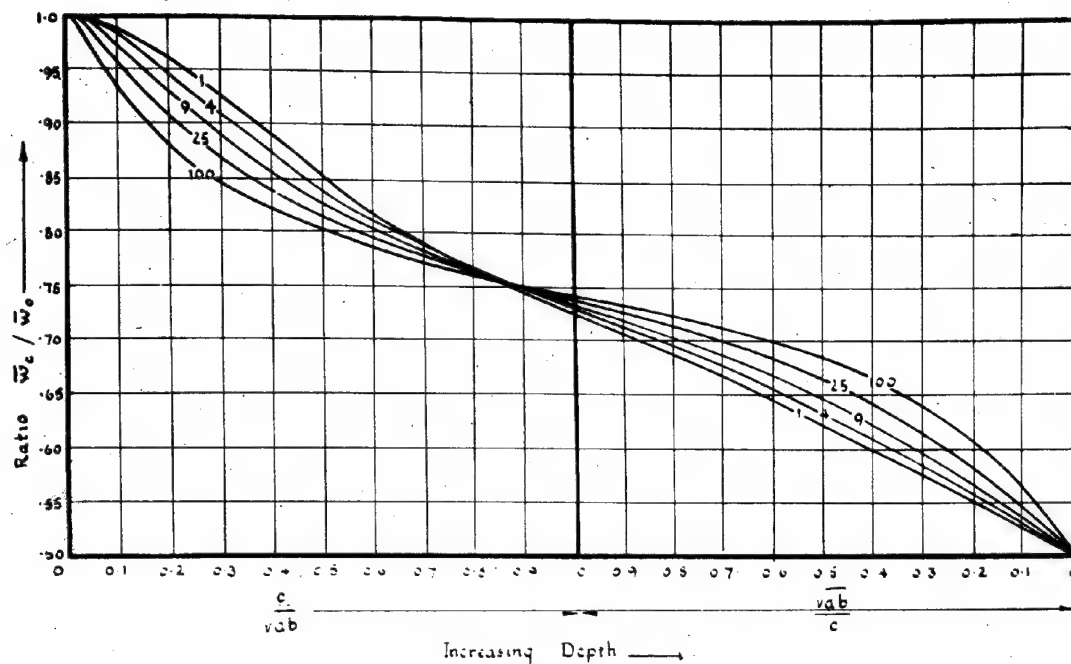
Calculations have been carried out to enable the relatively complicated solution for  $\bar{w}_c$  to be used in practice. Thus for the surface footing we can obtain  $\bar{w}_0$  simply from equation (15) and the curve for  $m$  given in Figure 1. (We choose  $\sqrt{b/a}$  rather than  $b/a$  as

abscissa in order to spread the curve near the origin for greater accuracy in use). Thence we require the ratio  $\bar{w}_c/\bar{w}_0$  which depends on Poisson's ratio  $\nu$  and on the ratios  $a:b:c$ . Calculations have been performed for



Mean settlement  $\bar{w}_c$  of Flexible Surface Footing. Uniform Pressure  $q$  on Rectangle of Sides  $a, b$

FIG.1



Ratio of Mean Settlements of Flexible Rectangular Footing  $a \times b$  at Depth  $c$  and similar Footing at Surface

(Numbers on curves denote value of ratio  $a/b$  which is constant along any one curve)

FIG.2

$\nu = 1/2$  and are shown plotted in Figure 2.

It may be noted firstly, that the abscissa in this figure changes from  $c/\sqrt{ab}$  to its inverse at unit abscissa in order that the infinite range of depth may be covered in a finite range of plotting. Secondly, the ratio  $c/\sqrt{ab}$  has been chosen rather than  $c/a$  or  $c/b$  since the curves for different constant  $a/b$  become relatively close with consequent small errors when interpolating. For practical purposes it might well be considered that one mean curve, say that for  $a/b = 9$ , is sufficiently accurate for all shapes of rectangle from the square to the long narrow strip. It has not been considered of sufficient practical value in foundation engineering to carry out calculations for other values of Poisson's ratio in view of the overall approximation inherent in assuming soil to be an elastic medium.

#### PROOF OF EQUATION (9)

Consider first the  $x$  and  $x_0$  integrations for which  $y - y_0$  is constant and need not be written. We put  $x_0 = x - X$  and integrate by parts as follows:

$$\begin{aligned} \int_0^a dx \int_0^a f(x-x_0) dx_0 &= \\ &= \int_0^a dx \int_0^x f(X) dX + \int_0^a dx \int_{a-x}^a f(X) dX = \\ &= \int_0^a \left[ (x-a) \int_0^x f(X) dX + x \int_{a-x}^a f(X) dX \right] + \end{aligned}$$

$$- \int_0^a (x-a) f(x) dx + \int_0^a x f(x-a) dx \quad (20)$$

The integrated terms vanish at both limits and if we change the variables of integration in (20) by writing  $\zeta$  for  $x$  in the first  $x$ -integral and  $\zeta$  for  $(a-x)$  in the second  $x$ -integral, we obtain

$$\begin{aligned} \int_0^a dx \int_0^a f(x-x_0) dx_0 &= \\ &= \int_0^a (a-\zeta) [f(\zeta) + f(-\zeta)] d\zeta \end{aligned}$$

= 0 when  $f$  is an odd function

$$\text{and } = 2 \int_0^a (a-\zeta) f(\zeta) d\zeta \quad (21)$$

when  $f$  is an even function

This equation (21) is a mathematical relation in which  $x$ ,  $x_0$ ,  $y$  and  $a$  have no special meaning and can equally be replaced by  $y$ ,  $y_0$ ,  $\eta$  and  $b$  respectively. Thus, if we apply (21) first to the  $x$ ,  $x_0$  integrations in (9) and then to the  $y$ ,  $y_0$  integrations we obtain equation (9) as stated.

The preceding proof assumes that the order of integration may be changed, conditions for which are discussed in books on pure mathematics. It is valid, in particular, when the integrand is a continuous function as in the integral  $J_2$  of our present problem.

**ACKNOWLEDGEMENT.**

The work described in the paper was carried out at the Building Research Station of the Department of Scientific and Industrial Research, and the results are published by permission of the Director of Building Research.

**REFERENCES:**

- 1) S. Timoshenko, "Theory of Elasticity", McGraw-Hill, New York, 1934.
- 2) R.D. Mindlin, "Force at a Point in the Interior of a Semi-infinite Solid", Physics, 1936, 7(5), 195-202.

-o-o-o-o-o-o-

## SUB-SECTION I :

### MISCELLANEOUS

I i 1

#### THE CONCEPT OF SOIL MOISTURE DEFICIT

R. K. SCHOFIELD AND H. L. PERMAN

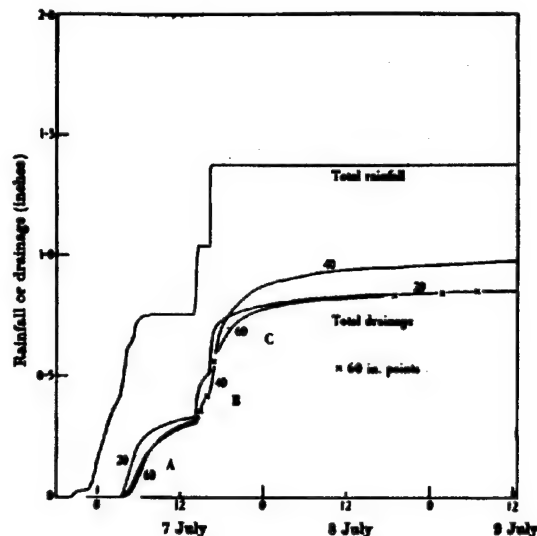
Rothamsted Experimental Station, Harpenden, Herts

When evaporation takes place, either directly from a bare soil surface or from the leaves of plants rooted in the soil, water is withdrawn from the soil. Water applied to the soil surface, or falling on it as rain, must first make good the loss due to evaporation before through drainage occurs. No doubt the broad truth of the above statement is generally conceded, but it is not easy to cite quantitative data from which the precision of the statement may be judged.

#### 1. SOIL MOISTURE DEFICIT IN BARE SOIL.

A recent examination of the records of the Rothamsted Drain Gauges (Pepman and Schofield, 1941) has been of value in this connection. These installations contain three blocks of undisturbed soil, each 1/1,000th acre (4 square metres) in area and respectively 20 in. (0.5 metres), 40 in. (1 metre) and 60 in. (1.5 metres) deep. The soil blocks rest on perforated plates, and are separated from the surrounding soil by impermeable side walls. Collecting funnels under the perforated plates lead the drainage water into measuring tanks. Daily records of drainage have been made since 1871 and continuous recording gear was installed in 1925. During the whole period the soil surfaces have been kept free of vegetation by hand-weeding.

In order to illustrate the type of evidence furnished by these drain gauges, Fig. 1 has been prepared from the automatic traces of drainage and rainfall for the period July 6-9, 1927. The effect of previous evaporation from the bare soil surface is shown in the difference between rainfall and drainage. Since the "die away" curves for the drainage have a form that is constant except for a seasonal variation, it is possible to estimate that the rain, totalling 0.76 in., that fell up to noon on July 7 would have caused a total drainage of 0.35 in. had no more rain fallen during the next 48 hours. Thus we obtain a value of 0.41 in. for the soil moisture deficit existing on the night of July 6 when rain first started to fall. Drainage in the 20 in. gauge did not start until 0.45 in. of rain had fallen. This is a reflection of the time taken for water to move down from the surface sufficiently to produce the pressure head needed to cause



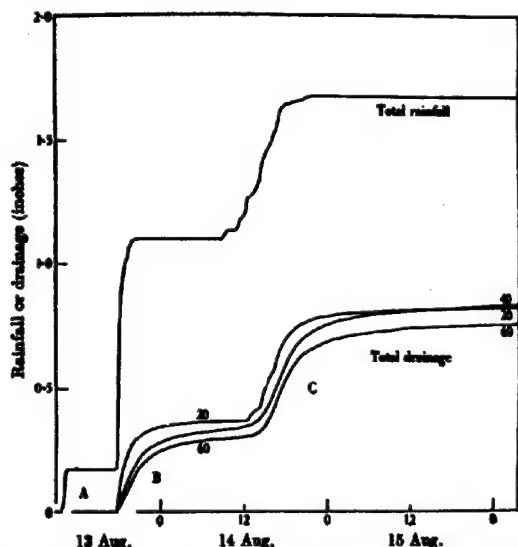
Typical continuous records of rainfall and drainage from Rothamsted gauges (July, 1927).

FIG. 1

drainage. Two further falls, totalling 0.62 in., caused the total drainage in both the 20 in. and 60 in. gauges to increase to 0.83 in., indicating that the soil moisture deficits at the times when the two rains began together amounted to 0.14 in. This represents the amount of water evaporated from the soil surface during July 7, which was on the whole a sunny day. There is, unfortunately, a leak through which foreign water enters the 40 in. gauge: records from this gauge are unreliable.

In the great majority of cases the estimates of soil moisture deficit obtained in these two ways are consistent and give amounts of evaporation that are reasonable. From time to time, however, usually when sudden heavy rain falls on a dry soil surface, drainage occurs before the deficit has been fully made good. Thus very heavy rain (0.17 in. + 0.93 in.) fell

in two periods during the evening of August 13, 1937, and the corresponding drainage was 0.38 in.



Continuous records showing drainage where there was still a soil moisture deficit (August, 1937)

FIG. 2

There was a further 0.58 in. of rain spread over about 12 hours on August 14, but the further drainage was only 0.44 in. As 0.14 in. is improbably high for the evaporation during the night and early morning before rain started again, part of it must be attributed to the failure of the earlier heavy rain to wet the profile completely. It can also be seen from the automatic records that the first drainage actually started at a time when there was still a soil moisture deficit of some 0.5 in. Most of this was made good by the rest of the rain of August 13, which was more gentle towards the end, but a small residue still remained unsatisfied when this rain ceased.

The records of the summer of 1921 are of special interest. Three months of almost continuous drought ended early in September when 2.0 in. of rain fell steadily during one day. The weather again became fine, and drainage ceased after 0.70, 0.63 and 0.59 in. had been collected from the 20, 40 and 60 inch gauges respectively. Under these exceptionally favourable conditions it was possible to evaluate rather precisely the soil moisture deficits as 1.30, 1.37 and 1.41 in. respectively. From the long series of records it is possible to obtain the soil moisture deficits developed by surface evaporation during dry periods of various lengths under different weather conditions. The figures given in Table I are representative of soil moisture deficits produced by evaporation from bare soil at Rothamsted in summer. Briefly, it may be said that the

first half inch of deficit is produced in 3 to 5 days, depending mainly on the amount of sunshine, the deficit only reaches one inch after several weeks, and even in three months did not reach 1.5 in.

Compared with other drain gauges, those at Rothamsted are peculiarly favourable for the determination of soil moisture deficits owing to the rapidity with which drainage dies away after rain. This is partly because the soil of these gauges is in its natural structure. Thus the bare soil gauge at the Cambridge Water Works at Fleam Dyke, of rammed chalk filled-in, may run for three weeks after rain. The drain gauges at Craibstone, Aberdeen and at Pusa and Campore, India, were all built round undisturbed soil but these too give a slower die-away than the Rothamsted gauges, showing that natural soils differ considerably in this respect.

## 2. SOIL MOISTURE DEFICIT IN CROPPED SOIL.

It might be thought that soil moisture deficits in soils carrying grass, arable crops, or even forest, could readily be determined by finding the moisture contents of soil samples taken to the depth of root penetration, and using for comparison similar samples taken at a time when the soil moisture deficit could be taken as zero. In practice this method can only be applied with advantage in places where the soil is exceptionally uniform, as is the case in Youngmans Pasture on the Cambridge University Farm. From repeated samplings and observations on the performance of field drains Mr. H.H. Nicholson and his students have secured valuable data from which the total soil moisture deficit and its distribution with depth have been obtained on more than a dozen occasions during several seasons. Some of these data are used in a later section and are included in Fig. 4.

At Rothamsted the soil is not uniform enough for the same method to be applied, and a new technique has been developed. The soil samples are taken in the form of "clods" in their field structure, are immediately weighed, and are then allowed to take up moisture in the laboratory against a controlled "suction" of 50 cm. of water (pF 1.7). Clods taken in winter, when the soil moisture deficit was considered to be zero, neither lost nor gained weight on the average under these conditions. Clods of the same size taken from the same depth did not all take up exactly the same amount of water in the laboratory, but a fairly accurate measure of the soil moisture deficit could be obtained from the mean of the results.

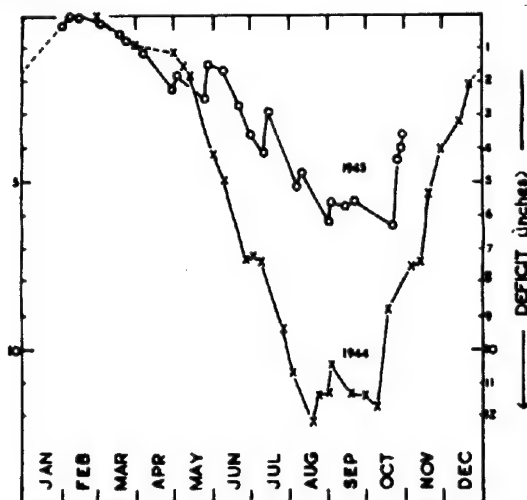
## 3. EVAPORATION FROM GRASS AND OPEN WATER.

Seeing that any method based on the examination of soil samples is very laborious it is fortunate that soil moisture deficits under vegetation can be obtained to an accuracy that will be sufficient for many practical purposes by an indirect method based on estimates of evaporation. This estimate is possible because the evaporation from a green crop that

TABLE I  
Typical soil moisture deficits built up  
during rain-free periods in summer:  
bare soil at Rothamsted

Length of period (days)	2	5	10	20	30	40
Deficit (inches)	0.30	0.50	0.65	0.80	0.90	1.00

effectively covers the soil and is not short of water depends on the weather but not on the height or rate of growth of the crop so long as it remains green. The truth of this statement has been proved by experiments at Rothamsted in which grass growing in soil tanks sunk flush with the surrounding grass covered soil has been continually supplied with water from a water table at 16 in. (40 cm). Each soil tank is in communication with a covered reservoir in which the water level is accurately measured. During rainless periods in summer a small moisture deficit develops in the top few inches of soil above the capillary fringe, but during a normal summer rain is sufficiently frequent and plentiful to wipe this out at times and cause a rise in the water table. From the records we know the net amount of water that was added to the reservoir (or taken from it) between two such occasions in order to keep the water at the standard level. In this way a measure is obtained of the excess of evaporation over rainfall for each interval between rises of the water table. The accumulated excess for the summers of 1944 and 1945 are plotted in Fig. 3.



Accumulated excess over rainfall of evaporation from sub-irrigated grass at Rothamsted.

FIG. 3

Alongside the soil tanks is an open water surface. The correspondence between the evaporation from the grass and the same area of open water is so close that the weather must be the controlling influence in both cases. The actual ratio is not fixed, but exhibits a seasonal trend. Values of the ratio appear in Table II. It is possible, therefore, to make a close estimate of the evaporation that would have taken place from grass plentifully supplied with water if the records are available for the evaporation from a well sited water surface.

At the Harrogate Water Works, situated at 549 ft. on Blubberhouses Moor, there is a grass-covered drain gauge and an open water evaporimeter alongside. Rain is sufficiently frequent to make it likely that the grass is rarely short of water and the records can be used to provide a check on the considerations of the foregoing paragraph. The monthly amounts of evaporation from the open water

TABLE II

Comparison of estimated evaporation from grass with excess of rainfall over drainage.

Month	$E_o$ in.	$f$	$E_o f$ in.
Jan.	0.41	0.6	0.25
Feb.	0.45	0.6	0.27
Mar.	0.98	0.7	0.68
April	1.78	0.7	1.25
May	2.71	0.8	2.18
June	3.28	0.8	2.62
July	3.38	0.8	2.70
Aug.	2.73	0.8	2.17
Sept.	1.94	0.7	1.36
Oct.	1.25	0.7	0.88
Nov.	0.62	0.6	0.38
Dec.	0.43	0.6	0.26
Year	19.96		15.00

$E_o$  = mean evaporation from open water.

$E_o f$  = estimated mean evaporation from grass.

inches

Mean annual rainfall	30.64
Mean annual drainage	15.45
Difference	15.19

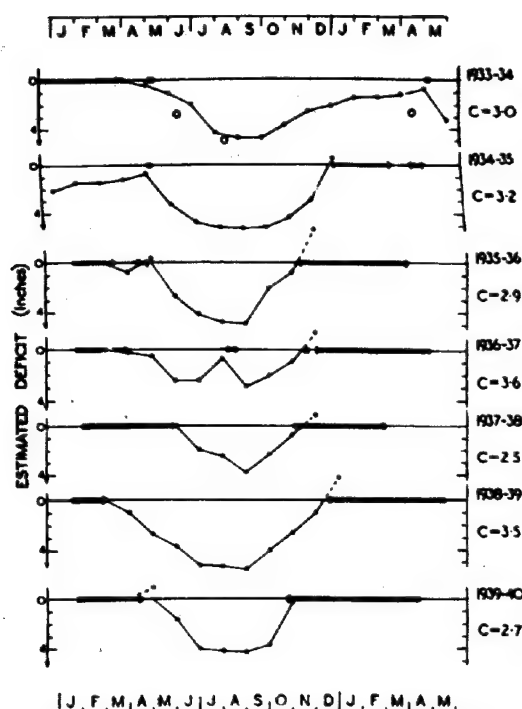
surface, entered under  $E_o$  in Table II are the means for 21 years up to 1943. The factors under  $f$  were obtained from the observations at Rothamsted. The entries under  $E_o f$  are, therefore, estimates of mean monthly evaporation from the grass-covered drain gauge, which total 15.0 inches for the whole year. This estimate is in close agreement with the mean excess of annual rainfall over annual drainage which was 15.2 in. for the same 21 years.

Even when the evaporation from open water has not been observed on the site it is possible, with the aid of recent developments in the theory of evaporation, to make a close estimate of open water evaporation from records of hours of sunshine, mean wind speed, mean air temperature and dew-point (Penman, 1948).

#### Soil Moisture Deficit Obtained from Estimates of Evaporation.

In arriving at an estimate of the soil moisture deficits in places where rainfall is often insufficient to maintain full evaporation from grass, it seems reasonable to assume that until the soil moisture deficit has reached a value,  $C$ , the evaporation is that for a plentiful water supply, but that for deficits greater than  $C$  the evaporation falls progressively below that for plentiful supply.

The result of an attempt to estimate the trend of the deficit during summer appears in Fig. 4. Details are being published elsewhere, but it should be noted that the value of  $C$  was chosen empirically to have slightly higher values for years in which a dry spring would encourage root developments. A successful estimate of  $C$  would result in the estimated deficit being reduced to zero when the soil reached field capacity in the autumn: in Fig. 4 the return to zero deficit is represented by



Estimated and observed soil moisture deficits in grassland at Cambridge. Thick horizontal lines show when the field drains were running. Open circle show values of deficit measured by soil sampling (1933-34).

FIG.4

the onset of autumn running of the field drains.

It is both reasonable and necessary to consider that  $C$  depends on the character of the soil, the nature (mainly the rooting habit) of the crop and perhaps the nature of the growing weather early in the year. Table III gives the values of  $C$  for a number of grass-covered surfaces together with the dates and amounts of the largest soil moisture deficits.

In some cases the distribution of rain throughout the year prevented large deficits from being built up and the readily available water can only be stated to be at least as great as the maximum estimated deficit. Otherwise the value of  $C$  for grass surfaces appears to be about 3 or 4 in. The large value (6.0) deduced for the 48 in. deep gauge at Farlington is unexpected. It may reflect the properties of disintegrated chalk studied recently by Locket (1946), but further investigation is needed to elucidate this case.

#### 4. DIFFICULTY IN SANDY SOILS.

The clay soil of the Cambridge University Farm is favourable for studies of soil moisture deficit because of the rapidity with which the discharge of the mole drainage system dies away after rain. Here it is easy to distinguish the times when the soil moisture deficit is zero. It is, however, much harder to do this when the soil is sandy with a deep water table. In such cases downward movement of water may persist below the level of root penetration throughout the year, although the rate of movement varies considerably. Where this occurs there is no state of moisture that

TABLE III  
Value of Readily Available Water, and Maximum Water Deficit for Grass-Covered Surfaces (inches).

Site	Nature of surface	Year	Readily available water (C)	Max. deficit	Date of maximum deficit
Graigstone, Aberdeen	Turfed gauge, 40 in. deep granitic soil, undisturbed	1938	>1.5	1.5	August
Harrogate, Yorks	Turfed gauge, 36 in. deep, clay soil, filled in	1921	2.0	3.6	July
		1941	>2.8	2.8	July
		1942	>1.7	1.7	June, July
University Farm, Cambridge	Pasture on clay mole-drained	1933	3.0	4.7	September
		1934	3.2	5.2	August
		1939	2.7	4.3	August
Harpden, Herts	Catchment area clay over chalk	1944	3.5	4.7	June
Compton, Sussex	Grassed gauge, 36 in deep chalk filled in	1933	4.0	5.5	August
		1934	3.0	4.6	July
Farlington, Hants.	Grassed gauge, 24 in. deep chalk filled in Ditto 48 in. deep	1933	2.0	3.9	August
		1934	2.0	3.5	June, July, Aug.
		1933)		7.5	August
		1934)	6.0	7.3	July, August

can be uniquely identified as the condition of zero deficit, although it may be possible to select a condition more or less arbitrarily which will serve as a zero of reckoning for practical purposes.

REFERENCES.

- 1) Penman, H.L. and Schofield, R.K. (1941). J. Agric. Sci., 31, 74 - 109.
- 2) Penman, H.L. (1948). Proc. Roy. Soc. (A) (In the press)
- 3) Locket, G.H. (1946). J. Ecology, 33, 222 - 229.

-o-o-o-o-o-o-



## SECTION II

### LABORATORY INVESTIGATIONS

## SUB-SECTION II a

### GENERAL

#### EFFECT OF NATURAL HARDENING ON THE UNCONFINED COMPRESSION STRENGTH OF REMOLDED CLAYS

II a 1

( A laboratory investigation carried out at the  
University of Illinois, U. S. A. )

ORESTE MORETTO (Dr. Ing.)  
of the Argentine

#### 1) PURPOSE.

In the literature of soil mechanics, much discussion has centered on where lies the source of the strength and rigidity of undisturbed clays. Until recently, this question appeared to have only academic importance. The results of field observations carried out during the last few years have emphasized, however, that it might have very important practical implications in cases such as the consolidation of hydraulic fill dams, effect of remolding due to driving of piles, etc.

The great decrease in strength experienced by some clays when remolded at unaltered water content was first observed by the Swedish Geotechnical Commission during the investigation of landslides. Subsequently, A. Casagrande 1) observed that the consolidation characteristics of undisturbed and remolded clays were also markedly different, and he concluded that such disturbing events as the driving of piles into soft clay are likely to increase the compressibility of the clay to such an extent that the piles may actually be detrimental.

In order to explain the difference in the physical properties of undisturbed and remolded clays, Casagrande proposed a theory according to which the clay particles settle during the process of sedimentation into a definite arrangement called the "clay structure". His conception of the structure is that of a coarse-grained skeleton cemented together by highly compressed clay whose interstices are filled with soft clay. Casagrande states that "the building up of such a structure is chiefly dependent on the exceedingly slow process of natural sedimentation and consolidation" because a rapid increase of pressure during sedimentation would displace the grains before they could become bonded by highly consolidated clay. Remolding is presumed to destroy the connecting links between the large soil grains and to replace them by the unconsolidated soft clay that fills the interstices. Since the development of the links was dependent on the exceedingly slow process of sedimentation, Casagrande was led to the conclusion that, "if we destroy the structure which nature has taken many centuries to build up, we cannot restore it".

A fundamentally different explanation of the manner in which undisturbed clays acquire their strength and rigidity has been given by K. Terzaghi 2). According to his theory, the strength and rigidity are acquired primarily by "slow physico-chemical processes" which are due to the surface activity of the mineral grains. As a consequence of its surface ac-

tivity, each clay particle is surrounded by a shell of adsorbed water, almost solid near the particle, and quite viscous within a somewhat greater distance. During sedimentation, the mass of clay consolidates and the viscous layers merge. Upon further consolidation, the solid parts of the water shells may come into contact and merge at a number of points in the clay mass and, as a consequence, the mass becomes stiff. Remolding breaks the contacts between the solid water shells, displaces the grains, and introduces viscous adsorbed water between them, whereupon the clay becomes plastic.

Field evidences have been advanced in support of both conceptions 3). Since these evidences have been questioned, laboratory experiments were designed to furnish pertinent data on the subject with the purpose of throwing some light on this much discussed problem.

#### 2. MATERIALS AND PROPERTIES.

The results on four types of clay, identified by their places of origin, are reported in this paper.

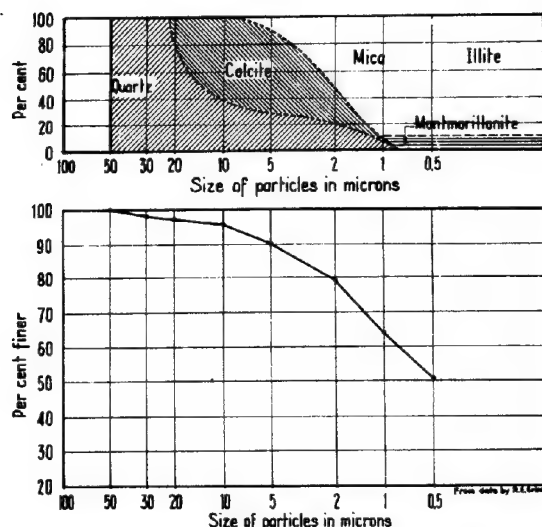
Figures 1 to 4 give the grain-size distribution and the mineralogical composition of those clays, plotted as a function of the size of the particles. The mineralogical composition was determined by the differential thermal method of studying minerals.

Table 1 gives the physical properties of the clays. The natural sensitivity indicated in column 4 denotes the ratio between the unconfined compression strength of the undisturbed material to the unconfined compression strength after remolding at constant water content.

Figure 5 shows the stress-strain relation for unconfined compression tests of the clays in the undisturbed and remolded conditions at the same water content. The natural sensitivity was derived from those tests taking as the strength of the remolded samples, and of those undisturbed that failed by bulging, the stress corresponding to 10 % strain.

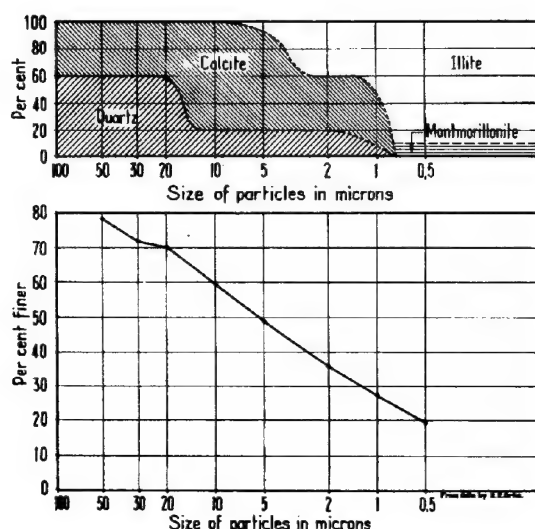
#### 3. PROCEDURE OF TESTING.

The investigation consisted of determining the unconfined compression strength of the clays when, after complete remolding, the material had been allowed to rest at constant water content for different periods of time. Tests of this kind were made for various water contents or relative consistencies of the materials (the relative consistency = r. c. =



Grain-size curve and mineralogical composition of Laurentian clay.

FIG. 1

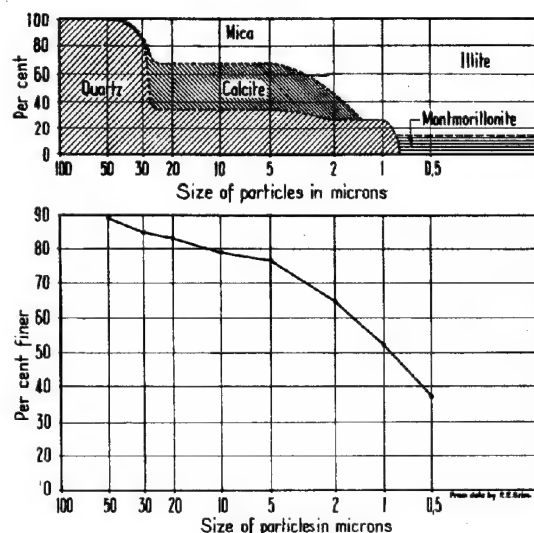


Grain-size curve and mineralogical composition of Detroit I clay.

FIG. 2

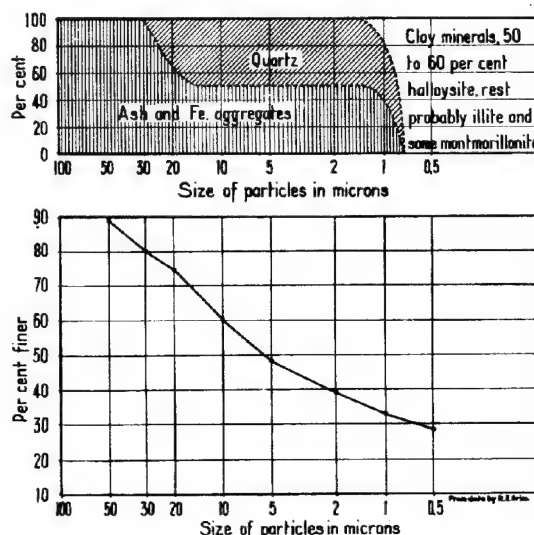
the ratio between the water content minus the plastic limit, and the index of plasticity.). For each type of clay enough material was mixed together to furnish a uniform mass sufficient for all the series of tests performed on it. This procedure was not followed in the case of the Laurentian clay, and as a consequence, the material employed was slightly different for the different series. The difference in the properties of the various Laurentian clay samples used was not great enough however to influence very prominently the results, and they can be compared between each other.

With each clay compression specimens were prepared in prismatic molds, Figure 6, con-



Grain-size curve and mineralogical composition of Detroit II clay.

FIG. 3



Grain-size curve and mineralogical composition of Mexico clay.

FIG. 4

sisting of a bottom plate of glass, two L-shaped side plates of brass, and a top plate of glass. All the plates were lined with ordinary waxed paper to avoid sticking of the clay to the mold. Later on this lining was substituted by a thin coat of mineral vaseline.

One of the specimens so made was tested immediately after it had been molded (0-day test). The rest were sealed in their molds by welding the brass and glass plates together with a fillet of paraffin, and the entire assembly placed in a tin can containing paraffin on the verge of solidifying. The tin can was later sealed full of paraffin.

The specimens stored in this manner to

TABLE 1

PHYSICAL PROPERTIES OF CLAYS						
Type of clay	Specific gravity of solid matter	Natural water content %	Natural sensitivity	Liquid limit %	Plasticity index %	Origin of clay sample
(1)	(2)	(3)	(4)	(5)	(6)	(7)
Laurentian	2.67	85 <sup>±</sup>	14.0 <sup>±</sup>	66.0	41.0	Beauharnois, Quebec, Canada 6 to 9 ft. below ground
Detroit I	2.73	24 <sup>±</sup>	2.5 <sup>±</sup>	29.2	12.7	Detroit, U.S.A. 40 to 70 ft. below ground
Detroit II	2.77	47 <sup>±</sup>	6.0 <sup>±</sup>	51.2	26.4	Detroit, U.S.A. 25 to 40 ft. below ground
Mexico	2.69	54 <sup>±</sup>	5.0 <sup>±</sup>	60.8	20.4	Mexican Dam 40 ft below crest of dam

TABLE 2

UNCONFINED COMPRESSION TESTS ON LAURENTIAN CLAY. SERIES 1. ( Relative consistency = 0.99 )				
Tested after a resting period of (days)	Water content %	Ultimate strength (for 10 % strain or less) (gm/cm <sup>2</sup> )	Type of failure	Acquired sensitivity
(1)	(2)	(3)	(4)	(5)
0	66.7	25.7	bulge	1.0
3	66.3	49.4	shear and splitting	1.92
7	66.0	51.0	"	1.98
14	66.0	56.2	"	2.19
28	65.5	63.0	"	2.45
60	65.0	83.0	"	3.22
120	65.3	90.1	"	3.51
240	65.5	109.0	"	4.25
610	65.6	114.0	"	4.45

keep them at constant water content, were tested after periods of rest of 3, 7, 14, 28, 60, etc. days to determine the increase in strength they had experimented with respect to the specimen tested at 0 day.

The procedure of testing gave in general good results. The tests indicate, however, a slight general trend of the moisture content of the clay to decrease with age, due mainly to absorption of water by the waxed paper. This decrease was small and did not influence practically the results.

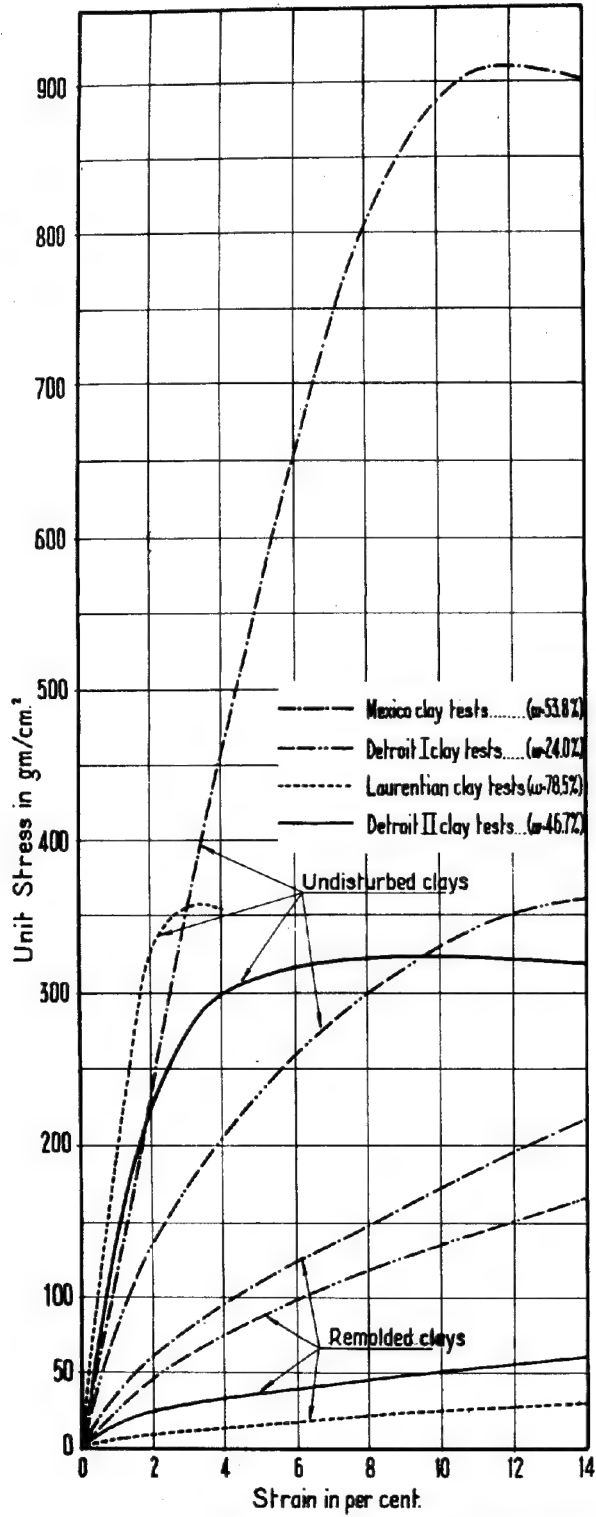
#### 4. RESULTS OF TESTS.

The test results are given in Tables 2 to 5 and Figures 7 to 15. The ultimate strength

of the specimens that did not reach a maximum before, was taken as the stress corresponding to 10 % strain. The acquired sensitivity is the ratio between the ultimate strength of the clay after a certain period of rest and the same strength immediately after the specimens had been molded (0-day test).

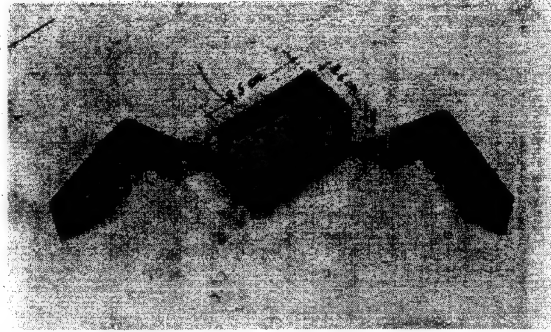
##### a) Laurentian clay.

The experiments on Laurentian clay comprise 7 series testing the material at different water contents. Series 1 constitutes the main series. Its results are given in Table 2, Figure 7 and Figure 8. Figure 7, that gives the stress-strain curves obtained for these tests, shows very plainly the tremendous increase on both strength and rigid-



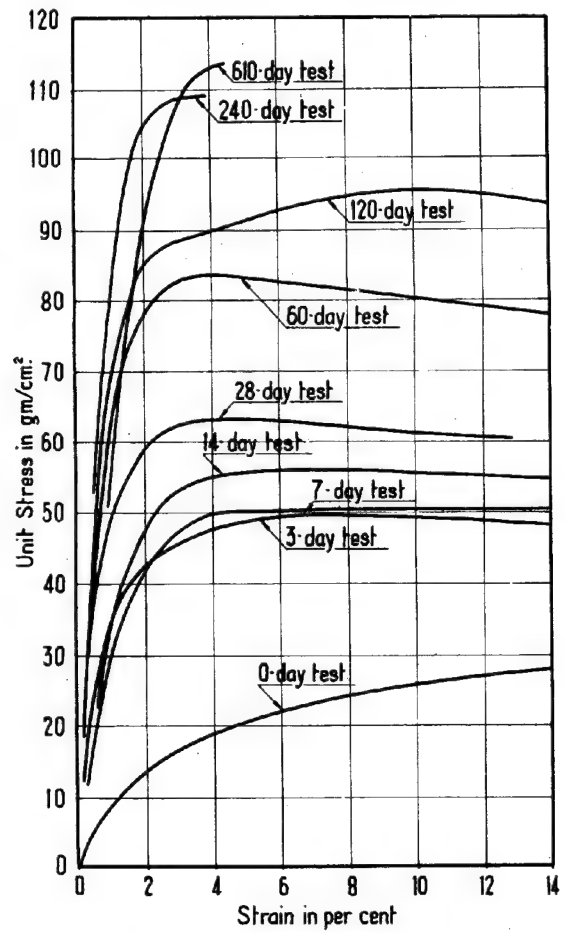
Compression tests of clays in the undisturbed and remolded state at natural water content.

FIG. 5



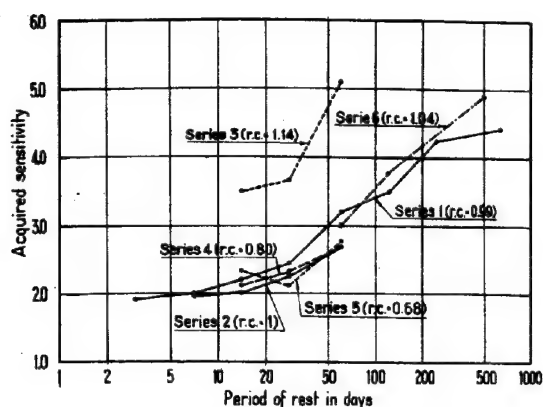
Molds for compression tests

FIG. 6



Laurentian clay tests.

FIG. 7



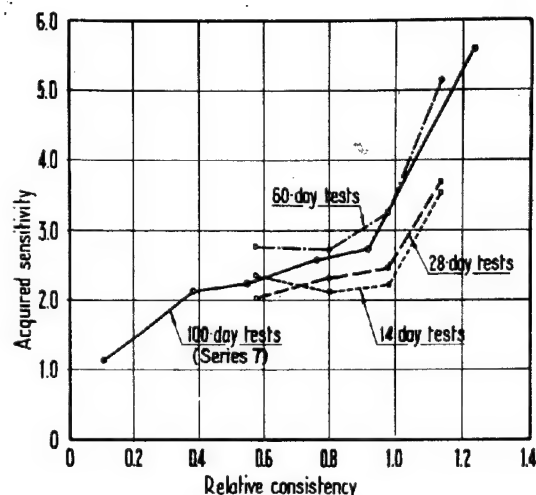
Acquired sensitivity as a function of the period of rest-Laurentian clay tests.

FIG. 8

ity that the clay experimented, from the very beginning, when it was simply allowed to rest at constant water content. The sensitivity acquired after 610 days of rest reached a value of 4.45, nearly one third of the natural sensitivity of the undisturbed material as given in Table 1.

The results of Series 2 to 6 are given in Figure 8 and they indicate increases in strength similar to those recorded in Series 1. Series 7 was undertaken to determine the relation between the increase in strength and the relative consistency, after a fixed period of rest. Its results are given in Figure 9, where are also included results deducted from the other series. For Series 7, the 0-day strength was obtained after testing the specimen that had tested, by remolding it at constant water content and testing it again. In this way, the influence of the small loss in moisture experimented with time by the specimens of the other series was entirely eliminated.

All the curves of Figure 9 indicate that, for a given period of rest, the relative increase in strength increases with the relative consistency of the clay. In other words,



Relation between relative consistency and acquired sensitivity-Laurentian clay tests.

FIG. 9

in the range of consistencies tested, the rate of hardening increases with the water content. This phenomenon may partly explain the reason for the high natural water content of the Laurentian clay, which was higher than any of those tested. If under the slow process of sedimentation and subsequent consolidation by which the clay strata was formed, hardening could have taken place in a manner similar to that in the test specimens, the clay would have tended to stabilize itself at a critical water content for which the rate of hardening is the greatest. This critical water content is evidently higher than any used in this investigation, but the natural water content of the clay is also higher.

#### b) Detroit I clay.

Tests on Detroit I clay comprise four groups designated as Series a to d. The results are given in Table 3 and Figures 10 to 12. Table 3 and Figure 10 give the results of

TABLE 3

UNCONFINED COMPRESSION TESTS ON DETROIT I CLAY. SERIES a. (Relative consistency = 0.98)				
Tested after a resting period of (days)	Water content %	Ultimate strength (for 10 % strain or less) <sub>2</sub> (gm/cm <sup>2</sup> )	Type of failure	Acquired sensitivity
(1)	(2)	(3)	(4)	(5)
0	29.1	34.2	bulge	1.0
3	29.1	49.0	"	1.43
7	29.0	51.5	"	1.51
14	28.9	49.4	"	1.44
28	28.9	58.0	"	1.70
60	28.3	68.6	"	2.00
120	28.6	64.2	"	1.88

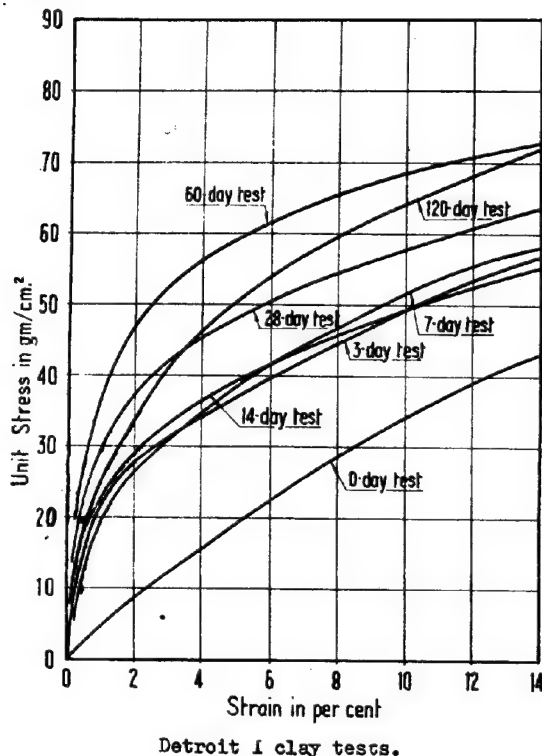
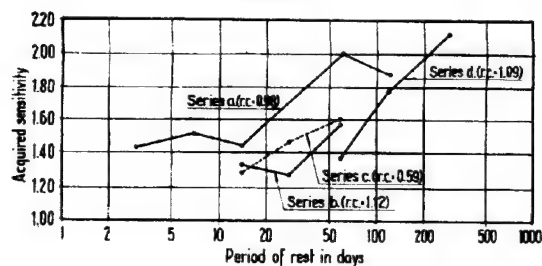


FIG. 10



Acquired sensitivity as a function of the period of rest-Detroit I clay tests.

FIG. 11

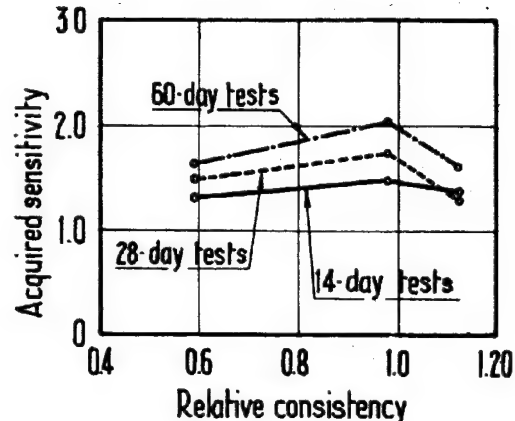
Series a that was the main series of tests on this clay.

The maximum acquired sensitivity measured in these series of tests reached a value a little over 2.10, which compared with the natural sensitivity of about 2.5 of Table 1, indicates that this clay may regain with time a very great part of its original strength lost by remolding.

The results given in Figure 12 are not extensive enough to permit a definite conclusion, but they seem to indicate that this clay has its maximum rate of hardening for a water content near the liquid limit. The water content of the clay in the ground is smaller than this value.

#### c) Detroit II clay.

Only one series of tests was made on this clay, at a relative consistency a little higher than that corresponding to the natural water content of the clay in the ground.



Relation between relative consistency and acquired sensitivity Detroit I clay tests.

FIG. 12

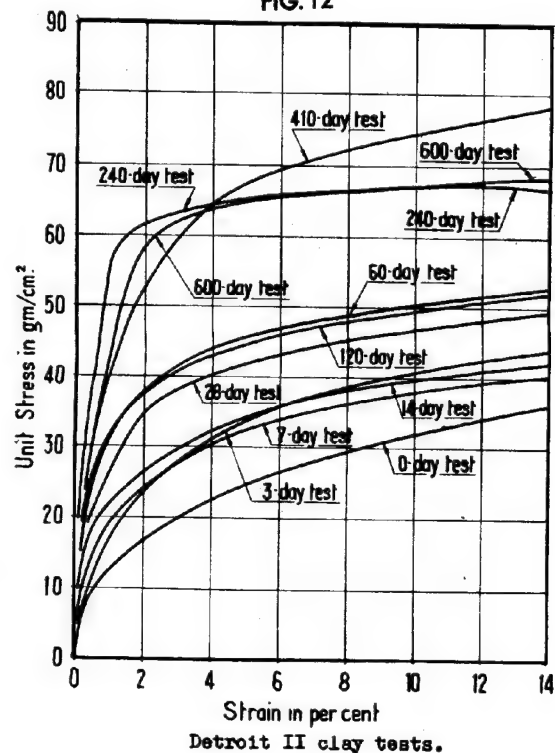


FIG. 13

The results are given in Table 4 and Figures 13 and 14.

The rate of increase on strength and rigidity was for this clay comparatively slower than for the other two types of clay already reported. Only after 240 days of rest the stress-strain curve acquired a shape similar to that of the undisturbed material. The acquired sensitivity reached, however, values up to 2.36, about one third of the natural sensitivity of the undisturbed material.

#### d) Mexico clay.

Tests on this clay include only a short series whose results are given in Table 5 and Figure 15. The increase in strength experi-

TABLE 4

UNCONFINED COMPRESSION TESTS ON DETROIT II CLAY. ( Relative consistency = 0.94 )				
Tested after a resting period of (days)	Water content %	Ultimate strength (for 10 % strain or less) (gm/cm <sup>2</sup> )	Type of failure	Acquired sensitivity
(1)	(2)	(3)	(4)	(5)
0	50.7	31.6	bulge	1.0
3	49.3	40.6	"	1.29
7	48.9	37.7	bulge and splitting	1.19
14	50.2	39.6	bulge shear and splitting	1.25
28	49.8	46.7	"	1.48
60	49.6	50.2	bulge and shear	1.59
120	50.3	49.4	"	1.56
240	49.9	67.0	"	2.12
410	50.1	74.5	"	2.36
600	48.9	67.2	shear	2.13

TABLE 5

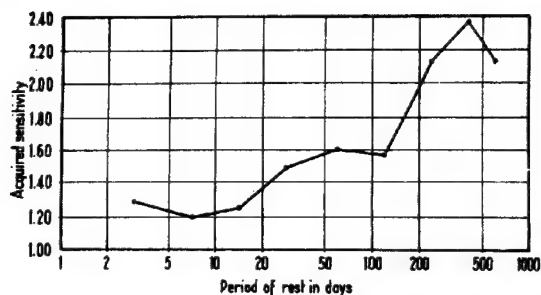
UNCONFINED COMPRESSION TESTS ON MEXICO CLAY ( Relative consistency = 1.03 )				
Tested after a resting period of (days)	Water content %	Ultimate strength (for 10 % strain or less) (gm/cm <sup>2</sup> )	Type of failure	Acquired sensitivity
(1)	(2)	(3)	(4)	(5)
0	61.5	44.4	bulge	1.0
14	---	58.5	"	1.32
28	---	55.7	bulge and shear	1.25
60	---	61.8	"	1.39

mented by the material during the 60-day extension of this series was small when compared with the natural sensitivity of the clay. These results were rather disappointing because the clay came from the core of a hydraulic fill dam constructed many years ago, where a recent investigation showed that the consolidation of the clay core did not proceed as would have been expected from existing theories. The water content of the core, more than 30 years after construction, remained practically independent of the depth below the crest at a value close to the liquid limit. Yet, the unconfined compressive strength was found to increase with depth and the strength of the material near the base of the core at

a depth of 80 ft. was nearly three times as great as the strength of the material in the upper part.

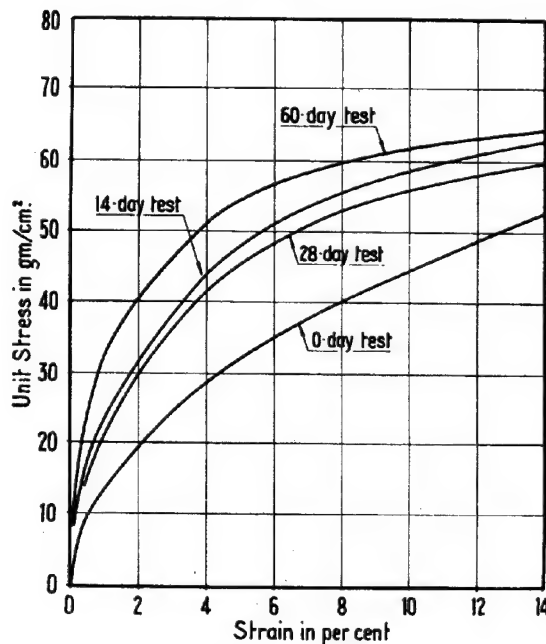
It is believed that the increase in strength experimented by the remolded clays when kept at constant water content may partly explain that phenomenon. The results of this series of tests do not warrant completely this ascertainment. The series of tests run is not extensive enough, however, to draw any conclusion. Besides, the tests on Detroit II clay indicate that if allowed to rest longer, the Mexico clay might still experiment considerable increases in its strength and rigidity, should it behave as the above mentioned material.





Acquired sensitivity as a function of the period of rest-Detroit II clay tests.

FIG. 14



Mexico clay tests.

FIG. 15

##### 5. DISCUSSION AND CONCLUSIONS.

The results of the tests indicate that, if a clay that has lost a great part of its original unconfined compressive strength by a process of complete remolding, is later kept for a certain period of time at constant water content, the clay regains a sensible part of its lost strength. Depending on the type of clay, this phenomenon may, in some cases, restore the greatest part of the original strength of the undisturbed material. This

fact is in complete contradiction with the theory that assigned most of the difference in strength between undisturbed and remolded clays to a structure that being destroyed could never be recovered.

Since the clays did not have an opportunity to build up any kind of a structure, it must be admitted in order to explain the results, that the period of rest permitted the clay to restore or improve the contacts among the shells of adsorbed water surrounding each particle, that were disturbed by remolding. This explanation is in agreement with Terzaghi's concept of the cause of the strength and rigidity of undisturbed clays, referred to in Part I. The results, however, do not warrant completely this concept. It is believed that in the affirmative case, the thixotropic phenomena studied in this investigation should have, on the basis of the above hypothesis, restored practically all of the original strength of the undisturbed clay. This was nearly so in the case of the Detroit I clay, but not so for the other materials tested. It remains no doubt, however, that the test results appear to indicate that a sensible part of the strength and rigidity of undisturbed clays depend on the physico-chemical processes resulting from the surface activity of the mineral grains.

The most important practical conclusions to be deduced from this investigation are as follows:

- The natural sensitivity may be a controlling clay property in some problems of soil mechanics such as landslides. It may not be of such significance in problems of foundation engineering where the critical period of behavior of the clay occurs some time after remolding has taken place. Since some clays may recover a sensible part of their strength in a relatively short time after remolding, the natural sensitivity may be no indication of the behavior of the soil.
- In all cases in which the method of construction involves remolding of clay material, such as driving of piles in or through clay strata, the importance of remolding may be much less than what Casagrande's concept of the clay structure would suggest.

##### 6. ACKNOWLEDGEMENT.

Thanks are due to Dr. K. Terzaghi and R.B. Peck for continued guidance throughout this investigation.

##### REFERENCES:

- 1) A. Casagrande, "The Structure of Clay and its Importance in Foundation Engineering", Journal of the Boston Society of Civil Engineers, April, 1932.
- 2) K. Terzaghi, "Undisturbed Clay Samples and Undisturbed Clays", Journal of the Boston Society of Civil Engineers, July 1941.
- 3) See also discussion of "Application of Soil Mechanics in Designing Building Foundations" by A. Casagrande and R.E. Fadum, Trans. A. S. C. E., 1944.

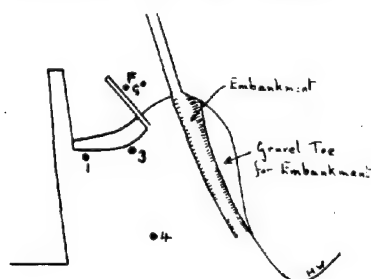
## || a 2 THE GEOTECHNICAL PROPERTIES OF A DEEP STRATUM OF POST-GLACIAL CLAY AT GOSPORT

A.W. SKEMPTON M.Sc., A.M.I.C.E., F.G.S.

University Reader in Soil Mechanics and Assistant Professor at Imperial College,  
University of London.

### 1. INTRODUCTION.

In 1942 following the collapse of a steel sheet pile wall in the Royal Clarence Yard at Gosport, the Admiralty requested the Building Research Station to report on the causes of failure and to advise on the re-design. Three borings were made, in the positions shown in Fig. 1. and they revealed



Key Plane

FIG. 1

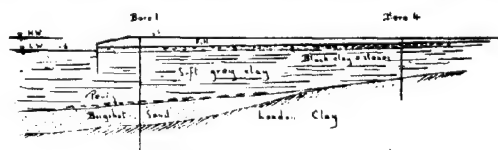
about 60 ft. of soft, post-glacial clay, overlying the Bagshot Sands and London Clay. A number of undisturbed samples of the soft clay were obtained and tested in the laboratory. The results show that this stratum consists of a normally consolidated clay (as defined by Terzaghi 1941) in which the shear strength and preconsolidation load increase with depth in a regular manner. This increase in strength and pre-consolidation load would be expected from general soil mechanics principles, yet the author does not know any other published examples giving complete data on a normally consolidated clay stratum.

In contrast, however, there have been descriptions of several cases where a bed of clay which might be expected to be normally consolidated has shown no regular increase in strength with depth (Terzaghi 1941, Casagrande 1944 (a) and 1944 (b)). Consequently the present results are published in order to show that the expected behaviour of a normally consolidated clay can be observed in nature. If this conclusion is accepted it follows that the other published results relate to strata which are not true normally consolidated clays, and that there must be a reason for their apparently anomalous behaviour. Casagrande (*loc.cit*) has suggested one possible reason, involving the drying of the clays to depths of 30 or 40 ft. below their surface. Whether this is correct or not, the Gosport clay at least shows the necessity for some such explanation of the anomalous strata, and discounts the assumption that an approximately constant shear strength with depth is the standard behaviour pattern of geologically recent clays.

### 2. GEOLOGY.

From the borings made in the Royal Clarence Yard and from the records of several

wells in the neighbourhood the geological section shown in Fig. 2 has been prepared. The



Geological Section

FIG. 2

Bagshot Beds and the London Clay are of Tertiary Age. Overlying these deposits there is a thin bed of peat. A sample of this peat, from Borehole No. 3 was submitted to Dr. H. Godwin F.R.S. for pollen analysis. He found (Godwin 1945) that the peat was of Pre-Boreal age; Zone IV in the British classification. At this period, about 9,000 or 10,000 years ago, the sea was substantially lower than at present. Various submerged peats around the coast show, however, that shortly after Zone IV peat was formed, a comparatively rapid rise in sea level took place and the soft clays found in many of the estuaries were deposited during this period. The marine transgression was probably almost complete by the end of Boreal times, roughly 7000 years ago; since when only minor oscillation have occurred, with a general slight rise in sea level. Evidence from a peat surface at Amberley Wild Brooks, not far from Gosport, (Godwin 1943) suggests that the transgression has not increased during the past 2000 years.

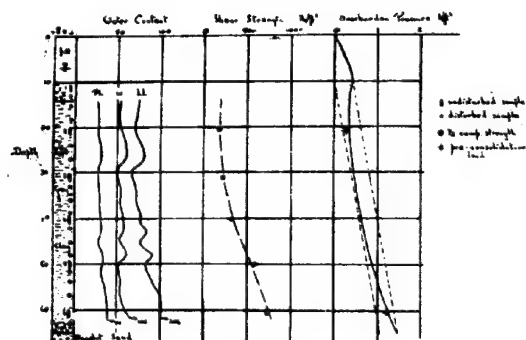
The Gosport clay is therefore post-glacial in age; deposited mainly if not entirely during the Boreal transgression. Therefore there can be no doubt that it is fully consolidated under its own weight. In about 1890, however, a fill was placed on the clay, in the area of the borings, to +6 O.D. and in 1936 the fill was raised by another two feet.

### 3. BORINGS.

The boring and sampling operations were carried out by Messrs. Soil Mechanics Ltd., under the supervision of Mr. H.J.B. Harding and the author. The boreholes were 6 ins. diameter, lined with casing tubes. Undisturbed samples were taken at the depths shown in Figs. 3, 4 and 5 with the tool described by Cooling (1946). This has a diameter of 4 1/2 in. and an area ratio of 23%. Visual examination showed that distortion of the samples was limited to the outer 1/10 inch, although some slight disturbance of the clay is inevitable in sampling owing to the change in stress conditions.

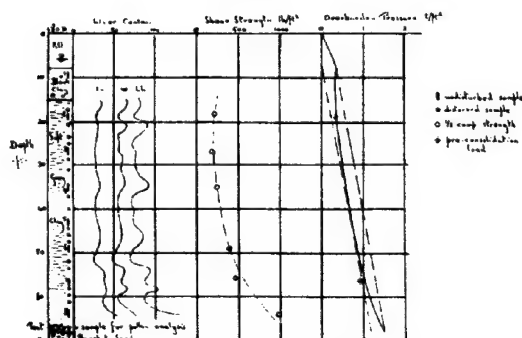
In addition, small samples were taken at about every 2 or 3 ft. in depth, for determination of water content and Atterberg Limits.

The author also took two samples of the clay (samples F and G) where it was exposed on the foreshore, at low water mark. Here the



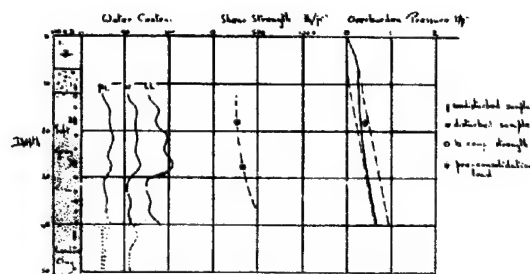
Bore no. 1

FIG. 3



Bore no. 3

FIG. 4



Bore no. 4

FIG. 5

Table I.

	Average	Range
Water content w	56	46 - 73
Liquid Limit LL	80	62 - 127
Plastic Limit PL	30	25 - 50
Consistency index $\frac{LL - w}{LL - PL}$	C. 48	0.31 - 0.73

In Boreholes 1 and 3 there is a general tendency for the Atterberg Limits to increase with depth, but the water content remains essentially constant. The consistency index therefore increases with depth. In Borehole 4 no general drift can be seen. The variations in water content are reflected by variations in the Atterberg Limits to a very marked extent. The relation between liquid limit and plasticity index, except for a few of the high liquid limit clays, is typical of that given by Casagrande (1947) for inorganic clays.

#### 5. PARTICLE SIZE.

Mechanical analyses were carried out on four samples, all from Borehole No. 1. The results are given in Table II.

TABLE II

Sample	Liquid Limit	Fine sand .2-.06 mm	Silt .06 - .002 mm	clay <.002 mm	H <sub>2</sub> O <sub>2</sub> loss	HCl loss
1 - 2	71	2.9	48.3	42.6	5.9	0.3
1 - 3	65	6.1	44.7	37.6	5.4	6.2
1 - 5	82	0	27.8	50.9	2.6	18.7
1 - 6	98	0.3	22.9	59.0	9.7	8.1

clay was very soft, and the samples were obtained by carefully pressing into the clay a thin walled tin tube 5 ins. diameter and 15 ins. long. This tube had an area ratio of only 4% and the samples were not visibly disturbed in any way.

#### 4. ATTERBERG LIMITS AND WATER CONTENT.

Water contents were determined on every test specimen and on each of the small samples. Atterberg Limits were determined on at least two and in some cases on every test specimen cut from the undisturbed samples and on each of the small samples.

The results are plotted in Figs. 3, 4 and 5. Average values and total ranges are given in Table I (excluding the foreshore samples).

These results show a definite correlation between liquid limit and clay fraction, typical of marine clay (Cooling 1946). They also show that the liquid limit is influenced more by the clay fraction than by the organic content (H<sub>2</sub>O<sub>2</sub> loss)

#### 6. MINERALOGY.

The four samples on which mechanical analyses had been made were submitted to Dr. Nagelschmidt for X-ray analysis. For the whole clays he found chiefly quartz and calcite, the calcite content corresponding roughly with the HCl loss given in Table II. For the clay fraction all the samples were similar and consisted of 50 - 70% Illite and 30 - 50% Halloysite. There was a general and low-angle scattering

due either to organic matter or amorphous inorganic material. No montmorillonite was found.

### 7. SPECIFIC GRAVITY.

Specific gravity determinations were carried out on seven samples. The average value was 2.67 with a range of 2.62 to 2.70.

### 8. OVERBURDEN PRESSURE.

In Figs. 3, 4 and 5 the effective overburden pressure before placing the fill is shown as a dotted line. The effective overburden pressure, if consolidation under the fill had been complete, is also shown. In calculating these pressures the following densities have been adopted.

fill above G.W.L.	105 lb/ft <sup>3</sup>
fill below G.W.L.	65
black clay and stones below	47
grey clay G.W.L.	42

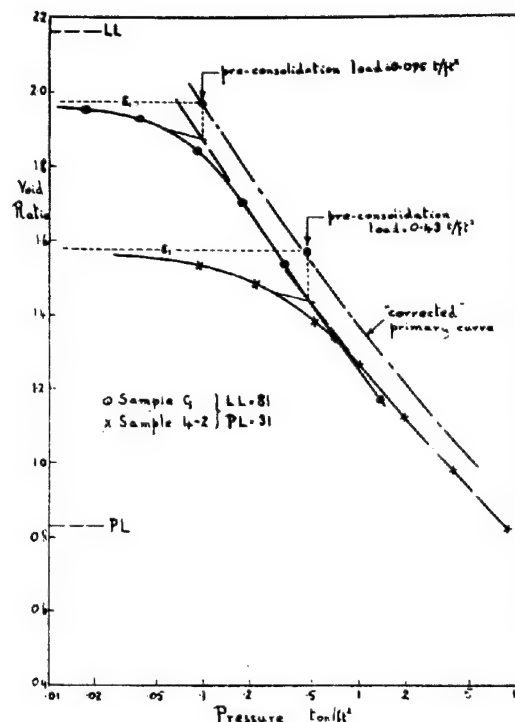
Consolidation under the fill, at the time of sampling, cannot be complete, however, and the effective overburden pressure has therefore been calculated from the theory of consolidation (Terzaghi and Frohlich 1936). Tests showed a reasonably constant coefficient of consolidation equal to 0.004 cm<sup>2</sup>/min, and using this value it is an easy matter to estimate the effective pressure at any depth. The results are shown by the full lines in Figs. 3, 4 and 5.

### 9. PRE-CONSOLIDATION LOAD.

Consolidation tests were carried out on five samples from the boreholes and on the two foreshore samples. Representative  $p - e$  curves are shown in Fig. 6. These are typical of undisturbed soft clays with a moderately high initial water content and an estimate of the pre-consolidation load can be found by the graphical construction suggested by Casagrande (1936). In Table III these values are compared with the calculated effective overburden pressure; and also in Figs. 3, 4 and 5, they are plotted on the same graph as that relating overburden pressure to depth. It will be seen that a reasonable agreement is obtained, probably within the range of accuracy of the construction and the inevitable slight disturbance in sampling.

TABLE III

Sample	Depth	Consistency				Calculated Overburden Pressure	Estimated Overburden Pressure (Casagrande)
		W	LL	PL	$\frac{LL - W}{LL - PL}$		
F	7 ins.	77	75	29	-.05	-	0.093 t/ft <sup>2</sup>
G	9 ins.	74	81	30	+.14	-	0.095
1 - 2	21 ft.	54	69	25	.34	0.37 t/ft <sup>2</sup>	0.28
1 - 6	61	60	100	36	.62	1.24	1.22
3 - 2	19	52	71	28	.44	0.34	0.30
3 - 7	56	60	86	33	.49	1.05	0.84
4 - 2	17	59	81	32	.45	0.32	0.44



Consolidation Test Results

FIG. 6

The two foreshore samples gave definite pre-consolidation loads, which are assumed to be an indication of the capillary pressures existing in the clay at a depth of about 8 ins. The correlation between calculated and experimental pre-consolidation loads for the bore-hole samples is good evidence for the conclusion that the stratum is a true normally consolidated clay.

### 10. DECREASE IN VOID RATIO WITH OVERBURDEN PRESSURE.

Owing to the variations in liquid limit

with depth a plot of water content (or void ratio) against overburden pressure would be of no value. Consequently the consistency index  $(LL-w)/(LL-PL)$  was calculated for each sample and the water content was then found which gave this same consistency index with average

# 11. SHEAR STRENGTH.

Triaxial compression tests carried out under different lateral pressures with no water content change during the test showed an angle of shearing resistance equal to zero. Typical results are given in Table IV.

TABLE IV

Sample 3 - 2 LL = 82      PL = 29			Sample 4 - 3 LL = 107      PL = 36		
$\sigma_v$	$\sigma_1 - \sigma_v$	w	$\sigma_v$	$\sigma_1 - \sigma_v$	w
0 lb/in <sup>2</sup>	2.90 lb/in <sup>2</sup>	61	0 lb/in <sup>2</sup>	4.7 lb/in <sup>2</sup>	70
20	2.94	58	10	4.3	68
40	2.88	59	20	5.1	73
			30	4.8	68

liquid and plastic limits of 80 and 30 respectively. In this way the variations were smoothed out.

The void ratio (water content  $\times 2.67/100$ ) calculated in this manner is plotted against overburden pressure in Fig. 7. As would be expected there is a considerable scatter, but the general decrease in void ratio with increasing pressure is quite definite. The results are in good agreement with data on other clays of a similar type (Skempton 1944).

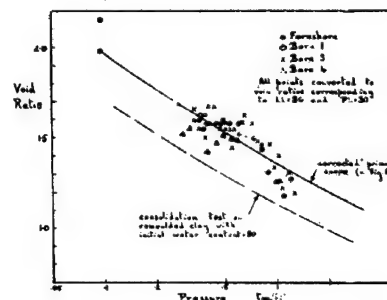
Fortunately sample G from the foreshore and sample 4-2 both had a liquid limit almost exactly equal to the average value of 80, and results of the consolidation tests on these samples can therefore be compared directly with the data in Fig. 7.

Referring to Fig. 6 it will be seen that a "corrected" primary  $p - e$  curve has been drawn through the two points corresponding to the natural void ratio and pre-consolidation load, and parallel to the experimental primary curve. This represents an attempt to obtain, as far as a laboratory test is concerned, a true primary  $p - e$  curve for the clay. The "corrected" curve is plotted in Fig. 7 and it is, rather surprisingly, found to agree well with the observed data. It is considered that this result constitutes a second indication that the clay is normally consolidated.

The curves in Fig. 6 are also of interest in that they show that the primary curve of Sample 4-2, which was taken from a depth of 17 ft., is an almost exact continuation of the primary curve of sample G. A comparison of this nature is not often possible, owing to the rare chance of finding two samples of the same stratum with the same liquid limit and with such widely different pre-consolidation loads.

In contrast a  $p - e$  curve obtained from a consolidation test carried out on the clay, remoulded with an initial water content equal to the liquid limit, lies well below the point.

These results show that a test made on the undisturbed clay, in the natural state in which it was deposited, corresponds closely to the actual consolidation under pressure in the ground, and that its structure is not seriously affected by the test.



Pressure-Void Ratio Relationship.

FIG. 7

Shear strength is therefore equal to one-half compression strength and it was determined by carrying out unconfined compression tests on at least two specimens from each sample. In about half the samples the compression strengths of the clay after remoulding was also measured. The results are given in Table V. Remoulding index equals the ratio of remoulded to undisturbed strength.

In Fig. 8(a) shear strength is plotted against calculated overburden pressure and, in Fig. 8(b) against pre-consolidation load. In both cases there is an approximately linear relationship, represented by the equation

$$c = p \cdot \tan 15^\circ = 0.27 p$$

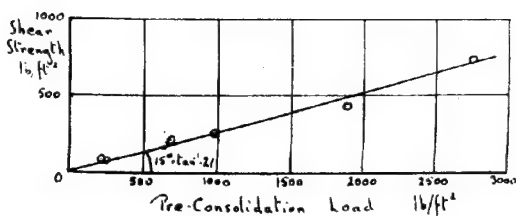
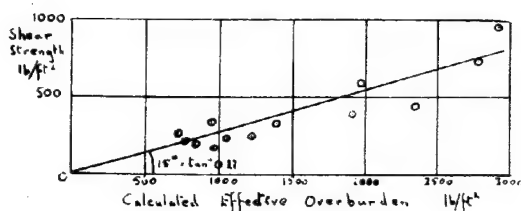
where  $15^\circ$  is the angle of shearing resistance of the clay.

This linear relationship is a third indication that the clay is normally consolidated. So far as the author is aware, Fig. 8 is the first published information on the increase in strength with overburden pressure obtained from field data on a thick stratum of clay.

The variation of strength with depth is shown in Figs. 3, 4 and 5. The increase with depth is quite obvious, and is especially apparent when it is remembered that the foreshore samples had a strength of only about 100 lb/ft<sup>2</sup>.

TABLE V

Sample	Consistency				Calculated Overburden Pressure lb/ft <sup>2</sup>	Pre- con- solid Load lb/ft <sup>2</sup>	Shear Strength lb/ft <sup>2</sup>	Remoulding Index
	W	LL	PL	$\frac{LL-W}{LL-PL}$				
F - 1	75	73	27	-.06	-	-	70	-
F - 2	77	75	29	-.05	-	210	90	-
F - 3	72	77	27	+.10	-	-	120	0.23
G	73	74	28	+.02	-	210	85	0.24
1 - 2	55	73	29	.41	830	630	190	0.47
1 - 3	49	66	27	.44	1050	-	225	0.51
1 - 4	57	76	30	.41	1390	-	325	0.41
1 - 5	51	82	34	.65	1970	-	595	0.45
1 - 6	62	98	40	.62	2780	2730	735	0.51
3 - 2	58	82	29	.45	760	670	210	-
3 - 3	55	77	27	.43	960	-	160	-
3 - 4	62	94	33	.52	1230	-	245	-
3 - 6	50	71	28	.49	1910	-	390	-
3 - 7	55	86	33	.58	2350	1880	440	-
3 - 8	70	127	50	.74	2920	-	975	-
4 - 2	63	96	35	.54	710	980	260	.43
4 - 3	69	107	36	.53	940	-	340	.40



Relation between Shear Strength and Consolidation pressure.

FIG. 8

The effect of remoulding seems to decrease with increasing strength. For the very soft fore-shore samples the remoulding index is about 0.25, while for the deeper samples taken in the borings the index is about 0.45. It will at once be asked whether this is not simply due to disturbance during sampling from the borings. Some slight disturbance is, of course, inevitable but the stability calculations on the embankment failure, described in the following section, show that the drop in strength in the borehole samples is unlikely to be more than 10 per cent.

In the author's opinion the true relation between shear strength and overburden pressure allowing for this possible disturbance may be

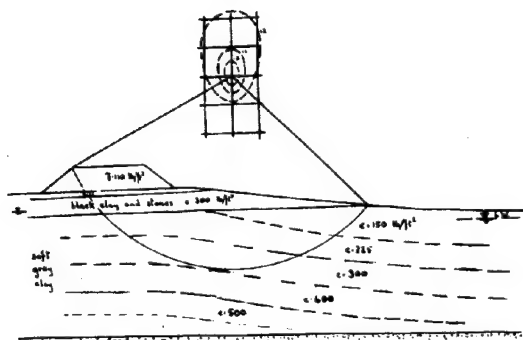
$$c = p. \tan 17^\circ = 0.30 p.$$

but is it improbable that the angle of shearing resistance could be appreciably higher.

## 12. EMBANKMENT FAILURE.

The embankment shown in Fig. 1 and in Fig. 9 was built in 1910 to a height of 8 ft. But immediately on reaching this height it subsided catastrophically. It was rebuilt successfully by forming a gravel toe simultaneously with the formation of the bank.

In Fig. 9 the contours of shear strength have been drawn from the data in Fig. 8, and an analysis of stability has been made on the



$\phi = 0$  Analysis of Embankment Failure  
Min. Factor of Safety = 0.93  
For strata above L.W. = 105 lb/ft<sup>3</sup>

FIG. 9

$\phi = 0$  assumption (Skempton 1948). It will be seen that the minimum factor of safety is 0.93. The correct value should be 1.00 and it is therefore possible that the average strength of the clay has been underestimated by about 7 per-cent. This can probably be attributed to slight disturbance of the samples, as mentioned above, but in general the evidence provided by this failure lends support to the values of shear strength as measured in the laboratory, and the maximum effect of disturbance is probably not in excess of 10 per-cent.

### 13. SHEET PILE WALL FAILURE.

The analysis of the sheet pile wall was rather complicated but the result is in agreement with this conclusion.

### 14. CONCLUSIONS.

- a) The following results show that the deep stratum of soft, post-glacial, clay at Gosport is normally consolidated.
- 1) the experimentally determined pre-consolidation loads are of the same order as the effective overburden pressures throughout the depth of the stratum
- 2) the primary p-fourve derived from consolidation tests on the clay as deposited in its natural state agrees with the p-frelation deduced from overburden pressures and water contents on samples taken from the boreholes.
- 3) shear strength is directly proportional to overburden pressure, and hence also to pre-consolidation load.

- b) Shear strength  $c$ , corrected for possible disturbance on sampling, and overburden pressure  $p$  are related by the expression  $c = p \tan 17^\circ = 0.30 p$ , where  $17^\circ$  is the angle of shearing resistance of the clay.
- c) The clay is moderately sensitive to remoulding, the sensitivity decreasing with increasing strength.

### ACKNOWLEDGEMENT.

The data given in this paper is published by permission of the Director of Building Research, Department of Scientific and Industrial Research.

The author is greatly indebted to Dr. Godwin F.R.S. and Dr. Nagelschmidt for their kindness in carrying out the pollen analysis and X-ray determinations.

### REFERENCES.

- CASAGRANDE, A. 1936, "The determination of the pre-consolidation load and its practical significance", *Proc. Harvard Conf. Soil Mech.* Vol. III p. 60.
- CASAGRANDE, A. 1944(a), "Application of Soil Mechanics in Designing Building Foundations", *Tr. Am. Soc. C.E.* Vol. 109 p. 463.
- CASAGRANDE, A. 1944(b), "Seventh Progress Report on Cooperative Research on Stress-Deformation and Strength Characteristics of Soils", Harvard University.
- CASAGRANDE, A. 1947, "Classification and Identification of Soils", *Proc. Am. Soc. C.E.* Vol. 73 p. 783.
- COOLING, L.F. 1946, "The development and scope of soil mechanics". *The Principles and Application of Soil Mechanics.* Inst. C.E.
- GODWIN, H. 1943, "Coastal Peat Beds of the British Isles and North Sea", *Journ. Ecology.* Vol. 31. p. 199.
- GODWIN, H. 1945, "A submerged peat bed in Portsmouth Harbour". *New Phytologist* Vol. 44 p. 152
- SKEMPTON, A.W. 1944, "Notes on the Compressibility of Clays", *Quat. J. Geol. Soc.* Vol. 100 p. 119
- SKEMPTON, A.W. 1948, "The  $\phi = 0$  Analysis of Stability and its Theoretical Basis", *Proc. 2nd Int. Conf. Soil Mechanics.*
- TERZAGHI, K. 1941, "Undisturbed Samples and Undisturbed Clays", *Journ. Boston Soc. C.E.* Vol. 28 p. 211
- TERZAGHI, K. and O.K. FROHLICH 1936, "Theorie der Setzung von Tonschichten", Vienna (Deuticke).



II a 3

LABORATORY STUDIES RELATING TO THE CLAY FRACTION OF COHESIVE SOILS \*)

K.E. CLARE

Department of scientific and industrial research  
Road Research Laboratory

SUMMARY.

This paper outlines the effect of the clay fraction on such engineering properties of cohesive soils as the strength, compactibility and permeability, and refers to the physico-chemical properties of individual clay particles which are important in this connexion.

Experimental results and data obtained at the Road Research Laboratory relating to the properties of the clay fraction are presented. These include results of Liquid and Plastic Limit tests, which have been grouped according to the general geological areas from which the soils were taken. When the Liquid Limits were plotted against the Plasticity Indices for particular groups, it was found that there were two relationships corresponding to the equations  $PI = 0.75(LL - 15)$  and  $PI = 0.8(LL - 15)$ .

Tests are also described in which samples of soil free from organic matter and carbonates were ignited to about 800°C. and the loss in weight expressed as a percentage of the total soil and of the clay fraction. With British soils most of the loss appears to take place in the clay fraction, the values falling into two distinct groups which are thought to correspond to different chemical and mineralogical groups. The loss during ignition of some of the other soils studied, particularly those of morainic origin from Scandinavia appears to be uniformly distributed throughout the soil fraction, from which it is inferred that the clay fractions of these soils contain particles derived from the primary weathering of rocks. The minerals in the clay fractions of British soils, however, presumably contain the more hydrated products of secondary weathering.

Data are included that were obtained with a method for determining the particle size distribution of the coarser clay particles, involving the use of a hypodermic syringe for sampling sedimenting clay suspensions, and some preparatory work in this investigation indicates the effect of the variation of the dispersing agent concentration on the deflocculation of suspensions of kaolin and montmorillonite clays.

Finally electron micrographs taken at the National Physical Laboratory of various types of clay particles are shown.

INTRODUCTION.

This paper outlines the effects of the clay fraction (particles smaller than 0.002 mm equivalent diameter) on the engineering properties of cohesive soils, and indicates how these effects depend on the physico-chemical characteristics of the individual clay particles. The results of some preliminary investigations undertaken at the Road Research Laboratory and having a bearing on this subject are presented.

EFFECT OF THE CLAY FRACTION ON THE ENGINEERING PROPERTIES OF COHESIVE SOILS.

From a consideration of the results of measurements of the engineering properties of cohesive soils in relation to their particle size analyses, it is possible to draw certain general inferences as to the effect of the clay fraction on these properties.

Thus, the major part of the mechanical strength of cohesive soils is derived from films of water surrounding the clay particles. When such soils are relatively dry, these films are thin and impart a high strength to the soil structure. An increase in moisture content, increases the film thickness resulting in a loss in strength, and the stability is therefore considerably dependent on the moisture content. This component of the stability is referred to as the cohesion, and is almost entirely a function of the clay fraction.

In the case of compaction, the results obtained with the standard compaction test indicate that soils having a high clay content cannot be compacted to such high densities as soils containing less clay, presumably due to the increased cohesion between the particles.

The average pore size in cohesive soils is less than that in granular soils, and their permeability is therefore less. The consolidation properties and the susceptibility of such soils to damage by frost, as well as their drainage characteristics are dependent on the permeability, and therefore indirectly on the clay content.

The water films surrounding the clay particles have a tendency to grow at the expense of free, capillary water and therefore contribute considerably to the soil suction (pF), differences between which cause moisture movements in unsaturated soil. When the films grow, the volume of the particles, and hence the bulk volume of the soil, increases, and when they diminish due to the drying of the soil, the particle volumes decrease. The phenomena of swelling and shrinkage are thus intimately bound up with the clay fraction.

PHYSICO-CHEMICAL CHARACTERISTICS OF CLAY PARTICLES.

The behaviour of the clay fraction in relation to the properties indicated above is determined by the physico-chemical characteristics of the individual clay particles. Amongst the more important of these is the surface area, which is dependent on the size and shape of the particles. Both these factors may alter in certain types of clay mineral, owing to an expansion or contraction of the particles, depending on the composition of the surrounding solution. Further, many of the effects of the clay fraction on the behaviour of the soil mass may be explained by the existence of a thin film of adsorbed water on the surfaces of the clay particles. The properties

\*) Note: Crown Copyright reserved.

of these adsorbed films will depend upon the mineralogical and chemical composition of the clay particles as well as the quantity and nature of any ions adsorbed on their surfaces.

#### RESULTS OF INVESTIGATIONS HAVING A BEARING ON THE CLAY PROBLEM.

In the course of soil investigations at the Road Research Laboratory, results have been obtained having a bearing on the clay problem, and relevant data have also been collected during the routine examinations of soils at the Laboratory. A review of these results and data are given below.

##### 1. ANALYSIS OF LIQUID AND PLASTIC LIMIT DATA.

These test were performed according to the A.S.T.M. procedure. 1) 2)

Both the Liquid and Plastic Limit are known to be dependent on the amount and type of the clay fraction in a soil, but the difference between them, the Plasticity Index is a function of the amount of clay only (xa). Therefore, if the Liquid Limits of a number of different soils are plotted against their Plasticity Indices, any variation in the relationship between these factors will be due to the presence of different types of clay mineral in the soils. This forms the basis for some of the soil classification systems used in Soil Mechanics, the most widely known being that due to A. Casagrande. 3)

Figs. 1a, 1b and 1c show the results of Plasticity tests on a large number of British soils plotted in this way, and grouped according to the general geological areas from which they were taken. The equations corresponding to the relationships for a number of such groups are given in Table 1.

Table 1.

Equations to the Plasticity Index/Liquid Limit relationships obtained for some groups of British Soils.

Recent and Pleistocene	$PI = 0.74(LL-17)$
Oligocene and Eocene	$PI = 0.74(LL-13)$
Upper and Lower Greensand	
and Gault	$PI = 0.82(LL-17)$
Chalk and Wealden	$PI = 0.80(LL-16)$
oolitic and Liassic	$PI = 0.75(LL-15)$
Marl and Sandstone	$PI = 0.72(LL-15)$

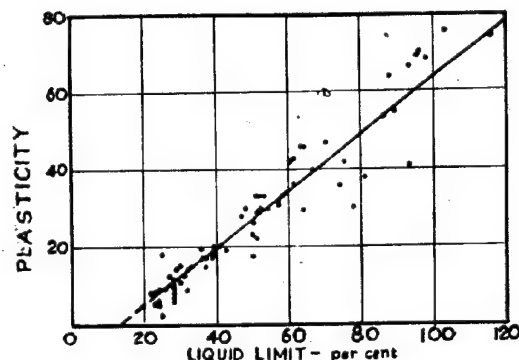
PI = Plasticity Index  
LL = Liquid Limit

It will be noted that although all the equations are similar, there appear to be two relationships corresponding to  $PI = 0.75(LL-15)$  and  $PI = 0.80(LL-15)$  approximately, but it is difficult to say whether these differences are significant, bearing in mind the possible experimental errors in simple tests of this type and the considerable scatter of the points. This variation in relation to the clay content, is brought out in Fig. 2, which shows the Liquid and Plastic Limits of the Oolitic and Liassic group plotted against the clay contents.

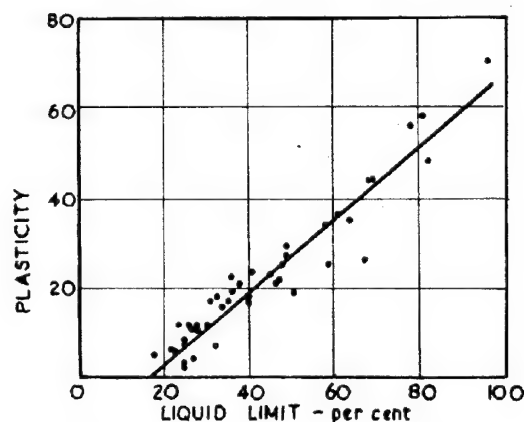
##### 2. ANALYSIS OF LOSS ON IGNITION DATA.

Data obtained from loss on ignition determinations have also been examined in an at-

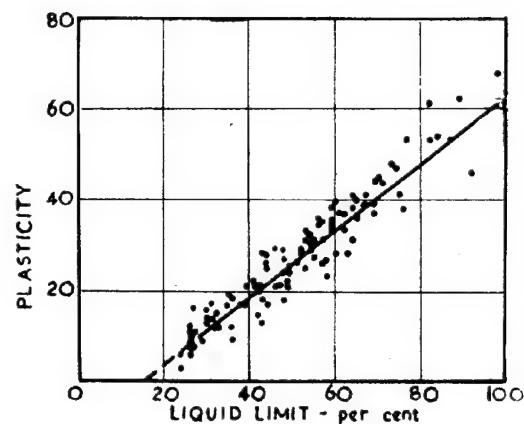
xa) L.F. Cooling and A.W. Skempton have correlated the liquid limit and the clay fraction. (L.F. Cooling "The development and scope of soil mechanics" Instn. Civ. Eng. 1946).



a Oligocene and Eocene



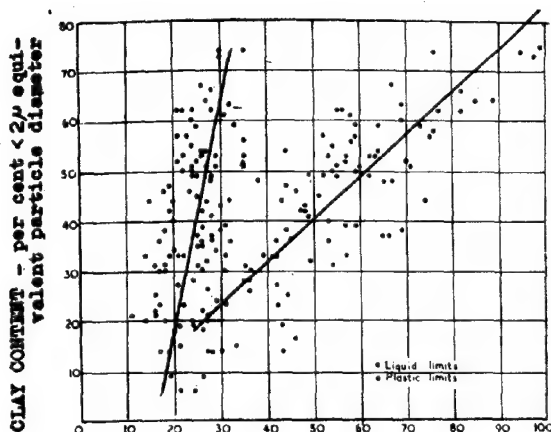
b Upper and Lower Greensand and Gault



c Oolitic and Liassic

Relations between Atterberg plasticity index and liquid limit for three groups of English clays.

FIG. 1



MOISTURE CONTENT-- per cent of dry soil weight  
Relation between clay content and Atterberg  
liquid and plastic limits for soils in oolitic  
and liassic areas.

FIG. 2

tempt to classify clays. Samples of soil, dried at 105°C., from which carbonates and organic material had been removed, were heated to temperatures between 700°C. - 800°C. in an electric furnace, and the loss in weight determined. Since the silt and sand fractions of most British soils are believed to contain only particles of silica or primary silicates derived from igneous rocks, it was assumed that all the loss on ignition would be from secondary hydrated alumina-silicates of the types found among the clay minerals. The loss in weight was therefore calculated as a percentage of the fraction having equivalent particle diameters less than two microns the proportion of which had previously been obtained from a particle size analysis. The results of these calculations are given in Table 2.

Table 2.

Ignition losses of some British cohesive soils.

Geological Group	Number of Samples tested	Loss at a percentage of the clay content
Recent and Pleistocene	3	13
Oligocene and Eocene	2	14
Wealden	3	21
Lower Greensand and Gault	2	14
Oolitic and Liassic	2 (1)	20 (13)

Three other soils from Marl and Magnesian Limestone areas gave values of 13%, 14% and 16% respectively.

The results suggest that again there may be two main groups, one giving a loss of about 14% and the other about 20% on ignition, comparable to the two Liquid Limit/Plasticity Index relationships. However, if the geological grouping used is accepted and the results compared with those given in Table 1, it will be noted that there are certain differences. Thus, while soils from Recent and Pleistocene, Oligocene and Eocene, and Marl areas and one soil from the Oolitic and Liassic areas gave ignition losses of approximately 14% corresponding to a slope of 0.75 on the LL/PI line, the two soils from the Greensand and Gault

area gave the same loss but had a slope of 0.80. The Wealden soils appeared to have entirely different characteristics in both respects, i.e., a loss on ignition of 21% and a slope of 0.80. These discrepancies may be due to incorrect geological classification, or to the fact that this classification was not made with the use of the detailed drift map, but was based on the geological type of the underlying strata.

A second, rather more extensive, series of experiments was made with soils of known mineral content from Britain, and with soils from Europe, Asia and Africa. The results, shown in Table 3, are given as the total loss on ignition of the whole soil, and the ignition loss as a percentage of the clay content.

It will be seen that the total loss of the kaolin clays from St. Austell was constant at about 13 - 14%, whereas the losses in terms of the clay contents were variable. This suggests that the whole soil and not merely the clay fraction contains kaolinite. Similarly, the moraine soils from Scandinavia gave a constant, rather low, total loss of 3 - 4%, which was also variable when expressed as a percentage of the clay fraction. In this case the clay fraction probably consists of the same material as the sand and silt components, that is, comminuted primary rock fragments derived from gneisses and granites by glaciation.

A constant total loss of 4% was generally obtained for the samples from West and South Africa, but the soils from North Africa appeared to contain more hydrated minerals, giving total losses of 6 - 8%. It does not appear possible to relate these losses to the clay contents of the soils, however.

The kaolin clay from Hong Kong had a similar percentage loss, on the clay content basis, as the total loss figures for the British kaolin clays, suggesting that in this case kaolinite was only present in the clay fraction.

Further ignition tests were made on the clay fractions isolated from a number of cohesive soils. The clay was separated by sedimenting suspensions of the soils dispersed with sodium oxalate, and converted to hydrogen-clay by leaching first with dilute acid and then with water. The ignition tests were performed in duplicate on the clay, after drying at 105°C., and the results are shown in Table 4 below:

Table 4

Ignition losses on the clay fractions (<0.002μ) of some cohesive soils.

Soil	Source	Ignition loss %
Kaolin clay, Montmorillonite	St. Austell, Cornwall	14
clay,	Redhill, Surrey	9
Gault clay,	Culham, Oxfordshire	12
Oolitic clay,	Stewartby, Bedfordshire	15
Moraine clay,	Göthenburg, Sweden	4
-----	Greyvillers, France	8
Lateritic clay,	Cape Province, South Africa	7

These results confirm the figure of 14% loss for kaolin clay, and the value of 4% for the moraine clays from Scandinavia. The montmorillonite clay had a very low loss (9%), which appears to correspond with that calculated for the alluvial clay from Denmark (Table 3), and possibly with the clay fraction of the soil from Greyvillers.

The ignition losses of the Oolitic and

TABLE 3

## Ignition losses of some cohesive soils

Soil	Source	Clay content ( $<0.002\mu$ ) %	Ignition loss %	Loss as a percentage of the clay content %
<u>Great Britain</u>				
Kaolin clay,	St. Austell, Cornwall	45	13	29
" "	" "	72	13	18
" "	" "	92	14	15
Montmorillonite Redhill, clay, Surrey		11 x)	8	73
" "	" "	35	11	31
x) Clay content not reliable				
<u>Scandinavia</u>				
Alluvial clay, Røgle, Denmark		75	7	9
" sand, - , Denmark		20	1	5
Moraine clay, - , Denmark		14	3	21
" " , Kungsbacka, Sweden		45	3	7
" " , Gothenburg, Sweden		68	4	6
" " , Stockholm, Sweden		63	4	6
" " , Trondhjem, Norway		12	3	25
<u>Western Europe</u>				
---	, Cologne, Germany	12	3	25
---	, Greyvillers, France	8	2	25
<u>Africa</u>				
---	, Duzère, Tunisia	15	6	40
---	, Souk-el-Arba, Tunisia	35	8	23
---	, Oudemaine, Algeria	26	8	31
---	, Philippeville, Algeria	69	12	18
---	, ---, Gambia	14	9	64
---	, Brikama, Gambia	27	4	15
---	, Yundum, Gambia	26	4	15
---	, Tow's River, South Africa	8	4	50
Lateritic Cape Province, South Africa		34	4	12
<u>Asia</u>				
---	, Hongkong	22	8	36
Kaolin clay, ---, Hongkong		40	6	15
Decomposed granite, Kistak, Hongkong		21	7	33
" " , ---, Hongkong		10	5	50

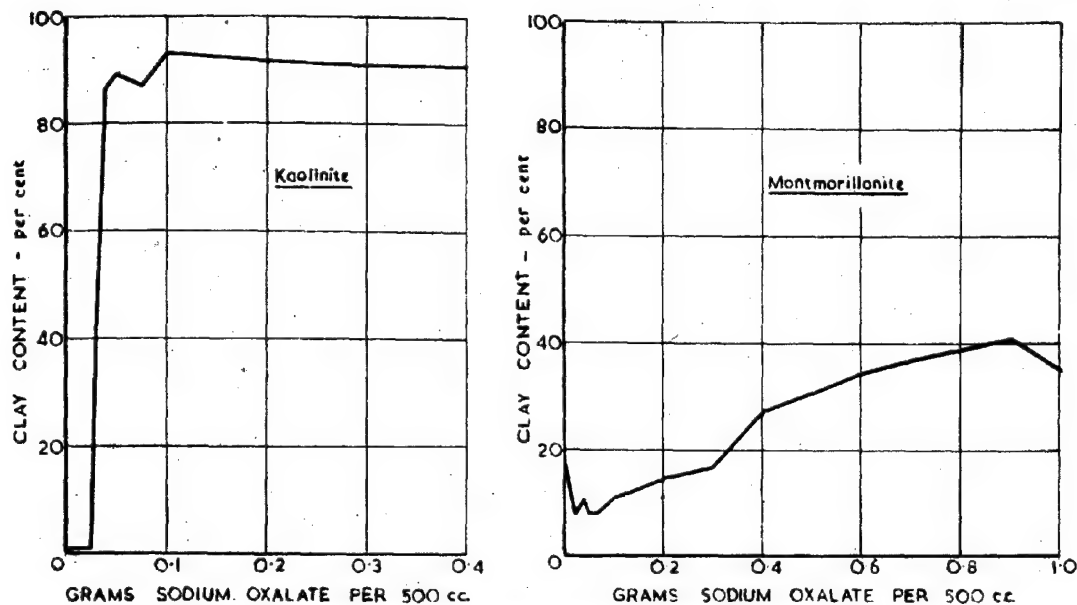
Gault clay fractions were both somewhat lower than the values obtained by the ignition of the complete soils from these areas (Table 2), suggesting that some additional losses occurred in the silt fractions. This is also the case with the lateritic clay from South Africa.

### 3. PARTICLE SIZE ANALYSIS BY MICRO-SEDIMENTATION METHOD.

A more fundamental approach is to consider the size distribution and shape of the

particles in the clay fraction. Some preliminary work on these lines has been carried out at the Road Research Laboratory, using a modification of the usual sedimentation technique for particle size analysis.

For this purpose, it was first necessary to obtain some idea of the correct amount of dispersing agent to employ in order to obtain maximum dispersion. A series of experiments was therefore made in which the particle size distributions of a kaolin clay soil and a montmorillonite clay soil were determined,



Effect of sodium oxalate concentration on apparent clay content in particle size analysis of kaolinite montmorillonite clays.

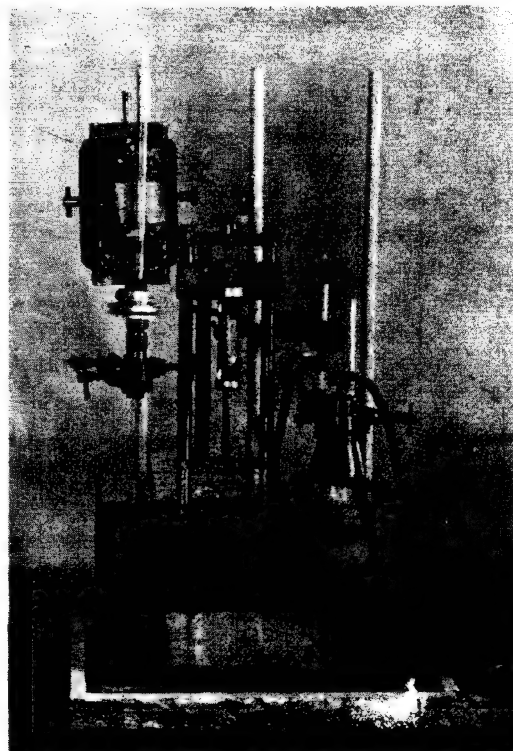
FIG.3

using varying quantities of sodium oxalate as the deflocculating agent. A series of experiments was also made with the kaolin clay using sodium hexametaphosphate for dispersion. The sedimentation analysis was done in the manner employed at the Road Research Laboratory for routine testing. In this, an Andreasen pipette is used for taking samples of a suspension containing 10 gm of soil in 500 cc.

The results of the experiments with sodium oxalate are shown in Fig. 3. The experiments with sodium hexametaphosphate are not shown, as the results obtained were almost the same as those obtained with the oxalate. It will be seen that a maximum dispersion of the kaolin clay occurred over a range of concentrations of from 0.1 to 0.4 gm of oxalate, for approximately 9 gm of clay particles. On the other hand, the dispersion of the montmorillonite clay increased slowly with the concentration of dispersing agent, until a maximum was reached corresponding to 0.9 gm of sodium oxalate for about 4 gm of clay. It appears, therefore, that unit weight of the montmorillonite clay requires about twenty times the quantity of dispersing agent needed by the kaolin to produce maximum deflocculation. It was also concluded that 0.1 gm of sodium oxalate could be used to deflocculate 10 gm of a kaolin clay of this type having a clay content in the range 22% - 90% under the experimental conditions employed. It was felt that such a generalization could not be applied to montmorillonite clays and that separate experiments to determine the optimum dispersing agent concentration are required for each soil.

The apparatus constructed for extending the particle size analysis into the clay fraction is shown in Fig. 4. The technique employed is similar to that used by Puri and Puri (4) and E.W. Russell (5).

The sampling device consists of a 10 ml.



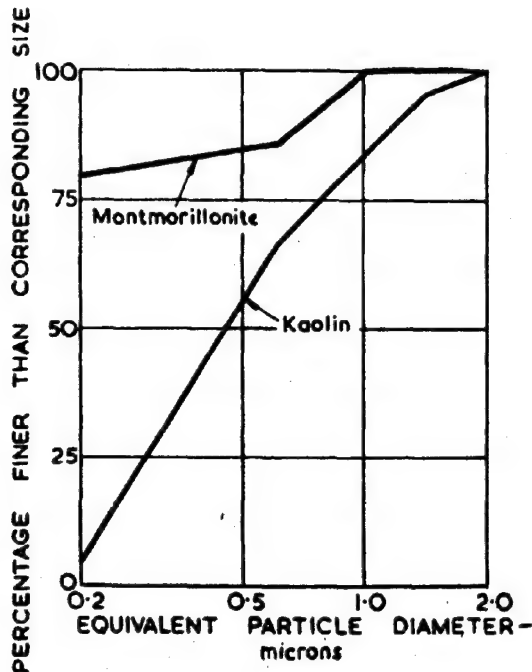
Micro-sedimentation apparatus for particle size analysis of clay soils using a hypodermic syringe.

FIG.4

hypodermic syringe, the tip of which can be set at various depths below the surface of the suspension with an accuracy of 0.01 cm. A sample of approximately 1 ml is taken from a depth of 1 cm after appropriate periods of sedimentation, and discharged into a weighed glass weighing bottle. The weight (and hence the volume) of the aqueous component of the sample is determined from the loss in weight after drying at 105°C. The weight of the solid residue is also determined, from which the volume of the solid component of the sample can be calculated, knowing the specific gravity of the particles and allowing for the presence of the dispersing agent. The concentration of the suspension in the sample is then calculated in the ordinary way, from the weight of the particles and the total volume of the sample.

This technique has been compared with the normal method for particles of 0.006 mm and 0.002 mm equivalent diameters, and the two procedures were found to give results that differed by not more than 1% of material in the case of two soils investigated. The accuracy of the syringe was found to be of this order even at sampling depths of 2 mm.

In a preliminary investigation the method was used to determine the size distribution in the coarser part of the clay fractions of the kaolin and montmorillonite clays previously referred to. The quantities of sodium oxalate employed for deflocculation were those giving maximum dispersion. The results (Fig. 5) show the size distribution in the range



Size distribution in clay particles from kaolin and montmorillonite soils.

FIG. 5

2.0 - 0.2 microns equivalent particle diameter (1 micron = 0.001 mm). It will be seen that the particle diameter decreased very rapidly in the kaolin clay below 2.0 microns, but that about 80% of the montmorillonite particles were smaller than 0.2 microns equivalent diameter.

#### 4. ELECTRON MICROGRAPHS OF CLAY PARTICLES.

Attempts have been made to study the shape and size of particles of clay by means of the electron microscope, and for this purpose the Metallurgical Division of the National Physical Laboratory has taken 48 photographs of clays from eight British soils supplied by the Road Research Laboratory. Samples of the fraction having equivalent particle diameters smaller than 2 microns were prepared from the complete soils by sedimentation. For the examination, a small quantity of this material was shaken up in a N/100 sodium citrate solution, a drop of which was allowed to dry on the thin nitro-cellulose film that forms the object support in the microscope. The dispersing agent was then removed by washing the specimens in distilled water.

Figs. 6 and 7 show the photographs obtained with clay fractions from five different localities, the lines at the side of each photograph representing a length of 2 microns at the magnification given. Sharp outlines were in general only obtained with the larger particles (>1μ) but the thin plate-like nature of the particles is evident from the transparent images. However, in spite of the blurred nature of the outlines, two facts may be noted regarding the larger particles. One is the frequent occurrence of the 120° interfacial angle at the crystal edges, which may be found in all the photographs to some extent, but which is particularly visible in the samples from Cheddington (6c) and Brentwood (7d). The resulting similarity to micrographs of china clay and kaolin obtained both at the National Physical Laboratory and elsewhere, suggests that a proportion of kaolin-type minerals may be present in all the clays examined, and although the evidence is inconclusive it tends to support the evidence obtained from the loss on ignition determinations. More experimental work is required, however, before definite conclusions can be reached. The second point of interest is the occurrence of rod-shaped particles in the samples from Cheddington (6c) and Brentwood (7d), four such particles being distinctly visible in the latter. The large elongated particle in Fig. 6c which is 0.8μ long is very similar to the particles of halloysite shown by Shaw and Humbert in a recent paper to the American Society of Soil Science (6).

#### ACKNOWLEDGEMENT.

The work described in this paper was carried out at the Road Research Laboratory of the Department of Scientific and Industrial Research as part of the programme of the Road Research Board. The paper is presented by permission of the Director of Road Research.

#### REFERENCES.

- 1) Standard method of test for Liquid Limit of soils. A.S.T.M. designation: D.423-39. A.S.T.M. Standards Part II. Non-metallic materials - Constructional. The American Society for Testing Materials, Philadelphia, Pa., 1944 (The Society).
- 2) Standard method of test for Plastic Limit

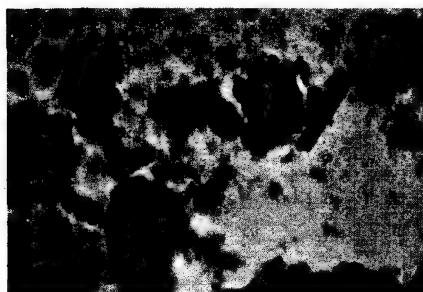




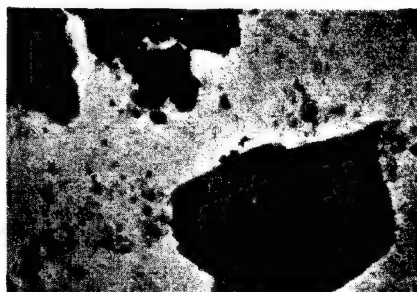
(a) Selby, Yorks x 13.000



(b) Selby, Yorks x 9.000



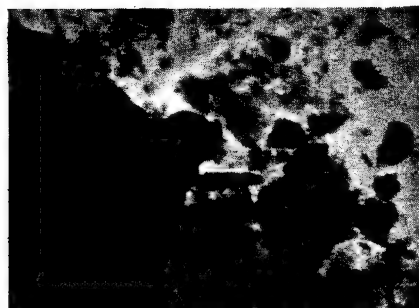
(c) Cheddington, Bucks x 15.000



(d) Cheddington, Bucks x 9.000

Electron micrographs of the 2 equivalent  
particle diameter fraction of some English clays.

FIG.6



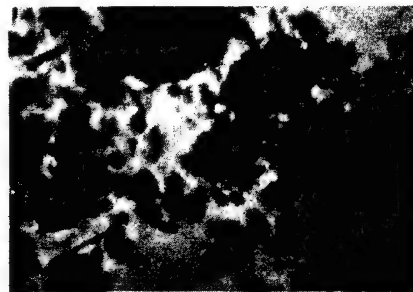
(a) Maidstone, Kent x 13.000



(b) Maidstone, Kent x 9.000



(c) Laindon, Essex x 13.000



(d) Brentwood, Essex x 9.000

Electron micrographs of the 2 equivalent  
particle diameter fraction of some English clays.

FIG.7



- And Plasticity Index of soils. A.S.T.M. designation: D.424-39. A.S.T.M. Standards. Part II. Non-metallic materials - Constructional. The American Society for Testing Materials Philadelphia, Pa., 1944 (The Society).
- 3) Classification and Identification of Soils. Casagrande, A: Proc. Am. Soc. Civ. Eng. 1947, 73, pp. 783-810.
- 4) Ultra-mechanical analysis of soils: Puri, A.N., and B.R. Puri: J. Agric. Sci., 1941, 31, 171-7.
- 5) The Sub-division of the clay fraction in mechanical analysis: Russell, E.W.: J. Agric. Sci., 1943, 33 (3), 147-54.
- 6) Electron micrographs of clay minerals: Shaw, B.T., and R.P. Humbert.: Proc. Soil Sci. Amer. 1941, 6, 146-9.

-0-0-0-0-0-0-

## SUB-SECTION II b

### IDENTIFICATION TESTS

#### II b 1

#### AN EXPERIMENTAL STUDY OF THE MAXIMUM AND MINIMUM POROSITIES OF SANDS

J.J. KOLBUSZEWSKI DIPL.ING.

Imperial College, University of London

#### INTRODUCTION.

This paper presents the results of research to determine limiting porosities for any given sand.

These limiting porosities (maximum and minimum) if obtained by simple and reliable methods should provide convenient and useful values not only for the description of a sand but should serve as criteria for its expected behaviour, in other words should provide the same sort of comparable values as Atterberg's limits in case of clays.

It may, for example, be known that the porosity of sand in the field is  $n\%$ , but by itself this value conveys little, and for its significance to become apparent it must be related to the maximum and minimum porosities at which the sand can exist in stable packing.

The main factors which have been considered in this study include the size of measuring vessel, the rate of pouring, the difference between pouring in air and water, the influence of tamping and vibration. Many tests were run to study these factors and the results were averaged so as to assure representative values. Every effort was made to keep all other minor variables constant (temperature, moisture content).

In all experiments special care was taken to repeat exactly the developed techniques.

A limited number of tests have been run to obtain supplementary information.

It must be clearly recognized that some of the results will require further investigation in order to complete the general picture of the research since this appears to be a first attempt to deal systematically with this problem.

#### THE SAND SAMPLES.

The sands which have been used are as follows:

1. Leighton Buzzard 18 - 25 B.S.S.
2. Stone Court 18 - 25 B.S.S.

3. Stone Court 52 - 100 B.S.S.
4. Stone Court Medium-Uniform
5. Stone Court Well-graded
6. Ham River 25 - 52 B.S.S.

Fig. 1 shows grain distribution curves for all of these sands. The roundness and sphericity of the grains were determined by inspection of the projected shapes, as outlined by KRUMBEIN 8) and 9).

S A N D	Mean Roundness	Mean Sphericity
1. Leighton Buzzard 18 - 25	0'5	0'840
2. Stone Court 18 - 25	0'3	0'803
3. Stone Court 52 - 100	0'3	0'787
4. Stone Court Med.-Unif.	0'3	0'800
5. Stone Court Well-Graded	0'3	0'786
6. Ham - River 25 - 52	0'4	0'772

Specific gravities of the Sands are:

- Leighton Buzzard 2'6  
Stone Court 2'7  
Ham River 2'7

Other Sands have been used for checking the results and techniques.

#### LOOSE PACKING.

##### Pouring in Air.

At an early stage of the research it was found that quick pouring of the same quantity (weight) of sand through air results in higher porosities than those obtained by slow pouring.

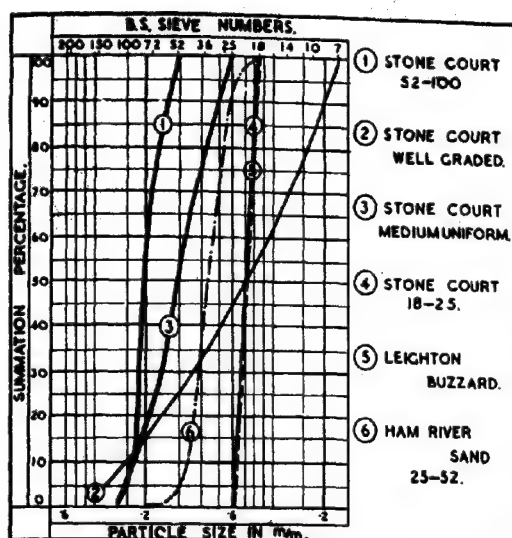
A series of tests thus were carried out and special techniques developed to investigate the rate of pouring through air.

The final technique was as follows:

1. Apparatus (see diagram No. 2)

The apparatus consisted of the following:

- a) A series of paper funnels perforated to provide an uniform rain of sand partic-



Sands used in the experiments.

FIG. 1

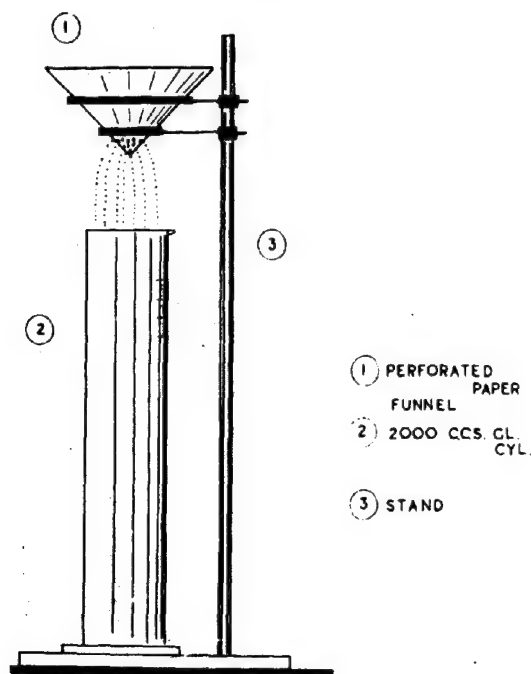


FIG. 2

les and permitting control of the time of pouring.

b) Glass graduates.

- i) volume 1000ccs. having 2" in diameter
- ii) volume 2000ccs. having 3" in diameter

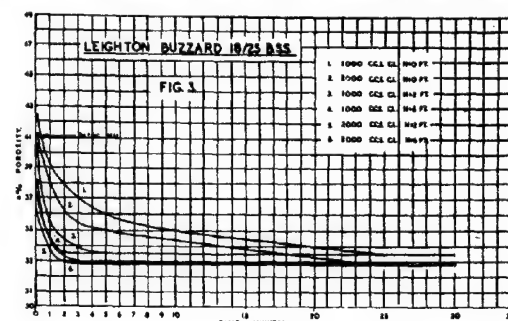
c) Laboratory stand with funnel support, suitable for changing height of pouring from 0 to 6 feet.

## 2. Procedure.

A sample weighing 1000gms. taken from the

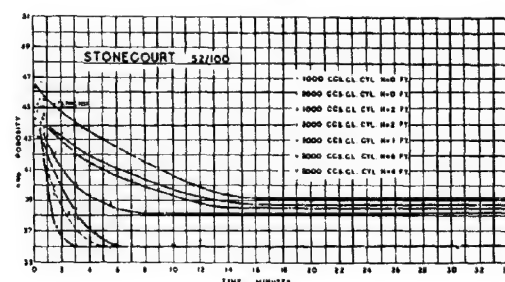
thoroughly mixed portion of the air-dried sand was poured through the funnels from different heights. Time of pouring and volume obtained were recorded. The weight of sample was recorded after the experiment and the porosity calculated. Each test has been repeated not less than 10 times and mean value calculated.

The results obtained for three of the 6 above mentioned sands are represented in this paper by figures No. 3, 4, 5, where porosities



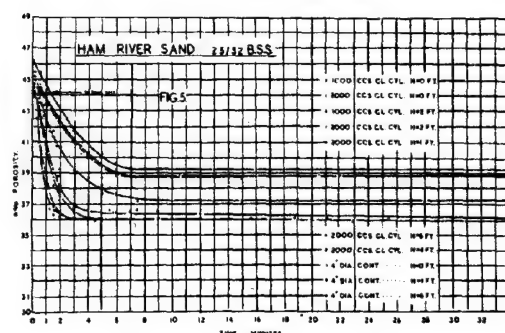
Leighton Buzzard 18/25 B.S.S.

FIG. 3



Stonecourt 52/100

FIG. 4



Ham river sands 25/52 B.S.S.

FIG. 5

have been plotted against time of pouring for each height of pouring.

Undoubtedly the Leighton Buzzard Sand showed the greatest response to small changes of time of pouring and was the most difficult material from the point of view of repeating results. This seems to be very important as

Leighton Buzzard Sand is being used as a Standard for field volume and other measurements.

The more angular Stone Court and Ham River sands were more satisfactory from this point of view and generally speaking sands possessing high roundness and high sphericity appear to be more sensitive than those with both values of lower degree.

As has been mentioned it is very important that the technique should be exactly repeated. Any slight disturbances during the test - for example when taking readings of volume-may disturb sand structure and give inaccurate results.

It will at once be seen from Figs 3, 4 and 5 that the rate of pouring and the height of drop have a profound influence on the porosity. For any given height of drop the porosity decreases with time of pouring, to some limiting value, and this limiting value itself tends to decrease with increasing height of drop, at least up to 6 ft. Indications were obtained that further increase in height produced little or even negative effects.

These phenomena appear to be of considerable importance, especially in laboratory work on sands, and they are at present being more fully investigated. The porosities obtained in 1000ccs. glass cylinder (2" dia) are in general slightly higher than those obtained in 2000ccs glass cylinder (3" dia). This was investigated separately and is reported below.

Since it had been shown that the porosity increased with decreasing time of pouring it was decided after discussion with Prof. Skempton to try a very simple technique involving the following procedure:

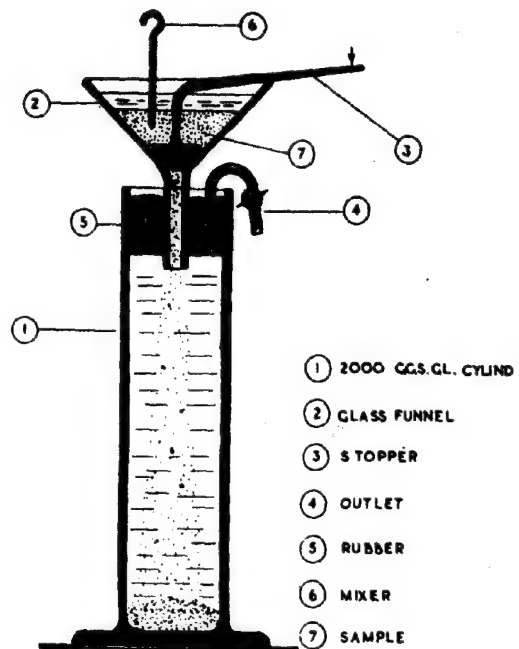


FIG. 6



a



b

FIG. 7

Place 1000gms. of sand in a 2000ccs. cylinder (3" dia) and place a stopper in the top of the cylinder. Tip the cylinder upside down, and then quickly tilt it back to its original vertical position. The porosities obtained in this way corresponded reasonably closely to the limit towards which the curves in Figs 3, 4 and 5 are tending for zero time of pouring. The test can be easily repeated many times and it is therefore suggested that it could be adopted as a standard method for obtaining the loosest packing. As will be seen later very slightly greater porosities can be obtained by depositing the sand through water, but the differences are not important from a practical point of view.

#### Pouring in Water.

Ordinary tap water was used for this part of experiments, having room temperature. The range of temperature in the laboratory was very small and could not have any effect in the results. It is necessary to point out that the effect of comparatively big changes in temperature, in this part of tests, was not investigated.

Attention was given to the effect of entrapped air when pouring sand through water and a special device was developed for pouring without air (see Fig. 6).

The results obtained by pouring sand through water with (Fig. 7) and without entrapped air are shown on Fig. 8. In all cases

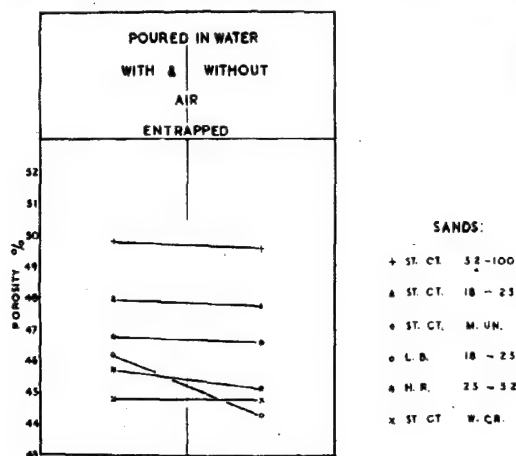


FIG. 8

the porosities are lower when no air has been trapped, but the differences were not great except for Leighton Buzzard Sand, possessing high roundness and high sphericity which shows again "sensitiveness".

It has been noted that in case of Leighton Buzzard Sand the air bubbles (see Fig. 9) are being formed not only at the surface of the water, where the surface tension is broken by grains, but some of the grains are adsorbing air from water when at comparatively big depth in the vessel. That phenomenon was not noted in the case of other sands and the author is of the opinion, that this may be explained by assuming that the more equal distribution of surface molecular forces, in the case of grains with high sphericity, enables the air dissolved in water to form bubbles around sand grains.

The stability of sand structure formed



FIG. 9

in water with and without entrapped air has been investigated. Results obtained showed: a) water moving slowly downwards in the container, after the sample has been settled, does not affect structure of the sample at all and leaves porosity unchanged, and that b) slight movements of the water upwards caused a decreasing of porosity to a certain constant value for each sand.

That was investigated in the device represented in Fig. 10.

The effect described under b) the author explains as in Fig. 11 which shows how arches formed by sand grains are being destroyed by water moving upwards.

The author feels that the porosities obtained with entrapped air are to some extent "artificially" high, and that the more fundamental result is that obtained by depositing the sand without this air. Although the difference between the results obtained by this technique and by rapid pouring in air are not very large, the former gives somewhat higher porosities and the results are probably the closest approximation to the loosest packing so far obtained, but this does not alter the suggestion, made above, that the "tipping" test should be used as a standard for the loose state, since the differences are not large and the tipping test is so very simple.

A limited number of tests were run to study the porosities of sands poured through a solution of bentonite (1.2 gms/100ccs) and the results obtained showed no essential difference in comparison with pouring through ordinary water. This should not be regarded as a final result and further investigations

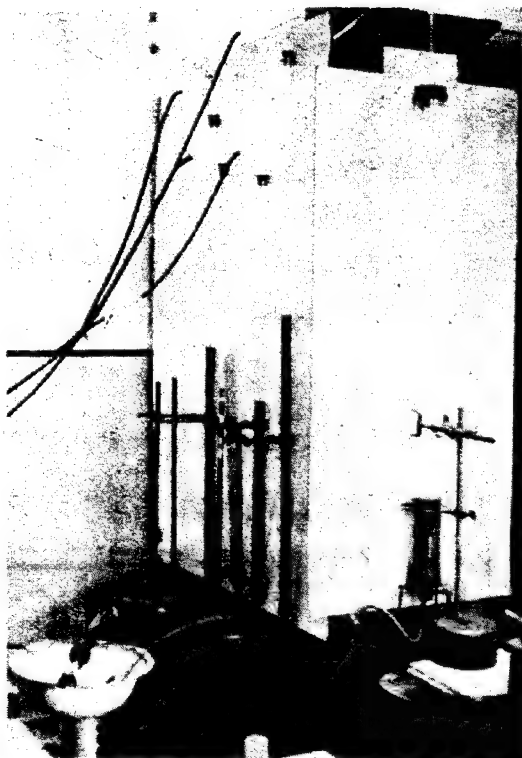
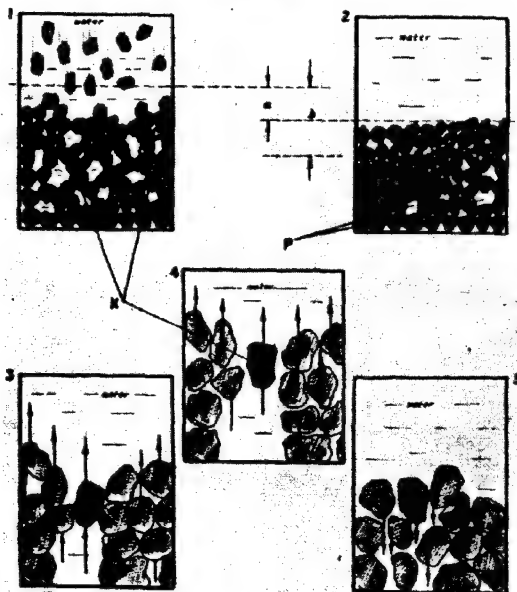


FIG.10



Pouring in water.

FIG.11

should be made in future, especially with fine sands.

#### Influence of the size of the Container.

The following containers were used in

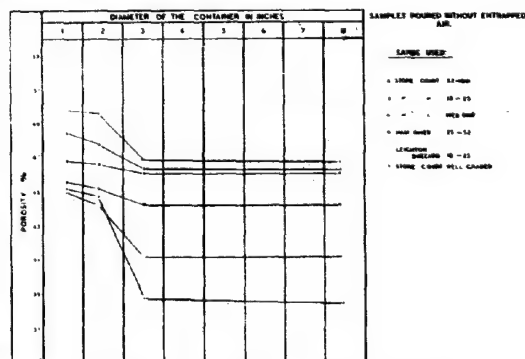
the above described experiments:

- 1" dia glass tube
- 2" dia 1000ccs glass cylinder
- 3" dia 2000ccs glass cylinder
- 3" dia glass tube
- 8" dia glass vessel

It was found that in all techniques, whether dry or wet, the porosity decreases when the diameter of the container increases and that changes are bigger in case of containers having the diameter smaller than 3 inches.

In case of diameters bigger than 3 inches changes are very small and it can be, in the authors opinion, assumed for practical purposes that for sand work the vessels 3" in diameter can be used and the influence of the container neglected.

Fig.12 shows the influence of the containers' diameter in the case of pouring sands without water without air.



Influence of size of the container.

FIG.12

The influence of the container has been mentioned by other investigators and is usually explained by the wall friction (14).

Observing the sand grains falling through water in vessels of 1, 2 and 3 inches in diameter the author was not convinced that comparatively big changes in porosity could be caused by wall friction: firstly because the experiment can be carried out in such a way that practically no grains will touch the walls of the container. Yet in all cases influence of the container was distinctly noted.

At the beginning of the research an experiment with packing of ideal spherical grains showed that large empty spaces may be established, tridimensional arching supported by the walls occurring. That sort of arching is easier in case of smaller containers and therefore gives higher porosities. That explanation, in case of grains with  $\frac{1}{2}$  inch diameters and 1, 2 & 3" dia containers is easy to understand, but in case of small sand grains also appeared to be insufficient. Finally when powdered mica has been introduced to the experiments it was noted that during the settlement of particles in the water some very characteristic vertical channels were formed, through which water from the bottom of the container moved upwards, being replaced by the settling material. The amount of the channels is always bigger in case of a smaller container when the same quantity of material is settling and in case of a large container only a few of those channels occur. It was also found that these channels remain in the settled material after the end of the



settling proces. It was observed that in case of very fine sand (100 - 150 B.S.S.) the same sort of channels are in operation but cannot be clearly seen after the end of settling process.

The author suggests that different amounts of those vertical channels are affecting porosities in different containers. Fig. 13 diagrammatically shows the described process.

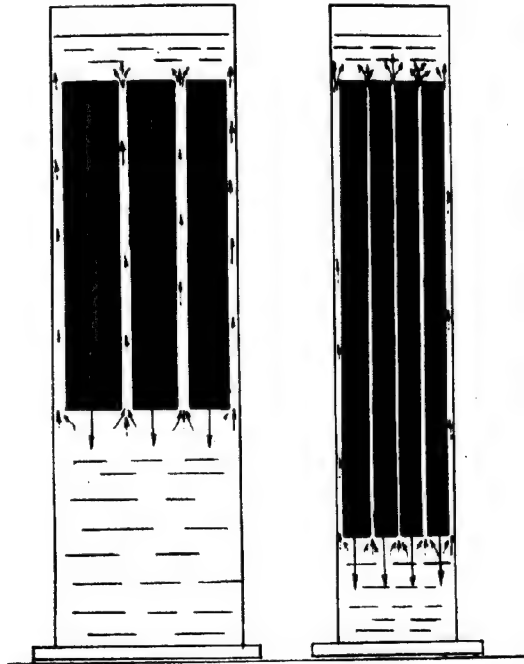


FIG.13

#### Influence of the Inclination of the Container.

It was found that the inclination of the container affects porosity in the following way:

##### 1) Pouring in Water inclined.

All sands formed lower porosities. In case of Well Graded Stone Court differences obtained were comparatively big.

##### 2) Pouring in Air inclined.

Generally gives very slightly higher porosities than when poured vertically. Increased speed of pouring increase porosity in all sands except in case of Well Graded sand where distinct lowering of porosity has been observed when the sand was poured quickly.

The different behaviour of Well Graded sand is explained by diagram No.14, where four techniques of producing porosity are represented.

No. 1 shows structure of sand sample built by pouring vertically in water. No. 2 shows how sand poured in water into the inclined container forms a comparatively denser structure because smaller floating particles are filling small gaps formed by bigger grains sliding on sample's surface.

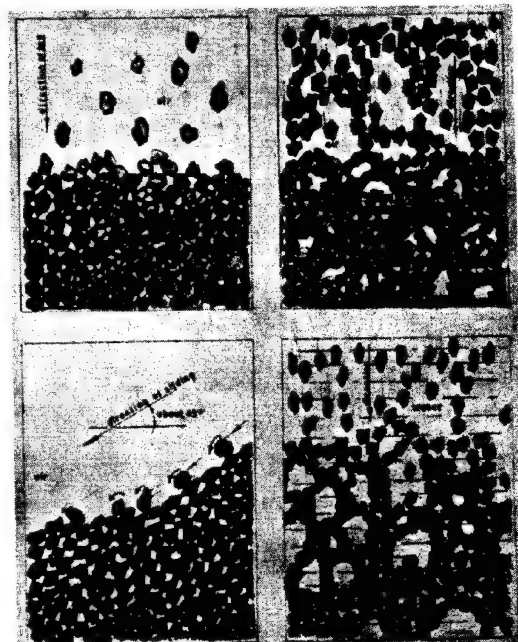
No. 3 shows how a moving part of quickly poured sand presses the stable part of sample and causes bigger density.

Slowly poured Well Graded sand in technique No. 4 builds itself into a looser structure. In case of uniform sands inclination is, in contrast, very much less important.



Stone court well-graded.

FIG.14



Structures caused by different techniques.

FIG.15

Fig. No. 15 explains generally how loose structures of sands are produced by: 1) slow pouring in air, 2) quick pouring in air, 3) pouring inclined and 4) pouring in water.

**DENSE PACKING.**

For obtaining dense packing following techniques were used:

1. Hand tamping and vibrating
2. Proctors compaction cylinder
3. Vibrating table
4. Pneumatic and electric hammers.

1. Results obtained in glass cylinder by
  - a) tamping dry sand with hand tamper in 100 ccs layers, 100 times each layer,
  - b) tamping dry sand by hand tamper as under a), and vibrating by hand each layer 10 times,
  - c) tamping by hand in water each 100 ccs layer 100 times
 are shown on Fig. 16

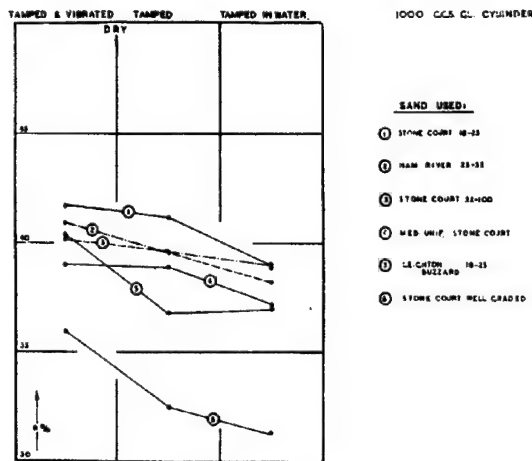


FIG.16

2. Results obtained in Proctors' Compaction Cylinder by tamping with 5 lbs. rammer having 12" drop
  - a) applying 25 blows of the rammer at the top of the dry sample,
  - b) applying 50 blows of the rammer at the top of the dry sample,
  - c) applying Proctors' Standard procedure, varying water content obtain maximum density,
 are shown on Fig. 17.

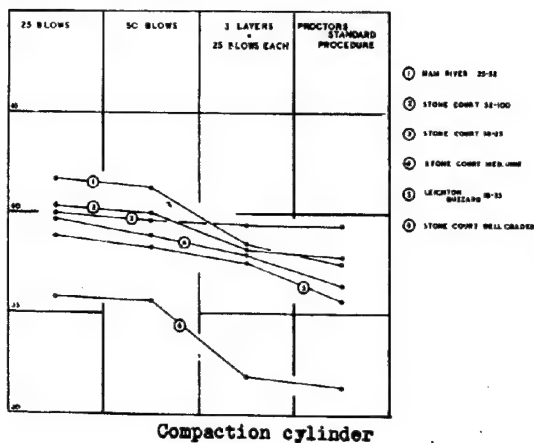


FIG.17

3. Results obtained by vibrations in steel compaction Cylinder (Proctors' type) on the vibrating table

- a) pouring dry sand quickly into the container during vibration,
- b) pouring dry sand slowly into the container during vibration,
- c) tamping during vibration with 5 lbs rammer in 3 layers 25 times each layer,
- d) vibrating with 25 lbs load at the top of the sample,

are represented on Fig. 18.

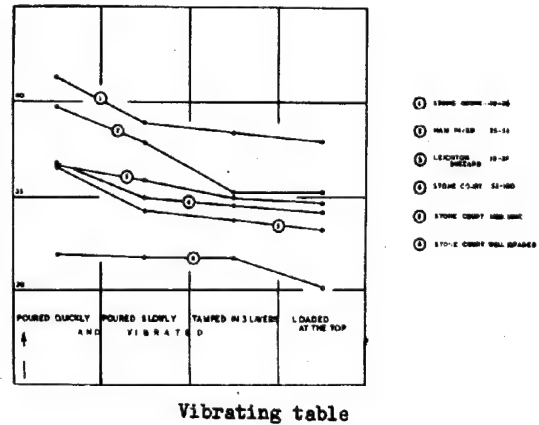


FIG.18



FIG.19



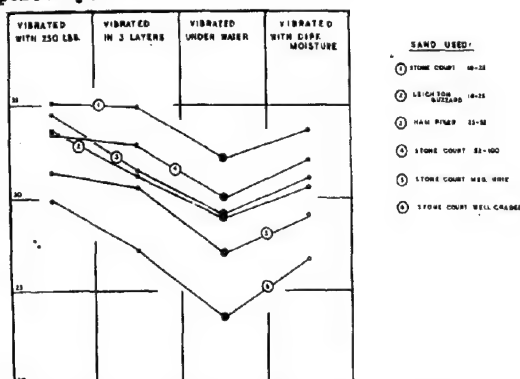
#### 4. Results obtained by vibrations in steel compaction cylinder with Pneumatic and Electric hammers

- vibrating in 3 layers dry sample for about 15 minutes each layer,
- vibrating dry sand with load (250 lbs) at the top for about 15 minutes (Fig. 19),
- vibrating sample in 3 layers for 15 minutes each layer and repeating test with different moisture contents,
- vibrating sample in 3 layers, 15 minutes each layer, submerged in water,

are shown on Fig. 20 (No crushing of grains occurred in any of those tests).

Graphs No. 16, 17, 18 and 20 show that lowest porosities were obtained by vibrations under water.

This procedure is here suggested tentatively for obtaining lower limiting state of sands porosity.



Vibrations pneumatic and electr. hammer

FIG.20

#### CONCLUSION.

It is tentatively suggested that following procedures be used for obtaining limiting porosities of sands:

1. Loose 1000 gms of dry and thoroughly mixed sand should be placed in 2000 cc glass cylinder and a rubber stopper should be put on the cylinder. The cylinder with the sample should be shaken a few times and turned upside down, then very quickly turned over again. Volume of the sample should be read and porosity calculated ( $P_{max}$ ).

Experiments have shown that porosities thus obtained are not very different from those obtained by pouring in water without entrapped air (see Fig. 21 and Figs 3,4,5,).

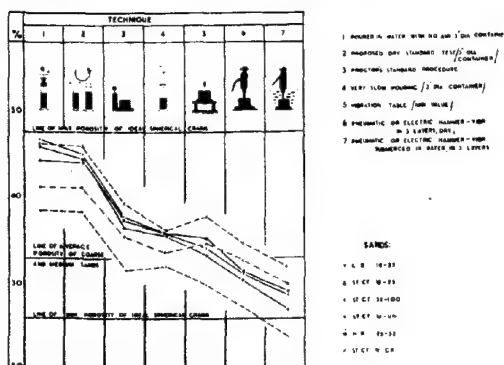


FIG.21

#### 2. Dense. Compaction Cylinder (Proctors' type)

should be placed in the water tank and sand sample should be vibrated in 3 layers (15 minutes each layer) with pneumatic or electric hammer ("Kango hammer" type).

1/30 cu.ft. sample should be thus obtained and porosity calculated ( $P_{min}$ ).

Porosity of sand found in the field be expressed in terms of Maximum and Minimum Porosities and be called Relative Porosity.

#### ACKNOWLEDGEMENTS.

The work described has been carried out during the years 1945 - 1947 in the Soils Laboratory of the Imperial College, University of London.

The author would like to express his gratitude to Prof. A.J.S. Pippard D.Sc., M.I.C.E. Head of Civil Engineering Department for permission granted in 1944 to start research in the College. The work has been directed by Asst. Prof. A.W. Skempton M.Sc., A.M.I.C.E. to whom the author is indebted for his most valuable suggestions, encouragement and constant help.

#### BIBLIOGRAPHY.

- Bagnold R.A., The Physics of Blown Sand and Desert Dunes, London 1941.
- Burminster D.M., A Study of the Physical Characteristics of Soils - with special Reference to Earth Structures, Columbia University, 1938.
- Fraser H.J. Experimental Study of the Porosity and Permeability of Clastic Sediments, Journal of Geology, Vol. XLIII, No. 8, P.I. Nov. Dec. 1935, p.p. 910 - 1010.
- Harper H.J. & Volk G.W., A method for Microscopic Examination of the natural structure and Pore space in Soil, Proc. Soil. Sci. Soc. Am., 1936 - 39 - 42.
- Hatch T. & Choate S.P., Statistical description of the size properties of non-uniform particulate substances, I. Frank Inst., 1929, 207, 369 - 87.
- Glossop R. & Skempton A.W., Particle Size in Silts and Sands, Inst. of Civil Eng. London, 1945.
- Green H., The effect of non-uniformity and particle Shape on "Average Particle Size", I. Frank Inst., 1927, 204, 713-29.
- Krumbein W.C., Measurement and Geological Significance of Shape and Roundness of Sedimentary Particles, Journ. of Sed. Petrol. Vol. II, No. 2, 64-72, 1941.
- Krumbein & Pettijohn, Manual of Sedimentary Petrology, The Century Earth Science Series, Appleton Century.
- Loos, Comparative Studies of the Effectiveness of Different Methods for compacting cohesionless Soils, Proc. of the Int. Conf. on Soil Mech. June 22-26, 1936.
- Martin G., Research on the theory of fine grinding. Law governing the connection between the number of particles and their diameters in grinding crushed sand, Fr. Brit. Ceram. Soc. 1923, 23, 61 - 109.
- Rittenhouse G., A Visual Method of Estimating Two Dimensional Sphericity, Journ. of Sed. Petrology, Vol. 13, No. 2, pp. 79 - 81.
- Terzaghi Karl, Theoretical Soil Mechanics, 1943.
- Tschebotariof G.P., Effect of Vibrations on the Bearing Properties of Soils, Highway Research Board, Proc. of the 24th annual meeting, Washington 1944, p. 404 - 425.
- Graton L.C. & Fraser H.J., Systematic Packing of Spheres with particular Relation to Porosity and Permeability, Journal of Geology Vol. XLIII, No. 8, P.I. Nov. Dec. 1935, p.p. 785 - 909.

## SUB-SECTION II c

CONSOLIDATION TESTS

## II c 1

SECONDARY TIME EFFECT IN THE COMPRESSION OF UNCONSOLIDATED  
SEDIMENTS OF VOLCANIC ORIGIN

ARRIGO CROCE

Italy

INTRODUCTION

The foundation soils of broad areas of Italian Peninsula consist mainly of volcanic non-cemented or slightly cemented materials.

These materials, ejected in cenozoic era or in the present one by the many volcanoes along the Thyrrenian coast, were often carried by the wind in lands very far from their origin. Sometimes the running water worked on the deposits so formed and, mixing volcanic materials with other kind of products, made them settling as soon as the water speed went slowing down.

Important built-up areas, as ROME and NAPLES, mostly lay on soils of this kind.

Similar conditions occurred in other lands of the globe and, hence, similar foundation problems must arise there. That is why we believe it could be useful to expose to the Congress some observations on the behaviour of such materials which, as far as we know, have not yet been observed from the mechanical point of view.

Our observations have been done by studying the foundation soils of the town of NAPLES which, as is known, lays between the two important volcanic districts of VESUVIUS and CAMPI PLEGREI.

The cohesionless volcanic materials, which can be found in this area, are composed by grains of very different size. However, they have two common characteristics:

- 1) The main part consists of isotropic substance (volcanic glass);
- 2) this isotropic substance has a spongy texture particularly notable in pumices.

Consequently grains may be easily broken.

The various deposits formed by such materials differentiate in particle-size distribution and in the rate of porosity of the volcanic glass. Furthermore, it may happen that the material has undergone rock decay; but in the volcanic district we are speaking of, material is generally unaltered or altered at a very low rate. At last we can find in the above materials a certain amount of organic substances.

Difficulties may arise in studying foundation problems in such soils, owing to the fact that only in few cases we find homogeneous beds of a notable thickness; but very often the soil consists of a series of very thin beds (some centimeter). Constituent materials have a different particle-size distribution and sometimes they did suffer a high rate of diagenesis until they reached a remarkable stage of lithification.

While carrying on our researches in order to have an almost large view of the behaviour of such materials under the load of buildings, we believe interesting to call attention on a peculiar phenomenon we have repeatedly observed either on undisturbed or on disturbed samples of different origin.

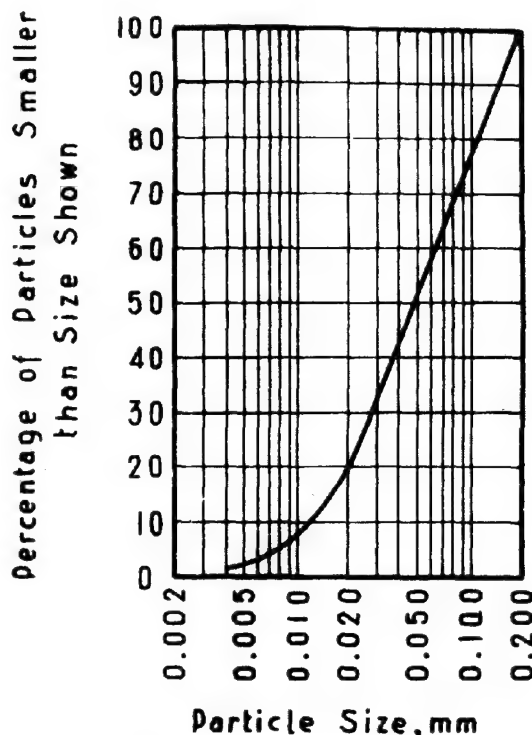
DESCRIPTION OF TESTS

In order to facilitate comparisons, we will expose results of a confined compression test on a typical volcanic material, the so called "pozzolana di BACOLI". The tests have been performed on the fraction passing the 0,2 mm sieve.

The particle-size distribution is shown in fig. 1. The mechanical analysis has been done with sieves down to 0,07 mm diameter. For smaller fractions Andreasen pipette has been used, distilled water being the dispersion medium.

As shown, the grain size accumulation curve mainly develops in the fine sand fraction.

The grains composing the material under test are fragments of angular volcanic glass (fig. 2) sometimes compact and clear, more often porous for holes caused by the expansion and escape of gases from the interior of the magma piece, while this late was rapidly cooling. These holes are variously shaped; often they are considerably long and minute and have



Grain size accumulation curve

FIG. 1



Photomicrograph showing different textures of grains.

FIG.2

no external outlets. The texture is more or less spongy, according to the frequency and dimensions of the holes.

On the basis of the particle-size distribution and microscopic analysis, it can be rejected that in the tested material there was any appreciable content of clay substance.

The confined compression test has been done on a test sample of 56,2 mm diameter and 20 mm initial thickness, fitted upside and downside with drainage porous stones. The

used extensometer permitted to evaluate settlements until 1/500 mm. The successive applied loads were in  $\text{kg/cm}^2$ :

0,04; 0,015; 0,19; 0,50; 1,00; 2,01; 4,02

The settlements  $s$  and the time  $t$  are plotted in fig. 3 for some values of the applied pressure  $p$ ; either time and settlement have been measured from time-moment in which the last load increment was applied. Drawings show that:

- 1) About one half of the settlement occurs in a very short time, less than 30 sec.
- 2) Consecutively the settlement proceeds approximately straight with the  $\ln t$ .
- 3) Lately this straight development shows a trend to change in slope towards the final setting (see the last points of graph).

The phenomenon described in 1 and 2 can be expressed by the relationship:

$$s = a + b \cdot \ln t$$

Coefficients  $a$  and  $b$  have been calculated by the method of least squares and following results obtained:

applied load $\text{kg/cm}^2$	$a$ mm	$b$ mm	probable error mm
1,00	0,0812	0,00830	0,0009
2,01	0,1054	0,01051	0,0010
4,02	0,1276	0,01280	0,0009

With the falling head permeameter the permeability coefficient  $k$  has been measured at various loads. Values of  $k$  are shown in the following table, together with inverse values

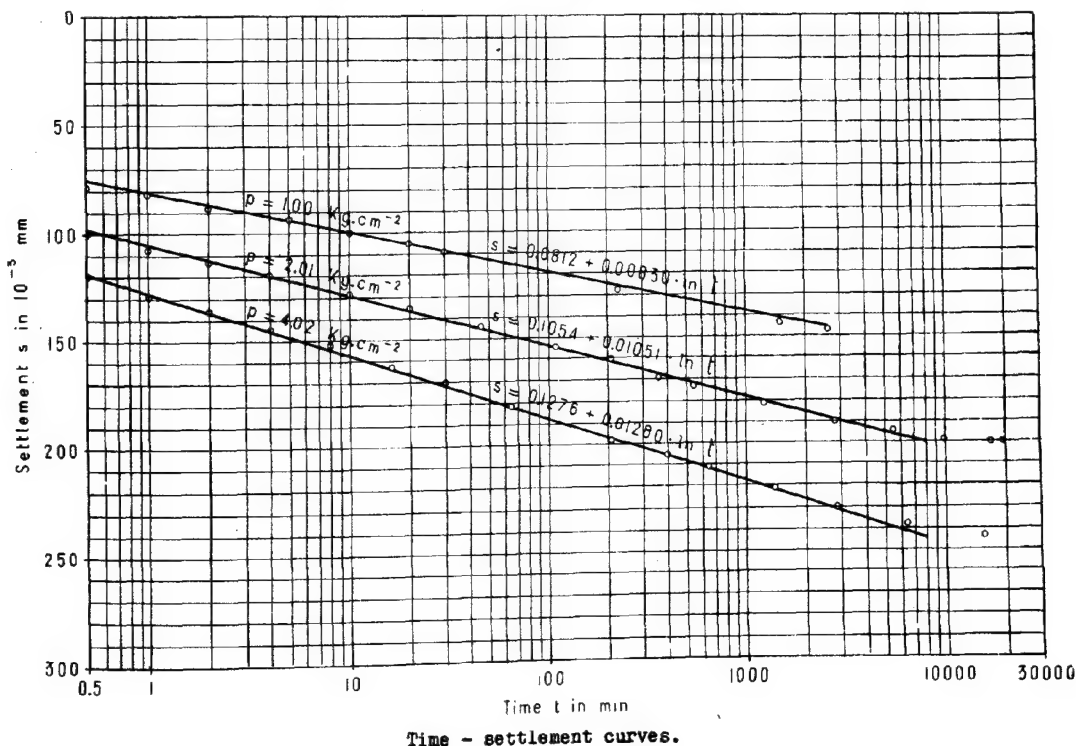


FIG.3

of moisture specific loss  $v$ , reckoned according to the final settlement observed.

applied load Kg/cm <sup>2</sup>	k cm/min	1/v Kg/cm <sup>2</sup>
1,00	$3,72 \times 10^{-4}$	63
2,01	$2,47 \times 10^{-4}$	91
4,02	$1,60 \times 10^{-4}$	147

#### DISCUSSION

According to our present knowledge on the progressive settlement of soil samples subjected to a constant load in a consolidation device, two typical schemes are usually distinguished:

- 1) Sand The necessary time for the final adjustment of grains is very short and can be generally neglected.
- 2) Clay The time, required for reaching the test sample equilibrium under the applied load, is quite long. Up to the first half of yielding, the time-settlement curve has a typical trend that, with much approximation, is explained by the well known TERZAGHI's theory of consolidation. This part of the phenomenon is called primary time effect. Beyond this, the time settlement curve is almost straight, when time is plotted on logarithmic scale. This is called secondary time effect and was particularly observed in clays with a certain amount of organic substances.

Volcanic material, we have tested, certainly is not a clayey material, for its grain size distribution, as for its mineralogical composition. Yet, under constant load, it reaches the final settlement with a remarkable slowness and, for this respect, behaves like a clay.

Since TERZAGHI's theory of consolidation is applicable both to sands and clays, it is interesting to ascertain if the observed phenomenon of compression could be a primary time effect and then interpreted by such theory. The fact that the actual settlement  $s$  is a linear function of  $\ln t$  shows immediately that the theory of consolidation is not applicable to the observed process. In order to illustrate this point, we have plotted in Fig. 4 the theoretical consolidation curve, expressed by means of the dimensionless variables:

$$\begin{cases} \sigma = \frac{s}{s_1} & (\text{degree of consolidation}) \\ T = \frac{c}{H^2} t & (\text{time factor}) \end{cases}$$

where:  $s_1$  indicates the final settlement produced by the load increment;

$c$  the coefficient of consolidation given by  $\frac{k}{\gamma v}$ , where  $\gamma$  is the unit weight of water;

$H$  the half thickness of the test sample.

If we express the empirical relationship we have found for our volcanic material through the above dimensionless variables, we obtain the straight lines of fig. 4. The observed phenomenon develops within an interval of values of the time factor  $T$ , which is clearly subsequent to the range of values of  $T$ , which limits the primary time effect. We believe, therefore, that the process of compression, we have experimentally noticed, must be considered as a secondary time effect. Likely, a primary time effect, as conceived in the theory of consolidation, took place in our test in a time inferior to 30 sec.

#### CONCLUSIONS

Our observations lead us into the opinion that unconsolidated sediments of volcanic origin, although they have, when unaltered, no petrographic characteristic in common with clayey materials display a secondary time effect like that of clays. Furthermore, it is possible that in the compression of volcanic materials a primary time effect takes place also. Nevertheless, some peculiarities for these materials have to be emphasised: the primary time effect, owing to the high permeability of such materials, occurs in a negligible time and is difficult to reveal by observation. Probably it could agree with the theory of consolidation. From technical standpoint this effect is of small importance on account of its quickhappening: the secondary time effect develops slowly in time and can be easily noticed by way of experiments. The settlement due to this part of the compression process may not be disregarded in comparison to the settlement corresponding to the primary time effect.

Some other experiments have been undertaken to throw more light on the subject. Since the laws, that rule the moisture movements, can also decisively influence soils accommodation process, as the theory of consolidation has clearly shown for clays, we intend to mea-

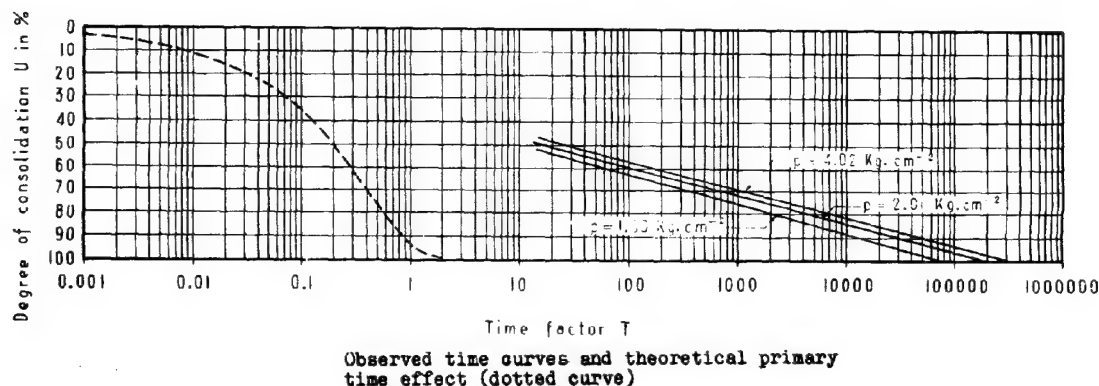


FIG.4

sure the pore water pressures in function of time.

Moreover, remounting to causes of the phenomenon now called secondary time effect, it seems that material's nature should be of

peculiar importance, and precisely its brittleness and the fact that possibly, on account of breaking of single grains, the volume of solid constituents of the soil may be no more considered as constant.

-0-0-Q-0-0-0-

|| c 2

### CONSOLIDATION TESTS ON SOILS CONTAINING STONES

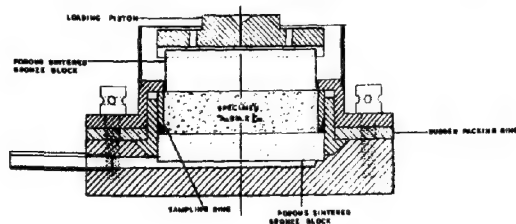
L.J. MURDOCK, Ph.D., M.Sc., A.M.I.C.E.

The test normally adopted in the determination of the consolidation characteristics of a soil, utilises a specimen of 3 inch diameter and approximately  $\frac{1}{2}$  inch thick. This thin specimen is used and drainage allowed both from the top and the bottom, in order to shorten the time required for the test.

Soils containing stones, e.g., boulder clays, are common to many parts of the world and estimates of settlement under load can only be made from consolidation tests on thin specimens (1) by selection of a portion of the main sample free from stones, (2) by patching, if only an odd stone needs removal, or (3) by removal of the stones and remoulding. None of these methods can be considered satisfactory, especially when the high cost entailed in taking the sample, is considered. Investigations were, therefore, made to determine the effect of the presence of stones and the possibility of using larger test specimens, or other methods of testing.

#### Consolidation Apparatus.

Specimens of 3 in., 4 in., and 6 in. diameter were tested by the conventional method, using a cylindrical mould with porous stones at each end, and the load applied vertically through a piston. The apparatus used for the 3 in. diameter specimens was not materially different from that used by other investigators, and is illustrated in Fig. 1. The method adopted to obtain the sample was to press the sampling ring into the soil being extruded from a 4 in. diameter sampling tube normally used for obtaining undisturbed samples in the field, and then to trim off the two ends. The finished thickness of the sample was  $\frac{1}{2}$  inch.

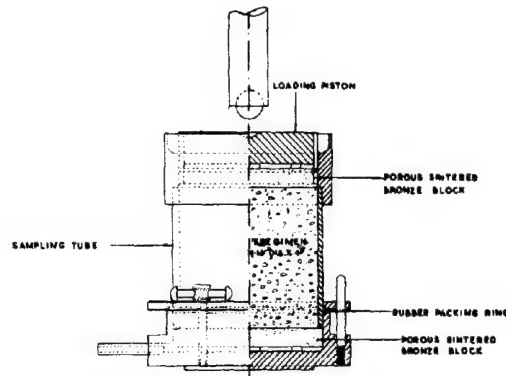


Consolidation box 3in. Dia.

FIG.1

The apparatus for the 4 in. diameter specimen is illustrated in Fig. 2. In this case the sample was pushed direct into the 4 in. nominal bore sampling tube from another

longer tube of the same diameter. The ends were then trimmed to give a finished thickness of approximately 4 in., and the load applied through porous blocks in the usual way.



Consolidation box 4in. Dia.

FIG.2

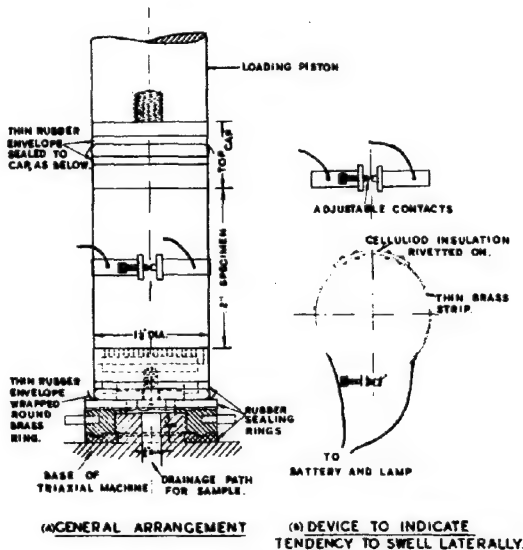
In view of the difficulties described later in connection with the use of the 4 in. apparatus, only one 6 in. diameter specimen was tried. The sample was contained in a mould normally used for C.B.R. tests. A piston was used for the vertical load in the usual way, and porous stones made from brick dust and cement provided drainage.

The effects of friction in the 4 in. diameter apparatus were found to be serious and the following methods of overcoming this were considered:

- 1) coating the inside of the tube with glue or other similar material to reduce friction.
- 2) pouring molten paraffin wax round the soil specimen placed inside a sampling tube of larger diameter, the object being to provide an incompressible container, but with comparatively low side friction. This method was not effective.
- 3) the use of the triaxial compression testing machine utilising the water pressure to maintain a specimen of constant diameter. The object of this arrangement was to eliminate friction entirely, while still obtaining one dimensional compression.
- 4) the use of the triaxial compression testing machine with fixed end pistons, and an ar-

rangement to measure the change in diameter of the sample when compressed by means of the water pressure.

Of these four methods, 3) was considered the most likely, and the arrangement shown in Fig. 3 was adopted. The soil specimen 2½ in. high x 1½ in. diameter, was encased in a rubber envelope sealed to the end caps shown, the lower one of which was porous to allow drainage under atmospheric pressure. The specimen was then placed inside the perspex cylinder of the triaxial compression testing machine and the thin metal band and contact device shown in Fig. 3(b), was attached. This contact was adjusted so that any lateral swelling of the specimen, broke the contact and put out the light. By using a small current, electrolysis and arcing at the points was avoided.



Adaptation of triaxial testing machine for consolidation tests.

FIG. 3

During the test, pressure was applied through a 1½ in. diameter piston, and any tendency on the part of the specimen to bulge was corrected by increasing the lateral water pressure until the light just came on again. In this way the diameter of the specimen could be maintained constant within very narrow limits, and the vertical compression of the specimen measured from a dial gauge calibrated in 0.0001 in. divisions reading on a mounting at the top of the piston. It was found that the device was sufficiently sensitive to react to changes in the vertical pressure of less than 1 lb., and in the lateral pressure of 0.1 lb. per sq. inch.

The method is experimental and requires regular attention to the water pressure in the perspex cylinder. There is, however, no difficulty in fitting an automatic relay and pumping arrangement.

#### Details of Soil and Stones Used.

One type of soil was used throughout the investigations described; this was a clay with the following characteristics:

Liquid Limit 39  
Plastic limit 19

Mechanical analysis:	per cent
Coarse sand (2mm - 0.6 mm)	13
Medium sand (0.6 mm - 0.2 mm)	11
Fine sand (0.2 mm - 0.06 mm)	16
Silt (0.06 mm - 0.002 mm)	24
Clay (Smaller than 0.002 mm)	36
Specific gravity of clay particles	2.73
Dry density as used	105 lb. per cub. ft.
Saturated moisture content	23.0 per cent.
Initial voids ratio = $e_0$	0.628

The stones were all sieved from a flint river gravel of irregular 1) shape. The sizes adopted were ¾ - ⅜ in. for use in the 4 in. diameter specimens only, and ⅜ - ⅜ in. The specific gravities and moisture contents of the stones are as follows:

	¾-⅜ in.	⅜-⅜ in.
Apparent specific gravity	2.48	2.45
Moisture content, saturated surface wet, per cent.	3.6	6.2

In all the experiments the soil mixture was compacted to a predetermined volume, in order to obtain the specified dry density in the clay, i.e., the initial voids ratio of the clay was kept constant.

#### Percentage Compression of ¾ in. Samples.

Consolidation tests were made on ¾ in. samples ½ in. thick with drainage both top and bottom, using clay and 0, 20, 40 and 60 per cent of gravel by weight of total mix. In order to obtain a reasonably constant voids ratio on the clay for the series of tests, dry clay was mixed with the necessary quantity of water and was then mixed with the saturated surface wet gravel. The sample was next compressed in a cylinder to a predetermined volume.

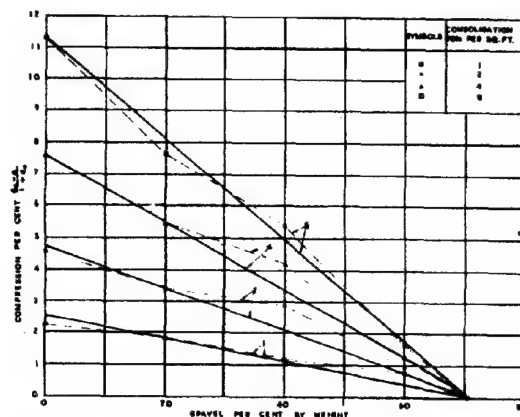
In order to present the data obtained in a form as closely related as possible to a final estimate of settlement, the results of the tests are given as the percentage compression, that is

$$\frac{e_0 - e}{1 + e_0} \times 100$$

where  $e_0$  = initial voids ratio

$e$  = voids ratio at end of consolidation due to applied load.

In Fig. 4 the percentage compression of



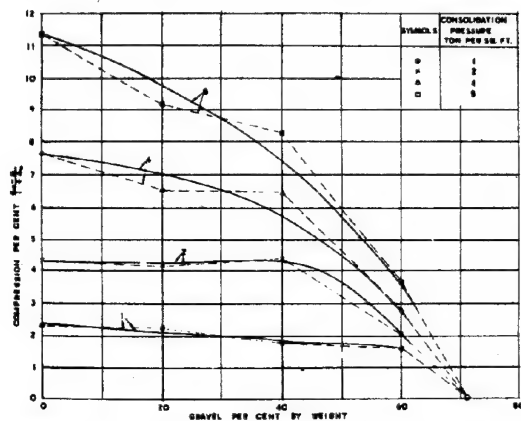
Effect of increasing proportions of gravel ¼ in. - ⅜ in. on percentage compression of ¾ in. specimens, ½ in. thick.

FIG. 4



the soil as a whole is plotted against the gravel content for four increments of consolidation pressure, 1, 2, 4, and 8 tons per sq. ft. As may be seen, the percentage compression varies inversely with the percentage of gravel by weight, and the compression becomes zero at a gravel content of about 71 per cent. This is the point at which the gravel particles make contact, and the load is therefore carried entirely by the gravel. There is a tendency for the percentage compression to fall less between 20 and 40 per cent than is expected from a straight line relationship. This tendency is even more marked in the 4 in. samples (see Fig. 6), and requires further investigation.

Curves have been plotted in Fig. 5 showing the percentage compression in the clay alone. At the lower loads of 1 and 2 tons per sq. ft., it appears that percentages of gravel up to 40 per cent have little or no effect on the consolidation in the clay. At 4 and 8 tons per sq. ft., however, and more especially with the higher load, the percentage compression decreases even with small proportions of gravel. It is, therefore, evident that errors are incurred if it is assumed that settlement in a soil can be computed from consolidation tests on samples from which stones have been removed, or on samples selected from a portion of the main sample free from stones, and that any such estimates are likely to be in excess of the settlements which actually occur.



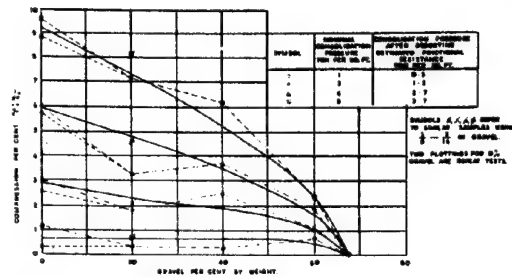
Effect of increasing proportions of gravel  $\frac{1}{2}$  in. -  $\frac{3}{4}$  in. on percentage compression of soil fines only, 3 in. Dia. specimens,  $\frac{1}{2}$  in. thick.

FIG. 5

#### Percentage Compression of 4 in. Specimens.

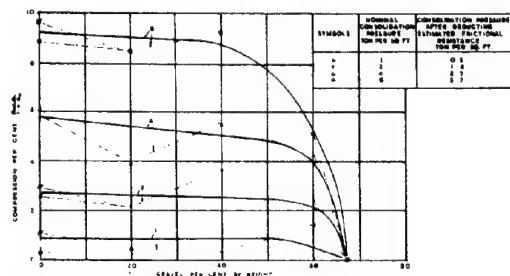
The results of tests on 4 in. specimens are given in Figs. 6, 7, and 8. Specimens 3 in. diameter and  $\frac{1}{2}$  in. thick are normally fully consolidated after 36 hours. Terzaghi 2) has shown that the time factor is dependent on the square of the thickness, and it follows that for specimens 4 in. thick, the comparative consolidation period is about 1,000 hours. In order to save time during testing, this period was not strictly adhered to, when it was found that little or no movement was occurring, and the compression was extrapolated by plotting on semi-logarithmic paper. It is felt that any error incurred is likely to be of minor importance.

The form of the curves obtained in Figs. 6 and 7 are somewhat similar to those given in Figs. 4 and 5 for 3 in. specimens. It is evident,



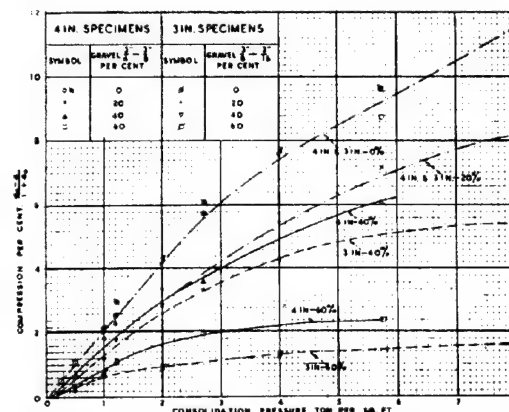
Effect of increasing proportions of gravel,  $\frac{1}{2}$  in. -  $\frac{3}{4}$  in. on percentage compression of 4 in. Dia. specimens  $\frac{1}{2}$  in. thick.

FIG. 6



Effect of increasing proportions of gravel,  $\frac{1}{2}$  in. -  $\frac{3}{4}$  in. on percentage compression of soil fines only 4 in. Dia. specimens,  $\frac{1}{2}$  in. thick.

FIG. 7



Comparison of percentage compressions of 3 in. & 4 in. specimens with various gravel contents.

FIG. 8

ent, however, that the percentage compression in each increment was lower than would be expected from the nominal loading, and that side friction had become much more serious than it was in the 3 in. specimens. Taylor 3) in discussing the effects of side friction, showed that inaccuracies in the pressure in Boston Blue Clay could amount to 6 to 11 for remoulded soil and 5 to 7 per cent for the undisturbed state, when using samples only  $\frac{1}{2}$  in. thick. Other investigators 4) 5) have designed special apparatus in connection with investigations of side friction, and indic-



ations have been obtained that the friction is of larger magnitude than is generally believed. The result was, therefore, anticipated and the following approximate method of making an allowance was adopted.

After testing, the pressure required to push the sample out of the tube was determined, and shear box tests were also made to find the cohesion and angle of friction of the material. Estimates were then made of the value of the constant  $K$  in the equation:

$$A_{CP} = A_s (c + Kp \tan \phi)$$

where  $A_c$  is the cross-sectional area of the sampling tube

$A_s$  is surface area of tube in contact with the specimen.

$p$  is the applied pressure

$c$  is the cohesion

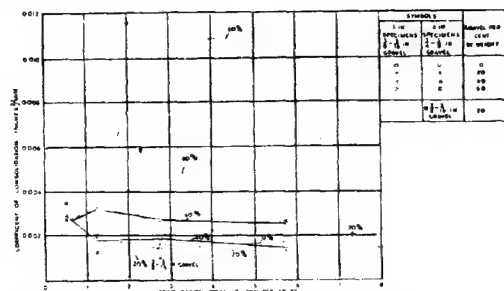
$\phi$  is the angle of friction

For all practical purposes with the material used in the tests, it was found that  $K$  could be taken as equal to 0.5,  $c$  equal to 2.87 lb. per sq. in. and  $\phi$  equal to  $19^\circ$ . From this data, the actual load transferred to the bottom of the specimen for any load applied at the top can be calculated. Taylor 3) has shown that the consolidation is then equivalent to that due to the average of the pressures at the top and the bottom. Values for nominal loadings of 1, 2, 4, and 8 tons per sq. ft. are given in Figs. 6 and 7.

With these corrections the percentage compression is plotted against consolidation pressure in Fig. 8, and it is shown that for 0 and 20 per cent gravel, the agreement between the 4 in. and 3 in. samples is good. Then, however, the percentage of gravel is increased to 40 and 60 per cent, a greater compression is obtained in 4 in. samples than in 3 in. This appears reasonable, since with specimens  $\frac{1}{2}$  in. thick, more arching and resistance to movement are to be expected when large quantities of gravel are present.

#### Rate of Consolidation.

Coefficients of consolidation were calculated using the time fitting method 3) 6) plotting degree of consolidation against  $\sqrt{t}$ . The coefficients are shown plotted against the consolidation pressure in Fig. 9.



Comparison of coefficient of consolidation of 3 in. & 4 in. specimens with varying gravel contents.

FIG. 9

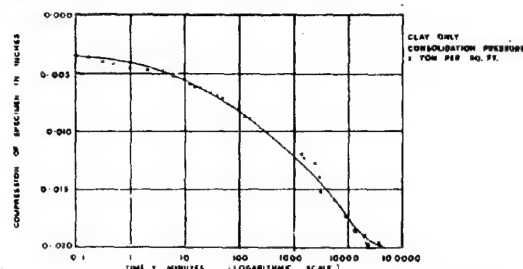
The most important point indicated by the plottings is the difference in the time rate of consolidation of 3 in. diameter specimens  $\frac{1}{2}$  in. thick, as the percentage of gravel increases. In comparison there is little change for 4 in. diameter specimens, 4 in. thick, until the proportion of gravel reaches 60 per cent.

The large increases in the coefficient of consolidation for 3 in. diameter specimens when gravel is present, are attributed to arching and uneven consolidation, which results in a lowered resistance to the flow of water. Greater freedom of movement of the gravel is possible in 4 in. thick specimens, and any uneven consolidation in the thin layer adjacent to the porous stones top and bottom, is of less importance. Serious errors in time-settlement curves are therefore likely to result from the use of thin specimens of stony soil.

#### Use of Triaxial Compression Testing Machine.

The method evolved for this test has already been described under "Consolidation Apparatus". Preliminary experiments were made with a sample of clay  $1\frac{1}{2}$  in. diameter and 2 in. high. The piston through which the load was applied, was made the same diameter as the specimen in order to avoid vertical compression when the lateral water pressure was increased. The use of the contact device at the centre of the specimen is based on the assumption that any increase in diameter is likely to be greatest at the centre, as is found in the normal change of shape of specimens in triaxial compression tests.

An example of the consolidation time curve obtained is given in Fig. 10. Owing to the fact that the experimental apparatus only had one drainage path, however, and the time required for full compression is estimated to be about 50 days for each increment, insufficient evidence is as yet available concerning the comparison with the normal consolidation apparatus. The results, are, however, encouraging and modifications are being made to provide drainage at the top and bottom of the specimen, and the contact device has been improved. Apparatus has also been designed to deal with larger specimens in the same way. In this case further modifications have been made to the loading piston arrangement, and a relay system is incorporated for automatic correction of any lateral swelling of the specimen.



Example of consolidation / time curve obtained when using triaxial compression machine.

FIG. 10

#### Discussion of Results.

The investigations described show that the consolidation characteristics of a soil are affected by the presence of stones, and that computations of settlements cannot be made accurately by testing samples of the soil fines, and assuming that the compression is reduced in proportion to the volume of stones present. Errors are likely to be particularly serious in estimates of the time rate of settlement. It is, therefore, evident that for clays containing gravel or boulders, e.g., boulder clays, use of the standard apparatus

with comparatively small samples is unsatisfactory.

When larger specimens are used, difficulties are encountered due to side friction in the consolidation box, but it appears that for a rough evaluation, corrections can be made from estimates of the reduction in pressure due to friction, and the assumption that the consolidation is due to the average of the pressure at the top of the specimen and the resultant pressure at the bottom. It is impossible to eliminate friction in the normal type of consolidation box, and the use of the triaxial compression type of machine with a device such as that used by the author appears likely to provide a solution of the difficulty.

The investigations described were regarded as exploratory and were made on one type of remoulded soil and one shape of gravel. Further investigations are necessary to determine the effect of the shape of the solid particles, effect of remoulding, and other properties before any definite conclusions on the general effect of the presence of stones and other coarse particles on the consolidation can be reached. This further research is dependent, however, on the final development of a suitable form of test for the large samples necessary.

#### ACKNOWLEDGMENT.

The Author is indebted to the Directors of Messrs. G. Wipey and Co. Ltd., for permission to publish the data contained in the Paper.

#### BIBLIOGRAPHY.

- 1) British Standard Specification No. 882, 1944, p. 53.
- 2) K. Terzaghi. Theoretical Soil Mechanics. John Wiley and Sons, New York, 1942.
- 3) D.W. Taylor. Research on Consolidation of Clays. Massachusetts Institute of Technology, August, 1942.
- 4) W.P. Kimball. Discussion of Progress Report of Special Committee on Earths and Foundations. A.S.C.E. Proceedings, Aug. 1933, p. 1063.
- 5) W.L. Wells. An Investigation of Side Friction on the Consolidation Test on Clay. Unpublished S.M. Thesis, Department of Civil and Sanitary Engineering, 1936.
- 6) G.Gilboy. Improved Soil Testing Methods. Engineering News-Record, vol. 116, 21st May 1936, p. 732.

-0-0-0-0-0-0-

## SUB-SECTION II d

### TRIAxIAL TESTS

#### II d 1

#### CORRELATION BETWEEN THE RESULTS OF CELL-TESTS AND COMPRESSION TESTS

E. DE BEER

Ghent (Belgium).

#### INTRODUCTION.

In the cell-tests performed at Delft and Ghent the sample is subjected to a certain number of vertical loads, and for each of these loads the minimum lateral pressure, necessary to still maintain the sample in equilibrium, is determined. When quick cell-tests are performed on clays, the obtained envelope of Mohr consists of two straight lines intersecting in the so called "singular point" of the diagram of Mohr. When the sample is given opportunity to consolidate under the last applied load, the necessary minimum pressure is decreasing with time. The circle obtained after consolidation is complete, is tangent to the first straight line of the envelope. The first line gives the cohesion  $c$  by its ordinate at the origin, and the angle of internal friction  $\phi$  by its inclination. The second straight line gives the so called apparent cohesion  $c'$  and apparent angle of friction  $\phi'$ . The ordinate  $W_0$  of the singular point should be the shearing-resistance of the material in its natural state in the ground, while the circle tangent to the two straight lines should give the natural vertical effective pressure  $\sigma_t$ .

For several clays the quick-test may not be performed too quickly. Indeed, because of phenomena at the surface of the very small clay-particles, the shearing-resistance of these clays under an instantaneously applied load can be larger than that existing under a remaining load. The velocity of performing the cell-test must be so, that the maximum value of the minimum lateral pressure, necessary to maintain the equilibrium under a given vertical load, can be measured, after what a new increase of the vertical load shall be applied as quickly as possible. In this way the normal cell-diagrams dealt with in this report have been obtained.

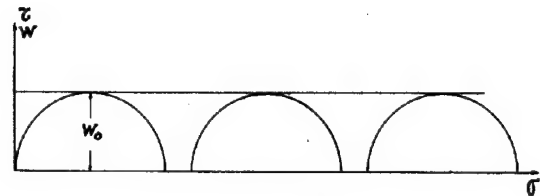
In the U.S.A. and in several other countries the shearing-resistance is computed from compression-tests. If  $q$  is the crushing strength of a sample, it is admitted that the shearing-resistance of the sample in its natural state in the ground  $W_0$  is given by

$$W_0 = \frac{q \cos \phi}{2} \quad (1)$$

In the same countries the shearing-resistance is also computed from triaxial compression tests. In the quick tests the sample enclosed in a rubberbag, is subjected to an overall

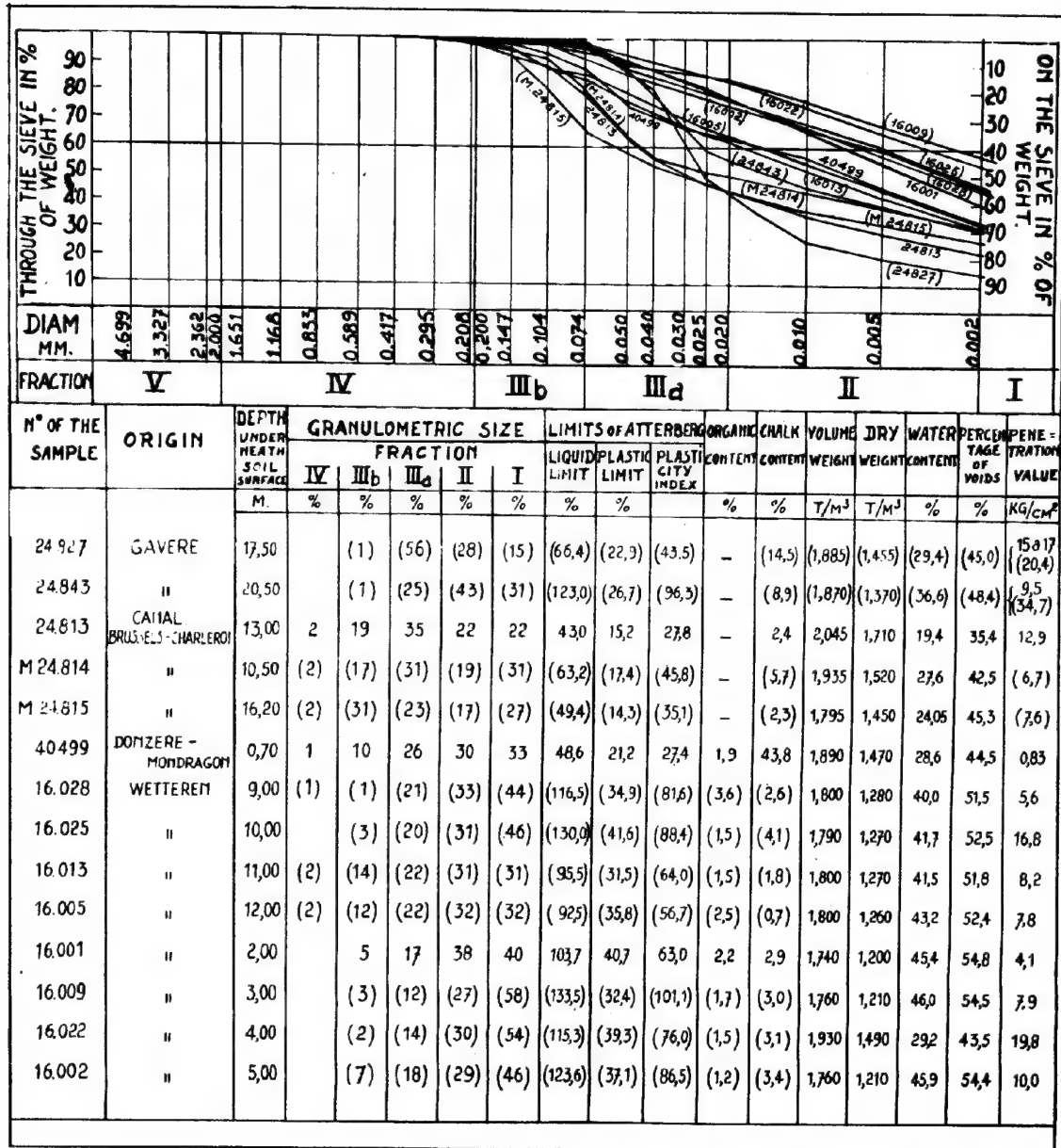
pressure; after what the vertical stress is increased till rupture. The overall pressure seems to have no influence on the shearing-resistance. When the test is repeated on different parts of the same sample, circles with the same radius  $W_0$  are obtained (fig.1). The quick triaxial tests should give the same results as the ordinary compression tests.

In order to compare the results of the cell-tests and of the ordinary compression tests, at our laboratory at Ghent a certain number of samples were subjected to both tests.



Quick triaxial test

FIG.1



Granulometric size

FIG.2

For all the tests the dimensions of the samples are the following:

height -  $h = 14,5$  or  $15$  cm.

diameter -  $\phi = 6,54$  or  $6,57$  cm.

The samples were tested in their undisturbed state unless otherwise specified.

The cell diagrams show a certain number of circles, indicated by numbers. The time taken to obtain the state of stress corresponding to a given circle is indicated in the corresponding table of each cell-diagram.

The diagrams of the compression tests give the vertical deformations of the sample in function of the applied vertical pressures, and also the variation of these pressures with time. If possible the diagrams give the angle  $\alpha$  between the shear plane and the horizontal direction. The natural vertical effective stress computed from the weight of the overburden, or from direct data, is indicated by  $\sigma_{k,0}$ .

#### A. SAMPLES OF YPRESIAN CLAY (Tertiary clay).

Two samples of Ypresian clay, 24827 and 24843 taken at a depth of 17,50 m, resp. 20,50 m under the soil surface were tested. The

mechanical analysis and the physical properties of samples taken in the same layer and in the neighbourhood of the two samples are given on fig. 2.

When the data of fig. 1 are written between brackets, it means that the physical properties are concerned, not with the tested samples itself, but with samples taken in the neighbourhood. The results of sample 24843 are given in fig. 3a and 3b; the results of sample 24827 in fig. 4a and 4b.

#### SAMPLE 24843.

The values of  $c, \phi$ , deduced from fig. 3a are given in table I. It is worthwhile to note the following special facts:

- 1) The circle (1) (fig. 3a) doesn't correspond to an extreme state of stress; indeed, to obtain this state under a vertical stress  $\sigma_v = 0,894$  kg/cm<sup>2</sup>, it should be necessary because of the large cohesion, to exert an horizontal pull, what it is impos-

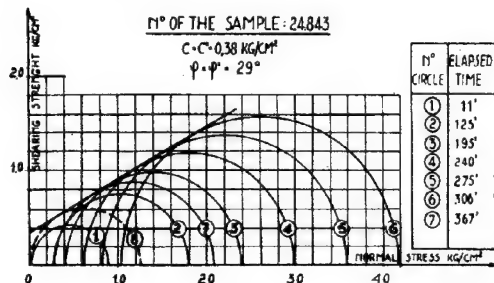


FIG.3a

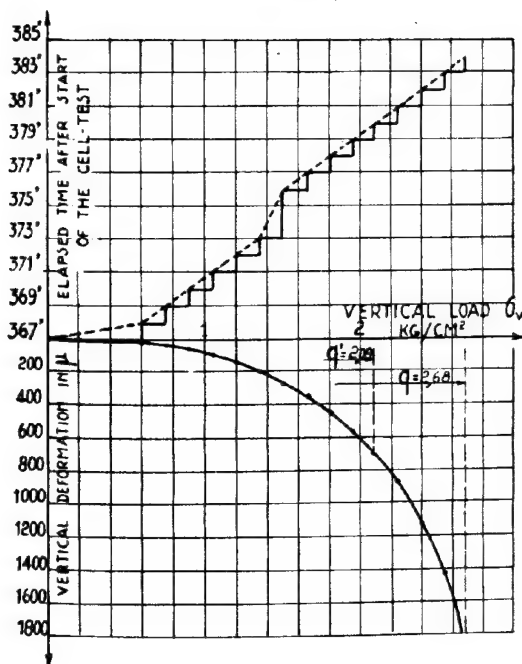


FIG.3b

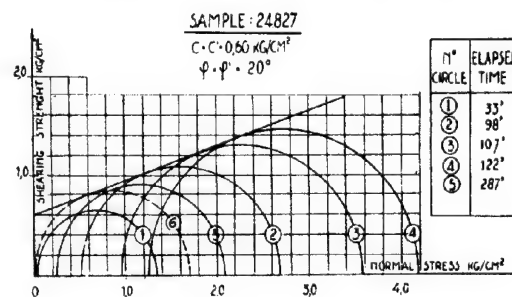


FIG.4a

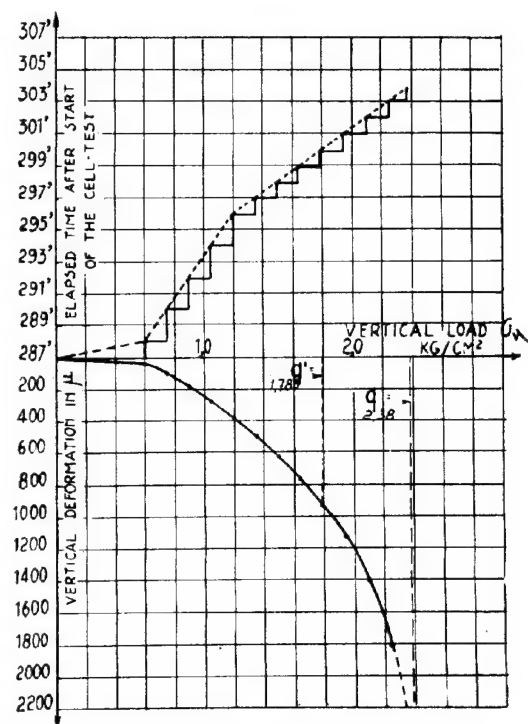


FIG.4b

- sible to do in the cell-apparatus.
- 2) The circle (2) (fig. 3a) is also probably not a limit-circle, because, in a quick test, underneath the natural effective pressure, the lateral stress can be produced by lateral expansion.
  - 3) After having been loaded to  $4.18 \text{ kg/cm}^2$ , the sample was unloaded to  $2.080 \text{ kg/cm}^2$ . The circle (7), nearly tangent to the straight line  $\phi = 29^\circ$ ,  $c = 0.4 \text{ kg/cm}^2$  is obtained.
- After having reached the stress-state of circle (7), the sample was farther unloaded to  $0.595 \text{ kg/cm}^2$ . Then the lateral pressure was reduced to zero and a compression test was performed on the sample previously subjected to the described cell-test.

Fig. 3b indicates that the sample collapsed under  $q = 2.68 \text{ kg/cm}^2$ , but that the increase of the deformations becomes very rapid from a pressure  $q' = 2.08 \text{ kg/cm}^2$ . Thus according to formula (1) the shearing-resistance should be  $W_{0,r} \sim 1.34 \text{ kg/cm}^2$  or  $W'_{0,r} \sim 1.04 \text{ kg/cm}^2$ . In the compression test there is a doubt concerning the value to adopt for the shearing strength. It can be the value  $W_{0,r}$  corresponding to failure, or the value  $W'_{0,r}$  corresponding to the rapid increase of the deformations. When it is the latter value, it can be seen from fig. 3b that it is very difficult to make an exact choice.

The circle (7) of fig. 3a corresponding to the value  $\sigma_k = 2.08 \text{ kg/cm}^2$ , gives  $W_c = 0.85 \text{ kg/cm}^2$ . This value of  $W_c$  is much smaller than the value  $W_{0,r}$  and even  $W'_{0,r}$  of the compression test.

Drawing the limit-circle (8) corresponding to zero horizontal pressure, one gets  $\sigma_v = 1.24 \text{ kg/cm}^2$ , and the corresponding shearing-resistance is  $0.54 \text{ kg/cm}^2$ . Comparing these values to those of the compression test, it is concluded, that in the compression test, at rupture, the effective horizontal stress is not zero.

In quick tests with constant watercontent the shearing strength should remain invariable; on the contrary the quick cell test indicate that in function of the applied loads and of the allowed deformations the shearing-resistance even by clays can vary rapidly with time.

A cone test performed on the sample 24845 gives a penetration value  $C_{k,0} = 9.5 \text{ kg/cm}^2$ . The penetration value is given by the formula

$$C_{k,0} = 1.3 (V_{bpc} + V_{cc}) \quad (2)$$

where  $p_c$  = capillary pressure at the moment of penetration. In accordance with the properties of structural deformability of the sample under shear stresses,  $p_c$  can be located between 0 and  $\sigma_{k,0}$ .

$$\text{For } \phi = 29^\circ \quad V_c = 27.5 \quad V_b = 16.4 \\ c = 0.38 \text{ kg/cm}^2 \\ \sigma_{k,0} \sim 1.58 \text{ kg/cm}^2$$

thus  $0 \leq p_c \leq 1.58 \text{ kg/cm}^2$

$$1.3 \times 27.5 \times 0.38 \leq C_{k,0} \leq 1.3(16.4 \times 1.58 + 27.5 \times 0.38)$$

$$13.6 \text{ kg/cm}^2 \leq C_{k,0} \leq 47.2 \text{ kg/cm}^2.$$

Comparing the computed limits of  $C_{k,d}$  with the measured value of  $9.5 \text{ kg/cm}^2$ , it is concluded that for the sample tested in the cone test the vertical effective stresses at the moment of rupture are nearly zero.

When the penetration value should be computed from the compression test, then the  $\phi = 0$  method has to be applied. For  $\phi = 0$ ,  $V_c = 5.14$ . Thus

$$C_{k,0} = 1.3 \times 5.14 \times 1.04 = 6.95 \text{ kg/cm}^2$$

$$\text{or } C_{k,0} = 1.3 \times 5.14 \times 3.14 = 9.06 \text{ kg/cm}^2.$$

The values so obtained are smaller than the measured value.

#### SAMPLE 24827.

The values of  $c$ ,  $\phi$ , deduced from fig. 4a are given in table I.

Special facts are:

- 1) The circle (1) fig. 4a is not a limit-circle, for the same reason as given for circle (1) of sample 24843.
- 2) After having been loaded to  $4.18 \text{ kg/cm}^2$ , the sample was unloaded to  $2.080 \text{ kg/cm}^2$ ; the circle (5) (fig. 4a) nearly tangent to the straight line  $\phi = 20^\circ$ ,  $c = 0.6 \text{ kg/cm}^2$  is obtained.

After having reached the stress-state of circle (5), the sample was farther unloaded to  $0.595 \text{ kg/cm}^2$ . Then the lateral pressure was reduced to zero and a compression test

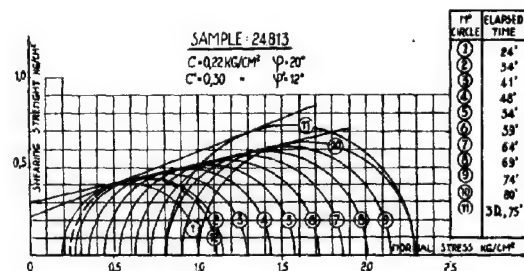


FIG.5a

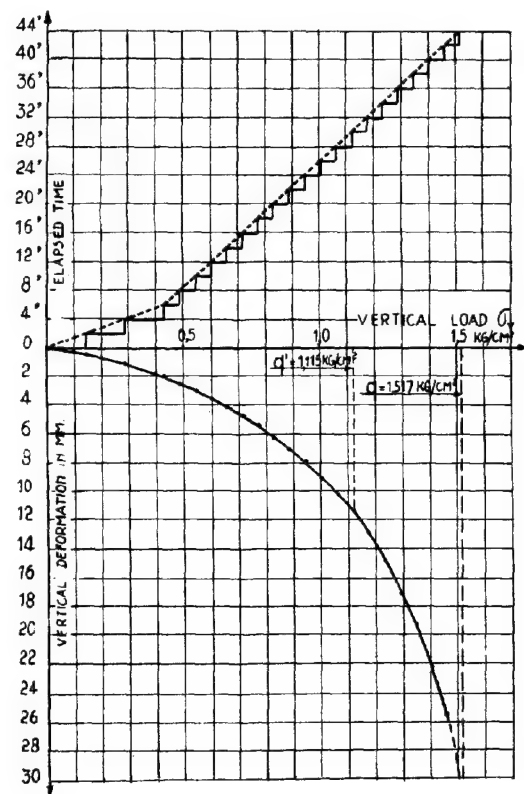


FIG.5b

was performed on the sample previously subjected to the described cell-test.

Fig. 4b indicates that  $q = 2,38 \text{ kg/cm}^2$

$q' \approx 1,64 \text{ à } 1,785 \text{ kg/cm}^2$

Thus  $W_{0,r} = 1,19 \text{ kg/cm}^2$ .

$W'_{0,r} \approx 0,82 \text{ kg/cm}^2$ .

Again there is a doubt in the compression test concerning the value to adopt for the shearing-resistance. The limit-circle (6) fig. 4a, corresponding to  $\sigma_h = 0$ , gives  $\sigma_v = 1,72 \text{ kg/cm}^2$ , and a shearing-resistance of  $0,76 \text{ kg/cm}^2$ . Comparing these values to those of the compression test, it is concluded that in the compression test, at the rupture, the effective horizontal stress is not zero. The cell-test shows again that even with constant watercontent in function of the applied loads and the allowed deformations the shearing-strength of clays can vary rapidly with time. The ome test gives a penetration value of 15 à 17  $\text{kg/cm}^2$ .

$0 \leq p_c \leq \sigma_{k,0} = 1,34 \text{ kg/cm}^2$ .

$\phi = 20^\circ$   $V_b = 6,4$   $V_c = 14,8$

$C = 0,6 \text{ kg/cm}^2$

$13 \times 14,8 \times 0,6 \leq C_{k,0} \leq (1,9 \times 6,4 + 14,8 \times 0,6) 1,3$

$11,5 \text{ kg/cm}^2 \leq C_{k,0} \leq 27,4 \text{ kg/cm}^2$ .

The measured value is located between the computed limits. At the moment of rupture, there still remains some value of the capillary pressure, namely:

$$\frac{15 - 11,5}{6,4} \leq p_c \leq \frac{17 - 11,5}{6,4}$$

$$0,547 \text{ kg/cm}^2 \leq p_c \leq 0,86 \text{ kg/cm}^2$$

When the  $\phi = 0$  method is applied, with the results of the compression-test

$$1,3 \times 5,14 \times 0,82 \leq C_{k,0} \leq 1,3 \times 5,14 \times 1,9$$

$$5,47 \text{ kg/cm}^2 \leq C_{k,0} \leq 7,96 \text{ kg/cm}^2$$

The values computed with the  $\phi = 0$  method are much smaller than the measured values.

#### B. SAMPLES CONSOLIDATED IN A PRESSURE BOX.

Three series of tests were run on remolded samples which were first consolidated during several days to a known-overall pressure.

The samples having an height  $h = 14,5 \text{ cm}$ , a diameter  $= 6,67 \text{ cm}$ , were placed in a rubber bag with a larger diameter; inside the bag the samples were surrounded by Rhine sand allowing free drainage. The samples were then put in a pressure box and subjected to a known overall pressure. From the same sample there were as many specimens consolidated, as tests had to be performed.

##### SAMPLE 24813.

physical properties: fig. 1.

Two identical specimens of this sample were subjected during 4 days to an overall pressure  $\sigma_{k,0} = 1,08 \text{ kg/cm}^2$ . Thereafter one of the specimens was subjected to a cell test, the other to a compression test. The diagrams are respectively given in fig. 5a and 5b, and the results therefrom in tabel 1.

The singular point of the cell-test, gives, by means of circle (12),  $\sigma_t = 1,12 \text{ kg/cm}^2$  and  $W_c = 0,42 \text{ kg/cm}^2$ .

In the compression test complete failure is obtained for  $q = 1,517 \text{ kg/cm}^2$ . When  $q' = 1,115 \text{ kg/cm}^2$  small fissures were observed. It can be noted that it is practically impossible to discern a discontinuity in the diagram deformations versus pressures of fig. 5b for

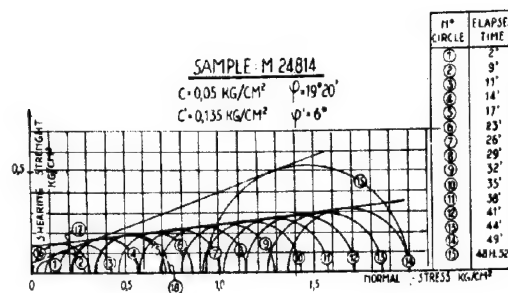


FIG.6a

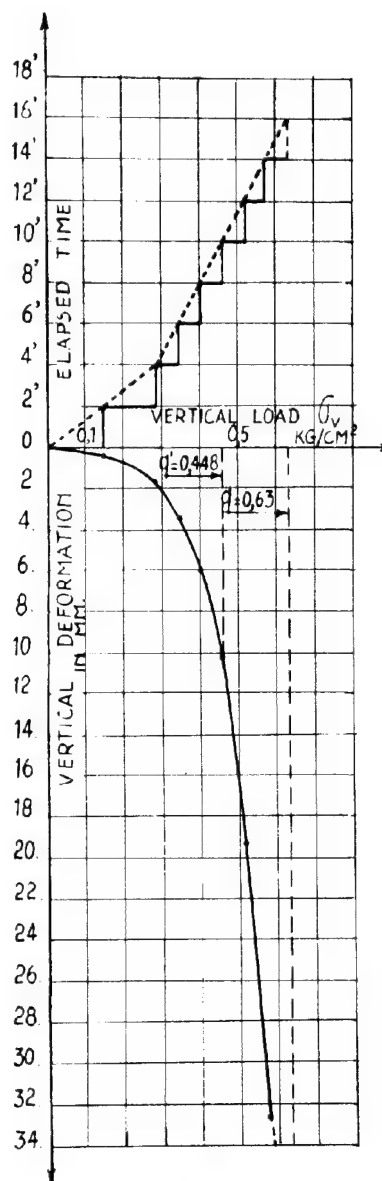


FIG.6b

TABLE I

Number of Sample	Nature	Depth under soil surface	Compu- ted ef- fective vertical stress $\sigma_{k,0}$	$\sigma_t$	compression test		cell- test		$\phi$	$\phi'$	$w_c$	compression-test		$\phi''$
					q	q'	kg/cm <sup>2</sup>	kg/cm <sup>2</sup>				kg/cm <sup>2</sup>	kg/cm <sup>2</sup>	
		m	kg/cm <sup>2</sup>	kg/cm <sup>2</sup>	kg/cm <sup>2</sup>	kg/cm <sup>2</sup>	kg/cm <sup>2</sup>	kg/cm <sup>2</sup>	de- grees	de- grees	de- grees	kg/cm <sup>2</sup>	kg/cm <sup>2</sup>	degrees
24843	Ypresian clay	20,50 ± 20,90	1,58	-	2,68	2,08	0,38	0,84	29	-	0,84	1,34	1,04	-
24827	id.	17,50 ± 17,90	1,34	-	2,38	1,785	0,6	0,85	20	-	0,85	1,19	0,82	-
24813	Remolded clay	-	1,08	1,12	1,517	1,115	0,22	0,42	20	12	0,42	0,71	0,52	-
M24814	id.	-	0,52	0,57	0,63	0,448	0,05	0,135	19°20'	6	0,17	0,293	0,22	-
M24815	id.	-	0,6	0,70	$q_w = 0,457$ $q_w = 0,8$	0,63	0,05	0,16	24	10	$w = 0,195$ $w = 0,22$	0,372	0,3	30 $\phi'' = 20$
40500	Clayey Marl	1,50-1,70	-	0,45	0,477	0,416	0,005	0,10	34	14	0,229 0,15	0,232	0,19	24
40499	id.	0,70-1,10	-	0,29	0,357	-	0	0,07	26	7	0,09	0,178	-	8
40497	id.	0,50-0,90	-	0,52	0,357	-	0,03	0,13	27	9	0,17	0,179	-	6
16028	Tertiary clay	9,00-9,40	1,24	0,62	1,042	0,74	0,02	0,12	23	9	0,18	0,501	0,355	16
16025	id.	10,00-10,40	1,32	1,10	0,744	-	0,19	0,27	18	11	0,40	0,354	0,354	18
16013	id.	11,00-11,40	1,40	1,49	1,31	1,19	0,05	0,28	26	12	0,46	0,635	0,577	14
16005	id.	12,00-12,40	1,48	1,15	1,25	1,071	0,10	0,23	22	12	0,36	0,611	0,524	12
16001	id.	2,00-2,90	$\geq 0,27$	0,54	0,417	-	0,01	0,11	27	11	0,17	0,200	0,200	16
16009	id.	3,00-3,40	$\geq 0,35$	0,92	0,536	0,476	0,04	0,18	25	11	0,28	0,264	0,234	10
16022	id.	4,00-4,40	$\geq 0,43$	1,32	1,37	1,25	0,05	0,16	27	19	0,40	0,643	0,587	20
16002	id.	5,00-5,40	$\geq 0,51$	0,87	0,595	0,535	0,08	0,18	24	13	0,29	0,288	0,259	14

unloaded  
years old  
at cut



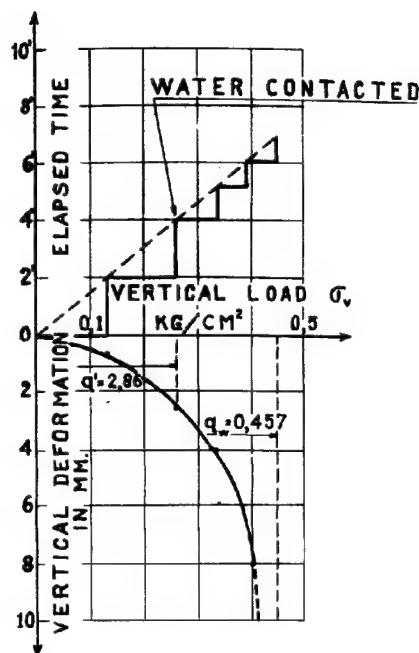


FIG. 6c

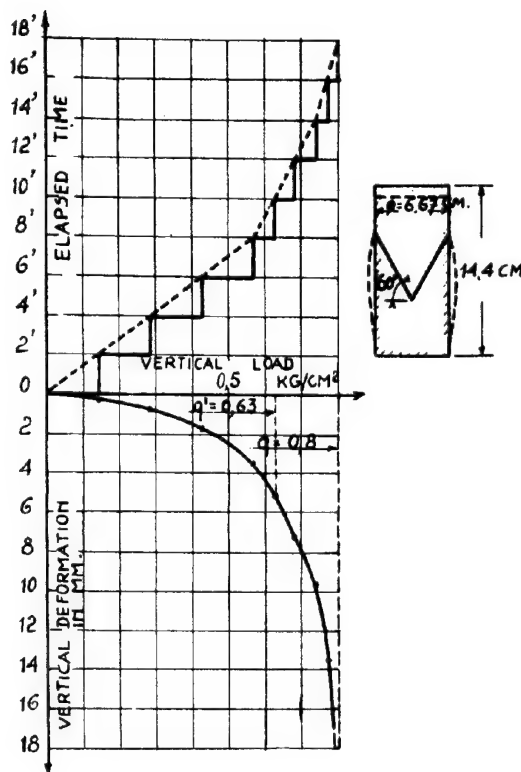


FIG. 7b

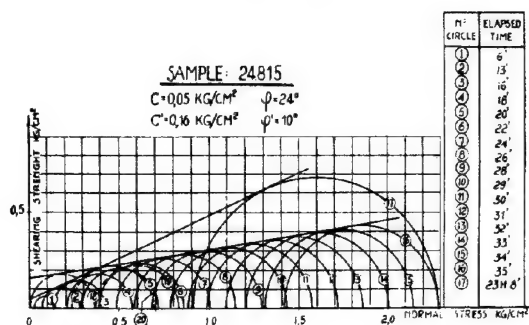


FIG. 7a

$\sigma_v = 1.115 \text{ kg/cm}^2$ . Only a visual inspection of the sample during the test gives this value.

Table I shows that the value  $W'_o$  and especially  $W_{o,r}$ , which is the only exactly measurable quantity, is noticeably larger than the value  $W_c$ .

#### SAMPLE M 24814.

physical properties: fig. 1.

Four identical specimens of this sample were subjected during 18 days to an overall pressure  $\sigma_{k,o} = 0.52 \text{ kg/cm}^2$ . Directly afterwards the specimens were subjected to an ordinary cell-test, an ordinary compression test, a compression test under water and a special cell test.

Ordinary cell-test: fig. 6a and Table I.

Ordinary compression test: fig. 6b and Table I.

Collapse of the sample occurred by  $q = 0.63 \text{ kg/cm}^2$ , but a fissure was detected at the base of the sample by  $q' = 0.448 \text{ kg/cm}^2$ .

The values  $W_{o,r}$  and even  $W'_o$  are larger than  $W_c$ .

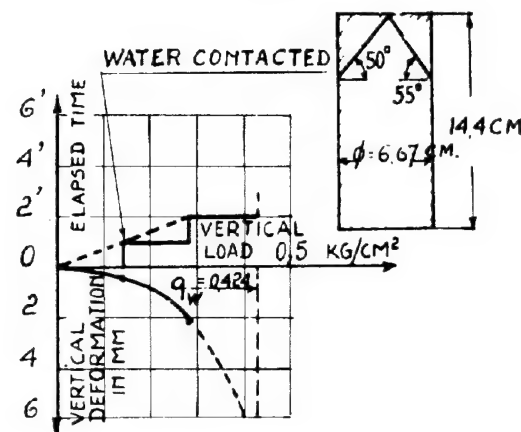


FIG. 7c

#### COMPRESSION TEST UNDER WATER: fig. 6c.

The sample is first loaded with  $\sigma_v = 0.286 \text{ kg/cm}^2$ , and then its base is contacted with a free waterlevel. Now the vertical pressures are rapidly increased. Seven minutes after the start of the test and three minutes after contacting with water, the sample collapsed under a pressure  $q_w = 0.457 \text{ kg/cm}^2$ . This is nearly the same value as  $q'$ , i.e. the pressure producing the first fissure in the ordinary compression test.

It is worthwhile to note that the circle

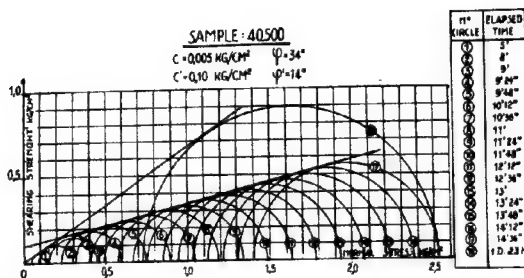


FIG. 8a

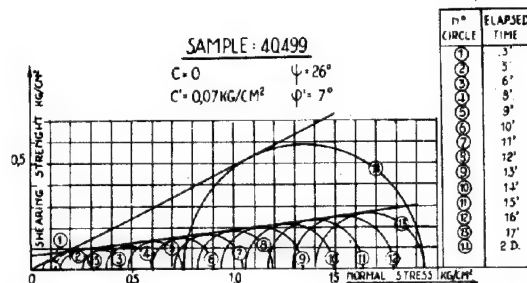


FIG. 9a

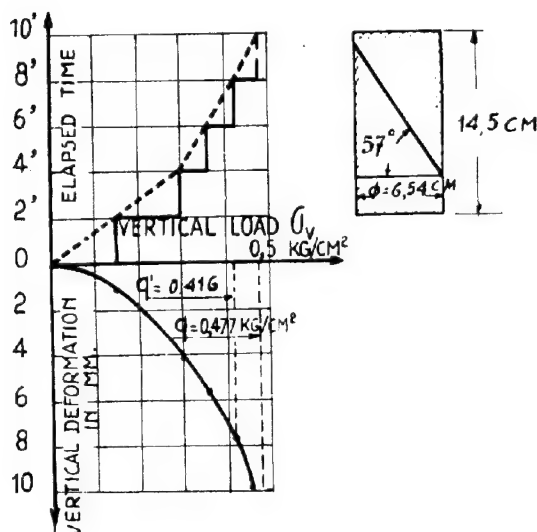


FIG. 8b

(16) of fig. 6a, corresponding to zero horizontal pressure, gives  $\sigma_v = 0.32 \text{ kg/cm}^2$ .

Special cell test: fig. 6a - circle (18)

In this test the sample is first brought in the cell-apparatus under an overall pressure of  $0.503 \text{ kg/cm}^2$ . Then the vertical pressure is increased by successive increments of  $0.057 \text{ kg/cm}^2$ , and the horizontal pressure at the same time decreased with the same quantity. A limit-state is obtained for  $\sigma_v = 0.73 \text{ kg/cm}^2$ ,  $\sigma_h = 0.34 \text{ kg/cm}^2$ , giving  $w_4 = \frac{0.73 - 0.34}{2} = 0.195 \text{ kg/cm}^2$ . This value is a little larger than  $w_c$  (table I).

#### SAMPLE M 24815.

physical properties: fig. 1.

Four identical specimens of this sample were subjected during 14 days to an overall pressure  $\sigma_{v,0} = 0.6 \text{ kg/cm}^2$ . For the rest see sample M 24814.

ordinary cell-test: fig. 7a and Table I.

ordinary compression test: fig. 7b and Table I.

The total failure occurred by  $q = 0.8 \text{ kg/cm}^2$ , but vertical fissures appeared already by  $q' = 0.63 \text{ kg/cm}^2$ . After then inclined fissures started, until the total failure by  $0.8 \text{ kg/cm}^2$ . The plane of rupture was rather rough, but its mean inclination to the horizontal is  $\alpha = 60^\circ$ . Thus  $\phi'' = 2(\alpha - 45^\circ) = 30^\circ$ .

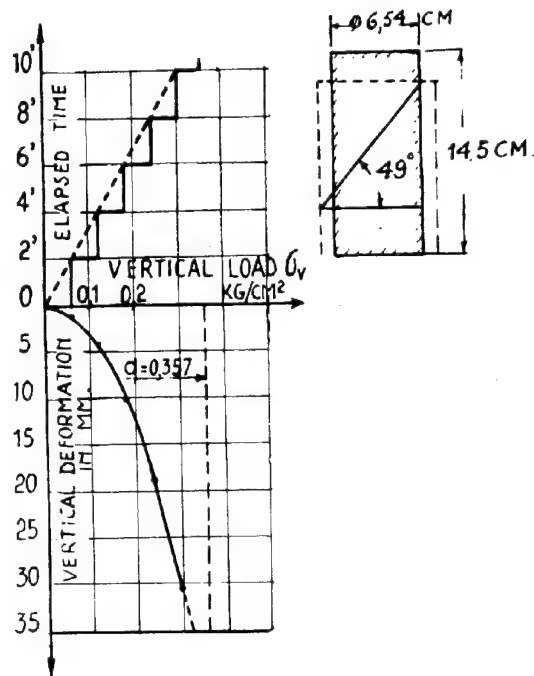


FIG. 9b

It is worthwhile to note that it is practically impossible to discern a abrupt change in the diagram deformations-stresses of fig. 7b for  $q' = 0.63 \text{ kg/cm}^2$ . Only a visual inspection of the sample during the test allowed to detect this value.

The values  $w_{0,r}$  and even  $w'_0$  are larger than  $w_c$ .

compression test under water: fig. 7c.

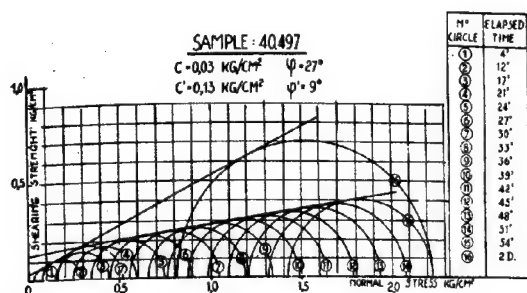
The sample was first contacted at its bases to a free water source and was then loaded rapidly vertically. The specimen failed under a stress  $q_w = 0.424 \text{ kg/cm}^2$ , 2' after the start of the test.

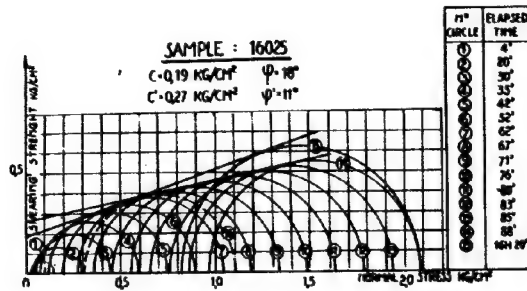
Angles  $\alpha = 50^\circ$  and  $\alpha = 55^\circ$  were measured, giving  $\phi'' = 20^\circ$ .

The limit circle (18) of fig. 7a, corresponding to  $\sigma_h = 0$ , gives  $\sigma_v = 0.37 \text{ kg/cm}^2$ , value which is a little smaller than the measured value  $q_w = 0.424 \text{ kg/cm}^2$ .

special cell-test: fig. 7a - circle (19)

The same procedure as for the sample M 24814 was followed, but the initial overall





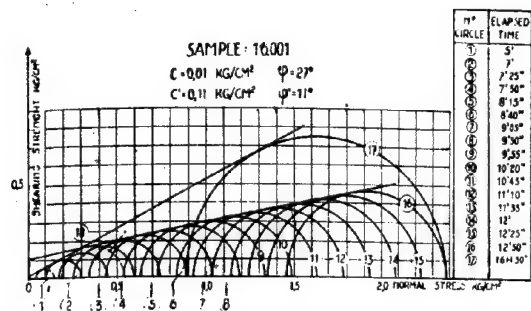


FIG. 15a

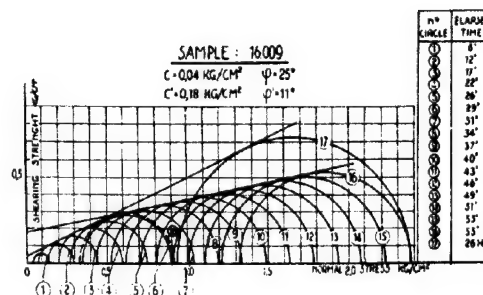


FIG. 16a

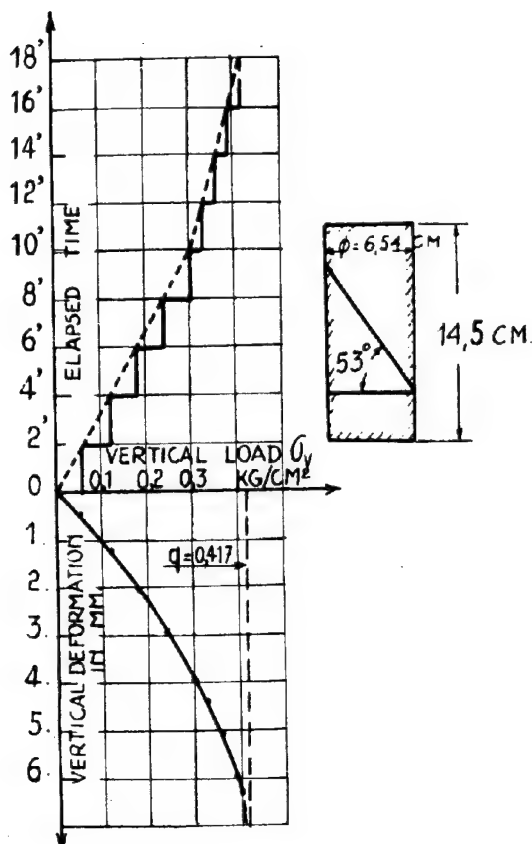


FIG. 15b

the load of failure  $q$ , the measured angle  $\alpha$ , and the quantities  $W_{0,r}$  and  $\Phi''$  deduced from the measurements.

A trial was also made to deduct from the shape of the compression diagram a value  $q'$ , from which the deformations start to increase rapidly.

It is difficult to determine exactly the value of  $q'$ ; thus this value is more or less arbitrary.

From these values  $q'$  the quantities  $W'_0$  are computed. Comparing the results of the compression tests with those of the cell-tests for the 8 samples tested, the following conclusions are obtained:

- 1) The values  $W_{0,r}$  are generally noticeably larger than the values  $W_c$  of the cell-tests.
- 2) The values  $W'_0$ , which are difficult to de-

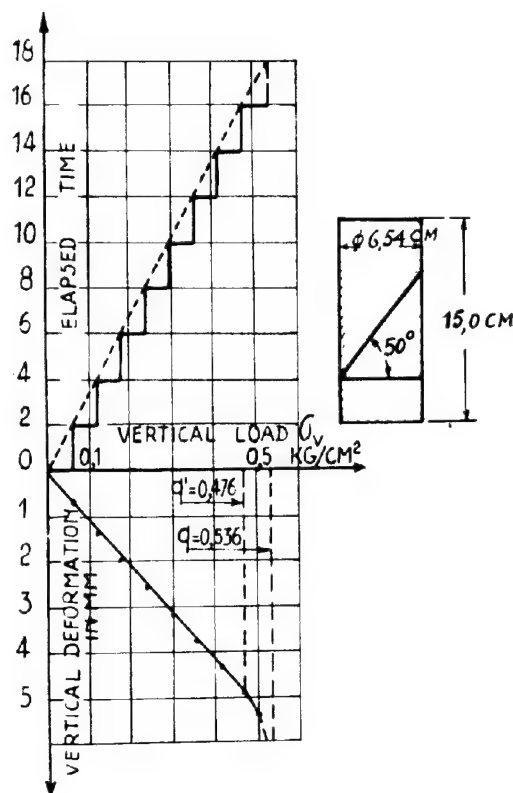


FIG. 16b

termine exactly, are generally larger than or equal to those of  $W_c$ . For  $W_c$  the central value is located between 0.36 and 0.29  $\text{kg/cm}^2$ , and the mean value is 0.318  $\text{kg/cm}^2$ . For  $W'_0$  the central value is 0.354  $\text{kg/cm}^2$ , and the mean value 0.386  $\text{kg/cm}^2$ .

3) The values of  $\Phi''$  deduced from the planes of rupture are generally located between those of  $\Phi$  or  $\Phi'$ , but are sometimes equal to one of these quantities.

#### GENERAL CONCLUSIONS.

- 1) The shearing-resistance deduced from the load of failure in compression tests is larger than that corresponding to the singular point of the cell-tests. If the latter is considered to be the shearing-resistance of

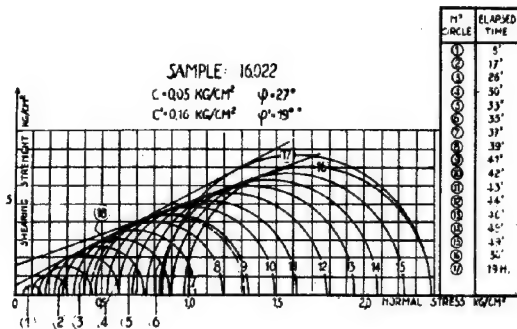


FIG. 17a

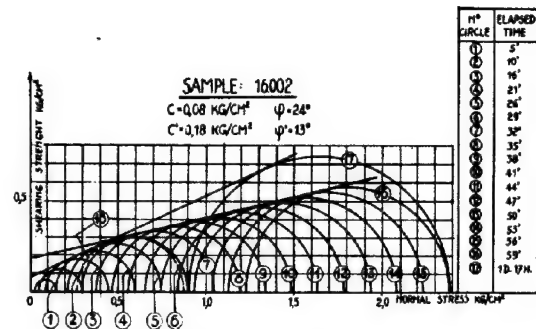


FIG. 18a

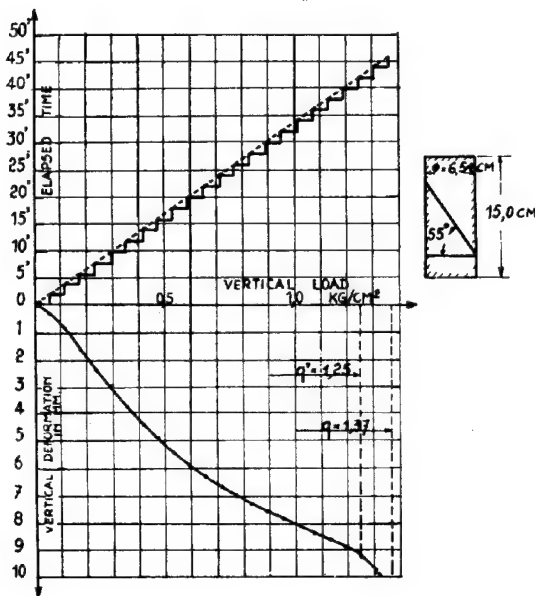


FIG. 17b

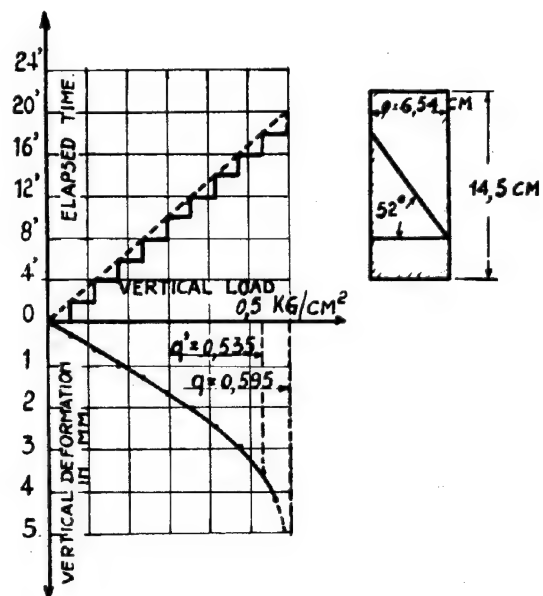


FIG. 18b

the soil in its natural state, it is concluded that, for the tested samples of very various origin, the shearing-resistance increases in the compression test with the applied load, even when the watercontent remains constant. This increase becomes especially important when the deformations of the sample are large and is thus correlated to a structural resistance.

2) In the compression tests it is possible to fix, though in a rather arbitrary and not very exact manner, the load  $q'$  under which the first fissures appear, or from which in the diagram deformations-loads the former start increasing rapidly. The shearing-resistance  $W'_0$  corresponding to this load  $q'$ , is generally still a little larger than the value  $W_0$  of the cell-test, but approaches more to this latter value. The better accordance is to be correlated to the fact that the deformations by constant volume being smaller for loads smaller than  $q'$ , the influence of the structural resistance is less than for values higher than  $q'$ .

3) The influence of the structural resistance is also indicated by the results of the special cell-tests, where, by smaller deformation under the same state of stress, the shearing-resistance is smaller.

4) The apparent angles of friction  $\phi'$ , obtained in very quick cell-tests, thus practically performed by constant watercontent, are also considered to be produced for a large part by the influence of the structural resistance.

5) Finally, the good agreement between the values of the natural effective pressures  $\sigma_{k,0}$  and the values  $\sigma'_t$  deduced from the cell-tests, and also the good agreement of the magnitude of the values  $W_0$  and  $W'_0$ , indicate that the results of the cell-tests are at least as reliable as those of compression tests and of the quick triaxial tests. But the cell-tests have the advantage that they give much more complete information concerning the shearing-resistance, and that they can be rapidly performed on one and the same sample.

11 d 2

THE ANGLE OF SHEARING RESISTANCE IN COHESIVE SOILS  
FOR TESTS AT CONSTANT WATER CONTENT

H.Q. GOLDER, M.Eng., A.M.Inst.C.E.

A.W. SKEMPTON, M.Sc., F.G.S., A.M.Inst.C.E.

One very simple method of analysing stability problems in cohesive soils, which is much used in England, is that known as the  $\phi = 0$  method. 1) In this method it is assumed that under conditions of no water content change, the soil shows an angle of shearing resistance  $\phi$  equal to zero. However, it is known that tests do not always show  $\phi = 0$  and the choice of the values of the shear characteristics to be used in the analysis is usually the most difficult part of the problem. The authors have examined several hundred sets of test results on very diverse soils and have found that they can be conveniently classified into groups which are given below.

The tests were all immediate triaxial compression tests. The technique employed in England in this test is different from that in use in some other countries, although it corresponds to the "quick" triaxial test as used in the U.S.A. 2) The sample of soil is a cylinder  $1\frac{1}{2}$ " in diameter and  $3\frac{1}{4}$ " in length. It is surrounded by a rubber membrane 0.01" thick which is sealed to solid metal end plates in contact with the ends of the sample. The amount of water inside the membrane cannot change during test. Thus the mean water content of the sample must remain constant, although migration of water within the sample is not prevented by the conditions of the test. The sample, sealed inside its rubber membrane and end plates, is then placed in a cell in which it is surrounded by water under pressure. This fluid pressure acts all round and on the ends of the sample. The vertical pressure is then increased by means of a piston, until failure occurs. During the test the sample is completely isolated and no measurements of volume change or internal pore-water pressures are made. The rate of strain during test is about 1 per cent per minute and failure is reached, with most soils after about 10 minutes.

The test results fall into the following groups:-

- I. Soft fully-saturated clays
- II. Stiff fully-saturated clays
- III. Fully-saturated remoulded clays
- IV. Partially saturated undisturbed soils
- V. Partially saturated remoulded soils
- VI. Clay shales & siltstones
- VII. Saturated undisturbed silts.

I. SOFT FULLY-SATURATED CLAYS  $\phi = 0$ .

Many examples of this type of material were met with. Most of them were soft recent alluvial clays in some cases containing peat. They were nearly all completely saturated and all had liquid limits greater than about 38%. In all cases  $\phi$  was equal to zero, although cases occurred where variation in strength of

the material from one test to another resulted in an unusually large or small Mohr circle under one lateral pressure. Seven examples are given in Table 1. Example b may be only 98% saturated and may exhibit a small  $\phi$  of 1°. Example f is London clay (Eocene) softened by weathering near the surface, all the others are recent marine or river alluvium. The Mohr circles for example c are shown in Fig. 1.

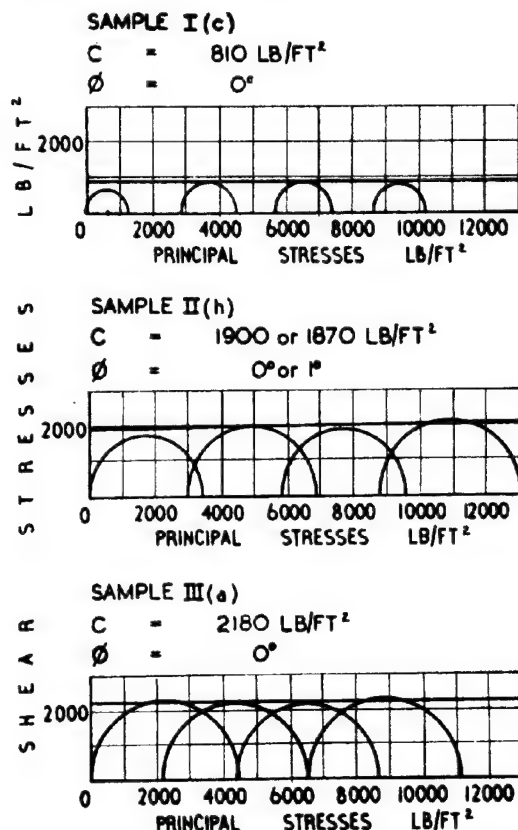


FIG.1.2.3

II. STIFF FULLY-SATURATED CLAYS  $\phi = 0$ .

Many stiff clays occur in England, the most important being the stiff fissured London clay. A large number of test results were available on this material, and these establish without doubt that although a considerable variation may occur between single results, the mean of a large number of tests is the same whatever the lateral pressure. The strength



under zero lateral pressure is, however, consistently lower by about 20% than that under any other pressure. This is attributed to the effect of the fissures and does not occur with the same material when remoulded. Other stiff clays also occur, some of which are not fissured, and eight examples of different types are given in Table II. All the samples are fully or almost fully saturated and in each case  $\phi = 0$  or very slightly more, but never exceeds 2°. The liquid limits range from 34 to 111 but all the samples with liquid limits below 40 are boulder clays of glacial origin.

### III. FULLY SATURATED REMOULDED CLAYS $\phi = 0$ .

When testing clays containing stones, the authors have sometimes found it necessary to remove the stones and remould the clay before testing. This procedure is permissible in soils such as boulder clays which have little structure, and also in the case of material which is to be used, or has been used as fill. By very heavy compaction it is possible to reduce the air voids practically to zero in

which case  $\phi$  is found to be zero. Four examples are given in Table III. Example d has a liquid limit of 26% and is only 95% saturated and there are indications of a small  $\phi$  of  $\frac{1}{2}^\circ$ .

### IV. PARTIALLY SATURATED UNDISTURBED SOILS

#### $\phi > 0$ .

Clay soils which contain some air, normally exhibit a  $\phi$  in immediate triaxial tests. Four examples of tests on undisturbed samples of soil are given in Table IV and example c is plotted in Fig. 4.

### V. PARTIALLY SATURATED REMOULDED SOILS $\phi > 0$ .

Remoulded soils which contain air also exhibit a  $\phi$ . Five examples of different soils are given in Table V. Examples d and e are taken from a series of tests in which the soil was compacted in a standard manner at different moisture contents and then tested. Fig. 5 shows the values obtained for  $c$  and  $\phi$  at different moisture contents. The density curve is also given.

TABLE I  
SOFT FULLY SATURATED CLAYS

Description	Saturation %	Liquid Limit %	Plastic Limit %	Moisture Content %	$\sigma_{in}$ lb/in <sup>2</sup>	$\sigma_{in} - \sigma_{in}^2$ lb/in <sup>2</sup>	$C$ lb/in <sup>2</sup>	$\phi^\circ$
8 a) Gosport. Very soft recent marine clay. Normally consolidated.	100	82	29	58	0 20 40	2.90 2.94 2.88	210	0
9 b) Fens. Soft lagoon silty clay. Normally consolidated	98 to 100	46	25	41	0 15 30 45	6.8 6.8 7.2 8.1	500	1°
10 c) Neath. Soft recent marine clay. Normally consolidated.	97 to 100	168 (peat in sample)	60	105	0 20 40 60	9.5 12.0 12.2 11.0	810	0
10 d) Clyde Estuary. Soft recent silty clay. Normally consolidated	100	56	22	46	0 20 40 60	2.5 4.5 3.4 3.0	250	0
10 e) Avonmouth. Soft recent silty clay. Normally consolidated.	96 to 100	60	23	45	0 30 60	7.8 7.8 7.8	560	0
10 f) Wembley. Soft weathered London clay. Eocene. Over-consolidated.	100	59	19	29	0 20 40 60	11.5 12.5 12.0 11.0	850	0
10 g) Newport, Mon. Soft intact grey clay. Recent river alluvium.	100	61	24	44	0 30 60	3.2 3.2 4.2	250 or 230	0 $\frac{1}{2}^\circ$

**TABLE II**  
**STIFF FULLY SATURATED CLAYS**

Description	Saturation %	Liquid Limit %	Plastic Limit %	Moisture Content %	$\sigma_{11}$ lb/in <sup>2</sup>	$\sigma_1 - \sigma_3$ lb/in <sup>2</sup>	$c$ lb/ft <sup>2</sup>	$\phi$
11 a) Durban. Firm estuarine clay. Highly over-consoli- dated	100	111	28	58	0 15 30 45	15.7 16.8 15.9 17.2	1,180 or 1,150	0 1°
12 b) Peterborough Very stiff laminated Oxford clay. Intensely over- consolidated.	100	87	30	21	0 30 60	93 86 86	6,300	0
10 c) Cambridge. Stiff fissured clay. Gault. Over- consolidated	98	74	29	30	0 30 60	25.3 27.5 28.1	1,950	0 or 1°
10 d) Conisborough. Stiff weathered clay.	100	42	14	13	0 30 60	34.7 34.7 34.8	2,500	0
10 e) Manchester. Stiff sandy boulder clay.	100	34	14	16	0 30 60	33.6 32.9 36.0	2,450	1°
12 f) Wrexham. Stiff laminated clay. Pleistocene. Normally consolidated.	100	36	18	28	0 20 40 60	28.0 33.0 27.0 29.0	2,100	0
13 g) Walton. Stiff fissured London clay. Eocene. Over-consoli- dated. Mean of 50 tests at each pressure.	100	70	25	27	0 20 40 60	26.4 31.7 32.9 34.1	2,250 or 2,160	0 2
10 h) Leyton. Stiff fissured. London clay. Eocene. Over-consoli- dated. Single tests.	97 to 98	66	20	27	0 20 40 60	23.9 27.1 25.6 29.1	1,900 or 1,870	0 1°

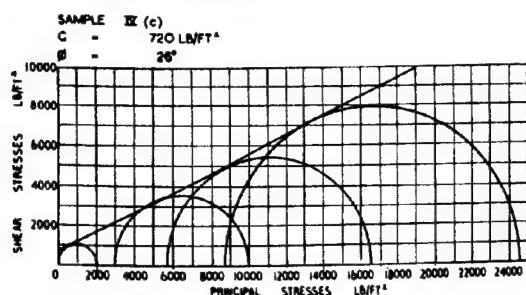


FIG.4

#### VI. CLAY-SHALES & SILTSTONES $\phi > 0$ .

It has been shown by Terzaghi 3) that the area of contact between the grains in most soils is very small (less than 1%), but it is probable that in materials with very low porosities, such as slates the area of contact is appreciable. Between these types are shales and clay-shales in which it is possible that some small area of contact occurs. If so, these soils would be expected to show a  $\phi$  in immediate triaxial tests. The seven examples given in Table VI all show a  $\phi$ . Some of these soils do not appear to be saturated although

**TABLE III**  
**FULLY SATURATED REMOULDED CLAYS**

Description	Saturation %	Liquid Limit %	Plastic Limit %	Moisture Content %	$\sigma_v$ lb/in <sup>2</sup>	$\sigma_v - \sigma_{v2}$ lb/in <sup>2</sup>	$c$ lb/ft <sup>2</sup>	$\phi^\circ$
12 a) Muirhead. Boulder clay. Optimum moisture content 16.5%	100	40	17	17	0 15 30 45	30.3 29.9 29.7 31.3	2,180	0
				21	0 15 30 45	10.7 11.8 10.6 10.3	780	0
13 b) Hyde Park. Brown London clay. Mean of 10 tests at each pressure.	100	82	23	33	0 30 60	26.9 28.3 27.6	2,000	0
10 c) Ireland. Gravel, sand and clay. Optimum moisture content 16%	100	42	20	22	0 20 40 60	5.8 - 5.0 5.0	380	0
10 d) Ireland. Gravel sand & clay. Optimum moisture content 10%	95	26	11	15	0 20 40 60	10.3 14.5 15.5 15.5	1,050	0 or $\frac{1}{2}$

**TABLE IV**  
**PARTIALLY SATURATED UNDISTURBED SOILS**

Description	Saturation %	Liquid Limit %	Plastic Limit %	Moisture Content %	$\sigma_v$ lb/in <sup>2</sup>	$\sigma_v - \sigma_{v2}$ lb/in <sup>2</sup>	$c$ lb/ft <sup>2</sup>	$\phi^\circ$
14 a) Blue Mountain Derm, U.S.A. Reddish brown mottled clay.	87	30	19	19	0 14 42 125	20 58 91 234	820	28
10 b) Soulthorpe. Brown fine sand with some silt and clay.	72	18	11	13	0 20 40 60	14.1 44.1 65.2 87.0	1,570	19
10 c) Prestwick. Soft brown sandy clay.	90	65	17	25	0 20 40 60	14.5 48.7 74.9 110.0	720	26
10 d) Conisborough. Firm clay and weathered siltstone.	80	36	20	12	0 30 60	33.5 58.5 91.6	1,700	20

**TABLE V**  
**PARTIALLY SATURATED REMOULDED SOILS**

Description	Saturation %	Liquid Limit %	Plastic Limit %	Moisture content %	$\sigma_v$ lb/in <sup>2</sup>	$\sigma_v - \sigma_h$ lb/in <sup>2</sup>	$c$ lb/in <sup>2</sup>	$\phi^\circ$
10 a) Brynmawr. Boulder clay.	61	c <sub>35</sub>	c <sub>23</sub>	15	0 30 60	71.5 88.0 97.0	4,400	10
10 b) Newport, Mon. Devonian Marl.	92	33	20	18	0 20 40 60	75.0 85.0 110.0 120.0	4,200	17
10 c) Newport, Mon. Weathered clayey Devonian Marl.	92	56	20	22	0 20 40 60	34.3 75.0 90.0 115.0	1,700	24
10 d) Ireland. Gravel, sand and clay.	46	42	20	10	0 20 40 60	85 123 164 203	3,500	30
10 e) Ireland, Gravel, sand and clay.	37	27	12	6	0 20 40 60	78 124 175 225	3,000	33

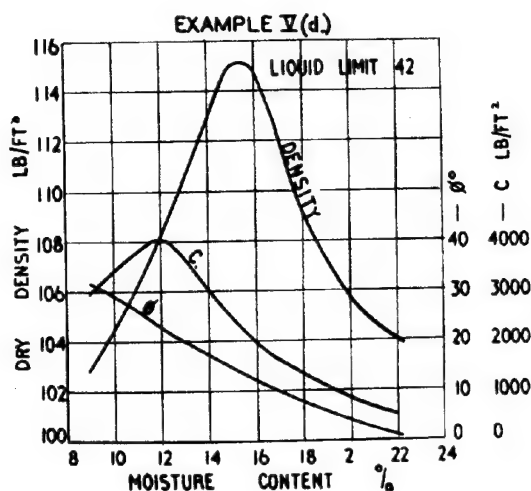


FIG.5a

they occur well below ground water level and in these cases the  $\phi$  may of course be due to an air content. However, three of them are definitely saturated. The liquid limits of all these soils are about 30 - 35.

**VII. SATURATED UNDISTURBED SILTS  $\phi > 0$ .**

The last group is most interesting. A few silts have been tested which give a  $\phi$  even though saturated. Not many of these materials have been found and some results have had to be rejected since the water contents were lower in the stronger samples, although

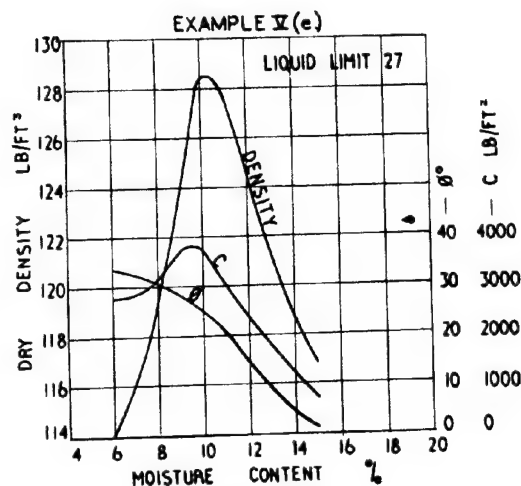


FIG.5b

the authors are of the opinion that this did not account completely for the increase in strength. Five examples are given in Table VII. Sample a is a recent marine alluvium. Samples, b, c and d are Eocene silts taken from a depth of about 40 - 50 feet on the same site but not at the same time. They are permeable and definitely frictional. Sample e was taken from a Pleistocene deposit formed in a glacial lake. The soil becomes more silty with increasing depth and samples above sample e showed no  $\phi$  but had a higher liquid limit. A typical test result is given in Fig. 7.

**TABLE VI**  
**CLAY SHALES AND SILTSTONES**

Description	Saturation %	Liquid Limit %	Plastic Limit %	Moisture content %	$\sigma_u$ lb/in <sup>2</sup>	$\sigma_u - \sigma_v$ lb/in <sup>2</sup>	$c$ lb/ft <sup>2</sup>	$\phi$
10 a) Portishead. Stiff red clay shale Kemper Marl.	81	41	27	20	0 30 60	30 71 110	1,440	23
10 b) Portishead. Stiff red & green clay shale, Kemper Marl.	100	29	23	19	0 20 40 60	38 69 109 133	1,600	27
10 c) Newport, Mon. Hard fissured red siltstone. Devonian.	91	30	17	9	0 20 40 60	23.0 49.7 90.0 125.0	900	28
10 d) Newport, Mon. Firm red weathered siltstone. Devonian.	100	32	16	10	0 20 40 60	24.5 47.2 55.0 57.5	1,440	16
10 e) Severn Estuary. Firm red clay shale. Kemper Marl.	100	30	17	15	0 20 40 60	41.5 62.0 78.0 85.5	2,300	16
10 f) Waun-y-Gilfach. Laminated grey clay shale. Coal measured.	86	Not known		9	0 20 40 60	17.6 63.1 90.7 121.5	1,600	25
10 g) Dormanstown. Hard grey shale	90	$c_{36}$	$c_{22}$	18	0 40 60	13.5 60.5 86.5	700	22

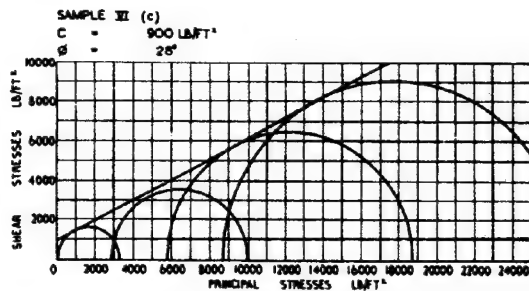


FIG.6

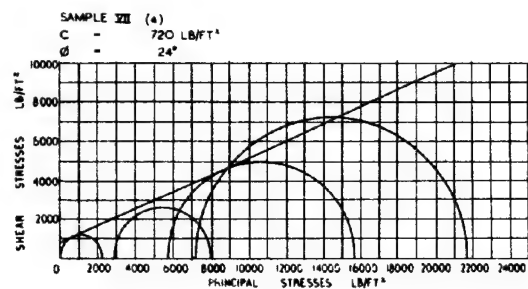


FIG.7

### DISCUSSION.

The results quoted in this paper were obtained in the course of routine tests on a large number of samples tested for the analysis of very diverse problems. The classification suggested in this paper was not envisaged when the tests were carried out and in some cases the lack of some piece of in-

formation or doubt about a test result has forced the rejection of several examples which could have been included had check tests been carried out at the time of test.

With saturated clays, whether soft or stiff, undisturbed or remoulded, sufficient tests have been done to prove that there is no increase in shear strength for the conditions of this test. This result is confirm-

**TABLE VII**  
**SATURATED UNDISTURBED SILTS**

Description	Saturation %	Liquid Limit %	Plastic Limit %	Moisture content %	$\sigma_v$ lb/in <sup>2</sup>	$\sigma_v - \sigma_h$ lb/in <sup>2</sup>	$c$ lb/ft <sup>2</sup>	$\phi^\circ$
10 a) Clyde Estuary. Compact slightly clayey silt. Recent.	100	31	21	24	0 20 40 60	16.0 35.5 68.8 100.0	720	24
10 b) Poole. Compact grey-white silt. Eocene.	100	23	19	21	0 20 40 60	13.0 115.0 110.0 200.0	450	38
10 c) Poole. Firm silty-clay.	100	32	15	19	0 30 60	19.1 81.4 185.0	750	34
10 d) Poole. Firm very silty clay.	100	30 to 35	12 to 15	15	0 20 40 60	77.5 97.4 110.5 129.0	4,040	18
10 e) Wrexham. Firm silty clay. Pleistocene.	100	23	15	16	0 20 40 60	18.8 38.3 34.8 75.0	1,000	19

ed by the results of a large number of tests carried out in the U.S.A. under similar conditions. 2) This result presumably means that the effective pressure does not increase with the lateral pressure, as shown by Terzaghi, 3) 4) Rendulic 5) and Jurgenson, 6)

It is significant that no soil in Table I has a liquid limit lower than 46%. A careful search through several hundred test results showed that no soil which would fall into Group I had a liquid limit less than about 38%. In Group II the only soils with liquid limits below 40% were boulder clays or were of glacial origin i.e. soils in which the clay fraction was not very active being composed of mechanically comminuted rock flour. Cooling 7) has shown that the particle size distribution of these soils is likely to be the same as that of a "normal" clay soil with a higher liquid limit.

In Group VII the number of tests is small but  $\phi$  is definitely greater than zero. No sample in this Group had a liquid limit greater than 35%. The authors' tentative explanation is that these silts have a dilatant structure. This phenomenon is familiar in dense sands and is the name given to an expansion of the material consequent upon shear deformation. Such an expansion, which need only occur on the plane of shear failure, can result in a drop in pore-water pressure which may even become negative. Since the total pressure remains unchanged the effective pressure must increase by a corresponding amount. The shear strength therefore increases with lateral pressure. This effect would only be expected in soils with a pronounced structure and may not occur with the same soil when remoulded. Further it is likely to be restricted to soils of a certain particle size. In

this respect it should be noted that the liquid limit is not an index of particle size and the particle size of the various soils in Group VII may be considerably more alike than would be expected from the liquid limits.

In the partially saturated soils of Groups IV and V the increase in strength with lateral pressure is easily explained by immediate compaction and what might be called "micro-consolidation" into the air voids.

In the case of the clay-shales and siltstones of Group VI it seems possible that there may be an appreciable area of grain to grain contact, in which case the effective pressure can increase immediately with increase in lateral pressure. On the other hand the possibility of dilatancy in these materials cannot be ruled out.

The authors are aware that in the type of triaxial test in use in Holland and Belgium angles of shearing resistance greater than zero are habitually obtained for fully saturated clays. The authors are of the opinion that the evidence indicates that this is due to a certain amount of consolidation occurring during the test. This point is important and the authors hope that full discussion will result in agreement.

#### TENTATIVE CONCLUSIONS.

- 1) All clays which are fully saturated, whether soft clays of recent origin or stiff fissured clays which have been over-consolidated, have an angle of shearing resistance of zero for the conditions of these tests, where no water content change is allowed to occur under the applied stress.
- 2) All clays which are partially saturated, either because they exist above present

ground water level or because they have been excavated and recompact, exhibit an angle of shearing resistance always greater than zero.

3) Clay-shales and siltstones give a value of  $\phi$  greater than zero. In some cases this may be due to partial saturation, but the evidence suggests that there may also be some other cause such as appreciable area of contact between the grains.

4) Some saturated silts give values of  $\phi$  greater than zero even when tested under conditions of no water content change. These silts have liquid limits less than about 35%. The reason for this result is not known but it is suggested that it may be connected with the phenomenon of dilatancy which could cause an increase in effective pressure due to a decrease in the pore-water pressure.

#### REFERENCES TO BIBLIOGRAPHY.

- 1) Skempton A.W. and H.Q. Golder "Practical Examples of the  $\phi = 0$  Analysis of Stability in Clays". Paper to this Conference.
- 2) Rutledge P.C. "Triaxial Shear Research." Waterways Experiments Station, Vicksburg U.S.A. (1947)
- 3) Terzaghi K. "Simple Tests determine Hydrostatic Uplift." Engineering News Record 116

- p. 872. (1936)
- 4) Terzaghi K. "Tragfähigkeit der Flachgründungen." Int. Assoc. Br. Str. Eng. p. 659. Paris (1932).
- 5) Rendulic L. "Ein Grundgesetz der Tonmechanik und sein experimenteller Beweis." Der Bauingenieur 18 p. 459 (1937).
- 6) Jürgenson L. "The Shearing Resistance of Soils." Jour. Bost. Soc. C.E. July 1934.
- 7) Colling L.F. "Development and Scope of Soil Mechanics." Inst. C.E. London 1946.

#### REFERENCES TO TEST RESULTS IN TABLES 1 TO 7.

- 8) A.W. Skempton "The Geotechnical Properties of a Deep Stratum of Post-glacial Clay at Gosport." Proc. 2nd Int. Conf. on Soil Mechanics 1948.
- 9) A.W. Skempton "A Slip in the West Bank of the Eau - Brink - Cut." J. Inst. C.E. Vol. 24 No. 7 1945.
- 10) Soil Mechanics, Ltd., Unpublished Records.
- 11) A.W. Skempton Unpublished Tests at Imperial College.
- 12) A.W. Skempton Unpublished Tests at B.R.S.
- 13) H.Q. Golder "The Shear Strength of Clay and its Measurement." Inst. C.E. Glasgow Association, 9th March, 1945.
- 14) A. Casagrande "Progress Report No. 4 on Cooperative Triaxial Shear Research." Harvard University, 1941.

-o-o-o-o-o-o-

## II d 3

### A STUDY OF THE IMMEDIATE TRIAXIAL TEST ON COHESIVE SOILS

A.W. SKEMPTON M.Sc., A.M.I.C.E., F.G.S.

University Reader in Soil Mechanics and  
Assistant Professor at Imperial College,  
University of London

#### 1. INTRODUCTION.

Two basic types of compression test are used for investigating the shear characteristics of cohesive soils. Firstly the immediate triaxial test, in which the specimen is stressed under conditions of no water content change. The unconfined compression test is a special case of the immediate triaxial test, where the applied lateral pressure is zero.

Secondly, the equilibrium triaxial test in which the specimens is allowed to attain equilibrium under an applied hydrostatic pressure before being tested in compression  $\bar{\epsilon}$ .

The immediate triaxial test is, from the practical point of view, the more useful and provides the basis for the  $\phi = 0$  analysis of stability in saturated clays. The equilibrium test is less easily interpreted and may, indeed, be misleading in the evaluation of stability problems (Terzaghi 1947).

In the present paper an attempt is made to study the immediate triaxial test from three points of view:

- i) to assess the significance of the inclination of the shear planes in compression specimens of cohesive soils
- ii) to obtain a theoretical expression for the pore water pressure set up in a saturated clay when stressed under conditions of no water content change
- iii) to obtain a theoretical expression for the compression strength of a saturated

clay, as measured in the immediate triaxial test, in terms of the true cohesion and true angle of internal friction as defined by Hvorslev (1937).

The treatment is approximate, but it is presented in the hope that it may prove useful in further research work.

#### 2. THE IMMEDIATE TRIAXIAL TEST.

In the immediate triaxial test a cylindrical specimen initially in equilibrium at some particular water content under a capillary pressure  $x_a$  p, is placed between non-porous end pieces and covered with a thin rubber envelope. The specimen is subjected to a hydrostatic pressure  $\sigma_3$  and the axial pressure is then progressively increased until failure occurs under a total applied axial pressure  $\sigma_1$ . No water content change is allowed to take place during the test.

With saturated clays the compression strength ( $\sigma_1 - \sigma_3$ ) is found to be a constant,

x) In the U.S.A. these two types are referred to as the "quick" and "consolidated" triaxial tests (v. Triaxial Shear Research 1947).

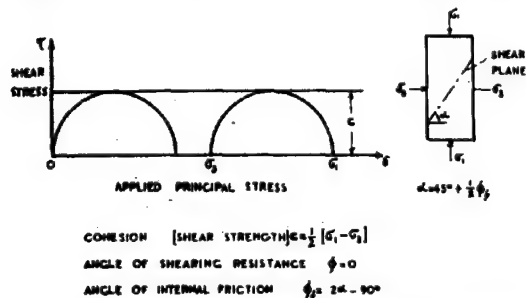
xa) In Laboratory work on remoulded clays p is the pressure under which the specimen has been consolidated prior to the test.



for any given water content, and the clay is therefore behaving with respect to the applied stresses at failure as a purely cohesive material, with an angle of shearing resistance  $\phi$  equal to zero. The apparent cohesion or "shear strength" of the clay is thus (v. Fig. 1a).

$$c = \frac{1}{2} (\sigma_1 - \sigma_3) \quad (1)$$

and this criterion of failure is the basis of the  $\phi = 0$  analysis of stability in saturated clays.



Typical results of immedial triaxial test on saturated clay.

FIG. 1a

It is clear from Fig. 1a that the unconfined compression strength (where  $\sigma_3 = 0$ ) is identical with the strength found in the immediate triaxial test even when  $\sigma_3$  is large. This result was proved experimentally by Terzaghi in 1932.

With saturated silts and partly saturated clays the angle of shearing resistance is greater than zero, in spite of the fact that no water content change takes place. The reasons for this behaviour are believed to be (i) that dilatancy occurs in silts and the pore water pressure can therefore decrease with a corresponding increase in effective pressure; and (ii) that the presence of air voids in a partially saturated clay results in an almost instantaneous increase in effective pressure, although the overall volume change may be small (Golder and Skempton 1948).

In all types of cohesive soils it is often observed that failure takes place by shearing along quite well defined diagonal planes (Luders' lines) and that, with very few exceptions, these planes are inclined at angles of more than  $45^\circ$  to the horizontal ( $\sigma_1$  being taken as vertical).

### 3. INCLINATION OF THE SHEAR PLANES.

According to Mohr's theory of failure the shear planes in a compression specimen should be inclined at  $(45^\circ + \frac{1}{2}\phi)$  where  $\phi$  is the slope of the envelope curve, (see Fig. 1b). This is in reasonable agreement with observations on those materials which fail in shear, such as steel and (xb) marble and it might be expected that the shear planes in a saturated clay tested at constant water content would be inclined at  $45^\circ$  while the angle would be steeper than  $45^\circ$  for silts (and for saturated clays in the equilibrium triaxial test where  $\phi$  is greater than zero). Terzaghi in 1936 demonstrated, however, that the inclination of the shear plane depends upon the true angle of friction of the soil and is entirely independent of the angle of shearing resistance.

This important fact is not widely appreciated and the following analysis has been presented to emphasise the point and also to provide a basis for the mathematical treatment

in sections 4 and 5. As the initial condition it will be assumed that the specimen is in equilibrium under the pressure  $p$ . During the applications of the pressures  $\sigma_1$  and  $\sigma_3$  pore water pressure will be established, as observed by Rendulic (1937) and Taylor (1947). If at the time of failure the pore water pressure is  $u$  then the effective principal stresses ( $\sigma'_i$ ) will be

$$\left. \begin{aligned} \sigma'_1 &= p + \sigma_1 - u \\ \sigma'_3 &= p + \sigma_3 - u \end{aligned} \right\} \quad (2)$$

It will now be assumed that failure takes place on a particular plane when the shear stress on that plane is equal to the shear strength of

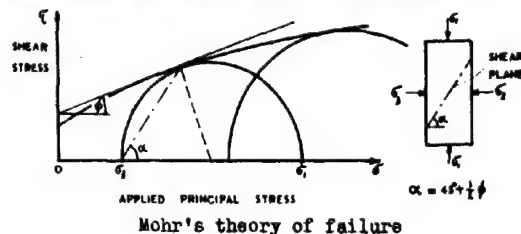


FIG. 1b

the soil, defined by the equation

$$s = c_e + n' \tan \phi_f \quad (3)$$

This is the Coulomb criterion of failure in which, following Hvorslev (1937),  $c_e$  and  $\phi_f$  are the true cohesion and true angle of internal friction of the soil at the water content, or porosity, of the test specimen, and  $n'$  is the effective pressure normal to the plane. Both  $c_e$  and  $\phi_f$  will vary with water content but at any given water content they can be taken as constants.

Now the effective normal pressure and the shear stress on any plane inclined at  $\alpha$  to the horizontal are:

$$\left. \begin{aligned} n' &= \sigma'_1 \cos^2 \alpha + \sigma'_3 \sin^2 \alpha \\ \tau &= \frac{1}{2} (\sigma'_1 - \sigma'_3) \sin 2\alpha \end{aligned} \right\} \quad (4)$$

Thus from equation (2)

$$\left. \begin{aligned} n' &= p + \sigma_1 \cos^2 \alpha + \sigma_3 \sin^2 \alpha - u \\ \tau &= \frac{1}{2} (\sigma_1 - \sigma_3) \sin 2\alpha \end{aligned} \right\} \quad (5)$$

For limiting equilibrium along this plane

$$\frac{1}{2} (\sigma_1 - \sigma_3) \sin 2\alpha = c_e + (p + \sigma_1 \cos^2 \alpha + \sigma_3 \sin^2 \alpha - u) \tan \phi_f \quad (6)$$

and failure will take place along that plane where  $\sigma_1$  in equation (6) is a minimum. The value of  $\alpha$  satisfying this condition can be

found by equating  $\frac{d\sigma_1}{d\alpha}$  to zero, and is

$$\alpha = 45^\circ + \frac{\phi_f}{2}$$

(xb) v. Nadai (1931), Mohr's theory does not strictly apply to materials such as concrete which fail partly by shear and partly by splitting. (Terzaghi 1945).

(xc) As defined by Terzaghi (1936).

Hence the shear plane is inclined at  $(45^\circ + \frac{1}{2} \phi_r)$  to the horizontal; and this result is independent of the pore water pressure  $u$  and the angle of shearing resistance  $\phi$ . Equation (4) therefore applies, theoretically, to any cohesive soil.

In tests on individual undisturbed specimens it is often difficult to obtain consistent values of  $\alpha$  owing to lack of homogeneity (xd). The author has, however, plotted in Fig. 2 the results of tests known to him where this angle was reasonably consistent in a number of specimens of the particular clay. It will be seen that there is a marked tendency for  $\phi_r$  to decrease with increasing porosity. The relationship is particularly clear with remoulded soils where anisotropy and structural effects are reduced to a minimum.

Four points may particularly be noted:

i) Bentonite consists almost exclusively of very small particles of the clay mineral montmorillonite which are probably surrounded by layers of adsorbed water. It would be difficult to see how any appreciable frictional forces could develop in such a material and, as will be seen, the shear planes in the specimens of Bentonite are, alone of all the cases recorded in Fig. 2, inclined at very nearly  $45^\circ$ . It is possible, however, that any clay at water contents approaching the liquid limit will show angles close to  $45^\circ$ . This requires further investigation.

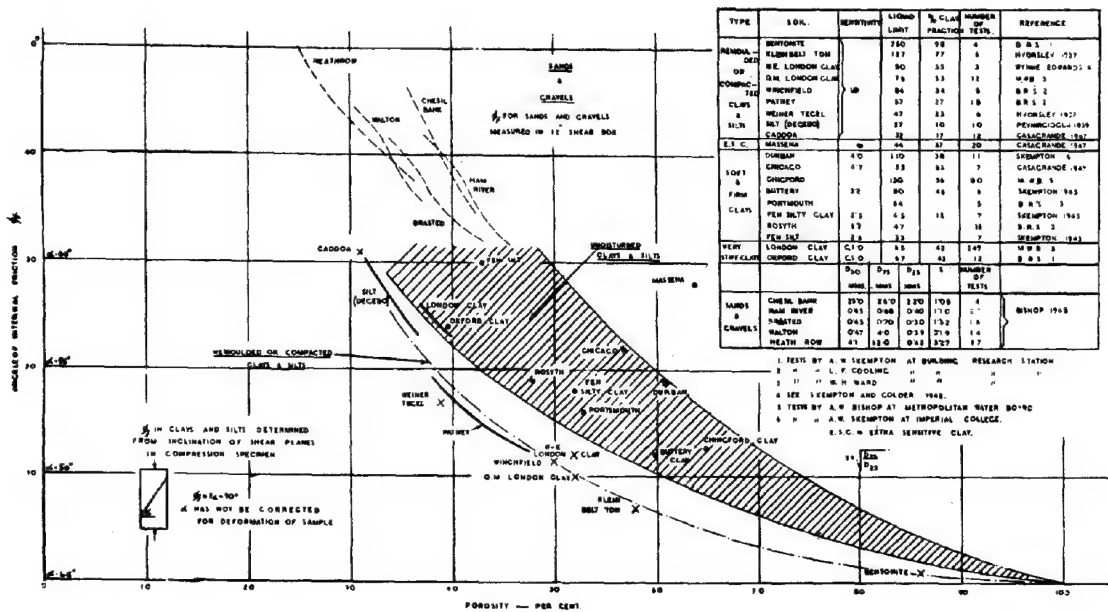
ii) Other factors than porosity are obviously involved. There is for example a definite tendency for clays with a greater sensitivity to  $\alpha$ ) remoulding to exhibit a higher  $\phi_r$ , at any given porosity, than those with a less sensitive structure. The Massena clay is an extreme example, showing a complete loss in strength on remoulding, and there may be another zone in Fig. 2 characteristic of these extra sensitive clays.

iii) It is perhaps significant that the sands and gravels appear to link in with and form an extension of the relationship shown by the undisturbed silts and clays. This suggests that in cohesive soils the frictional properties are of a similar character to those in sands, although less pronounced owing to the greater porosities. Terzaghi's views on clay structure (Terzaghi 1947) seem to be in accord with this suggestion.

iv) Most of the clays (LL greater than 40) have been proved to show a zero angle of shearing resistance in the immediate triaxial test.

xd) The inclination of the shear planes is also influenced by anisotropic strength properties. (Casagrande and Carrillo, 1944).

xe) Sensitivity =  $\frac{\text{undisturbed strength}}{\text{remoulded strength}}$



2 Relation between angle of internal friction and porosity.

FIG. 2

The total evidence presented in Fig. 2 indicates that, in spite of the inevitable difficulties of determination and interpretation, the inclination of the shear planes in cohesive soils has a real physical significance and is a measure of the angle of internal friction. Internal friction is a directional property. The angle of shearing resistance is not. It is simply the rate of increase in shear strength with pressure.

#### 4. PORE WATER PRESSURES.

In the foregoing analysis, which applied to all cohesive soils, it was sufficient to assume the presence of a pore water pressure  $u$ . In the case of non-dilating saturated clays, however, it is possible to derive an expression for this pressure from the condition that no volume change takes place when the clay is stressed under conditions of no water content change. In the following treatment it is necessary to realize that a saturated clay is a 2-phase system consisting of a compressible structure of mineral particles (the "clay structure") and water, filling the voids of the clay structure. The water can be taken as incompressible in comparison with the clay structure.

It will be seen from equation (2) that the changes in effective pressure during the test are

$$\Delta \sigma'_1 = (\sigma_1 - u) \quad (8)$$

$$\Delta \sigma'_3 = -(u - \sigma_3)$$

The change  $\Delta \sigma'_3$  is actually a decrease in pressure since, as will be shown,  $\sigma_3 < u < \sigma_1$ .

Now a change in effective pressure is accompanied by deformations in the clay structure, and the pore water pressure  $u$  must consequently be such that the specimen, although subject to deformations, remains at constant volume. With respect to increasing effective pressure (causing consolidation) the modulus of compression and Poisson's Ratio, of the clay structure, will be taken as  $E_c$  and  $\mu_c$  while with respect to decreasing effective pressure (causing swelling) the modulus and Poisson's Ratio will be  $E_s$  and  $\mu_s$ .

The strains are therefore

$$\left. \begin{aligned} \epsilon_1 &= \left[ \frac{(\sigma_1 - u)}{E_c} + 2\mu_s \left( \frac{u - \sigma_3}{E_s} \right) \right] \\ \epsilon_3 &= - \left[ \mu_c \left( \frac{\sigma_1 - u}{E_c} \right) + (1 - \mu_s) \left( \frac{u - \sigma_3}{E_s} \right) \right] \end{aligned} \right\} \quad (9)$$

Consequently the volume change is

$$\epsilon_1 + 2\epsilon_3 = \frac{C_c}{3} \left[ (\sigma_1 - u) - 2(u - \sigma_3) \right] \frac{C_s}{C_c} \quad (10)$$

where  $C_c = \frac{3(1 - 2\mu_c)}{E_c}$  is the compressibility (volume decrease per unit all-sided effective pressure increase) and  $C_s = \frac{3(1 - 2\mu_s)}{E_s}$

is the expansibility (volume increase per unit all-sided effective pressure decrease) of the clay structure. But the volume change is approximately zero, and, since the compressibility of the clay structure with respect to an increase in effective pressure is not zero if it is seen that the following relationship must exist:

$$(\sigma_1 - u) - 2(u - \sigma_3) \frac{C_s}{C_c} = 0 \quad (11)$$

$$\text{or if } \frac{C_s}{C_c} = \lambda$$

then

$$u = \frac{\sigma_1 + 2\lambda\sigma_3}{1 + 2\lambda} \quad (12)$$

The pore water pressure can therefore be evaluated if  $\lambda$  is known. For soft clays  $\lambda$  approaches zero, since the compressibility is far greater than the expansibility, while the upper limit of  $\lambda$  is unity. The condition  $\sigma'_3 < u < \sigma'_1$  is therefore satisfied.

The effective principal stresses in a saturated clay, stressed under conditions of no water content change by applied principal stress  $\sigma_1$  and  $\sigma_3$ , are therefore

$$\left. \begin{aligned} \sigma'_1 &= p + (\sigma_1 - \sigma_3) \frac{2\lambda}{1 + 2\lambda} \\ \sigma'_3 &= p - (\sigma_1 - \sigma_3) \frac{1}{1 + 2\lambda} \end{aligned} \right\} \quad (14)$$

For most clays  $\lambda$  probably does not exceed about 0.5 and the practical limits of the effective principal stresses are thus

$$\begin{aligned} \lambda = 0: \quad \sigma'_1 &= p \\ \sigma'_3 &= p - (\sigma_1 - \sigma_3) \\ \lambda = \frac{1}{2}: \quad \sigma'_1 &= p + \frac{1}{2}(\sigma_1 - \sigma_3) \\ \sigma'_3 &= p - \frac{1}{2}(\sigma_1 - \sigma_3) \end{aligned}$$

These conclusions are in agreement with experimental observations by Rendulic (1937) and Taylor (1947) and are, moreover, in general accord with the "working hypothesis" put forward by Casagrande (1947).

Equations (14) are approximate in so far as linear stress-volume relationship have been assumed, see equation (10). Where  $(\sigma'_1 - \sigma'_3)$  is small compared with  $p$ , as in a clay beneath a foundation, the approximation is probably reasonable and equation (14) provides the basis for calculating immediate settlements. In the triaxial test, however, a more exact solution would have to be based on finite stresses and non-linear stress-volume relationships.

It should be noted that when the hydrostatic pressure  $\sigma_3$  is applied to the test specimen the principal effective pressures remain unaltered at the initial value  $p$ . This provides an explanation of the experimental result that  $\phi = 0$  for saturated clays in the immediate triaxial test.

#### 5. COMPRESSION STRENGTH IN TERMS OF $c_{\alpha}\phi_f$ AND $\lambda$

It will now be seen from Equation (5) and (14) that

$$\left. \begin{aligned} n' &= p + (\sigma_1 - \sigma_3) \frac{2\lambda \cos^2 \alpha - \sin^2 \alpha}{1 + 2\lambda} \\ \tau &= \frac{1}{2} (\sigma_1 - \sigma_3) \sin 2\alpha \end{aligned} \right\} \quad (15)$$

Assuming, as before, the Coulomb-Hvorslev equation, failure will take place on any plane when

$$\frac{1}{2} (\sigma_1 - \sigma_3) \sin 2\alpha = c_e + \left[ p + (\sigma_1 - \sigma_3) \frac{2\lambda \cos^2 \alpha - \sin^2 \alpha}{1 + 2\lambda} \right] \tan \phi_f$$

if This must not be confused with the compressibility of the whole specimen with respect to applied pressure. This is of course equal to zero.

The condition  $\frac{d\sigma_1}{d\alpha} = 0$  again leads to the solution  $\alpha = 45^\circ + \frac{\phi_f}{2}$

and putting this value of  $\alpha$  in Equation (16) it is found that

$$\frac{1}{2}(\sigma_1 - \sigma_3) = \frac{c_e \cos \phi_f + p \sin \phi_f}{1 + \sin \phi_f \frac{(1-2\lambda)}{(1+2\lambda)}} \quad (17)$$

This equation is the criterion of failure, based on the assumption of linear stress-volume relationships for the clay structure, for saturated clays in the immediate triaxial test.

Since  $c_e$ ,  $\phi_f$  and  $\lambda$  are constants for the clay at any given water content, corresponding to a definite value of  $p$ , it follows that

$$\frac{1}{2}(\sigma_1 - \sigma_3)$$

is a constant at any given water content: which agrees with test results.

It is interesting to note that the effective normal pressure on the shear plane is

$$n' = p - \frac{1}{2}(\sigma_1 - \sigma_3) \left[ \sin \phi_f + \frac{(1-2\lambda)}{(1+2\lambda)} \right] \quad (18)$$

Thus this pressure does not remain unaltered during the test; but the change is directly proportional to  $(\sigma_1 - \sigma_3)$  which is itself constant, and the change in effective normal pressure is therefore independent of  $\sigma_3$ .

## 7. A METHOD OF DETERMINING $c_e$ AND $\phi_f$ .

The author would suggest the following method of determining  $c_e$  and  $\phi_f$  for saturated clays. A sample is consolidated under a pressure  $p$  and then subjected, at constant water content, to an increasing axial pressure until failure occurs.

Thus  $\sigma_3 = 0$  and

$$\frac{1}{2}\sigma_1 = \frac{c_e \cos \phi_f + p \sin \phi_f}{1 + \sin \phi_f \frac{(1-2\lambda)}{(1+2\lambda)}} \quad (19)$$

But if  $\sigma_3 = 0$  then

$$u = \frac{\sigma_1}{1+2\lambda} = j\sigma_1 \quad (20)$$

and

$$\frac{1}{2}\sigma_1 = \frac{c_e \cos \phi_f + p \sin \phi_f}{1 + \sin \phi_f (2j-1)} \quad (21)$$

Both  $\lambda$  and  $j$  can be measured experimentally, thus providing a check on equation (20) and providing two methods of evaluating the compression strength in terms of  $c_e$  and  $\phi_f$ . In addition  $\phi_f$  can be found, at least approximately, from the inclination of the shear planes, and thus  $c_e$  can be determined.

The above procedure can be compared with results obtained by the method of Hvorslev (1937). It can not be used for dilating silts or partially saturated clays.

## 8. CONCLUSIONS.

1) The inclination of the shear planes in a compression specimen of cohesive soil is a function of the angle of internal friction and

is independent of the angle of shearing resistance, which is a non-directional property.

2) For saturated clays, stressed under conditions of no water content change, the pore water pressure can be evaluated in terms of the applied stresses and the ratio of expansibility and compressibility of the clay structure.

3) Knowing the pore water pressure, either from the theoretical expression or by direct measurement, the compression strength of a saturated clay in the triaxial test can be expressed in terms of the true cohesion and internal friction of the clay at the water content of the test specimen.

## 9. ACKNOWLEDGEMENTS.

The author is indebted to Mr. L.F. Cooling, M.Sc., and Mr. A.W. Bishop, M.A., A.M.I.C.E. for sustaining helpful discussions on the subject of this paper.

## REFERENCES.

- BISHOP, A.W. 1948. "A Large Shear Box for Testing Sands and Gravels".  
Proc. 2nd Int. Conf. Soil Mechanics.
- CASAGRANDE, A. 1947. Summary of a Harvard Report, published in "Triaxial Shear Research".  
U.S. Corps of Engineers.
- CASAGRANDE, A. and CARRILLO, N. 1944. "Shear Failure in Anisotropic Materials".  
Journ. Boston. Soc. C.E. Vol. 31. 0.74
- GOLDER, H. and SKEMPTON, A.W. 1948. The Angle of Shearing Resistance in Cohesive Soils for Tests at Constant Water Content".  
Proc. 2nd Int. Conf. Soil Mechanics.
- HVORSLEV, M.J. 1937. "Über die Festigkeitseigenschaften gestörten bindiger Boden".  
Ingéniovidenskabelige Skrifter. A.No. 45. Copenhagen.
- NADAI, A. 1931. "Plasticity".  
McGraw Hill, New York.
- PEYNERCIOGLU, H. 1939. "Über die Scherfestigkeit bindiger Boden".  
Ver. Inst. Deut. Forsch. Bodenmechanik. Vol. 7. p. 28
- RENDULIC, L. 1937. "Ein Grundgesetz der Tonmechanik".  
Bauing. Vol. 18. p. 459.
- SKEMPTON, A.W. 1945. "A Slip in the West Bank of the Eau Brink Cut".  
Journ. Inst. C.E. Vol. 24. p. 267.
- TAYLOR, D.W. 1947. Summary of a M.I.T. Report published in "Triaxial Shear Research".  
U.S. Corps of Engineers.
- TERZAGHI, K. 1932. "Tragfähigkeit der Flachgründungen".  
Int. Assoc. Br. Struct. Eng. p. 659 Paris.
- TERZAGHI, K. 1936. "The Shearing Resistance of Saturated Soils and the Angle between the Planes of Shear".  
Proc. Harvard Conf. Soil Mech. Vol. 1. p. 54.
- TERZAGHI, K. 1945. "Stress Conditions for the Failure of Saturated Concrete and Rock".  
Proc. A.S.T.M. Vol. 45 p. 777.
- TERZAGHI, K. 1947. "Shear Characteristics of Quicksand and Soft Clay".  
Proc. 7th Texas Conf. Soil Mechanics.
- U.S. CORPS OF ENGINEERS. 1947 "Progress Report on Triaxial Shear Research".  
Waterways Expt. Station, Vicksburg.

11 d 4

## A CONTRIBUTION TO THE STUDY OF THE ELASTIC PROPERTIES OF SAND

GUTHRIE WILSON, S.M., B.Sc.,

and

J.L.E. SUTTON, B.A.

## NOTATION

- $\sigma_1, \sigma_2, \sigma_3$  = major, intermediate, minor principal stresses.  
 $\tau$  = sum of principal stresses.  
 $\tau$  = greatest shear stress.  
 $\epsilon$  = linear strain.  
 $E_{sec}$  = secant Young's Modulus =  $\frac{\tau}{\epsilon}$  for a mass  
 $E_{tan}$  = tangent Young's Modulus =  $\frac{d\tau}{d\epsilon}$  of sand grains  
 $G_{sec}$  = secant modulus of rigidity  
 $E_m$  = Young's Modulus for the material of which grains are composed.  
 $\mu$  = Poisson's ratio  
 $e$  = void ratio  
 $D_R$  = degree of compaction =  $\frac{e_{max} - e}{e_{max} - e_{min}}$

$$G_{sec} = c_1(\mu) \quad (1)$$

$$\mu = \frac{1}{2}$$

In 1897 August Föppl 3) described some classic tests made in the yard of his laboratory at Munich: he measured surface deflections at various distances from a small circular loaded area and found that these deflections did not agree with those deduced elsewhere by Boussinesq 4) for the case of an elastic half space.

Since then many tests have been carried out with the object of determining the distribution of stress in a loaded sand stratum and appear to have shown that the load is not dispersed so widely as would be the case in an elastic medium, but the resisting stresses are concentrated more closely around the vertical axis through the loaded area and are, consequently, greater in the neighbourhood of the axis.

All these tests were carried out in artificial sand fills placed on a rigid base and the vertical pressures were measured at the bases.

It remained for Cummings 5) to point out, in 1941, that it had been shown by Biot 6) that the presence of a rigid base under an elastic medium would produce similar stress concentrations.

In the meantime much effort had been expended in deriving expressions for the stress distribution that would accord better with the results of these tests than those derived by Boussinesq for the case of a semi-infinite elastic solid. The best known of these expressions are those of Griffith 7) and Fröhlich 8) in which a concentration factor  $\gamma$  is introduced.

## INTRODUCTION

It has long been recognised that the modulus of elasticity of sand is not constant, but varies with the state of stress, and that, therefore, sand does not obey Hooke's Law.

Boussinesq 1) in 1876 was the first to recognise this fact and to make an assumption regarding the variation of the modulus of elasticity. Todhunter and Pearson 2) state: "Boussinesq bases his theory of pulvulence on the hypothesis that masses of pulverulent material stand midway between solid and fluid bodies and act like fluids when not subjected to pressure, but when subjected to pressure gain an elasticity of form as well as of bulk, and act like solids. Boussinesq considers the slide modulus to be proportional to the mean pressure". Boussinesq also assumes the dilatation to be zero, or negligible. His assumption may be written

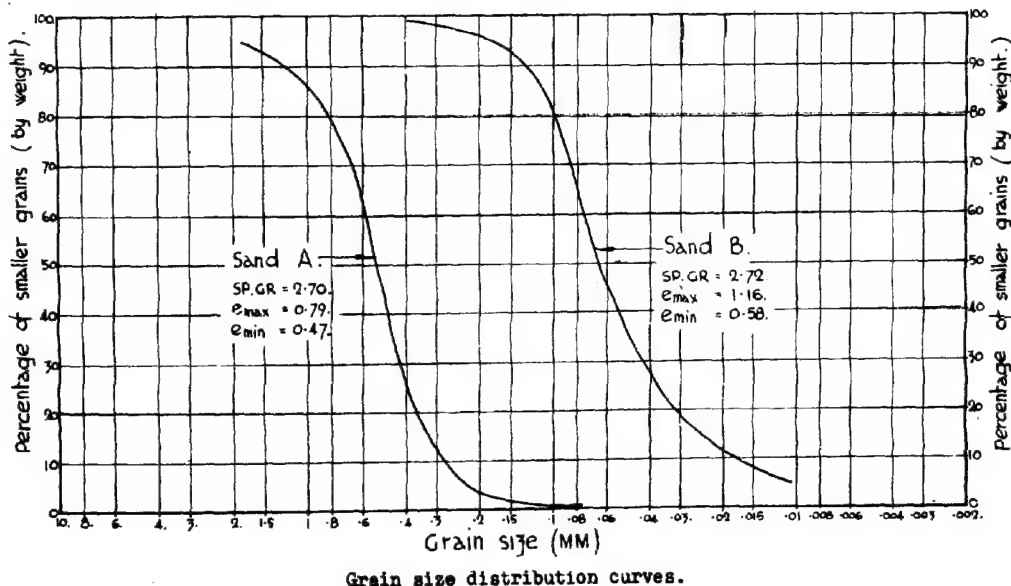


FIG.1

Fröhlich shows that if the concentration factor is equal to 3, the case reduces to that of a semi-infinite isotropic elastic solid, and if it is 4, it is equivalent to the case of a semi-infinite solid in which the modulus of elasticity increases in direct proportion to the depth. This would be true for the modulus of elasticity of the soil, before the application of any external load, if eqn. (1) were to hold.

It appears to the Authors that the problem of the distribution of stress due to a surface load on a pulverent medium has not been solved either theoretically or by test and that the whole question should be reconsidered. It would be necessary to carry out loading tests with stress measuring devices inserted at various depths within a sand stratum of considerable extent and to compare the results of these with those of a theory based on the actual elastic properties of sand. The Authors having had the opportunity to make a number of triaxial tests on sand and having studied the results of a number of other tests have assembled such information as they can on the elastic properties of sand and offer it as a contribution towards the data that it will be necessary to collect.

#### FACTORS AFFECTING THE ELASTICITY OF SAND

The principal factors which may affect the elastic modulus of a mass of freely draining sand are the following:

- a) the material of which the grains are composed. It seems reasonable to assume that this is not important, since the range of materials is not great.
- b) the sizes and shapes of the grains. Though this factor is important, the infinite variety of size and shape makes it difficult, if not impossible, to reduce it to simple mathematical terms.
- c) the degree of saturation. This is probably unimportant.
- d) the degree of compaction of the sand (or its void ratio or porosity)
- e) the stresses imposed on the sand.

In the triaxial tests from which the results given in this Paper are derived, the measured stresses are, of course, the principal direct stresses  $\sigma_1, \sigma_2, \sigma_3$ , the last two being equal; but they are generalised into  $\sigma$ , the sum of the principal stresses, and  $\tau$ , the greatest shear stress.

#### RANGE OF INVESTIGATION. SAMPLES USED.

The Authors have investigated the values assumed by the tangent Young's modulus

$E_{tan} = \frac{d\sigma}{d\epsilon}$  in the course of triaxial compression tests on two widely differing sands, under different combinations of stress and at different degrees of compaction.

One series of tests (A) was carried out by the Authors themselves on a sample of Ham River Sand from Richmond, Surrey, England; the other (B) was performed by Prof. A. Casagrande and Mr. John D. Watson at the Harvard University Soil Mechanics Laboratory on sand from Franklin Falls, N.H., U.S.A. and published by the U.S. Army Corps of Engineers (9). The grain size curves of the two samples are given on figure 1, and the specific gravity of the material of each, and their limits of compaction, are also noted on the figure.

#### RESULTS

The results of Series A are summarised in figures (2a) to (10a), and corresponding re-

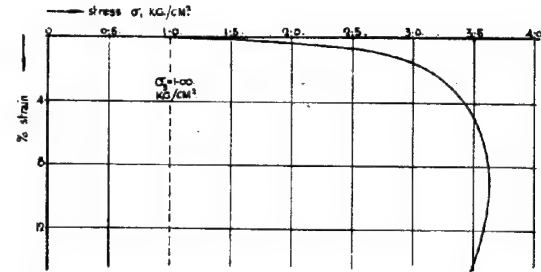


FIG.2a (Sand A:  $D_R=28\%$ )

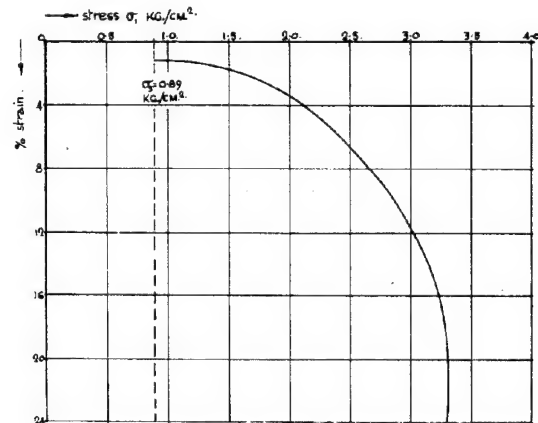


FIG.2b (Sand B:  $D_R=48\%$ )

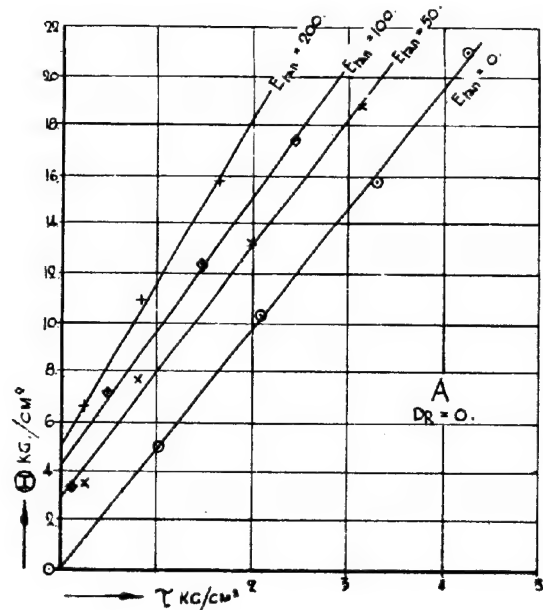


FIG.3

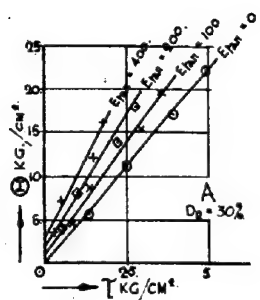


FIG.4a

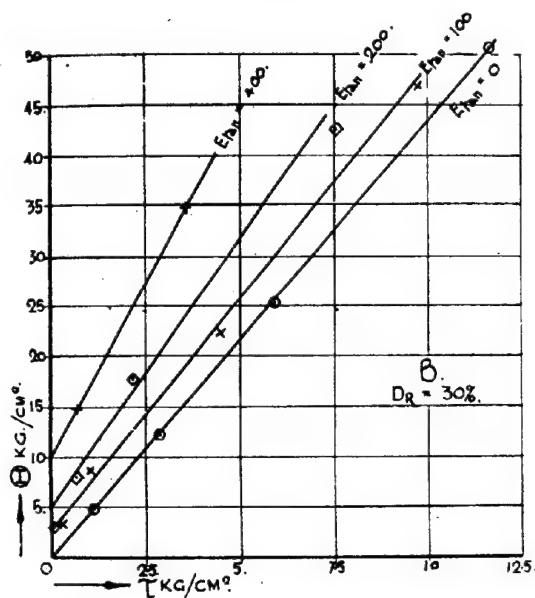


FIG.4b

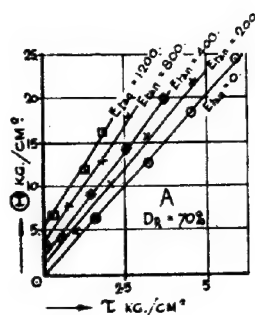


FIG.5a

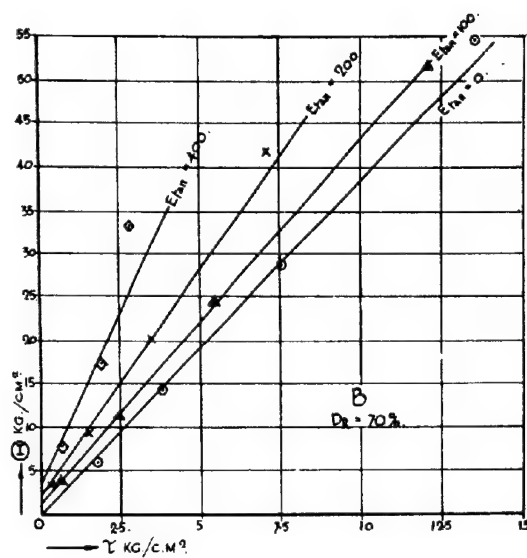


FIG.5b

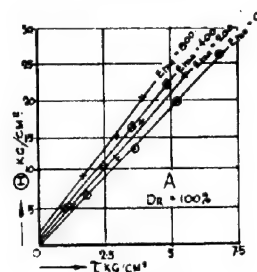


FIG.6a

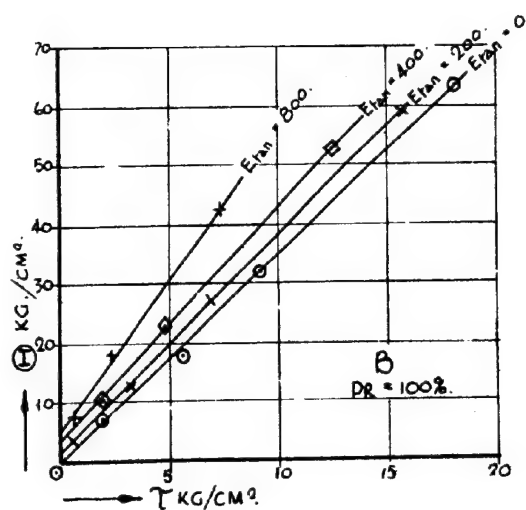


FIG.6b



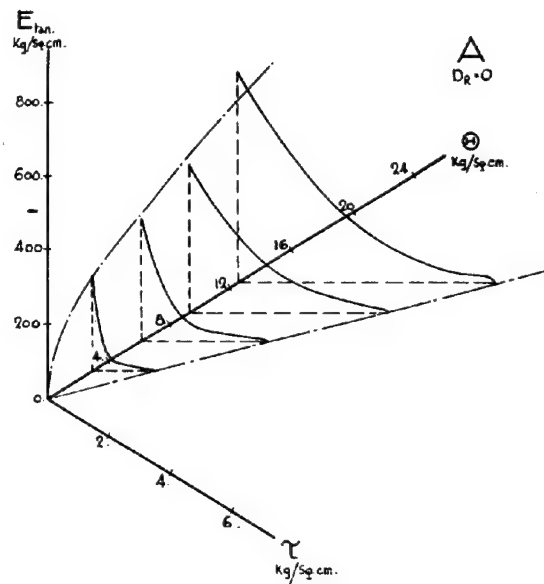


FIG. 7

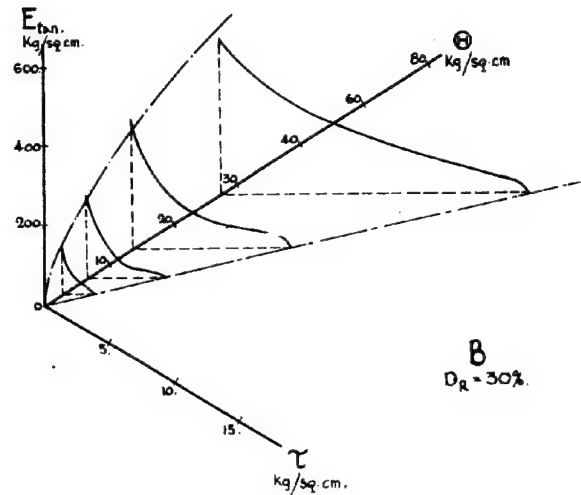


FIG. 8b

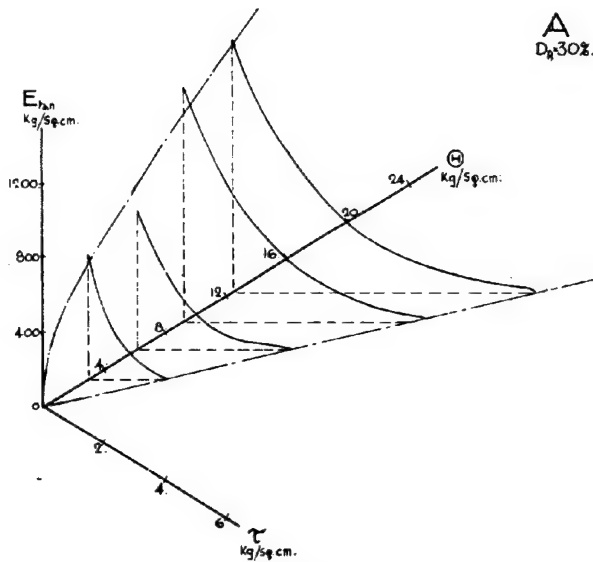


FIG. 8a

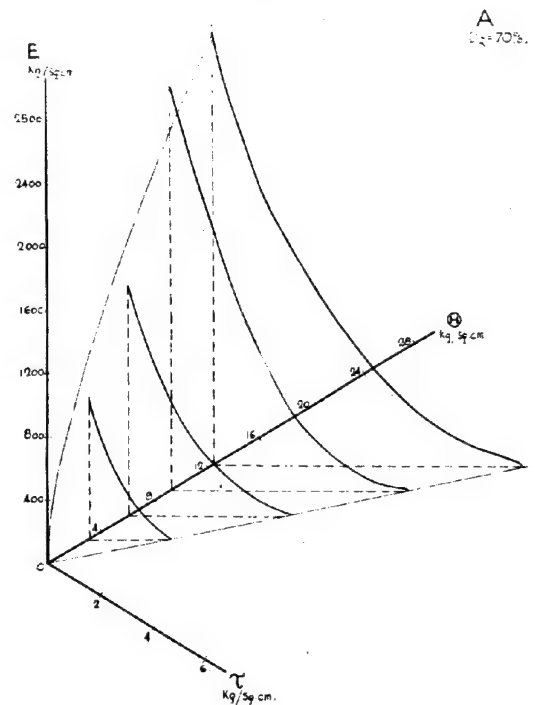


FIG. 9a

sults of Series B are given in figures (2b) to (10b).

Figures 2 are typical stress strain curves resulting from the triaxial tests.

Figures 3 to 6 give contours of  $E_{tan}$  on axes of  $\sigma_3$  and  $\tau$  for four different values of the degree of compaction.

Figures 7 to 10 are axonometric diagrams of the  $E_{tan}, \sigma_3, \tau$  surface.

#### COMMENT ON RESULTS

The results presented show the overwhelming importance of the shear stress, which was not taken into account by Boussinesq.

Starting from eqn. (1) it is easy to deduce that

$$E_{tan} = c_2 \frac{\sigma_3}{\sigma_3} \quad (2)$$

if  $\sigma_3 = \sigma_2$  be one of two equal minor principal stresses.

On the  $E_{tan}, \sigma_3$  plane, i.e. where  $\sigma_1 = \sigma_2$ , eqn. (2) reduces to

$$E_{tan} = 3c_1 \sigma_3 \quad (3)$$

It will be seen from figures 7 to 10 that this also is not true. A closer approach

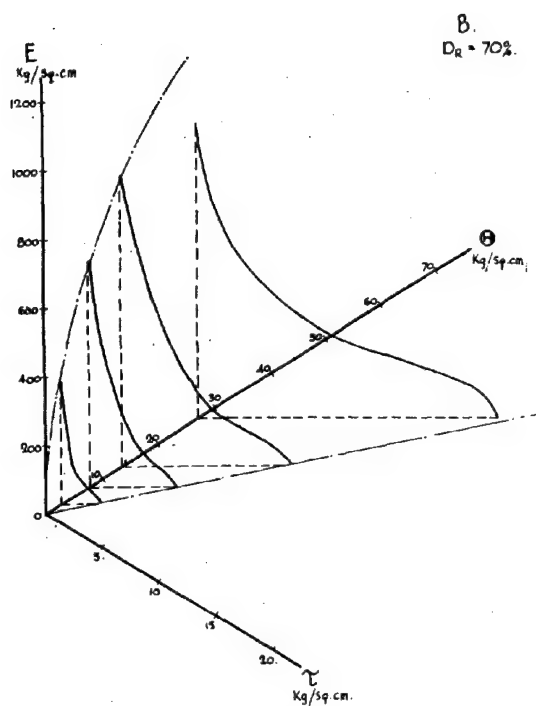


FIG.9b

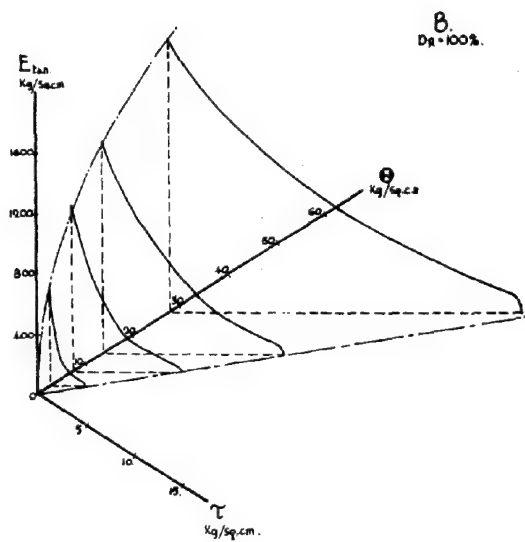


FIG.10b

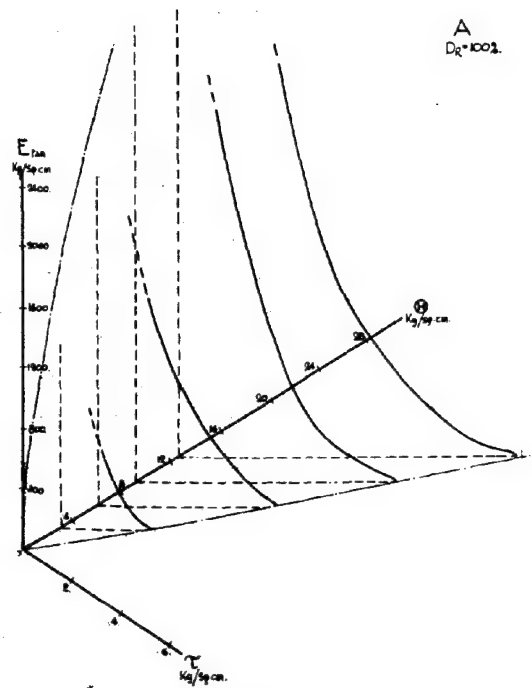


FIG.10a

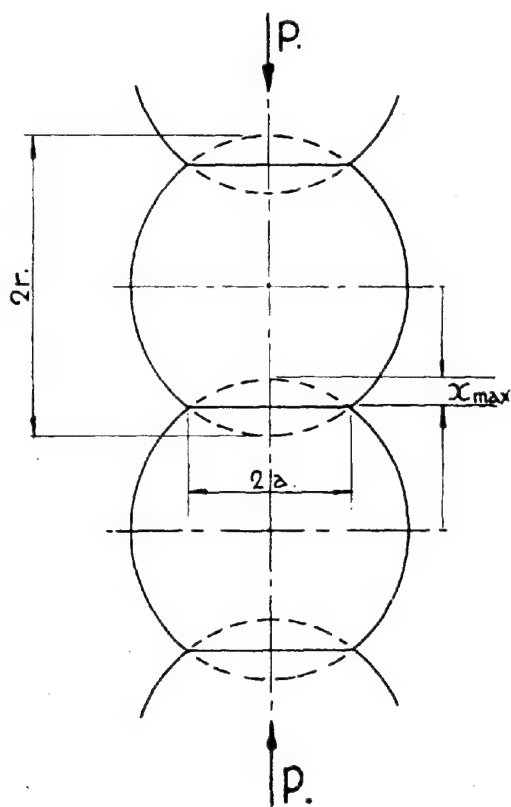


FIG.11

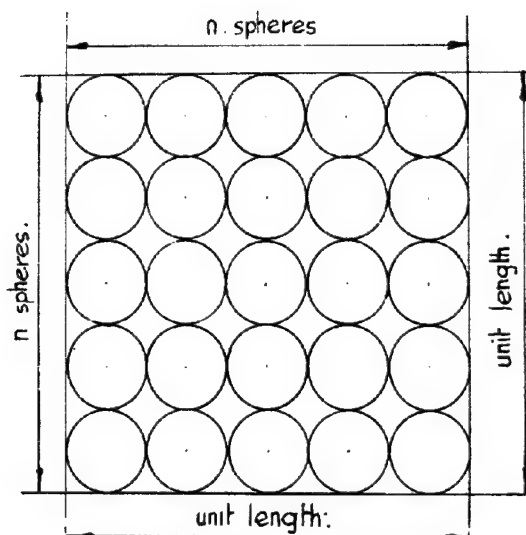


FIG.12

to the actual form of the trace on this plane can be derived from consideration of the behaviour of a mass of equal elastic spheres, in the loosest state, subjected to hydrostatic pressure.

Consider first a column of equal spheres subjected to compression, fig. 11. A. & L. Föppl 10) give the elastic deformation of each sphere as:

$$2x_{\max} = \frac{a^3}{r} = 4.23 \sqrt{\frac{P^3}{E_m^2 r}} \quad (4)$$

where  $E_m$  is the modulus of elasticity of the material of the spheres.

Hence the strain,

$$\epsilon = \frac{2x_{\max}}{2r} = 0.615 \sqrt{\frac{P^3}{E_m^2 r^4}} \quad (5)$$

If the diameter of each sphere is  $1/n$  of the unit of length, fig. 12 and  $\sigma$  be the stress per unit of gross area, we find the  $P$ , the load on each column of spheres, is given by

$$P = \frac{\sigma}{n^2} = \sigma(2r)^2 \quad (6)$$

since  $n = 1/2r$ .

Therefore,

$$\epsilon = 0.615 \sqrt{\frac{16\sigma^3 r^4}{E_m^2 r^4}} = 0.615 \sqrt{\frac{16\sigma^3}{E_m^2}} = 0.615 \left(\frac{4\sigma}{E_m}\right)^{2/3} \quad (7)$$

The longitudinal compressive strain will

be reduced by the effect of the lateral stresses. This reduction will be a constant fraction of  $\epsilon$ . We can, therefore put

$$\epsilon = C_2 \sigma^{2/3} \quad (8)$$

where  $C_2$  is a constant.

$$E_{\tan} = \frac{d\sigma}{d\epsilon} = \frac{1}{\frac{d\epsilon}{d\sigma}} = \frac{1}{\frac{2}{3} C_2 \sigma^{-1/3}} = \frac{3}{2C_2} \sigma^{1/3} = \frac{3}{2C_2} \left(\frac{\sigma}{3}\right)^{1/3} \quad (9)$$

The trace of the  $E, H, \tau$  surface on the  $E, H$  plane has, therefore, been represented on the diagrams by a cubic parabola.

Each line on figures 3 to 6 is, of course, a section of one of figures 7 to 10 by a plane parallel to the  $\sigma, \tau$  plane. The remarkable thing about these sections is that they appear to be, at least very nearly, straight lines.

From this fact it appears that  $E_{\tan}$  might be represented by an empirical formula similar to

$$E_{\tan} = a E_{\tan}^3 + (b + c E_{\tan}^n) \tau \quad (10)$$

where the index  $n$  is not much different from unity: if it were equal to 1.5, eqn. 10 could be solved for  $E_{\tan}$ , but such a formula does not seem worth elaboration at this stage when the influence of the intermediate principal stresses has not been investigated.

#### REFERENCES:

- 1) Boussinesq. "Essai theorique sur l'équilibre d'élasticité des massifs pulvureux comparé a celui de massifs solides et sur la poussée des terres sans cohesion". Memoires Couronnes et memoires des savants étrangers publiés par l'academie ... de Belgique. Tome XL., Bruxelles, 1876.
- 2) Todhunter & Pearson. "A History of the Theory of Elasticity and of the Strength of Materials." Vol. II, part II, Camb.U.P.1893, p. 313.
- 3) Föppl. "Versuche über die Elastizität des Erdbodens." Zentralblatt der Bauverwaltung, June 19th, 1897.
- 4) Boussinesq. "Application des Potentials a l'Etude de l'Equilibre et du mouvement des solides elastiques" - Paris, 1885.
- 5) Cummings. "Foundation stresses in an elastic solid with a rigid underlying boundary." Civil Engineering, November, 1941.
- 6) Biot. "Effect of certain discontinuities on the pressure distribution in a loaded soil." Physics, Vol. 6, pp. 367-375 (1935)
- 7) Griffith. "The pressures under substructures." Engineering & Contracting, Vol. 68, pp. 113-119 (1929)
- 8) Fröhlich. "Druckverteilung im Baugrunde." Vienna, 1934.
- 9) Casagrande & Watson, "Compaction tests and Critical Density Investigation of Cohesionless Materials for Franklin Falls Dam" - U.S. Engineer Office, Boston, Mass., 1938.
- 10) A. & L. Föppl, "Drang und Zwang", Berlin 1928, Vol. II. eqns. (10), p. 225 and (13) p. 226

11 d 5

THE DETERMINATION OF THE SHEARING STRENGTH OF VARVEDCLAYS AND OF THEIR SENSITIVITY TO REMOULDING

GREGORY P. TSCHIBOTARIOFF x)

and

JOHN R. BAYLISS xa)

SUMMARY.

The paper outlines previous differences of opinion concerning the use of unconfined compressive strength tests to determine the effective shearing strength of varved clays.

An investigation is described which was performed in 1946 relative to two building sites located on the same deep deposit of glacial varved clay. Photography was used extensively to check and to record the condition of each sample and to select samples for testing. Most of the specimens extracted by thin walled samplers were found to be in good condition, but most of those extracted by means of samplers with inner lining tubes serving as containers were found to have undergone distortion.

The shearing strength was determined by controlled stress unconfined compressive strength tests. Photographs showed that most of the specimens extracted by thin-walled samplers had definite shear failure planes after testing which intersected the planes of stratification. The strength of these specimens was in good agreement with the value computed from an earlier failure of a vertical cut in an excavation.

The average strength of specimens extracted by samplers with inner lining tubes reached only 55% of the average value of specimens extracted by thin-walled Shelby tube samplers. This finding explains some previous puzzling discrepancies between theoretical considerations, laboratory soil test results and full-scale field observations.

A definition of the term "Sensitivity Ratio" is proposed which is based on the ratio of the strengths of the undisturbed and the remoulded samples at equal strains, rather than their ultimate strains at failure.

The concept advanced by Dr. Terzaghi according to which the effective shearing strength of plastic clays is approximately equal to one half of their unconfined compressive strength has now been generally accepted. Some doubts have however existed concerning varved clays.

An analysis of an actual slide in plastic glacial varved clay reported by the senior author on p. 1077 of Ref. No. 5 showed that a cohesion value taken as one half of the unconfined compressive strength of the clay could account for only 50% of the shearing strength required to ensure the stability of the bank prior to failure. It therefore appeared likely that some friction was also present. On p. 1094 of Ref. No. 4 Dr. Terzaghi expressed in reply the opinion that unconfined compressive strength tests may perhaps be unsuitable for investigating varved clays.

Clarification of this question is of considerable practical importance. Most clays are stratified to some extent. Varved clays represent a condition of extreme development of stratification. If their shearing strength, as actually effective in a large mass of soil, cannot be determined in the laboratory by means of unconfined compressive strength tests, then it would become necessary to develop some other practical method of making such determinations. It would be necessary to establish criteria concerning the extent of stratification in other clays which would still permit the effective use of the unconfined compressive strength tests.

Some light has been thrown on this whole matter as a result of two investigations which were performed in 1946 on different building sites located on the same deep deposit of gla-

cial varved clay. These two sites will be referred to as "Site No. 1" and as "Site No. 2" in this paper.

The samples from both sites were tested in the Princeton Soil Mechanics Laboratory. Photography was extensively used, after partial drying, along the lines developed by Dr. Hvorslev's pioneer work in that field (Ref. No. 3), to check and to record the condition of each sample tested. Controlled stress unconfined compressive strength tests were performed twice on all suitable samples. They were tested first in their undisturbed condition, after which they were completely remoulded at the same water content and tested again. This was necessary to determine the degree of sensitivity of the clay to remolding.

It should be noted in this connection that tests performed earlier by the senior author in Egypt had shown that in one particular deposit some clay specimens could be unfavorably affected by remolding, whereas specimens from other layers of a similar type could even be strengthened by remolding (compare Fig. 14 and 15; Ref. No. 2).

Dr. Terzaghi has proposed (Ref. No. 6) to define the degree of sensitivity of a clay to remolding by means of the sensitivity ratio "S", defined as:

$$s = \frac{q_u}{q_{ur}} \quad (1)$$

where: S = sensitivity ratio based on ultimate strengths.

$q_u$  = unconfined compressive strength at failure of the undisturbed sample.

$q_{ur}$  = unconfined compressive strength at failure of the remolded sample.

x) Associate Professor of Civil Engineering, Princeton University, Princeton New Jersey, U.S.

xa) Research Assistant and Graduate Student in Civil Engineering, Princeton University, Princeton, New Jersey, U.S.

Most naturally deposited undisturbed clays exhibit brittle types of failure at relatively small strains ( $\Delta h/h$ , where "h" is the height of the sample) ranging from 4% to 8% (Ref. No. 1). Remolding usually increases the strain at failure of sensitive clays up to the ultimate value of 20% which characterizes fully plastic failure. In many cases it may be advisable to base the definition of the sensitivity of clays on the ratio,  $S'$ , of strengths of the undisturbed and the remolded samples at equal strains:

$$S' = \frac{q_u}{q_{ur}} \quad (2)$$

where:  $S'$  = sensitivity ratio based on strengths at equal strains;

$q_{ur}$  = unconfined compressive strength of the remolded sample at the strain corresponding to the failure of the undisturbed sample.

The direct use of formula (2) is predicated on the construction of stress-strain diagrams of the type illustrated by Fig. 8, and is more time consuming as compared to the use of formula (1). However, the approximate value of  $S'$  can be estimated from formula (1) and the following data:

If strain corresponding to  $q_u$  equals 5%;  $S'$

may vary from 2.50  $S$  to 3.00  $S$

If strain corresponding to  $q_u$  equals 10%;  $S'$

may vary from 1.50  $S$  to 2.00  $S$

If strain corresponding to  $q_u$  equals 15%;  $S'$

may vary from 1.05  $S$  to 1.50  $S$

If strain corresponding to  $q_u$  equals 20%;  $S' = S$

Fig. 8 and formulas (1) and (2) refer to controlled stress tests. In the case of controlled strain tests, " $q_u$ " should refer to the maximum stress reached and not to the stress at final failure. " $q_{ur}$ " should then refer to a corresponding value.

The samples from site No. 2 were extracted from 6 in. diameter bore holes which were lined with steel pipe. The 3-3/8 in. diameter samplers, 18 in. long were made of steel Shelby tubing 1/16 in. thick with slightly curved in cutting edges. Most of the samples thus extracted were in perfect condition, (Fig. 1 and Fig. 2). A few showed visible signs of slight disturbances and consequently were not used.

The general characteristics of this clay are as follows. Because of its stratified nature there is much variation from varve to varve. Within one inch depth the natural water content frequently changes by some 20% and in

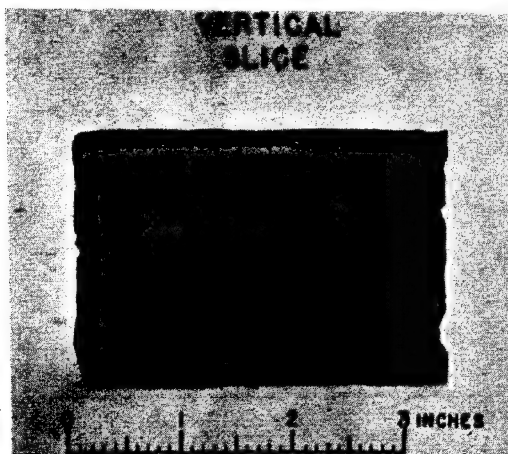


FIG.1



FIG.2

one case was found to have changed from 20% to 60%. The natural water content,  $w_n$ , usually is very close to the liquid limit value,  $w_L$ , and sometimes even exceeds it. At the same time the clay has a high unconfined compressive strength which varied from 0.50 to 2.40 tons/sq. ft. with an average value of 1.05 tons/sq. ft. and a corresponding average value of 9.3% strain at failure. The clay is very sensitive to remolding. The comparable average values of all samples tested in a remolded condition are 0.18 tons/sq. ft., and 20% strain. The average value of the Sensitivity Ratio,  $S'$ , as defined by formula (2) is 12.0 and the highest value recorded is 48.6.

The grain-size analysis indicated a very high clay content, even in the so-called "silt" varves. An attempt was made to separate various layers. A coarser grained layer was found to consist of 70% of clay sized particles - (smaller than 5 microns) - and had a liquid limit of 29% and a plasticity index of 9%; a finer grained layer had 85% particles of clay size, a liquid limit of 51% and a plasticity index of 23%. The low values of the plasticity indexes of all samples, combined with a corresponding high percentage of clay size particles, indicate the probability that they are of "rock flour" type. This is likely, considering their glacial origin, and may be a possible cause of the sensitivity of this clay to remolding. Other possible causes of such sensitivity are the subject of a cooperative study at Princeton. (Ref. No. 8).

The majority of undisturbed samples from site No. 2 which were subjected to unconfined compressive strength tests showed definite planes of shear failure which intersected the planes of stratification, (Fig. 3 and Fig. 4). Even when the planes of stratification had a natural inclination the plane of failure intersected some varves (Fig. 5). Only a very few samples failed by crushing and lateral squeez-

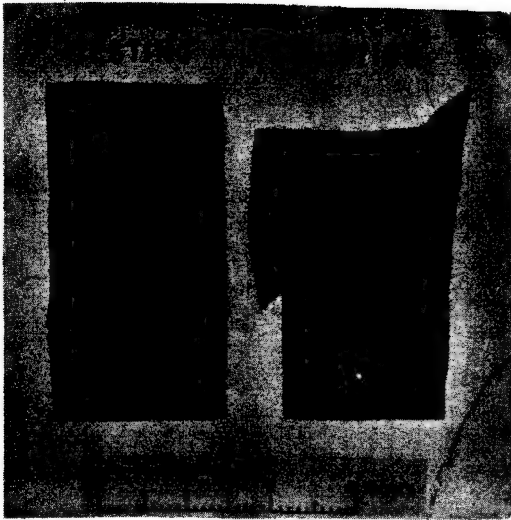


FIG.3

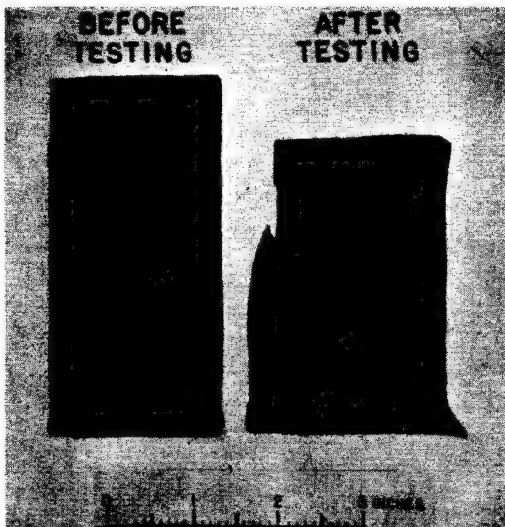


FIG.4

ing out of a single varve, (Fig. 6). It should be noted that this latter essentially plastic type of failure occurred suddenly at a strain of only 4.7% which is usually taken as an indication of brittle failure.

The fact that the types of failures in most varved clay samples from site No. 2 did not differ from the ones usually encountered elsewhere in non-stratified cohesive soil specimens is in itself an indication that the unconfined compressive strength test should be equally suitable for use on both stratified and non-stratified clays. Further confirmation, however, has been obtained by an analysis of the failure of an excavation cut which occurred in the immediate vicinity of Site No. 2 eighteen years ago; a photograph of which, taken immediately after the failure, is shown by Fig. 9. The 22.0 ft. vertical cut on the left hand side of the picture remained stable.

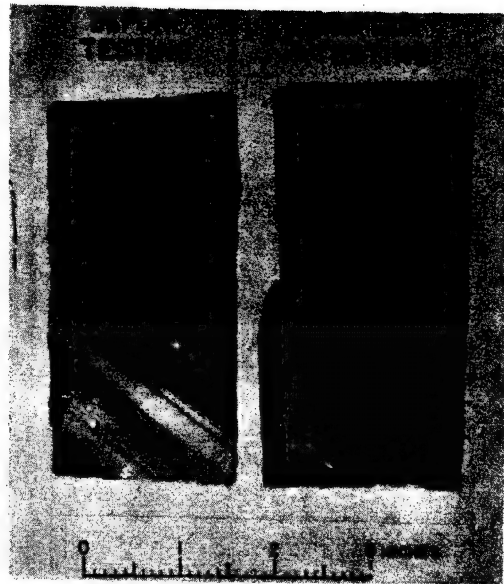


FIG.5

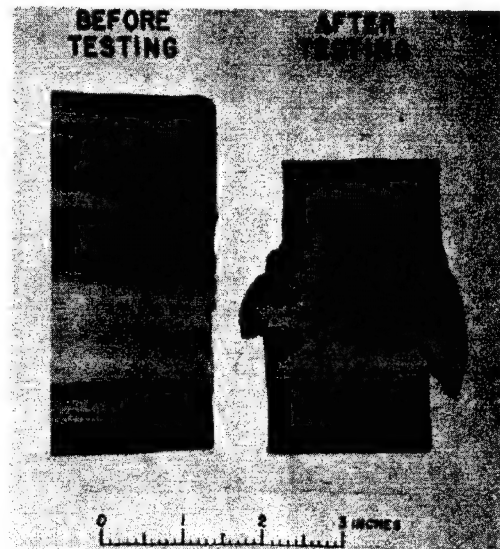


FIG.6

The 31.5 ft. vertical cut on the right hand side collapsed while the timber cross-bracing was being installed.

Dr. Terzaghi (Ref. No. 7, p. 154) shows that the theoretical maximum height,  $H'_c$ , of a bank which has been weakened by tension cracks at the surface is:

$$H'_c = 2.67 \frac{c}{\gamma}; \quad (3)$$

where:  $c$  = unit cohesion of the soil  
 $\gamma$  = unit weight of the soil.

For a clay with a zero value of friction the cohesion is determined from:

$$c = q_u/2; \quad (4)$$



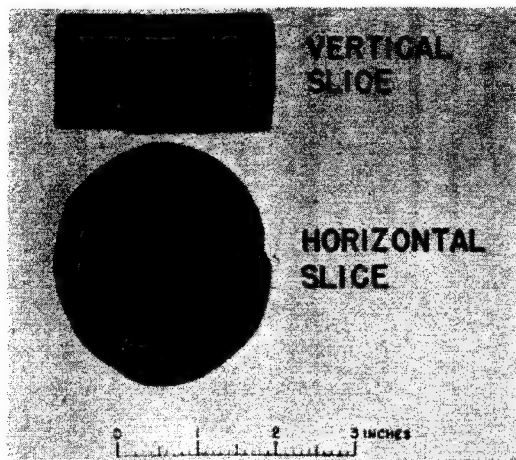


FIG. 7

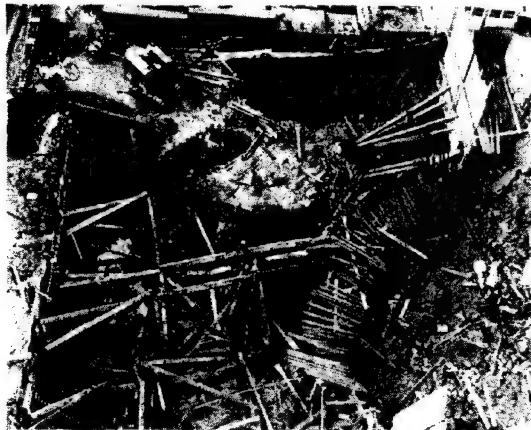


FIG. 9

so that:

$$H'_c = 1.34 \frac{q_u}{\gamma}; \quad (5)$$

Similarly, it follows from earlier studies by Fellenius (Ref. No. 7, p. 155) that the maximum height,  $H_c$ , of a bank which had not been weakened by tension cracks at the surface is:

$$H_c = 3.85 \frac{c}{\gamma} = 1.93 \frac{q_u}{\gamma} \quad (6)$$

Laboratory test on samples from the nearby site No. 2 gave average values of  $q_u = 1.05$  T/sq. ft. and  $\gamma = 120$  lbs./cu. ft. =  $0.06$  T/cu. ft. These values inserted into formulas (5) and (6) give  $H'_c = 23.5$  ft. and  $H_c = 33.8$  ft. This is in quite good agreement with the situation illustrated by Fig. 9 where a 22.0 ft. cut stood up and a 31.5 ft. cut collapsed. It is possible that the value of  $q_u = 1.05$  T/sq. ft. is too low by some 10% since this average included several undisturbed samples with strains at failure exceeding 15%, which in this clay may be taken as a sign of some remolding. If we discard these samples, then the average value of " $q_u$ " is raised to 1.16 ton/sq. ft. with a corresponding theoretical value of  $H'_c = 26.0$  ft. which is equal to 8% of the depth at which failure had actually occurred. The agreement is quite good since it is probable that tension cracks do not form immediate-

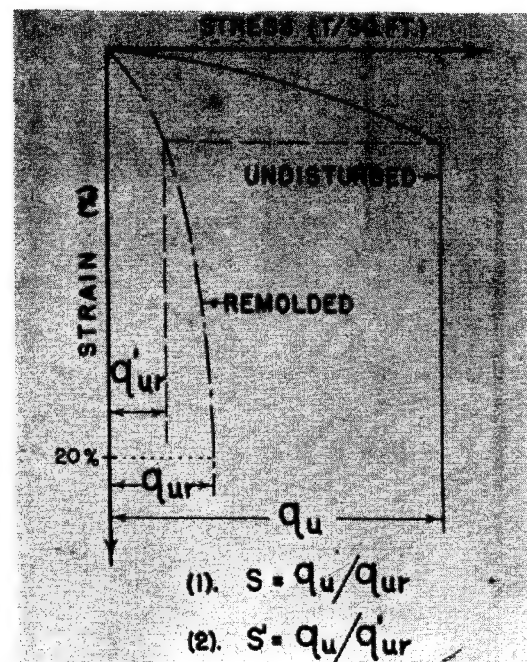


FIG. 8

ly after the depth  $H'_c$  is exceeded during excavation but only at some greater depth and that they develop gradually.

Thus the investigation as carried out at Site No. 2 brings out the suitability of the unconfined compressive strength test for the testing of varved clays. Further information about Site No. 2 can be obtained from Reference No. 9.

The results of an investigation performed on another nearby site (No. 1) on the same deposit appear to provide an explanation for the case which led to the incorrect adverse opinion concerning the use of unconfined compressive strength tests on varved clays as expressed on p. 1094, Ref. No. 4 and on p. 1077 Ref. No. 5. The sampler type used on the Site No. 1 was identical to the one employed for the extraction of samples at the site of the slide referred to in Ref. No. 5. It was 18 in. long, its inner diameter was 3.0 in., and it had a total wall thickness at its lower end of 5/16 in. or a five times greater wall thickness than the sampler used on Site No. 2. Most of the samples extracted on Site No. 1 were found to have undergone some distortion (Fig. 7), and to have failed at high strains; the average value was 17.6%. The average value of the unconfined compressive strength correspondingly dropped to 0.65 T/sq. ft. or to 61% of the 1.05 T/sq. ft. average of all samples from Site No. 2 and to 55% of the 1.16 t/sq. ft. average of the specially selected samples from the same site; the value of  $S'$  dropped to 4.9 (average).

The low laboratory shearing strength value reported on p. 1077 of Ref. No. 5 as being equal to only 50% of the strength required to ensure stability of the bank during the years preceding its failure was therefore probably not due to any inherent defect of



unconfined compressive strength tests when applied to varved clays, but to the disturbance produced by the type of sampler employed.

#### CONCLUSIONS.

- 1) Unconfined compressive strength tests are suitable for the determination of the shearing strength of varved clays and of other stratified cohesive soils.
- 2) In order to obtain reasonably correct strength values from really undisturbed specimens only modern types of thin-walled ("Shelby Tubing") samplers should be employed, especially on clays which are sensitive to remolding.
- 3) The comparison of the sensitivity of different clays to remolding should preferably be based on a ratio of the strengths of the undisturbed and of the remolded samples at equal strains, instead of on the ratios of their respective ultimate strengths at failure.

#### REFERENCES.

- 1) "The Structure of Clay and Its Importance in Foundation Engineering" by A. Casagrande; Journal of the Boston Society of Civil Engineering April, 1932.
- 2) "Comparison between Consolidation, Elastic

and Other Soil Properties Established from Laboratory Tests and from Observations of Structures in Egypt," by Gregory P. Tschobotarioff, Proceedings 1st. International Conference on Soil Mechanics and Foundation Engineering, Paper D-1, Vol. 1, 1936.

- 3) "The Present Status of the Art of Obtaining Undisturbed Samples of Soil" by M. Juul Hvorslev. Supplement to Proceedings of the Purdue Conference on Soil Mechanics and Its Applications, July 1940.
- 4) "Liner Plate Tunnels on the Chicago (III) Subway" by Karl Terzaghi. Transactions, Am. Soc. C.E., 1943, p. 970-1008 and 1090-1097.
- 5) Discussion of Ref. No. 4, by Gregory P. Tschobotarioff, Ibid., p. 1075-1078.
- 6) "Ends and Means in Soil Mechanics" by Karl Terzaghi. Journal of the Engineering Institute of Canada, December 1944.
- 7) "Theoretical Soil Mechanics" by Karl Terzaghi, New York, 1943.
- 8) "Sensitivity of Clay to Remolding and its Possible Causes" by Hans F. Winkler and Gregory P. Tschobotarioff, Proceedings Highway Research Board, 1947.
- 9) "Comparison of the Extent of Disturbance Produced by Driving Piles into Plastic Clay to the Disturbance Caused by an Unbalanced Excavation" by Gregory P. Tschobotarioff and James R. Schuyler. Proceedings 2nd. International Conference on Soil Mechanics and Foundation Engineering., 1948.

-0-0-0-0-0-0-

## SUB-SECTION II e

### DIRECT SHEAR TESTS

#### A LARGE SHEAR BOX FOR TESTING SANDS AND GRAVELS

#### II e 1

ALAN W. BISHOP, M.A., A.M.I.C.E.

Lecturer in Civil Engineering, Imperial College, University of London.

#### I. INTRODUCTION.

The design of new reservoirs in the Thames Valley by the Metropolitan Water Board necessitated the examination of the stability of a number of proposed earth dams on sites overlain by a stratum of gravel. In addition the dams were to be constructed of rolled gravel fill.

As no satisfactory test results for gravel were available, or could be obtained with existing testing machines, a constant rate of strain shear box 1 foot square taking samples 6 inches in thickness was designed by the author and constructed by the Metropolitan Water Board.

Tests are at present being carried out with this apparatus in the Soils Laboratory at Imperial College, with two main purposes in view.

- a) For immediate design purposes, to determine:
  - 1) the shear strength of in situ gravel by the correlation of field density measurements with laboratory tests over a range of densities.

- 2) the shear strength of samples of gravel under various degrees of compaction for the design of the rolled fill.

b) For a general research programme:

- 1) to examine the effects of grading and grain shape on the relation between shear strength and porosity, and extend knowledge in this field into the range of materials containing particles up to  $1\frac{1}{2}$  inches effective diameter.
- 2) by comparative tests in the large and small (6 cm. square) shear boxes to examine scale effects in testing.

#### II. DESCRIPTION OF THE MACHINE.

The shear box (fig. 1 and plates I & II) is constructed of standard channel sections electrically welded and machined on the contact faces. The lower half of the box is carried in a steel tank which slides forward on two ball bearing tracks under the action of the loading jack. This provides the shearing force.



Foot Square Shear Box.

PHOT. 1



Shear Box Details.

PHOT. 2

The reaction is carried by two tension bars to the cross-head where it is measured by the deflection of the proving ring.

The normal load is applied by a simple lever system, and has a working range up to 3 tons per square foot. The loading jack is operated by a  $\frac{1}{2}$  H.P. electric motor, isolated by rubber couplings and mountings to eliminate vibration. The rate of horizontal displacement is 2 inches per hour, the usual range during a test being 1 inch. The displacement is measured by a revolution counter on the jack. A correction can be made for the deflection of the proving ring, but this is only  $72 \times 10^{-4}$  inches per ton, and this does not make an appreciable difference to the shape of the load-deflection curves.

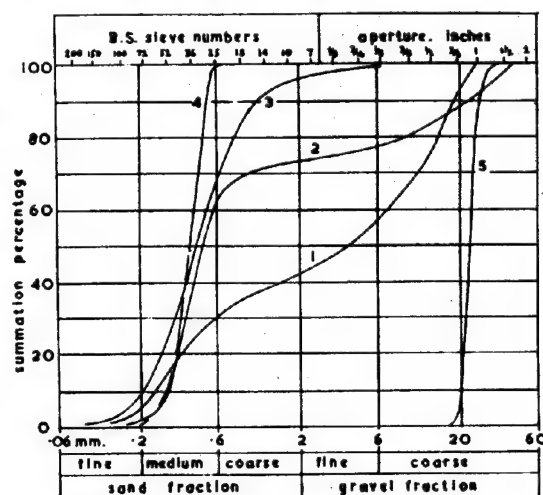
### III. TESTING PROCEDURE.

Testing techniques have been developed to enable the preparation of a homogeneous sample and to ensure accurate measurement of its weight and volume. High porosities are obtained by rapid pouring, and low porosities by tamping in a number of layers by hand, though in the case of sands low porosities are also obtained by slow pouring (Kolbuszewski 1948). Sufficient tests have not yet been done to determine whether the angle of internal friction (at a given normal stress) depends only on the porosity or whether the method of packing affects it. The tests up to date indicate that the magnitude of any such effect is probably small.

### IV. TYPICAL RESULTS.

Typical results are given in figs. 3 - 9 for 5 sands and gravels whose grading curves are shown in fig. 2. They are:

1) Heathrow gravel - a well graded Thames Val-



Sieve analysis.

1. Heathrow
2. Walton
3. Brasted
4. Ham River
5. Chesil Bank

FIG. 2

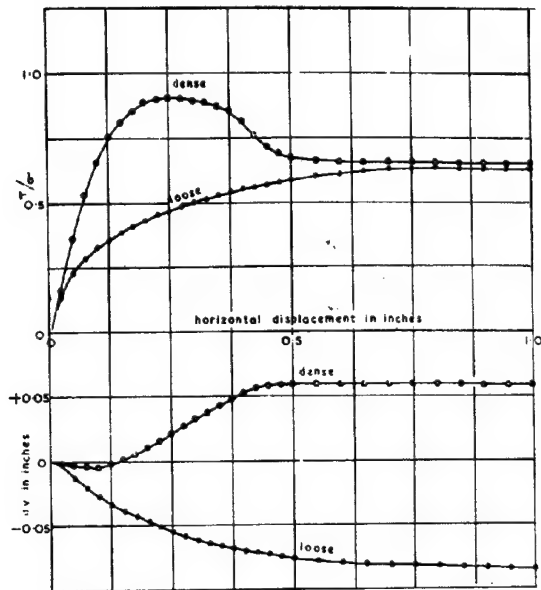
ley gravel. (For this series of tests, particles greater than 1" were removed).

- 2) Walton gravel - a sandy gravel from the Thames Valley, possibly a mixture of thin adjacent lenses of sand and coarse gravel.
- 3) Brasted sand - a well graded sand of the Folkestone beds.
- 4) Ham River sand - a uniform sieved fraction from the Thames Valley gravels.
- 5) Chesil Bank pebbles - a uniform coarse beach gravel, consisting of rounded particles about 1" in diameter.

### V. DISCUSSION OF RESULTS.

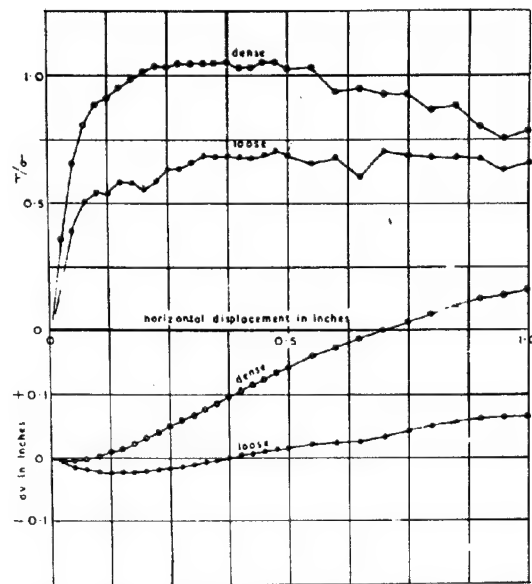
a) For the purposes of present design work the results shown in fig. 7 indicate that angles of friction of up to  $45^\circ$  may be obtained, even in not very well graded gravels at moderate porosities. The insitu porosity in this gravel from Walton could not be repeated in the laboratory by tamping the dry material.

Fig. 9 includes a similar curve for the well graded Heathrow gravel which gave angles



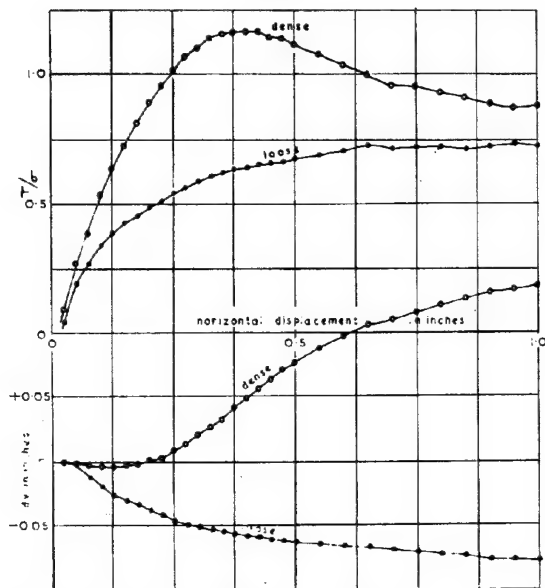
Shear tests on graded sand. Brasted.  
 Test no. 43. loose.  $n = 44.4\%$   $\phi = 32.3^\circ$   
 Test no. 44. dense.  $n = 33.3\%$   $\phi = 42.1^\circ$   
 $\sigma = 2$  tons / sq.ft.

FIG. 3



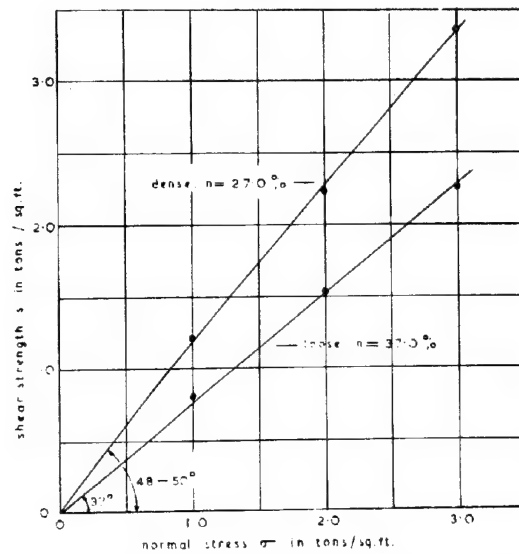
Shear tests on uniform gravel. Chesil Bank.  
 Test no. 96. loose.  $n = 42.0\%$   $\phi = 35.3^\circ$   
 Test no. 97. dense.  $n = 35.0\%$   $\phi = 46.5^\circ$   
 $\sigma = 0.5$  tons / sq.ft.

FIG. 5



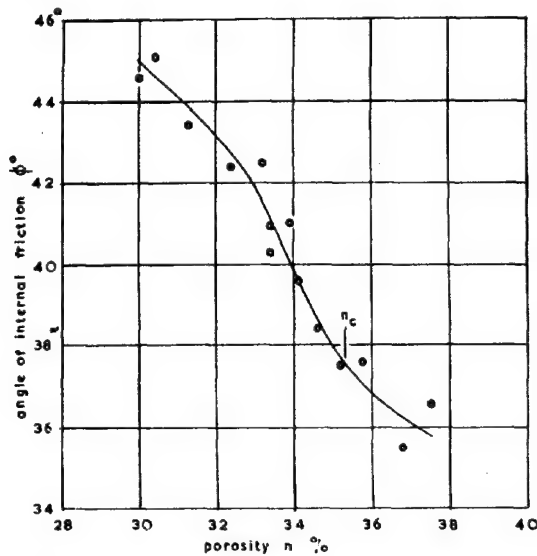
Shear tests on gravel. Heathrow.  
 Test no. 114. loose  $n = 36.8\%$   $\phi = 36.5^\circ$   
 Test no. 119. dense.  $n = 26.3\%$   $\phi = 49.5^\circ$   
 $\sigma = 3$  tons / sq.ft.

FIG. 4



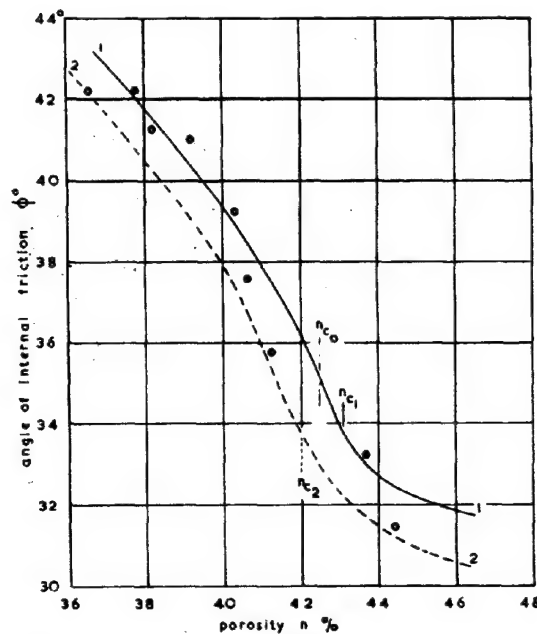
Relationship between shear strength and normal stress. Heathrow gravel.

FIG. 6



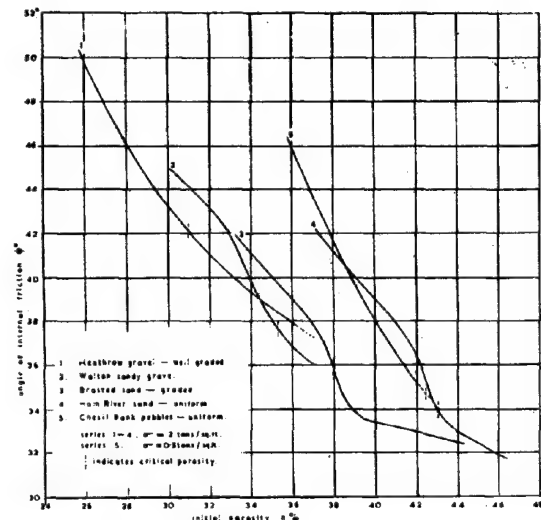
Variation of angle of internal friction with porosity. Walton gravel.  $\sigma = 2$  tons / sq.ft.

FIG.7



Comparison of testing machines.  
0..0. 6 cm. square. constant rate of strain.  
1..1. 1 ft. square. constant rate of strain.  
2..2. 6 cm. square. dead load.  
Ham River sand.  
 $\sigma = 2$  tons / sq.ft.

FIG.8



Relationship of angle of internal friction to porosity for various gradings.

FIG.9

of friction of about  $50^\circ$  at porosities a little greater than those measured in the formation in which the material was being rolled.

Fig. 4 shows typical test results for this material, and Fig. 6 gives the relationship between shear strength and normal stress for two different porosities. It is noteworthy that the high angle of internal friction ( $\alpha$ ) does not decrease much within the range of stresses met with in earth dam design in this country.

b) 1. As pilot tests for a more detailed investigation the results given in Fig. 9 indicate that in the relation of angle of friction to porosity, graded and uniform materials separate out into two definite groups, between which a transition zone will presumably lie.

It is very striking that the tests on the Chesit Bank pebbles ( $\alpha$ ) give results very similar to those of the Ham River sand, which though about  $1/60$  in linear dimensions, has a similar grading curve. Tests results in Fig. 5 indicate that the shearing action (with the pebbles) is becoming jerky and that they probably represent an upper limit to the size of uniform material that can be tested accurately in this machine. In a graded material, however, the larger particles do not seem to control the behaviour, and it will be seen from Fig. 4 that the shearing action is remarkable smooth, and the expansion of the sample ( $dv$ ) is smaller.

2. A comparison is also made in Fig. 8 with results obtained on the small (6 cm. square) boxes using both constant rate of strain (Golder 1942) and dead loading. The methods of compaction in this set of results are similar in the 3 cases.

It is seen from the figure that the results of the smaller box scatter on both sides of the average line for the large machine, although they tend to give a slightly lower value of  $\phi$ .

$\alpha$ ) defining  $\phi$  as  $-\tan^{-1} \frac{1}{\alpha}$  at failure.

$\alpha$ a) these were tested at 0.5 ton/sq.ft. initially to avoid damage owing to the few contact points, but this will not materially affect the comparison.

There is, however, a much bigger difference between the two methods of testing in the same size box. This is also borne out by a few tests carried out at a very rapid constant rate of strain, which also gives lower values of  $\phi$ . This indicates that the value of  $\phi$  obtained does not depend to any great extent on the size of the machine (over a limiting size), but that discrepancies between measured values of  $\phi$  and the results of field or model loading tests etc., may lie in the different types of failure induced.

3. The stress distribution within the sample and along the failure plane is not discussed in this paper, but preliminary examinations of the type of failure plane by Kotter's equation indicate that the deviation from the average of the normal stress on the failure plane is not serious.

#### VI. CONCLUSIONS.

A full range of cohesionless soils, ranging from sands to gravels and sandy gravels, has been tested in a shear box taking samples 1 foot square and 6 inches thick. For sands it has been found that the results obtained in the standard 6 cm. shear boxes are in good agreement with those obtained in this large box. It should be noted however that in the standard boxes the results appear to depend to some extent on the manner of applying the shear force.

It was found that materials with a uni-

form grain size, whether a medium sand or pebbles about 1 inch in diameter, gave similar results when plotted in the form of  $\phi$  against porosity which were quite distinct from the relationships found for the graded materials.

The graded sands and sandy gravels lay more or less in the same general zone, but the lower porosities of the well graded sandy gravels resulted in higher angle of friction than the graded sand. The sandy gravels were found to have angles of friction as high as  $50^\circ$  at a dense packing.

#### VII. ACKNOWLEDGEMENTS.

For permission to publish details of the machine and of the Walton tests the Author is indebted to H.P. Cronin, M.I.C.E., Chief Engineer of the Metropolitan Water Board.

The Author is grateful to J.B. Miners, A.C.G.I. B.Sc. (Eng.) A.J. Smallman, A.C.G.I. B.Sc. (Eng.) and M.A.A. Hafez B.Sc., for carrying out much of the testing programme referred to, and to Assistant Professor A.W. Skempton for his constant interest.

#### VIII. REFERENCES.

- Golder, H.Q. 1942 "An Apparatus for Measuring the Shear Strength of Soils". *Engineering*, Vol. 153, p. 501 (26 June 1942).  
 Kolbuszewski J.J. 1948 "An Experimental Study of the Maximum and Minimum Porosities of Sands". *Proc. 2nd Int. Conf. Soil Mechanics*.

-o-o-o-o-o-o-

## II e 2

### THE SHEARING RESISTANCE OF SOILS AS DETERMINED BY DIRECT SHEAR TESTS AT A CONSTANT RATE OF STRAIN

J. MAC-NEIL TURNBULL, Assistant Research Officer  
 State Rivers and Water Supply Commission, Victoria, Australia.

- Three samples of soil, compacted at or near the optimum density, have been tested in direct shear in accordance with the latest developments of the procedures described elsewhere 1). Tests were made at three rates of strain: namely, 0.22, 0.055, and 0.007 inch per hour
- Specimens were tested under normal stresses between 570 and 27,000 lb. per sq. ft., and after the determination of the maximum shearing resistance the cohesion, if any, was obtained by a new method 1).
- The results were checked by tests wherein specimens were preconsolidated at a particular normal stress before testing at reduced normal stresses, also for conformity with certain geometrical requirements.
- The same soils were also tested by means of the triaxial compression test in the Research Laboratory of the Melbourne and Metropolitan Board of Works in accordance with procedures described by D. F. Glynn 2).

- The particle size distribution curves of the three soils are shown in Figure 1, and the classifications 3), Atterberg Limits, and compaction data are given in Table I.
- The results of direct shear tests at various rates of strain are shown in Figures 2, 3, and 4; and the test curves, including the determination of the cohesion, are shown in Figures 5, 6 and 7. Data for tests on sample No. 2 are given in Table II. In order to check the values obtained by this new method for obtaining the cohesion of each specimen

under a particular normal stress, several tests were made after preconsolidation and unloading to a lower normal stress.

It will be seen that the results by the two methods of testing are in close agreement in Figures 2(a) and 4(a). In Figure 3(a) agreement is also obtained when the particle displacement correction is made, and indicates one advantage of the additional information obtained by the new method. The curves of Figures 5(a) and 6(a) show the effect of a partial breakdown of the soil particles during

TABLE I

## PHYSICAL CHARACTERISTICS OF THE SOILS TESTED

Sample No.	Classification Soil	Sp. Gr.	L.L.	P.I.	S.L.	Optimum Moisture Content <sup>1</sup> Per Cent.	Optimum Density <sup>1</sup> lb./cu.ft.	Shear Test Specimens Compacted At	
								Moisture Per Cent.	Density lb./cu.ft.
1	0.184mm./2.781	2.75	44	23	17	18.9	105.1	20.2	104.2
2	0.736mm./3.787	2.71	18	1	13	11.2	123.7	12.0	122.4
3	0.368mm./3.339	2.72	28	6	19	-	-	16.6	107.3
1 Compacted under 40 blows per layer.									

TABLE II

## DATA FROM TESTS ON SAMPLE NO. 2 IN FIGURE 6.

Fig. No.	Test No.	Applied Normal Stress		Load and Strain after Figure 9.						Max. Shearing Resistance Corrected lb./sq.ft.	Cohesion lb./sq.ft.
		Consolidation lb./sq.ft.	Test lb./sq.ft.	S <sub>m</sub> lb.	l <sub>m</sub> in.	a <sub>1</sub> lb.	l <sub>1</sub> in.	a <sub>2</sub> lb.	l <sub>2</sub> in.		
6(a)	1	1,500	1,500	175	0.106	70	0.349	83	0.814	1,270	0
	2	2,500	2,500	239	0.092	72	0.198	81	0.800	1,950	25
	3	4,500	4,500	376	0.098	83	0.250	99	0.702	3,410	10
	4	10,000	10,000	773	0.157	156	0.308	244	1.110	7,160	215
	5	12,000	12,000	875	0.128	139	0.255	228	1.103	8,520	250
	6	18,500	18,500	1,165	0.236	37	0.315	86	0.891	12,920	290
	7	27,000	27,000	1,754	0.197	116	0.320	-	-	18,840	-
6(b)	8	18,500	3,000	257	0.104	66	0.316	-	-	2,250	-
	9	18,500	4,500	413	0.101	107	0.254	-	-	3,570	-
	10	18,500	6,000	486	0.115	114	0.325	-	-	4,360	-
	11	18,500	9,000	703	0.123	161	0.442	-	-	6,430	-
6(b)	12	4,500	4,500	334	0.134	52	0.327	-	-	3,270	N.D.
	13	18,500	18,500	1,105	0.205	0	-	-	-	12,670	N.D.

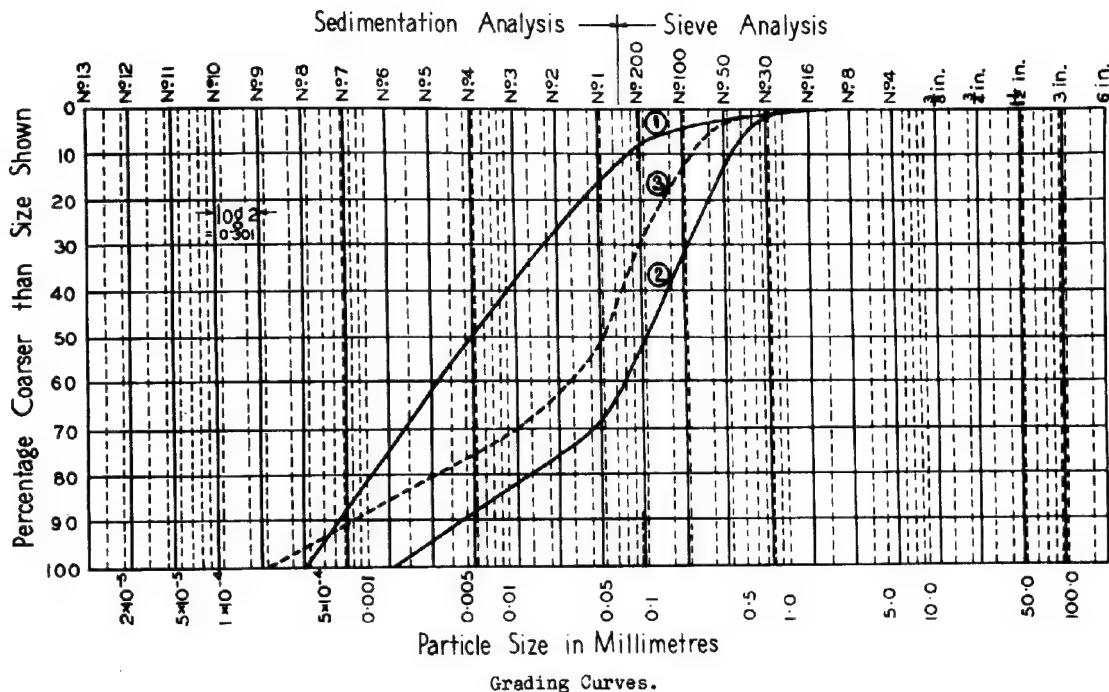




TABLE III  
RESULTS OF DIRECT SHEAR TESTS.

Sample No.	Rate of Strain in. per hr.	Applied Normal Stress lb. per sq. ft.	Capillary Stress lb. per sq. ft.	Total Normal Stress lb. per sq. ft.	Cohesion lb. per sq. ft.	$\phi$	$\tan \phi$
1	0.22	18,500	3,500	22,000	1,800	15° 35'	0.279
		10,000	3,500	13,500	1,100	15° 35'	0.279
		4,500	3,500	8,000	650	15° 35'	0.279
1	0.055	18,500	1,500	20,000	2,300	18° 10'	0.329
		10,000	1,500	11,500	1,300	18° 10'	0.329
		4,500	1,500	6,000	700	18° 10'	0.329
1	0.007	18,500	900	19,400	2,500	19° 25'	0.352
		10,000	900	10,900	1,400	19° 25'	0.352
		4,500	900	5,400	700	19° 25'	0.352
2	0.22	18,500	230	18,730	290	34° 00'	0.674
		10,000	230	10,230	160	34° 00'	0.674
		4,500	230	4,730	75	34° 00'	0.674
2	0.055	Same as for 0.22 in. per hr.					
3	0.22	18,500	800	19,300	1,100	27° 50'	0.528
		10,000	800	10,800	620	27° 50'	0.528
		4,500	800	5,300	300	27° 50'	0.528
3	0.055	18,500	400	18,900	1,330	28° 45'	0.549
		10,000	400	10,400	730	28° 45'	0.549
		4,500	400	4,900	340	28° 45'	0.549

TABLE IV  
RESULTS OF TRIAXIAL COMPRESSION TESTS.

Sample No.	Cohesion lb. per sq. ft.	$\phi$	$\tan \phi$
1	2,700	20° 50'	0.38
2	2,600	39° 20'	0.82
3	1,600	29° 40'	0.57

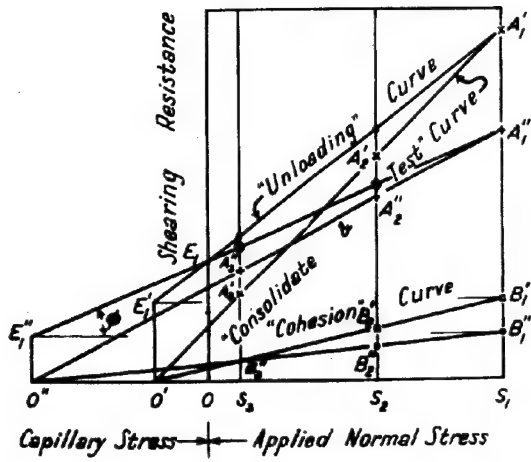
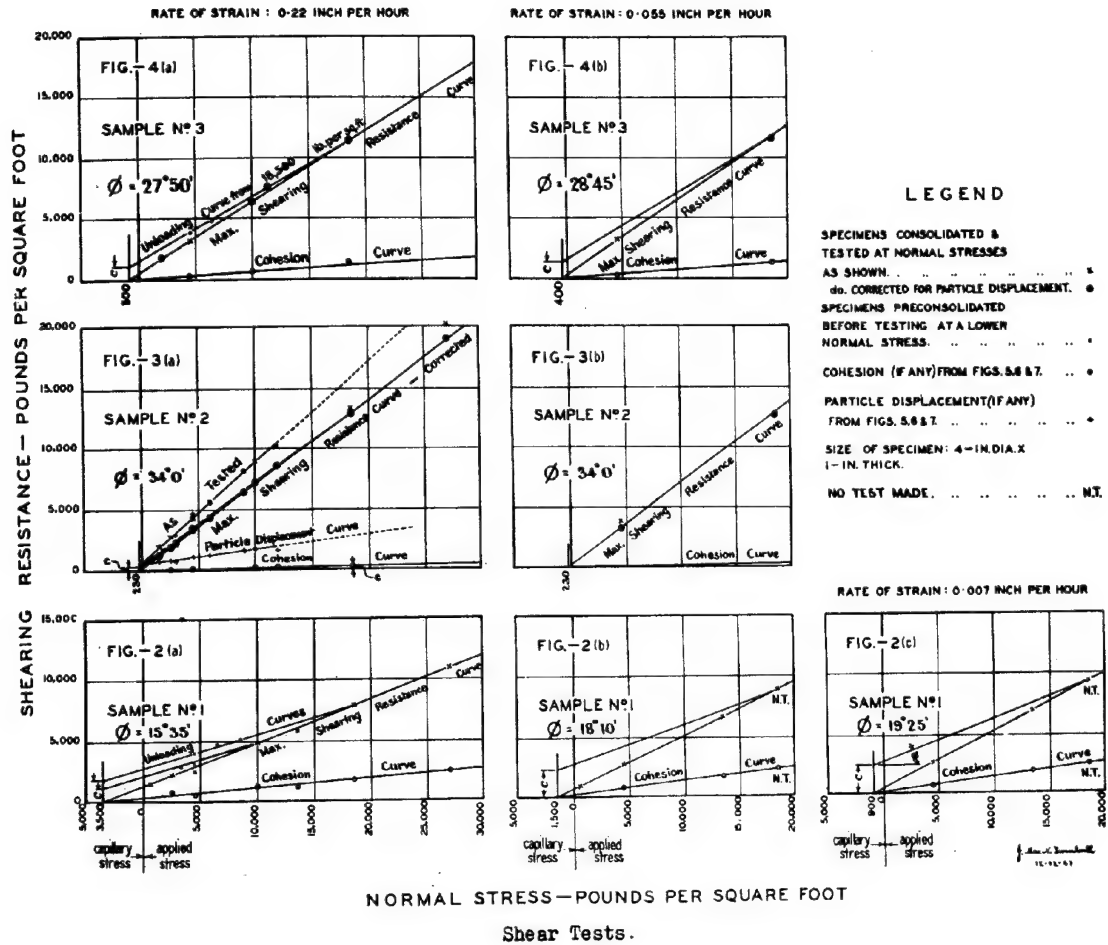


FIG.8

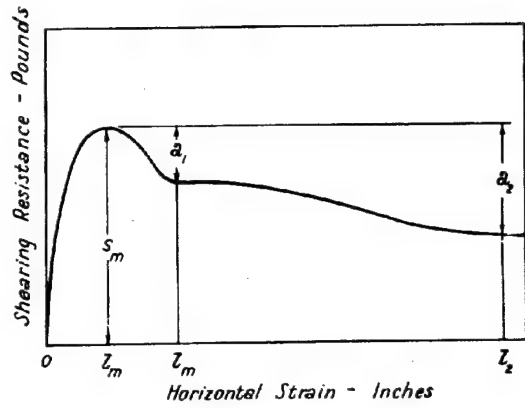
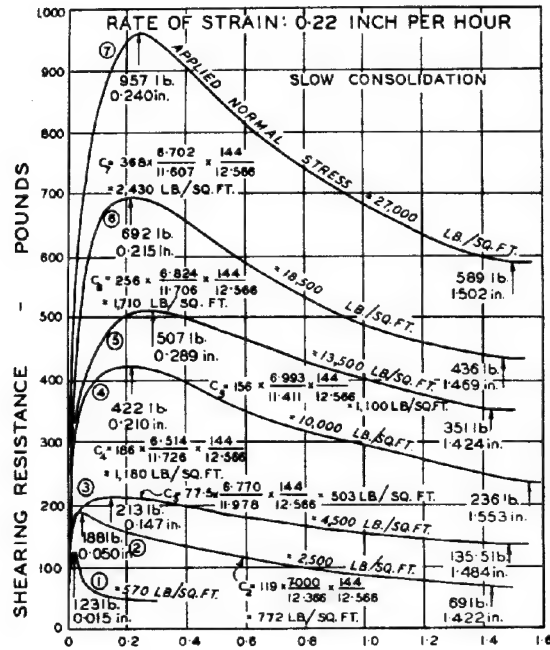


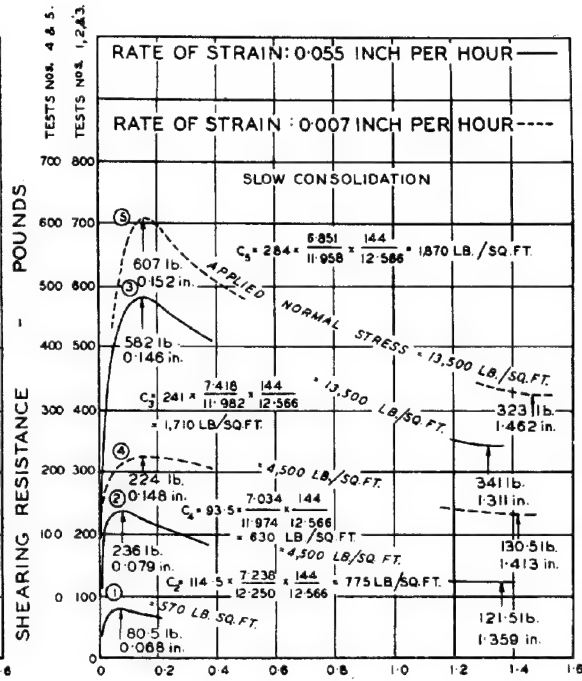
FIG.9



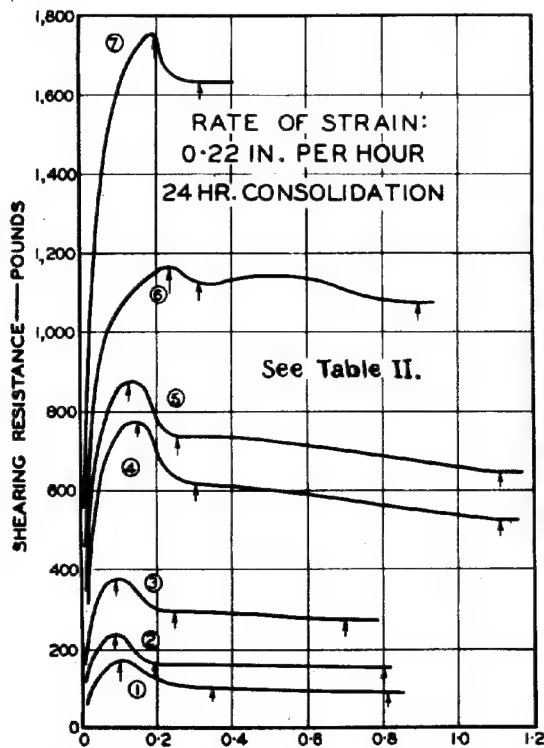
a. Horizontal strain-inches.

Cohesion Tests on Sample no. 1.

FIG. 5



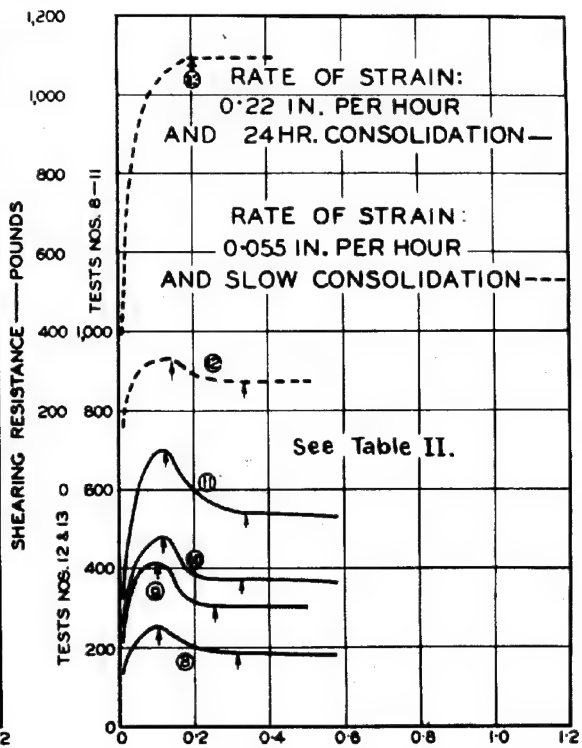
b. Horizontal strain-inches.



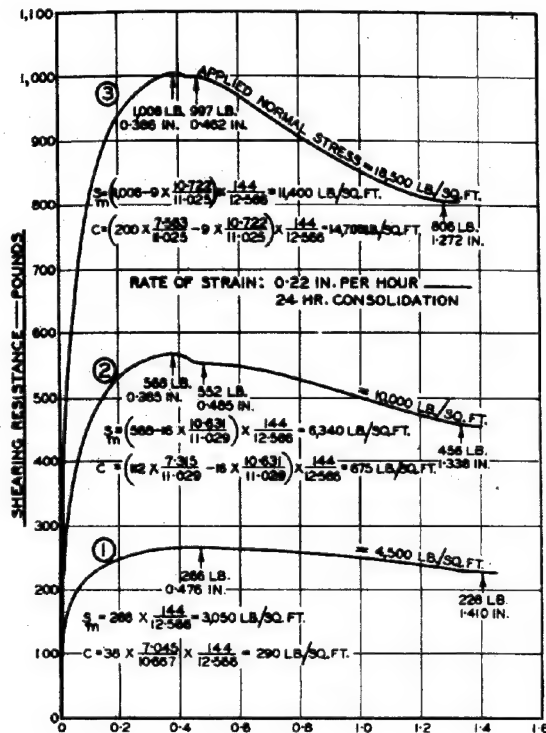
a. Horizontal strain-inches.

Cohesion Tests on Sample no. 2.

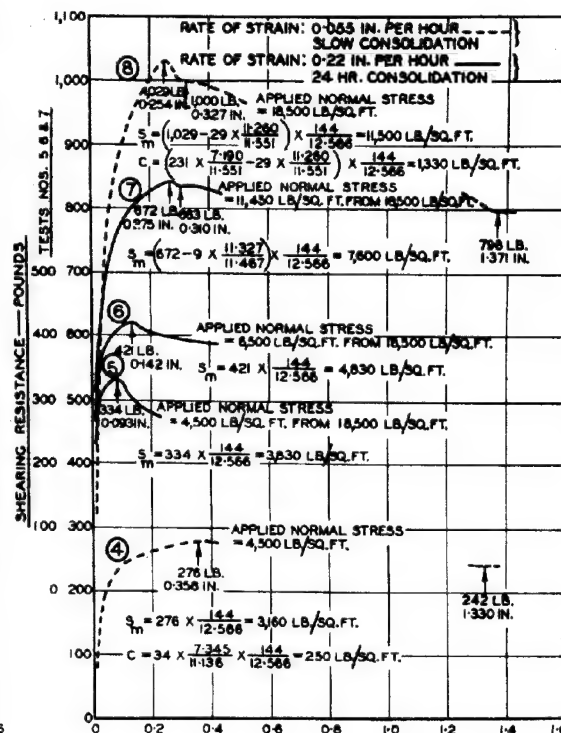
FIG. 6



b. Horizontal strain-inches.



a. Horizontal strain-inches.



b. Horizontal strain-inches.

Cohesion Tests on Sample no. 3,

FIG. 7

The maximum shearing resistance is reduced by the particle displacement correction expressed by the last term in the above equation, which vanishes when there is no particle displacement as in the curves of Figure 5. The maximum shearing resistance and the cohesion are reported in lb. per sq. ft. on the assumption that the load is carried by the initial cross-sectional area of the specimen. The applied normal stress remains constant throughout the test.

8. Appreciation is expressed to Lewis R. East, Chairman, State Rivers and Water Supply Commission, for permission to publish this paper; and W.J. Corrigan who made all the tests; also D.F. Glynn for permission to quote the results of his tests.

#### SUMMARY.

- Direct shear tests were made on samples of soil under several normal stresses at various rates of strain.
- The cohesion was determined for each particular normal stress by a new method.
- The accuracy of these determinations of the cohesion was checked by a series of tests in which specimens were preconsolidated

at the normal stress for which the information was desired, and the maximum shearing resistance was determined at reduced normal stresses.

- The results of tests on a homogeneous sample of soil must comply with certain geometrical requirements.
- Comparison of these results with those obtained on the same soils by means of triaxial compression tests shows that the latter make no allowance for the effects of particle displacement or capillary stress.

#### BIBLIOGRAPHY

- Turnbull, J. MacNeil, "Handbook of Methods of Testing Soils", Government Printer: Melbourne, 1945. (Distributed by Tait Book Co.: Melbourne.)
- Glynn, D.F., "Application of Triaxial Compression Tests to Stability Analysis of Rolled Fill Earth Dams", Proceedings of the Second International Conference on Soil Mechanics and Foundation Engineering, 1948.
- Turnbull, J. MacNeil, "A New Classification of Soils Based on the Particle Size Distribution Curve", Proceedings of the Second International Conference on Soil Mechanics and Foundation Engineering, 1948.

## SUB-SECTION II f

ELECTRO-OSMOSIS

II f 1

ELECTRO-OSMOSIS

DR. ING. L. CASAGRANDE

Department of Scientific and Industrial Research  
Building Research Station.

SUMMARY.

- 1) The electro-osmosis flow can be represented by an equation similar to Darcy's law, the coefficient of permeability being dependent mainly on the porosity and the  $\zeta$ -potential.
- 2) From the results of laboratory investigations it may be concluded that the quantity of flow does not vary considerably in view of the great differences in the soil materials tested and that for practical purposes in civil engineering it may be assumed to be of the magnitude of  $k_e = 5 \times 10^{-5}$  cm./sec./volt/cm.
- 3) The osmotic flow does not seem to take place through the individual pores of clay-size or less, but through fissures, which develop throughout the soil between the electrodes, even under a small potential gradient. This movement leads to the development of a hydraulic pressure which is the same for soils containing more than a certain proportion of colloidal particles.
- 4) Though the osmotic permeability is very much higher than the hydraulic permeability for many soils, it is not sufficient to make the consolidation of soils within a brief period a commercial proposition. Nevertheless, the fact that by these means it is possible to divert the flow of pore water away from unstable slopes and cuttings makes its use in this manner a valuable and highly economical method for earthworks and foundation engineering.
- 5) Mention is made of the fact that the osmotic flow of water causes a laminated structure to develop in clayey soils and colloidal materials, apart from the random fissures. These laminations resemble strikingly some natural deposits of laminated clays.

II. INTRODUCTION.

Although the application of the principle of electro-osmosis to assist in the drainage of soils has been used for a number of years 1) it was realised that a more detailed knowledge of the process was required in order to assess its full possibilities. With this end in view the author undertook a laboratory investigation of electro-osmosis in soils and the main results of his work are summarised in the paper.

This work has not led the author to change his earlier opinion that the field of practical application of this method is likely to be limited on account of economic factors. In contrast other workers in the subject 2) have indicated the possibility of a much wider field of application including the drying out and consolidation of soils. The author considers that for economic use the rate of removal of water is too small to permit the consolidation of large soil masses within the short period which is usually available in building practice. However, the original use of the method for overcoming difficulties in excavations in water-logged ground is both practicable and economical.

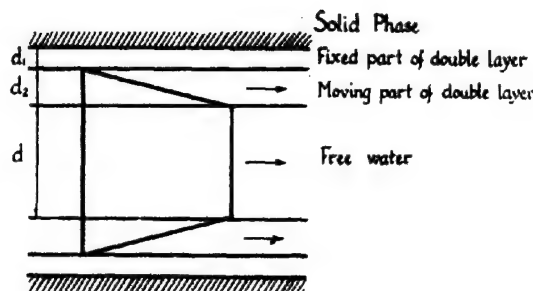
The scope of this paper is rather limited, but it may be mentioned that a more comprehensive publication on this subject is being prepared at the Building Research Station.

III. THEORY.

The quantity of liquid "Q" moved in unit time under a potential difference "E" can be derived from the modified Helmholtz equation 3) (Fig. 1):-

$$Q = \frac{EDr^2}{4\eta l} \quad (1)$$

which is similar in form to Poiseuille's law for the flow through a single capillary. If applied to a bundle of capillaries of a cross



Electro - osmotic flow in capillaries

FIG.1

sectional area "A" the corresponding flow; unlike the hydraulic flow, is independent of the individual pore sizes. The equation for the electro-osmotic flow in soils, therefore, may be built up similar to Darcy's equation

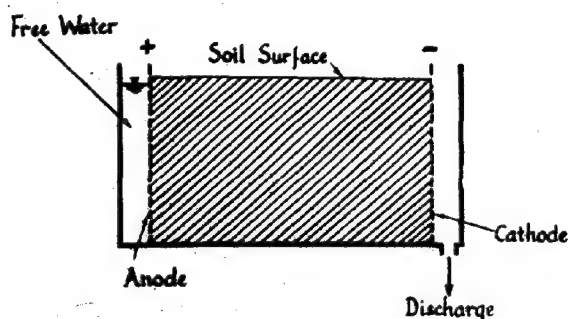
$$Q = k_e \times i_e \times A \quad (2)$$

with a coefficient of "osmotic" permeability " $k_e$ " which is mainly dependent on the porosity and the  $\zeta$ -potential and independent of pore size.

IV. DESCRIPTION OF LABORATORY TESTS.

The apparatus used for general investigations of parallel flow is shown diagrammatically in Fig. 2. It had no cover; it was fitted with electrodes at both ends and had an outlet for the water in the base near the cathode.

For measurements of the hydrostatic pres-



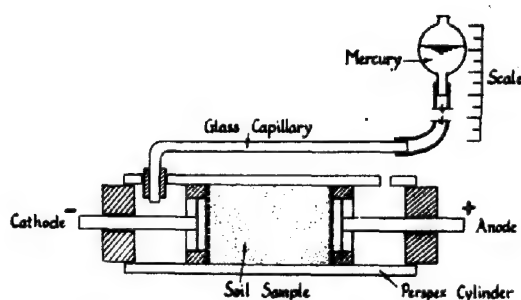
Sketch of apparatus for investigations on parallel flow.

FIG.2

sure developed by electro-osmosis the soil samples were tested in a perspex cylinder, connected to a rubber tube and mercury reservoir which allowed pressure to be applied artificially (Fig. 3).

In most of the tests the electrodes consisted of a simple iron gauze with meshes 1 - 2 mm wide and covered on its inner face with a coarse filter paper or with a permeable cotton fabric to prevent the passage of material through the electrodes.

A series of tests has been made with the soils of Table 1 and in addition with kaolin powder (80 per cent. smaller than  $1\mu$ ) and with common table gelatine. The curves of the grain size distribution of the soils in Table 1 are plotted in Fig. 4.



Apparatus for measurement of hydrostatic pressure.

FIG.3

the type shown for a clayey silt in Fig. 6. These curves seem to converge on two points A and B, except for certain more or less pronounced irregularities in the neighbourhood of the electrodes. In the course of an experiment the distribution curve changes gradually from "a" to "f" and finishes approximately as a straight line; no further reduction then occurs i.e. a steady condition has been reached. From the very instructive results obtained with the materials of Table 1 the following condensed statement may be made:-

- 1) The inclination of the straight line A - B depends on the potential gradient and is the same for all soils with equal " $k_e$ ".
- 2) For a given potential gradient the water contents at the cathode and at the anode

TABLE 1

Soil	Permeability $k$ cm./sec.	Liquid Limit L.L.%	Plastic Limit P.L.%
(a) Sodium-bentonite	$1 \times 10^{-11}$	600	38
(b) Fat clay (London clay)	$7 \times 10^{-9}$	80	27
(c) Clayey silt (organic)	$8.5 \times 10^{-8}$	46	24
(d) Clayey sand (loam)	$3.1 \times 10^{-7}$	37	21
(e <sub>1</sub> ) Sandy silt	$1.2 \times 10^{-6}$		
(e <sub>2</sub> ) Quartz powder (ground quartz sand)	$7.9 \times 10^{-5}$		
(f) Coarse silt	$6.2 \times 10^{-4}$		
(g) Fine sand	$2.9 \times 10^{-3}$		
(h) Mica powder			
Vertical	$5.6 \times 10^{-3}$		
Horizontal	$8.0 \times 10^{-3}$		

a) Quantities of Water Moved and its Distribution between the Electrodes.

The results obtained for the osmotic flow are very similar for most materials which were tested. From Fig. 5 a magnitude of " $k_e$ " of about  $5 \times 10^{-5}$  cm/sec. per volt/cm may be determined. The highly colloidal Wyoming bentonite shows a greater deviation from this value for very small and very high water contents, reaching  $12 \times 10^{-5}$  cm/sec. per volt/cm with a water content of about 2000 per cent. of dry weight.

The measurements of the water distribution between the electrodes indicate conditions of

are equal for all soils with equal " $k_e$ " (Fig.7)  
3) The water content at the cathode approaches zero with very small potential gradients. As the potential gradient increases the distribution curve rotates about the centre M (Fig.7) and it becomes uniform throughout the specimen with very high (infinite) potential gradients. Under a very high potential gradient the water content at the cathode appears to approach a value to 28 per cent. of the dry weight. The value "a" for the potential gradient "zero" is imaginary, since in that state a considerably higher pore-water content exists. "a" can therefore not be considered otherwise

ccv

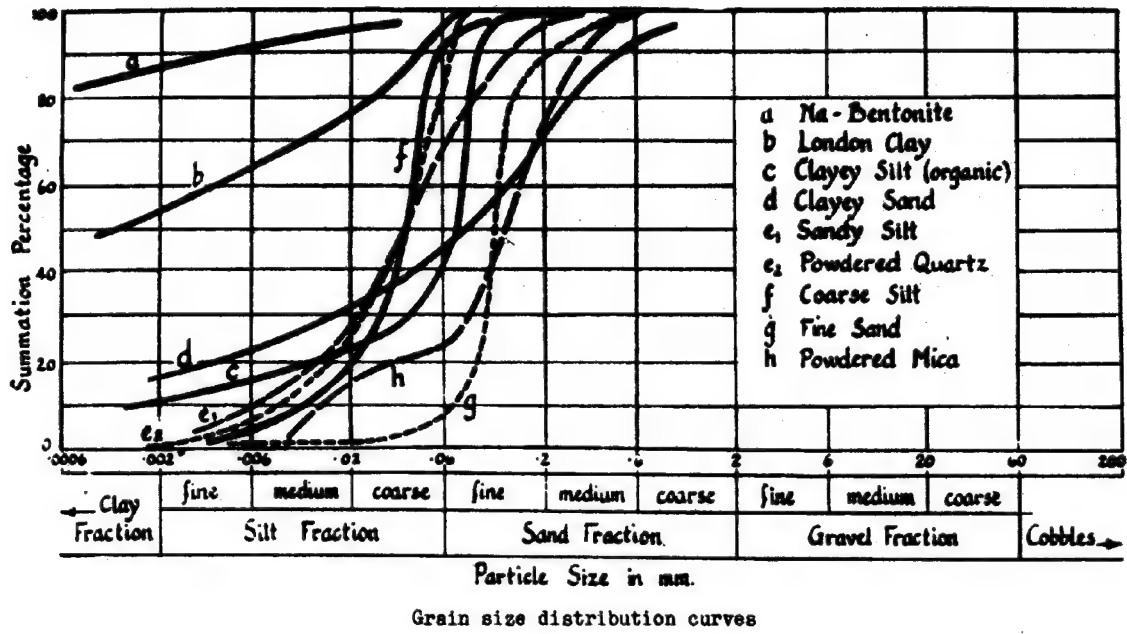


FIG.4

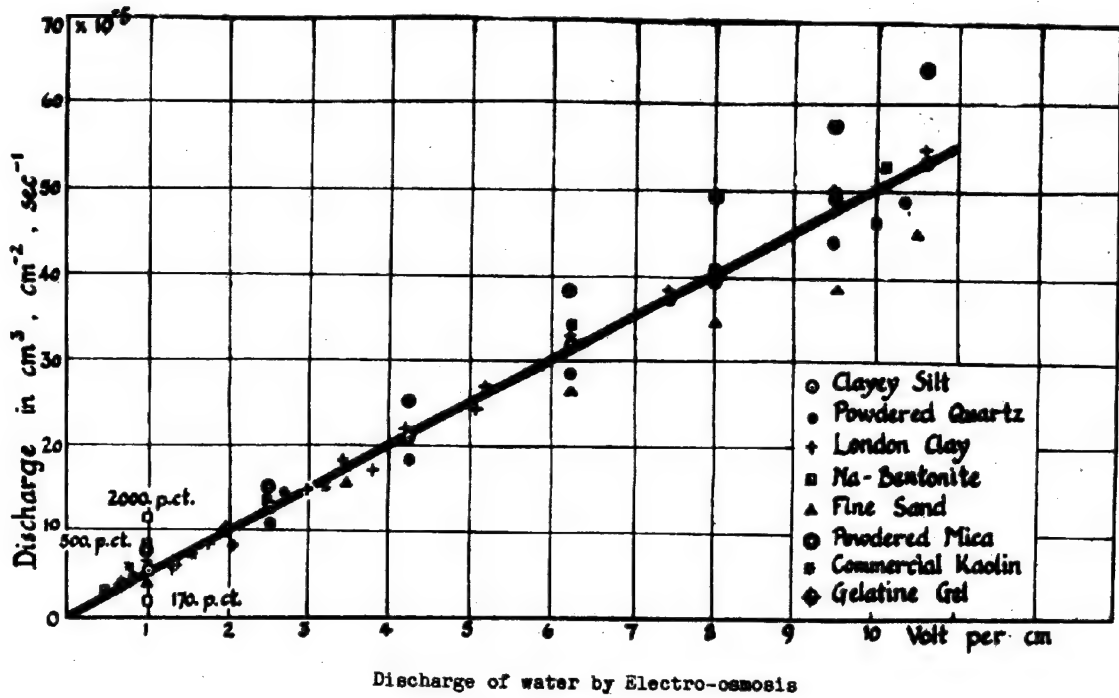
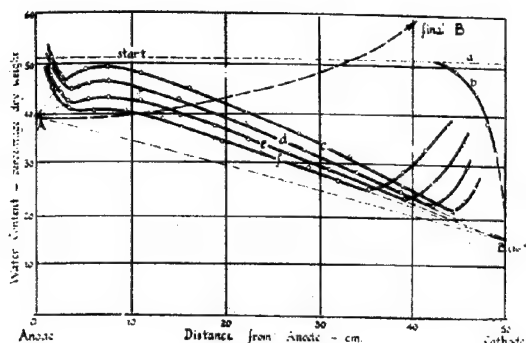
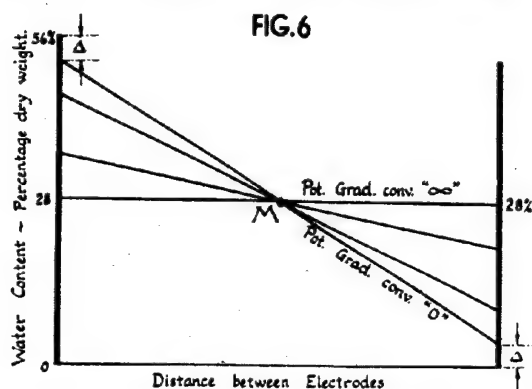


FIG.5





Distribution of water content for a clayey silt at different times after start of test.



General relation between the distribution of water content and potential gradient

FIG. 7

search Laboratory 4). In a much lesser degree this phenomenon seems to develop also in pure silts.

#### b) Consumption of Energy.

Though the results prove that the osmotic effect depends primarily upon the potential gradient, the current flowing through the soil, i.e. the amount of current associated with any potential, is conditioned by the type of soil and the electrolytic content. Continuous measurements on natural soils and on pure mineral powder with the use of mains water led to the following results:-

- 1) The amount of current passing  $1 \text{ cm}^2$  of soil depends largely on the grain size of the soil (Fig. 10).
- 2) The amount of the current is almost independent of the magnitude of the pore water content. A noticeable decrease occurs only after the water content has been reduced to a state far below the magnitudes which have any application in building practice.

#### c) Determination of the Electro-osmotic Pressure.

According to the Helmholtz theory the hydrostatic pressure "p" developed at the cathode 3), represented by the equation

$$p = \frac{2 \frac{1}{2} E D}{\pi r^2} \quad (3)$$

is inversely proportional to the square of the radius of the capillary.

The difficulties in practical tests, caused by shrinkage of the sample due to electro-osmotic action, were avoided by building up the equilibrium pressure within a short time by raising the water or mercury head artificially (Fig. 3). Thus very accurate results were obtained (Fig. 8).

For soils with single grain structures such as sand, silt and kaolin, these results compare well with the theoretical values as shown in Table 2.

TABLE 2

Type of Soil	Magnitude of Pressure Head in Equilibrium with 20 volts in cm. Water	
	Theoretical Value (Helmholtz)	Test Result
Fine sand (passing 100 mesh)	1	1
Sandy silt	$10^2$	$10^2$
Kaolin (80 per cent. below $1\mu$ )	$4.5 \times 10^3$	$5 \times 10^3$
Clayey silt	$\gg 2 \times 10^3$	} $10^3$
London clay	$\gg 5 \times 10^3$	
Sodium-bentonite	$\gg 5 \times 10^4$	

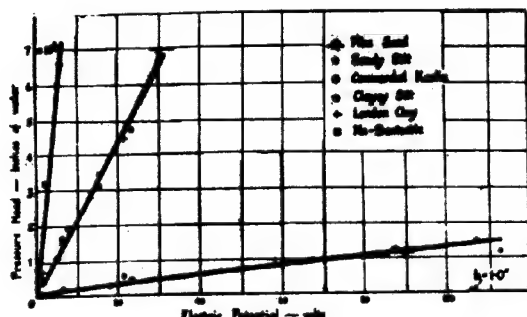
than in connection with the general problem of electro-osmosis.

After a certain time of constant flow, the discharge at the cathode slowly but steadily decreases with clayey soils. While the water content is still decreasing at some distance from the cathode it starts increasing in its immediate neighbourhood. This increase moves slowly back until, specially with clays and bentonite, the point B in Fig. 6 lies well above A. This end stage was observed also during experiments carried out at the Road Re-

#### d) Development of Natural Structures in Soils.

In 1931 the author observed for the first time the development of a structure in remoulded clays, after an electrical potential was applied. From these observations and recent investigations the following general results emerged:-

- 1) In conformity with the natural occurrence fissures develop under electro-osmotic treatment only in plastic materials. A natural structure cannot be formed, unless a certain amount of colloidal matter is present.



Hydrostatic head developed by Electro-Osmosis.

FIG.8

- 2) The higher the potential gradient applied to the soil the sooner the natural structure appears. Very small potential gradients, however, prove to be just as effective over a longer period of time.
- 3) Under a given potential gradient the fissured structure develops more effectively the greater the colloidal content and the greater the water content.

Fig. 9a shows a sample of London clay at its liquid limit, with distinct fissured structure, developed under a small potential gradient. If carefully handled a colloidal sludge still containing 800 per cent. of water displays a similar structure after having been treated electro-osmotically (Fig. 9b). While this sample of sludge gives the impression of being fairly rigid if not disturbed, it turns into a thick fluid when remoulded, without water being added.

Apart from the fissured structure parallel cracks are formed under the conditions outlined above 5). These cracks start to develop at the cathode and gradually form at regular intervals towards the anode. If such a soil is broken up the boundaries between two adjoining soil sections display a thin layer of fine crystals, apparently deposited from the pore water under electro-osmotic influence. These laminations are 4 - 5 mm thick for a potential gradient of 0.2 volt/cm and decrease in thickness with increasing potential gradient to a fraction of a mm for about 1 volt/cm.

#### V. DISCUSSION OF THE RESULTS.

##### a) Quantity of Discharge

The important general result which emerged from the investigations described is the fact that, within fairly narrow limits, from a practical point of view, the discharge of water is equal for all soils. It may be suggested, that highly plastic minerals such as Montmorillonite which have a considerable amount of water bound by molecular forces owing to their lattice structure, are possibly responsible for the wider range observed for bentonite.

##### b) Water Accumulation at the Cathode

The concentration of water at the cathode seems to be partly dependent on the design and permeability of the cathode. An incrustated cathode gauze augments the concentration of water considerably. However a gradual concentration at the cathode cannot be prevented even with the cathode gauze working satisfactorily.

As the concentration increases, the volume of drained water decreases, and simultaneously



Fissured structure in London clay developed by Electro-Osmosis. (3x nat. size)

FIG.9 a

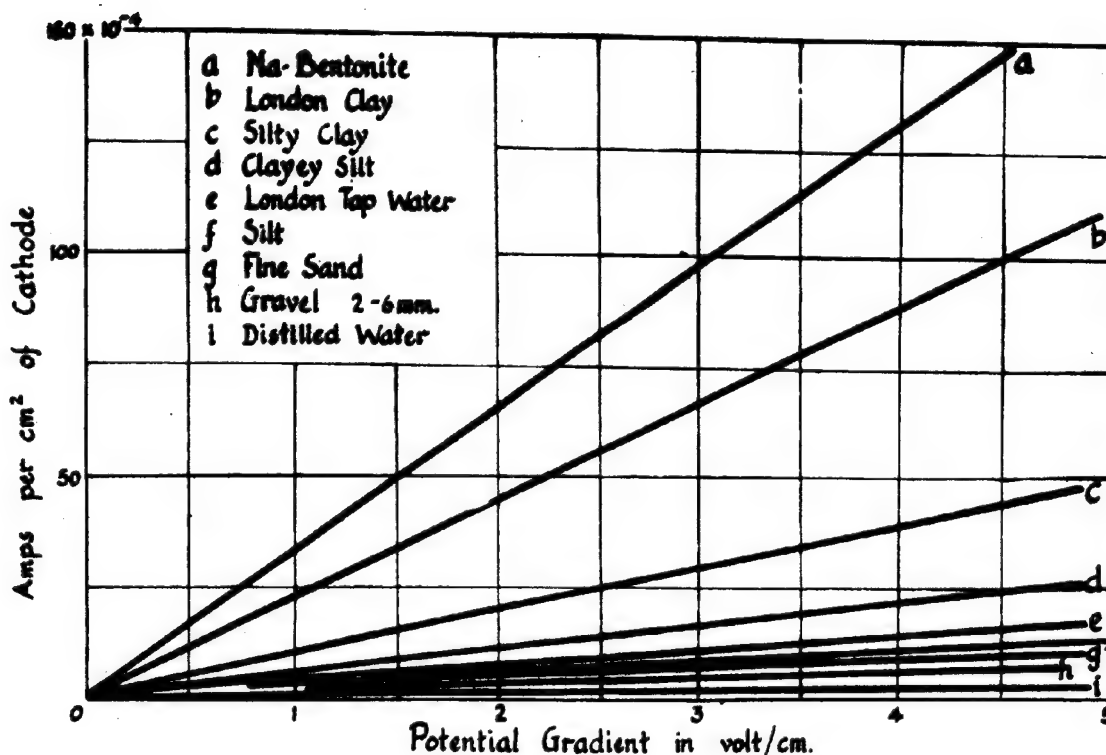


Fissured structure in colloidal sludge developed by Electro-Osmosis. (3x nat. size)

FIG.9b

the electrical current. A simple experiment proves that the reduction of the osmotic effect is in direct proportion to the concentrated water volume. This is important for the correct understanding of the electro-osmotic water movement since the decreasing efficiency combined with the decreasing intensity of the current may easily conceal the fundamental connections.

The author noticed a very close relation between the accumulating water behind the cathode and the development of laminations. These parallel and equally spaced cracks start forming as soon as the water content of the soil begins to increase again at the cathode. Besides, the rate with which additional cracks appear seems to be the same as the progress of water accumulation from the cathode towards the anode. From these facts and the observations that the cracks are filled with free water it may be concluded that the stresses developed by the water which accumulates are probably responsible for the formation of cracks.



Flow of current for various soils.

FIG.10

The development of similar cracks following equipotential surfaces was observed in colloidal gels 5) even when very small potential gradients were used.

When such samples are broken up they resemble in a striking manner some natural deposits of laminated clay.

#### c) The Hydrostatic Pressure at the Cathode

The hydrostatic pressure with fine sand, sandy silt and kaolin, derived from direct tests, show fairly good agreement with the theory (Table 2). However, such agreement has not been found with soils containing a certain proportion of clay or colloidal particles, such as a clayey silt, London clay or bentonite. For these soils the pressure head developed at the cathode was found to be about 10<sup>3</sup> cm of water for a potential of 20 volts.

This water head corresponds to a flow in capillaries of a diameter of about 0.4  $\mu$ , in other words through a system of channels which are relatively coarse compared with the size of the particles. Together with the fact that clayey and colloidal soils develop a distinctly fissured structure under electro-osmosis, and the observation that these fissures are filled with free water, it may be concluded that the water draining from the cathode is transported through the soil in these fissures. In that case the formation of the fissures could be feasibly explained on the assumption that in clayey and colloidal soils the water does not flow according to Fig. 1 but rather prefers to open up cracks (fissures) to produce a freer passage.

#### ACKNOWLEDGEMENTS.

The work described in this paper was carried out at the Building Research Station, Department of Scientific and Industrial Research, under the general supervision of Mr. L.F. Cooling, M.Sc. The author is especially indebted to Mr. L.F. Cooling, Mr. W.H. Ward and Mr. A.G. Ward for their valuable advice and help, and to the director of Building Research for his permission to publish this paper.

#### REFERENCES.

- 1) Casagrande, L., The Application of Electro-osmosis to Practical Problems in Foundations and Earthworks, Building Research Technical Paper No. 30, 1947, H.M. Stationery Office, London.
- 2) Schaad, W. and R. Haefeli, Die Anwendung der Elektrizität zur Entwässerung und Verbesserung feinkörniger Bodenarten, Bulletin der Vereinigung Schweiz. Petrologen u.-Ing., No. 42, 1946, and, Strasse und Verkehr, No. 23/24, 1946.
- 3) Schaad, W. and R. Haefeli, Elektrokinetische Erscheinungen und ihre Anwendung in der Bodenmechanik, Schweizerische Bauzeitung, 65, No. 16 - 18, 1947.
- 4) Freundlich, H., Colloid and Capillary Chemistry, London, 1926.
- 5) Maclean, D.J. and D.W. Rolfe, A Laboratory Investigation of Electro-osmosis in Soils, The Philosophical Magazine, Vol. 37, 275, 1946.
- 6) Casagrande, L., Structures Produced in Clays by Electric Potentials and their Relation to Natural Structures, Nature, Vol. 160, 1947, p. 470.

## SUB-SECTION II 9

II 9 1

MISCELLANEOUSLABORATORY COMPACTION TECHNIQUE

A.L. LITTLE B.Sc.(Eng)., A.M.I.C.E.

SUMMARY.

The paper discusses the Dietert method of compaction in the Laboratory and describes ways of measuring shear strength of the compacted soils. Reference is made to the relation between the Proctor and Dietert techniques, and tentative suggestions are made for a modification of the Dietert technique.

INTRODUCTION.

The original Laboratory Compaction Apparatus was devised by Proctor and was described by him in 1933. 1)

The test is used as a method of control when building earth embankments or compacting the subgrade of roads etc. It is proposed to adopt the Proctor technique as a Standard of the British Standards Institution. It has also been adopted by the American Association of State Highway Officials and is known as AASHTO T - 99 - 38. A full discussion of the test may be found in a paper by Markwick. 2)

For various reasons, another type of Compactor manufactured by Dietert 3) (originally for Foundry Sands) has been adopted for use in the Laboratory of Messrs. Soil Mechanics, Ltd., London, and has been correlated with the Proctor Apparatus.

THE PROCTOR TECHNIQUE.

The Proctor technique is well-known, but briefly it consists of mixing soil to a known water content and ramming it into a mould 4-inches diameter with a volume of  $1/30$ th cubic foot. The rammer weighs 5½-lbs and is dropped through 1 foot. The mould is filled in three approximately equal layers each layer being struck 25 times with the rammer. In order to make sure that the mould is filled, a loose collar is provided to accommodate surplus soil which is removed when the compaction is complete. The weight of soil in the mould is measured and the density is determined. The operation is repeated for a number of different moisture contents and a graph is drawn (as in Fig. 3) showing the variation between density and moisture content.

It is usual to express the density as dry density, i.e. the amount of dry soil contained in unit volume of the mixture - soil and water. This avoids the masking effect of the moisture content.

The graph indicates a maximum dry density at a definite moisture content known as the "optimum". Both the maximum dry density and the optimum moisture content are characteristics of the soil and depend to some extent on its Liquid Limit.

THE DIETERT TECHNIQUE.

Figure 1 shows a photograph of the Dietert machine and its accessories. Figure 2 is an outline drawing showing the principal features. A weight "A" slides freely up and down the guide "B" and is actuated by the cam "C". This cam which moves up and down with the guide ensures that the weight always falls through the same distance whatever the initial thickness of the soil pat. Detachable "foot" "D" and "E" may be screwed on to the guide rod to be used in con-

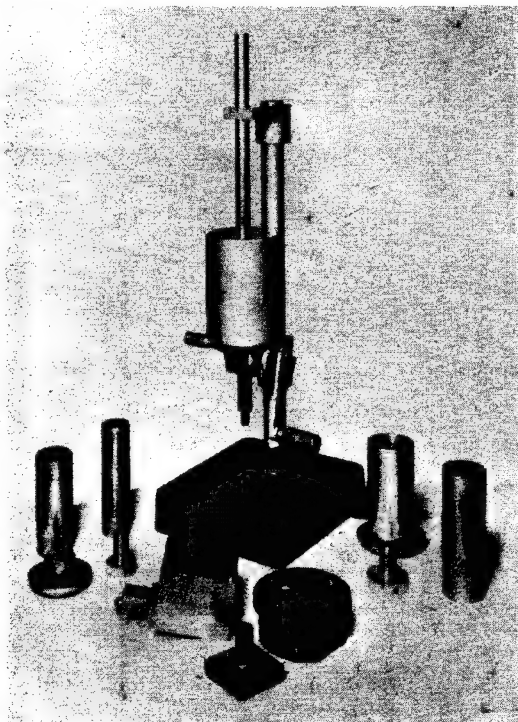
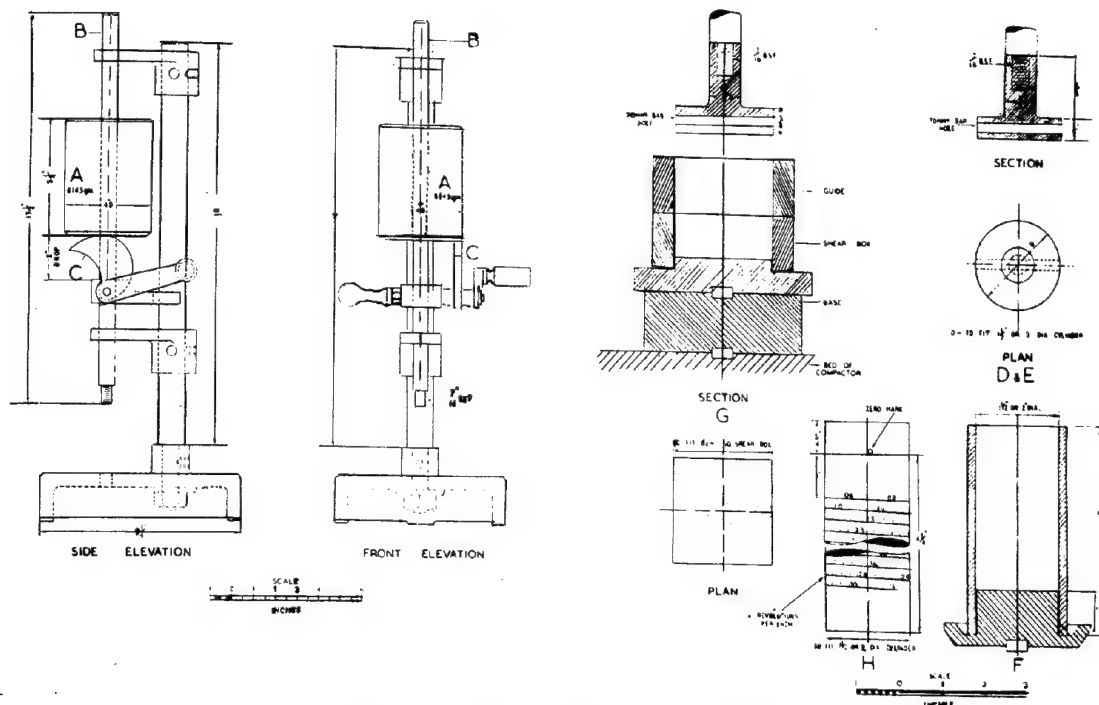


FIG.1

junction with either 1½-inch diameter cylinders (F) or the shear box (G). "H" is a spiral depth gauge used to measure the length of the samples. It is calibrated so that the "wet" density in pounds per cubic foot is given by dividing the weight of the soil pat in gms by the gauge reading.

The Dietert machine as originally used had a single fixed "foot" of 2-inches diameter and was used to compact soil pats in connection with soil stabilisation tests. The following technique was finally evolved for this purpose:

- 1) A quantity of soil was mixed to the required moisture content.
- 2) 150 gms of this wet soil was put into the 2-inch diameter cylinder.
- 3) This soil was compacted by allowing the weight to fall on it 10 times.
- 4) The cylinder was inverted and ten blows struck on the other side of the pat.
- 5) The weight and length of the pat was meas-



Drawing of Dietert apparatus and accessories

FIG.2

ured and hence its density determined.

A typical compaction curve is shown in Fig. 3.

Owing to the smaller size of the cylinder, the Dietert technique cannot deal with such coarse material as the Proctor. In this Laboratory, the practice has been to limit the use of the Dietert to material passing 1/8-inch sieve (about 3 mm). For coarser material it is necessary to use the Proctor technique, or to sieve the material and use only the finer fraction. In this latter case care must be used in interpreting the results.

#### RELATION BETWEEN PROCTOR AND DIETERT TESTS.

It was realised that as the Dietert test required only 150 gms of soil it had considerable advantages from the Laboratory point of view over the Proctor machine which required about 1500 gms. Only one tenth of the weight of soil requires to be mixed, and since thorough mixing is an essential in compaction tests, a great deal of labour is saved and accuracy is probably increased. Accordingly, parallel tests were carried out on various

soils using the Dietert and Proctor techniques as described above. Table I gives typical results which were obtained on soils with Liquid Limits ranging from 18% to 87% and a typical pair of compaction curves is given in Fig. 3.

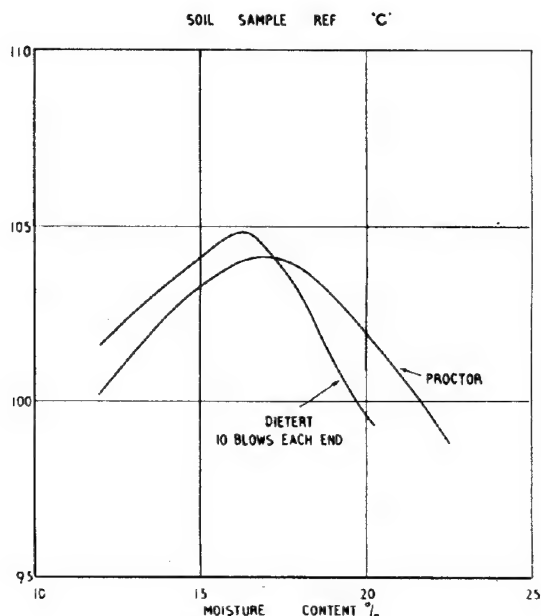
It will be seen from the table that the Dietert technique tends to give higher dry densities and somewhat different optimum moisture contents from the Proctor technique. From the practical point of view these differences are not great and either method can be used.

However, it is desirable to obtain the closest possible correlation between the two methods and further tests are being carried out.

The results obtained so far are summarised in Figs. 9, 10 and 11. A "Proctor" test was carried out on the soil in the normal manner and the curve obtained is shown. The Dietert test was carried out as described above, except that a series of tests was made, the first using 4 blows total instead of 20 and so on. In the case of the "normal compaction" soil "B" (Fig. 9) it will be seen that a total of 5 blows using the Dietert technique closely corresponds to the Proctor case. This is also

TABLE I

Soil ref	Description	Liquid Limit %	Plastic Limit %	Proctor technique		Dietert technique	
				Optimum moisture content %	Maximum dry den- sity lb/ft <sup>3</sup>	Optimum moisture content %	Maximum dry den- sity lb/ft <sup>3</sup>
A	Brown very sandy clay	18	12	12.0	122.5	10.0	125.0
B	Brown sandy clay	25	13	10.7	125.8	9.3	129.9
C	Brown silty clay (top Soil)	33	20	17.0	104.2	16.5	104.9
D	Brown silty clay (top Soil)	33	15	17.0	105.7	16.2	108.0
E	Brown silty clay (top Soil)	34	19	15.3	104.3	15.5	106.0
F	Brown silty clay (top Soil)	40	25	20.5	57.5	17.0	103.0
G	Grey Blue silty clay (Recent Alluvium)	46	21	19.5	105.0	20.0	105.2
H	Slightly silty Grey Clay (London Clay)	67	20	23.4	100.6	20.5	107.2
J	Yellow Brown Clay (Recent Alluvium)	87	28	34.5	85	24.3	55.7



Typical compaction curves

FIG.3

borne out by soil "H" (Fig. 10). A departure, however, is seen in the case of the soil "J" (Fig. 11). This was an active clay with a Liquid Limit of 87 and represents a type unlikely to be used in actual field compaction.

Further correlation tests are being carried out, and although the gap between the density and optimum obtained by the two techniques (in their original form) appears to increase with increasing Liquid Limit, it appears that good agreement is obtained between the Dietert and Proctor techniques by a suitable modifica-

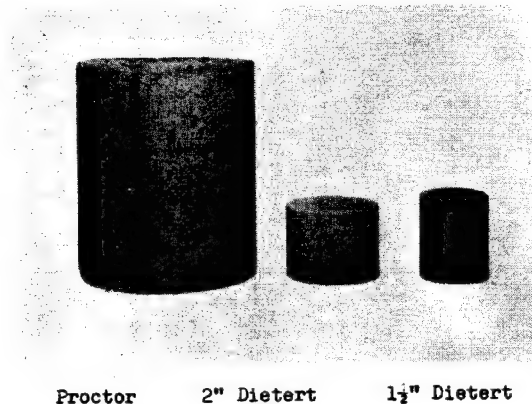


FIG.4

tion. This modification consists of reducing the total number of blows struck in the Dietert technique, to an amount tentatively fixed at a total of 5. Otherwise, the techniques should remain as described above.

Results have been published 4) showing increases in density obtained by increasing the work done in the case of the Proctor technique and it is interesting to note that such results bear a general similarity to those described here.

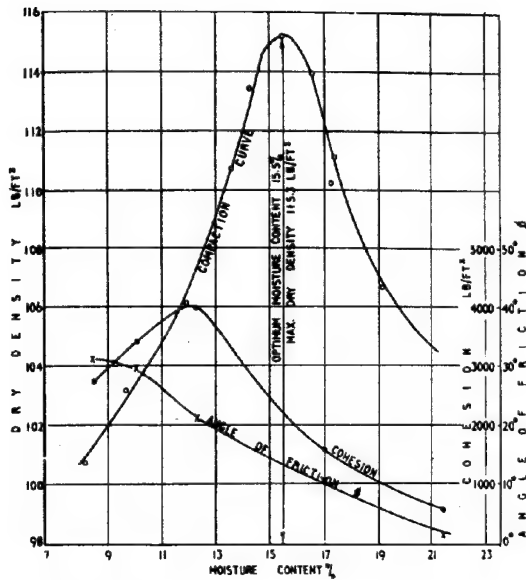
#### MEASUREMENT OF SHEAR STRENGTH.

##### a) Triaxial Samples.

As originally devised, the Proctor technique included an empirical method of estimating the strength of the compacted material by pushing into the soil bearing plates of various sizes, and such measurements can be correlated with shear strength. However, the advantages of measuring the shear strength directly are obvious and a simple modification of the Dietert machine enables this to be done.

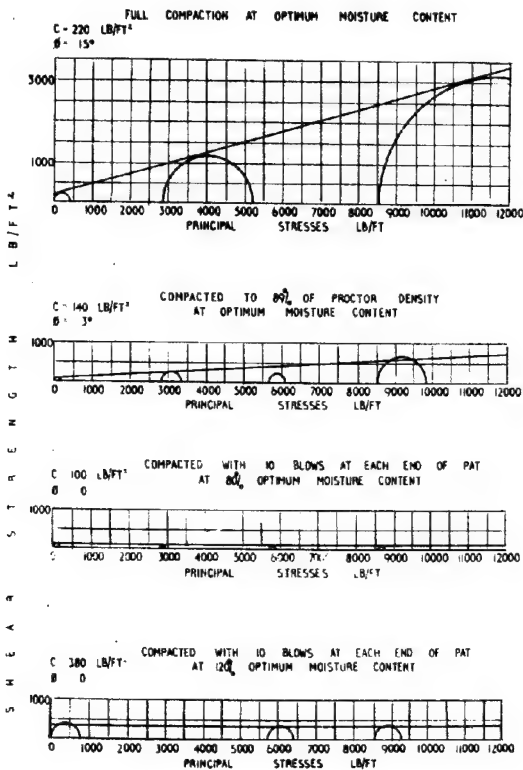
Instead of compacting the material into a





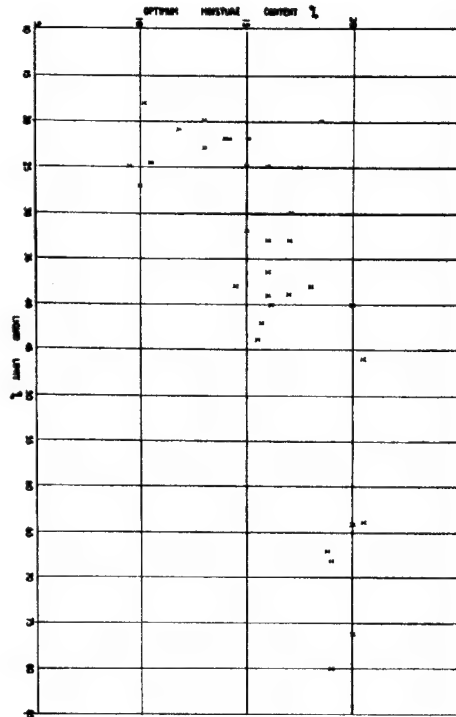
Compaction shear strength characteristics

FIG.5



Mohr's diagrams of samples tested after softening up.

FIG.6



Relation between liquid limit and optimum moisture content.

FIG.7

2-inch diameter cylinder it was compacted into a 1½-inch diameter cylinder. It was found that in order to secure the "Dietert" density, the work done had to be reduced to 4 blows on each end of a soil pat, weighing 92 gms. This gave a pat at least 1½-inches long. Two of these pats placed together (and trimmed if necessary), give a cylindrical sample 3-inches long by 1½-inches diameter which can be enclosed in a rubber envelope and tested in the Triaxial Compression Apparatus in the usual way. Fig. 5 shows the shear strength characteristics obtained at different densities.

Owing to the design of the machine it is not possible to compact a 3-inch long sample in one operation, but in any case it seems preferable to retain the 1½" long by 1½-inch diameter pat owing to its geometrical similarity to the 2-inch diameter Dietert pat and the Proctor sample (Fig. 4).

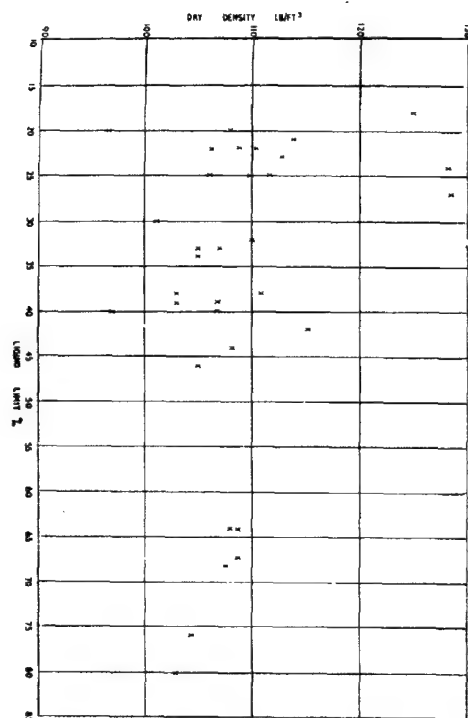
The Proctor apparatus has also been modified so that triaxial samples may be prepared from it, but so far very few tests have been carried out.

#### b) Shear Box Samples.

Compacted Shear box samples may also be prepared by the Dietert technique by ramming the soil direct into the shear box using the 6 cm square piston shown in Fig. 2.

In this case, in addition to reaching a given density at the "optimum" moisture content it is also necessary to obtain a pat approximately 2 cm thick. This condition, of course, controls the weight of soil which may be used. So far, it has been found that 12 blows on either side of the pat give the Dietert density when using the amount of soil





Relation between liquid limit and maximum dry density.

FIG. 8

calculated to give a 2 cm thick pat. It may be, however, that when soils of low density are compacted by this method, a different number of blows will be necessary to secure the correct compaction. Work on this aspect is continuing.

This technique was designed to enable compacted samples to reach their equilibrium moisture content under any given overburden before being tested for shear strength. It was not intended to measure the "immediate" shear strength of compacted samples by this method, since this is best done by using the triaxial technique described.

#### SOFTENING TESTS.

In order to estimate the effect of a softening on the stability of a compacted bank, the technique of the softening tests was developed.

After compaction of the 1½-inch diameter sample, it was put into a rubber jacket with open ends and immersed in water. It was found that one days immersion was usually sufficient for the majority of the softening effect to occur and the samples were taken out after this time and tested.

In Fig. 5, it will be noted that the maximum shear strength will in general be attained at a moisture content somewhat below the optimum. However, the practice of compacting soils at or near their optimum moisture content is amply justified when the results of the softening tests are considered.

Fig. 6 shows the Mohr's diagrams obtained from the triaxial tests on the same samples under different conditions of moisture content and compaction. It can be clearly seen that the

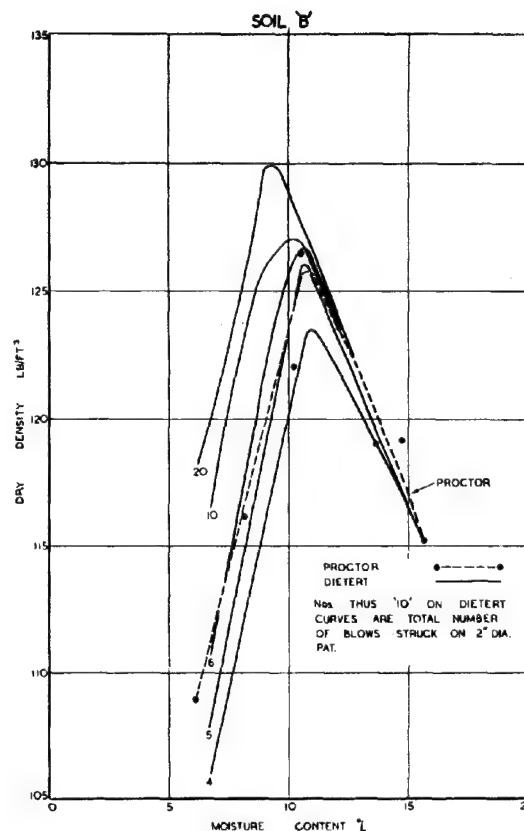


FIG. 9

softening effect is worse where the material is compacted at 80% of its optimum moisture content. Worse, in fact, than where the work done is reduced so as to give 89% of the Proctor density at the optimum moisture content. It is also interesting to note that from this point of view it is much worse to compact at 80% of the optimum moisture content than 120%. Similar results have been obtained with other materials.

#### EFFECT OF LIQUID LIMIT.

Figs. 7 & 8 respectively show the variation between Liquid Limit and Optimum Moisture Content and between Liquid Limit and Maximum Dry Density.

The results although not very clear cut do indicate a definite tendency for the optimum moisture content to increase with increasing Liquid Limit. The Maximum Dry Density on the other hand, reduces with increasing Liquid Limit.

Table II gives the relationship between Grain size distribution and compaction characteristics. As would be expected from the Liquid Limit relationship, the optimum moisture content tends to decrease and the maximum dry density to increase with increasing content of coarse material.

#### FUTURE TRENDS.

The trend in the field is to use heavier

TABLE II

SOIL REF	LIQUID LIMIT %	PLASTIC LIMIT %	OPTIMUM MOISTURE CONTENT LB/FT <sup>3</sup>	MAXIMUM DRY DENSITY LB/FT <sup>3</sup>	GRAIN SIZE DISTRIBUTION %		
					COARSER THAN 0.06 mm	0.06 mm to 0.002 mm	FINER THAN 0.002 mm
A	18	12	10.0	125.0	56	28	16
	20	18	18.5	96.6	90	10	0
	22	17	14.0	110.2	60	34	6
	23	18	13.0	112.9	70	12	18
	24	10	10.5	128.2	100	0	0
B	25	13	9.3	129.9	100	0	0
	25	16	17.5	109.9	69	15	16
	27	12	10.0	128.5	42	33	25
	30	15	17.1	101.1	39	50	11
C	33	20	16.5	105.0	13	71	16
	39	14	17.0	103.0	16	64	20
F	40	25	17.0	103.0	18	68	14
	42	20	15.7	115.2	37	38	25
	68	25	19.0	107.8	18	38	44

x Sandy Peaty Topsoil

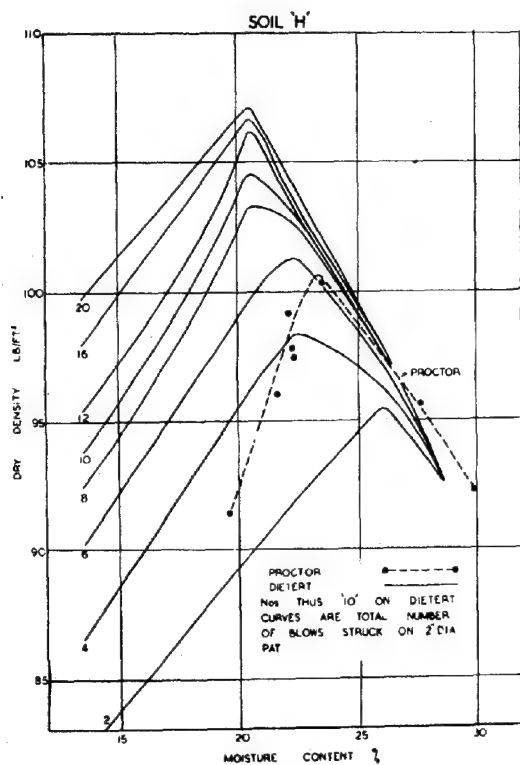


FIG.10

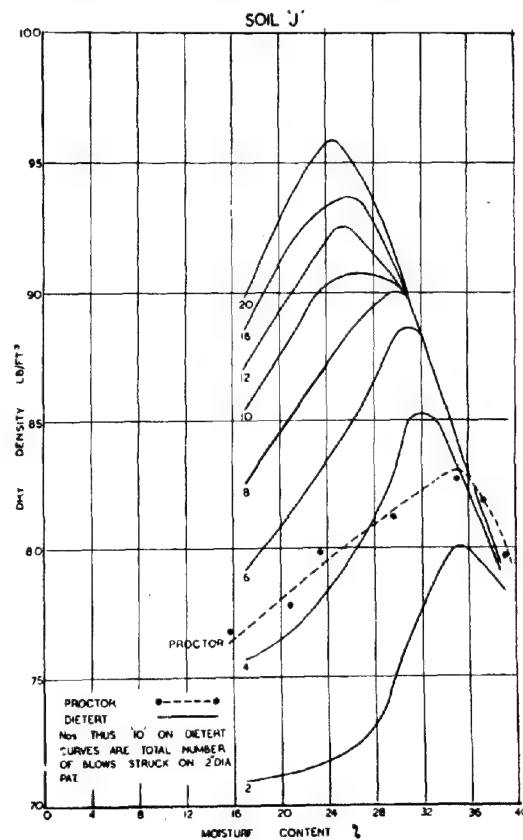


FIG.11

compaction machinery and obtain densities considerably in excess of those possible a decade ago. Complementary to this the "Heavy Proctor" has been introduced into the Laboratory. 2) This utilises a 10-pound rammer dropped through 18-inches instead of a 5½-pound rammer dropped through 12-inches.

It may be necessary to modify the Dietert technique to correspond to this test and further work will then be required to correlate the two.

By using the method described of compacting in the shear box, it will be possible to allow samples to swell or consolidate under given overburden loads, and it will be interesting to compare results of such tests with the softening tests carried out on the 1½-inch cylindrical samples.

In general, the approach to compaction problems is still largely empirical, but there is now no reason why estimates of stability should not be based on shear strength calculations as well as previous experience.

#### ACKNOWLEDGEMENTS.

The work described was carried out in the Laboratory of Messrs. Soil Mechanics, Ltd., and the author wishes to express his thanks to his Assistant - Mr. T.G. Clark - who carried out most of the tests, and to the Directors for permission to publish the results.

#### REFERENCES.

- 1) R.R. Proctor, "Four Articles on Soil Compaction". Engineering News Record, Vol. 59. 1933.
- 2) A.H.D. Markwick, "The Basic Principles of Soil Compaction and their application". Institution of Civil Engineers (London) Road Paper No. 16.
- 3) American Foundrymen's Assoc., "Foundry Sand Testing Handbook." A.F.A. 1944.
- 4) W.E. Curtis, "Soil Compaction Experiments point way toward stronger, more economical subgrades".

-O-O-O-O-O-O-

## || 9 2

### SOME LABORATORY EXPERIMENTS IN THE WATERPROOFING OF SOILS

K.E. CLARE

Department of Scientific and Industrial Research  
Road Research Laboratory

#### SUMMARY.

The note points out the value of reducing the ability of moisture to enter soil, as for instance, in the case of road subgrades, and it deals in detail with two waterproofing agents which have been investigated at the Road Research Laboratory. These are "Vinsol"-resin, which is a solid in powder form, and a waxed fuel oil. Both these materials have surface-active properties, that is, they can spread over the surface of water in thin films. It is suggested that the waterproofing of soils when admixed with these materials is due to the formation of such films at the air/water interfaces in the pores of the soil.

A description is given of the Capillary Water Absorption test developed at the Road Research Laboratory for evaluating the waterproofing properties of such stabilizers. Results obtained with this test in the case of a sandy clay soil are given, indicating, that under ideal laboratory conditions, 1 per cent of the resin and 3 per cent of the waxed oil by weight of the soil impart a maximum degree of waterproofing to the soil.

In the Capillary Water Absorption test, account is taken, in preparing the specimens, of the influence of the waterproofing agent on the compaction properties of the soil. Laboratory compaction tests made on mixtures of the sandy clay and the two stabilizing agents referred to, show that both reduce the maximum dry soil density.

Attention is drawn to the importance of the pH of the soil-water in the waterproofing of soil with resinous materials. Curves are given showing that the water absorption is greater in alkaline soils than in soils having an acidic reaction. However, some very alkaline soils and also chalk can be waterproofed using sodium stearate or tall oil emulsions.

A study has also been made of the soil waterproofing properties of several resins from tropical areas. Of these, only a Manila Copal resin was found to have an effect of the same order as "Vinsol"-resin. The waterproofing properties of Wallaba resin from British Guiana were found to be considerably improved by treating the resin with acetyl chloride.

In spite of the pH effect, the addition of "Vinsol"-resin appears to impart to chalk some resistance to damage by frost, to which chalk is particularly susceptible. Experiments are described in which cylindrical specimens of powdered chalk were frozen from the top downwards, while in contact with a source of free water. After 16 hours, ice-lenses were formed in specimens of the untreated material, while specimens containing resin were unaffected.

Box shear test results obtained with the sandy clay soil are given, showing that the addition of resin does not increase the natural stability of the soil, by increasing either the cohesion or the angle of internal friction.

#### INTRODUCTION

In road engineering it is important that bases and subgrades constructed of cohesive soils should have an adequate stability when

laid, and that this stability should be subsequently maintained. Such soils are stable if well compacted at suitable moisture contents, but they may become less stable owing to the

ingress of water. While the provision of an impermeable road surfacing will prevent the entry of water from above, moisture content increases may occur from water rising from a water-table. A method of reducing and delaying such moisture content increases is to mix waterproofing agents with the soil. This paper is concerned with laboratory investigations made at the Road Research Laboratory into the properties of some of these soil waterproofing materials.

#### WATERPROOFING AGENTS

Among the more important waterproofing agents studied are resinous materials, of which "Vinsol"-resin is the most well-known, and bituminous materials, of which waxed fuel oil is a typical example.

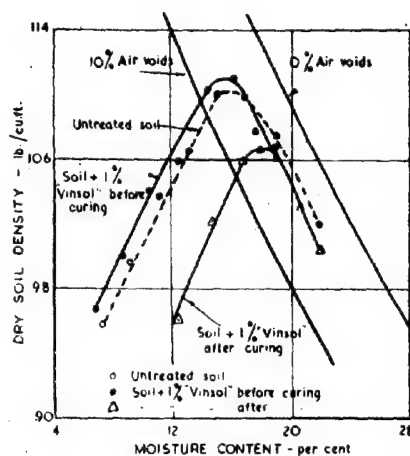
"Vinsol" is a brown resin obtained by the solvent extraction of the residue left after the distillation of pine-tree roots for turpentine 1), and it is available commercially in the form of a fine powder. Although its exact chemical constitution is not known, it contains, like abietic acid, the main constituent of rosin, a carboxyl group which confers polar properties on the molecule as a whole. By virtue of this property the resin is able to spread over the surface of water in the soil in a layer of molecular thickness. The waterproofing action of "Vinsol"-resin and other resinous materials which behave in a similar way, is believed to be due to the resistance to displacement offered by this layer to additional water entering the soil. The spreading action of resin on water can be demonstrated by dusting a small quantity of French chalk on the uncontaminated surface of some distilled water contained in a photographic developing dish. When a few grains of the resin are dropped lightly from a penknife, on to the water surface, the chalk particles will be seen to move slowly away leaving a clear area near each grain.

A bituminous material that has been found to have a very effective waterproofing action when mixed with many types of soil is a fuel oil containing about 4 per cent of paraffin wax 2). The commercial product has a viscosity of 30 seconds B.R.T.A. at 25° C. when measured on the 4 mm cup, and has been used in conjunction with a flocculating agent such as lime 3). The mechanism of the waterproofing action has been dealt with by Jackson 4) who concluded that the oil spreads out on the air/water interfaces in the soil, in very thin films. A layer of paraffin wax micro-crystals possessing some rigidity is then thought to develop on the surface of the oil films. A rigid water-repellant layer formed in this way on the soil particles would present a hydrophobic surface to water entering the soil and would not be displaced by it.

#### CAPILLARY WATER ABSORPTION TEST

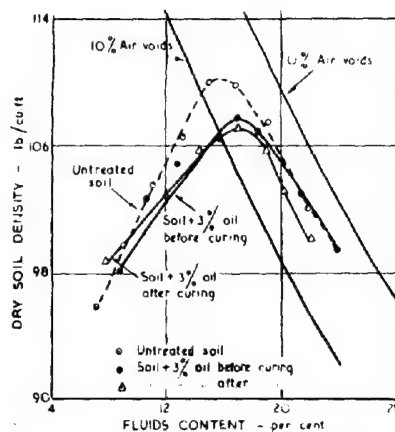
The method developed at the Road Research Laboratory for assessing the effectiveness of stabilizing agents for waterproofing soil is known as the Capillary Water Absorption test. In this method a standard compaction test 5) is first made on the soil having a stabilizer content in the middle of the range that it is intended to investigate; i.e., a stabilizer content of 3 per cent would be selected if absorption tests were to be made over the range 0-6 per cent. The compaction test is required for the purpose of determining the dry density and moisture content at which to prepare speci-

mens for studying the water absorption of the treated soil; these should approximate to conditions obtainable in practice, and research at the Road Research Laboratory has shown that of the available laboratory tests, the standard compaction test most closely reproduces field conditions in Great Britain. It is not possible to use the results of a standard compaction test on the untreated soil, as waterproofing agents of the types being considered make the soil more difficult to compact, resulting in a different moisture density relation. This is illustrated in Fig. 1 and 2, in which compaction curves are shown for a sandy loam soil from Harmondsworth, with and without the addition of, respectively 1 per cent "Vinsol"-resin and 3 per cent of waxed oil. Curves are shown for the treated



Moisture / density relations for Harmondsworth sandy loam containing 1% "Vinsol" resin, before and after curing.

FIG.1

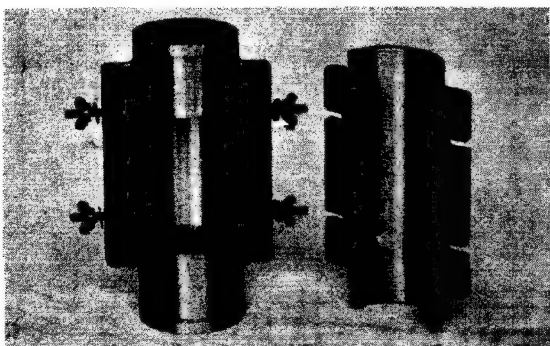


Moisture / density relations for Harmondsworth sandy loam containing 3% of waxed fuel oil, before and after curing.

FIG.2

soil when freshly mixed with the stabilizer and after having been allowed to cure for 1 week. It will be seen that the addition of the stabilizer causes a reduction in the maximum dry soil density in both cases, the reduction being obtained immediately with the waxed oil, but only after curing with the soil treated with "Vinsol"-resin.

The dry soil density and moisture content at which the water absorption specimens are prepared are those selected by drawing the 10 per cent air-voids content line on the same graph and finding the co-ordinates of the point at which this line and the relevant compaction curve intersect. The use of a 10 per cent air content ensures a condition in which the untreated soil can absorb water. If the soil in the field is to be compacted as soon as mixing has finished, the curve for the uncured mixture is used, but if the mixture is to be allowed to stand unrolled, as for example in a stock pile, the second curve for the cured material is used. Duplicate specimens



Split Cylindrical Mould, with a constant internal volume, for preparing capillary water absorption specimens.

FIG.3

are then made up in the split cylindrical mould shown in Fig. 3, which has a known internal volume (3 in. long and 2 in. diameter), when the two plungers are pressed home; it is thus possible to obtain a required dry density by compressing a calculated weight of the treated soil in the mould. The use of the split mould enables specimens to be removed rapidly without damage. The bulk density of specimens are checked by weighing and measuring after moulding.

Specimens are then kept in a humid atmosphere for three days since some stabilizing agents have been found not to develop their full waterproofing effect immediately. The curved surfaces of the specimens are then given a thin coating of paraffin wax, and the cylinders are weighed and stood in about 2 mm of water in a closed tank. The amount of water absorbed is determined by measuring the increase in weight after periods of 1, 3, 7, 14 and 28 days.

Since the specimens are made up to a constant volume (154 cc.) and a fixed air-voids content (10 per cent) it follows that the volume of air-voids is 15.4 cc. This is also the volume of water required to saturate each specimen if it is assumed that water enters all the air-voids and that no swelling takes place. The volume of air-voids that are unfilled at the end of the test can thus be used as a criterion by which the efficiency of a stabilizing agent can be compared.

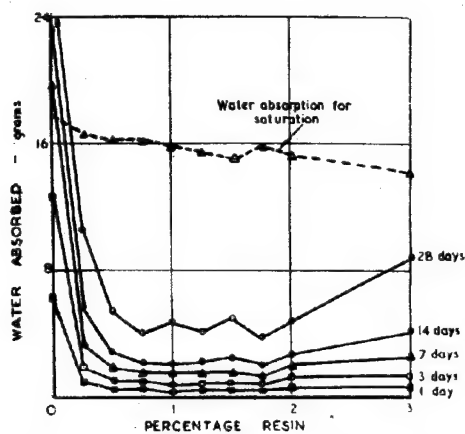
Typical results from two series of tests with "Vinsol"-resin and a waxed fuel oil are shown in Fig. 4 and 5. The soil used in the tests was a sandy loam from Harmondsworth having the characteristics shown in Table 1 below.

From Fig. 4 it will be seen that the water absorption is considerably reduced by the addition of about 1 per cent of "Vinsol", but that additional resin effects no further improvement, and in fact the addition of 3 per cent causes an increase in water absorption. The specimens of untreated soil are fully saturated after 7 days, whereas those contain-

TABLE 1

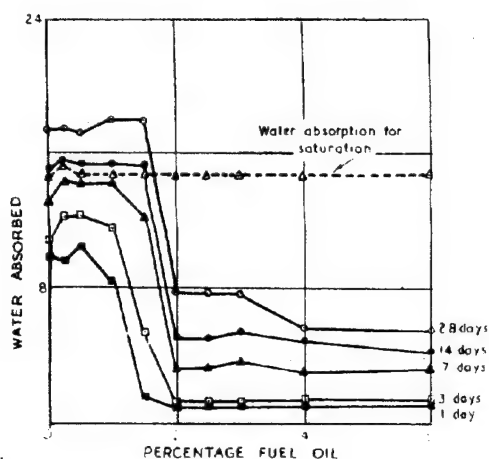
Particle size analysis, index 6), and compaction test 5) results  
for a sample of Harmondsworth sandy loam

Particle size analysis		
Coarse Sand (2.0 mm - 0.2 mm)	(%)	4
Fine Sand (0.2 mm - 0.02 mm)	(%)	57
Silt (0.02 mm - 0.002 mm)	(%)	14
Clay (< 0.002 mm)	(%)	25
Total	(%)	100
Index tests		
Liquid Limit	(%)	32
Plastic Limit	(%)	18
Plasticity Index	(%)	14
Compaction test		
Maximum dry soil density(lb./cu.ft.)		110
Optimum moisture content	(%)	16
(Mechanical Analysis by International method)		



Water absorption of specimens of Harmondsworth sandy loam containing various percentages of "Vinsol" resin.

FIG.4



Water absorption of specimens of Harmondsworth sandy loam containing various percentages of waxed fuel oil.

FIG.5

ing 1 per cent of resin are less than 10 per cent saturated after the same period.

The shape of the curve for the specimens treated with the waxed oil (Fig. 5) is different from that for the "Vinsol"-resin. The amount of water absorbed after 14 days is constant for oil contents up to 1.75 per cent, and completely saturates the soil. The water absorption is much less at 2 per cent oil content when the soil is only 20 per cent saturated.

Experience at the Road Research Laboratory with a number of such tests has indicated that a soil that can be waterproofed satisfactorily will absorb about 6 gm. of water after a period of 28 days.

#### THE INFLUENCE OF THE pH OF SOIL ON THE WATER-PROOFING EFFECT OF RESINOUS MATERIALS

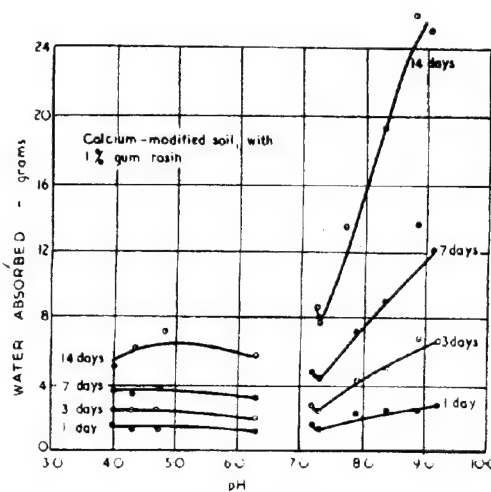
The reaction of the soil water, that is

to say its acidity or alkalinity, is conveniently expressed on the pH scale. The pH value of a solution is defined as the logarithm to the base 10 of the reciprocal of the hydrogen ion concentration. A completely neutral solution has a pH value of 7, while acids and alkaline solutions have pH values below and above this figure respectively. The reaction of most British soils varies between about pH 4 for acid heath and fen soils and pH 8 for alkaline chalky soils.

The pH of water as it exists in the soil is difficult to measure directly, and for most engineering purposes it is sufficient to determine the reaction of a soil suspension. Since the pH of such aqueous suspensions varies with the concentration, the practice at the Road Research Laboratory is to determine the reaction of a standard suspension containing 1 part of soil by weight in 3 parts of distilled water. The determination is carried out electrometrically by measuring the potential difference between the suspension and a glass electrode, using a saturated calomel electrode as a reference level.

To investigate the effect of soil reaction on the waterproofing properties of resinous materials, capillary water absorption specimens were made up with a 1 per cent admixture of gum rosin in an acid sandy loam soil from Oaklands, Hertfordshire. The pH of this soil was adjusted to different values by the addition of calcium hydroxide. The various specimens were subjected to capillary water absorption test for periods from 1 to 28 days.

The results of these are shown in Fig. 6.



Relation between water absorption and hydrogen ion concentration (pH) for a sandy loam soil treated with 1% gum rosin.

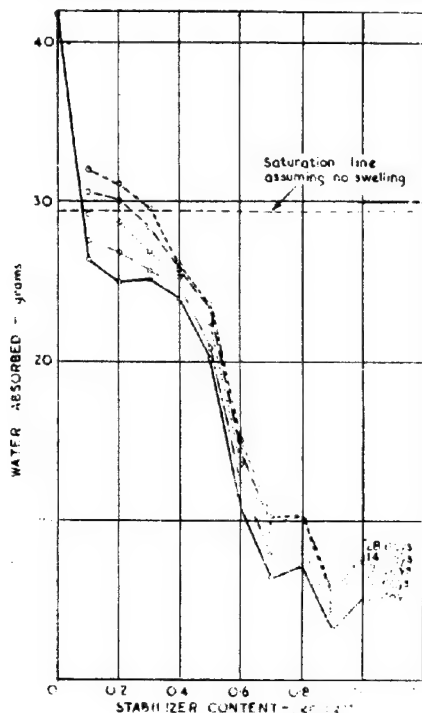
FIG.6

It will be seen that the rosin exerts a waterproofing effect in all cases where the soil reaction was acid, whereas when the pH value exceeded 7 there was a definite increase in water absorption, the amount absorbed increasing with a numerical rise in pH value. Similar results were obtained when "Vinsol"-resin was employed. It is therefore concluded that natural (i.e. unmodified) resins of this type can only exert a waterproofing action when used with acid soils.

### THE WATERPROOFING OF ALKALINE SOILS

Recognising the limitations imposed by the pH effect described above, it was felt that a method should be found for waterproofing alkaline soils, particularly in view of the wide occurrence of such soils in Southern England. As a result of observations made during another investigation involving cation-active materials, it was decided to determine the effect of anionic soaps as waterproofing agents for alkaline soils.

Capillary water absorption tests were therefore made to determine the waterproofing effect obtained by mixing sodium stearate in powdered natural chalk. The results (Fig. 7) showed that the untreated specimens absorbed 40 gm. of water after 1 day, whereas the addition of 0.9 per cent of stearate reduced this figure to about 3 gm., or less than one-tenth of the original value. The effect was



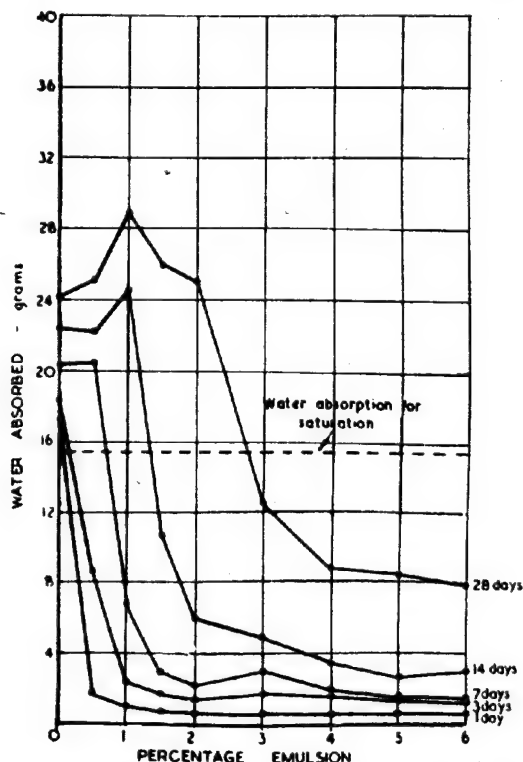
Relation between stabilizer content and water absorption for capillary water absorption specimens of chalk treated with sodium stearate.

FIG. 7

still operative after 28 days. Similar results were obtained when this chemical was added to laterized soils containing a proportion of free iron oxide, and it is thought that the waterproofing is due either to the adsorption of the soluble stearate ions on to the surfaces of the soil particles or to the formation of water-insoluble calcium or iron stearates at the water/air interfaces in the soil pores.

There are now a number of commercial soil stabilization processes, many of them patented (?), involving the use of water-soluble soaps of organic acids of different types. Metallic salts such as calcium hydroxide and the sulphates of aluminium and iron are often added to precipitate the required water-insoluble soaps, and these will also presumably have a

flocculating action on the clay particles in the soil. One of those materials, a commercial resinous emulsion derived from the tall oil or liquid rosin obtained as a by-product in the manufacture of paper was found to have a waterproofing action when mixed with soils having chalk contents of 4 per cent or more. Fig. 8 shows the results of capillary water absorption tests on a sandy loam soil containing 4 per cent of chalk when admixed with this emulsion.



Variation of water absorption of a sandy loam soil containing 4% of chalk when treated with a resinous emulsion.

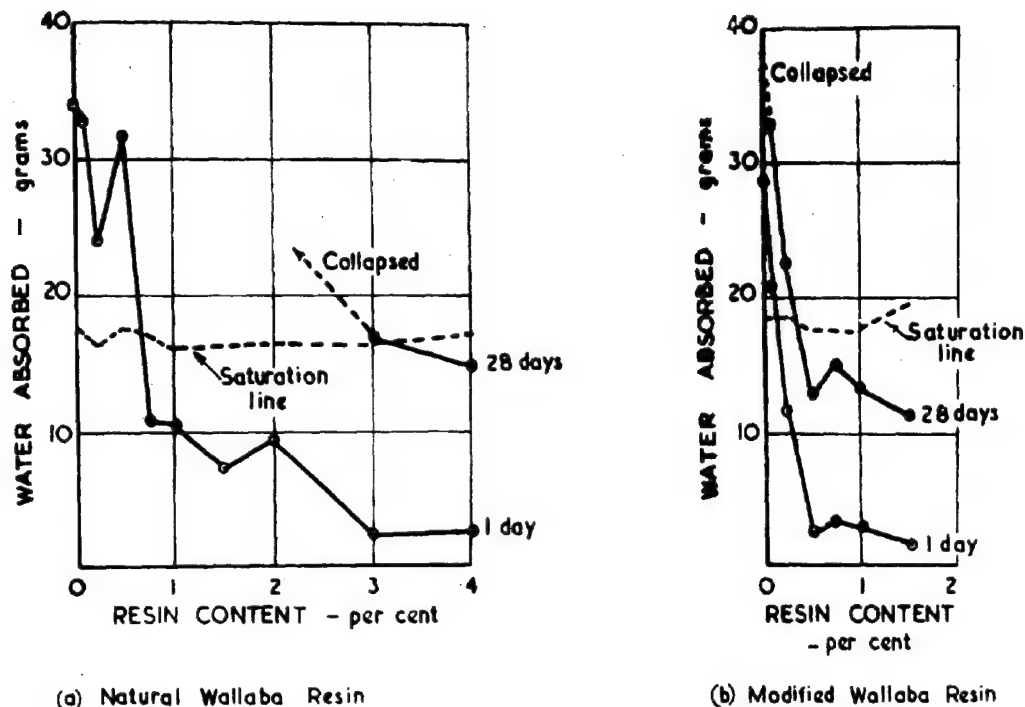
FIG. 8

### THE USE OF TROPICAL RESINS

Both "Vinsol"-resin and gum rosin are obtained from pine trees, which occur in temperate climatic conditions. The waterproofing properties of several other resinous materials from tropical regions have, however, also been studied. Among the materials investigated were Copal and Damar resins from the Dutch East Indies and the Belgian Congo, and resins from Ceylon and Nigeria. The only resin having waterproofing properties comparable with "Vinsol" under the conditions of test was a Manila Copal resin.

An interesting aspect of this work was the improvement of the waterproofing characteristics of a rosin obtained by the modification of its molecular structure. Fig. 9(a) shows the results of water absorption tests on specimens of Harmondsworth sandy loam containing resin from the Wallaba tree of British Guiana. Fig. 9(b) shows the results of similar tests with a derivative of the rosin obtained by treating





Effect of modification of chemical structure on the waterproofing properties of wallaba resin from British Guiana.

FIG.9

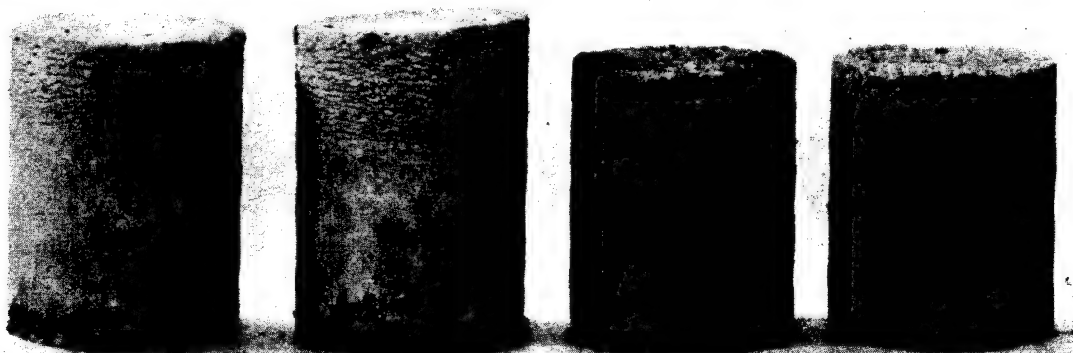
it with acetyl chloride. An improvement in both the minimum resin content required and in the permanency of waterproofing was obtained, presumably because the film formed by the modified resin has greater stability than that of the natural material.

#### EFFECT OF "VINSOL"-RESIN ON FROST RESISTANCE OF CHALK

A particular characteristic of chalk is

its susceptibility to damage by frost, and several cases have been observed in Southern England in which roads on chalk subgrades have been disrupted during severe winters. Experiments were therefore carried out at an early stage to determine whether resinous treatment of chalk could reduce this susceptibility.

Fig. 10 shows four specimens of powdered natural chalk which were prepared in the standard compaction mould, and subsequently



Chalk specimens after being subjected to a temperature gradient freezing test for 16 hours. The two specimens on the left are made with the original material, while the two on the right contain 1% "Vinsol" resin.

FIG.10

subjected to a temperature gradient by allowing the top surfaces to come into contact with air at  $-10^{\circ}\text{C}.$ , while the lower surfaces were immersed in water maintained at a temperature slightly above  $0^{\circ}\text{C}.$  Two of the specimens were prepared from the natural chalk, while the others were made with the same material containing 1 per cent of "Vinsol"-resin. It will be seen that under the conditions of the test the resin-treated specimens remained unchanged, whereas ice-lenses were formed in the untreated specimens as a result of which they increased in height about half an inch. It was concluded therefore, that the addition of resin may inhibit the damage of chalk by frost to some extent, but the mechanism by which this is accomplished is not yet known.

#### EFFECT OF "VINSOL"-RESIN ON THE STABILITY OF SOIL

It was originally thought that the addition of resinous material might increase the stability of a soil by raising the inter-particle friction, by analogy with the use of rosin on pulleys and belts. A series of box shear tests were therefore made with untreated and treated samples of Harmondsworth sandy loam to investigate this possibility. The results are given in Table 2 below:

TABLE 2

Results of box shear tests on specimens of Harmondsworth sandy loam soil, with and without the addition of "Vinsol"-resin

Resin content	(%)	0	0.5	1.0
Moisture content	(%)	10.3	9.6	10.1
Dry soil density (lb./cu.ft.)		103	104	105
Cohesion (c) (lb./sq.in.)		16	16.5	18
Angle of Internal Friction ( $\phi$ )	( $^{\circ}$ )	40	40	41

It will be seen that, within the limits of experimental error, neither the angle of internal friction nor the cohesion are changed by the addition of the resin.

#### ACKNOWLEDGEMENT

The work described in this paper was carried out at the Road Research Laboratory of the Department of Scientific and Industrial Research as part of the programme of the Road Research Board. The paper is presented by permission of the Director of Road Research.

#### LIST OF REFERENCES

- 1) United States Patent No. 2,193,026 and United States Patent No. 2,221,540.
- 2) British Patent No. 537,567.
- 3) British Patent No. 561,266.
- 4) Recent developments in connexion with the application of soil stabilization in practice. JACKSON, J.S. J. Soc. Chem. Ind., Lond., 1944, 63, (6).
- 5) Tentative Method of Test for Moisture-Density Relations of Soils. A.S.T.M. Designation D 698-42T. Part II Non-metallic materials-Constructional. American Society for Testing Materials, A.S.T.M. Standards, Philadelphia, 1944. (The Society).
- 6) Standard Methods of Test for Liquid Limit, Plastic Limit and Plasticity Index of Soils. A.S.T.M. Designations D 423-39 and D 424-39. Part II Non-metallic materials-Constructional. American Society for Testing Materials,

A.S.T.M. Standards, Philadelphia, 1944 (The Society).

- 7) British Patents Nos. 575,479; 575,484-5; 575,798.

# AN INVESTIGATION OF THE BEARING CAPACITY OF SHALLOW FOOTINGS ON DRY SAND

G.G. MEYERHOP, M.Sc.(Eng.), A.M.I.C.E., AM.I.Struct.E.

Department of Scientific and Industrial Research  
Building Research Station

## INTRODUCTION.

Although several investigators 1), 2), 3), 4) have carried out small-scale loading tests on sand, their experiments were restricted to surface loads. The bearing capacity of footings and piers located below the surface does not appear to have been determined experimentally, nor is a rigorous analysis of this problem available owing to its mathematical difficulties. In order to assess the value of approximate methods, a preliminary series of model experiments has been made on square and rectangular footings on dry sand, at depths of up to six times the footing width. These tests are briefly described below and the results are analysed on the basis of the observed movements in the sand mass and shear strength of the sand.

## METHOD AND RESULTS OF LOADING AND ANCILLARY

### SHEAR TESTS.

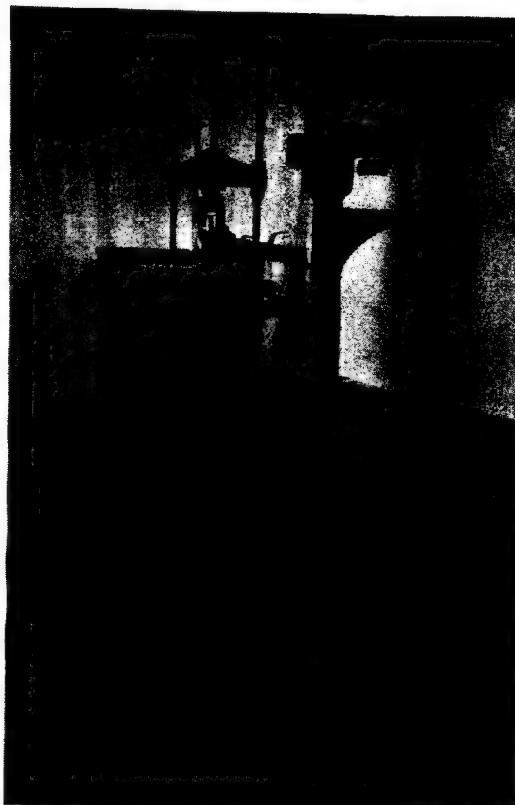
The loading tests were carried out in a stiffened steel tank (Fig. 1) 18 in. long, 15 in. wide and 18 in. deep, which was filled in 3 in. thick layers with a clean and dry medium river sand. The grading lay between 0.3 and 0.6 mm, with 50 per cent. passing a 0.4 mm sieve; the specific gravity of the particles was 2.70. Each layer was tamped with a vibrating hammer, and a fairly uniform density was obtained, the average porosity being 37.1 per cent.

The footings were brass sections  $\frac{1}{2}$  and 1 in. wide; their lengths and depths varied from  $\frac{1}{2}$  to 6 in. They were placed at the required depth in the centre of the tank and loaded by a jack through a proving ring. The load was applied in small steps, each increment being maintained until the settlement was sensibly complete. The tests were continued beyond the ultimate bearing capacity and the final smallest value until the additional surcharge effect became noticeable and the failure surface was well developed. More information about the extent of the failure surface was obtained from similar tests on footings in a wooden box with a glass front, the inside face of which had been smoked to record the movement of the soil particles.

The principle results of the loading tests are summarized in Table 1 below.

Some typical tests are illustrated by their settlement-pressure curves in Fig. 2. When a footing was loaded, its settlement increased at an increasing rate until the ultimate bearing capacity was reached. That happened at a settlement of 0.05 to 0.2 times the width of the footing, the lower limit relating to shallower and the upper limit to deeper footings. The final bearing capacity occurred at about twice the above settlement by which time a failure surface usually became noticeable at ground level. With square footings, however, no failure surface was observed for depths greater than twice the footing width.

In plan the failure surface was circular for square and elliptical for rectangular footings, the sand surface rising uniformly for shallow foundation depths (Fig. 3) and as a flat dome for greater depths (Fig. 4). Failure rarely took place with the formation

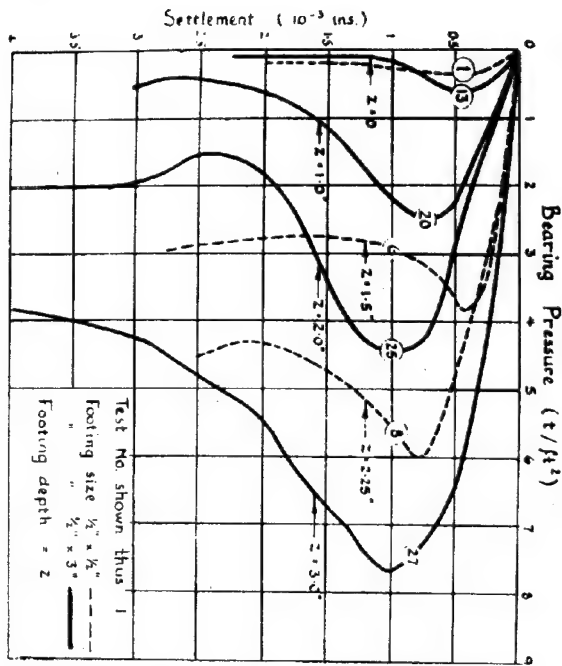


Arrangement of Loading Test.

FIG.1

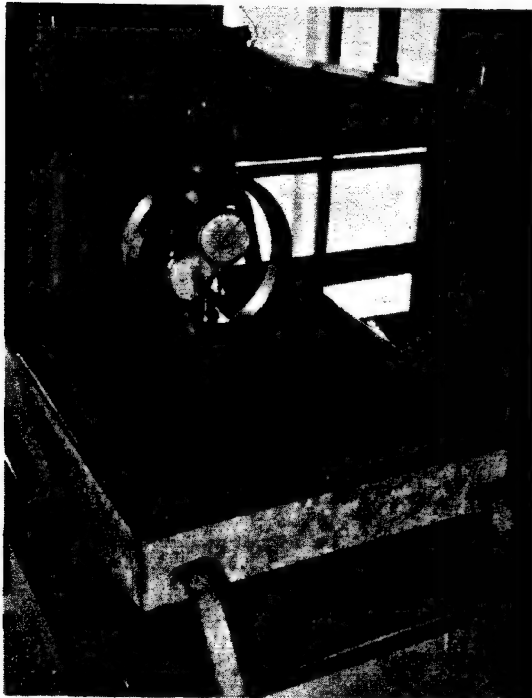
of two rupture surfaces, but generally the footing tilted slightly to one side, on which a small crater was produced, with a single failure surface on the other side of the footing (Fig. 5). The corresponding ground movements extended to depths of 2 to 3 times those of the failure surfaces below the foundation base.

The angle of internal friction  $\phi$  of the sand and the angle of skin friction  $\delta$  of sand on brass were determined in a constant rate of strain shear box 5) for various porosities and vertical pressures. The results (Fig. 6 upper curves) agreed with previous investigations 6), 7) in that although the ultimate (or maximum) (or residual) value  $\phi_u$  increased with smaller porosities and pressures, its final value  $\phi_f$  was independent of them. In the present tests  $\phi_f$  was  $30.5^\circ$ , and the critical porosity varied from 41 per cent. under a normal pressure of  $\frac{1}{2}$  t/ft.<sup>2</sup> to  $43\frac{1}{2}$  per cent. under 4 t/ft.<sup>2</sup>. Similarly the ultimate value  $\phi_u$  (Fig. 6 lower curves) increased with smaller porosities and pressures, while the final value  $\phi_f$  was independent and was found to be  $18.5^\circ$ .



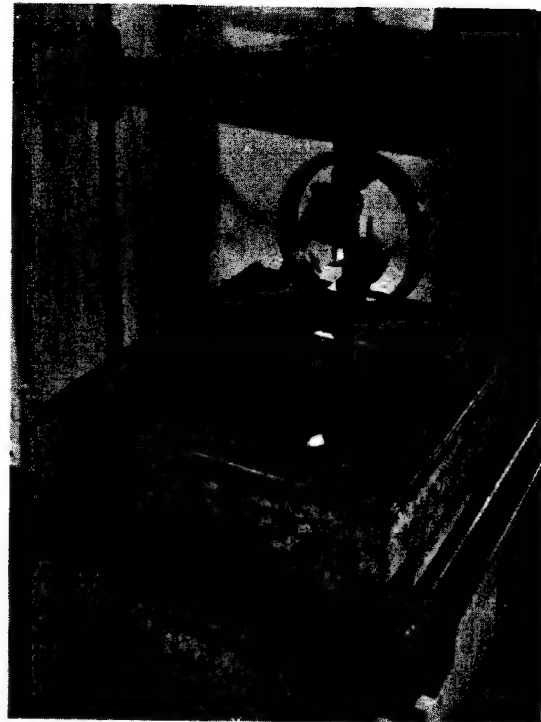
Typical settlement-pressure curves.

FIG.2



Failure of Footing at Depth equal to Width (Test no. 52).

FIG.3



Failure of Footing at Depth equal to 6 times width (Test no. 28).

FIG.4



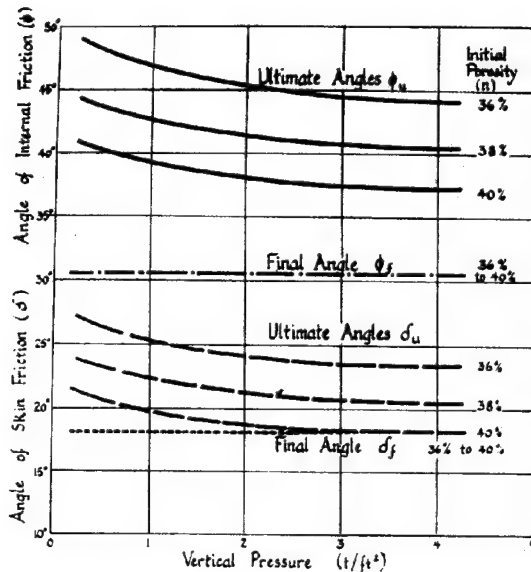
Failure Zone below Surface Footing (Test no. 49).

FIG.5

TABLE 1.

## Results of Loading Tests

Test No.	Footings Size	Initial Depth Z	Average Porosity n	Bearing Capacity		Failure Surface	
				Ultimate	Final	Width	Length
				$q_u$ t/ft. <sup>2</sup>	$q_f$ t/ft. <sup>2</sup>	$b_f$ in.	in.
1	1 x 1	0	37.0	0.36	0.18	0.5	
2	"	"	37.0	0.39	0.30	0.6	
3	"	"	37.1	0.38	0.35	0.5	
4	"	"	37.1	0.33	0.32	0.5	
5	"	"	36.9	0.35	0.22	0.5	
6	"	1.5	36.5	3.81	2.73	-	
7	"	"	36.5	4.09	2.71	-	
8	"	2.25	36.5	6.0	4.25	-	
9	"	3.03	37.4	6.5	5.3	-	
10	"	3.02	37.3	7.9	6.1	-	
11	1 x 1 1/2	0	37.4	0.35	0.17	1.1	2.2
12	"	"	36.6	0.35	0.22	1.0	1.9
13	1 x 3	"	37.1	0.61	0.10	2.2	3.6
14	"	"	37.0	0.51	0.07	2.1	3.3
15	"	"	37.0	0.46	0.11	1.7	3.2
16	"	"	37.0	0.58	0.26	1.6	3.2
17	"	0.48	36.5	1.52	0.42	3.1	4.2
18	"	0.5	36.9	1.32	0.42	3.2	4.5
19	"	0.9	36.7	2.92	1.54	3.5	5.4
20	"	1.0	36.9	2.52	0.42	4.7	5.8
21	"	1.37	37.3	3.74	0.72	4.8	5.7
22	"	1.42	36.6	3.81	0.65	5.6	7.2
23	"	"	37.1	3.81	0.54	5.2	6.7
24	"	1.95	36.8	4.61	1.51	7.4	6.6
25	"	2.0	36.9	4.41	1.51	6.7	7.6
26	"	2.95	36.8	7.2	2.53	8.0	8.8
27	"	3.0	37.1	7.7	3.29	8.4	9.8
28	"	"	37.0	6.8	2.93	8.2	9.4
29	1 x 4 1/2	0	36.5	0.78	0.20	2.0	5.0
30	"	0.5	36.9	2.01	0.44	3.4	5.3
31	1 x 6	0	36.6	0.48	0.15	2.0	7.0
32	"	"	36.6	0.77	0.14	2.1	6.7
33	"	0.5	36.6	1.87	0.36	3.5	8.0
34	"	0.7	36.8	1.81	0.16	4.8	8.3
35	"	0.88	36.7	2.53	1.34	5.3	8.6
36	1 x 1	0	37.0	0.61	0.46	1.0	
37	"	"	37.8	0.60	0.41	1.1	
38	"	"	37.8	0.60	0.42	1.0	
39	"	"	37.8	0.60	0.41	1.1	
40	"	"	37.8	0.61	0.39	1.0	
41	"	0.8	37.0	2.43	1.38	2.1	
42	"	1.5	38.2	3.68	1.90	3.0	
43	"	"	37.6	3.31	2.41	2.8	
44	"	2.05	36.6	6.7	3.86	3.8	
45	"	3.0	38.3	5.8	4.52	-	
46	"	3.1	37.6	6.8	4.82	-	
47	"	4.45	37.6	8.4	7.5	-	
48	"	6.0	38.1	13.2	12.1	-	
49	1 x 3	0	37.2	1.15	0.23	2.8	4.8
50	"	"	38.0	0.50	0.18	2.6	4.0
51	"	1	36.9	4.15	1.23	7.0	8.2
52	"	"	37.1	3.01	1.17	5.3	6.2
53	"	2	37.5	5.7	1.76	7.6	9.3
54	"	3	37.4	6.6	3.47	11.1	14.7



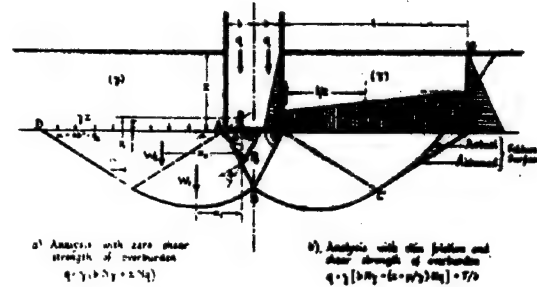
Relation of angles of internal and skin friction and vertical pressure.

FIG. 6

In general,  $\tan \delta = \frac{1}{2} \tan \phi$  for the same porosity and normal pressure.

#### ANALYSIS OF RESULTS OF LOADING TESTS.

A comparison by the author 8) of different theories of bearing capacity of shallow foundations indicated that Prandtl's (logarithmic spiral) method 9) was the most promising. Prandtl assumed that the footing edges form the centres of the spiral portions of the failure surface. This assumption does not give the minimum bearing capacity for sands so that such mathematical analyses 10), 11), 12) yield unsafe results. Terzaghi suggested 13) that these centres should be determined by a graphical trial and error method along a line inclined at an angle of  $45^\circ - \phi/2$  to the horizontal (Fig. 7a) the corresponding analytical determination of the bearing capacity is summarized in the Appendix and leads to a rather involved closed expression from which the coefficients in column 2 of Table 2 have been computed.



a. Analysis with zero shear strength of overburden.  
 $q = \gamma(b N_\gamma + z N_q)$

b. Analysis with skin friction and shear strength of overburden.  
 $q = \gamma[b N_\gamma + (z + p/\gamma) N_q] + F/b$

Analysis of bearing capacity.

FIG. 7

The above mentioned values do not, however, represent the worst failure condition, for which the centres of rotation should not be restricted to a line. In this way the lower coefficients in column 3 of Table 2 were obtained together with the width and depth of the failure surfaces. While the difference between the previous and new values is small at low angles of internal friction, it increases rapidly to about 20 per cent. at  $\phi = 50^\circ$ .

It is somewhat difficult to compare the results of the present tests on surface footings with the theoretical values because  $\phi$  varies with the normal pressure along the failure surface. When an allowance is made for the proportion of the total resistance developed by the various zones of plastic equilibrium, the average normal pressure along the failure surface is of the order of 1/10th of the applied average foundation pressure ( $45^\circ < \phi < 46^\circ$ ). For that pressure (about 0.1 t/ft. per inch width of footing) and the average porosity used (37 per cent.), Fig. 6 indicates an average  $\phi_u$  of  $46^\circ$ , giving an ultimate bearing capacity by the modified analysis of  $q_{su} = 0.75$  t/ft. per inch width of footing. This value is in good agreement with the average experimental result of 0.82 t/ft. The average observed final bearing capacity  $q_{sf} = 0.38$  t/ft. which corresponds to  $\phi_f = 42.3^\circ$  is practically the same as that obtained from subsidiary loading tests on the sand in the plastic zone. Although these tests showed that the shearing action occurred

TABLE 2

#### Theoretical Bearing Capacity and Failure Surface

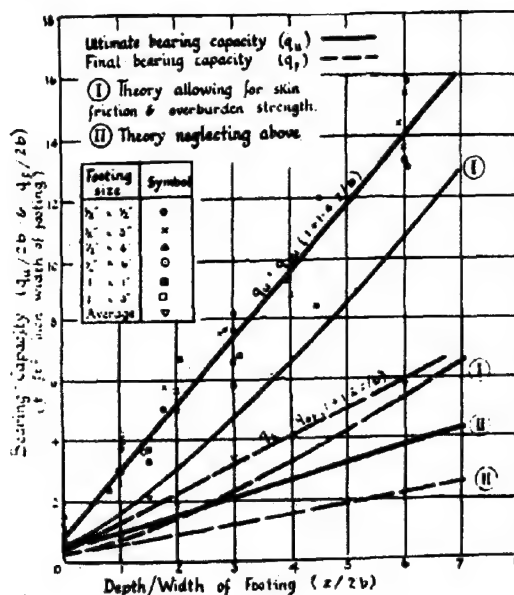
(Base Angle  $\psi = 45^\circ + \phi/2$ )

Angle of Internal Friction $\phi$	Bearing Capacity Coefficient $N_\gamma$		Failure Surface (modified Analysis)	
	Equation 1	Modified Analysis	Width $b/2b$	Depth $d/2b$
0	0	0	1.0	0.71
5	0.05	0.05	1.1	0.72
10	0.6	0.6	1.2	0.74
15	1.8	1.8	1.4	0.78
20	4.9	4.8	1.7	0.86
25	11.1	10.7	2.2	1.0
30	24.0	22.9	3.0	1.15
35	51.8	48.4	4.1	1.4
40	128	116	4.6	1.7
45	355	305	8.0	2.2
50	1800	1455	12	3.1

throughout that zone, it appeared to be of a partial and progressive nature at different points, as compared with the simultaneous failure along the whole rupture plane in the box shear tests, which gave the much lower  $\phi_r = 30.5^\circ$ . The observed maximum depth and width of the failure surface for strip footings were about  $2/3$ rd of the theoretical values for a base angle  $\psi = 45^\circ + \frac{1}{2}\phi$ . Since in the preliminary tests footings of different roughnesses showed sensibly the same failure surface, the corresponding variation of the base angle suggested by Terzaghi (13) is not supported by this investigation, but the discrepancy must be sought in the theory, which neglects the effect of the weight of the soil on the shape and extent of the failure surface.

The experimental ultimate and average final bearing capacities per unit width of footing are plotted in Fig. 8 against the ratio of depth to width of footing ( $z/2b$ ). In spite of some scatter of the results, which is largely due to variations in porosity of the sand, the bearing capacities increase in direct proportion with the footing depth within the range investigated. These relations can, with good approximation, be expressed by  $q_u = q_{ou} \cdot (1 + 1.4z/b)$  and  $q_f = q_{of} \cdot (1 + 1.2z/b)$  for the ultimate and final bearing capacities, respectively. There was a tendency for the ultimate bearing capacities of square footings to be rather less than those of rectangular ones, particularly at ground level where the ratio of the corresponding values was 0.7. The ratio of final to ultimate bearing capacity decreased a little with increasing footing depth and averaged 0.4.

A theoretical estimate of the bearing capacity of shallow footings can be made for the limiting conditions of zero and full shear strength of the sand above foundation level. In the first case a mathematical solution (14) (Appendix equation 2) is available from which the ultimate and final bearing capacities are  $q_u = q_{ou} \cdot (1 + 0.44z/b)$  and  $q_f = q_{of} \cdot (1 + 0.49z/b)$



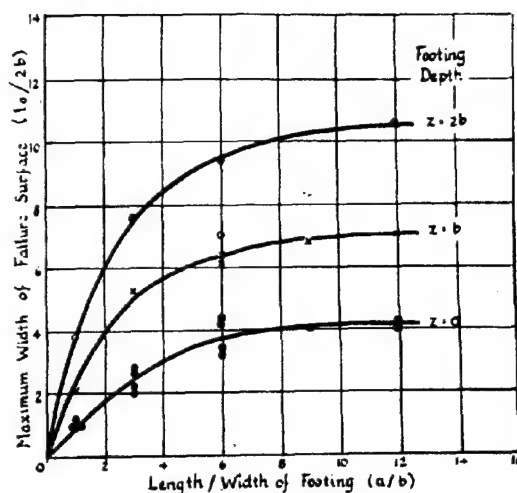
Bearing capacity. Depth relations.

FIG.8

respectively, for  $\phi_r = 45^\circ$  and  $\phi_r = 41.5^\circ$ , which would be the upper limits for the higher bearing pressures obtained. These relations have been plotted in Fig. 8 (curves II) and when compared with the test results show that the observed effect of foundation depth is about three times the theoretical one. The shear strength of the overburden cannot, therefore reasonably be neglected, even for very shallow foundations.

Assuming that the skin friction on the footing and the shear strength along vertical ends of the failure surface are fully mobilized, an approximate analysis can be made on the basis of Terzaghi's method (13) (Appendix equation 3). Preliminary investigation of skin friction in conjunction with the shear test results indicated that nearly the full passive pressure is effective, i.e.  $K_0 = K_1 = 5.83$  for  $\phi_r = 45^\circ$  and 4.4 for  $\phi_r = 41.5^\circ$ . The distance ( $l$ ) of the assumed vertical part of the failure surface from the footing edge can be estimated from the observed movements of the sand mass. The experimental ratio of maximum failure surface width (at ground level) to footing width is plotted in Fig. 9 against length/width ratio ( $a/b$ ) of the footings. These curves show that for a given foundation depth the failure surface width increases with footing length at a decreasing rate, and approaches a maximum for a long strip; for  $a/b \geq 6$  this increase appears to be small. Further, Fig. 10, which has been obtained from these curves and Table 1, shows that for a given ratio  $a/b$  the failure surface width ( $l_0$ ) is directly proportional to the footing depth ( $z$ ), and that for a long strip this relation approximates to  $l_0 = 8b + 3z$ . At depths greater than those investigated a maximum  $l_0$  seemed to be reached, while later no failure surface at all developed at ground level (e.g. for the deepest square footings tested) owing to the small shear stresses induced there. Since neither depth nor width ( $l_0$ ) of this surface at base level were appreciably affected by footing depth, i.e.  $l_0 \approx 8b$  for a long strip, an average distance  $l = (l_0 + l_1)/2 = 8b + 1.5z$  may be taken as a rough approximation.

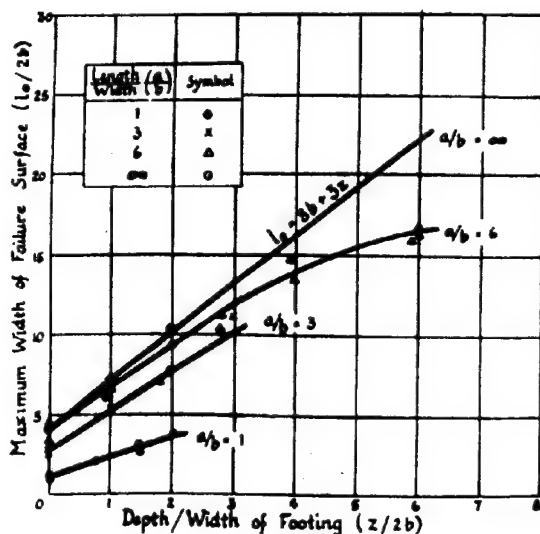
The upper theoretical curves (I) of Fig.8 have been computed from the above results for



Relation of failure surface width and length of footing.

FIG.9





Relation of failure surface width and depth of footing.

FIG.10

the ultimate and final bearing capacities. While the rate of increase of the bearing capacities with footing depth agree closely with that observed in both cases, the estimated values are conservative, particularly for the ultimate condition. This under-estimation may be due to the neglect of greater skin friction and shear resistance near base level caused by the foundation stresses; furthermore, the deformation conditions there might allow the passive pressure ratio to be exceeded locally.

#### CONCLUSION.

The present model tests show that the ultimate bearing capacity of footings on the surface of dry sand agree fairly well with the theoretical value for the worst failure condition and ultimate shear strength of the soil. The final bearing capacity is considerably greater than that estimated from the final shear strength, probably owing to partial progressive failure with a limited relative movement of the particles. The width of the failure surface at ground level increases with footing length to a maximum for a long strip when it is less than the value predicted by the modified analysis.

While the bearing capacities of shallow foundations are about three times greater than the values estimated on the assumption of zero shear strength of the overburden, they agree fairly well if the maximum skin friction and full shear strength above base level along a vertical failure plane at the mean observed distance from the footing edge are included. Although the extent of the failure surface varies considerably with bearing areas of different shapes, the corresponding bearing capacities appear to differ mainly for foundations at the surface and at very shallow depths.

#### ACKNOWLEDGEMENT.

The author is indebted to his colleagues for their assistance in the tests. The work was carried out as part of the programme of the Building Research Board of the Department of

Scientific and Industrial Research, and the paper is published by permission of the Director of Building Research.

#### BIBLIOGRAPHY.

- 1) Fellenius, W. "Jordstatiska Beräkningar för vertical Belastning". Teknisk Tidkrift, 1929, Nos. 21 and 25.
- 2) Kogler, F. and A. Scheidig, "Baugrund und Bauwerk". Ernst, Berlin, 1938, p.177.
- 3) Meischneider, H. "Über den Einfluss der Flächenform auf die Tragfähigkeit von Fundamentplatten". Bauingenieur, 1940, vol.21, p.83.
- 4) Golder, H.Q. "The Ultimate Bearing Pressure of Rectangular Footings". Journ. Inst. C.E., 1941, vol. 17, p.161.
- 5) Golder, H.Q. "An Apparatus for Measuring the Shear Strength of Soils". Engineering, 1942, vol. 153, p.501.
- 6) Cassagrande, A. and S.G. Albert. "Research on the Shearing Resistance of Soils". Report M.I.T., September 1930.
- 7) Taylor, D.W. and T.M. Leps. "Shearing Properties of Ottawa Standard Sand". Proc. Soils and Found. Conf., U.S. Corps of Engineers, 1938, p.C-1.
- 8) Meyerhof, G.G. "The Bearing Capacity and Consolidation of Soils and Settlement of Foundations". M.Sc. Thesis, University of London, 1944.
- 9) Prandtl, L. "Über die Härte plastischer Körper". Nachr. Kgl. Ges. Wiss., Göttingen, Math.-Phys. Kl., 1920, p.74.
- 10) Palmer, L.A. and E.S. Barber. "Principles of Soil Mechanics Involved in Fill Construction". Proc. Highw. Res. Bd., Washington, 1937, vol. 17, p.503.
- 11) Raes, P.E. "Het Oppersingsvraagstuk bij een Stroomvormig Fundament". Techn. - Wetensch. Tijdschr., 1941, No. 10, p.1.
- 12) Boulton, N.S. "Plastic Stresses in a Semi-Infinite Cohesive Mass". Phil. Mag., 1946, vol. 37, p.733.
- 13) Terzaghi, K. "Theoretical Soil Mechanics". Wiley, New York, 1940, p.118.
- 14) Reissner, H. "Zum Erddruckproblem". Proc. 1st. Int. Congr. Appl. Mech., Delft, 1924.

#### APPENDIX.

##### Analyses of the Bearing Capacity of a Strip Footing on Sand.

- 1) Load at Ground Level (Fig. 7a with  $z = 0$ )  
When the bearing capacity is  $q$ , the plastic equilibrium to the left of the footing centre is found by balancing the moments about O (on CA produced and defined by angle  $\theta$  between CO and the vertical) of the overturning resultant  $P_0$  on AB and the resisting sector ABC (force  $W_1$  and wedges ACE ( $W_2$ ) and CDE ( $P_1$ )).

$$\text{Thus } M_0 = M_1 + M_2 + M_3$$

$$\text{where } M_0 = P_0 x_0, M_1 = W_1 x_1, M_2 = W_2 x_2 \text{ and } M_3 = P_1 y_1$$

Omitting details of the analysis and using the notation illustrated in Fig. 7, it can be shown that

$$M_0 = \frac{(2q + \gamma \tan \psi) \gamma^2 \tan \psi}{2 \cos(\psi - \phi)} \left[ \frac{2 \cos \phi}{3 \sin \psi} \frac{(\cot \psi - \tan \theta) \cos(\alpha + \psi - \phi)}{(\cot \alpha + \tan \theta) \sin \alpha} \right],$$

$$M_1 = M'_1 - M''_1, \text{ where}$$

$$M_1' = \frac{\gamma^3 \tan^3 \psi (\cot \alpha + \cot \psi)^3}{3(\cot \alpha + \tan \theta)^3 \cos^2 \theta (9 \tan^2 \frac{\psi}{2} + 1)} \left[ \left( 3 \tan \frac{\phi}{2} \cos \alpha - \sin \alpha \right) e^{3(45^\circ + \frac{\phi}{2} + \theta) \tan \frac{\phi}{2}} + 3 \tan \frac{\phi}{2} \sin \theta + \cos \theta \right] \quad \text{and}$$

$$M_1'' = \frac{\gamma \nu \tan^2 \psi (\cot \psi - \tan \theta) (1 + \tan \psi \cot \alpha)}{3(\cot \alpha + \tan \theta)} \left[ \frac{(\cot \psi - \tan \theta) \cot \alpha}{\cot \alpha + \tan \theta} - \frac{\cot \psi}{2} \right],$$

$$\text{and } M_2 = M_3$$

$$= \frac{\gamma \nu^3 \tan^3 \psi}{6} \left[ (A-B)^2 \cot^2 \alpha (2A+B) \right]$$

$$\text{where } A = \frac{\cos \alpha + \sin \alpha \cot \psi}{(\cot \alpha + \tan \theta) \cos \theta} e^{(45^\circ + \frac{\phi}{2} + \theta) \tan \frac{\phi}{2}}$$

$$\text{and } B = \frac{\cot \psi - \tan \theta}{\cot \alpha + \tan \theta}$$

Substituting the above into the equilibrium equation and simplifying,

$$q = \gamma \nu N_y \quad (1)$$

where  $N_y = \frac{\tan \psi}{3} [C]$  the expansion of C being

$$\left[ \frac{\tan \psi}{(\cot \alpha + \tan \theta)^3} \left\{ \frac{\cos \alpha + \sin \alpha \cot \psi}{\cos \theta} e^{(45^\circ + \frac{\phi}{2} + \theta) \tan \frac{\phi}{2}} - \cot \psi + \tan \theta \right\}^2 \right. \\ \left. + \frac{(\cos \alpha + \sin \alpha \cot \psi)}{\cos \theta} 2 e^{(45^\circ + \frac{\phi}{2} + \theta) \tan \frac{\phi}{2}} + \cot \psi - \tan \theta \right) \cot^2 \alpha \right] \\ + \frac{\tan \psi}{(\cot \alpha + \tan \theta)^3} \left\{ \frac{(\cot \alpha + \cot \psi)^3}{(9 \tan^2 \frac{\psi}{2} + 1) \cos^2 \theta} \left[ 3 \tan \frac{\phi}{2} \cos \alpha - \sin \alpha \right] \right. \\ \left. + 3 \tan \frac{\phi}{2} \sin \theta + \cos \theta \right\} \\ - \frac{1}{(\cot \alpha + \tan \theta)^2} \left\{ \cot \psi - \tan \theta \left[ \left( \frac{\cot \psi}{2} - \tan \theta \right) \cot \alpha - \frac{\cot \psi}{2} \tan \theta \right] (1 + \tan \psi \cot \alpha) \right\} \right] \\ \frac{3}{2} \\ \left[ \frac{2 \cos \frac{\phi}{2}}{3 \sin \psi} - \frac{\cos(\alpha + \psi - \frac{\phi}{2})}{\sin \alpha} \left( \frac{\cot \psi - \tan \theta}{\cot \alpha + \tan \theta} \right) \right] \div \cos(\psi - \frac{\phi}{2})$$

The worst  $\theta$  is found by solving  $dN_y/d\theta = 0$ , which has been done for two special cases:-

$$1) \psi = 45^\circ + \frac{\phi}{2} \quad \text{when } \theta = \frac{4\alpha}{3} = 60^\circ - \frac{2\phi}{3}$$

$$\text{and } 2) \psi = \frac{\phi}{2} \quad \text{when } \theta = \frac{2\alpha}{5} = 18^\circ - \frac{\phi}{5}$$

By substituting either of these equations into the general equation of the bearing capacity above, it can be simplified a little.

## 2) Load at Depth $z$ below Ground Level

### a) Zero shear strength of overburden (Fig. 7a)

$$q = \gamma (\nu N_q + z N_q) \quad (2)$$

$$\text{where } 14) N_q = \frac{\cos(\psi - \frac{\phi}{2})}{\cos \psi \tan \alpha} e^{(270^\circ + \frac{\phi}{2} - 2\psi) \tan \frac{\phi}{2}}$$

$$\therefore N_q = \cot^2 \alpha e^{160^\circ \tan \frac{\phi}{2}} \quad \text{for } \psi = 45^\circ + \frac{\phi}{2}$$

$$\text{and } = \frac{\cot \alpha}{\cos \frac{\phi}{2}} e^{(270^\circ - \frac{\phi}{2}) \tan \frac{\phi}{2}} \quad \text{for } \psi = \frac{\phi}{2}$$

### b) Full skin friction and shear strength of overburden (Fig. 7b)

The bearing capacity is increased from the value of equation (2) by the skin friction  $F$  on the footing and the average surcharge pressure  $p$  due to  $F$  and the shear strength  $S$  along the vertical part D'G of the failure surface.

$$\text{Hence } q = \gamma \left[ \nu N_q + \left( z + \frac{p}{\gamma} \right) N_q \right] + \frac{F}{b} \quad (3)$$

$$\text{where } \begin{cases} F = K_0 \tan \delta \frac{1}{2} \gamma z^2 \\ S = K_1 \tan \frac{\phi}{2} \frac{1}{2} \gamma z^2 \\ p = \frac{F + S}{l} \end{cases}$$

$K_0$  and  $K_1$  are the

earth pressure coefficients at the footing side and vertical part of the failure surface, respectively.

# SECTION III

## FIELD INVESTIGATIONS

### SUB-SECTION III a

#### BORING AND SAMPLING

#### III a 1 FIELD TESTS WITH NEW COMBINED LOADING TEST SAMPLER FOR HARBOUR EXTENSION WORK

A. MORTENSEN, Harbour Engineer  
Aalborg, Denmark

#### SUMMARY.

In heterogeneous samples from deep waterfilled borings the porewater may migrate from sandy to clayey parts of the sample and sandy samples may be lost in the casing or damaged during the lifting operations or shipment due to lack of capillary pressure.

A new combined loading test sampler with short piston rod for undisturbed sampling in cohesive soils and for test loading f. inst. in cohesionless soils is described.

The measured values for shear,  $\tau_s$  (skin friction on outside of cylinder) and vertical soil pressure,  $\sigma_v$ , in uniform heavy-textured late glacial clay with thin layers of sand (Yoldia clay), in heterogeneous glacial chalky clay and in chalk are compared with results from sample tests in the field and on the laboratory.

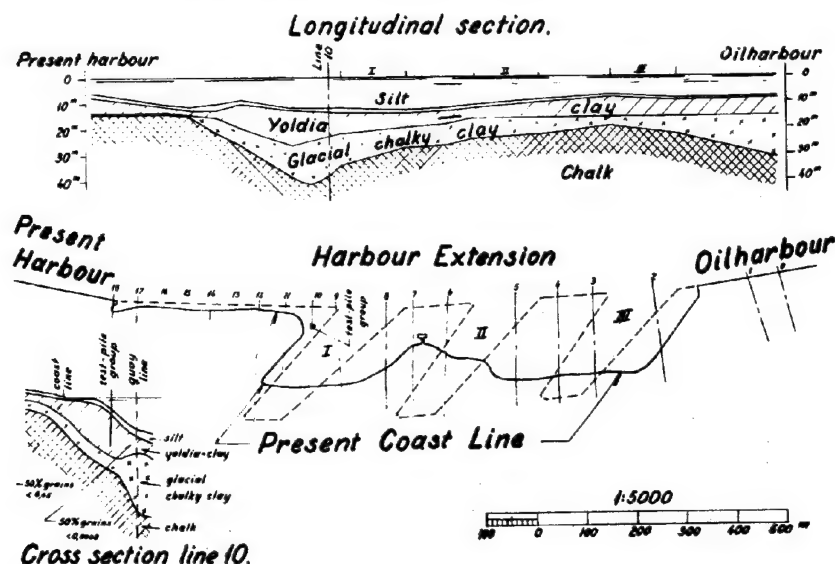
The average values for all tests of the relation between  $\tau_s$  and  $\sigma_v$ , respectively, and the natural soil pressure (geostatic soil pressure - weight less buoyancy)

$p_n = \Sigma(\gamma - 1) \cdot \Delta h$  ( $\Delta h$  is the stratum thickness) were for Yoldia clay:

$$\begin{array}{ll} \tau_a = 0.5 + 0.5 p_n \text{ kg/cm}^2 \text{ for } p_n < 1 \text{ kg/cm}^2 & \left. \begin{array}{l} \text{average for} \\ 169 \text{ samples} \\ \text{from 40 hec-} \\ \text{tars harbour} \\ \text{extension area} \end{array} \right\} \\ \tau_a = 0.8 + 0.2 \cdot p_n - - - p_n > 1 - & \\ \sigma_a = 12.5 + 7.4 \cdot p_n^2 - - - p_n > 1 - & \end{array}$$

for glacial clay:

$$\begin{array}{ll} \tau_a = 0.5 + 0.5 \cdot p_n \text{ kg/cm}^2 \text{ for } p_n > 1 \text{ kg/cm}^2 & \left. \begin{array}{l} \text{average for} \\ 114 \text{ samples} \\ \text{(same area)} \end{array} \right\} \\ \sigma_a = 12 + 45 \cdot p_n - - - p_n > 1 - & \end{array}$$



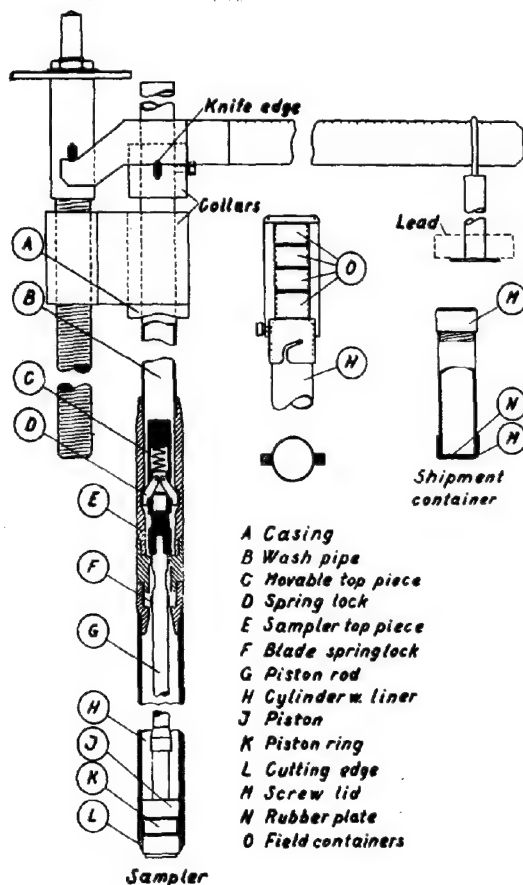
Plan of harbour extension with longitudinal and cross section.

FIG. 1

### INTRODUCTION:

On a coast stretch of 1,3 km (fig.1) plans were in 1943-45 prepared for the extension of Aalborg Harbour with 3 bassins outside the coastline. Old wash borings (73) with dry sampling to 15 m depth in 21 lines perpendicular to the coast gave by individual judgement the result, that the bottom consisted of solid clay of good bearing capacity but from later pile-driving results suspicion arose about the reliability of these results. The borings were then supplemented by 37 new borings to until 40 m depth with undisturbed samples (1,5 - 2 m intervals for determination of the shear strength and other soil properties, but in order to eliminate errors from changes in pressure and consistency it was decided simultaneously to carry out loading tests just below the casing shoe.

A combined loading test sampler was constructed - fig.2 -



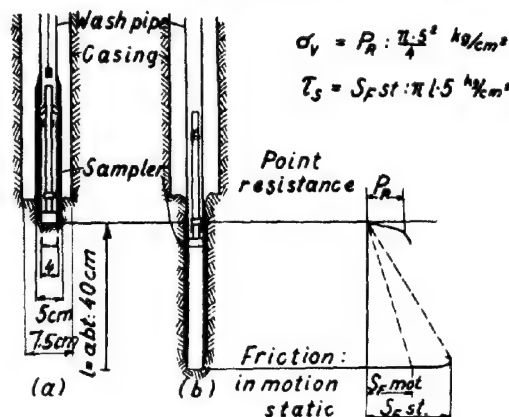
Combined sampler and loading tests cylinder

FIG. 2

with a short piston, locked in bottom position by a helical spring lock D, which may be released by sinking a lead suspended in a string down on the top of a tubular top piece C. When loading the top spring the two lock levers D are pulled back from the lock grooves in the top piece through the two slots in the top pipe and the piston is then released and ready for sampling.

After the sampler is filled (40 cm) two blade springs E lock the piston in upper position, because an enlargement of the piston rod G. passes between the two blade springs.

When the casing has been brought down to the wanted depth, the sampler is screwed on the wash pipe and sunk down to rest on the bottom of the borings (fig. 3 a). To the casing top is fastened a collar with a lever knife with a downwards turning edge, movable by a helical screw, and to the wash pipe is fixed a collar with an upwards turning knife edge (fig. 2). A 2 m lever with movable lead is used to press the sampler 2 - 5 cm down into the soil. The lever is kept level by turning the helical screw and moving the lead simultaneously. Corresponding values of load and depression are read on the lever scale and on the screw scale. When the initial static point resistance,  $P_R$ , thus has been determined - fig. 3 a & c - the piston is released and the sampler by the lever pressed 40 cm down until the blade springs are heard locking the piston in upper position. The lever is then turned opposite and the sampler withdrawn. The corresponding values of the pulling force and the lift are measured, and the static skin friction,  $S_F$ , determined - fig. 3 b & c. The sampler is then brought up and the sample taken out for field and laboratory tests.



Loading test.

FIG. 3

The loading test skin friction,  $\tau_s$ , is compared with the following field tests on samples under capillary pressure:

1) spring scale cone test by which the cone load,  $K_{sc}$ , for a 10 mm steady impress of a 60° steel cone in a sample in natural state is measured on the spring scale. The drop cone weight,  $K_3$ , is the cone load, that gives a 10 mm imprint after a 10 mm drop. The former (size of a fountain pen) is practical for field testing, and the relation between  $K_{sc}$  and  $K_3$  is for Yoldia-clay  $K_{sc} : K_3 = 2,3$  and for Glacial chalky clay  $K_{sc} : K_3 = 1,4$ .  $i_1$  denotes in the same way the drop cone weight, when the clay structure has been broken by kneading without change in natural water content. The ratio  $K_3 : K_1$  is for Yoldia-clay 2,1 and for heterogeneous glacial clay about the same value but ranging between wider limits. The relation between  $K_3$  and the ultimate shear stress,  $\tau_{sc}$ , due to the capillary pressure ( $p_c$ ) was found to be:

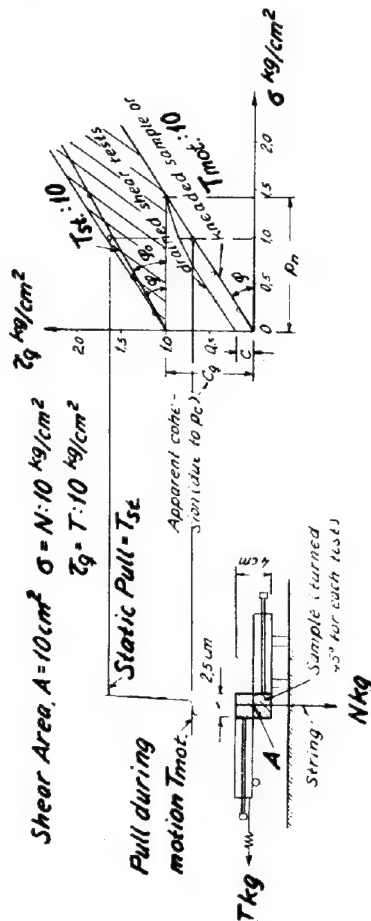
for Yoldia-clay

$$\tau_{sc} = \frac{K_s}{4.3} = \frac{K_{sc}}{4.3 \cdot 2.3} = \frac{K_c}{10}$$

glacial chalky clay

$$\tau_{sc} = \frac{K_s}{4.3} = \frac{K_{sc}}{4.3 \cdot 1.4} = \frac{K_c}{6}$$

2) Quick shear tests with the apparatus fig. 4 a gave the



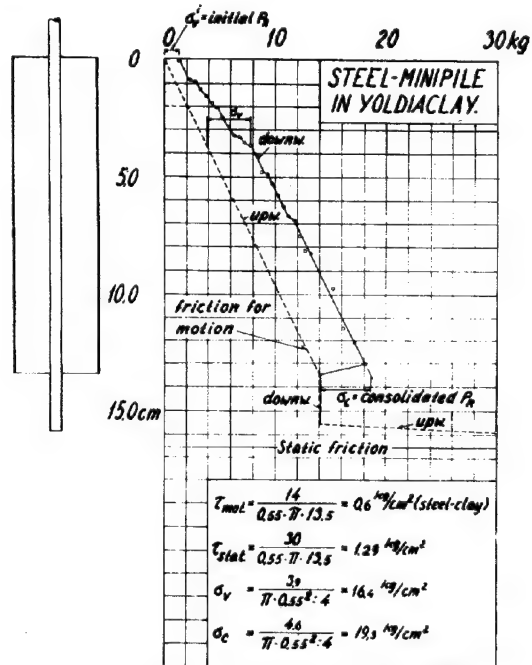
Quick shear test.

FIG. 4

result, that the shear value,  $c_0$  corresponding to the capillary pressure  $p_c$  (in Yoldia-clay same as the geostatic pressure  $p_n$ ) could be determined from the  $\sigma_v - c_0$  graph - fig. 4 b - as the apparent cohesion. A minimum value,  $\phi_0$ , for the angle of internal friction,  $\phi$ , was found by turning the sample  $45^\circ$  and varying the vertical pressure. Generally  $\phi_0$  was found on or near the upper limit ( $\tau_0$  in upper part of cross hatched section.) for sandy and chalky clay was practically found  $\phi_0 = \phi$  and  $\tau_0 = c + \sigma \tan \phi$  as in Casagrande shear tests.

For some of the samples  $\tau$  further was controlled by 3) cork screw tests: the shear,  $\tau_c$ , corresponding to the capillary pressure  $p_c$ , was determined by  $\tau_c = \frac{P}{\pi d l}$ , where  $P$  is the pull in the cork screw,  $d$  is the outside screw

diameter and  $l$  the length screwed into the sample. The cork screw shear value was the same as by the quick shear test or slightly higher. The same result was obtained 4) by pulling a model or MINI-pile ( $d = 5$  mm) out of a clay sample in a container.



Model of Mini-pile test

FIG. 5

The point resistance,  $\sigma_v$ , found by the loading tests, was checked by the Mini-Pile tests as the initial point resistance in 2-3 cm depth or as the drop in pressure  $\sigma_c$  - fig. 5 - when the pile breaks through the sample (consolidated point resistance). The ratio  $\sigma_v$  for a Mini-Pile is a measure for the consolidation during the penetration of a pile.

In fig. 6 a is given the average  $\tau_a - p_n$  graph in Yoldia-clay for the relation between the soil pressure  $p_n = \sum (\gamma \cdot h)$  and the shear  $\tau_a$ , determined by average curves for 1) loading test  $\tau_s$ , 2) spring scale cone tests,  $K_{sc}/10$ , and 3) quick shear tests,  $c_q$ , each determined from about 200 uniform tests results in homogeneous Yoldia-clay. The average shear value corresponds to the straight line  $\tau_a = 0.5 + 0.5 p_n$  kg/cm<sup>2</sup> for  $p_n < 1$  kg/cm<sup>2</sup> and  $\tau_a = 0.8 + 0.2 p_n$  kg/cm<sup>2</sup> for  $p_n > 1$  kg/cm<sup>2</sup> and seems also to include same clay type outside the new harbour area - cf. tests results for  $\tau_a$  in fig. 6 b from a quay 1000 m from the investigated area. The point resistance found by loading tests and Mini-piles gave for the harbour extension area the average value  $\sigma_v = 12.5 + 7.4 p_n^2$  kg/cm<sup>2</sup> and for the quay in question  $\sigma_v = 12.5 + 9.2 p_n^2$  kg/cm<sup>2</sup>.

This late glacial Yoldia-clay has 50 % - 70 % grains less than 0.002 mm, specific gravity 1.92, voids ratio  $f = 0.95$ , coefficient of permeability  $k = 3.10^{-7}$  cm/min and for  $\sigma = 1$  kg/cm<sup>2</sup> is the confined compression modulus of elasticity  $E_c = \frac{\Delta \sigma}{\Delta \epsilon} (1 + e_m) = 40 - 80$  kg/cm<sup>2</sup>. The grain size decreases with the water depth and above water is the Yoldia-clay very sandy

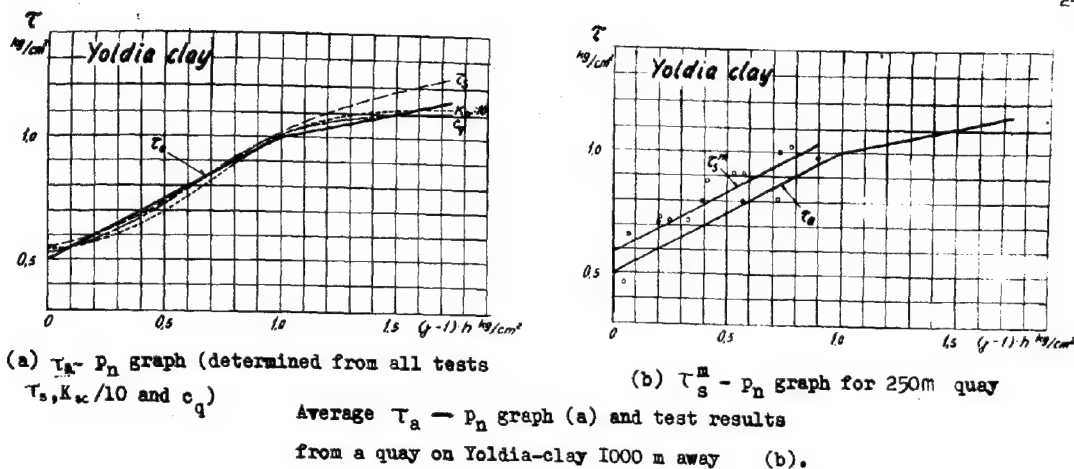


FIG. 6

(50 % over 0,05 mm).

For a chalky glacial clay with 10-20 % grains less than 0,002 mm (50 % over 0,05 mm), specific gravity 2,23, voids ratio  $e = 0,35$ ,  $k = 5,10^{-5}$  cm/min,  $E_2 = 100 - 200$  kg/cm<sup>2</sup>, the average shear  $\tau_a$  was found  $\tau_a = 0,5 + 0,5 \cdot P_n$  - cf. (fig. 7) - and the average point resistance  $\tau_a = 12 + 45 \cdot P_n$  kg/cm<sup>2</sup>, but the individual test results are here more spread due to the heterogeneous character of glacial clay and the varying capillary pressure, and this applies still more to chalk, where  $K_v/K_h$  is about 10,  $K_v/10$  about 1,20 and  $\tau_s = 0,85 \tau_a$  and  $c_a = 40 + 15 p_n$ .

In clay types with high fragmental content - as chalky glacial clay - an onion-shaped consolidated body is formed under the loading test sampler as under piles, and an increase in the point resistance thereby produced. This important soil property for piles

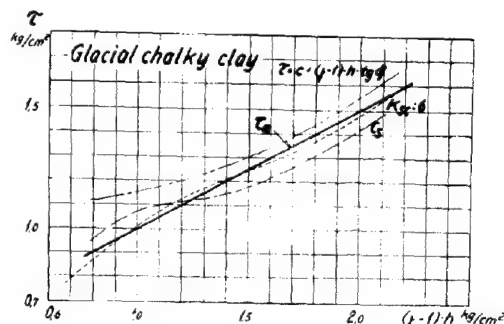


FIG. 7

TABLE I  
FIELD TESTS

Boring 1234 February 1946		same day			n days later				$\frac{K_{sc}^n}{K_{sc}^0}$	$\frac{c_q^n}{c_q^0}$	Loss $\Delta w$ in W % water content
depth m	Yoldia-clay with sand layers.	$K_{sc}^0$	$c_q^0$	$\varphi^0$	n	$K_{sc}^n$	$c_q^n$	$\varphi^n$			%
1,98	fine lay	8,8	1,1	30	11	7,0	1,1	30	0,8	1,0	0
2,93	thick -	1,8	0,42	31	7	9,0	0,88	27	5,0	2,1	3
4,45	- -	12	0,8	30	10	7,5	0,8	30	0,6	1,0	4,7
6,12	few & fine lay	9,5	0,87	33	8	6,5	0,77	33	0,7	0,9	2,3
8,40	thick -	9,0	0,7	30	7	10,2	0,8	32	1,1	1,1	2,4
10,0	- -	9,0	1,08	29	8	8,0	1,0	30	0,9	0,9	2,4
13,97	few thinner layers	7,3	1,2	27	5	10,0	1,95	27	1,4	1,6	4
15,72	-	11,0	1,3	24	5	12,0	1,67	29	1,1	1,3	4

TABLE II

Field tests.					Laboratory tests, Copenhagen.							
Boring	depth	Late glacial Yoldia-clay.	$K_{sc}^o$	quick shear tests $c^o/q$	$\gamma$ $t/m^3$	w % water	after days	$K_3^L$	$K_{sc}^L$	quick shear test $c^L/q$	$K_{sc}^L$ $\frac{K_{sc}^L}{K_{sc}^o}$	$c^L/q$ $\frac{c^L}{c^o}$
1046	- 7,94	thin sand layers	5,5	0,60	1,97	25,2	8	4,8	(11,2)	1,58	2,04	2,63
-	-16,54	- " -	8,0	0,60	1,91	31	8	2,7	(6,3)	0,51	0,79	0,64
-	-18,65	- " -	8,0	1,00	1,96	30,1	9		10	1,73	1,25	1,73
1248	-16,35	Yoldia-clay	2,0	0,30	1,91	30,9	8	4,3	10	1,50	5,00	5,00
-	-19,60	-	6,0	0,70	1,93	31,8	-	5,7	13	1,65	2,17	2,36
-	-23,31	Heavy Texture	11,0	0,85	1,98	33,7	-	6,1	14	1,66	1,28	1,96
1048	-17,70	traces of sand	8,5	0,68	1,93	31,1	9	5,4	(12,7)	1,79	1,50	2,63
-	-19,96	Spots sand & chalk	10	0,74	1,92	30,7	22	6,15	(14,3)	1,70	1,43	2,30
-	-21,78	homogeneous	10	0,48	1,91	32,1	-	6,95	(16,2)	2,56	1,62	5,36
-	-23,60	many thin sand layers.	11	0,31	1,99	31,8	-	4,9	(11,3)	1,52	1,03	4,90
Average . . .											1,81	2,56

may be determined by cone tests in the upper part of a loading test sample, where the cone weight  $K_{sc}$  in chalky clay may be increased with 50 - 100%, gradually decreasing to the normal value in a depth of abt. 4 x the point diameter, and ordinary tests should only be taken from the lower 15 cm of the sample.

The loading tests in Yoldia-clay give very uniform results and only in greater depth are the loading test results slightly higher than the cone and quick shear sample tests, probably due to insufficient capillary pressure on the samples to develop the natural pressure from overlying weight. The importance of testing the samples as soon as possible - even in tight containers with rubber cushions between the lids and the container - was confirmed by repeating the cone tests ( $K_{sc}$ ) and quick shear tests ( $c_q$  and  $q$ ) 5 to 11 days later - of table I - and by comparing the field tests with laboratory tests 8 - 22 days later - table 2. The greater changes in table 2 may be due to damage during shipment of containers and difference in testing outfit and procedure, but in both tables are found cases of drying out and cases of migration of pore-water from sandy layers to clayey parts of the sample, which is the most common cause to a decrease in shear strength of a heterogeneous sample.

In glacial chalky clay the loading test results are lower than the cone and quick shear test results, which for the shear value may be explained by the fact, that while there in Yoldia-clay always is found a thin clay skin on the outside of the sampler, this is not the case in glacial chalky clay. In fragmental soil is proposed to weld a helical groin on the outside cylinder surface and in order to prevent loosening samples is proposed to surround the wash pipe with a rubber collar

near the sampler.

#### CONCLUSION.

The described loading test is simple, speedy and reliable and gives 1) the skin friction and point resistance under actual conditions without depending on a certain capillary pressure, 2) samples of test loaded soil (upper sample) for investigation of consolidation and 3) undisturbed soil sample (lower part).

The shear stress  $\tau^m$  is for each sample determined as an average of 1) a loading test and 2) 8 - 10 sample tests (spring-cone, quick shear, Mini-pile and cork screw tests) immediately after it has been brought up. The vertical soil stress  $\sigma_v^m$  is found as an average of a loading test and a Mini-pile-test.

In heavy-textured homogeneous Yoldia-clay the deviations of the individual tests from the  $\tau^m - p_n$  and  $\sigma_v^m - p_n$  - curves are insignificant. The stresses increase uniformly downwards with the weight  $p_n$  and the curves are generally parallel to the average curves ( $\tau_a$  and  $\sigma_a$ ) for all borings in the area.

By comparing the individual tests with  $\tau^m$  and  $\sigma_v^m$  and these again with  $\tau_a$  and  $\sigma_a$ , errors are eliminated and important historic informations about the clay (earlier overburden, disturbances etc.) obtained.

In chalky glacial clay and in chalk same procedure is used, but the deviations are greater due to the inhomogeneous character, but the loading test results may here replace lost or insufficient samples.

The loading test results were found more reliable than the other field tests and these - especially the shear tests - again more reliable than Laboratory tests a week or more later due to drying out or migration of porewater.



III a 2

EXTRACTOR FOR TAKING DISTURBED SAMPLES IN HARD GROUND

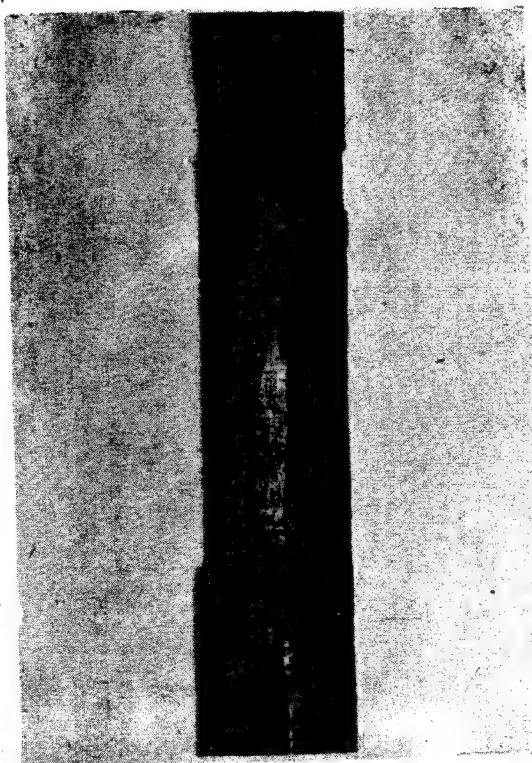
OLEG WAGER

The Royal Swedish Geotechnical Institute

In this paper a new extractor is described, by means of which very long and almost continuous disturbed samples can be taken quickly in hard ground.

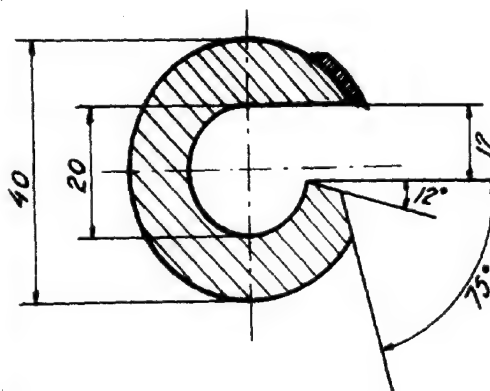
The extractor consists of a series of 1 m long tubes, joined by screwed muffs, flush with the tubes, fig. 1. The wall thickness of the tubes is very considerable. Each tube is

cut open longitudinally in the form of a slot along the whole length excepting at the ends. A small lip is welded along one side of the slot, fig. 2. In order to permit connecting up of the tubes flats for a spanner are machined on them towards the ends. The muffs are made of special steel in order to be equal in strength with the tubes, in spite of their



Connection between tubes

FIG. 1



Crosssection of the extractor.

FIG. 2

small wall thickness. The extractor is made with a removable point at its lower end.

When the extractor is driven down, the empty tube space is occupied by a series of rods, screwed together. After the depth required has been reached, the rods are withdrawn, use being made of a jack if necessary. After that the extractor is rotated, so that soil is forced into it by the action of the lips and then it is withdrawn. The soil is removed from the extractor as far as possible in one piece and gives a good picture of the soil strata.

The extractor is intended to be used specially in very hard grounds, containing sand and gravel. It has shown great ability to penetrate such grounds and has been frequently used in order to ascertain whether or not clay is present in a gravel esker.

-0-0-0-0-0-0-

## CONCERNING THE PHYSICAL PROPERTIES OF CLAYS

RALPH E. PADUM

Professor of Soil Mechanics-Purdue University

It is the writer's purpose to present data that will indicate the effects of sample disturbance on the stress-strain and consolidation characteristics of inorganic clays and to present data that will show how the natural water content of an apparently homogeneous deposit of soil may be expected to vary with depth. To these ends, the results of field loading tests are compared with the results of unconfined compression tests of specimens prepared from test pit and bore-hole samples of soil similar to that subjected to the field loading tests. The data obtained from consolidation tests of specimens, that were prepared from samples obtained by three different sampling techniques, are compared, and data obtained from detailed investigations of the variations in natural water content are presented.

The data reported herein were obtained during the period from 1936 to 1941 in connection with subsoil investigations that were made during the planning and construction of several large buildings in Boston. All of the laboratory data presented in this paper were obtained from tests performed in the Soil Mechanics Laboratories of the Graduate School of Engineering of Harvard University under the direction of Professor Arthur Casagrande and in cooperation with Mr. L.S. Homer of the Turner Construction Company and Mr. H.A. Mohr of the Raymond Concrete Pile Company.

# I. COMPARISON OF DATA OBTAINED FROM FIELD LOADING TESTS AND UNCONFINED COMPRESSION TESTS OF TEST PIT AND BORE-HOLE SAMPLES.

## A. Description of Tests.

During the construction of the New England Mutual Life Insurance Company Building in Boston, extensive tests were made of the load bearing characteristics of a hard yellow clay stratum, 5 to 10 feet in thickness, which existed 40 feet below the ground surface and upon which the wall footings of this building were to be supported. These tests consisted of field loading tests as well as unconfined compression tests of specimens prepared from hand-cut, test pit samples and from bore-hole samples.

The field loading tests were conducted in a test pit 4.5 feet square at the bottom that extended from the ground surface to the top of the hard clay stratum. Load was applied to a platform erected at the top of the pit and supported by timber columns resting directly on a loading plate 18 inches square which was placed level on the surface of the hard clay. The settlement of the plate was measured by a precision dial gage that was supported by a rigid timber, which spanned the center of the pit at the level of the ground surface, and that was in direct contact with the top of a  $\frac{1}{4}$  inch pipe, which extended downward to the top of the center of the pad where it was screwed into a flanged fitting.

Two load tests were performed. The first of these was conducted by placing pig iron on the platform in increments of 2.25 tons at intervals of 15 minutes until a total load of 19.9 tons was obtained on the platform. The settlement of the pad was recorded 15 minutes after

the application of each increment of load. Load was then removed from the platform in increments of 2.25 tons per 15 minutes until the platform was completely unloaded. The second test, which was conducted in essentially the same manner as the first test, was performed at a depth of 3 feet below that at which the first test was made.

After the completion of each test, samples were obtained by carefully cutting one-foot cubes of undisturbed soil from the region adjacent to the loaded areas. Unconfined compression tests were performed on specimens prepared from these samples, having a length-diameter ratio of 2 to 2-1/2.

When exploratory borings were made at this site, samples of this stratum of hard clay were also obtained. These samples were secured by ramming a sampling tube 2 feet in length, 5 inches in internal diameter, and 1/4 inch in wall thickness into a cased hole by means of a 185 lb. weight dropping 30 inches. Three tests were performed on specimens prepared from samples obtained in this manner.

## B. Interpretation of data.

The average settlement of a uniformly loaded, square area on the surface of a semi-infinite, elastic and isotropic mass due to the elastic deformation of the mass is expressed by the following equation: 1)

$$S = 0.95 (1 - \mu^2) \cdot \frac{P}{E} \cdot b \quad (1)$$

wherein

$\mu$  = Poisson's ratio  
 $P$  = intensity of pressure  
 $E$  = modulus of elasticity  
 $b$  = width of loaded area

The axial deformation,  $S$ , of an unconfined compression test specimen of elastic material is expressed by the following equation:

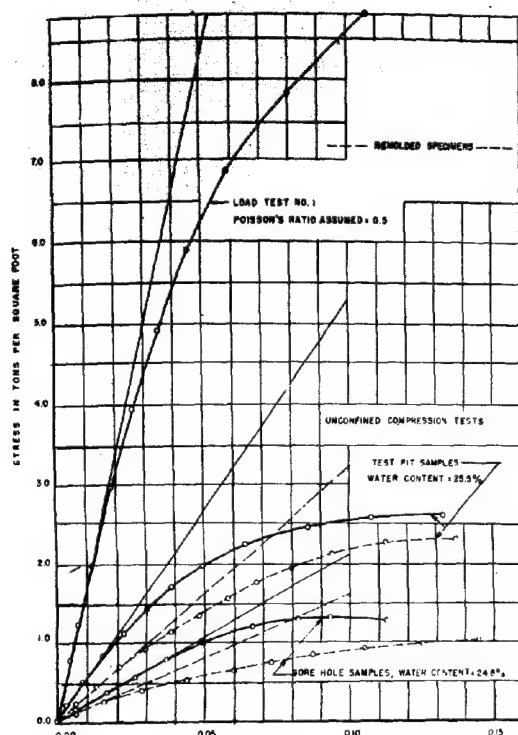
$$S = L \cdot \frac{P}{E} \quad (2)$$

wherein

$L$  = the length of the specimen.

Comparing equations (1) and (2), it is seen that the settlement obtained by applying a load of uniform intensity to a square area on the surface of a semi-infinite elastic mass is equal to axial deformation of a prismatic specimen of the same material subjected to the same intensity of load having a height equivalent to  $0.95 (1 - \mu^2) b$ . For Poisson's ratio equal to 0 this equivalent height is equal to  $0.95 b$ , and for Poisson's ratio equal to 0.5, the equivalent height is equal to  $0.71 b$ . If it can be assumed that the mass, which is loaded, is elastic and homogeneous to a depth equal to at least 1-1/2 times the width of the loaded area, it is possible to obtain a reasonable estimate of the equivalent strain from surface load test data by utilizing equation (2) and substituting for  $h$  its equivalent value, i.e.,  $0.95 b$  to  $0.71 b$ , depending upon the value assigned to Poisson's ratio.

The procedure as outlined above was followed in evaluating the load test data. The stress-strain curve for load test No. 1, for an assumed value of Poisson's ratio equal to 0.5, is shown in Fig. 1 by the curve design-



Stress- strain curves

FIG. 1

nated "Load Test No. 1". The modulus of elasticity  $x$ ) for the limiting values of Poisson's ratio and corresponding to the slope of the initial position of the stress-strain curves for both tests are shown in Table I.

The moduli of elasticity as determined from the unconfined compression tests prepared from the hand-cut test pit samples are summarized in Table 2 and the stress-strain curve obtained from test No. 3, which is typical, is shown in Figure 1.

The data obtained from the specimens prepared from the bore-hole samples are tabulated in Table 3 and the stress-strain curve obtained from test No. 2, which is typical, is also shown in Fig. 1.

The data tabulated in Tables 1, 2, and 3 and the typical curves shown in Fig. 1 indicate the effects on the stress-strain characteristics of a soil that are due to sample disturbance. By comparing the moduli of elasticity obtained from the so-called "undisturbed" bore-hole samples with those obtained from the remoulded specimens of the test pit samples-

$x$ ) The term "modulus of elasticity" is used herein to describe the resistance that a material offers to deformation. It is specifically defined as the slope of the linear portion of the stress-strain curve. The term "modulus of deformation" would be more appropriate to describe this property of a material but the term "modulus of elasticity" is retained because of its general acceptance in other fields of civil engineering.

TABLE I

Moduli of Elasticity Obtained from Loading Tests

Test Number	Poisson's Ratio = 0	Poisson's Ratio = 0.5
1	220 tons per square foot	165 tons per square foot
2	240 tons per square foot	180 tons per square foot
Average	230 tons per square foot	173 tons per square foot

TABLE II

Moduli of Elasticity Obtained from Unconfined Compression Tests of Specimens Prepared from Test Pit Samples

Test Number	Area of Specimen sq. in.	"Undisturbed" Specimen tons per sq. ft.	Remoulded Specimen tons per sq. ft.
1	1.64	58	---
2	1.67	58	23
3	6.20	53	25
4	6.16	84	17
5	1.73	51	---
6	2.34	58	30
7	1.27	85	---
8	1.35	53	---
Average		63	26

TABLE III

Moduli of Elasticity Obtained from Unconfined Compression Tests of Specimens Prepared from Bore-Hole Samples

Test Number	Area of Specimen sq. in.	"Undisturbed" Specimen tons per sq. ft.
1	6.00	12
2	2.62	21
3	2.82	18
Average		17

les it is evident that the bore-hole method of sampling completely disturbed the samples. It is to be noted that the limiting values of the moduli of elasticity obtained from the field loading tests are equal to 3 to 4 times the average of the modulus of elasticity obtained from the test pit samples and 10 to 14 times that obtained from the bore-hole samples. Thus, the elastic deformations of such a mass as computed from the modulus of elasticity obtained from unconfined compression tests would not be even approximately correct.

## II. COMPARISON OF CONSOLIDATION DATA FROM SAMPLES OBTAINED BY THREE DIFFERENT SAMPLING TECHNIQUES.

### A. Description of Methods of Obtaining Samples.

In 1936, 1938, and 1941, samples of Boston Blue Clay were obtained by "undisturbed" sampling methods at three different locations within the Boston Basin. The geologic profile is essentially the same at all locations. The methods of sampling, however, were in each case different due to improvements that were made in sampling techniques during this period.

In 1936, the samples were obtained by a soil sampler designed by Casagrande, Mohr, and Rutledge 2). This sampler had a core barrel 2 feet in length, an internal diameter of 4.76 inches, and an area ratio ratio  $x_a$  of 44 percent. A sample was obtained by ramming this sampler a distance of 2 feet into a cased bore-hole. Due to the large area ratio of this sampler and the method of advancing it, the samples suffered considerable disturbance.

In 1938, a new type of sampler developed by H.A. Mohr  $x_b$ ) was used. This sampler had an over-all length of 9 ft. 2 in. that provided space for five one-foot removable liner sections approximately 4 inches in diameter and a two-foot section on top of the liner sections to serve as a reservoir for cuttings and shavings. The cutting edge section of this sampler was provided with four flap valves that prevented loss of the sample during the withdrawal operation. The area ratio of this sampler was the same as that used in 1936. To minimize disturbance, this sampler was ad-

$x_a$ ) The area ratio is defined as the ratio of the cross-sectional area of a sampler at its largest section minus the area of the opening through which the sample enters to the area of the opening through which the sample enters. It is thus a measure of the amount of soil that must be displaced by the walls of the sampler. Thus the smaller the area ratio the less is the disturbance to the sample.

$x_b$ ) loc. cit. Ref. 2, p.56.

vanced slowly in a cased bore-hole by jacking with levers.

In the latest sampling operations, a Shelby Tube of sampler  $x_c$ ) developed by H.A. Mohr was used. Tubes 3 inches in diameter, 18 gage wall thickness and from 3-1/4 to 5 feet in length were used. The ends of these tubes were sharpened and turned in slightly so as to provide a small inside clearance. The area ratio was equal to 8 to 9 percent. A sample was obtained by advancing the tube in a quick, continuous motion by a block and tackle system reacting against the casing. Laboratory inspection of these samples indicated that they were less disturbed than those obtained by the two methods described previously.

### B. Interpretation of Data.

Eleven consolidation tests were performed on specimens prepared from the 1936 samples, 33 from those obtained in 1938 and 24 from those obtained in 1941. The original water content, the original void ratio,  $e_0$ , and the compression index,  $C_c$ ,  $x_d$ ) of each sample was determined from these tests.

The relation between the original (natural) water content and the physical constants, which describe the consolidation characteristics of a soil, as expressed by the ratio

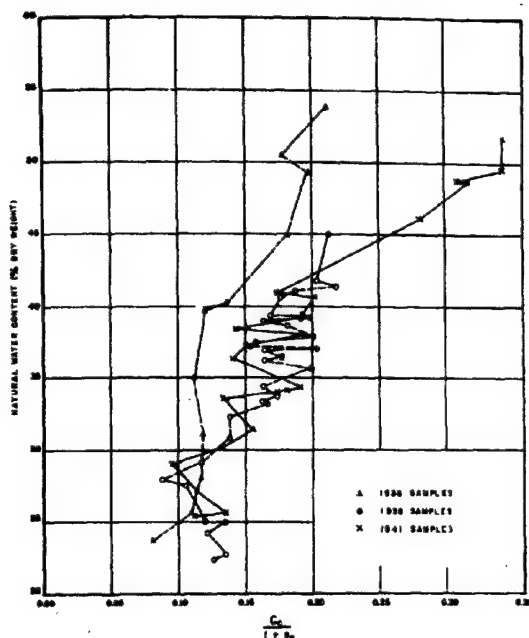
$C_c/(1 + e_0)$ , is shown in Fig. 2. Each point in this figure represents the data obtained from one consolidation test. Three different symbols are used to distinguish the data obtained from the three different series of samples. The symbols in each case are connected by straight lines to differentiate the data more clearly.

The broken line representing the data obtained from the 1936 samples, which were considerably more disturbed than those obtained in 1938 and 1941, shows the smallest change in the ratio  $C_c/(1 + e_0)$  with respect to the natural water content. Rutledge 3) found that the compression index obtained from remolded specimens (completely disturbed) is smaller than that obtained from an undisturbed specimen of the same soil. It is also known that, in general, the higher the natural water content of a clay, the greater will be the difference between the consistency when undisturbed as compared to the consistency when remolded. It is not surprising therefore, that the effects of disturbance to the samples, suggested by the difference in the values of  $C_c/(1 + e_0)$  for a

$x_c$ ) loc. cit. Ref. 2, p.44.

$x_d$ ) The compression index is defined as the slope of the linear portion of the void ratio vs. log of pressure curve:

$$C_c = \frac{e_1 - e_2}{\log P_2 - \log P_1}$$



Relation between natural water content and  $\frac{C_c}{1+e_0}$   
FIG. 2

given water content increases as the natural water content increases.

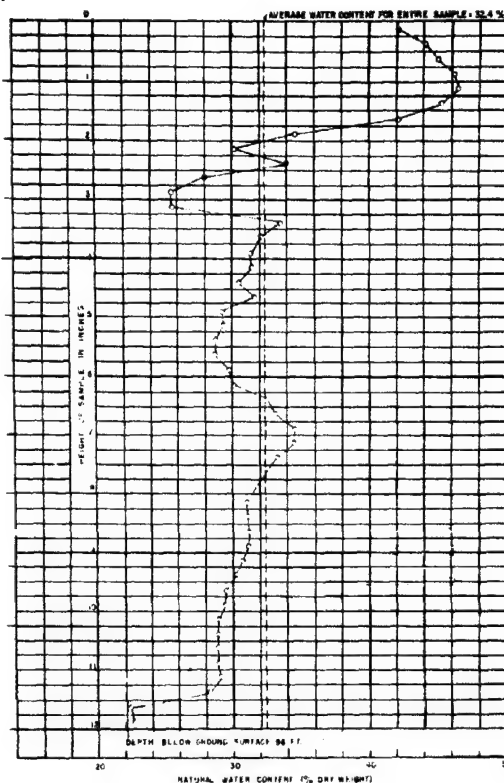
It can be seen from Fig. 2 that the range in values of  $C_c/(1+e_0)$  obtained from samples having approximately the same water content is such that the ratio of the value of  $C_c/(1+e_0)$  for the least disturbed sample to that of the most disturbed sample is in no case greater than 2 to 1.

It is to be noted, therefore, that the effects of disturbance on the consolidation characteristics of a clay, as expressed by the ratio  $C_c/(1+e_0)$ , are small as compared with the effects of disturbance on the stress-strain properties. It is also to be noted that the extreme range in values of the ratio  $C_c/(1+e_0)$  obtained from these samples of inorganic clay subjected to varying degrees of disturbance and having natural water contents ranging from 22 percent to 54 percent is approximately 0.10 to 0.35.

### III. VARIATIONS IN NATURAL WATER CONTENT IN A CLAY DEPOSIT.

A detailed examination of the variations in natural water content in a clay deposit was made from bore-hole samples obtained at the site of the New England Mutual Life Insurance Company Building. The samples were obtained by means of a Shelby Tube type of sampler, 3-1/2 inches in diameter and 4 to 5 feet in length. The sampler was driven by means of a 140 lb. weight falling 30 inches. Samples were taken as continuously as possible.

Water content determinations were made of each 1/2 inch length of these samples as soon as they were received in the laboratory. Typical variations in water content within a 12-inch length of sample are shown in Fig. 3. A summary of all tests made in this manner, approximately



Variations in natural water contents  
FIG. 3

1,400, is shown in Fig. 4. The maximum and minimum water contents found in each 12-inch length of sample are shown by the extremities of the horizontal lines in this figure. The average water content for each section is represented by a small circle.

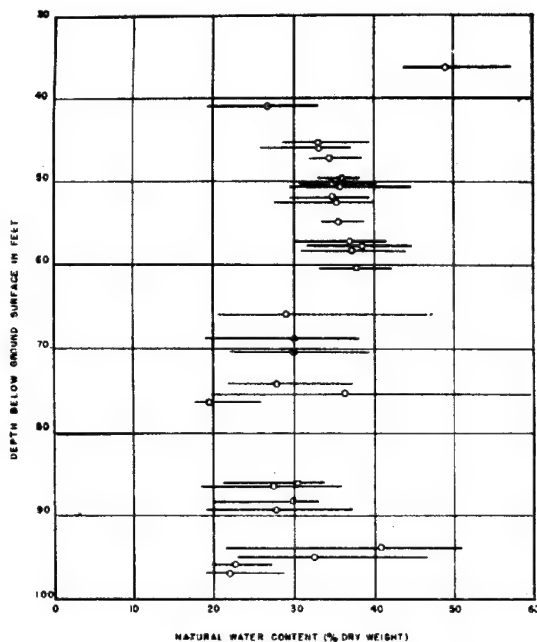
This detailed examination showed extreme variations in natural water contents of from 19.8 percent to 59.5 percent within a single 12-inch length of sample. The average water content obtained from each 12-inch length of sample ranged from 19.4 percent to 49.0 percent and the aggregate average of all samples tested was approximately 37 percent.

Many of the samples tested appeared homogeneous and uniform in their undisturbed condition. Yet, the variations in water content in some of these samples were found to be surprisingly great.

Since many of the physical properties of clays are related to the natural water content, it is evident that extreme care must be exercised in evaluating the overall performance characteristics of a given clay deposit.

### IV. SUMMARY AND CONCLUSIONS.

1. From a comparative study of the results of field loading tests and unconfined compression tests of specimens prepared from test pit and bore-hole samples of a hard, yellow, inorganic clay stratum similar to that subjected to the field loading tests, it was found that the modulus of elasticity determined from the field loading tests was equal to from 3 to 4 times that obtained from the test pit



Variations in natural water content. Extremities of each horizontal line represent maximum and minimum water contents in a 12 inch length of sample. O represents average of 48 water content determinations for each 12 inch length of sample.

FIG. 4

samples and 10 to 14 times that obtained from the bore-hole samples. It is evident, therefore, that the stress-strain characteristics of clay-like soils are extremely sensitive to disturbance. Since some disturbance is inevitable in the operations of sampling and in the preparation of test specimens for unconfined compression tests, the elastic deformation of a mass of such soil computed from the moduli of elasticity obtained from such tests will not be even approximately correct.

2. A comparison of the results of 68 consolidation tests performed on specimens prepared from samples of inorganic clay that were obtained by three different sampling techniques, in which the three series of samples were subjected to different degrees of disturbance, showed:

- that the consolidation characteristics of clays of high natural water content are more sensitive to the effects of disturbance than are those of low natural water content.
- that the range in values of the consolidation characteristics as expressed by the ratio  $C_c/(1 + e_0)$  obtained from bore-hole samples having approximately the same water content is such that the ratio of the value of  $C_c/(1 + e_0)$  for the least disturbed sample to that of the most disturbed sample is in no case greater than 2 to 1. Therefore, the effects of disturbance on the consolidation characteristics as expressed by the ratio  $C_c/(1 + e_0)$ , are small as compared with the effects of disturbance on the stress-strain properties, and
- that the extreme range in values of the ratio  $C_c/(1 + e_0)$  obtained from these samples, which were subjected to varying degrees of disturbance and which had natural water contents ranging from 22 percent to 54 percent, is approximately 0.10 to 0.35.

- A detailed investigation of the variations in natural water content of a clay deposit, approximately 60 feet in thickness, showed:
  - extreme variations of from 19.8 percent to 59.5 percent within a single 12-inch length of sample.
  - variations in the average water content obtained from each 12-inch length of sample ranging from 19.4 percent to 49.0 percent, and
  - no consistent variation with depth.

It was observed, furthermore, that even those clay samples that appeared homogeneous had large variations in water content. Therefore, it is imperative that extreme care be exercised in evaluating the over-all performance characteristics of a given clay deposit by means of laboratory test data.

#### REFERENCES.

- "Über die Berechnung der Fundamentdeformation," by F. Vogt, Avhandling utgitt av Det Norske Videnskaps...Academi 1, Oslo, 1, Math. naturv. Klasse 1925, No. 2, Oslo, pp. 9 and 10.
- "The Present Status of the Art of Obtaining Undisturbed Samples of Soil," Report by M.J. Hvorslev, to the Committee of Sampling and Testing, Soil Mechanics and Foundations Division, American Society of Civil Engineering, March 1940, p. 50.
- "Compression Characteristics of Clays and Application to Settlement Analysis", Thesis, Graduate School of Engineering, Harvard University, April, 1938.



W. KJELLMAN and T. KALLSTENIUS  
The Royal Swedish Geotechnical Institute

INTRODUCTION.

When investigating ground conditions, it would be useful to be able to extract long continuous cores of soil with undisturbed structure. If however, for this purpose an ordinary tube is driven down into the soil, it appears that the tube owing to friction and adhesion on its inside to a certain extent drags the core, thus formed, with it downwards. This means that part of the soil mass immediately beneath the mouth of the tube is diverted instead of caught by the mouth. This tendency is stronger, the softer the soil beneath the mouth is and the harder and longer the core already formed. Consequently, the natural soil layers will appear in the core with a thickness, which is reduced to an unknown degree, and with a structure, which is disturbed to an unknown extent. On the whole, in most soils only very short cores, i.e. samples, can be obtained in this way.

In order to reduce the friction and adhesion between the tube and the core, the tube usually has a small "clearance", i.e. the inner diameter is a little less at the lower end of the tube than in the rest of it; further, as proposed by Hvorslev, the tube is forced down by one single rapid drive. Undisturbed samples of a maximum length (as far as we know) of 1,8 m have thus been taken in cohesive soils. Whether the same measures have any effect in cohesion-less soils, we do not know.

PRINCIPLE OF THE CORE-EXTRACTOR.

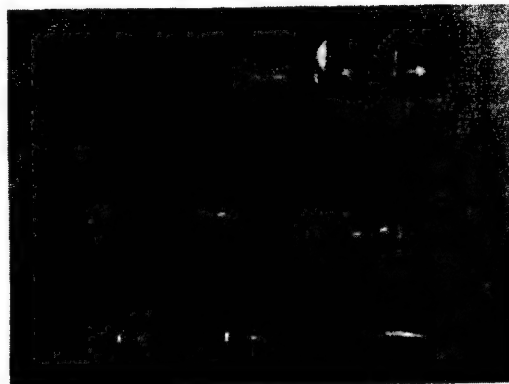
According to the method, described in this paper, the errors and difficulties caused by friction and adhesion between core and tube are eliminated by "insulating" the core from the tube by means of a number of thin axially running metal strips or foils, the upper ends of which are fastened to a piston, which is placed in the tube above the core and by means of a rod is attached to a driving scaffold on the soil surface. During the driving of the tube sliding occurs between the tube and the foils; friction thus produced causes a pulling force in the foils and their anchorage but does not affect the core. If for some reason the core should tend to move downwards or upwards, this movement is immediately prevented by friction and adhesion, which in such case arise between foils and core. Friction and adhesion, which hitherto were the main causes of all troubles, are in this way turned into useful agents, which compel each soil layer to keep its original thickness and structure unchanged on its way into the tube.

The lower part of the extractor is double-walled and serves as a magazine for the foils, being stored in a roll. Within the magazine each foil runs from its roll downwards to a horizontal slot, arranged in the inner wall at the bottom of the magazine. Here the foil runs through the slot and then in between the core and the wall, where it continues upwards to the piston.

DETAILS.

The inner diameter of the core-extractor is approximately 68 mm. Sixteen foils, each 12,5 mm broad, are used, together covering very nearly the whole circumference of the core. The foils are mostly made of soft iron, hard-rolled. Foils made from hardened steel have also been used with good result; these have a higher strength but will rust more easily. Foil thicknesses between 0,10 and 0,04 mm have been tried with good result. The maximum length of foil, that can be stored in each roll in the magazine, varies according to the thickness between 20 and 40 m.

In order to limit the maximum outer diameter of the extractor as much as possible, the foil rolls are placed, as can be seen on fig. 1, in four different stories, the axis



Core-extractor taken to pieces.

FIG. 1

of each roll being radially directed. Each roll is placed in a recess in the thick inner wall (as visible also in fig. 3) and kept in place by a vertical bar. Each foil on its way downwards from the roll to the slot is twisted 90° by means of guide slots, visible in fig. 2. (In fig. 3 the foils are shown only in the rolls.)

Below the magazine the extractor is extended downwards a certain distance, as shown in fig. 3. Here it is single-walled, the wall thickness being as small as advisable with regard to the strength. It ends in a thin and sharp steel cutting edge, kept in place by a threaded ring. By virtue of its shape the edge can easily be very well hardened. It is inexpensive and easily changed.

The outer wall is divided into an upper and a lower part, the former being kept in position by the latter, which is attached to the inner wall by four screws. The part below the magazine is screwed to the outer wall. Thus, by unscrewing the four screws and removing the outer wall, the rolls and foils are easily and quickly made accessible.

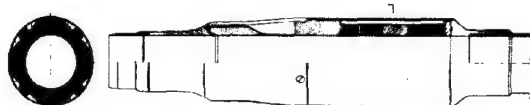
The inner wall is screwed to the single-





Inner wall with foil rolls and twisted foils

FIG. 2



Core-extractor in elevation, longitudinal section and cross section.

FIG. 3

walled tube above the magazine. This tube consists of 2,5 m long sections, connected by coupling-boxes, which are so made, that they can be removed by dividing longitudinally. Thus the sections of the tube can be taken apart without being turned in relation to each other.

The piston is seen on the left of fig. 1. The upper ends of the foils are wedged securely to it by means of a conical ring, visible halfway up on the piston. On its upper end the piston is provided with such arrangements, that it can be fixed in its lowest position relative to the extractor. In this position the lower end of the piston covers the lower mouth of the extractor, as seen in fig. 4, so that if desired the extractor can be driven down into the ground without producing any core. When the depth has been reached, where core-extraction is to begin, the rod, provided with a special catch, is lowered in the tube until it engages the head on top of the piston, visible in fig. 1 and 4. The piston is thereby released from the extractor and attached to the rod, which is then clamped to the driving scaffold, the lower mouth of the extractor being thus freed to admit the core.

A provisional driving scaffold, used so far, is seen in fig. 5. The driving force is produced by two chain-jacks, and the reaction force is taken by four screw-shaped soil anchors. (When the photo was taken, a thin chain was used instead of a rod for anchoring the piston to the scaffold.) A much better type of driving scaffold, mounted on a cart, is under construction.

#### STRESSES IN THE CORE.

If a tube without foils is driven down into clay, downward directed shear stresses are transmitted by adhesion from the tube to the core. These stresses increase the vertic



Core-extractor assembled.

FIG. 4



Driving scaffold.

FIG. 5

al normal stress in the core, so that at any given depth it will be greater than the stress outside the tube (at some distance from it). This difference increases with the driving depth, until no more soil can enter the tube.

By introducing the foils the core is protected from shear stresses, so that its stresses are reduced to equal those outside the tube. Because of the horizontal pressure from the clay on the foils, friction arises between the foils and the tube, causing a pulling force in the foils. As long as the depth is moderate, the foils can withstand this pulling force, but if very great depths are reached, the foils may break. (Probably the friction between the foils and the tube is reduced to some extent by remolded clay, coming from the core, but on the other hand some adhesion may appear.)

In order to reduce the pulling force in the foils a clearance is arranged in the core-extractor, amounting to a few thousandths of its diameter, i.e. essentially less than re-

commended by Hvorslev. In order to secure contact and adhesion between the core and the foils, the clearance begins only at a certain distance above the slot in the inner wall.

The clearance can reduce the horizontal pressure in the core considerably, only if the core adheres to the foils, so that the vertical pressure decreases. If the adhesion between the core and the foils exceeds  $0,003 \text{ kg/cm}^2$ , as it usually does, the entire weight of the core can hang on the foils, so that all stresses in the core become extremely small. In this borderline case there is no friction between the foils and the tube, and the foils need sustain the weight of the core only.

The pressure in the core must decrease from a certain value in the lower mouth of the extractor to a smaller value in the section, where the clearance begins. This decrease is effectuated mainly by adhesion and friction on the core between said sections. A length of this pressure-decreasing part of 2-4 times the inner diameter should do in clay, according to our experience so far.

When extracting cores from sand ground, the influence of the foils and of the clearance upon the stresses in the core is still more pronounced than described above.

Without foils the increase of the normal stresses in the core, caused by the friction from the tube, leads in its turn to an increase of the friction. This phenomenon is the reverse of the silo-effect and can be calculated in a corresponding way. It appears, that the stresses in the core increase enormously with the depth so that only very short cores, or rather samples, can be taken.

By introducing the foils the downward directed friction on the core is eliminated. Consequently the reversed silo-effect vanishes, so that the stresses inside the tube are reduced to the same values as outside it.

When in addition clearance is introduced, upward directed friction arises on the core. Thus the ordinary silo-effect comes into play reducing all stresses in the core to very low values.

#### DISCUSSION.

The rather considerable wall thickness of the core-extractor in cross section through the magazine may seem open to objection. However, according to our experience so far the distance from the magazine to the cutting edge is great enough to prevent the magazine from affecting the soil below the edge. The distance can easily be made still longer, if need be. Another model of the core-extractor, seen in fig. 6, is of extremely slender shape,



Special core-extractor for soft soil and small depth.

FIG. 6

and the foils are extended almost to the cutting edge. This model was made for softer ground and smaller depth than the robust model described above.

During the last two years a great number of cores have been taken by the core-extractor

in all kinds of soils varying from fat clay to coarse sand. Practically all cores seemed to be quite undisturbed. It may be mentioned, that the core-extractor is used now in Geochronology, which deals with counting and measuring the thin layers of the varved clay in such an accurate way, that up to now no sampler but only open shafts could be used.

The longest core so far was slightly above 20 m. Fig. 7 shows a core, 10 m long,



Core of clay 10 m long.

FIG. 7

resting in a wooden groove. Every core longer than 5 m is divided, when being lifted out of the ground, into sections of 5 m (or 2,5 m if desired) by removing the coupling-boxes and cutting the foils and the core. Such cores as are to be sent to the laboratory, are furnished with a cap and a seal on each end of the tube. The core is taken out of the tube by pulling the foils at one end of the tube. After it has been examined, recorded, photographed etc, representative samples for laboratory tests are cut out of its different layers.

Obviously a continuous core as described in this paper, gives a much better conception of the ground than any number of samples. Extracting one core, reaching from the soil surface to a given depth, needs less time and less work than taking one sample at each two metres down to the same depth. Even if sometimes one does not wish to take continuous cores from the surface to the firm ground, it may be of great help to be able to take cores of say 5 m length in order to be sure of obtaining samples of certain layers which are of special interest.

In very hard soils, where the driving of the core-extractor is difficult, a casing may be used and the soil, entering the interspace between the extractor and the casing, removed by jetting or otherwise. Hitherto ramming has been used in hard soils; the extractor and the foils have proved resistant to this hard treatment, and the cores have shown no sign of disturbance.

A core-catcher can easily be arranged in combination with the magazine. So far it was not found necessary.

#### SUMMARY.

The report deals with a quite new type of soil investigation device, called core-ex-

tractor. This device makes it possible to take very long continuous and undisturbed cores from any soil finer than gravel and not too hard. The extractor is described in principle and in detail. The stress system in the core during the driving of the extractor is analysed. Experience of the device, gained so far, is discussed.

-O-O-O-C-O-O-

## SUB-SECTION III b

### MEASUREMENTS OF SPECIAL SOIL PROPERTIES

#### III b 1

#### PERMEABILITY OF PEAT BY WATER

IR. J.L.A. CUPERUS  
Netherland Railways

Obtaining a better insight into the behaviour of soft peat, when a load of sand is brought to bear into it, by previously determining the permeability of the peat by water with a suitable apparatus.

When in tract of land, consisting of soft peat, a road or a dike is constructed or - with some other end in view - a load of sand is brought to bear, the water in the peat comes under pressure and under this pressure the water is driven out into and outside the marginal region of the load.

When in 1938 an experimental section was executed in behalf of the strengthening of the railway between Utrecht and Rotterdam near Gouda, it has been found, that disturbance of equilibrium occurs at a certain excess water pressure in that marginal region, in consequence of which extensive slidings of earth have taken place.

In the above-mentioned case (I) the condition was as indicated in fig. 1.

At that place the railway was situated in a tract of very soft peat and it had to be strengthened because of inadmissible subsidences. 1)

The existing ditches beside the track were dredged out to 2.50 m beneath the level of the ground water. Subsequently sand was dumped into the ditches and after these had been completely filled up to the level of the surrounding area, they were heightened still

further. When the heightening had reached about 2 m above the level of the ground water, a sliding took place (vide fig. 2).

At the commencement of this disturbance of equilibrium the excess pressure of the water in the pores in the marginal region of the load (point A) corresponded to a water pressure of about 1.50 m. 2)

During the further execution of the strengthening of the road-bed about 8 km east of the above-mentioned experimental section in a similar tract of land near Oudewater, (case II) an effort was also made to press away the soft layers of peat under the dumped sand, however, without any success. Even when heightening up to 3.50 m above the ground water no disturbance of equilibrium took place.

For the difference in behaviour three causes may be indicated:

- 1) Difference of thickness of the layer of peat.
- 2) Difference in the proportion of resistance of the peat.
- 3) Difference in the permeability of the peat by water.

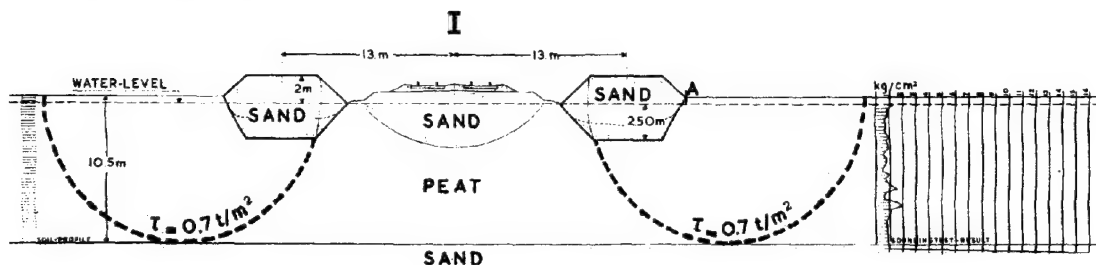


FIG. 1

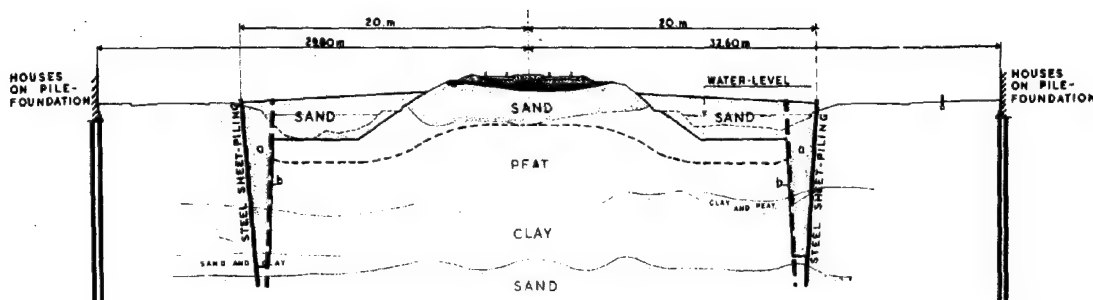


FIG. 2



FIG. 2 a

### 1. DIFFERENCE IN THICKNESS OF THE LAYER OF PEAT.

In case II the firm soil under the layer of peat lay considerably higher than in case I. One might imagine that this was the cause in consequence of which the disturbance of equilibrium failed to occur in case II.

The equilibrium computation executed in both cases, however, showed that in case I as well as in case II, despite the difference in situation of the planes of sliding a resistance against sliding of 0.7 ton/sq.m was necessary to retain equilibrium (fig. 1 and fig. 3).

3) , it appeared, that in both tracts the peat had to be considered equivalent in appearance and properties of resistance, so that this cause also failed to explain the difference in behaviour.

### 3. DIFFERENCE IN PERMEABILITY OF THE PEAT BY WATER.

As the difference in behaviour, when applying entirely equal methods of execution, could not be explained from what was described under 1 and 2, a third possibility was considered, viz. that in case I the pressing away of water took place with a lower velocity than in case II.

In the first case the excess pressure in the water of the pores might soon have reached the critical height (1.50 m) by insufficient flowing out, and disturbance of equilibrium might have occurred, which actually did happen.

In the second case flowing out of water under excess pressure might already have taken place to some extent immediately after the load had been brought to bear. The solid phase might have been more speedily adapted to the load and the resistance against sliding of the soil might have been increased sooner, simultaneously with compression of the soil.

In order to ascertain this the permeability by water of the peat was examined in both places.

This might have happened by taking undisturbed samples and by determining the permeability by water in a laboratory, but in that case one would have had to restrict oneself to a few points because of the expense.

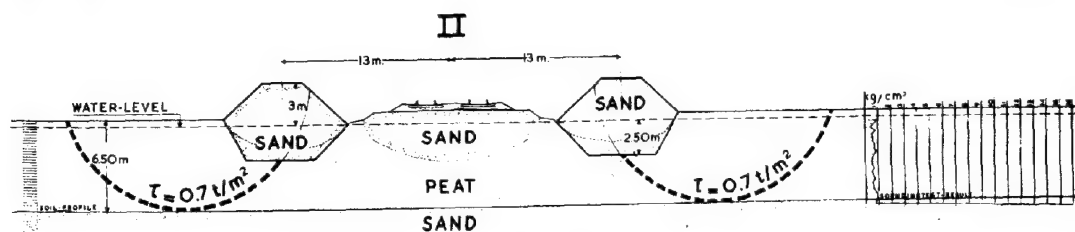


FIG. 3

### 2. DIFFERENCE IN THE PROPERTIES OF RESISTANCE OF THE PEAT.

From the borings as well as from the sounding tests with the Barentsen apparatus

That is why an apparatus was constructed with which the permeability by water of the soil might be determined in the field in a simple and swift manner. The values found with it were relatively applicable.

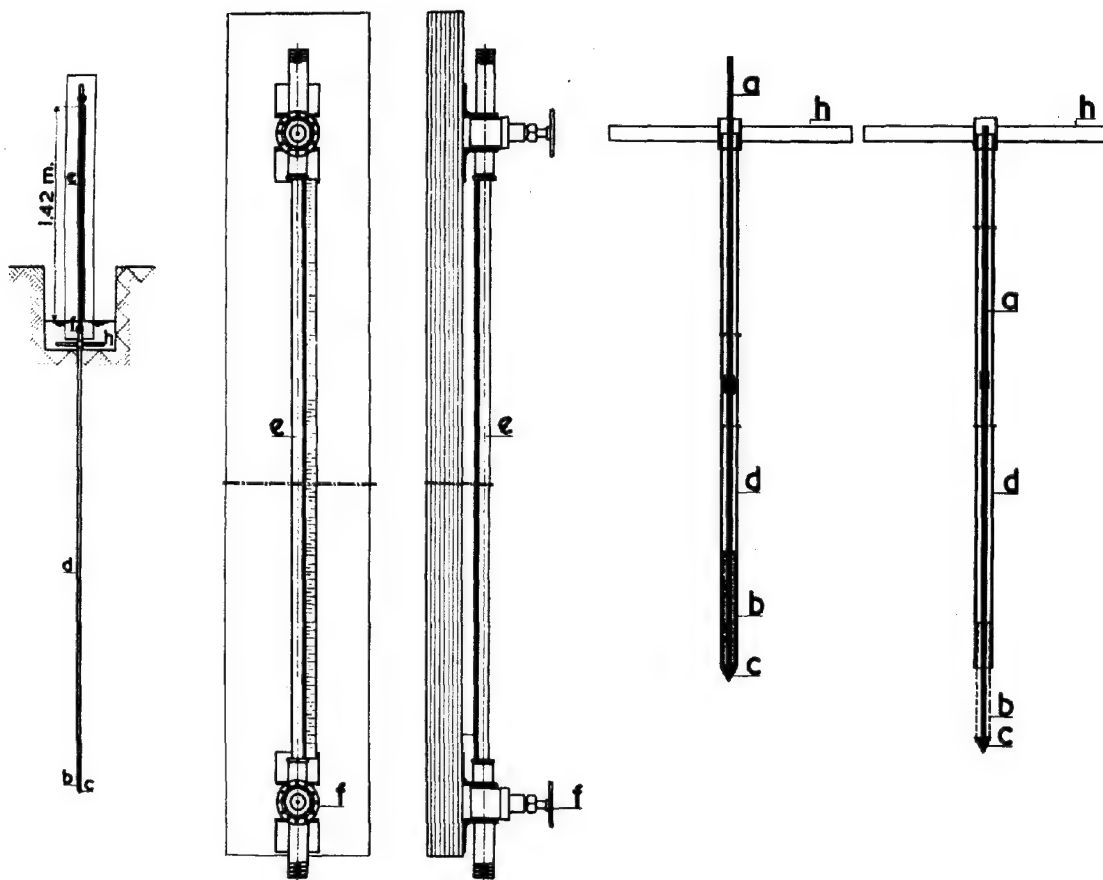


FIG. 4



FIG. 4 a

Description of the apparatus (vide fig. 4 and 4 a).

A steel rod (a) provided with a filter (b) at the bottom and ending in a conus (c) is protected by a mantle tube (d). The rod projects 10 cm above the mantle tube. The whole apparatus is pushed into the soil with

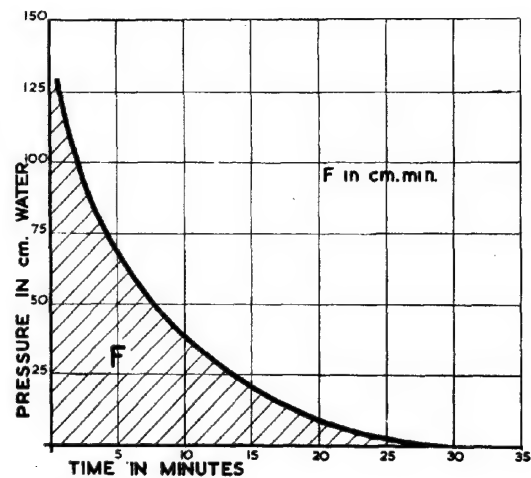
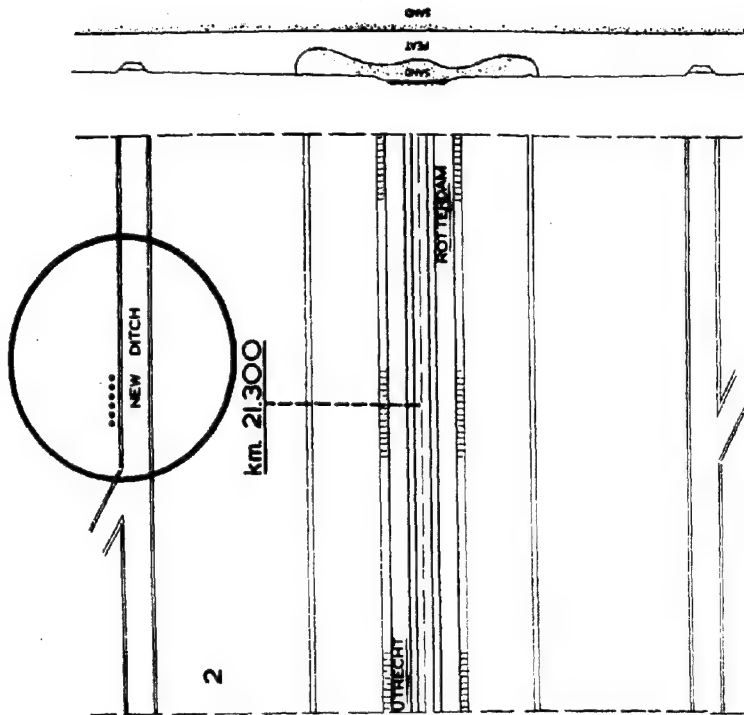
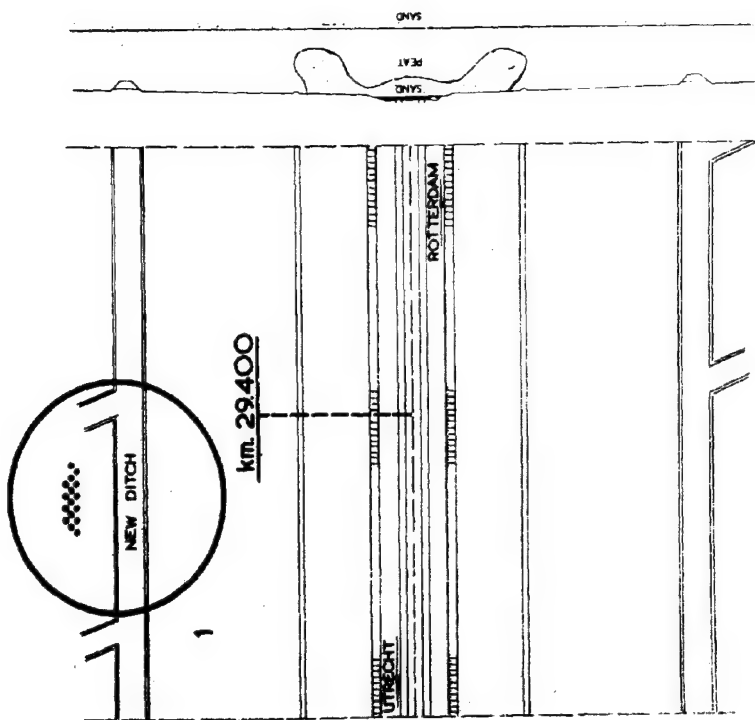


FIG. 5

a handle (h) and filled with water. When the filter has reached the desired depth the rod (a) is pushed down 10 cm and so the filter comes into direct contact with the soil. On



CASE I I



CASE I

FIG. 6

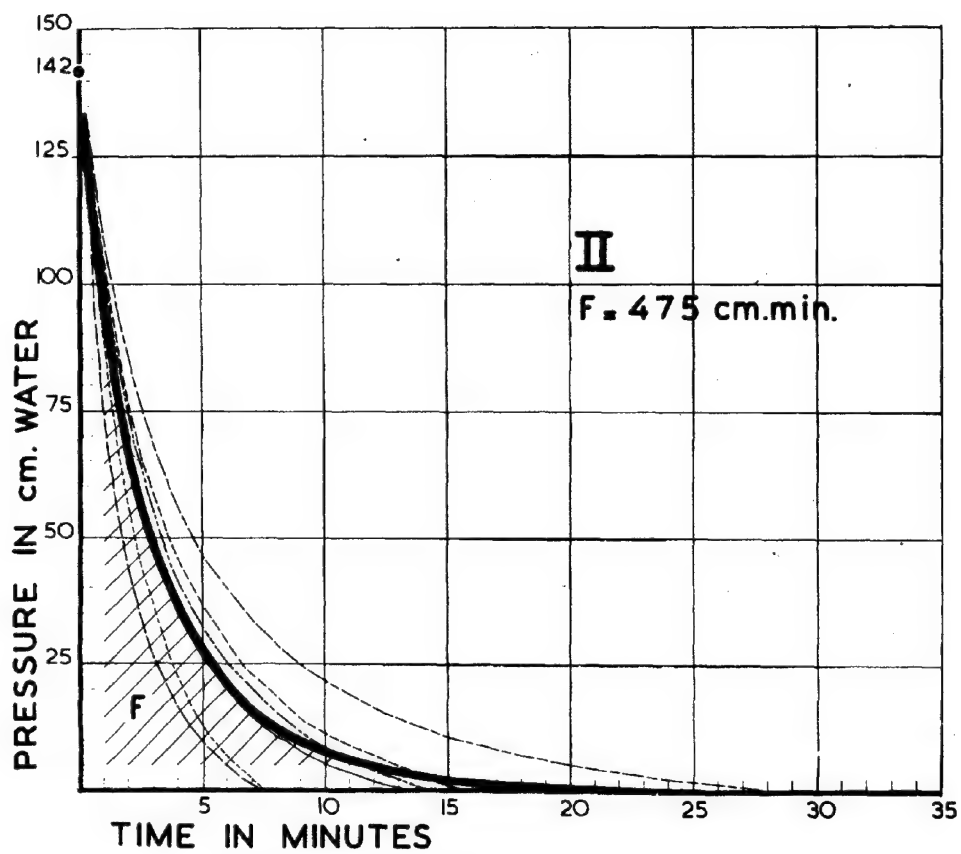


FIG.7 a

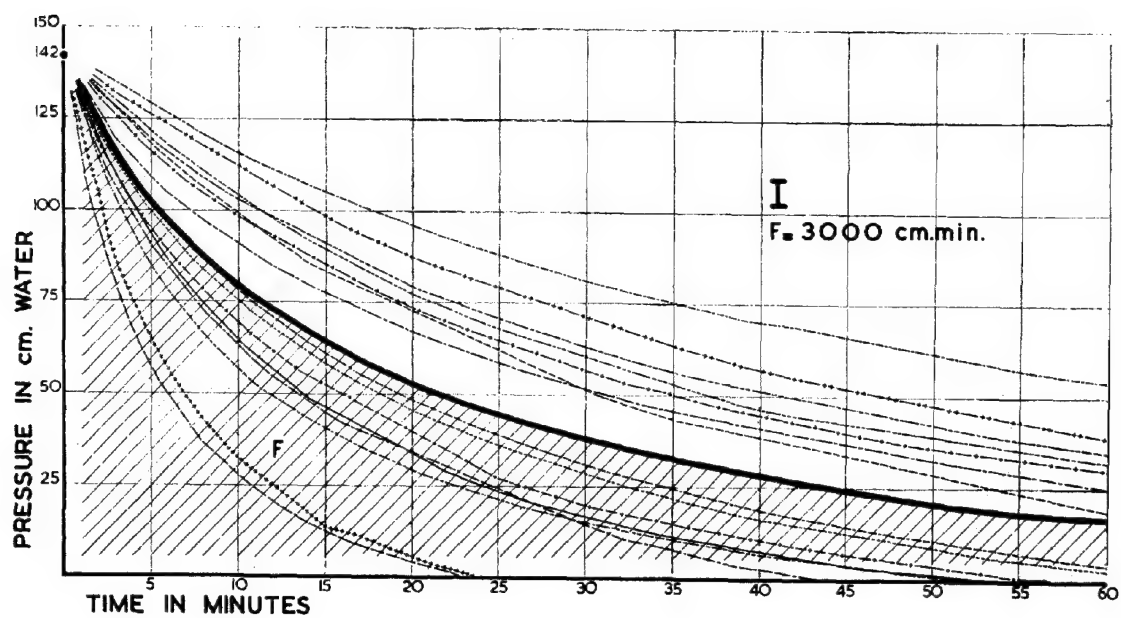


FIG.7 b



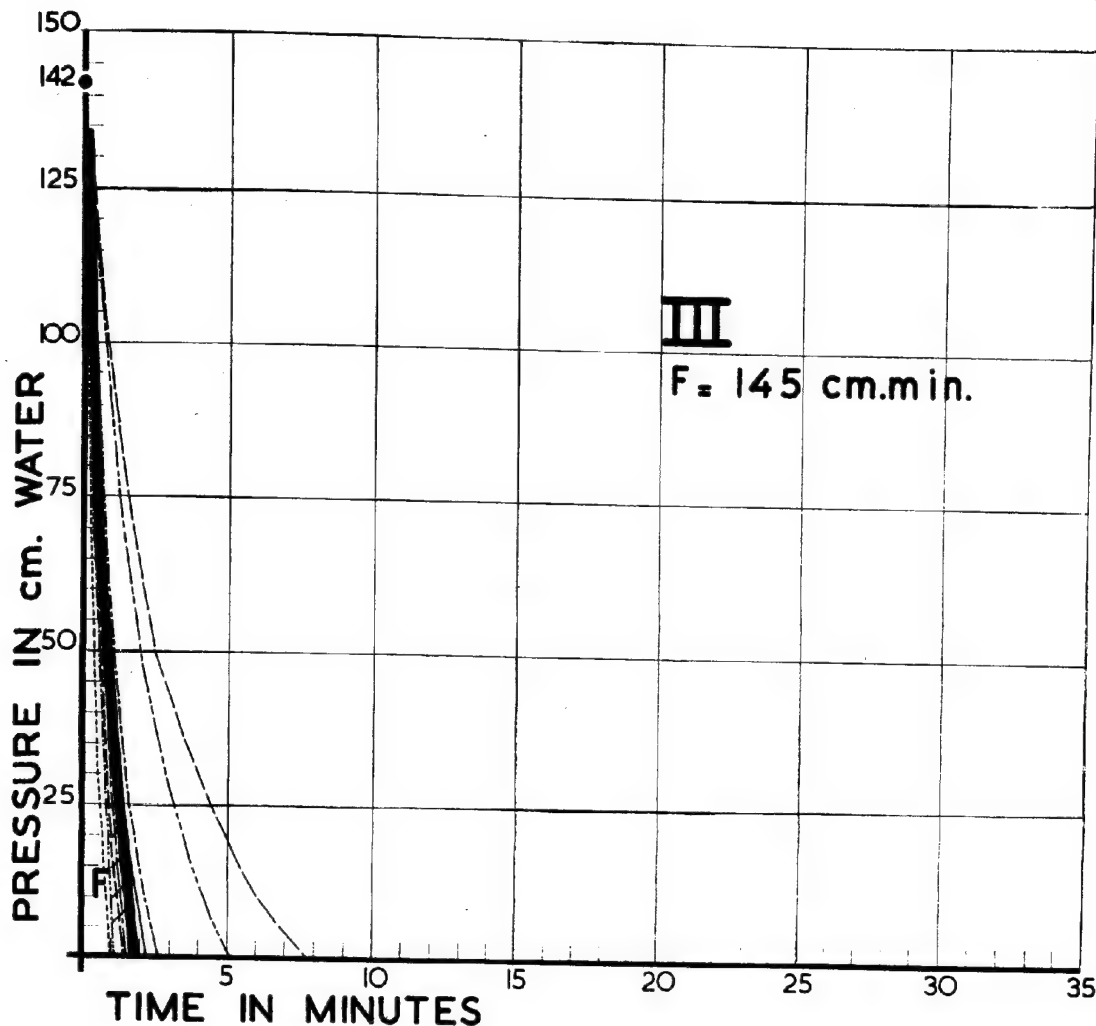


FIG. 8

the mantle tube, the top of which is placed at an equal level with the surface of the ground water, a glass tube (e) is attached by means of a cock coupling (f). The glass tube is open at the top. While the cock (f) is closed the glass tube now is filled up to a height of 1.42 m above the surface of the ground water. Behind the glass tube a scale has been fitted.

Now the cock (f) is opened and the reading of time is taken with a chronometer. Every minute the level of the column of water is read till the glass tube is empty and the observations which have been found are noted in a graph (vide fig. 5). As the relative value for the permeability by water, the superficies is taken of the figure enclosed by curve and axes, and expressed in the dimension cm.min.

At the aforesaid points of the railway, i.e. near km 29.400 (Gouda) case I and km 21.300 (Oudewater) case II (fig. 6) a number of measurements were carried out with this apparatus a little outside the newly dug ditch. All the measurements were carried out twice at the same places. Apart from a single ex-

ception the duplicates gave practically the same results as the first measurements. In the graphs of fig. 7 a and b the average values between first and second readings have been drawn with different types of lines. Moreover the total average value of all first and second readings has been indicated in the graph by a heavy line.

Near km 29.400 (I) 16 measurements and near km 21.300 (II) 6 measurements were carried out.

The reason for the great number of measurements near km 29.400 was to be found in the fact that the investigation at that place showed a considerable spreading of results. The presence of remains of wood and of vegetable fibre in the immediate neighbourhood of the filter will probably have strongly influenced the local permeability of the peat by water. Therefore it is imperative to choose a greater or smaller number of measurements, dependent on the local constitution of the soil, in order to obtain a reliable average value.

As a matter of fact, when comparing the results of the measurements I and II, it ap-

peared that there was a considerable difference between the average values  $F_I = 3000$  cm min and  $F_{II} = 475$  cm.min, that is to say that there was an important difference in the permeability by water of the two samples of peat.

The greater permeability by water of the peat near II will probably have been the cause that the disturbance of equilibrium which had been expected at the outset did not take place.

Further another 10 measurements were carried out near km 31.750 of this railway (III) where strengthening of the road-bed must be executed in the central part of the town of Gouda. 4)

From the values  $F_{III} = 145$  cm.min (fig. 8) found in this case III it appears that the kind of peat in this region has a good permeability, which enables the strengthening of this section of the railway to be very simple and inexpensive.

#### CONCLUSION.

Carrying out measurements of permeab-

ility by water with the apparatus as described above in peat at any place is possible without great expense and will clear the insight into the behaviour which may be expected of the liquid phase and therefore of the soil as a whole, when a load is brought to bear onto it.

As to how far measurements in clay and sand soils may have practical significance should be investigated further.

#### REFERENCES.

- 1) Vide the author's article under section VIII.
- 2) For further particulars concerning the execution of this experimental section near Gouda we refer to the author's publication in "de Ingenieur" of 1947 nos.26 and 27.
- 3) Vide Proceedings of the International Conference on Soil Mechanics 1936 Vol. I page 7).
- 4) Vide the author's article on this subject in section VIII.

-o-o-o-o-o-o-

### III b 2

#### SIMPLE FIELD TESTS FOR SOILS

A.H. GAWITH, M.C.E., A.M.I.E.Aust.

Engineer for Tests, Country Roads Board of Victoria  
Melbourne, Australia

1. Owing to the differences in soils encountered over a length of roadway it is not possible to perform the more elaborate soil tests on all the variations encountered. It is necessary to use those tests which give the greatest return of information for the least expenditure of time and labour in testing. Further, it is desirable that there should be established a system of tests which can be done by relatively unskilled operators, with a minimum of equipment, and which bear a known relation to the more difficult tests.

2. The simple linear shrinkage test has been used and provided that the mould is filled at a definite moisture content, e.g. either the Field Moisture Equivalent or the Liquid Limit, reproducible results are obtainable. The mould can be of any convenient length, e.g. 10 inches or 20 centimetres, and cross

section, and may be formed by splitting a piece of 1 inch internal diameter tube longitudinally and attaching end pieces.

The soil, sieved through a No. 36 B.S. (No. 40 U.S.) sieve is brought to the Liquid Limit by the addition of water, the consistency being checked by the hand liquid limit test, (A.S.T.M. D423-39), but the actual moisture content is not determined. The mould is filled, struck off level, and then allowed to dry in air overnight and then in an oven. The percentage reduction of length of the soil pat is measured. Results of experiments with 282 samples of soils indicate that the test can be used to give an indication of the liquid limit and plasticity index. Regression equations fitted by the method of least squares to the means of arrays of linear shrinkage are shown in Table 1.

TABLE 1

Percentage of all tests in which (a) or (b) occurs	(a) Actual Plasticity Index will exceed	(b) Actual Liquid Limit will exceed
1%	P.I. = $3.08(LS) + 3.6$	L.L. = $30.5 + 3.11(LS)$
5%	P.I. = $2.74(LS) + 2.8$	L.L. = $26.4 + 2.87(LS)$
10%	P.I. = $2.61(LS) + 2.3$	L.L. = $23.9 + 2.81(LS)$
50%	P.I. = $2.34(LS) - 0.49$	L.L. = $15.5 + 2.71(LS)$
90%	P.I. = $2.03(LS) - 2.9$	L.L. = $7.2 + 2.59(LS)$
95%	P.I. = $1.96(LS) - 3.7$	L.L. = $4.7 + 2.54(LS)$
99%	P.I. = $1.58(LS) - 4.3$	L.L. = $0.2 + 2.34(LS)$

3. An analysis was made of the results of tests on 533 samples of soils which had been tested by the Highways and Local Government Department of South Australia. For these samples the linear shrinkage test had been carried out on material passing the No. 7 B.S.

Y = logarithm of California Bearing Ratio  
 $X_1$  = linear shrinkage from the liquid limit on material passing No. 36 B.S. sieve  
 $X_2$  = percentage passing No. 36 B.S. sieve  
 $X_3$  = percentage passing No. 7 B.S. sieve  
 $X_4$  = percentage passing No. 200 B.S. sieve

TABLE II

Regression equation	Correlation Coefficient	Standard error of estimate of Y
1. $Y = 1.99 - 0.042X_1 - 0.0009X_2 + 0.0051X_3 - 0.0016X_4$	0.732	0.241
2. $Y = 2.00 - 0.042X_1 - 0.0074X_2 - 0.0021X_4$	0.732	0.241
3. $Y = 2.06 - 0.046X_1 - 0.0074X_2$	0.724	0.243
4. $Y = 1.44 - 0.052X_1$	-0.656	0.265

(No. 8 U.S.) sieve and California Bearing Ratio tests at 100 per cent of standard A.A.S.H.O. compaction had also been performed.

A correlation coefficient of -0.797 was found between linear shrinkage and the logarithm of the California Bearing Ratio, the regression equation being  $\log. (C.B.R.) = 1.68 - 0.085 (\text{Linear Shrinkage})$  with standard error of estimate 0.25. The results of sieve analyses of these soils were not available.

4. There were available the results of tests on 159 samples of soil on which the California Bearing Ratio test at 95 per cent of Modified A.A.S.H.O. compaction had been performed, as well as linear shrinkage tests on the material passing No. 36 B.S. (No. 40 U.S.) sieve, and sieve analyses on the No. 7, No. 36 and No. 200 B.S. sieves. These results were examined by the method of linear multiple correlation and the regression equations, correlation coefficients and standard errors of estimates are shown in Table 2, where

The percentage passing the No. 36 sieve ( $X_2$ ) had little effect on the estimate and equation 2. was used as the basis of an alignment chart for estimating the California Bearing Ratio.

5. It is realized that the California Bearing Ratio test is not in itself an entirely satisfactory basis for estimating the relations of the simpler tests to the actual stability of the soil. Further, the methods of statistical analysis used have been relatively simple and the work is now being extended to an examination of multiple curvilinear correlations between various tests, particularly with regard to the effect of the proportions of various particle sizes, in which case there is evidence that the relationship is not linear.

6. The objects of this investigation have been,

- a) to obtain information of immediate value in the control of works in the field.
- b) to establish relations between test methods preparatory to carrying out a field examination of pavement thicknesses and their relation to soil, traffic and climate.

-0-0-0-0-0-0-

### III b 3

#### DETERMINATION IN SITU OF THE SHEAR STRENGTH OF UNDISTURBED CLAY

##### BY MEANS OF A ROTATING AUGER

LYMAN CARLSON

The Royal Swedish Geotechnical Institute

#### INTRODUCTION.

The shear strength of clay is usually determined in the laboratory from samples taken from different depths of the ground. In Sweden the investigation is generally carried out by means of unconfined compression test or cone test. Usually the shear strength, thus obtained, increases only slightly with the depth under the surface of the ground. It is often smaller than the "real" strength,

calculated from slides that have occurred in the same soil. This discrepancy may depend partly on disturbance of the sample caused by the sampler, partly on changes in the sample due to decrease of pressure when the sample is extracted. The decrease of pressure is likely to have a considerable effect on the results as pointed out by S. Odenstand. 1)

These errors can never be entirely eliminated when the investigation is carried out on

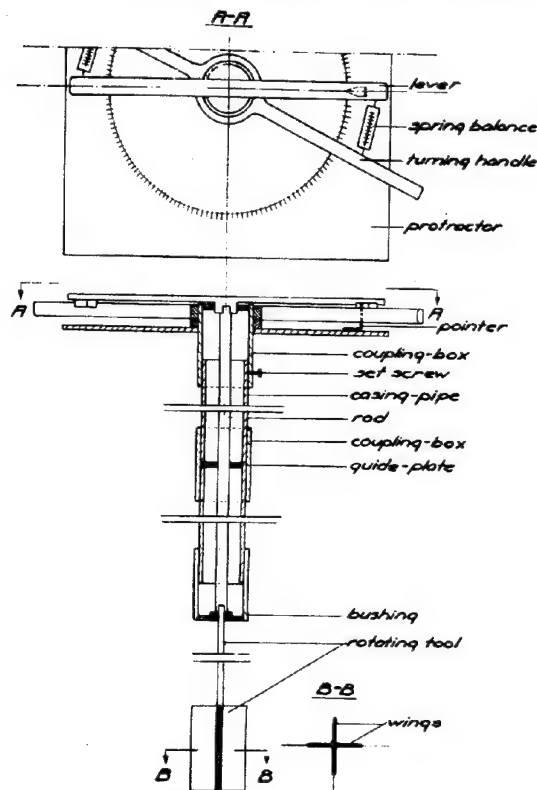
extracted samples. The only possibility of avoiding them, especially the latter one, is to determine the shear strength directly in the ground. Such a method whereby both errors are practically eliminated, is being developed at The Royal Swedish Geotechnical Institute, and is described below. The experiments are still in an early stage, but the method, as now can be judged, seems full of promise.

Similar experiments are said to have been performed in Sweden by professor Carl Forssell and in Germany by Deutsche Forschungsgesellschaft für Bodenmechanik (Degebo). But as far as is known they seem not to have taken due consideration to the sensitivity of the clay to disturbance.

#### THE TESTING APPARATUS AND ITS METHOD OF APPLICATION.

In this early stage of the experiments the apparatus was constructed in a very simple manner. Essentially it consists of parts from the Swedish piston sampler 2) and the Swedish sounding auger. 3)

The apparatus is shown in fig. 1. At its



The testing apparatus.

FIG. 1

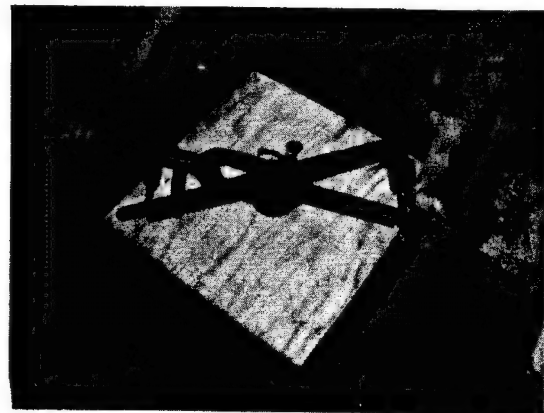
lower end it consists of a rotating tool made up of a steel shaft on which four thin rectangular wings are welded. The tool is lengthened upwards by means of suitable extension rods, each one metre long. The whole rod is surrounded by a casing pipe also in one metre sections. The shaft of the tool has such a length above the wings, that when the tool is in the position shown in fig. 1, the wings

will be in clay, which is not disturbed by the casing-pipe. Thanks to its thinness the tool itself does not appreciably disturb the clay to be tested.

The sections of the casing-pipe are joined by coupling-boxes, some of which are furnished with guide-plates for the turning rod. The shaft of the rotating tool is centred at its lower end by means of a bush fitted to the lower coupling-box. A protractor is mounted on the upper coupling-box which is located in position by means of a set-screw. At the same coupling-box a turning handle rests on a bearing. The turning rod is furnished with a lever, on which a pointer, for reading the protractor, is fastened. The lever is connected with the turning handle by means of two spring balances, so that when the turning handle is rotated, torsional moment is transmitted to the lever.

The apparatus is driven down into the ground by pressure or ramming. Before this procedure the turning handle, the uppermost coupling-box, and the parts attached to it are removed. In order to be protected while being driven down, the rotating tool is lifted, so that the wings rest against the lowest coupling-box.

When the soil layer to be tested is reached, the parts which were removed, are reassembled, and the rotating tool is pushed down to its lower position. The test proper is then carried out as follows (shown in fig. 2). The turning handle is turned at such a



The testing apparatus during operation.

FIG. 2

speed, that the velocity of the lever, controlled by means of a watch and the protractor, is kept constant. The forces, indicated by the spring balances, are noted at certain time intervals and; when the maximum readings are registered, the turning is stopped.

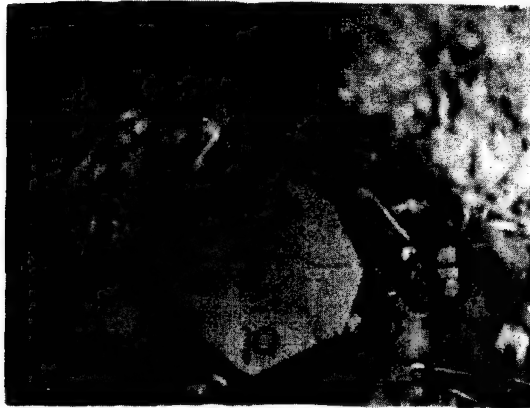
The apparatus is then driven down to the next testing depth, and the procedure is repeated.

#### THE SHAPE OF THE SURFACE OF RUPTURE.

Some simple experiments have been made in order to study the shape of the surface of rupture which is produced, when the tool is turned in clay.

A rotating tool with two wings was driven into clay soil, and turned until the maximum forces had been registered; then the turning was stopped, and the tool withdrawn. The piece

of clay in which the tool had been turned was excavated, and when it was cut at right angle to the previous direction of the axis of the rotating tool, a fairly clear surface of rupture was seen. Fig. 3 shows such a piece of excavated clay. As seen in the figure, the clay seems to have ruptured along a surface with oval, almost circular cross-section.

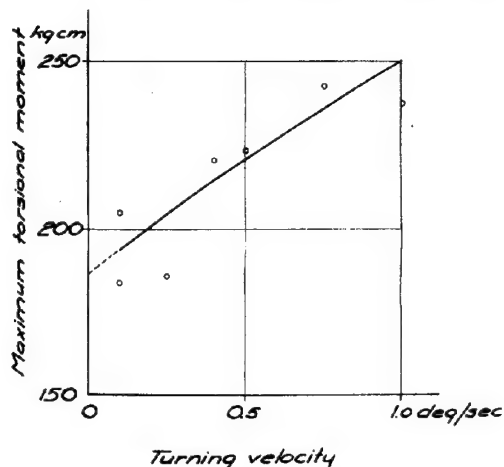


A piece of excavated clay in which the turning tool has operated.

FIG. 3

#### INFLUENCE OF THE TURNING VELOCITY.

In order to study the influence of the turning velocity of the lever on the maximum torsional moment, investigations have been carried out with different velocities but with the same rotating tool and in the same clay. Tests have been made at different depths, and all depths have given results similar in character. Fig. 4 shows a typical result. As



Maximum torsional moment at different turning velocities for a rotating tool with two wings.

FIG. 4

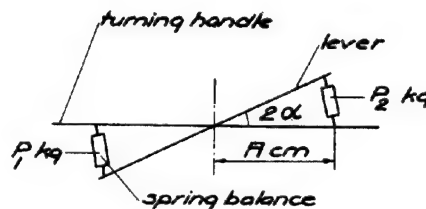
seen in the figure, the maximum moment decreases, as the velocity decreases. A velocity corresponding to actual cases may now be chosen and used in the tests.

In reality clay is generally loaded very slowly, so that a turning velocity approximating zero would correspond best to reality. For practical reasons however, it is impossible to use an infinitesimal velocity, particularly if the turning is to be done by hand. The velocity 0.1 degree per second seems in such case to be a practical lower limit, and for this reason this velocity has been chosen. In fig. 4 the maximum torsional moment at this velocity only slightly exceeds the moment obtained by extending the curve to zero. In all tests carried out up to now this difference seems to be less than 5 % of the maximum moment at the velocity of zero.

#### CALCULATION OF THE SHEAR STRENGTH

When loaded the spring balances extend, causing the moment arm to vary with the load. In order to calculate the real torsional moment ( $M$ ) in the turning rod, a correction for the variation of the moment arm is introduced. With designations as in fig. 5 then

$$M = (P_1 + P_2) A \cos \alpha$$

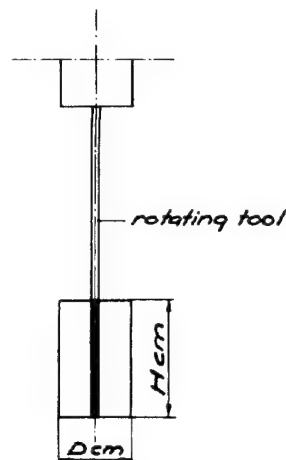


Upper part of the apparatus.

FIG. 5

The factor  $\cos \alpha$ , which varies with the load only, can be experimentally determined for different loads.

On the assumption, that the surface of rupture is a circular cylinder surrounding the tool, that at maximum torsional moment ( $M_{max}$ ) the shear strength is fully developed over



Lower part of the apparatus.

FIG. 6

the whole surface of the said cylinder, including its end surfaces,

that the torsional moment, exerted by the clay upon the shaft of the rotating tool can be neglected,

and with designations as in fig. 6, then

$$M_{\max} = \tau \left( \pi D H \frac{D}{2} + 2 \frac{\pi D^2}{4} \frac{2 D}{3} \right)$$

$$\text{and } \tau = \frac{M_{\max}}{C}$$

where C is a constant.

On account of the turning velocity,  $M_{\max}$  could be 5% too high, as previously found.

According to the tests the surface of rupture is somewhat smaller than the one assumed above. Furthermore, the shear strength is surely not fully developed in both end surfaces.

The influence of these factors may well counterbalance the increase of  $M_{\max}$  caused by the turning velocity.

As, further, torsional moment exerted by the clay upon the shaft of the rotating tool, is very small, and friction in the apparatus, according to several tests, is also slight,  $\tau$  calculated as above may not be impaired by errors of importance.

COMPARISON BETWEEN VALUES OF THE SHEAR STRENGTH OBTAINED BY THE ROTATING AUGER, BY CALCULATIONS FROM SLIDES AND BY LABORATORY INVESTIGATIONS ON EXTRACTED SAMPLES.

The rotating auger has been used in several localities. Among them are two sites where slides had taken place, and where ex-

tensive investigations were carried out. At these investigations samples were extracted by means of the Swedish piston sampler 2) and the shear strength determined by unconfined compression test and by the Swedish cone-test. 3)

Fig. 7 and 8 show results from two boreholes, viz. the shear strength according to the rotating auger and according to the laboratory methods. In the figures the shear strength according to calculations from the slides is also represented. The calculated values are approximate and obtained by the circular arc method. In the figures some soil data is also given.

From the figures it follows:

At shallow depths under the soil surface the shear strength, according to the rotating auger, roughly equals the shear strength determined by these laboratory methods;

at greater depths the shear strength, according to the rotating auger, exceeds laboratory values considerably;

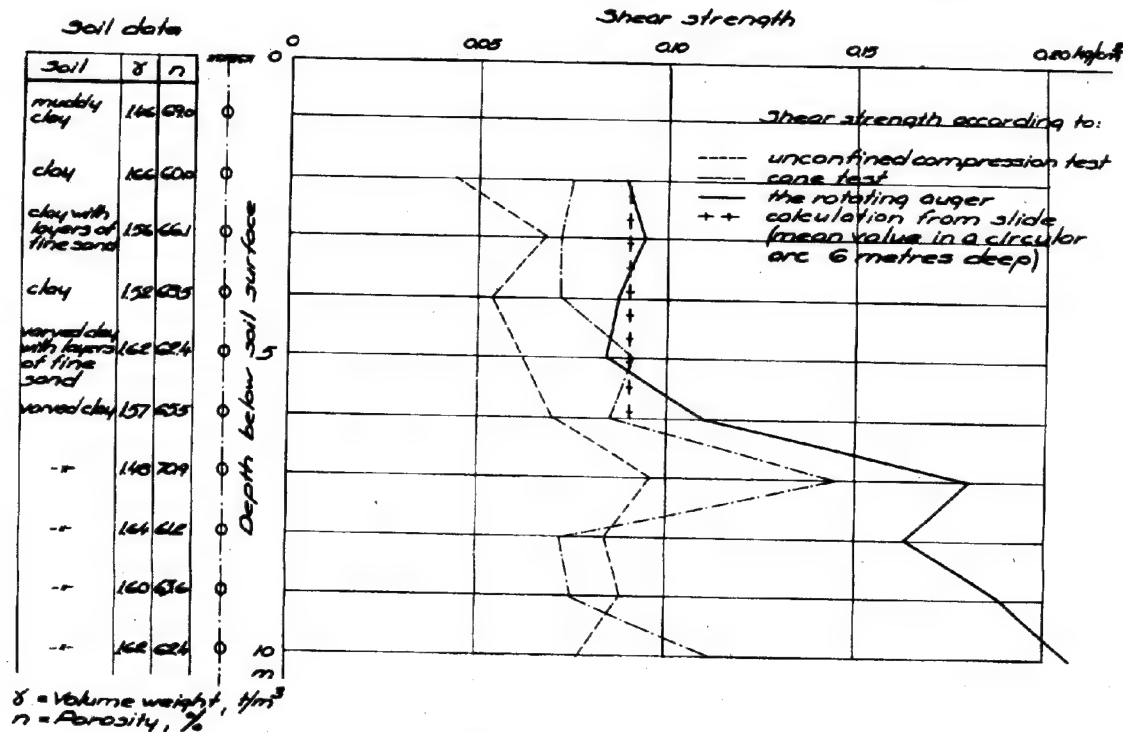
the shear strength, according to the rotating auger, seems to correspond with the strength calculated from slides, while the laboratory values are too small.

CONCLUSIONS.

The experiments carried out up to now are only few, but as all results are similar in character, the following conclusions might be drawn:

When a tool, like the one used, is turned in clay, a surface of rupture is formed with oval, almost circular cross-section.

The maximum torsional moment is influ-



The shear strength determined by different methods.

FIG. 7

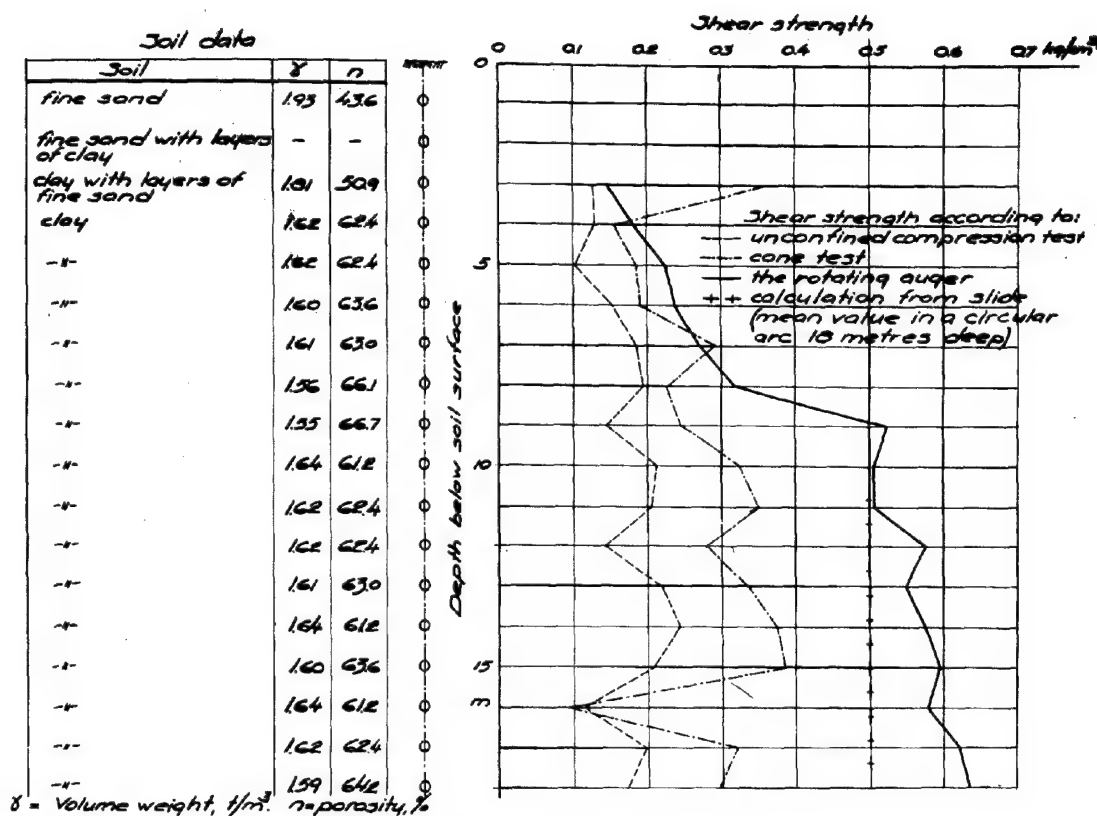


FIG. 8

enced by the turning velocity, and in such a way, that the moment decreases, as the velocity decreases.

At the velocity chosen (0.1 deg/sec) the maximum torsional moment seems to exceed by less than 5 % the value obtained by extracting the moment-velocity curve to zero.

At shallow depths under the soil surface the shear strength according to the rotating auger roughly equals the shear strength determined by laboratory methods.

At greater depths the shear strength according to the rotating auger exceeds the laboratory values considerably.

The shear strength according to the rotating auger seems to correspond with the strength calculated from slides, while the laboratory values are too small.

Or in other words, the method used to be a simple, quickly working method for determining the real shear strength of a clay soil.

#### SUMMARY

The shear strength of clay is usually determined in the laboratory from samples taken from different depths of the ground. In Sweden the investigation is generally carried out by means of unconfined compression test or cone test. Usually the shear strength thus obtained increases only slightly with the depth under the surface of the ground. It is often smaller than the real strength, calculated from slides that have occurred in the

same soil. This discrepancy may depend partly on disturbance of the sample caused by the sampler, partly on changes in the sample due to the decrease of pressure when the sample is extracted. These sources of error can never be entirely eliminated when the investigation is carried out on extracted samples.

On account of this a method for determining the shear strength of soil directly in the ground has been developed at The Royal Swedish Geotechnical Institute. According to this method a tool is first driven into the ground and then turned, the resistance against turning being measured. The shear strength is then calculated from the maximum resistance. The tool is shaped in such a way that, when being driven down, it disturbs as little as possible the soil to be tested, and, when being turned, it produces in the soil a surface of rupture of well defined shape. The tool is lengthened upwards by an extension rod, surrounded by a casing-pipe.

At shallow depths under the soil surface the shear strength determined by this in situ method roughly equals the strength determined by the laboratory methods. But at greater depths the former exceeds the latter considerably. The in situ values also seem to correspond with those calculated from slides, while the laboratory values are too small.

The experiments are still in an early stage, but the method, as now can be judged, seems full of promise.



REFERENCES.

- 1) Odenstad, Sten. Load tests on clay (Report to the Second International Conference on Soil Mechanics and Foundation Engineering).
- 2) Kortfattat kompendium i geoteknik 1946. Stockholm 1946. (Medd. nr 1 Stat.geot.Inst.)
- 3) Statens Järnvägar; Geotekniska kommissionen 1914-1922. Slutbetänkande. Stockholm 1922. (Stat.Järnv. geot.Medd". nr 2.)

-0-0-0-0-0-0-

### III b 4 A PRACTICAL METHOD OF RAPID MEASUREMENT OF SOIL MOISTURE AND ITS APPLICATIONS

KANO HOSHINO

Japan

#### I. THE METHODS USED BEFORE AND NEW METHOD.

It is essential to measure the content of soil moisture in the course of research or practise on soil mechanics. The oven-dry method has been used, but it takes at least a day or more before we can know results.

A few methods have been proposed for rapid measurement of soil moisture; for example, a method of measuring the electric resistance of soil sample and of measuring the temperature rise by mixing sulphuric acid with it, but none of which has been in common use because of the requirement of special instruments or because of the difficulty or inaccuracy of the process.

A new method of rapid measurement of soil moisture based on a physical principle can afford results in about ten minutes with ample accuracy for engineering purposes.

Principle of the method is very simple as well known, and is based on the fact that the net specific volume or the net volume per unit weight of a sample excluding air void changes in linear proportion to the percentage in weight of moisture to the total soil sample.

A practical procedure was devised by author for measuring the net specific volume of soil sample, which is to be called the index of moisture.

Equipments required for this method are not special made, but we can find them all on the shelf in our laboratory, such as flask, funnel, beaker, glass tube and balance, etc.

It is very easy to exercise this method both in laboratory and in field, and we can know results at once.

If the apparent specific density of soil is known, the index of dry density can be determined, which proportionates in linear relation with the dry density. In this case, the saturation curve can be drawn in the simplest form with no relation to the specific gravity of soil particles.

A number of results have been obtained successfully by this method both in laboratory and in field, especially in the field of compacting soil to obtain the maximum density at optimum moisture. Some examples of the results observed are reported in this paper.

#### II. PRINCIPLE AND PRACTICE OF NEW METHOD.

Let the specific gravity of soil particles be equal to 2.50 and that of water to 1.00, then the value of net specific volume of perfect dry soil sample is 0.4 and that of water is 1.0, and the corresponding percent-

ages of moisture content are zero and 100 respectively. In the case of mixing both in equal weight, it amounts to 0.7, corresponding to 50 percent of moisture content. We can know that the net specific volume of a soil sample has a linear relation to the percentage of moisture content to the total weight of sample. In general, if we use the following designations,

Gs-specific gravity of soil particles  
W-weight of a soil sample  
V-net volume of the soil sample, excluding air void

Ww, Ws-weights of water and soil particles contained in the soil sample

w-percentage of soil moisture to the total weight of the sample

$\Omega$ -net specific volume of the sample (index of moisture)

Gd, Gd-apparent specific gravity and dry density of the sample

$\Gamma$ -index of dry density

then we get the following relations

$$w = Ww/Ws \times 100 \text{ and } \Omega = V/W = Ww/W + (W - Ww)/GsW \quad (1)$$

Therefore

$$w = (\Omega - 1/Gs) / (1 - 1/Gs) \times 100 \quad (2)$$

We know from (2) that the moisture content  $w$  is in linear relation to the net specific volume  $\Omega$ , which is to be called the index of moisture.

If the apparent density of soil sample is known, the index of dry density can be defined by

$$\Gamma = (1 - \Omega) Gs \quad (3)$$

hence

$$Gd = (1 - w/100) Gs \quad (4)$$

$$= \Gamma / (1 - 1/Gs)$$

We can know that the dry density is in linear proportion to the index of dry density.

In the case of saturating the voids of a soil sample by water (no air void), the moisture content and the dry density stand in a relation of

$$w = 100(1 - Gd/Gs) / (1 + Gd - Gd/Gs) \quad (5)$$

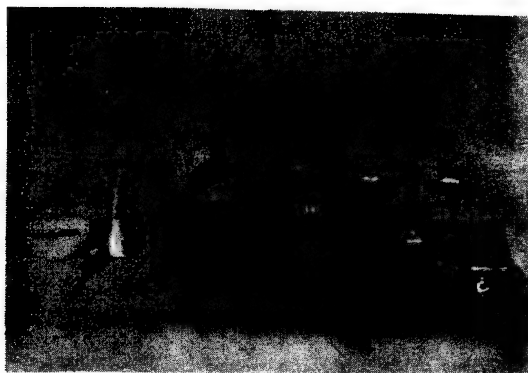
which gives the different saturation curve with the different value of  $Gs$ . Using the both indexes  $\Omega$  and  $\Gamma$  in the new method, we can express the saturation curve by

$$\Gamma = 1/\Omega - 1 \quad (6)$$

which has a simplest form easy to remember.

The equipments to be prepared for this method are as follows (Photo. 1):

Quantity	Unit	Equipment
1	each	glass flask, 400l ltr., slender necked
1	"	glass funnel, 45 mm dia., with a sharp point
2	"	glass beakers, 100 c.c. and 500 c.c.

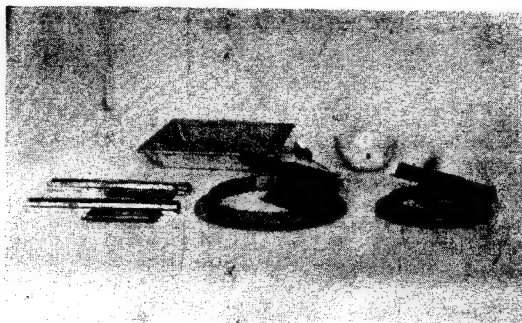


Equipments for the new rapid method of measuring soil moistures.

PHOT. 1

- 1 " glass tube, 3 mm inner dia., 15 cm long
- 1 " balance, 200 gr. capacity, 0.1 gr. sensibility
- 1 " steel wire rod, 2 mm dia., 25 cm long
- 1 " tin-plate funnel 7 cm dia., for throwing soil sample in a flask
- 1 " brass spoon of a large size

If the apparent specific density of a soil sample is to be known, its volume must be measured. An equipment of shaving type consisting of a ring frame and a shaving blade has been used by author conveniently for this purpose (Photo 2).



Shaving equipments for getting a fixed volume of soil sample.

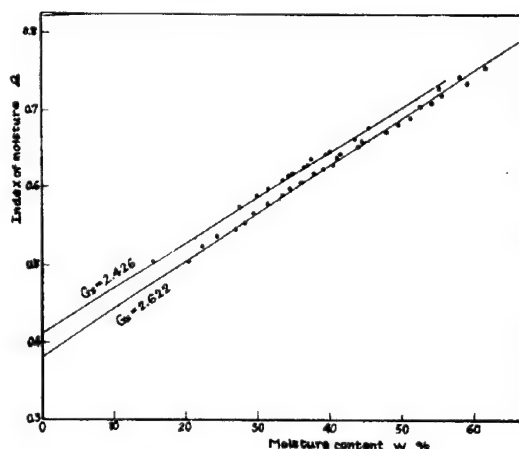
PHOT. 2

Practice of the new method is done in the following order.

Pour clear water in a flask up to its bottle neck. Adjust the level of water to coincide with the lower point of a funnel inserted, holding the flask in a right position. A glass tube can be used for adjusting a small quantity of water. We can suspend or release a drop of water in it by shutting or opening its upper opening with a finger. After a precise adjustment of water level, take out a part of water from flask to a beaker and throw a weighed sample of soil (about 100 gr.) into the flask, then stir up the mixture rotating the flask or inseting a steel wire rod moistened before. Remove the bubbles or lighter dirt risen up from soil sample to the surface of water into a glass tube filled with a bit

of water through its lower opening and then transmit them to the beaker. Rest the flask on a support for a while until the upper portion of contained water becomes clear. Then adjust again the level of water in the equal height in the same manner as before, adding water in the beaker to the flask. During the course of process, even a drop of water must not be lost. Measure the weight of water remained in the beaker, which represents the net volume of soil sample free from contained air void. The index of moisture or the net specific volume can be determined by dividing the weight of water in beaker by that of soil sample.

The data obtained by the new method were compared with those by the oven-dry method and the results showed the ample accuracy for engineering purposes (Fig. 1).



Accuracy of the new rapid method compared with the oven-dry method.

FIG.1

### III. APPLICATIONS OF NEW METHOD.

The new method of rapid measurement is applicable to all fields in soil mechanics when it is necessary to measure the soil moistures; but it is most useful when a lot of results are to be known in a very short time, especially in field works. Because of the easy receipt and lightness of equipments and the simple procedure of measurement, we can exercise the new method in any place at any time. Those jobs executing soil compactions will be most benefited by this method as we can know the moisture contents of soils quickly and precisely in the field and can adjust them to the optimum moisture for compaction.

Some examples of the results obtained by author are as follows:

- 1) Effects of drying and hydrating soil sample on the compaction and the strength of test piece.

It is a well known fact that the dry density of test piece compacted under a certain static pressure becomes heavier by mixing water to the soil sample and reaches to a maximum value at optimum moisture.

Experiments on the effects of drying and hydrating soil samples were done with a red loam soil in Chiba, Japan, physical properties of which are shown in Table 1.

Table 1.

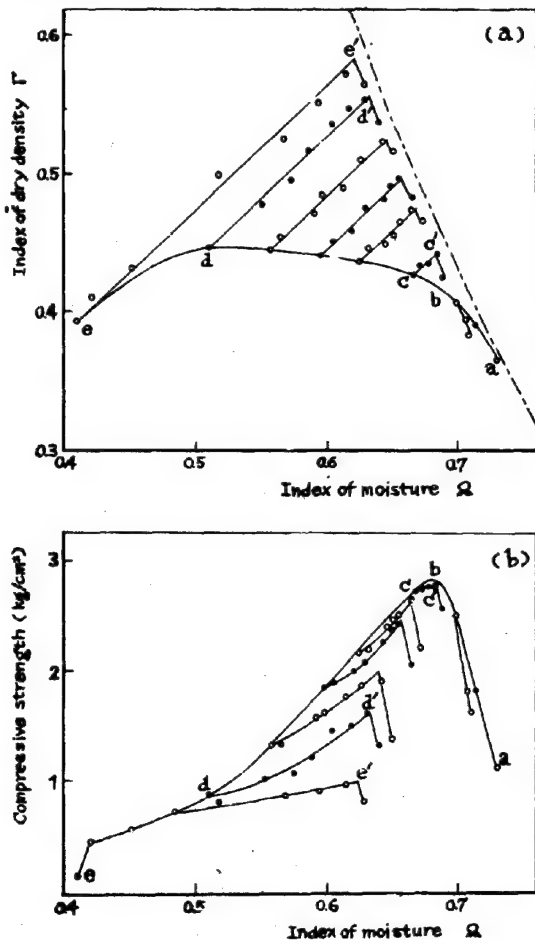
Items	District	Chiba
<b>Mech. Analysis</b>		
Sand (coarser than 0.074 mm)		41.3
Silt (0.074 mm - 0.005 mm)		21.4
Clay (finer than 0.005 mm)		27.3
Specific gravity		2.67

The results of both compaction and compression tests are as follows:

Test pieces, 5 cm dia., 10 cm high, were compacted in a brass cylinder under a 10 kg/cm<sup>2</sup> static pressure.

Both indexes of moisture and dry density of each test piece were measured.

Compaction of dry samples gives a moisture dry density curve abcde expressed by both indexes (Fig. 2a), on which points a, d, and e correspond to the no dry, air-dry, and oven-dry states separately. The dry density slightly increases by drying until air-dry, but decreases adversely by absolute dry. Mixing water to the dried samples gives a group of



Effects of drying and hydrating soil sample on the compaction and the compressive strength of the test piece.

FIG.2

straight lines cc', dd', ee', and so on. At optimum moisture is obtained the maximum density, which fairly differs each other by the degree of drying (c', d', or e'). Absolute maximum dry density can be obtained by absolute dry sample (e').

The compressive strength of each compacted test piece was measured. (Fig. 2b). With the reduction of moisture by drying, compressive strength rises steeply at first, and reaches to a highest value near a point b, then reduces gradually and comes to a lowest point e at absolute dry state. By mixing water, the compressive strength increases slightly and reaches to a maximum at optimum moisture (c', d', or e'). The higher degree of drying corresponds to the lower compressive strength, though it corresponds to the heavier dry density. It is to be noticed that the degree of drying gives a soil sample the quite different physical properties, and that to gain an absolute maximum compressive strength, the soil sample must not be dried in excess degree, though the absolute maximum dry density can be obtained by absolute dry sample.

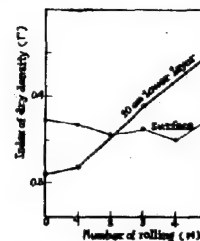
2) Effects of rolling soils observed both in a job and in a field.

The effects of rolling a natural soil layer by 10 ton macadam roller were observed in a job in Chiba district.

Results obtained are as follows:

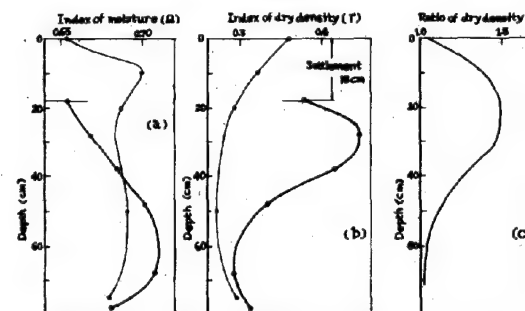
The effect of rolling did not appear on the ground surface, where the soils were rather in dry state and had already heavier densities by being stamped. But it appeared clearly in the 10 cm lower layer, giving heavier dry density with the repetition of rolling. (Fig. 3).

Vertical distributions of moisture and dry density of soils before and after rolling varied distinctly (Fig. 4a and b). The degree



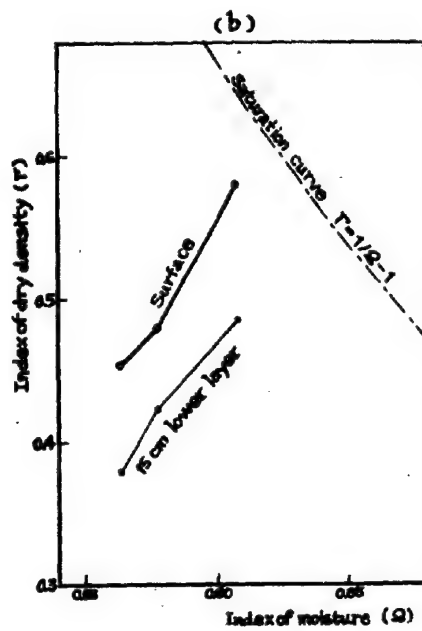
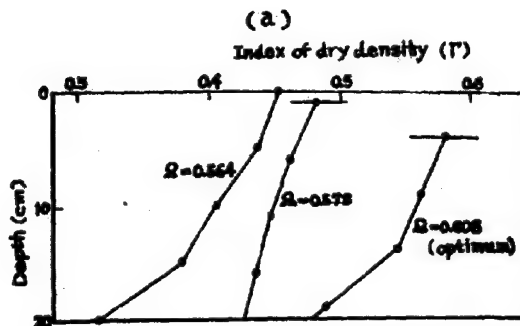
Effects of rolling a natural soil layer (number of rolling and depth).

FIG.3



Do (vertical distributions of moisture and dry density).

FIG.4



Effects of rolling moistened soil layers (moisture).

FIG.5 a b

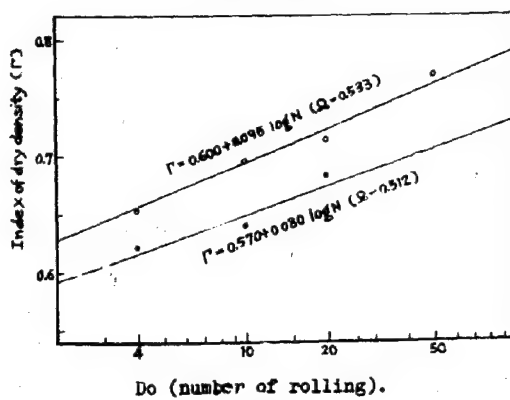
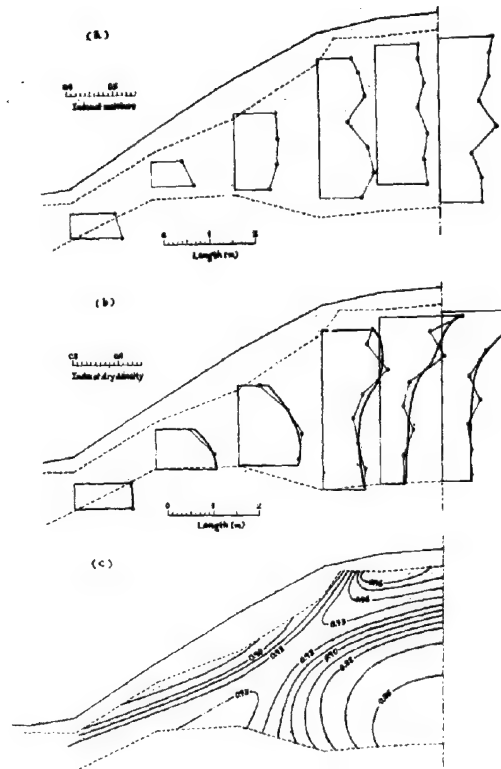
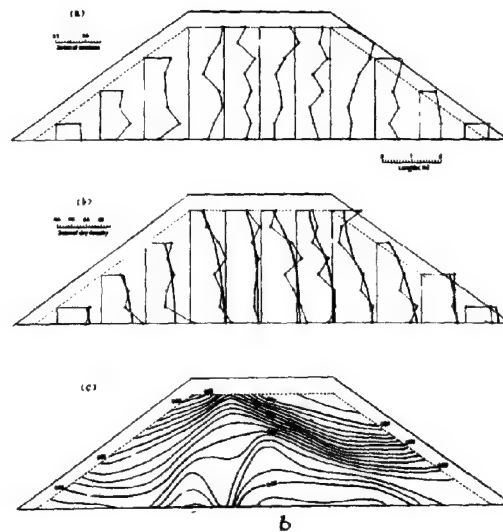


FIG.6



Distributions of moisture and dry density in the interior of an aged embankment.

FIG.7



Distributions of moisture and dry density in the interior of a new embankment.

FIG.8

of compaction in each depth of soil layer was calculated and the maximum value of the ratio of both in dry density before and after rolling was obtained at the 20 cm lower layer (Fig. 4c).

Another experiment of rolling soils by 375 kg hand roller in a field in Chiba city clearly showed the effects of mixed water and number of rolling (Figs. 5, 6).

We can know that the maximum rolling effect of uniformly moistened soil layer is obtained when an optimum moisture is given for the maximum density at the surface of layer corresponding to the number of rolling and that the rolling effect reduces gradually with the depth.

3) Distributions of moisture and dry density in the interior of embankments.

Distributions of moisture and dry density on the cross section of railroad embankments were measured at both fields in Mie and Fukushima districts, Japan. The former embankment has been compacted under traffic loads for about fifty years, the latter was executed only two years ago, being charged with no load yet.

At each point in the cross sections, two or three samples of a fixed volume were shaved and their indexes of moisture and dry density were measured in the field. The mean va-

lues of observations were plotted and the lines connecting the points of equal density were drawn in Fig. 7 (a) (b) and (c) for Mie and in Fig. 8 (a) (b) and (c) for Fukushima.

The upper portion of an aged embankment has heavier dry densities compacted by traffic loads in a long period, which may be assumed to be a main factor for the settlement of embankment. New embankment has loose densities in the upper layers and heavier densities in the lower layers being charged by its own weight only.

The physical properties of soils prevailing in both cross sections are listed in Table 2.

Table 2.

Items	District	Mie	Fuku-shima
Mech. Sand (coarser than 0.074mm)		58.0	84.8
Anal. Silt (0.074 mm - 0.005 mm)		29.0	14.4
Clay (finer than 0.005 mm)		13.0	00.8
Specific gravity		2.63	2.65
Liquid limit		35.0	54.0
Plastic limit		24.7	50.0
Plastic index		10.3	4.0

-O-O-O-O-O-

### III b 5

#### TESTING OF THE ELASTICITY AND STRESS PROPERTY OF ROCK SOIL

F. HORNLMANN Dipl. Ing.

Köniz bei Bern, Switzerland

According to the known methods for the establishment of the elasticity and stress property of rock, which serves for example as rock soil for dams, test samples are cut out of the rock, or partly separated from it and then subjected to the usual tests. They are relatively small, as already a crosscut of 5 ft<sup>2</sup> needs extraordinary high pressure tests, which up to the present can be made with complicated special appliances, which are very expensive. It is therefore necessary to confine oneself when testing the rock to the small test samples. The results of these tests indicate very roughly the real conditions of the above mentioned soil.

According to the author's proposal the tests on the rock itself are carried out with "pressure cushions" without bulbs. These cushions were developed by the author and already employed with success in 1934 for grid potential of the soil and later also for testing the strength of materials for great pressures.

The above mentioned cushions of pressure are flat, hollow bodies made of thin sheet metal and closed on all sides, which can be provided with pads at the edge. In the case of great compressibility of the rock, a number of cushions is placed one upon another, so that even when very high pressures are used a proportionately thin sheet may be employed. Each cushion possesses devices for admitting the pressure of a liquid and at the same time

expelling air.

To introduce such a cushion into the rock one or more large slits are made in the rock by means of boring or otherwise. These slits may have a depth and breadth of several yards and a height of a few inches. There is no difficulty in making cushions of 10 and more yards by 0.5. These are inserted in the slit side by side after which the free space between the cushions and the rock is filled up with cement mortar (pressed mortar).

After the hardening of the mortar the pressure of a liquid will be introduced into the cushions. As they can easily lose their shape, the pressure of the liquid is carried directly over on to the rock.

The elastic compressibility of the rock can then be exactly ascertained from the quantity of pressure liquid introduced into the cushion.

This quantity is ascertained during the testing of the different pressures.

If great value is attached to ascertaining the compressibility for example per 1.0 yd<sup>2</sup> at different points, cushions of 1.0 yd<sup>2</sup> are employed whereby each receives a separate feed pipe.

The duration of the particular testing can be spread over several days, months or even years without any difficulty. This is of a great importance.

In order to ascertain the resistance to

pressure of the rock soil, the cushions are arranged in the rock in two parallel slits. The distance between the two slits then corresponds to the thickness of the test sample.

Very often it will be possible to leave these appliances where they are after the construction has been completed and to continue to use them to ascertain the changes in tension occurring in the soil. For this it is only necessary to give the pressure cushions filled with a compressed liquid a degree of elasticity in the direction of the load, identical with that of the material surrounding the pressure cushion. For measuring strain in the soil or the material of a construction a concrete dam for example, special appliances (regulators) are used which make it possible to regulate the elasticity of the pressure cushions without any difficulty. The tension in the soil or the material of the construction can then be deduced from the degree of the pressure of the liquid in the pressure cushion. As such appliances can remain in use for years, changes of tension can be continuously registered over a long period of time.

In order to give the pressure cushion a particular degree of elasticity, it is attached by means of a pressure conduit to a regulator, for instance an iron pipe of particular dimensions closed all round. If the cushion filled with a liquid is then exposed to pressure from without, the liquid is subjected to tension. As a result of the pressure of the liquid, the above-mentioned pipe expands elastically in a special way and compressed liquid flows over into the pipe from the pres-

sure cushion. As, when the exterior load on the cushion changes, the tension of the liquid contained in it also changes, it is quite easy, by measuring the pipe to produce a particular degree of elasticity in the pressure cushion.

If suitable methods of construction are employed to ensure the tensile strength of the connection between the cushion and the surrounding material the degree of tensile stress occurring in the material can be ascertained by means of the appliance. It is then only necessary to measure the reduction in pressure of the liquid contained in the cushion.

The cushions employed are suitably gauged prior to use, the pressure of the liquid in the cushion being measured for a particular load and a particular change of volume. Cushions which have two smooth parallel surfaces for transferring the load (see fig. 1 and 2) can be gauged very simple by means of testing machines which contain parallel pressure plates.

The attached figures 1 and 2 show illustrations for the use of the devices described above.

In fig. 1 two parallel slits (1,2) are shown in the rock one on top of the other and a certain distance apart, into which pressure cushions have been inserted, the spaces between the cushions and the rock having been filled with compressed mortar.

In the upper slit (Section A-A) the length of the cushion (10) corresponds to the depth of the slit. In the lower slit (2) several pressure cushions (11) are arranged one

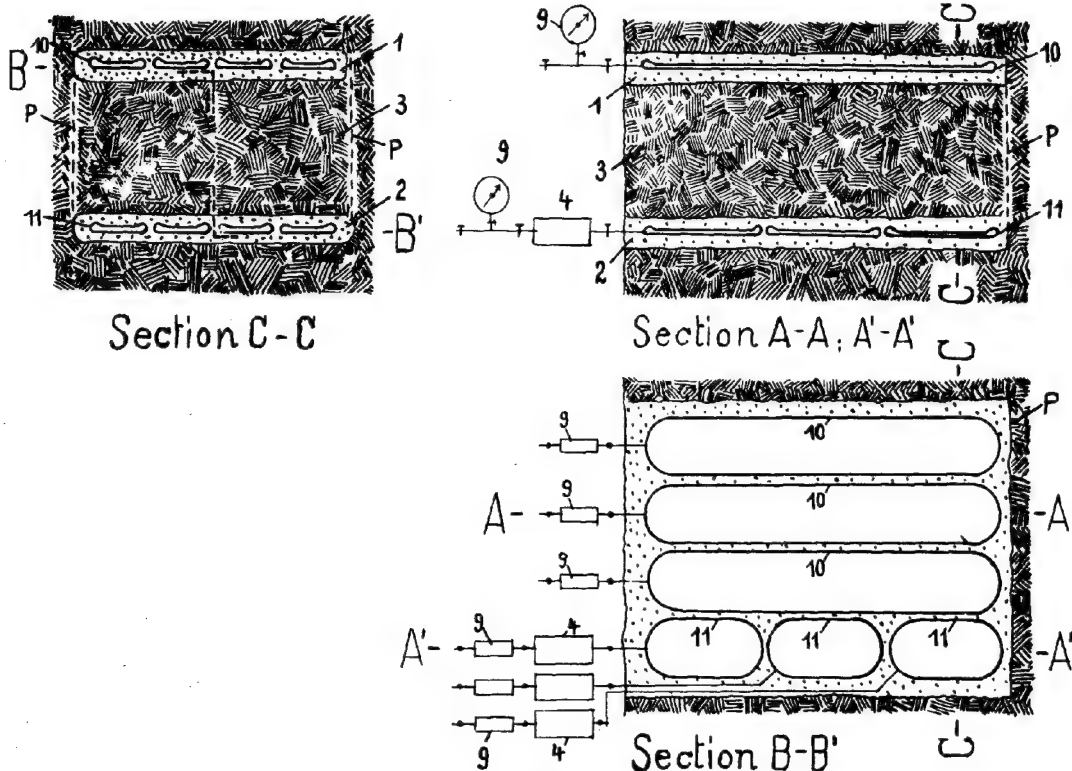
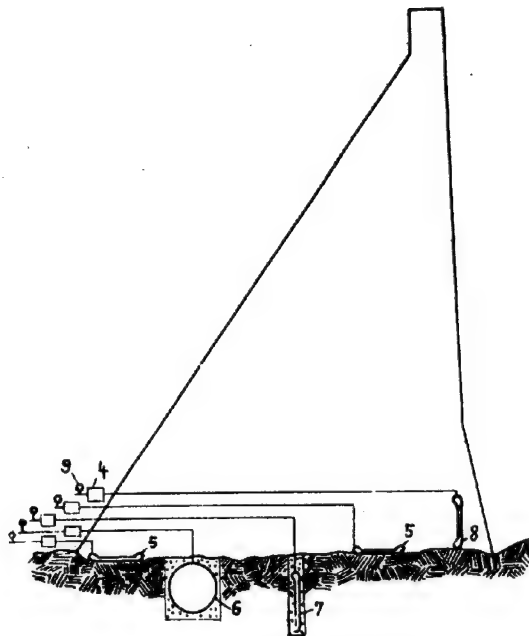


FIG.1





Pressure cushions not  
according to scale

FIG. 2

behind the other, so that the deformation of the rock can be ascertained for each section on the strength of the quantity of the liquid introduced into the various cushions.

If the slits are for instance 10 yards wide by 10 yards deep these 100 square yards of area can be filled with 20 cushions of 10 yards in length and  $\frac{1}{2}$  yard in width. After the compressed mortar inserted between the cushions and the rock has become hard, compressed liquid is introduced into the different cushions of for instance 5 atmospheres. The quantity of liquid introduced into each cushion is exactly measured and registered. Thereupon the pressure is increased by, say, 5 atmospheres more and the quantity of liquid introduced into each cushion is again measured. In this way it will be possible to ascertain the degree of contraction of the rock resulting from the increased inpressure of 5 atm. If the pressure of the liquid is similarly increased by the 5 atm. at a time and the contraction is measured at each degree of pressure on the basis of the quantities of liquid introduced, a very good general idea of the

capacity of contraction of the rock can be obtained. By gradually imposing and removing loads, it will be possible to ascertain the elasticity of the rock. If the imposition and removal of loads are also effected in the case of the cushions of the lower slit (2) of fig. 1 particular tests with loads can be made in this way with the part (3) of the rock between the slits (1,2).

The accuracy of the result of the test can of course be increased by appropriately separating this part (3) of the rock from the rest along lines P of fig. 1 but even without this separation these tests can produce valuable results if as large areas as possible covered with cushions are chosen.

If the loading of the rock is carried out within the limits of elasticity of the rock material, these appliances can be used during construction and after the completion of the structure for ascertaining the tension of the soil. At the same time the above-mentioned regulators (4) and tension meters (manometers) (9) are attached to the cushions and the extent of the tension in the soil can then be deduced from the pressure of liquid in the cushions. Such regulators (4) attached to the cushions are shown in the lower slit (2) of fig. 1 Sections (A - A', B - B'). For better control the regulators (4) and manometers (9) are arranged outside the areas to be tested.

For measuring the tension in the soil, it will often be sufficient to use round cushions of a diameter of say 0.4 by 0.8 yd. In fig. 2 such cushions (5-8) are arranged in the joint between the soil and the concrete of the construction (dam). The cushions can be placed straight on the soil (5) or in a vertical position in the plane of section of fig. 2 (6) or perpendicular thereto (7,8). By means of the arrangement indicated in fig. 2 the strain occurring in the three principal directions can be ascertained (5,6,7). There is of course no reason why the cushions should not be arranged in any other way.

The pressure cushions can naturally be arranged deeper underneath the foundations of a construction. If this is done, the cushions are sunk and concreted, together with the pressure conduit, in small shafts and slits, before the construction is erected. The pressure conduit of each cushion is then directed to the observation room and there provided with the regulator (4) and the tension meter (manometer) (9).

For measuring the strains in the masonry of the construction the cushions (8) of fig. 2 are appropriately built into the masonry during construction or sufficient room is left for inserting the cushions subsequently. In this way, the tension both in the soil and in the construction can be ascertained by means of fairly simple devices as shown in fig. 2 for a concrete dam.



III b 6

CONSTRUCTION AND METHOD OF OPERATING OF A NEW DEEPSOUNDING APPARATUS

Ir. G. PLANTEMA,

Engineer of City Engineers Dept., Sub-Dept. of Soil Mechanics, Rotterdam.

SUMMARY.

A deepsounding is performed by pushing a cone into the soil, and by measuring the resistance experienced. The resistances which are thus measured in the sand layers, form a measure for the bearing capacity of piles driven into them. Since pile loading tests have shown the reliability of the measured sounding values, it will be of importance to describe in this report a new type of a deepsounding apparatus, the characteristic difference of which with respect to the apparatus in use up till now, is a reliable soil-tight connection of the cone with the tube. A source of measuring faults is avoided with it.

INTRODUCTION.

When designing a pile foundation for constructions, it is of vital importance to know to what depths piles have to be driven, and what area the piletoe must have for the required bearing capacity. It is therefore necessary to get an idea of the bearing capacity of the subsoil.

During the last decade the results of deepsoundings have been used in the Netherlands for the above information. A cone with a top-area of  $10 \text{ cm}^2$  1) is hereby driven into the earth mass and the experienced resistance measured, (the cone is generally pushed down until a resistance of  $300 \text{ kg/cm}^2$  is obtained, which in Rotterdam occurs at a depth of 20 - 25 m). The cone is then pushed down with a rod which is guided through a tube, the latter taking the friction  $x$  (tubes and rods can be lengthened with pieces of 1 m each).

The method of operating is such that alternately first the cone is pushed down abt. 10 cm and afterwards the tube. By measuring, with a Bourdon gauge, the pressures necessary for pushing down cone, and cone and tube simultaneously, values are obtained of the extents of the cone resistance (measure for pile-toe resistance) and the friction of the tube (measure for the negative skin friction of the pile, if any). The relation between depth and resistance, plotted in a diagram will be an indication for the bearing capacity of subsoil.

The results of these soundings are an indication for the most favourable depth of the pile-toe, taking into account any negative skin friction, and a factor of safety of e.g. 2 - 3.

As for the reconstruction of Rotterdam, hundreds of deepsoundings have been performed, the figures of the measured resistances have been compared with an especially arranged pile-loading test, the so-called "pile-sounding" 2).

This comparison proved that the results of deepsoundings are reliable.

The City Engineers Dept. of Rotterdam has now designed a new sounding device, which differs from the one used up to now in:

- 1) a soiltight connection of cone and tube,
- 2) an accurate measuring apparatus, which registers electrically,
- 3) a manner of pushing the tube into the earth mass.

#### 1. SOIL-TIGHT CONNECTION OF CONE AND TUBE.

The apparatus in use up to now consists of a cone and a tube, which are pressed down alternately. On pushing down the tube, after registering the cone resistance, soil particles may penetrate the connection. See Fig.1. If the cone is pushed down and the resistance measured, not only the sounding resistance, but

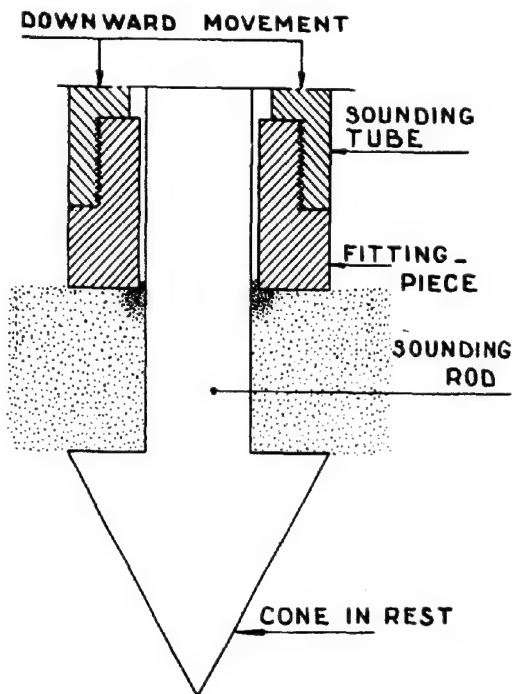


FIG.1

also the friction between the lower end of the tube and the rod are registered. (fig. 2) Due to this connection not being soil-tight, substantial reading-faults may be obtained and too favourable sounding values registered. It even happens that due to the penetration of soil into the above connection, the rod can no longer be pushed out of the tube and the sounding fails.

To obtain a perfectly soil-tight connection, it is necessary

- a) To introduce a cone construction as shown in Fig. 3 3).
- b) To operate this construction in such a manner that sounding tube and -rod are pushed down simultaneously, but the pressures are measured separately.

Sub a. A curiosity of the mantle is the outer surface, which is not cylindrical, but conical, in order to reduce the friction of the soil on the mantle to a minimum, when pressing down the cone. Moreover, the obli-

x) Netherlands Patent no. 43095, registered for Goudse Machinefabriek & P. Barentsen.

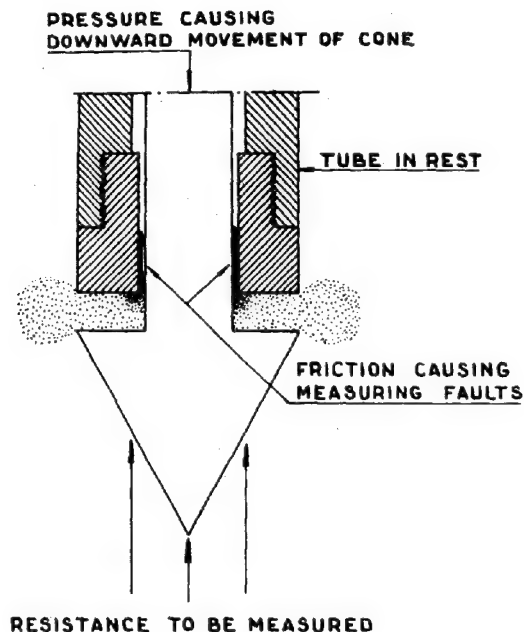


FIG.2

quity can be so great, consequently the frictional powers minimal, because with the method of working sub b, the mantle need only be short.

The mantle-construction on the cone has still an other advantage. When sounding with the ordinary cone an empty space develops over the cone, when the latter is pushed down. The surrounding soil will hereby influence the circumstance whether the hole - in the first instance arising over the cone - is filled with ground or not (fig. 4). This circumstance will influence the forming of the sliding surface resulting from pushing down the cone, and the shearing resistances occurring at the same time. Thus the nature of the soil may have an influence on the appreciation of the sounding resistance. This potential source of inequality of the sounding-resistance, however, is almost completely prevented by the mantle on the cone, which may be called an advantage for its interpretation. It is curious that on pushing down a mantleless cone always a discontinuous expiration of pressure was found as shown in fig. 5; on pushing down the cone below the maximum value, the resistance may drop due to a hole being formed over the cone. On pushing a cone with mantle this discontinuity, however, cannot be ascertained.

**Sub b.** When operating with the mantle-construction in the conventional manner, e.g. rod and tube pressed down alternately, soil particles are also bound to penetrate into the connection between mantle and tube. To avoid this, tube and rod must be pressed down simultaneously. Thus the soil particles are moving in an upward direction and will miss the connection between mantle and tube. Operating in this manner the mantle-construction can be considered as soil-tight.

When sounding the following procedure is applied:

Over the top of the tube a bowl-shaped part is screwed with the gauge box (fig. 3). If necessary, a second gauge box can measure

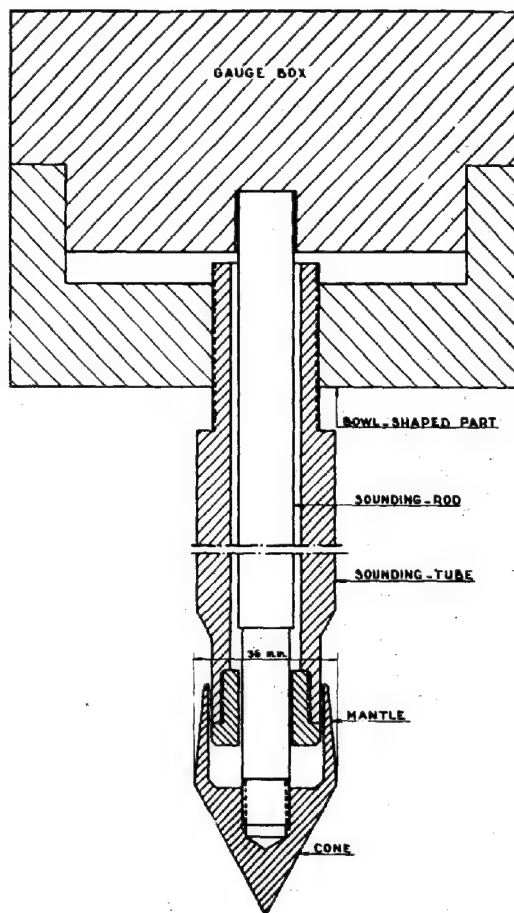


FIG.3

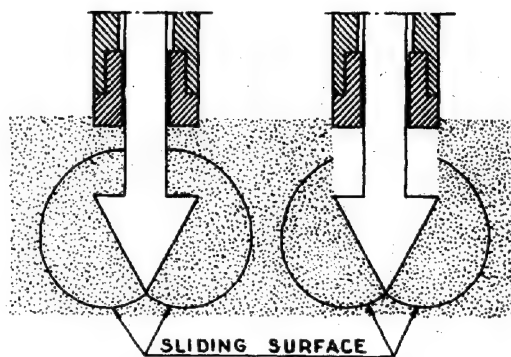


FIG.4

the total stress which is required for pushing down sounding rod and tube and the friction along the tube thus fixed. On the tops of the gauge box the forces are exercised necessary for the sounding operation. The bowl-shaped part presses down the tube, whereas the gauge box presses down the rod with the cone, registering at the same time.

The margin between upper part cone and lower part tube can also be checked by pushing

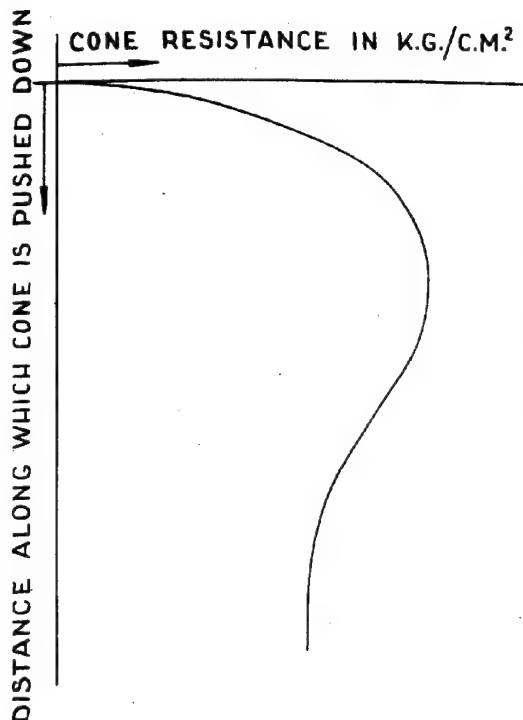


FIG. 5

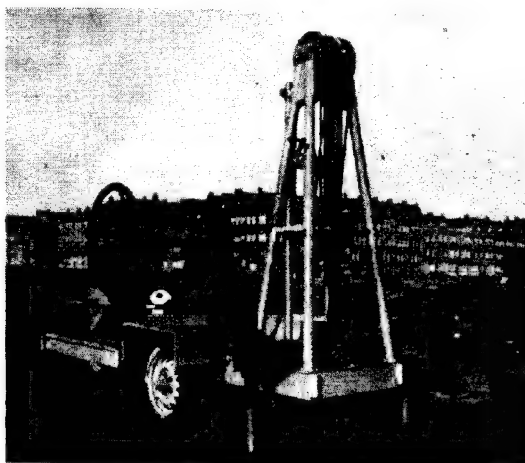


FIG. 7

down the bowl only, whereby the tube is pushed down into the earth, until the lower part of the tube meets the cone, and tube and rod are moved down simultaneously.

## 2. EXACT MEASURING APPARATUS.

Moreover the measuring apparatus can be applied to the requirements of modern measuring technics. It can be done by replacing the hydraulic measuring method with a Bourdon gauge in use up till now (with its adhering technical measuring errors) by a gauge box with wire resistance strain gauges, whereby the pressures are measured electrically (measuring faults only a few percents). Moreover,



FIG. 6

this measuring method has the advantage that for pressure measurements only a negligible pushing is necessary, so that, indeed, it is possible that tube and rod are pushed down at the same rate.

The gauge box is practically invulnerable and the registering apparatus full proof transportable, easily handled (unskilled labour). Gauge box and registering apparatus can be seen from fig. 6.

## 3. SPEED OF SOUNDING OPERATIONS.

In fig. 6 an apparatus is shown with which City Engineers Dept. of Rotterdam performs deepsoundings. By means of a specially designed rack-jack, the sounding tubes and -rods are pushed down one metre at a time.

To save time, in erecting and dismantling, the apparatus has been designed as shown in fig. 7. By means of a winch the tubes are pressed into the earth one metre at a time and afterwards pulled out. The wagon is anchored into the ground by means of screw anchors. The possibility of a motor sounding apparatus by means of which manipulations will take place still faster is, under consideration; with the latter apparatus deepsoundings are expected to be performed up to 25 m in depth in less than half a day.

## REFERENCES.

- 1) The predetermination of the required length and the prediction of the toe-resistance of piles - Lab. of Soil Mechanics, Delft - Vol. I, no. I, 1, Proceedings First Conference.
- 2) Results of a special loading test on a reinforced concrete pile, the so-called pile-sounding. Paper of Section VII.
- 3) Similar ideas were developed by J. Vermeiden, see paper no. III b 7. Improved sounding apparatus as developed in Holland since 1936.

IMPROVED SOUNDINGS APPARATUS, AS DEVELOPED IN HOLLAND SINCE 1936

J. VERMEIDEN

Head of Field Investigations, Delft Soil Mechanics Laboratory

a. SOUNDING APPARATUS.

In the Proceedings of the First International Conference on Soil Mechanics in 1936 a description has been given of the hand sounding apparatus of Barentsen 1) for the determination

of the penetration resistance of the soil. In view of the increased demand of modern field investigations this apparatus showed some imperfections.

A first imperfection is that the sounding tubes are forced down by hand, which limits the measuring range (up to 10 kg/cm<sup>2</sup>).



FIG.1a

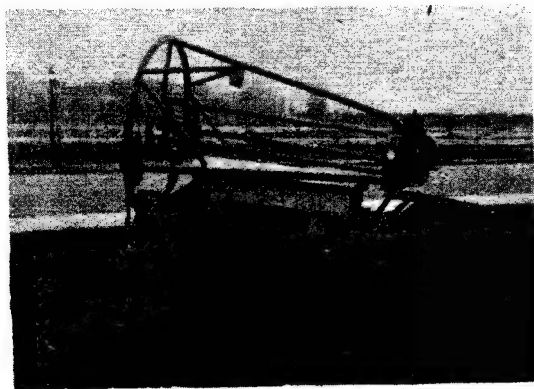


FIG.1b

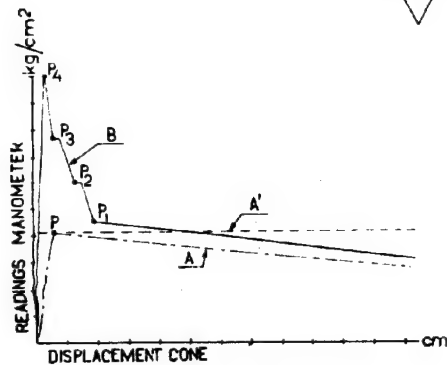
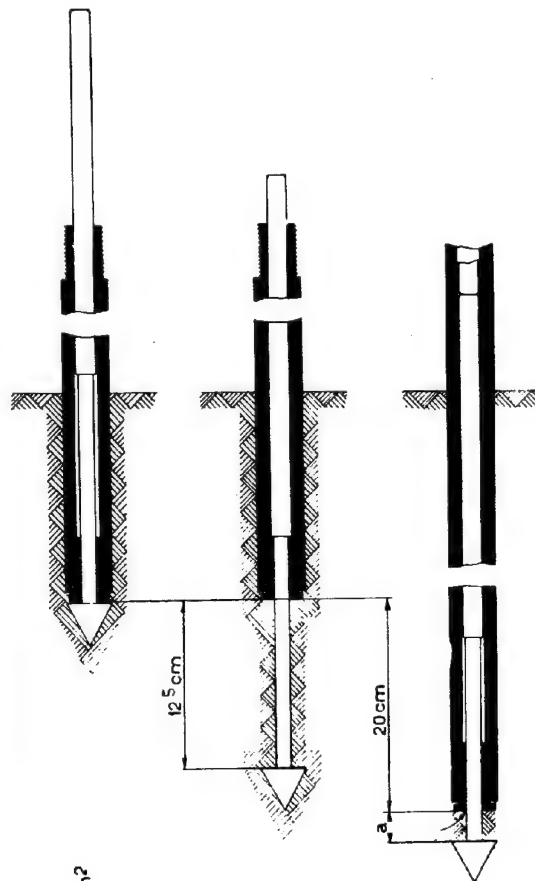


FIG.2

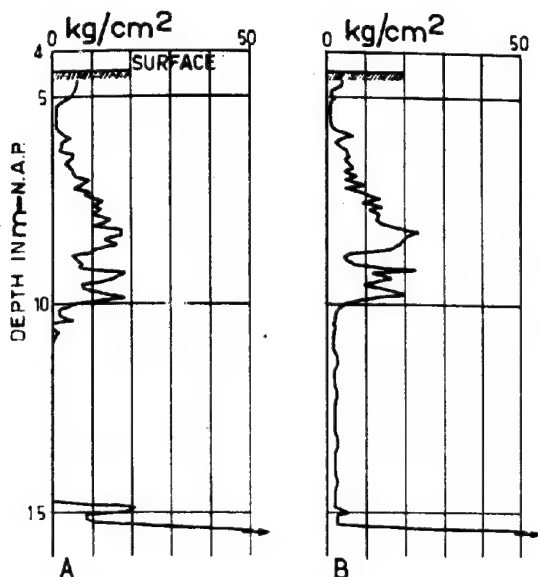


FIG.3

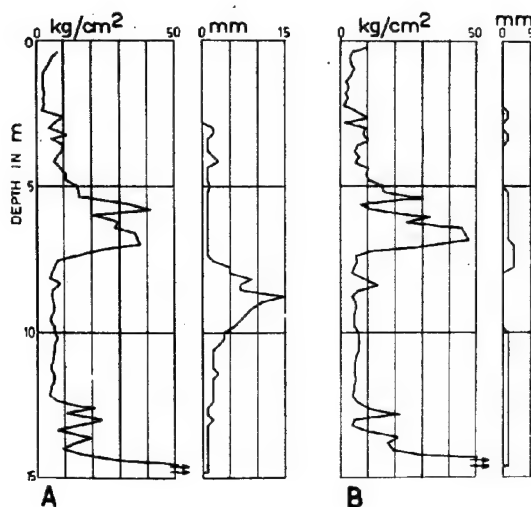


FIG.5



FIG.4

Secondly, when passing through a thin hard layer, increased pressure must be applied with the resulting danger that, after passing the layer, the apparatus is pushed through an underlying soft layer without registering its resistance.

Lastly, it has been observed that, while measuring high sounding resistances, the gland between sounding rod and sounding tube at the lower end influences the readings.

The first two imperfections were rectified at the Soil Mechanics Laboratory by constructing a pressure device so that the sounding tubes were forced down by mechanical means. Moreover, the pressure applied could now be increased appreciably and sounding resistances in sand layers up to  $50 \text{ kg/cm}^2$  could be measured, and by an adjustment at the head of the apparatus it became possible to perform continuous and discontinuous soundings. Fig. 1 (a) shows the apparatus.

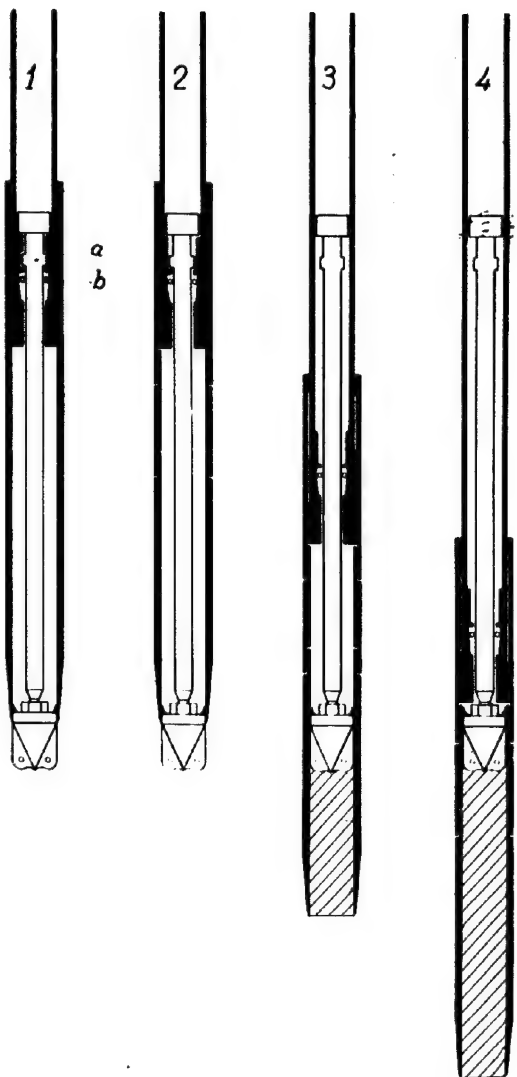


FIG.6

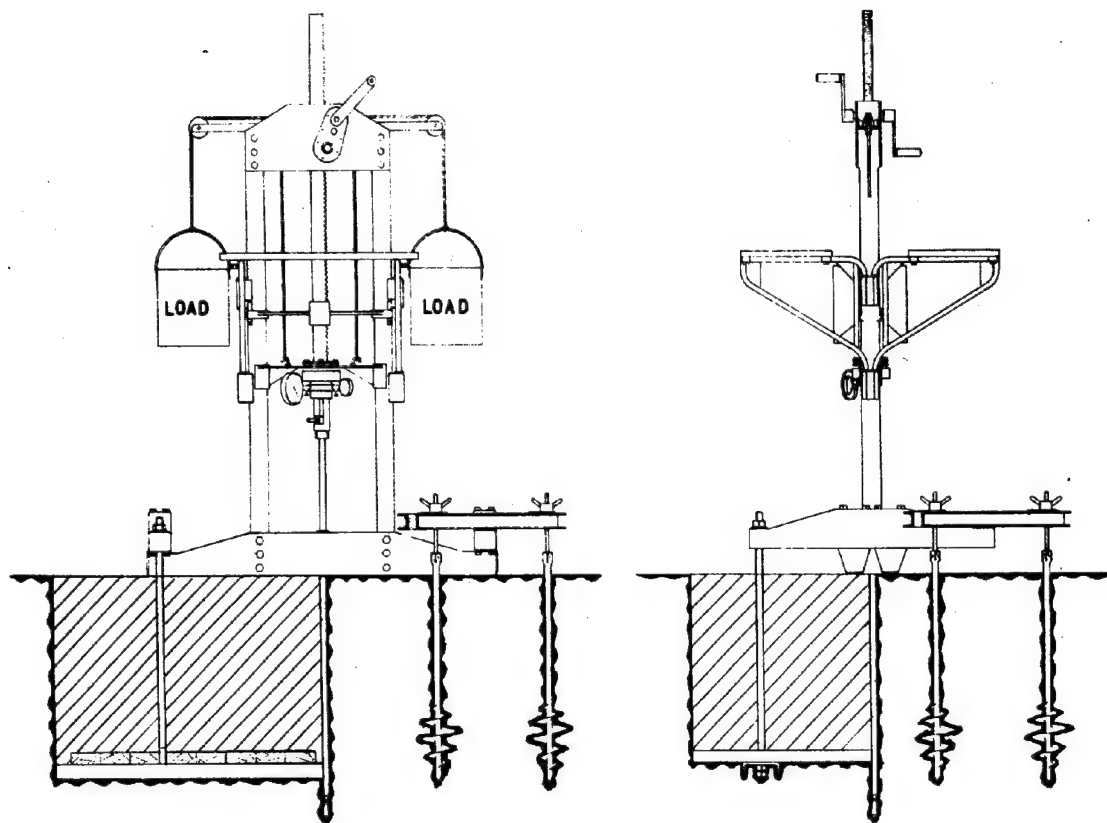


FIG. 7

Reaction forces are furnished by two screw-rods, screwed into the soil. The relatively small weight and the easy transport of this apparatus enables one to make field investigations at almost every spot (fig. 1, b).

To give an insight into the last mentioned imperfection viz. the gland between sounding rod and hollow tube, fig. 2 shows the various stages during sounding. Stage 1 shows the sounding tube with the cone at a certain depth below the ground surface. In order to find the cone resistance the rod (with cone attached) is pushed out 12½ cm (stage 2). The resulting cylindrical space between the cone base and the end area of the sounding tube can now be filled partly with soil. In order to measure the frictional resistance along the sounding tube, the tube is now pressed down over a distance of 20 cm, so that over a distance of 7,5 cm tube and cone are pressed down together. During this movement the soil between the two areas mentioned will be somewhat compressed, with the result that soil particles (especially fine sand) may be pushed into the space between tube and rod. This causes friction which has an effect on the accuracy of subsequent measurements of the cone resistances. This can be perceived when observing the readings of the manometer.

As an example a diagram of a set of readings is given in fig. 2. The movement of the cone is plotted horizontally against the readings of the manometer vertically. On this diagram line A represents the normal readings on the manometer and point P the reading that is registered. The falling off of the readings is

caused by the fact that at continued penetration of the cone the soil is given an opportunity to flow round the cone and this causes the resistance to drop.

However, when small sand particles penetrate between rod and tube, as indicated above, readings as represented by line B are obtained. The highest point of this line corresponds with the pressure on the sounding rod, necessary to overcome the friction between rod and tube. From then onward the forcing-down of the cone proceeds jerkily, as represented by points P<sub>1</sub> to P<sub>4</sub>, and it is possible that excessive values are registered.

The same thing might happen in reverse. Such is the case for the sounding of fig. 3(A). From 11.00 m to 14.80 m - N.A.P. the manometer gave no reading at all, and therefore it was concluded that the soil was so soft, that it could not carry the weight of cone and rods. Here also small sand particles of the overlying sandlayer had found their way into the space between tube and rod, and at the approach of the soft layer insufficient resistance was developed to overcome this friction.

These difficulties as well as the ensuing wear of the gland caused the author to shape the cone as shown in fig. 4. The object of this construction is that, by the presence of the protecting sleeve, the soil is prevented from penetrating between rod and tube and it has the additional advantage that continuous sounding can be performed more accurately. Similar ideas were developed by ir. G. Plantema. 2) The readings of the manometer follow now line

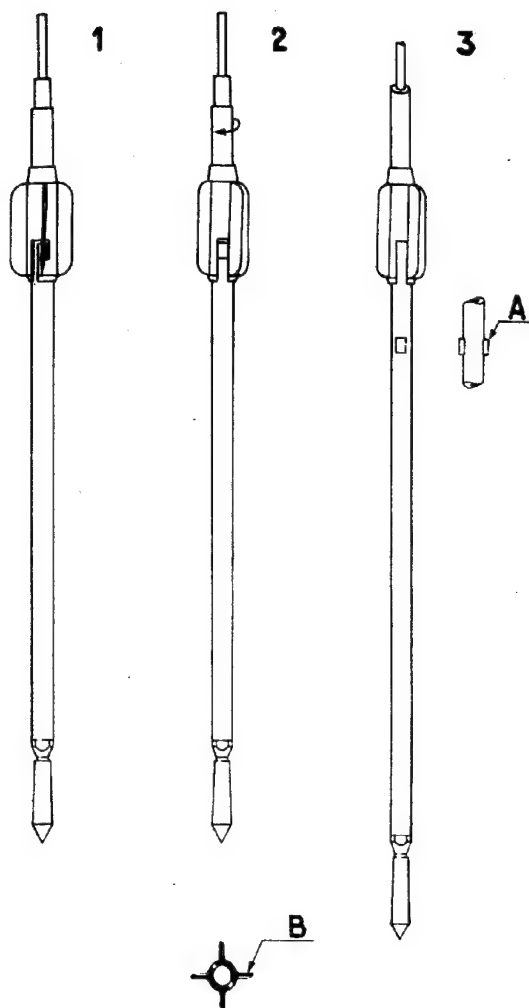


FIG.8

A<sup>1</sup> of fig. 2.

Fig. 3 shows the results of a sounding with this improved cone. The distance between the soundings A and B was 50 cm as measured on the ground surface. This shows that, at the same depth as at sounding A, with this new sealing device sounding resistances of 2-4 kg/cm<sup>2</sup> were measured.

An investigation is also made into the variation with the depth of distance  $a$  (see fig. 2) between the lower end of the tubes and the base of the cone, for the old and for the improved system. Fig. 5 shows the results of 2 soundings in close proximity. Sounding A is done with the old system, and B with the new system. The accompanying figures show the relationship of the variable distance  $a$  with the depth.

It is to be noted that with the new system the distance  $a$  remains always constant. The slight discrepancies are due to unavoidable measuring errors. With the old system the discrepancies are largest under the overlying sandlayer.

#### b. DRIVE SAMPLING APPARATUS.

In order to interpret successfully the

results of a sounding it is of prime importance to know also the nature and the properties of the soil layers. To this end the Soil Mechanics Laboratory of Delft has constructed a light soil sampler which is forced into the soil by means of the sounding apparatus (fig. 6). With this sampler undisturbed soil samples of 100 cm<sup>3</sup> may be obtained from any desired depth, without a casing.

In position 1 the sampler is ready to be forced into the soil. The lower end of the sampling tube is provided with a plug, attached to a rod which, while the sampler is forced down, bears by means of the notches  $a$  up against 2 similar notches on the inside of the extension tube. When the desired depth is reached, the apparatus is turned a quarter turn and the rod gets free from the notches in the extension tube. The turning of the plug itself is prevented by the wings on the plug (position 2). Now the sampler is lowered again, the plug disappears into the sampler and the latter is filled with soil (position 3).

In order to prevent that, at withdrawal the weight of the plug presses on the sample, the plug rod is kept up by means of the balls  $b$ , which find their support against a seat (position 4). After withdrawal the samples are pushed out of the sampling tube into zinc cylinders and sent to the laboratory for eventual tests.

#### c. DEEP-SOUNDING APPARATUS.

The deep-sounding apparatus for the determination of the bearing capacity of sandlayers, supporting foundation piles, is described in 1936 3) and has not been altered since in any essential respect. The improvements made to the apparatus as shown in fig. 7, aimed principally at a more economical working method. This has been achieved by using a more efficient pressure appliance and a frame built up from hollow steel beams, which reduces the weight and facilitates dismantling and transport.

An improvement in measuring technique is provided by the new hydraulic measuring device for reading the penetration resistances. The construction is based on past experience and special attention has been given to prevention of leakage and to low piston friction. It appears that the amount of friction works out at about 4% of the pressure at any moment. The anchoring of this apparatus may consist of a weighted floor underground or of screw-rods. If screw-rods are used, one should pay regard to the nature of the soil and the ground water level.

The results of several deep-soundings for one definite object often vary with respect to depth and strength of the sandlayers in which pile points must find their bearing.

In that case any desired supplementary investigation may only be concerned with the variation of the bearing value of the sandlayers with the depth, and measurement of the friction properties may be omitted, because the safe bearing value of a pile is mainly determined by the allowable stress under the point and the friction is usually not taken into account as a favourable influence.

In order to determine the bearing value in a simple way, the lower sounding tube has been provided with an enlarged section, which diminishes the friction along the tube surface. This enlarged section is constructed as a separate part which can be disconnected from the tube at any desired depth, mostly at the underside of the cohesive layers. Fig. 8 shows the position 1 of this "ring" just before it will



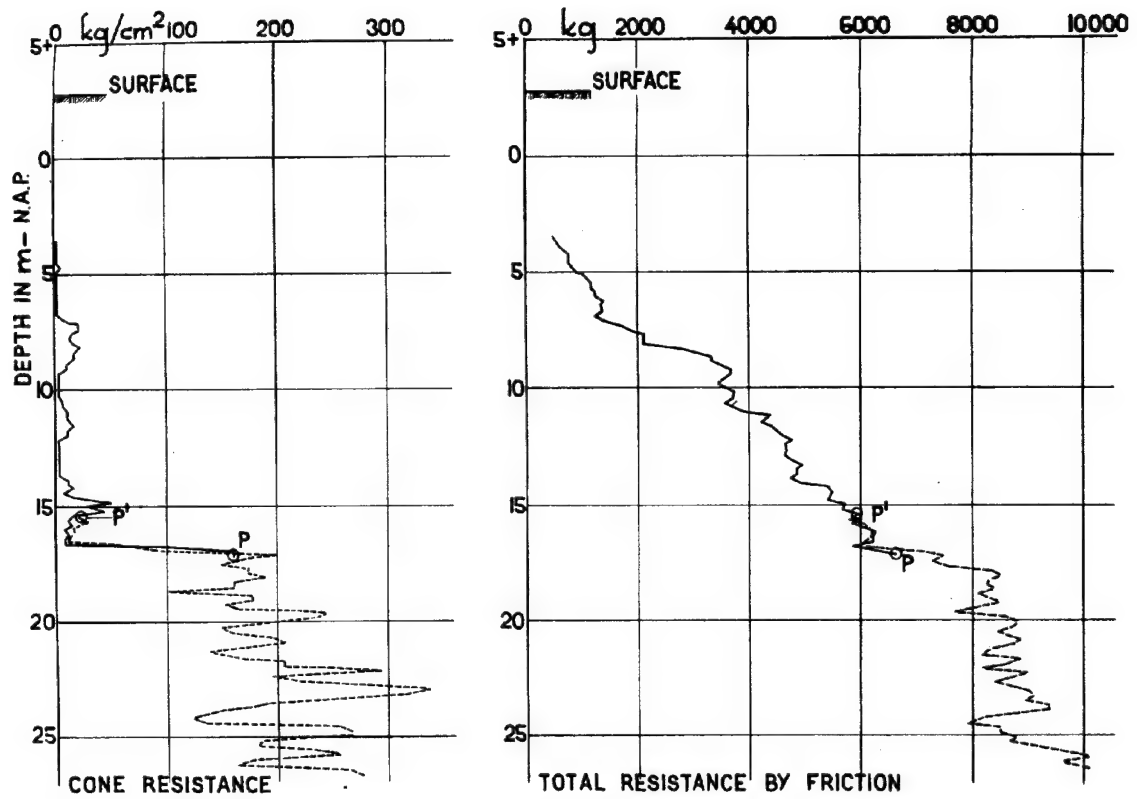


FIG.9

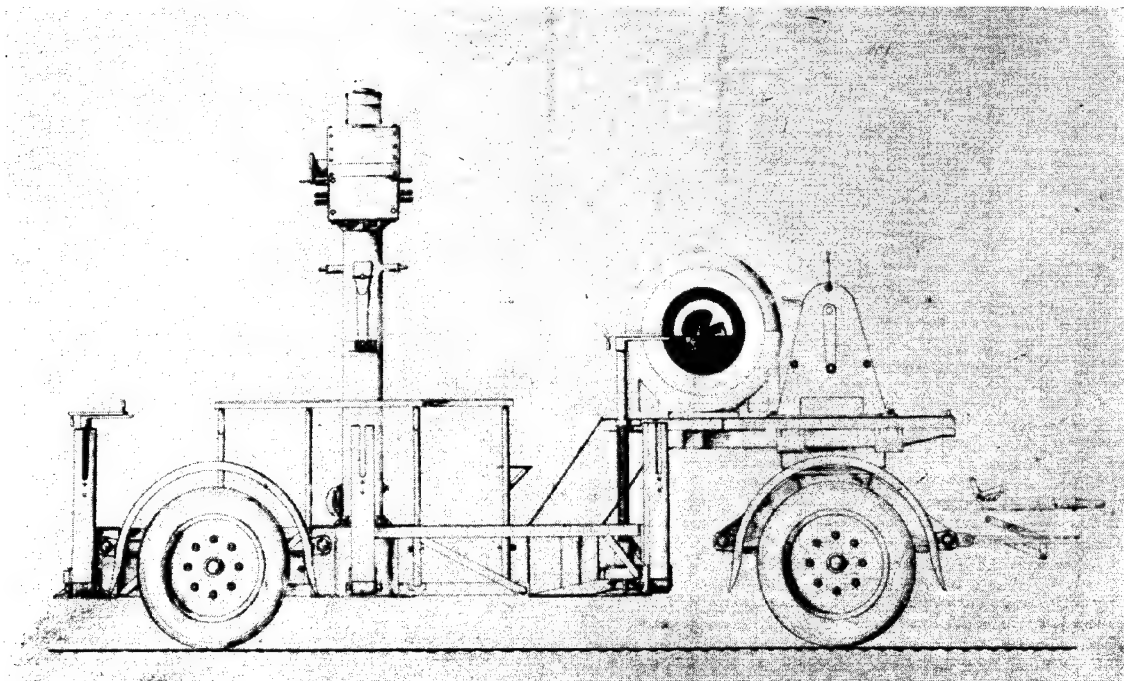


FIG.10 a

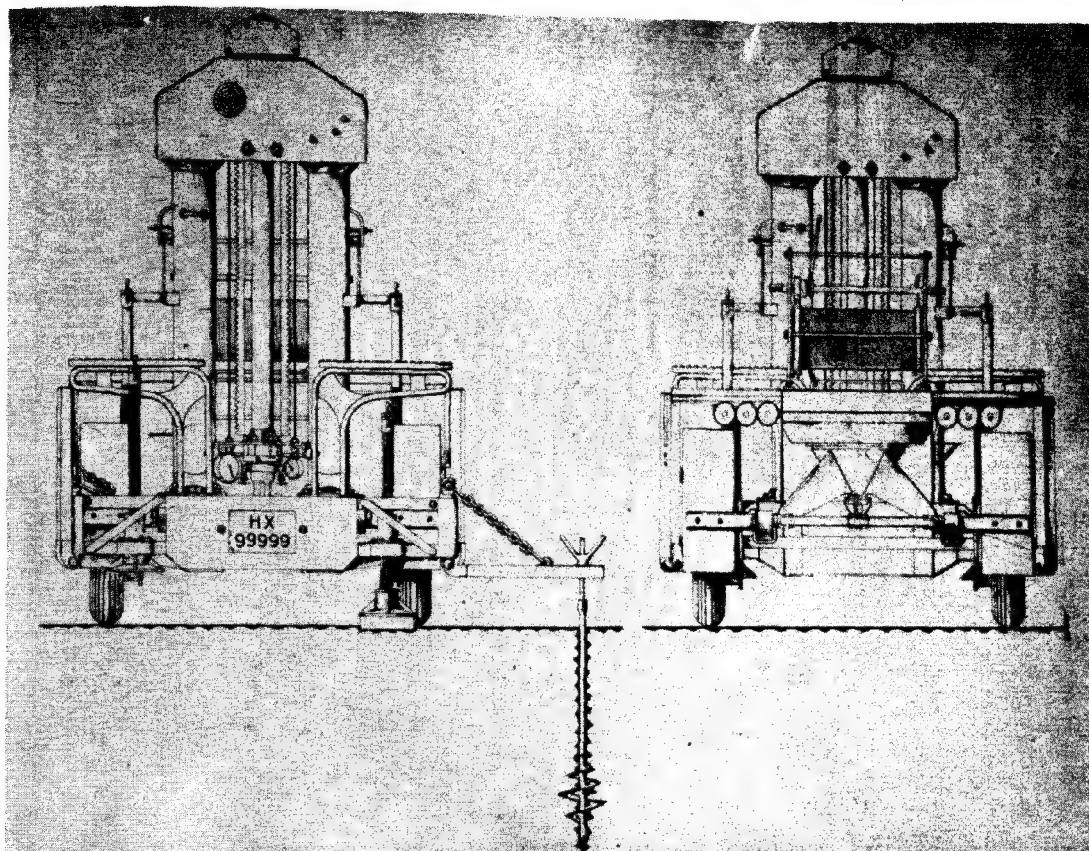


FIG.10b

be forced down. The notches A carry the ring with them. After the desired depth has been reached, the sounding tube is turned a quarter turn, so that the notches move in the slit (position 2). Subsequently the tube can slide freely through the ring and the sounding may start (position 3). While disconnecting the turning of the ring is prevented by the wings B.

Another advantage of this device is that deeper sounding becomes possible with the existing pressure arrangements. At the usual way of deep-sounding it is often seen that the friction along the surface of the sounding tubes is so high that the pressure capacity of the sounding apparatus is exhausted before layers of sufficient penetration resistance are found. Fig. 9 shows the results of such a deep-sounding. The full drawn line represents the results of sounding done in the usual way. At point P the tubes are with-drawn and a new start was made with the described device. From P1 downwards sounding has again proceeded after disconnection and the results are combined with the first results, as is shown by the dotted line in the figure.

For these "fast" soundings the sounding apparatus sketched in fig. 10 is now being designed. In order to facilitate transport, it is intended to place the apparatus on a specially constructed carriage, that will be pulled by a tractor. The reaction forces will be provided by 6 screw-rods, screwed into the ground. It is suggested to put the apparatus in position by raising the carriage to a truly hori-

zontal position by means of screw-spindles. This makes it also possible, when extracting the sounding tubes, to transmit the reaction forces directly to the ground via the spindles so that the springs of the carriage remain unstressed.

#### d. SOUNDING ON CANAL, RIVER, OR SEA BOTTOM.

In order to determine the bearing value of the soil in behalf of structures which are wholly or partly built in the water, it is necessary to carry out soundings under the water because the reduced load at that place has given rise to reduced effective soil stresses.

The problems to be solved consist mainly of the construction of adequate reaction supports and of a device against buckling of the sounding tubes. Special devices are required when working on tidal waters.

For the soil investigations in behalf of the reclamation of the former Zuiderzee a pontoon has been constructed by us in conjunction with the Department of the Zuiderzee Works. This pontoon is so designed that it can be sunk at any required spot. Fig. 11 shows the pontoon after sinking. The sounding can be done working from the deck.

The sinking is performed by opening a number of valves fitted on the deck; thereby the tanks are filled. After the completion of the sounding the tanks are emptied by means of a petrol driven pump (fig. 12).

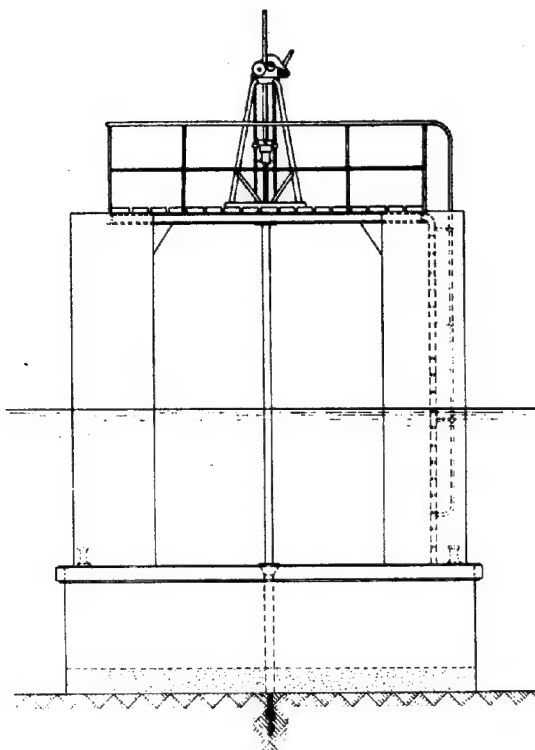


FIG. 11

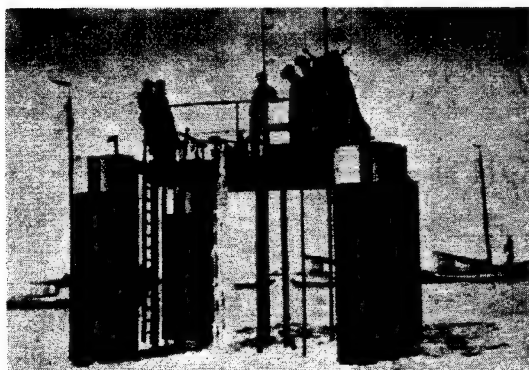


FIG. 12

This pontoon has the disadvantages that it can only be used on a flat bottom not deeper than 5 m under water, and in windy weather the structure tends to slide.

To overcome these disadvantages, for the investigations in behalf of the future tunnel under the Y at Amsterdam we have cooperated with the City Engineer's Department of Amsterdam in constructing a sounding tower, shown in fig. 13. The footing of this tower is ballasted and sunk with the aid of barges at the place of sounding (fig. 14). On this footing a hollow shaft is erected, connected to the footing with a cardan joint. The vertical position of the shaft is maintained by 3 steel wires, fastened to the corner points of the footing.

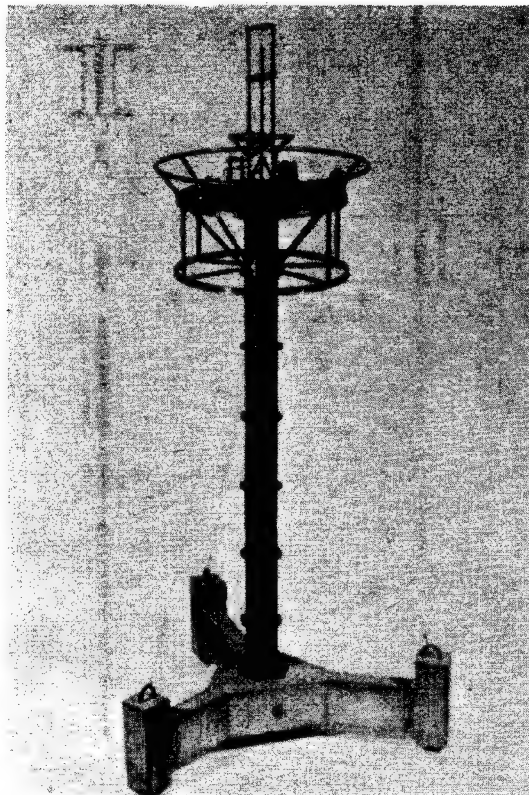


FIG. 13

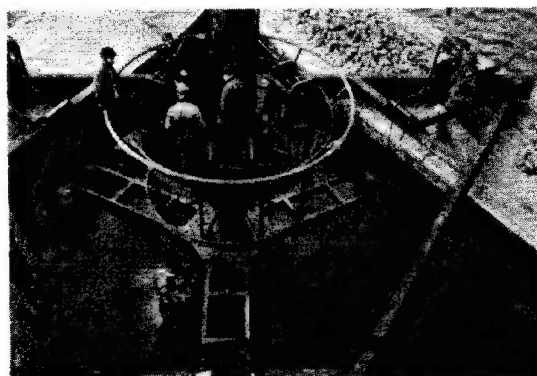


FIG. 14

The sounding apparatus is set up on the staging above the water line. To prevent the buckling of the sounding tubes, these are passed through a guide pipe running centrally through the shaft and supported at regular intervals. Thus a fairly stable arrangement is achieved which can be used at any water depth between 2 m and 16 m. However this is a costly construction.

In connection with the reconstruction of the war-damaged quay walls at Rotterdam, a large number of deep-soundings were required under the bottom of the river. The use of the sounding tower was impracticable, since the bottom

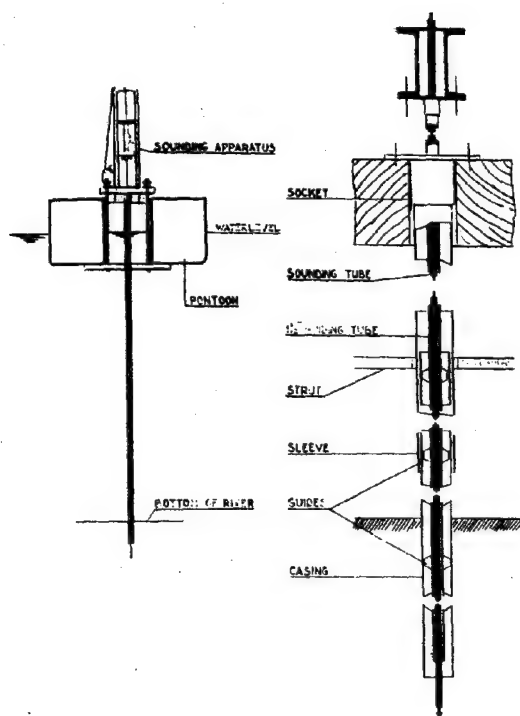


FIG.15

of the river was covered with debris from the destroyed quay walls. The City Engineer's Department succeeded in developing a method of deep-sounding, working from a pontoon barge, solving the problems arising out of the rise and fall of tidal water. The 300 ton barge is shown in fig. 15. A deep-sounding apparatus is set up above the cylindrical opening in the pontoon. The sounding proceeds as follows:

Working from the deck, first a 4" casing is placed to about 2 m under the river bottom. The top is then at about 20 cm above low water. Enveloping this casing, a 5" sleeve pipe is lowered, which is connected to the pontoon and takes part in the vertical tidal movement. The sounding tubes are prevented from buckling by a 1 1/2" guiding tube, which finds support against the casing by means of welded guides. All pipes together are secured against buckling by wooden struts in the hole in the pontoon.

During the sounding the rise and fall of ebb and flow is registered by a levelling apparatus set up on the shore and, with the aid of these readings, the results of the sounding are subsequently corrected.

#### REFERENCES.

- 1) Barentsen, P., Short description of a field-testing method with coneshaped sounding apparatus. Proc. Int. Conf. Soil Mech. 1936. Vol. I B-3
- 2) Ir. G. Plantema, Construction and Method of Working of a new Deep-sounding Apparatus, Proc. 2nd. Int. Conf. Soil Mech. 1948. Vol. I paper III b 6.
- 3) Laboratory of Soil Mechanics Delft. The predetermination of the required length and prediction of toe resistance of piles. Proc. Int. Conf. Soil Mech. 1936. Vol. I I-1

-O-O-O-O-O-O-

## SUB-SECTION III c

### MEASUREMENTS OF PRESSURES AND DEFORMATIONS

#### EXPERIENCE GAINED IN THE MEASUREMENT OF PORE PRESSURES IN A DAM AND ITS FOUNDATION

III c 1

MILTON G. SPEEDIE, M.C.E.

#### INTRODUCTION.

Fifteen piezometers have been installed in the embankment and foundation of the Eildon Dam, Victoria, Australia, to record pore pressures and so provide basic information for the design of an enlargement of this structure. It was necessary to select instruments suitable for installation through about 100 feet vertical thickness of rock and clay embankment and which would permit pressure reading to be made at the level of the embankment crest. They are of two types designated 1 and 2 as shown on drawing No. 1, and have been located in two cross-sections of the dam.

#### LOCAL CONDITIONS.

The dam was originally constructed in the period 1915 to 1929 and consists of a zoned clay and rock fill embankment with a central concrete core wall extending from the foundation rock to the top of the bank. For the most part the interbedded sandstones, slates and shales of Silurian age which form the foundation rock are overlaid by alluvial deposits consisting of about 6 feet of sandy gravel which in turn is covered by 15 feet of medium clay. Typical mechanical analyses of these materials are shown on drawing No. 3 and physical properties of the clay are as follows:

## Physical Properties of clay.

	6 feet above Piezometer 4	4 feet above Piezometer 7	Average Values
Wet Density lbs. per cub.ft.	124.6	118.3	125
Dry Density " " " "	99.7	86.4	102
Moisture Content %	24.9	36.7	
S.G. of Particles	2.72	2.74	2.72
Permeability Ft. per yr.			0.003

Only sufficient of the foundation materials were excavated to enable the core wall to be keyed into the rock. Immediately upstream of the concrete wall a clay blanket wall was constructed from the surface of the foundation clay to an elevation 5 feet below top of embankment, having a thickness of about 17 feet at the top and an upstream slope of 6 on 1.

The whole of the downstream and remainder of the upstream portions of the bank were composed of rock fill placed directly on the clay. This material is very permeable and free draining with an average density of 125 pounds per cubic foot.

An extensive subsidence occurred in the upstream portion of the embankment during a rapid draw down of the reservoir in 1929 when construction had been practically completed. This subsidence and the subsequent dam reconstruction involving the placing of much additional rock filling were described in detail elsewhere. (1) The greatest subsidence occurred at chainage 1550 feet for which the present profile is as shown in drawing No. 3 together with the locations and recordings of the piezometers installed at this cross-section. The present location of the clay zone does not agree with that previously reported on account of slow continuation of the subsidence for some time after completion of the original exploratory boring in the embankment.

PIEZOMETER INSTALLATION.

Two types of piezometers were installed, their constructions and details of the installation being as shown in drawing No. 1.

Piezometers type 1 closely follow a design used by the United States Bureau of Reclamation and consist essentially of a bronze body in which is mounted a diaphragm, subject to the hydrostatic pressure on its underside. A copper tube enclosing an insulated wire connects the upper portion of the body with the recording panel and air pressure is applied through the tube to the cell until deflection of the diaphragm breaks an electric circuit (through insulated wire, contact button, diaphragm, body, tube, lamp and battery) and extinguishes a lamp, the pressure of air being recorded by a Bourdon pressure gauge.

Piezometer type 2 is of similar construction but has two tubes instead of one thus permitting flushing out of any water which may leak past the diaphragm or condense from the air.

The piezometers were mounted in a steel tube fitted with a pointed shoe to assist driving. Coarse sand was packed around the piezometer heads and the voids filled with water.

The remainder of the steel tube was filled with concrete, rubber discs being provided at intervals to ensure that copper tubes retained their correct positions and did not contact the outer tube.

When placing the assembly in the clay wall or foundation the tube was jacked into position. No pilot hole was bored where the clay was soft but in hard or stiff clay a pilot hole was necessary and this was made at least an inch smaller in diameter than the tube. All copper tubes at each cross section were led to a panel mounted on the top of the embankment and fitted as shown in drawing No. 1 and illustrated in photographs No. I and II. Air pressure is supplied by an electric motorcompressor unit illustrated in photograph No. III, and air pressure measurement is by means of a calibrated Bourdon gauge.

PRECAUTIONS.

The following precautions were taken:

- 1) The use of dissimilar metals in the installation was avoided. Experience (2) with other equipment showed that a sealed galvanized pipe filled with water generated hydrogen by galvanic action, thus producing high pressures. For this reason the piezometers and copper tubes are insulated from the steel tube by rubber discs.
- 2) Diaphragms and contact buttons were carefully adjusted, and the cell subjected to pressure to test its operation and watertightness, prior to installation.
- 3) Each piezometer was calibrated to determine the pressure difference required to break the circuit. This varied from 1 to 4 feet of water and 8 feet for Piezometer No. 7, all corrections to be subtracted from air pressure readings to give pressure below diaphragm.
- 4) Copper tubes were joined by compression couplings or brazing. Sweating with solder was avoided.
- 5) Air pumped into the tube when taking readings was first dried by passing through calcium chloride crystals. It is doubtful whether this procedure provides adequate desiccation.

METHOD OF MAKING READINGS.

- 1) Air pump and gauge are connected to the large tube leading to piezometer. This is done by closing relief valve and connecting rubber tube to valve fitting.
- 2) Electric circuit is completed through piezometer battery and lamp by burning control knob to appropriate contact on multiple switch.
- 3) Valve on air line is slightly opened and air pressure very slowly built up until lamp is extinguished. Pressures at which lamp flickers or becomes dim are also recorded.





Front View

PHOT. 1



Rear View

PHOT. 2

4) Air pressure is slowly reduced until lamp again glows brightly. Dim and flicker pressures are again noted.

5) Tubes are dewatered by opening return tube to atmosphere and building up an air pressure of 150 feet head of water (65 lbs. per sq. inch) at top of down tube.

6) If the tubes are found to contain water repeat steps 1 to 4 above.

The first set of readings is used unless water is found in the cell, in which case the second set is adopted. Where the breaking of the circuit is not definite the points at which the lamp changes from bright to dim, or vice versa, are considered to indicate deflection. Flickering of the lamp shows instability of the diaphragm and when confirmed by recordings on other dates may indicate pore pressure.

#### EXPECTED PRESSURE VARIATIONS.

At the time of installation the soil disturbance due to forcing steel tubes into it must produce high local pore pressures. These would dissipate gradually while the pressure inside the tubes will build up until they attain that of the pore water in the soil. The pressure of the pore water and the water in contact with the piezometers will then still further reduce, until the effect of the soil disturbance disappears. Thereafter the pore water pressure should be governed by water level variations although this condition can only be definitely recognized when pressure recordings show increasing pressures for the second time.

The pore water pressures can vary with water level for two reasons.

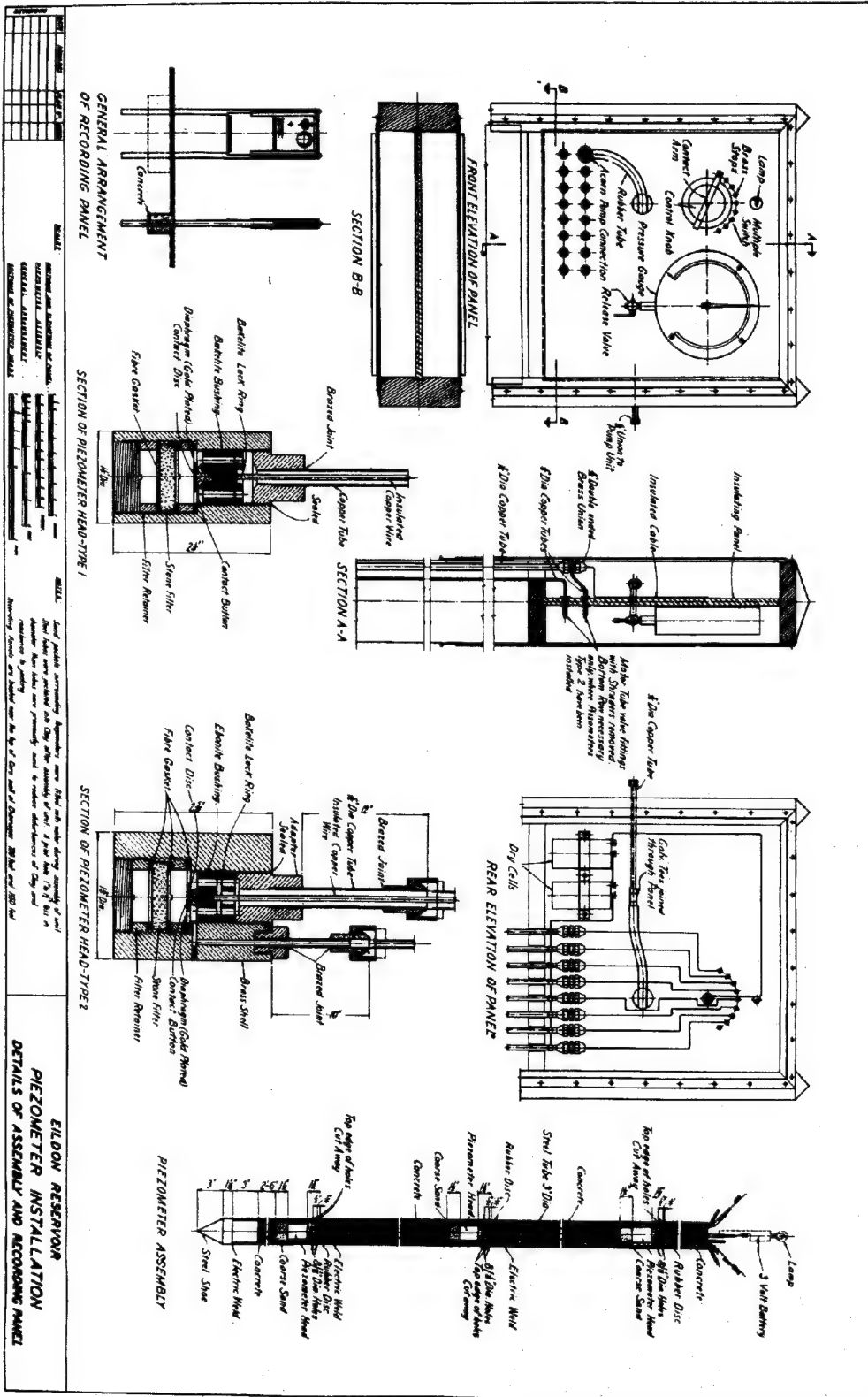
1) The loading on the surface of the clay varies and portion of this variation would be transmitted to the pore water. Where there is no rock filling the variation in water level represents the change in pressure on the clay expressed as hydrostatic head. Where rock fill overlies the clay to an elevation above water level the change in vertical pressure equals the weight of water contained in the voids of the filling within the range of water level variation i.e. about 27% of hydrostatic pressure variation. In addition to the vertical loading there will be a lateral component due to the embankment slope; this would be greater for low water levels than for high.

2) Hydrostatic pressure changes can be transmitted through the pore water of the clay mass. Pressure variations transmitted in this way are likely to exhibit a time lag with respect to the water level changes producing them.

#### RECORDINGS.

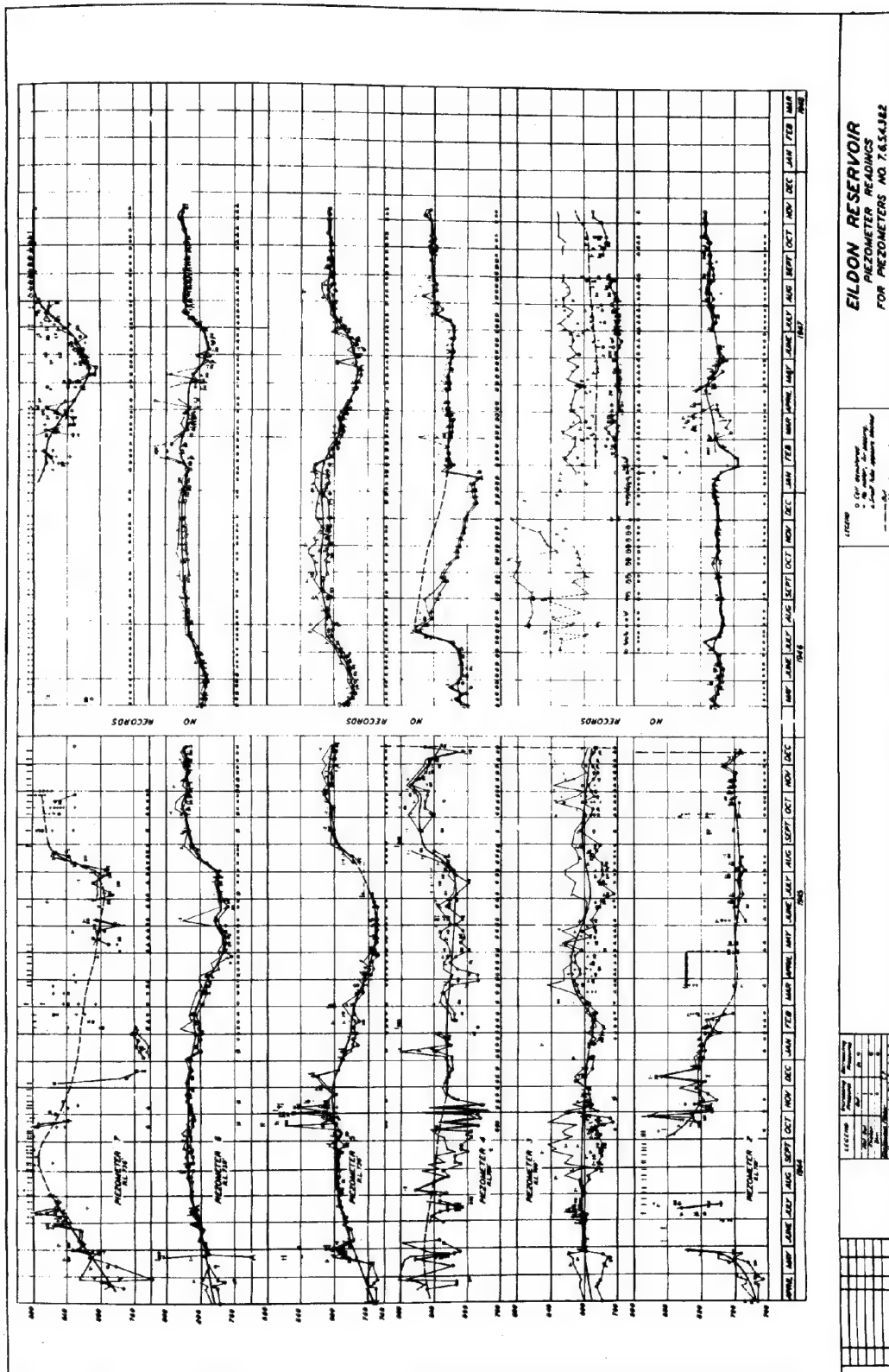
Details of the locations and recordings of type 2 piezometers are shown on drawings Nos. 2 and 3. Type 1 cells were placed at another location in the dam and their readings have been more consistent and showed lower pressures than for type 2 piezometers but are considered unreliable as stated below so the readings are not recorded here.

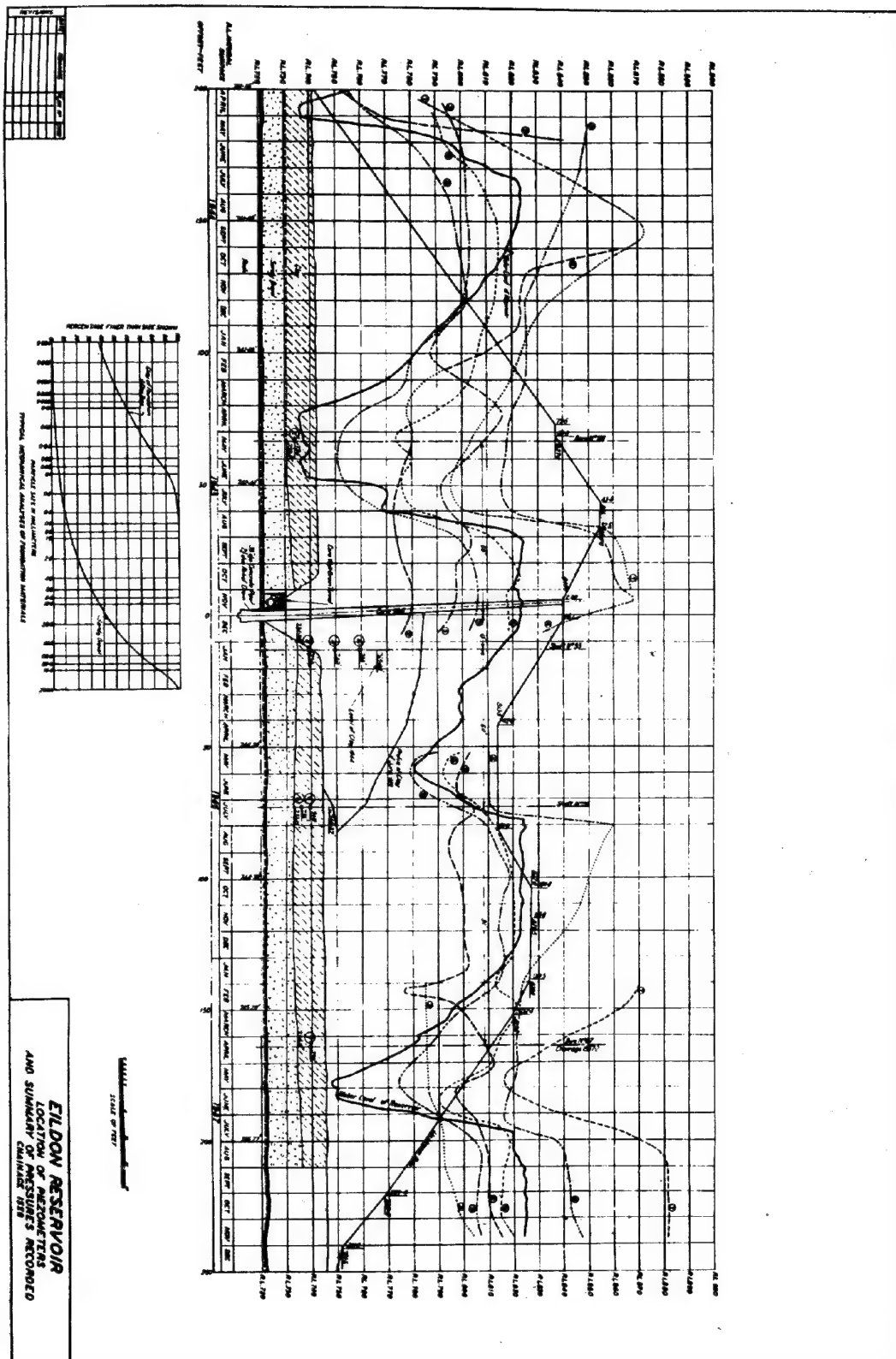
Recordings of type 2 cells show -  
a) About 15 months after installation the piezometers indicated increasing pressures for the second time. This is thought to make the



DRAWING 1









Portable Air-Compressor Unit.

PHOT. 3

commencement of the first definitely representative readings of pore water pressures in the embankment.

- b) Thereafter the pressure recordings increase and decrease with water level. Particular comments on individual cells are given below.
  - c) Piezometer 1 has shown zero pressure as would be expected downstream of the core wall.
  - d) Piezometer 2 has given readings which are generally consistent regarding pressures at which the diaphragm deflects with increasing and decreasing air pressure. No correlation with water level has been possible.
  - e) Piezometer 3 recordings have been very irregular and no conclusions can be drawn.
  - f) Piezometer 4 has given fairly consistent readings but considerable quantities of water have collected therein. In the period August 1946 to January 1947 water accumulated in the tubes as a result of inadequate flushing by an inexperienced operator. In January 1947 well over a pint of water was flushed from the tubes which would account for the whole of the 50 feet rise in pressure at that time.
  - g) Piezometer 5 has been consistent and pressures have varied with water level, generally with a small lag. The variation amounting to 45% to 87%, average 58%, of change in water level, is greater than the variation in vertical pressure on the clay surface.
  - h) Piezometer 6 also gave consistent readings with variations of 39% to 71% (average 55%) of change in water level. When the reservoir is full the hydrostatic head given by both piezometers 5 and 6 approximates that to water level.
  - i) Piezometer 7 has recorded very high pressures. For a long time the electric circuit could not be broken with air pressures up to 150 feet head of water and it was thought to have a short circuit or other fault. However, in 1944 a large quantity of water (estimated at 70 feet depth) collected in the tubes and some readings were then obtained again. During 1947 pressures were recorded and they varied with water level but were about 60 feet greater than hydrostatic from reservoir level.
- Slight upstream movements of the rock fill observed during draw down of water level are consistent with high pore pressure.
- The high pressures might be interpreted as indicating a condition of partial consolidation in the clay, but the large variation with water level seems inconsistent with this

interpretation. Lateral pressures should be greatest with low water level and might be expected to limit the pore pressure reduction during drawdown of water level. However, no such limitation has occurred.

#### CONCLUSIONS.

It is concluded that -

- 1) The diaphragm type of piezometer has given consistent readings over a period of 3½ years.
- 2) Water has been found to accumulate in the piezometers due to condensation from air pumped into the tubes, and/or as a result of leakage, consequently type 1 cells which are not capable of being cleared of water are considered unreliable and will give misleading readings.
- 3) The pressures in the foundation clay are high.
- 4) The variation in hydrostatic pore pressure in the foundation clay is less than the variation in reservoir water level but considerably more than the variation in total pressure (rock fill plus water) on the foundation.

#### ACKNOWLEDGEMENT.

The Author wishes to thank Mr. L.R. East, M.C.E., M.I.C.E., M.I.E.Aust., Chairman, State Rivers and Water Supply Commission, Victoria, for permission to publish the paper. All designs and investigation work are carried out under the direction of Mr. R.G. Knight, M.C., M.C.E., M.I.C.E., M.I.E.Aust., Chief Designing Engineer.

#### BIBLIOGRAPHY.

- 1) "The Subsidence of a Rock Fill Dam and the Remedial Measures Employed at Eildon Reservoir, Australia", R.G. Knight, Jour.Inst. Civ.Engrs., 1938.
- 2) "Pore Pressures in Earthen Embankments", Milton G. Speedie, The Commonwealth Engineer, December 1942.

#### SUMMARY.

Piezometers of two types, totalling fifteen in number, have been installed in the embankment and foundation of the Eildon Dam, Victoria, Australia, and readings are available for a period of 3½ years.

The dam consists of a zoned embankment of clay and rock fill with a central concrete core wall extending from the foundation rock to the embankment crest. The clay and rock fill embankment rests on a natural clay strata overlying sandy gravel and rock.

In both types of piezometers pore pressure is transmitted to the underside of a diaphragm while air pressure is applied to the top until deflection breaks an electric circuit and indicates equality of air and pore pressure. Type 2 cells differ from Type 1 in that two tubes lead to the upper side of the diaphragm and so permit removal of any water that accumulates there.

Precautions taken in manufacturing and installing the cells are listed together with the method of making readings. Illustrations give details of the equipment, installation, and readings, the latter being briefly discussed in the latter press.

Pore pressures were disturbed by installation of the piezometers but, after an adjustment period, consistent recordings were obtained

which varied with water level, but to an extent greater than the variation in total pressure on the clay surface and somewhat less than the corresponding variation in reservoir level. In general, the maximum pressures for each instrument corresponded with or were greater than hydrostatic from spillway crest level.

It is concluded that the diaphragm type of piezometer has given consistent readings over a period of 3½ years and that provision must be made for removing water which accumulates in the cells by leakage or condensation. Results obtained from cells without such provision are unreliable.

-0-0-0-0-0-0-

### III c 2

#### SOME RESULTS OF WATERPRESSURE MEASUREMENTS IN CLAY-LAYERS

E. DE BEER and H. RAEDSCHELDERS  
Ghent (Belgium)

##### INTRODUCTION.

To control the stability of deep cuts in clay-layers several waterpressure measurements were performed. Most of the tested clay-layers are situated between an upper and a lower sand layer or limestone layer, having a different hydrostatic pressure. Beforehand one should believe that the waterpressure in the clay-layer would be a mean between the upper and the lower watertable. The results of the measurements are often quite different from this expectation.

##### CANAL CUT AT GODARVILLE FOR THE CANAL BRUSSELS-CHARLEROI.

To allow navigation for 1350 ton ships, a deep cut of a depth of 43 m has to be constructed at Godarville. At this location the following layers are generally found, starting from the surface of the ground:

- 1) loam or loamy fine sand.
- 2) more or less sandy clay.
- 3) clayey sand.
- 4) more or less sandy clay.
- 5) limestone.

The physical properties of a typical sample of each of these layers are given in table I. None of the layers can be considered as homogeneous.

The loam or loamy fine sand (layer 1) belongs to the pleistocene, the layers 2 till 4 belong to the tertiary ypresian formation ( $\gamma_2 - \gamma_{1b} - \gamma_{1a}$ ). The limestone is of secondary age.

In some borings there was a sand layer belonging to the tertiary Lutetian formation ( $B_1$ ) between the pleistocene top-layer and the tertiary Ypresian sandy clay-layer. In one boring (group 605) a sand-layer of the secondary Wealdien formation ( $W$ ) was found between the limestone and the Ypresian clay formation.

A certain number of borings were performed. During the borings the water-level was accurately recorded, especially at morning before continuing the boring. Depending on the permeability of the soil the water had opportunity to come more or less to hydrostatic equilibrium. In this way the points indicated by a single circle in the fig. 1 are obtained and the points corresponding to a same boring are connected with a dotted line. In these figures the depth underneath the soil surface is taken as an ordinate, and the piezometric

waterheight corresponding to this depth as an abscissa.

The pressures so measured during the borings are not necessarily exact, because it is not sure that in one night the hydrostatic equilibrium has been reached. But from their variation with depth can be deducted how many independent watertables were met during the boring. Thus when a boring was finished, at a mutual distance of at least 2 m., there were performed a certain number of complementary borings, at least as many as different watertables were recognized. During the execution of these complementary borings the variation of the waterlevel was recorded as for the primary boring. The complementary borings were ended at different depths, and almost in different soil layers. Open tubes, 2" diameter, were put in place.

In these open tubes the fluctuations of the waterlevel were controlled during several months, thus giving a more exact value of the piezometric height at the level of the bottom of the tube. The so recorded values are indicated by crosses and a letter in the fig. 1.

Group of borings 601.

There is a different water-level in the loam layer and in the limestone layer. The pipes b and c, located at different depths in the sandy clay indicate that the waterpressure in this layer increases hydrostatically with depth, according to the water level in the loam. During the boring 601-a the waterlevel starts to drop underneath the level +115. Thus it is as if a more impervious skin existed near this level.

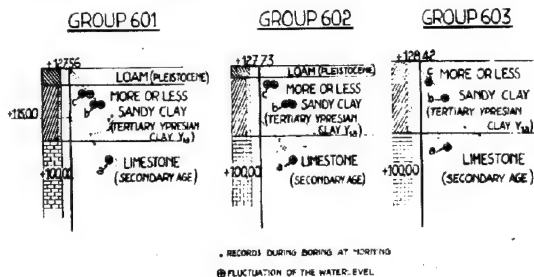


FIG.1

#### Group of borings 602.

There is a different water-level in the loam and in the limestone. The pipes b and c, and also the waterlevel variations recorded during boring a, indicate that the waterpressures in the sandy clay layer follow a hydrostatic law according to the waterlevel in the loam.

#### Group of borings 603.

Same conclusion as for group 602.

#### Group of borings 604.

Here the piezometric height in the limestone is nearly the same as that in the loam. Thus one gets a nearly hydrostatic law through all the layers.

#### Group of borings 605.

The pipes c, d give a hydrostatic law in the sandy clay with respect to the water-level in the loam. The pipes a and b both in the sand give a hydrostatic law in the sand. It is worthwhile to note that during the boring a, the recorded levels in the sandy clay follow an hydrostatic law, the fall of pressure being located in the sand.

#### Group of borings 606.

A sandy clay layer is located between a loam- and a clayey finesand layer, having distinct water-levels. Pipes b and c indicate a hydrostatic law in the sandy-clay layer with respect to the water-level in the upper loam layer.

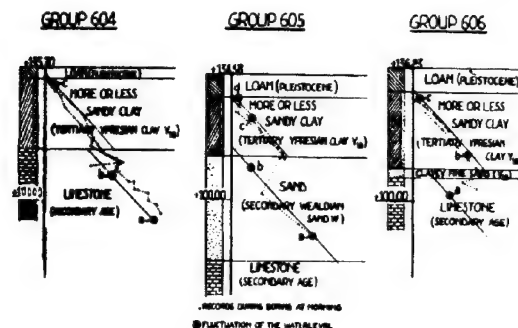


FIG.1

#### Group of borings 607.

This group is composed of 5 pipes and shows 5 distinct layers, and 3 distinct water-tables. The variations of the water-levels recorded during the borings themselves are rather erratic, but the measurements in the pipes give very concordant results.

The pipe d placed at the top of the clayey sand layer, sandwiched between the two sandy clay layers shows zero pressure. Pipe e shows a hydrostatic law in the upper sandy clay layer in respect with the open water-level found in this layer. Pipes b and c give a hydrostatic law in the lower sandy clay layer with respect to the water-level in the clayey sand layer.

#### Group of borings 608.

Pipes d and e show a hydrostatic law in the upper sandy clay with respect to the open water-level found in this clay. Pipes b and c in the lower sandy clay layer, and also pipe a in the limestone show a hydrostatic law with respect to the water-level in the clayey sand layer. In this case there should be no distinct water-level in the limestone.

#### Group of borings 609.

The waterpressures in the lower sandy clay

layer and in the limestone seem to follow the water-level in the clayey sand.

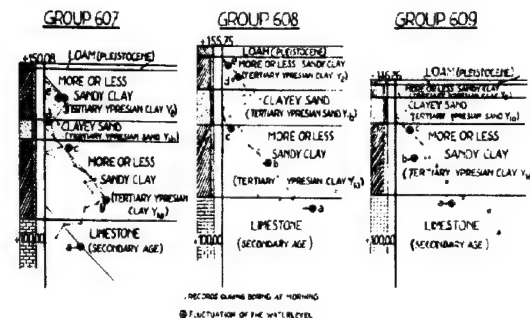


FIG.1

#### Group of borings 610.

The hydrostatic law in the lower sandy clay layer in respect with the water-level in the clayey sand layer, is shown by the pipes b and c, and also by the records during the boring 610a.

#### Group of borings 611.

The pipes b and c show a hydrostatic law in the lower sandy clay layer in respect with the water-level in the clayey sand layer. It must be noticed that the records during the borings themselves are very different from one boring to another especially in the clayey sand layer. Of course these records have only a relative value, as already has been explained.

#### Group of borings 612.

The only difference from the other groups is, that here a fine sand layer between the lower sandy clay-layer and the limestone has been encountered.

All other groups of borings and pipes of the cut at Godarville give analogous results.

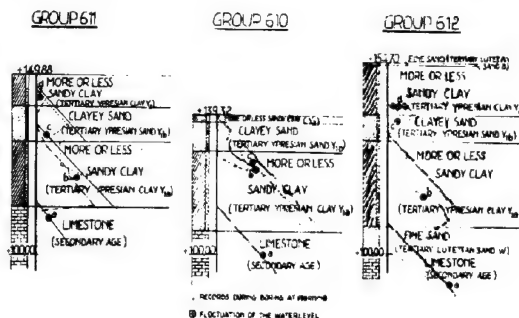


FIG.1

#### CANAL CUT AT EIGENBILZEN FOR THE ALBERTCANAL.

To cut the crest between the basins of the Meuse and the Scheldt a cut of a maximum depth of 29 m was dug at Eigenbilzen for the Albertcanal. At this location the following layers are generally found, starting from the soil-surface:

- 1) loam
- 2) in some places cobblestones, in other hill-sidewaste.
- 3) a pleistocene layer of fluvial origin (Pl<sub>2</sub>)
- 4) a pleistocene gravel (Pl<sub>1</sub>)

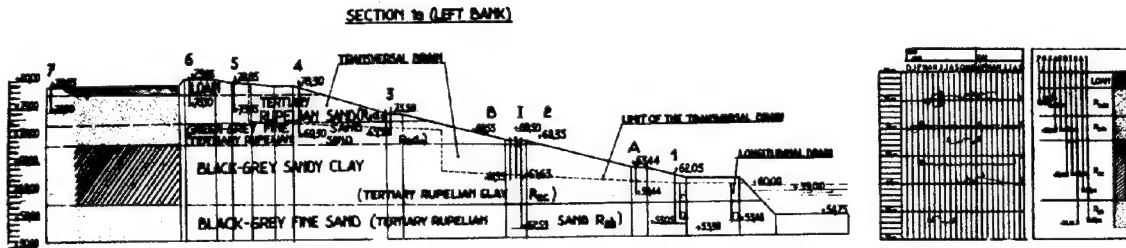


FIG.2a

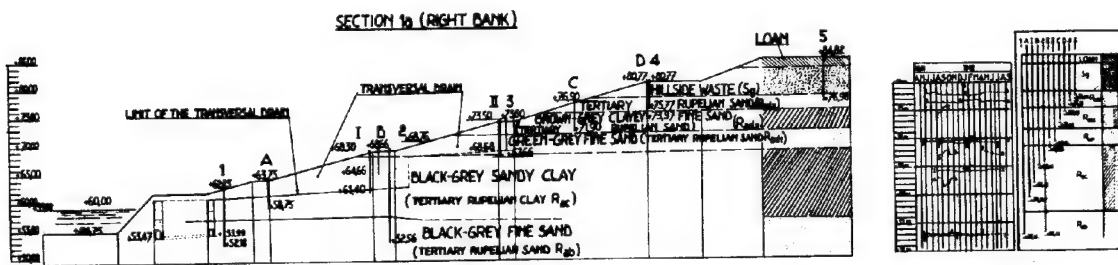


FIG.2b

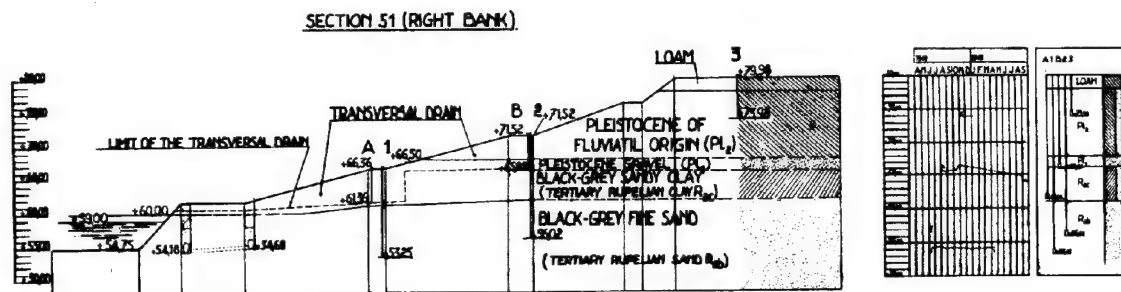


FIG.2c

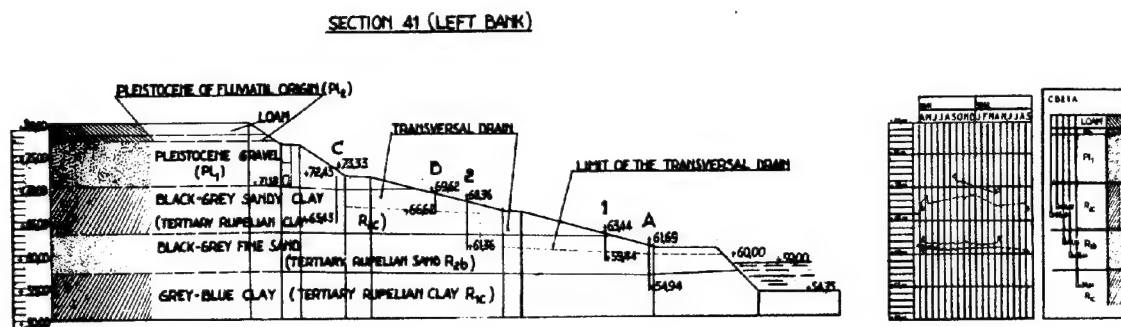


FIG.2d

CANALCUT AT EIGHENBILZEN FOR THE ALBERT CANAL



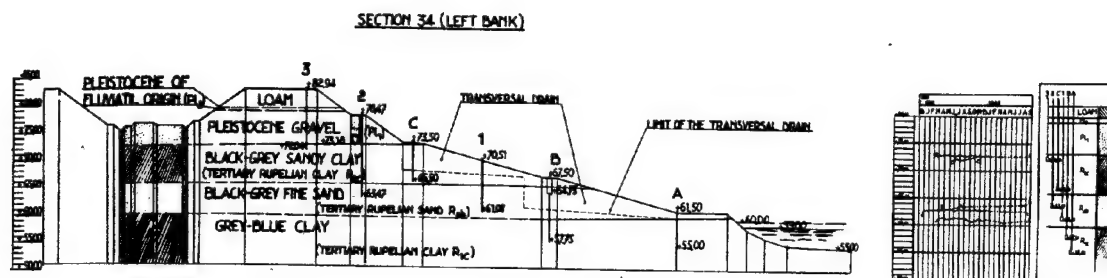


FIG.2e

- 5) a grey fine sand belonging to the tertiary Rupelian sand  $R_{2d3}$ .
- 6) a brown-grey clayey fine sand belonging to the tertiary Rupelian sand  $R_{2d2}$ .
- 7) a green-grey fine sand belonging to the tertiary Rupelian sand  $R_{2d1}$ .
- 8) a black-grey sandy clay belonging to the tertiary Rupelian clay  $R_{2c}$ .
- 9) a black-grey fine sand belonging to the tertiary Rupelian sand  $R_{2b}$ .
- 10) a grey-blue clay belonging to the tertiary Rupelian clay  $R_{1c}$ .

There, where the Rupelian sandlayers  $R_{2d1}$ ,  $R_{2d2}$  and  $R_{2d3}$  are found, the Pleistocene formations  $Pl_1$  and  $Pl_2$  don't exist.

The physical properties of a typical sample of the principal layers are given in table II.

To obviate the waterpressures in the different layers longitudinal and transversal drains were provided, as indicated on the sections of the figures 2. The transversal drains are located on mutual distances of about 20 m.

After the canal cut existed already several years, 34 piezometers were put in place, as indicated on the figure 4. Twenty piezometers have their end in more pervious layers and are of the open type; fourteen others have their end in clayey layers and are of the closed type.

The open piezometers are steel tubes with an internal diameter of 2". The end of each of the piezometers is perforated with holes and surrounded with a metal gauze over an height of 25 cm. After the tubes have been lowered in the hole of the boring, the filtering end is surrounded with clean coarse sand. Above the sand clay was put around the tubes and carefully compacted, while the boring tubes were extracted.

The closed piezometers consist of  $\frac{1}{2}$ " diameter steel tubes, connected to a capillary mercury gauge. At their end the tubes are perforated over an height of 15 cm and surrounded with metal gauze. A scheme of the closed piezometers is given in figure 3. The open piezometers are indicated by numbers, the closed by capital letters.

Before putting the 34 more accurate piezometers into place, some  $\frac{1}{2}$ " diameter tubes already had been put. The latter are indicated by Roman numbers.

Section 1 a (Left Bank) fig. 2a.

There are independent water-levels in the sandlayers  $R_{2d1}$  and  $R_{2b}$ . The open tube I and the closed piezometers A and B are put in the

clay layer  $R_{2c}$ . The recorded waterpressures in this clay-layer are much higher than those corresponding to the water-level in the lower sand layer  $R_{2b}$ . The waterpressures recorded with the closed piezometer B are higher than those recorded with the open tube I although located nearly at the same spot. In the fine sand layer  $R_{2d3}$  there is a water table independent from that in the fine sand layer  $R_{2d1}$ .

It is worthwhile to note that the locations of all the piezometers are not more distant than maximum 10 m from the transversal drains.

Section 1 a (Right Bank) fig. 2 b.

There are independent watertables in the sand layers  $R_{2d3}$ ,  $R_{2d1}$  and  $R_{2b}$ . In the brown-grey clayey finesand layer  $R_{2d2}$  are located the closed piezometers C and D. The waterpressures of these piezometers are not influenced by the waterlevel in the lower sand layer  $R_{2d1}$ .

The waterpressure given by D is even higher than that corresponding to the waterpressure in the upper sandlayer  $R_{2d3}$ , and the piezometer C, though located at the base of the clayey layer  $R_{2d2}$  gives practically a hydrostatic pressure in respect of the watertable in the sandlayer  $R_{2d3}$ .

In the claylayer  $R_{2c}$  are located the closed piezometers A and B, and the open pipe I. The recorded waterpressures don't correspond to the watertable in the lower sandlayer  $R_{2b}$ .

The waterpressures given by the closed piezometer B are higher than those deducted from the open pipe I, although having nearly the same location.

Section 51 (Right Bank) fig. 2c.

There are independent watertables in the layer  $Pl_2$  of fluvial origin, in the pleistocene gravel  $Pl_1$  and in the sandlayer  $R_{2b}$ .

In the claylayer  $R_{2c}$  was put the closed piezometer A. Although located at the base of the claylayer, the piezometer is practically not influenced by the waterlevel in the lower sandlayer  $R_{2b}$ .

Section 41 (Left Bank) fig. 2d.

There are independent watertables in the layer  $Pl_1$  of fluvial origin and in the sandlayer  $R_{2b}$ . In the claylayer  $R_{2c}$  are put the closed piezometers B and C. The waterpressures in them are not influenced by the watertable in the lower sandlayer  $R_{2b}$ .

In the claylayer  $R_{1c}$  is put the closed piezometer A. The recorded pressure is nearly



TABLE I

Sample	Nature of soil	Depth under-neath soil surface	Granulometric size						Limits of Atterberg			Organic content	Chalk content	Volume weight	Dry weight	Water content	Percentage of voids	Penetration value
			IV from 2 to 0.074 mm	III <sub>b</sub> from 0.074 to 0.02 mm	III <sub>a</sub> from 0.074 to 0.02 mm	II from 0.020 to 0.002 mm	I from 0.002 to 0.0002 mm		Liquid limit	Plastic limit	Plasticity index							
		m	%	%	%	%	%	%	%	%	%	%	%	t/m <sup>3</sup>	t/m <sup>3</sup>	%	%	kg/cm <sup>2</sup>
27749-266-4	loam	1,50		5	47	31	17		34,4	18,1	16,3	0,3	3,8	2,010	1,625	23,5	38,6	4,1
31549-266-640	loamy fine sand	4,45		51	35	8	6		35,8	23,4	12,4	0,5	2,4	1,920	1,510	27,1	43,0	6,2
31534-266-1567	more or less sandy clay	3,25	1	21	39	18	21		69,7	30,2	39,5	0,6	3,2	1,768	1,265	39,5	52,5	7,7
27772-266-1308	clayey sand	9,80		75	20	2	3		29,7	21,6	8,1	0,5	0,5	1,600	1,320	21,2	50,1	1,2
31521-266-1322	more or less sandy clay	16,20	9	50	10	11	20		49,8	19,3	30,5	1,1	4,4	1,990	1,625	19,8	38,6	14,5

TABLE II

Sample	Nature of soil	Depth under-neath soil surface	Granulometric size						Limits of Atterberg			Organic content	Chalk content	Volume weight	Dry weight	Water content	Percentage of voids	Penetration value
			IV from 2 to 0.074 mm	III <sub>b</sub> from 0.074 to 0.02 mm	III <sub>a</sub> from 0.074 to 0.02 mm	II from 0.020 to 0.002 mm	I from 0.002 to 0.0002 mm		Liquid limit	Plastic limit	Plasticity index							
		m	%	%	%	%	%	%	%	%	%	%	%	t/m <sup>3</sup>	t/m <sup>3</sup>	%	%	kg/cm <sup>2</sup>
1689-22-17	Clay E <sub>1c</sub>	4,30	1	23	17	28	31		61,4	20,5	40,9	0,53	6,5	2,090	1,730	20,7	34,7	41,2
4390-22-41	Sand E <sub>2b</sub>	7,00	13	71	4	6	6		23,6	no	no	1,5	2,8	1,850	1,680	10,0	36,6	6,9
4388-22-38	Clay E <sub>2c</sub>	3,00	1	38	18	18	26		43,2	20,2	23,0	2,1	1,4	2,020	1,660	21,5	37,4	15,8
1900-22-29	Sand E <sub>2d</sub>	3,50	5	82	3	3	7		26,2	no	no	-	-	1,930	1,680	14,6	36,6	5,9
4386-22-36	Sand E <sub>2e</sub>	5,00	6	77	5	5	7		25,4	no	no	0,65	2,5	1,980	1,860	10,7	29,8	5,5

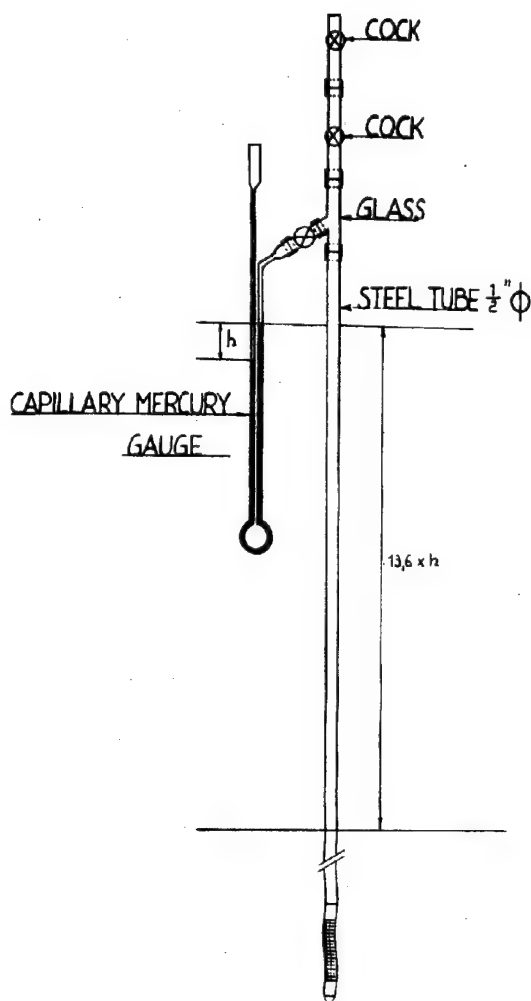


FIG. 3

hydrostatic with respect to the water-level in the upper sandlayer  $R_{2b}$ .

Section 34 (Left Bank) fig. 2e.

Independent watertables are found in the layer  $Pl_1$  of fluviatil origin and in the sandlayer  $R_{2b}$ .

In the claylayer  $R_{2c}$  was put the closed piezometer C. Although located very near the base of the claylayer, it doesn't show any influence of the waterlevel in the lower sandlayer, but the recorded pressure is nearly hydrostatic with respect to the waterlevel in the upper pervious layer  $Pl_1$ .

In the claylayer  $R_{1c}$  were put the closed piezometers A and B, which give nearly hydrostatic pressures with respect to the water-level in the upper sandlayer  $R_{2b}$ .

#### GENERAL REMARK.

All of the piezometers are not more distant than max 10 m from the transversal drains. Some are even located at only 4 & 5 m. from these drains. In spite of these very short distances, the piezometers located in the claylayers, and even those located in the clayey layers, are practically not influenced by the existence of these drains. At the contrary the waterpressures in all the sand- and gravel-layers are very influenced by the same drains.

#### GENERAL CONCLUSION.

The waterpressure measurements performed at Godarville and Eigenbilzen indicate that in case of claylayers located between more pervious layers, in which exist two independent water-tables, the waterpressures in the claylayer are practically not influenced by the water-level in the lower pervious layer, but are generally nearly hydrostatic with respect to the water-level in the upper more pervious layer. These results are surprising, because the waterpressure in the clay should be expected to be a mean between the upper and the lower watertable. The much higher recorded waterpressures are a very peculiar fact for the stability of slopes in claylayers. When deep cuts are to be made in such layers it is thus suggested to control the waterpressures in the claylayers by means of closed piezometers.

-O-O-O-O-O-O-

### III c 3

#### LOADING TESTS ON CLAY

STEN ODENSTAD

The Royal Swedish Geotechnical Institute.

#### SYNOPSIS.

This report deals with the strength of clay. In certain borderline cases, where ground rupture has occurred at a known load, the strength according to computation by tentative sliding surfaces is compared with the strength obtained in the laboratory by nonconfined compression tests and by Swedish cone tests on undisturbed soil samples taken from the same ground. A hypothesis is stated for the relation between the strength of the

soil sample and that of the native soil, indicating in principle how strength of soil may be obtained.

#### INVESTIGATIONS.

In the laboratory, nonconfined compression tests are made on "undisturbed" soil samples according to fig. 1. The vertical normal stress is increased from zero until either real rupture occurs, usually in an inclined sliding surface, or the height of

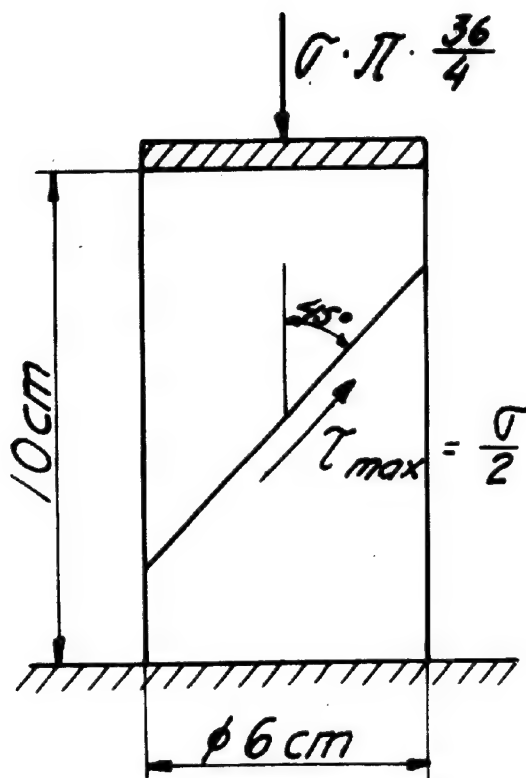


FIG. 1

the sample has been decreased 10%, this strain being considered equivalent to a real rupture. During the test the soil sample is placed in paraffin oil, preventing it from drying. The rate of the load increase is 0.05 kg/cm<sup>2</sup>h. For such fine-grained clays, as are now in question, this rate is great enough to render the consolidation of the sample negligible. The strength according to the test is  $\tau_{max} = \sigma/2$  at rupture.

The cone test is another method of obtaining the strength of clay, which to some extent is used in geotechnical laboratories in Sweden and also in the other Scandinavian countries. In this test one observes how deep a small metal cone with sharp point sinks in the soil sample, when released from the position where the point touches the surface of the sample. By means of stability computations of known borderline cases, where the soil is considered to be near rupture, one has obtained a relation between the impress depth of the cone and the strength of the soil. This relation is different for different kinds of clay.

Usually the strength, according to nonconfined compression tests in the laboratory, is lower than the real strength of the soil according to computation with sliding surfaces. As an example from practice a stability computation for a slope of a clay pit in a brickyard at Falkenberg (fig. 2) may serve. The slope is 14-15 m high and very long. After a slide, which raised the bottom of the pit 2 or 3 m, a geotechnical survey was made, the results of which are shown in fig. 2. The natural ground, in which the pit is dug, has a

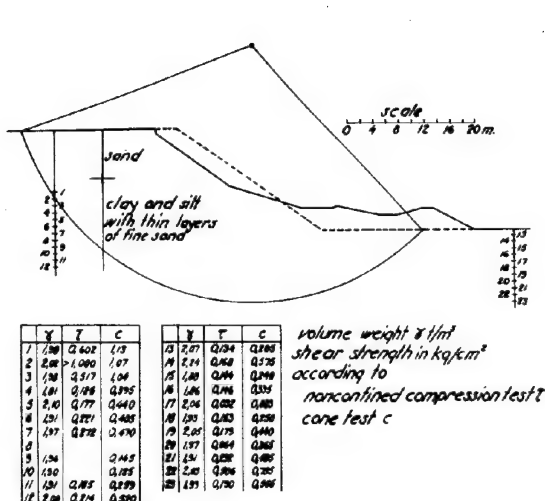


FIG. 2

top layer of sand, 7 m thick, and under it down to a great depth clay and silt with thin layers of "mo" (grain size 0.2-0.02 mm). A stability computation was made for the tentative sliding surface shown on fig. 2, assuming that the slope before the slide was as shown by a dashed line on the figure. Giving different importance to the different soil samples according to the length along the sliding surface which they represent, the average value for the cone tests is 0.52 kg/cm<sup>2</sup> and that of the nonconfined compression tests 0.28 kg/cm<sup>2</sup>. The stability computation shows that the shear stress along the tentative sliding surface in the part through the clay is 0.51 kg/cm<sup>2</sup>, and thus in accordance with the cone test but greater than the nonconfined compression test. These results are representative for many such cases.

In order to investigate further the relation between strength according to stability computations and strength according to laboratory experiments the author has made loading tests on clay in the field. These tests were conducted in pits 1.1 m deep and 2.0 m square, which were cut through the dry crust to the underlying soft clay. In the test place the ground has never been consolidated by any overburden. The soft clay was homogeneous in the thin layer, the strength of which was tested. The test slab was made up of steel beams and steel plates and was rigid compared with the clay. Its area was 2.0 x 0.4 m square, and it was placed on the levelled bottom of the pit along one of the sides. The load was applied on the centre of the slab from a steel bar 1 m in height, which had a bearing at each end and which before the test was made exactly vertical with water-level. The load was produced in a special loading test device by pouring water into a barrel, the total weight applied to the steel bar being enlarged 10 times by a lever arrangement. The device was arranged in such a way, that only the load from the test slab acted on the tested earth volume. The load was increased at such a rate, that the rate of the shear stress increase in the presumed sliding surface was the same as in the nonconfined compression test. The sinking of the slab was measured by micrometer dials at its 4 corners,

and the raising of the pit bottom beside the slab was measured at 8 points along a line at right angles to the length of the slab drawn from its centre. The load was increased until ground rupture occurred. The rupture was very distinct as seen in fig. 3, which for one of the tests shows the sinking of the corners of the slab and the corresponding load. The loading tests were made in 9 pits.

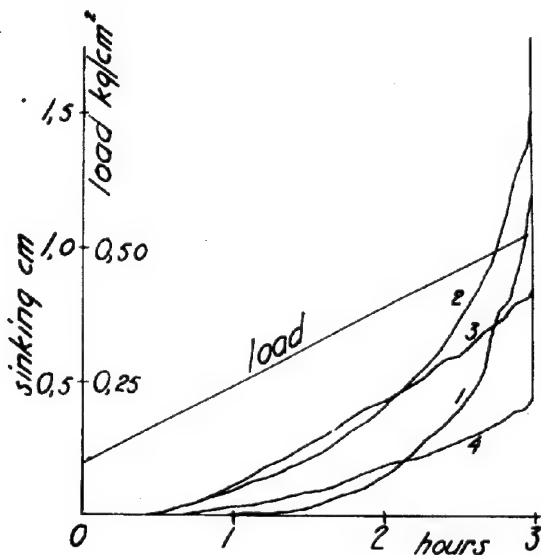


FIG.3

The load at rupture being  $q$ , the shear stress  $\tau_p$  in the circular arc sliding surface is computed to  $\tau_p = 0.173 q$  the stabilizing moment of the shear stresses in the end faces of the moving soil mass being taken into account. In each test pit 4 soil samples were taken, on which nonconfined compression test and cone test were made in the laboratory. The results from the loading tests and the laboratory tests are collated in fig. 4. The results of the nonconfined compression tests appear to correspond well to the real strength of the soil, while the values of the cone tests are somewhat too high.

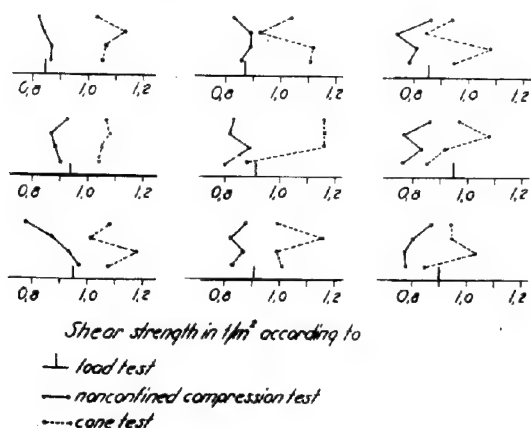


FIG.4

#### THEORETICAL EXPLANATION.

As mentioned above the nonconfined compression test usually gives too low strength values. The author will give a tentative explanation of this circumstance. This explanation also shows why in the loading tests described above the relation between the strength according to laboratory tests and the real strength of the soil (i.e. according to stability computation at ground rupture) diverged from its usual value. For this purpose the stress conditions of the soil before and after the sampling in the laboratory test are considered.

The clay is considered as a 2-phase system consisting of a solid phase, the grain skeleton, and a fluid phase, water. To the solid phase may then be assigned that part of the water which, owing to molecular forces, more completely adheres to the grains and possibly surrounds them as a more or less solid envelope. The fluid phase consists of ordinary water. The strength of the clay, i.e. its capacity for transmitting shear stress is then identical with the strength of the grain skeleton. The grain skeleton is considered as a somewhat yielding but yet solid body possessing cohesion, owing to internal molecular forces, and internal friction. Slow shear tests, which have been published, show that the angle of internal friction of clay, i.e. of the grain skeleton, usually is arc  $\text{tg } 0.2$  to arc  $\text{tg } 0.4$ . The rupture condition of the grain skeleton is shown in fig. 5 where Mohr's representation is used and the angle of internal friction is presumed as arc  $\text{tg } 0.3$ ; the principal stresses  $p_1$  and  $p_2$  then cause rupture if the relevant Mohr's circle touches the inclined straight line that is

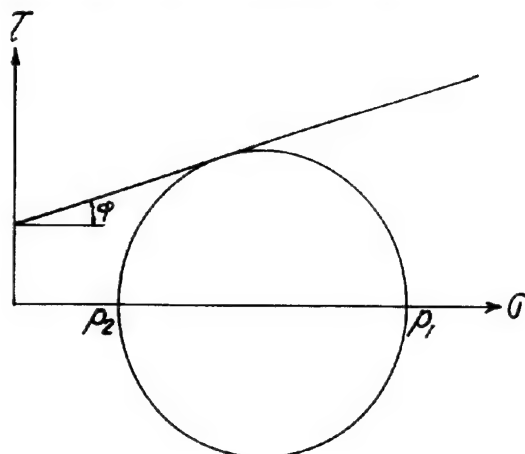


FIG.5

characteristic for the substance. In order to illustrate the stress conditions somewhat further we may assume that the grain pressure in the soil after sampling is  $p_a$  (fig. 6). This grain pressure is hydrostatic, i.e. equal in all directions. Furthermore we assume that the grain skeleton behaves like a homogeneous, isotropic elastic body following Hooke's law. The soil sample being subjected to nonconfined compression of the amount  $\sigma$ , the normal stress in the grain skeleton increases by  $\Delta p_1 = 2/3 \sigma$  in axial direction and decreases by  $\Delta p_2 = 1/3 \sigma$  perpendicularly to the axis, and the pore water pressure increases by  $1/3 \sigma$ . The total

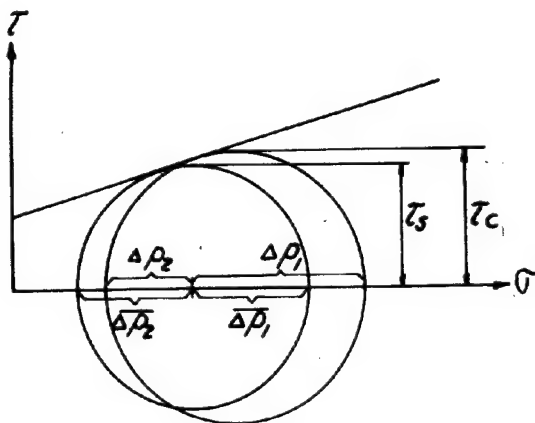


FIG. 6

change of pore water pressure and axial grain pressure then equals the load; further the equation  $\Delta p_1 - 2\Delta p_2 = 0$  is valid, i.e. the volume of the grain skeleton is unchanged, the pore water preventing volume change. The shear strength of the soil sample is found to be  $\tau_c$ . If, instead of this, the sample is subjected to direct shear test at constant water content, the equation  $\Delta p_1 = \Delta p_2$  is valid, and the shear strength  $\tau_s$  is obtained.

If an entirely undisturbed soil sample could be taken, the original vertical and horizontal grain pressures should be converted during the sampling to a hydrostatic average pressure  $p_a^1$  of such a magnitude that the volume would be unchanged. The shear strength  $\tau_a^1$  should then be obtained in the laboratory (fig. 7). In reality also an "undisturbed" soil sample becomes somewhat disturbed during the sampling, as is apparent inter alia from confined compression tests. The grain skeleton may now be compared to a kind of framework having the grains as bars and exposed in the ground to the internal average stress  $p_a^1$ . During the sampling the adhesion between the grains break down to some extent and thus the grains find a chance to avoid the pressure; they turn and slide one on another and the average pressure of the grain skeleton or the framework sinks to a lower value  $p_a$ . In the laboratory then a shear strength  $\tau_a$  is obtained which is lower than the shear strength  $\tau_a^1$  of the native soil. Evidently the decrease of the grain pressure mentioned can take

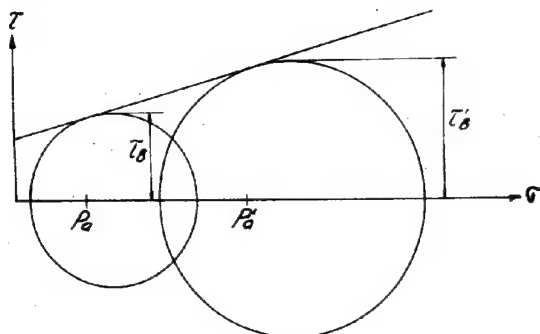


FIG. 7

place without volume change precisely as the decrease of strength when clay is remoulded at maintained water content.

It is to be expected that in entirely consolidated clay layers the grain pressure and thereby also the strength usually should increase downwards. Such is the position at those tests with a rotating auger which are published by Lyman Carlson in a report to this conference. In accordance therewith the absolute difference between the vertical and horizontal grain pressures of the soil probably increases downwards, at least in ordinary cases. Therefore if an entirely undisturbed soil sample could be taken, the change of the grain pressure during the transition to hydrostatic pressure also should increase with the depth, from which the sample was extracted. The injury to the soil sample, i.e. the reduction of the hydrostatic grain pressure from  $p_a^1$  to the lower value  $p_a$ , therefore seems to increase with the depth from which the sample was taken, provided that it is caused by the change of the grain pressure mentioned above. The injury can also be caused by the sampler acting on the earth mass out of which the sample is stamped; also in this case the injury seems to increase with the depth from which the sample was taken, as the greater average grain pressure makes possible a greater pressure reduction in the grain skeleton.

The hypothesis that the injury is greater at greater sampling depth explains why in the laboratory the nonconfined compression test and the rapid direct shear test give lower strength than corresponds to the real load in those cases, (e.g. Falkenberg) where the bearing capacity of the earth to a great extent depends on the strength of rather deep layers. The circumstance, that the cone test often gives a better result, is due to the fact that it is calibrated from such cases. Furthermore the hypothesis explains why on the other hand the load tests in the field and the nonconfined compression tests in the laboratory belonging thereto correspond fairly well; owing to the small sampling depth in this case no pressure reduction in the grain skeleton occurred at the sampling. The reason why the cone test gave somewhat too high values may be explained by the circumstance that it is calibrated from cases where the sampling involves strength reduction of the sample.

Thus, according to the stated hypothesis the following should be observed. Prior to executing the nonconfined compression test or the rapid direct shear test in the laboratory, the sample should consolidate in such a way, that its grain pressure is restored to the same value as in the native soil. Otherwise the strength should be determined in some way directly in the ground. (The reader may compare with the conference report by Lyman Carlson concerning a rotating auger).

#### SUMMARY.

Experience shows that nonconfined compression tests and rapid direct shear tests at maintained water content give lower strength than corresponds to those normal loading cases, where the bearing capacity of the earth at least partly depends on the strength of rather deep clay layers. The inferior strength of the soil sample is explained by the average grain pressure being reduced at the sampling. The grain skeleton is thereby

considered as a kind of framework under pressure in the earth, at the sampling the soil sample is injured in the manner that the "bars" of the framework, the grains, to some extent turn and slide one on another, whereby the

average grain pressure sinks from  $p_1$  to  $p_a$  and, according to fig. 7, the shear strength from  $\tau_1$  to  $\tau_a$ . This statement conforms also with loading tests which have been carried out.

-o-o-o-o-o-

III c 4

#### MEASUREMENT OF PORE WATER PRESSURE

Ir. T.K. HUIZINGA

Director of the Soil Mechanics Laboratory, Delft, Holland

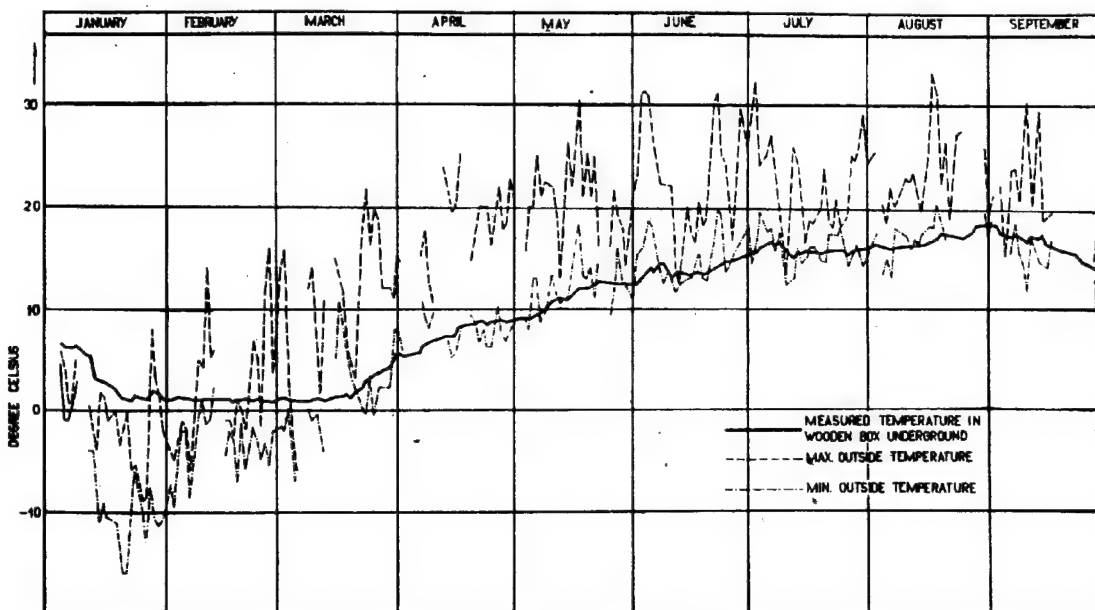
#### INTRODUCTION.

In the Proceedings of the First Conference on Soil Mechanics Ringeling and Bie-mond reported on the measurement of pore water pressure in peat and clay layers (F 8, F9). The importance of such measurements in view of the preparation, the design or the construction of civil engineering works needs hardly be stressed nowadays. Since then many measurements have been carried out in the Netherlands, in most cases under the guidance

or under the supervision of the Laboratory. In the course of these measurements we encountered various difficulties which had to be overcome, resulting in the gradual improvement of the apparatus.

#### OBJECT.

The measurements may serve several objects, e.g. to collect the necessary data for the estimation of the probability of earth failures in excavation works, both for a con-



Measured temperatures in 1942

FIG.1

stant and a variable hydrostatic pressure in the underlying layers of sand, to calculate the stability of slopes and hence to control the construction speed in earth works, to predict the continued settlement of a fill at any time after construction, to estimate horizontal forces on pile groups under abutments or other retaining walls, to evaluate pile driving data, for research, etc.

#### CONSTRUCTION.

At first the filters were placed in a previously made borehole and embedded in suitable graded sand in the same way as when installing ordinary water gauge pipes. Because it is to be feared that the soil fill in the borehole may permit communication with layers of different pore water pressure, nowadays the pipe with the filter is forced into the ground, resulting at the same time in less disturbance in the neighbourhood of the filter. Owing to the displacement of the soil round the filter, some initial excess pressure in the pore water will develop, so that one must wait one or more days before the correct value can be read. In the beginning the filter pipe was connected by means of a hollow lead-cable to a mercury pressure gauge erected away from the construction works. It appeared however that the cables were not sufficiently watertight. Now the pressure gauge is once more directly connected to the filter pipe.

#### EFFECT OF TEMPERATURE.

The mercury pressure gauges installed on the surface are in a vulnerable position and are liable to freeze during frost periods. To counteract this, they were at first placed in wooden boxes, which were heated during the winter. An other way was to use oil or liquid paraffine instead of water in the upper portion of the pipe. This required much attention and therefore nowadays the filter pipes are placed with their tops 80 cm to 1 m under the surface and an ordinary Bourdon type pressure gauge is used, the whole being covered by an insulated plate. Even during long and severe frost periods the temperature in the thus enclosed box did not drop below  $0^{\circ}\text{C}$ , due to the transfer of heat from the earth. The curve in fig. 1 shows the relation between recorded temperature in the box and above.

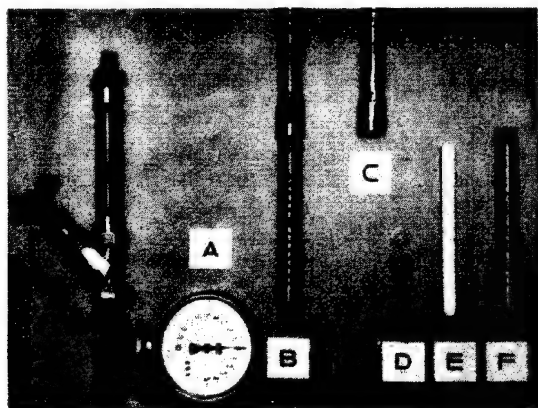


FIG.2

At the same time this arrangement reduces the rise of temperature due to the radiation of the sun, which would have caused expansion differences between the material of the pipe and the water, with the ensuing observation errors.

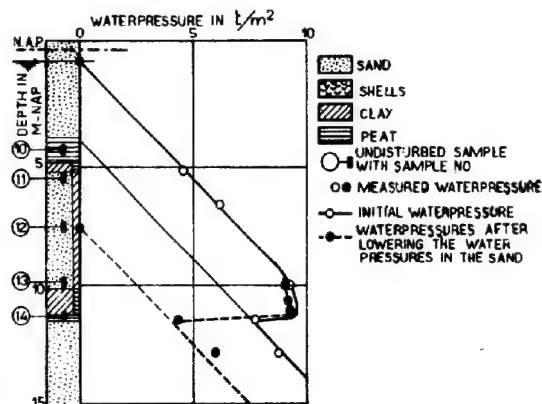
#### EFFECT OF GASCONTENT OF THE SOIL.

In soils containing gas, trouble has been experienced from gas bubbles rising in the pipe. The gas accumulates in the upper portion of the pipe, causing a time lag in the readings. To avoid this an air lock is provided, consisting of a glass tube in which the amount of gas present can be clearly seen. This gas can be locked out without appreciable change in the water pressure. In some cases the large amount of gas caught in the pipe necessitated frequent lock-out operations, resulting in unreliable readings. Furthermore, in fine grained soils it has been found that the soil particles entered the pipe through the filter. To counteract this a porous pot was placed inside the filterpipe. In this way we have reverted to the tensimeters of Schofield, used by him since long in agricultural work and by means of which even pressures above the phreatic water table can be measured down to a pressure of about  $\frac{1}{2}$  atmospheric pressure. Thus the water pressure meter has become a vapour pressure meter by means of which at the same time easily the relative humidity in moisture laden spaces can be measured. Fig. 2 shows a photograph of the described apparatus.

The most important advantage of a water pressure meter as compared to an open water gauge pipe is the improved registering of changes in pore water pressure, owing to the smaller amount of in- or out flowing water required.

#### VARIOUS INFLUENCES ON THE GROUNDWATER TABLE.

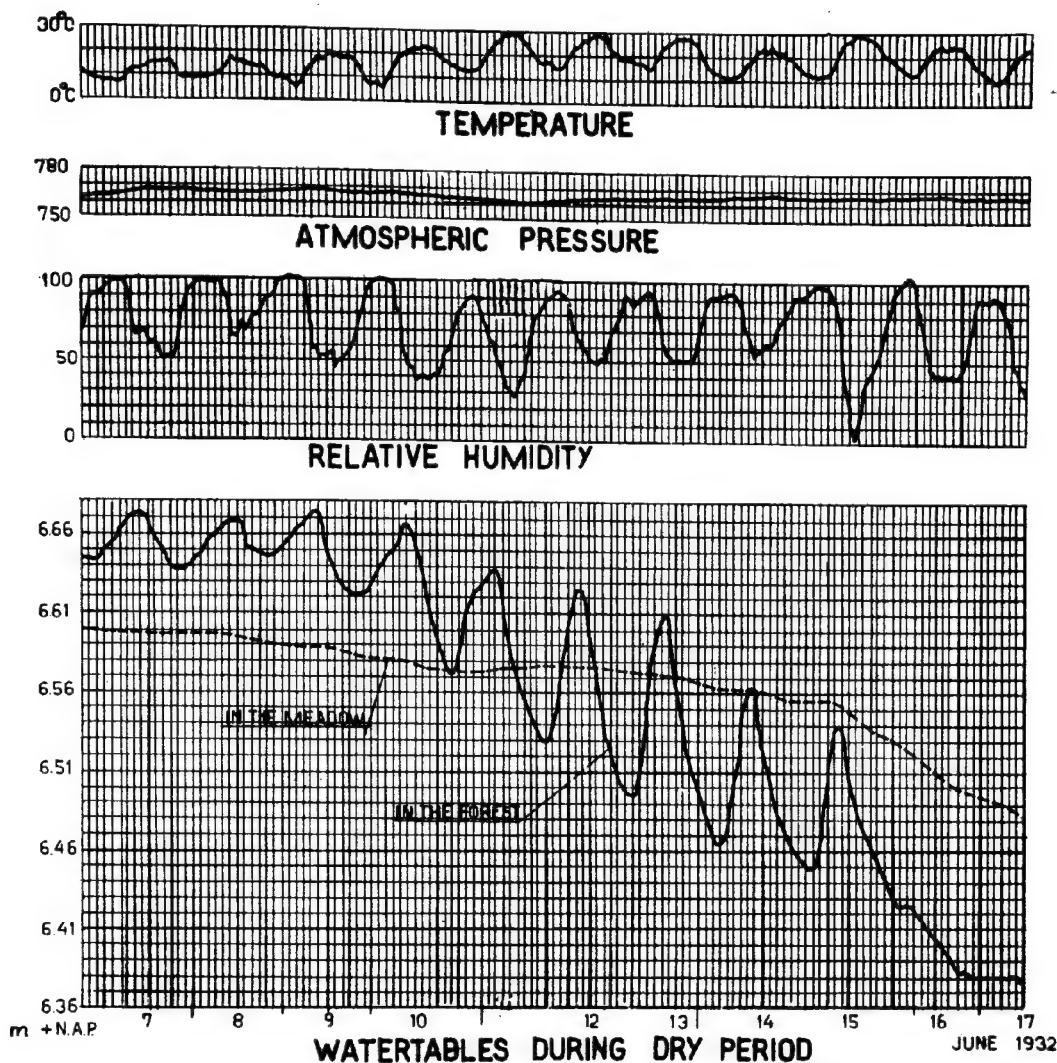
In the course of our observations we often found certain readings difficult to explain. Such readings do not necessarily result from faulty construction or arrangement of the apparatus because in the ground appreciable fluctuations of water pressure may occur, and we must also take account of the influences of temperature, atmospheric pressure, etc. When using Bourdon type pressure gauges or electrical pressure gauges we should remember that we measure the difference of pressure with the



Measured waterpressures at Amsterdam

FIG.3





Observations of groundwater table at Wageningen

FIG.4

atmospheric pressure obtaining at the time of the calibration of the gauge.

It is useful to form a clear idea of the various factors influencing the level of the phreatic water table or generally speaking the pore water pressure.

- 1) The soil conditions. Soils are composed of heterogeneous materials; they are built up from layers of different permeabilities giving rise to apparent water tables and to water pressures that sometimes do not correspond to the hydrostatic pressure. This may be associated with
- 2) The flow of the pore water. If the pore water pressure does not follow the hydrostatic law, the water is caused to flow through the soil. An example is furnished by the readings taken at Amsterdam and shown in fig. 3. It appears that a very thin layer of peat practically prevents communication between the two layers with different water pressures, so that

drainage of the underlying sandlayer will have little effect on the pressures in the layer above. Also in dewatering or irrigation works a vertical flow may be caused. A result of this can be that temporarily thicker or thinner capillary layers occur.

- 3) Excess hydrostatic pressure. Besides the excess water pressure caused by forcing the apparatus into the ground, we know excess pressure caused by loads on the surface, pile driving, etc. Here too the water will flow, mostly in several directions. Dependent on the depth of the filter and the time of placing, the readings will vary.

- 4) Strains within the soil. When measuring pore water pressures in the neighbourhood of pile groups in soft layers on which an overburden has been placed, we must be aware of the fact, that a certain friction may develop between the soil and the piles. The resulting displacements in the soil may take place rather irregularly causing corresponding sudden fluctua-

tions in the readings.

5) Rainfall. Dependent on the conditions of the soil and the amount of water entering the soil, rather sudden changes in ground water pressure may occur. An example of this is furnished by the so called Lisse-effect where it is assumed that between the zone of capillary rainwater entering from above and the existing capillary zone the air in the voids is compressed, causing a sudden rise of the phreatic watertable. This rise is limited both by the height of capillary rise in the upper layer and by the weight of this saturated layer which finally may burst, so that part of the compressed air can escape. An other example is the Wieringermeer-effect, where the soil is completely in a state of capillary saturation. A slight rainfall will break up the menisci causing the phreatic watertable to rise to the surface.

6) Relative humidity. Experiments of Professor Thal Larssen at Wageningen show that even the very slight amount of water resulting from dew may effect an appreciable rise of the phreatic watertable (fig. 4). On the other hand dessication of an upper layer consisting of several thin sub-layers, each with their own different heights of capillary rise, may re-

sult in sudden fluctuations of the phreatic watertable.

7) Frost action. It is well known that during frost periods the pore water pressure decreases appreciable. Observations made below the frost depth show that the relative humidity there is very low, perhaps due to the diffusion of the moisture upwards in the form of vapour with subsequent condensation and freezing. Wells run dry until immediately after the onset of the thaw when they start flowing again even without previous rainfall. Also in the drinkwater producing areas in the dunes this fact is well known although a satisfactory explanation has not yet been given.

8) Atmospheric pressure. It is also well known that with a fall of the atmospheric pressure wells may start flowing even without rainfall. A theoretical explanation may be found only when we associate this phenomenon with the presence in the water of gas bubbles or dissolved gases.

These water pressures vary fairly suddenly. For the proper study of these phenomena a quick registering water pressure meter is needed. It might be advisable therefore to use a meter, where the water volume remains practically constant.

-o-o-o-o-o-o-

### III c 5

#### AN ELECTRICALLY OPERATING PORE WATER PRESSURE CELL

R.G. BOITEN

Research-Engineer T.N.O. Dept. Stress-Analysis, Delft

G. PLANTEMA

Engineer of Public Works, Dept. Soil Mechanics, Rotterdam

#### SUMMARY.

For the solution of various soil mechanical problems exact and reliable water-pressure-meters are required. Up till now, the Dept. of Public Works of Rotterdam have made measurements by means of filters driven into the ground, provided with pipes, with Bourdon gauges, on which the water pressure can be read. As the use of this measuring system always forms an obstacle to the works being carried out, as it cannot be read at a distance, and has several other technical defects, an attempt has been made to develop another measuring system.

In this report a waterpressure meter is described which can be read electrically, and does not have the defects of the system in use up till now, and nevertheless is of such small size that it can easily be driven into the soil without using a bore hole, so that the subsoil is disturbed as slightly as possible. Moreover the meter is very robust, and can be read in a simple and exact way.

Hitherto Public Works of Rotterdam have determined water pressures in the subsoil by means of a filter, which is driven into the subsoil to the desired depth and is connected with a Bourdon gauge by  $\frac{1}{2}$ " tubes. After these tubes have been completely filled with water and connected with this gauge, the height of water or of suction which corresponds with the watertension around and in the filter, can be read on it. (fig. 1). 1)

However, several difficulties arise in using this system, such as:

- a) the being of an obstacle for the work being carried out;
- b) the impossibility to registrate at a distance, which is so troublesome that in cer-

tain cases, the experiments were given up, although they could have yielded valuable data;

- c) the possibility of leakage in the connections of the pipes, so that the measurements become unreliable;
- d) the freezing of accessories during a frost-period;
- e) on the one hand faulty indications owing to pressure differences in the water, on the other hand owing to differences in temperature of the water in the pipe, caused by differences in the temperature outside;
- f) faulty indications by the Bourdon gauge, in consequence of the overloading of the de-forming torus 2).

In view of these difficulties, a water-

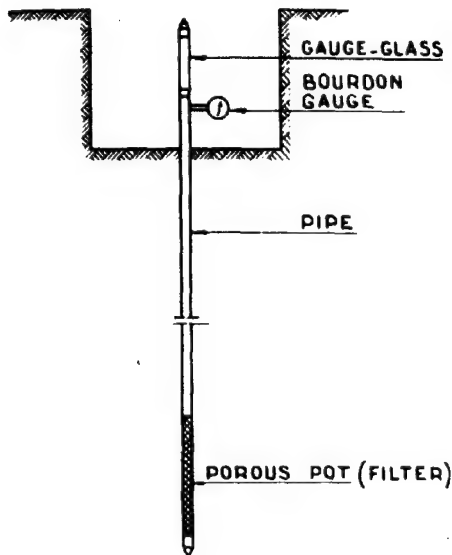


FIG. 1

pressure meter of quite another type was projected as shown in fig. 2.

After this apparatus has (prior to use) been filled with water and then driven into the ground, it is read electrically, so that the connection between the meter and the measuring apparatus only consists of an electric cable.

It is obvious that the faults inherent in the other system are surmounted here, and that nevertheless the dimensions of the meter have remained so small that it can easily be driven into the ground without using a borehole.

The requirements which are to be made to this meter, are the following:

- 1) The waterpressures must be measured in a part of the subsoil which is scarcely dis-

turbed.

- 2) After the meter has been driven into the subsoil, it must enable to measure as soon as possible the occurring watertensions, and moreover, to register fluctuations with as small a time-lag as possible.

- 3) The errors to be made must lie beneath abt. 1 or 2 percents, which can be realised with the present state of technics of measurement, and which suffices also for soil-mechanical purposes.

- 4) The meter as well as the registration-apparatus must be as robust as possible, while the use of it must be as simple as possible.

A brief description of the meter follows with reference to the figures 2 and 3.

Starting with the essential point it can be said that the water-pressure by means of the contact canals is transferred to the membrane. Its deformation is a measure for the water-pressure and it is this deformation which is registered by a wire-resistance strain gauge, cemented to the membrane. It must be observed that the water-room, connecting canal and contact canal of the meter, before the latter is pushed into the ground, are completely filled with water, for which purpose the point is first screwed off.

The contact-canals are capillaries, so that, after the meter has been completely filled with water, no water can run out of it, and no airbubbles can enter. After the meter has been put into the ground, neither bubbles of gas in the soil, if present, can enter. The flow of water into the contact-canals occurring with pressure-differences, viz., is too small for it; this point will be referred to afterwards. The position of the canals has been chosen in a slantingly upward direction, in order to prevent particles of soil from being pressed into it when driving the meter into the ground.

Over the membrane there is a space for the electrical circuit, which is kept dry by means of silicagels. The rest of the meter constitutes a perfectly watertight unit.

As well-known, the wire resistance strain-

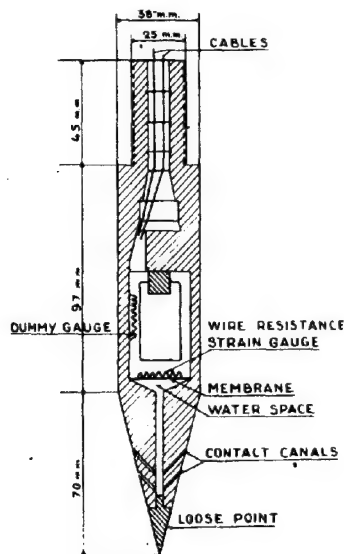


FIG. 2

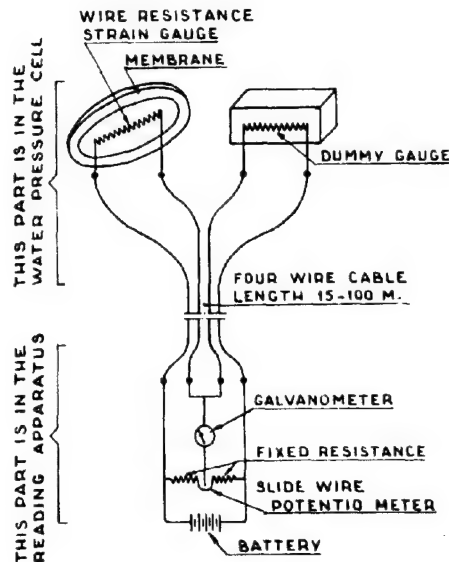


FIG. 3

gauge is a thin wire of a highly resistant metal, which is cemented to the construction. If the membrane becomes active, this wire undergoes an elongation, by which its resistance increases. This change of resistance is measured by means of a Wheatstone bridge (fig. 3).

Two arms of the bridge (2 strain gauges) are in the water pressure cell; the two fixed arms are in a small box, in which the power batteries of the bridge are placed. The scale of the slidewire potentiometer can, if desired, immediately be calibrated. With a small extension this measuring unit can be made suitable for successive reading of a great many water pressure cells.

Pushing the meter into the ground can be done with 1½" tubes by means of the apparatus shown in fig. 4.

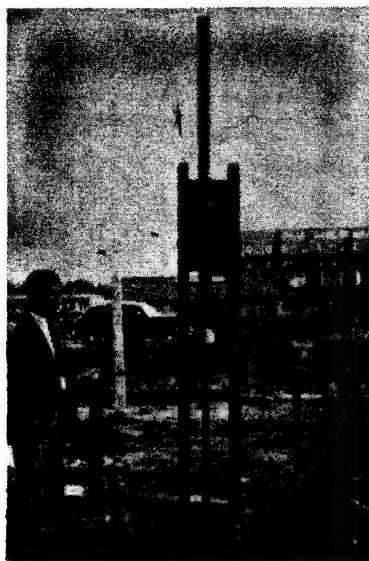


FIG. 4

Now that the description of the meter has been given, it can be seen to what extent the requirements sub 1 up to 4 have been met.

Sub 1. The water pressures must be measured in a part of the subsoil disturbed as slightly as possible. Therefore the diameter of the meter has been made very small (3.8 cm), so that it can be pushed into the ground to the desired depth with a small force and little disturbance of the soil. No use is made of a bore hole, which generally spoken changes the stress conditions in the subsoil, and therefore gives rise to less accurate measurements. Apart from a diameter as small as possible it can be said, too, that the contact of the meter with the surrounding pore water must take place in a part of the subsoil which is disturbed as slightly as possible, so that the contact canals are projected in the lower part of the sharp point of the waterpressure meter. However, the construction can still be improved, by the arrangement as shown in fig. 5. Here the water-pressure can be measured at a spot, where the ground is only slightly disturbed.

Sub 2. The condition that the meter must adapt itself soon to the pressure of the surrounding water, requires that the flowing of

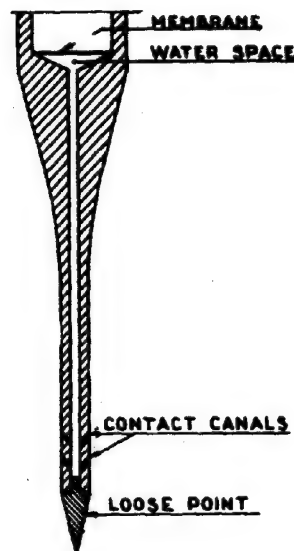


FIG. 5

pore water from the subsoil into the meter, (necessary to equal the pressure in and outside the meter and to stretch the membrane), be minimal.

The meter being entirely filled with water "before" it is pushed into the ground, the magnitude of this flow is determined by the deflection of the membrane. This membrane is constructed in such a way that for an increase of pressure of 10 t/m<sup>2</sup>, a flow of only 5,7 mm<sup>3</sup> is required, which safely may be called a small amount. Consequently, the time of adaptation is very short, as appears from the rough and ready calculation mentioned below.

Assuming that, e.g. : the pressure in the pore water rises by 10 t/m<sup>2</sup>, while the contact-canals (12 canals) when putting away the meter, have possibly been choked up by a piece of clay of very low permeability of e.g. 1 mm thickness, then, with a required displacement of 0.0057 cm<sup>3</sup> water, the time required for the displacement can be calculated from the equation

$$t = \frac{Q}{k \cdot i \cdot f} \quad 1 \text{ (d'Arcy)}, \text{ in which}$$

Q = quantity of inflowing water per contact-canal

$$= \frac{0.0057}{12} = 0.000475 \text{ cm}^3$$

k = coefficient of permeability of this clay

$$= 10^{-8} \text{ cm/sec.}$$

i = the hydraulic gradient in the piece of clay at the opening of the contact-canal

$$= \frac{1000}{0.1}$$

f = the surface of the contact-canal

$$= 0.0075 \text{ cm}^2.$$

From this it results that the time t-abt. 600 sec. or 10 min., which indeed can be regarded as quite satisfactory.

If the contact-canal is closed by a more permeable piece of soil, the time of adaptation becomes orders of magnitude smaller, and consequently will be seconds or fractions of them; a permeability of 10<sup>-8</sup> cm/sec. can be considered as a very low figure.

Moreover it has been proved from experiments that the piece of soil at the opening of the contact-canal has a thickness of less than 1 mm, so that this figure, too, in the equation of d'Arcy tends to a maximum time.

Sub 3. With respect to the measuring accuracy it can be said that with the new apparatus an exactness of 0.1 to 0.2 % can be reached, while with a more robust transportable unit an exactness of 0.5 % was realised. On account of other possible faults, in practical cases errors of 1 to 2 % will be probable. These faults originate in the following factors:

- a) The connection cable used between water pressure cell and recording apparatus may be imperfect;
- b) The air-volume over the membrane in the water pressure cell gives rise to pressures on the membrane, when changes of barometric pressure and temperature occur.

However, if necessary, these faults can be eliminated by measuring the open air-temperature when adjusting the zero point of the meter before it is brought into the soil and by reading the barometric height during the measurements. It is a favourable circumstance that the temperature of the groundwater practically is constant.

Sub 4. The recording apparatus can, indeed, be constructed sufficiently robust. The most sensitive part forms the galvanometer in the meter branch. By applying an electronic am-

plification, a stronger instrument can be used.

Recording can take place in two ways:

- a) By reading the result from the galvanometer; the deflection of the pointer is proportional to the change of resistance of the gauge, and therefore with the water pressure;
- b) By balancing the bridge with the slide-wire-potential meter (current through the meter zero). The angle of turning of the potential meter-knob is now proportional to the water pressure.

The method mentioned sub (a) requires not a single manual work; with the method mentioned sub (b) one knob must be turned. However, with the latter method more accurate recording is possible.

The actual construction is contained in a small portable box, and has proved to resist rather rough treatment. Moreover, as it requires very simple attendance, it is fully suitable for field work.

The pore water pressure cell itself is practically non-destroyable.

#### REFERENCES

- 1) Ir. T.K. Huizinga: "The measurement of water-tensions." Proc. Int. Conf. Soil Mech. 1948
- 2) C.B. Biezeno & J.J. Koch. On the elastic behaviour of the so-called "Bourdon" pressure gauge. Proceedings Nederlandse Academie voor Wetenschappen vol. XLIV no. 7 & 8, 1941.

-0-0-0-0-0-0-

## SUB-SECTION III d

### VIBRATION RESEARCH

#### III d 1 THE RESONANCE OF MACHINE FOUNDATIONS AND THE SOIL COEFFICIENTS WHICH AFFECT IT

GREGORY P. TSCHBOTARIOFF

Associate Professor of Civil Engineering, Princeton University, Princeton, New Jersey, U.S.

EDWARD R. WARD

Research Associate in Civil Engineering, Princeton University, Princeton, New Jersey, U. S.

#### SUMMARY.

Formulae published to-date for the determination of the natural frequency of machine foundations contain at least two coefficients which depend on the soil beneath them - the dynamic modulus of soil reaction and the average vibrating mass of the soil. It is customary to use separate formulae and coefficients for the cases of vertical and horizontal vibratory forces. No satisfactory methods have, however, been developed to-date for the determination of these soil coefficients in advance of design and construction.

The present paper gives a brief outline of published relevant model test results performed by the "Degebo" in Germany, by "Vios" in Russia, and by Princeton University in the United States. Also mentioned are some full-scale observations carried out in California and a so-far unpublished resonance case of compressor foundations in a pumping station in the U. S. is discussed in some detail.

Formulae are developed which show that for the case of vertical vibratory impulses the natural frequency of a foundation is dependent on the average unit pressure on the ground distributed over its entire area. These formulae can be used for the determination of the "reduced natural frequency"  $\omega_{nr}$ , which is equal to the natural frequency for a given size of foundation area and type of soil when the unit pressure on the ground is equal to unity. A graphical comparison of available data from different localities shows that this reduced natural frequency  $\omega_{nr}$  is primarily affected by the size of the foundation area and only to a somewhat lesser degree by the



properties of the soil. In some cases it does not seem to be affected at all by the direction of the vibratory impulses.

The effect of piles on the natural frequency of a foundation is briefly discussed.

#### PUBLISHED DATA ABOUT PREVIOUS STUDIES.

Very little experimental data has been published to date on this subject.

The conventional natural frequency formula for undamped vibrations reads:

$$\omega_n = \frac{1}{2\pi} \sqrt{\frac{k}{M}} \quad (1)$$

where:  $\omega_n$  = natural frequency of the vibrating system;

M = mass of the vibrating system;

k = linear spring coefficient of the support.

Resonance occurs when the frequency of the exciting forces is equal to the natural frequency of the system.

Lorenz 1) performed experiments with vibration-producing machines of the German Research Society for Soil Mechanics ("Degebo") and subsequently transformed formula (1) to read:

$$\omega_n = \frac{1}{2\pi} \sqrt{\frac{k' A g}{W_s + W_v}} \quad (2)$$

where: A = contact area between base of vibrator machine and the soil;

k' =  $k/A$  = dynamic modulus of soil reaction, or the volume spring coefficient.

g = acceleration of gravity;

$W_v$  = Weight of vibrator machine, including its foundation;

$W_s$  = Weight of vibrating soil.

During the experiments which led to the development of formula (2) the machines were employed to produce continuous vertical harmonic vibrations. Any possible damping effect of the soil was neglected in setting up the formula. Tests with one standard type of vibrator were performed on a wide range of soil types. Experiments were also performed by the "Degebo" whereby the machine was set to produce harmonic horizontal vibratory forces alternating with rotational vibratory forces around its horizontal axis. The natural frequency for this condition was equal to app. 50% of the value found for vertical vibrations 1)

No experiments with purely horizontal vibratory forces were reported.

In analyzing the results of the tests on footings ranging from 2.7 sq. ft. to 10.7 sq. ft. area subjected to vertical vibratory forces, Lorenz 1) arrived by indirect reasoning to the conclusion that a definite mass of soil took part in the vibration at resonance and that this mass neither depended on the unit contact pressure between the base of the vibrator and the soil, nor on the size of the contact area between the vibrator base and the soil. The vibrating soil mass, however, appeared to increase in size - (from four to ten times the weight of the vibrator) - with an increase in the magnitude of the vibratory forces. Lorenz further concluded that the natural frequency itself was only slightly affected by the size of the contact area between the soil and the base of the machine. 1) (Fig. 5). Most of the above conclusions were based on comparative computations which appear to involve the assumption that the dynamic modulus of soil reaction of a soil is independent of the intensity of the unit pressure on the surface of the ground.

Barkan 2) 4) reported the results of extensive large-scale model tests performed in Russia by the Institute for Engineering

Foundation Research ("Vios"). Tests were performed on one type of soil only - plastic clay. Three model machine foundations were used of 2 m<sup>2</sup>; 4 m<sup>2</sup> and 8 m<sup>2</sup> base contact area with the soil (21.5 sq. ft.; 43 sq. ft.; 86 sq. ft.) The determination of their natural frequency was performed by two methods. First by the use of a vibration producing machine. This method gave clear vibrographs for the case of vertical vibratory forces, but less clear ones for the case of horizontal vibratory forces. The latter tests were also performed by a second method whereby the vibration was induced by means of a single horizontal blow. In contrast to the "Degebo" results the natural frequencies thus obtained did not differ by more than  $\pm 11\%$  from the corresponding values produced by vertical impulses 2) (See tables No. 5 and No. 11).

The analysis of the results was performed mainly for the purpose of determining the values of the moduli of soil reaction both for the case of vertical forces and for the case of horizontal forces. To that end in the relevant computations the mass of the vibrating soil was assumed to be zero. However, by indirect reasoning the conclusion was also arrived at that the mass of the vibrating soil cannot be neglected, but that its value must lie between two-thirds and one and a half times of the combined mass of the vibrator and of the foundation. This is much less than the value estimated by Lorenz.

The U.S. Coast and Geodetic Survey 3) has published an extensive investigation of earthquakes in California. It includes a table of data concerning some 212 buildings and the soil types on which they were built. The table gives the recorded frequencies of horizontal vibration of these buildings as a result of wind pressures. Some 93 buildings of those submitted had a rectangular shape. The comparison of the records of these buildings shows that their horizontal natural frequencies decrease appreciably with the height of the building.

Extensive studies of the effects of vibrations on the bearing properties of soils were performed at Princeton University in 1943/46. 5) 6) They were carried out on a comparative basis and only few natural frequency determinations were made, mainly for the purpose of avoiding the performance of later tests at frequencies close to the resonance range of the vibrating system.

#### CASE OF COMPRESSOR FOUNDATION RESONANCE TROUBLE AT A PUMPING STATION.

The following analysis of a so-far unpublished case may serve to illustrate the factors which affect the resonance of a full-scale machine foundation.

A pumping station was recently erected on a deep river deposit of silt and clay. No soil tests appear to have been made at the site, but the characteristics of this type of deposit in the general vicinity are approximately as follows. In the same boring the liquid limit " $w_L$ " may vary from 30% to 110%; the plastic limit " $w_p$ " from 16% to 24%; the natural water content " $w$ " from 30% to 70%; the liquidity index =  $100(w - w_p)/(w_L - w_p)$  from 30% to 90%; the unconfined compressive strength from 0.40 T/sq. ft. to 1.10 T/sq. ft., with

an average strain at failure of 6%. This clay is not sensitive to remolding, the average value of the sensitivity ratio "S" being equal to 3 and sometimes dropping below unity.

The water level was less than a foot below the surface of the ground. Frictional timber piles of some 60 ft. length were employed, approximately two-fifths of them being batter piles. The vertical piles were embedded to a depth of 8 inches in the concrete of the foundation blocks and were not otherwise connected to them. The batter piles were provided with light metal clips bolted by a single bolt to the head of the pile. The concrete foundation blocks of the individual compressor units did not have any structural connection to each other.

Excessive vibration was found to take place after the pumping station began operating. Every indication pointed towards resonance phenomena of the compressor - foundation - soil system at the operating speeds of 300 r.p.m. The building and soil around the station shook violently, especially when the individual compressors happened to synchronize. Pipe connections were frequently damaged as a result.

This condition was remedied by the station engineers who provided a drainage system around it and by continuous pumping lowered the ground water table to approximately the elevation of the pile heads. Excessive vibrations were then reported to have stopped. Since this measure by removing buoyancy increased the effective weight of the foundation only by some 7%, the value of its natural frequency was well defined.

#### COMPARATIVE ANALYSIS OF ALL AVAILABLE DATA BY THE "REDUCED NATURAL FREQUENCY" METHOD.

An attempt to analyse by conventional methods the resonance case of the pumping station just described led to the realization that the problem as handled so far is an indeterminate one and that this circumstance probably accounts for some of the discrepancies in the conclusions arrived at by previous investigators.

A different approach to the problem appeared therefore advisable. After a few trials, the following procedure was developed. Formula (2) can be modified to read:

$$\omega_n = \sqrt{\frac{A}{W_f}} \cdot \frac{1}{2\pi} \sqrt{\frac{K'g}{1 + \frac{W_s}{W_f}}} \quad (3)$$

or:

$$\omega_n = \frac{\omega_{nr}}{\sqrt{p}} \quad (4)$$

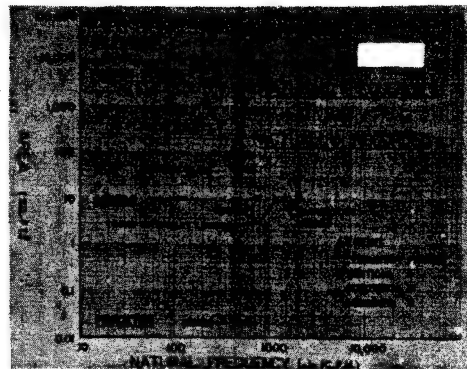
where:  $p = W_f/A$  - average unit pressure on the ground

$\omega_{nr}$  - "reduced natural frequency" or the natural frequency at an average unit pressure on the ground equal to unity, in this case to one ton/sq. ft.

Fig. 1 shows the recorded " $\omega_n$ " values plotted against size of foundation area. Presented are only tests concerning which complete information is available. Frequencies recorded due to vertical exciting forces are marked by circles; crosses indicate horizontal exciting forces. Combined forces are designated by a combination of both signs.

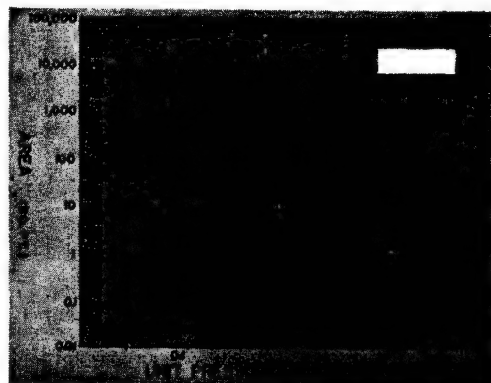
The Princeton value was obtained during tests with a 3 in. diameter plunger in a 15 in. diameter and 18 in. deep container filled with sand.

Two values are indicated for the pumping



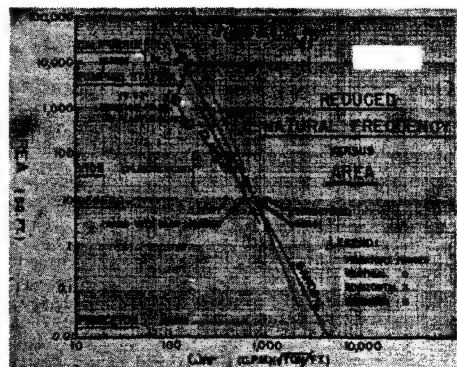
Natural frequencies as actually recorded.

FIG.1



Average unit pressures on soil surface or the cases recorded on fig. 1.

FIG.2



Reduced natural frequency versus area.

FIG.3

station. The one marked (1) is obtained if each compressor foundation is considered as acting separately; the one marked (2) is obtained if the entire station area is considered. Value (1) is believed to be the more logic-



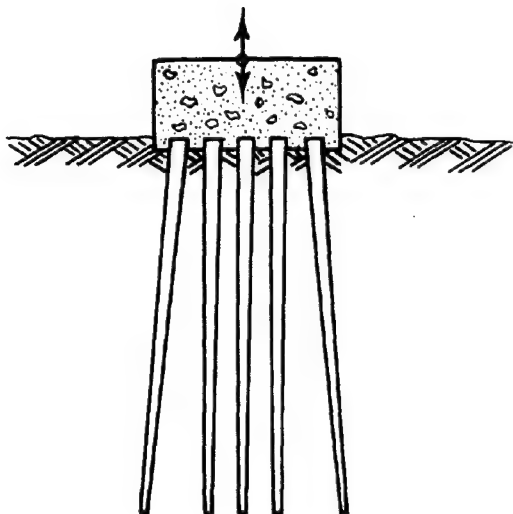


FIG. 4

al one.

The seven California buildings are the only rectangular buildings reported in Ref. 3 which were founded on sand and which had a height not exceeding their smallest dimension in plan.

Fig. 2 shows the corresponding unit pressures on the ground.

Fig. 3 gives the values of the reduced natural frequencies " $\omega_{rn}$ " computed from Fig. 1 and Fig. 2 according to formula (4). High values of vibratory forces, as in the case of the Princeton test data, can be included in the value of the unit pressure "p".

It can be seen that a definite pattern emerges. The most probable lines connecting values obtained on the same type of soil are shown in thick full lines, but a greater number of later observations may change them to the extent estimated by the thinner dash-dotted line since some scattering of results, similar to the one recorded in California, is to be expected.

The pattern shown by Fig. 3 may be explained as follows. For a given type of soil the value of the dynamic modulus of soil reaction " $k$ " in the formulas (3) and (4) changes with the size of the area. The ratio  $W_g/W_v$  either remains constant for areas of the same shape or varies only slightly.

The effect of damping is slight and is included in other characteristics of a given type of soil. Second and even third harmonics are of course possible but seem to lie outside of the normal operational range of most machines.

The effect of piles connected to the foundation in the conventional manner (Fig. 4) appears to be slight. A rigid tensile connection might take the mass of soil shown hatched on Fig. 5 participate directly in the vibrations of the foundation to the extent that its weight could be included in the value of the unit pressure "p" in formula (4). This point and its economic aspects, however, require experimental verification.

#### CONCLUSIONS.

- 1) Past attempts to determine from a few early

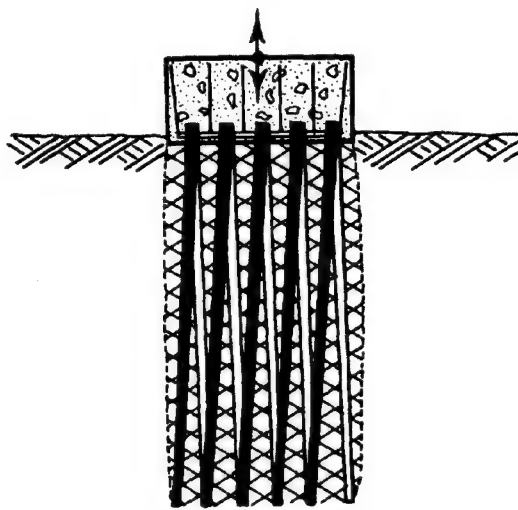


FIG. 5

experiments of limited range the numerical values of the individual soil coefficients which influence the natural frequency of machine foundations have led different researchers to conclusions which are at variance with each other and which, in some cases, are contradicted by later observations.

2) The cause of these contradictions lies in the impossibility of determining from any number of observations on one soil the numerical value of either one of the relevant soil coefficients - as the dynamic modulus of soil reaction, - without making some arbitrary assumptions concerning the value of the other, e.g. the average vibrating mass of the soil; - or vice-versa. Therefore, no greater success is to be expected from a continuation of this method of approach in the future.

3) Encouraging results have been obtained by means of the "reduced natural frequency ' $\omega_{rn}$ '" method presented in this paper. The diagrams of " $\omega_{rn}$ " values computed from the smaller number of so far available records on the matter appear to outline some definite relationships which may be used as a preliminary guide for design purposes.

4) Further experiments and observations along the same lines are needed to develop the method, to disclose possible limitations and to thereby permit its more precise use.

Acknowledgement is expressed to Prof. E.W. Suppiger, Princeton University, for a review of the manuscript of this paper.

#### REFERENCES.

- 1) "New Results of Dynamic Investigations of Foundation Soils" - (in German) - by H. Lorenz; Zeitschrift d.V.D.I., March 1934.
- 2) "Experimental Study of Vibrations of Mat Foundations Resting on Cohesive Saturated Soils" by D.D. Barkan - (in Russian with English abstract). - Transactions, Institute for Engineering Foundation Research ("V.I. O.S."); Moscow, U.S.S.R., 1934.
- 3) "Earthquake Investigations in California; 1934/35"; Special Publication No. 201; U.S. Coast and Geodetic Survey. Government Printing Office; Washington, 1936.

- 4) "Field Investigations of the Theory of Vibration of Massive Foundations Under Machines"; by D.D. Barkan, Proceedings First International Conference on Soil Mechanics and Foundation Engineering, Vol. II, 1936.
- 5) "Effect of Vibrations on the Bearing Properties of Soils" by G.P. Tschebotarioff, Proceedings, Highway Research Board, 1944.
- 6) "Vibratory and Slow Repetitional Loading of Soils" by G.P. Tschebotarioff and G.W. McAlpin, Proceedings, Highway Research Board, 1946.

-0-0-0-0-0-0-

## SUB-SECTION III e

### AERIAL PHOTOGRAPHING

III e 1

#### THE DETERMINATION OF SOIL CONDITIONS BY AERIAL PHOTOGRAPHIC ANALYSIS

DONALD J. BEICHER

Associate Professor of Civil Engineering, Cornell University, Ithaca, New York

#### ABSTRACT.

The development of aerial photography and the extensive coverage that has been accomplished in recent years has stimulated the use of airphotos to facilitate engineering planning and construction. The basis of this phase of development has been the identification of features that bear a relationship to the texture of the soil pattern although they include such elements as land form, drainage, soil color, erosion, and vegetative cover. Land form identification does much toward establishing general conditions of soil depth and texture, while surface drainage indicates relative permeability. Gullies assume various shapes and thereby reveal not only certain properties of the surface material but the existence of clay-pan developments or unrelated materials occurring below the surface. Soil color is related to texture and ground water conditions, and vegetation is a variable depending upon climate and local influences.

Assembled evidence shows that most soils can be distinguished by characteristic patterns regardless of their geographic distribution. Photographs illustrate the patterns, and test data are presented to permit the evaluation of interpretation.

#### INTRODUCTION.

Basically, airphoto analysis depends upon a well-versed acquaintance with ground features and soil characteristics. The aerial pictures provide a means of making a deliberate and a detailed study of an area and an evaluation of the land forms by an enlarged perspective. Theoretically, the same things that can be studied in the airphotos can be examined on the ground; time and limited information prevent this. The optimum condition is represented by a judicious ground investigation guided by a photo-analysis. In most instances, to see a ground feature in its entirety is to understand its origin, its composition, and its influence on the surrounding terrain. When standing on the ground, man is so dwarfed in size even by features of micro-relief that their outline and overall character is obscure or hidden.

The land forms mentioned are, in general, the land forms of geomorphology. The broad and general classification of land forms is not sufficiently specific for the detailed treatment of engineering projects; therefore, when the geologists stop with third order land forms (valleys, ridges, basins, etc.) this work requires identification of sub-forms or land forms of fourth and fifth order. This condition may be likened to two contour maps of the same area; one map with 100 foot contour intervals may present a picture of the area suitable for general use but the details

important to engineers are shown only on the map having a five-foot contour interval.

The land forms considered in this work deal with the individual materials. Where "plateau" may indicate one of several sedimentary rocks, engineers must deal specifically with limestone, or sandstone, or shale, or with combinations of these. Each is a rock differing from all others in physical and often chemical properties. Because of these differences, they weather differently to assume characteristic forms related to their individual properties.

Pedologists (soil scientists) have shown the relationship between the weathered soil profile (solum and the underlying parent material). In nearly all cases, the identification of the land form establishes the type of parent material and, therefore, the properties of the weathered soil material. In the development of this work it is necessary to work out the details of a particular land form and then to obtain a sufficient number of soil samples of the various types, within the land form, for the results to be statistically significant.

If we consider that the land form establishes the general (or exact, depending upon the origin) nature of the material, then, it has served much as the sliding adjustment in a camera serves to bring the object into approximate focus. It remains for the pedologic principles to serve as a micro-adjustment to bring

specific details of soil variations into focus.

These principles are simply expressed in the statement that, within a parent material (land form) area similar soils are developed on similar slopes. The fact that similar soils develop in similar positions i.e. depressions, or hillsides, is not confined to one particular area. Unless extremes of climate are introduced. It will be found that soils produced by the weathering of similar materials will be physiologically alike regardless of geographic locations.

The rock, the soil and the ground water are the three important factors influencing foundation sites. An illustration of the relationship between the land form and landslides is an example. Because of certain inherent characteristics, several land forms are highly susceptible to land slide failures at their unsupported margins. The identification of these land forms implies the possibility of landslides. An examination of aerial views such as that in Figure 1 will show the scars of old slides when they are present and indicate the probability of new or continued sliding.



(Scale: 1 in. = 1650 feet). This vertical photograph records the predisposition of these local materials to fail by sliding. The highway (white line) is located on sloping terrain. Recent (A) and old slides (B) along the unsupported face, running diagonally upper left to lower right, show that roads and structures near this face are susceptible to destruction by slides. Dense forest cover prevents adequate ground reconnaissance. The light gray area (C) which the road engineers attempted to circumvent is a shallow swamp; its upper border marks the approximate limit of material susceptible to sliding.

FIG.1

At present, rapid strides are being made in many areas to add to the knowledge of the various land forms and their soil and other engineering relationships. In many areas the correlations have now advanced to a point where grain-size characteristics, Atterberg limits, and natural and compacted density data can be anticipated.

#### TYPICAL LAND FORMS.

The earth's features may be divided into land forms so that each form presents separate and distinct soil characteristics, topography, rock materials, and ground water conditions.

The bedrock land forms follow the conventional delineation with several notable exceptions: granites are ultimately subdivided into low and high quartz granites; soluble limestones are separated from the dolomites and young coralline limestones. Glacial drift is subdivided into moraines, till plains, outwash plains, kames, eskers, drumlins, valley trains, peat bogs; aeolian materials into sand dunes and loess.

While the various forms are usually recognized as geologic units, each has been classified primarily upon its physical characteristics.

The following examples have been selected to illustrate the technique in representative land forms and in extreme climatic conditions of the arid and arctic regions.

#### SOLUBLE LIMESTONE.

The wide distribution of limestone on the surface of the earth, and the information existing regarding the soil material weathered from these rocks, are considerations that make this an excellent example of a bedrock land form.

The soluble limestones weather to forms having combined characteristics that set them apart from all other types. These features are recognizable in aerial photographs by those having the most elementary training, whereas, on the ground they may be indistinguishable to all but the expert. The identifying features are found in the cross-section and profile characteristics of the valleys supplemented by the presence of the sink holes in the upland (Figure 2) and the relatively angular outline of the land form. This is represented in a plan (aerial) view by the line marking



(Scale: 1 in. = 1650 feet) This vertical photograph records in exact detail the surface physical features on the numerous sink holes identifying the soluble limestone bedrock. Water standing in the sinks marks those blocked with eroded soil.

The majority are dry and free draining. The dark area (A) is a group of forested clay shale hills differing in every way from the adjacent limestone.

FIG.2

the contact between the alluvium and the upland, or between the limestone and an underlying formation. Modification of this is found in the tropics under advanced stages of weathering and also in tilted structures. Those limestones having exceptionally high quantities of

chert also have features distinguishing them from the average. The process of weathering reduces the limestone to a reddish silty-clay soil varying in thickness between one and twenty feet. Photo-analysis identifies the land form as limestone; the depth of the mantle is estimated by reference to outcrops. By the procedure outlined, the general texture of these soils has been established. Table I is an extract of data accumulated from the samples of these soils.

As a means of detecting significant variations from the general average, the relationship of soil colors (gray values on photographs), the degree of erosion and the "chert" pattern are used as an index.

#### WIND-TRANSPORTED MATERIALS.

The aeolian, or windblown soils, form extensive and important deposits in many parts of the world. They vary in size from the vast loess plains of north China, central Europe and the central United States, to relatively insignificant isolated deposits occurring in almost every country. The texture and the uniformity of these deposits has been shown by local investigations but only in isolated instances have there been efforts to bring the significance of these to the attention of engineers.

Table I  
Geographic Correlation of Limestone Soils  
Based Upon Some Atterberg Limits

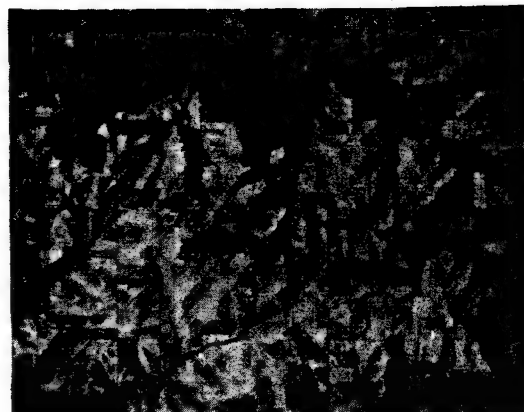
Geographic Location	Atterberg Limits	
	Liquid Limit	Plasticity Index
U.S. - Alabama	69.3	27.6
" - Arizona	57.4	33.9
" - Indiana	63.6	29.5
" - Kansas	56.8	28.4
" - Kentucky	59.1	20.3
" - Ohio	65.0	35.5
" - Oklahoma	60.0	40.9
" - West Virginia	54.1	31.7
W. Indies - Barbados (Tropical)	107.0	79.1
W. Indies - Puerto Rico (Trop.)	61.8	26.2
E. Indies - Papua (Tropical)	68.5	37.3

Without exact data, soils at the following locations have been classified as indicated.

Zanzibar, Tanganyika, N.W. Africa, Spain, Greece, Turkey, Palestine, Trinidad, Cuba, Haiti and Java as medium heavy clay to fat waxy clay ranging from plastic to very plastic in consistency.

In both the large and small areas, the photo-analysis establishes the identity of these materials. The loess and the sand dunes both have distinctive land forms. While there are some wide variations from the normal forms it has been observed in this work, that loess is usually deposited in ridges whose axes are approximately parallel.

See Figure 3. This tendency that is apparent in aerial photographs is lost to an individual on the ground. Supplementing the land form phase of the identification, there are the details of drainage and particularly the erosion forms shown in Figure 15 that are characteristic of silt. These can be relied upon to define the material and the extent of the area. In addition, gullies and slope details indicate the depth of the deposit.



(Scale: 1 in. = 4750 feet) A vertical photograph of deep loess near the source. The axis of individual ridges have been indicated to emphasize the parallelism of this land form. Studies have shown the presence of very fine sand near the source (flood plain) with a replacement by silt and clay at great distances. Samples listed in Tables II and III reflect their position with respect to the source by the amount of sand present or higher indices where sand was absent. Figure 15 shows a type of erosion typical in these loessial materials.

FIG.3

The data shown in Tables II and III illustrate the remarkable uniformity of texture and consistency regardless of geographic location. This is emphasized by the similar construction methods that are practiced in widely separated areas. These characteristics are so consistent that several highway departments have found that in the loess areas numerous elements of design and construction achieve identical results, even though widely separated. On this basis, the "shrinkage" of the material between the excavation and the embankment is relatively fixed since the natural density and the compacted density are nearly constant values. Likewise, limited data on the amount of portland cement required to stabilize loess indicates that over considerable areas ten to twelve percent by volume has been satisfactory. Figure 4 illustrates

Table II

Grain-size Data on Various Loess Deposits.

Geographic Location	Percentages of:		
	Sand	Silt	Clay
China	6.4	67.1	26.5
Germany	8.0	66.0	26.0
Iowa	6.5	76.0	17.5
Nebraska	13.0	75.0	12.0
Illinois	19.0	73.0	8.0
Missouri	15.0	67.0	18.0
Idaho	17.5	60.5	22.0
Tennessee	11.5	72.5	16.0
Mississippi	11.0	83.0	6.0
Kansas	9.0	71.2	26.6
Washington	6.8	64.0	29.2
Wisconsin	1.0	68.0	31.0
Colorado	11.0	68.8	20.2
South Dakota	2.0	76.3	20.4
Louisiana	4.0	88.0	8.0
Kentucky	0.6	88.8	10.6

a construction characteristic to be observed in all loess areas.



Bench-type construction in loess. The rule of vertical cut slopes introduces an element of instability in deep cuts. In sub-humid climates of the northwestern U.S. and China simple slopes in 80 to 100 feet cuts have been satisfactory. Excessively erosive, these soil materials require special protection from running water. The source area of the loess can be seen in the background. Back of the camera the loess extends as a gradually thinning deposit, for more than 100 miles. (Courtesy: The Highway Magazine)

FIG.4

Table III

Soem Physical Test Results on Loessial Materials

Geographic Location	Liquid Limit	Plasticity Index	Max.Wt. (Dry) lbs /Cu. Ft. (Proctor)	Optimum Moisture
China	29.	6.1	--	--
Tennessee	29.0	4.9	104.5	18.2
Mississippi	31.8	3.1	104.9	17.8
Illinois	26.2	3.9	106.2	15.5
Washington	30.7	7.5	99.5	21.4
Missouri	33.6	16.3	--	--
Nebraska	32.0	8.0	--	--
Indiana	29.6	7.6	--	--
Iowa	28.0	9.5	--	--

Dune sand also presents a remarkable uniformity that has been caused by the sorting action of the wind. The recognition of the dune form in airphotos establishes the limits of the grain size within a narrow range. Figure 5 shows a typical dune pattern in the sub-arctic. Similar dunes are commonplace in the tropics. Samples of dunes from the arctic coast to the southern hemisphere have furnished the statistical proof of their uniformity. A brief of this data is shown in Table IV. Having established the land form and the texture of these soils, observations and records indicate the best practice to be followed in dealing with them as subgrade or foundation material. Thus the concept of the land form provides a basis of comparison for extending experience and practice.

#### GLACIATED REGIONS.

The areas of the earth that have been in-



(Scale: 1 in. = 1650 ft.) This vertical photograph is of a heavily forested dune and swamp area. In spite of the cover the light gray of the dry sand is obvious. Recognizing the characteristic form of dunes and estimating their distance from the source permits reference to Table IV for a close approximation of the grain size distribution.

FIG.5

fluenced by glaciation may contain any or all of the land forms previously attributed to glacial or fluvioglacial origin. Of particular interest to engineers are the level, well-drained terraces or "valley trains". These gravel and sand plains offer excellent sites for airports and highways since the essential feature of this land form is its nearly level surface. While good sub-drainage is the rule in such areas an inspection of the aerial photos will show considerable variation in soil and drainage conditions, within the terrace area. Figure 6 illustrates such an area. Referring to the fundamental differences between the relatively clean (quartz) sands and the mineralogical heterogeneous gravel-sand mixtures it is possible to distinguish between areas that are preponderantly sandy and those that contain appreciable amounts of gravel. Differences in weathering characteristics and corresponding differences in gray tones are directly related.

In many areas large quantities of sand and gravel are required for construction work. As aggregate, as base course material, or as fill material these granular materials are often of utmost importance. One of the notable land forms in which gravel and sand is found is the esker.

Whether in heavily forested areas or in other surroundings, the esker is easily located in airphotos. Figure 8 illustrates the striking form of this type of glacial deposit.

#### CLIMATIC INFLUENCES.

In areas where extremes of climate are experienced there are numerous influences that are not present under moderate climatic conditions. In such areas airphotos are particularly valuable because of the limited knowledge of terrain conditions. Desert areas and the arctic regions are examples of extremes of climate that exert great influence on soil and foundation conditions.

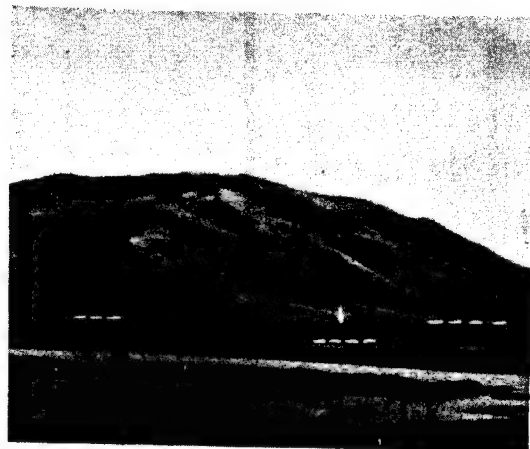
The particular problems of the arctic





(Scale: 1 in. = 6750 ft.) This vertical view presents the strong contrast in soil patterns found in relatively impervious silty clay and that associated with gravels. The integrated drainage pattern and the mottled black and white soil pattern mark two-fifths of the area as a silty clay. The relatively plain appearance of the central portion is a typical gravel pattern. The small irregular dark dots in this area are very slight depressions acting as "infiltration basins" for surface water. Although the area represents several square miles no surface run off occurs. Coarse gravel occurs in the light band that parallels the boundary between the two deposits.

FIG.6

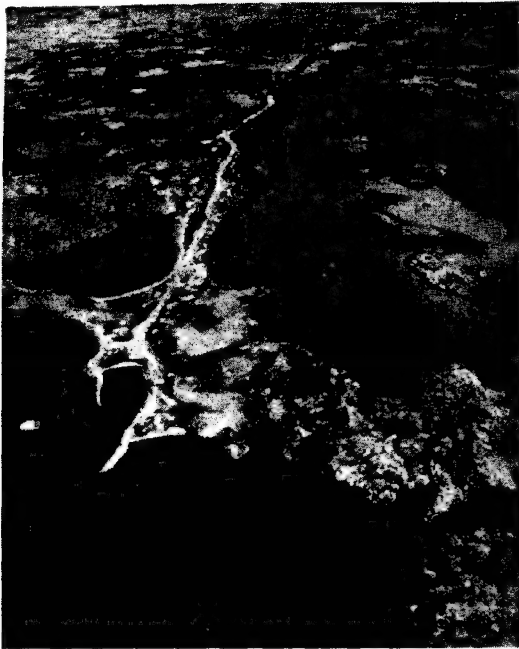


A ground view of a terrace showing the flat surface, the associated upland and the recent alluvium in the foreground. The well defined edges, lack of surface drainage, and absence of gullies on the terrace face indicate the presence of gravel. (Photo: H.E. Nelson)

FIG.7

TABLE IV

Mechanical Analyses Of Dune Sands						
Geographic Location	Number Samples	Plus 20	Sieve Analysis (Ave.)		Pass 60 Ret.100	Minus 100
			Pass 20 Ret.40	Pass 40 Ret.60		
U. S. Nebraska	20	Trace	5.9	20.8	66.1	6.9
" Wisconsin	3	0.4	20.8	33.4	36.6	8.6+
" Illinois	8	-	2.1	14.0	69.9	14.0
" N. Dakota	5	Trace	9.2	20.3	58.9	11.4
" Kansas	3	"	4.7	24.3	67.3	2.6+
" Massachusetts	2	"	5.5	23.4	67.6	2.3+
" Washington	1	6.0	14.0	41.0	27.5	11.5
" Alaska	2	-	-	21.8	58.2	20.0
British Columbia	1	-	6.5	31.2	43.6	17.5+
Peru, S. A.	1	-	Trace	0.3	87.3	12.3+
Laborador	1	-	3.2	26.6	59.2	11.0
Churchill Manitoba	1	-	6.6	38.5	54.7	0.2
Pan American Hwy. C. A.	1	-	0.5	5.4	59.2	34.7



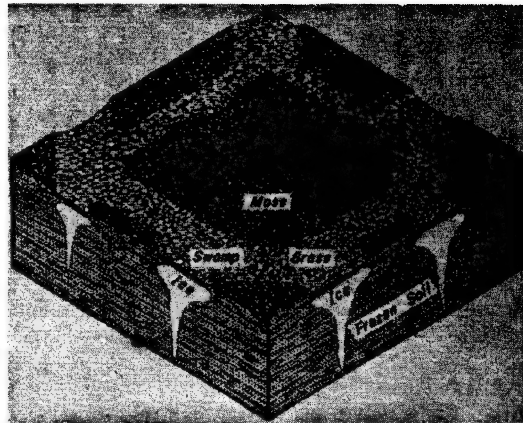
An oblique view of an esker. This gravel ridge resembling a long "fill" has an unmistakable land form. Some eskers reach the length of 100 miles, others a few hundred yards. Lakes interspersed among bare granite hills comprise the balance of the area. (RCAF photo).

FIG.8



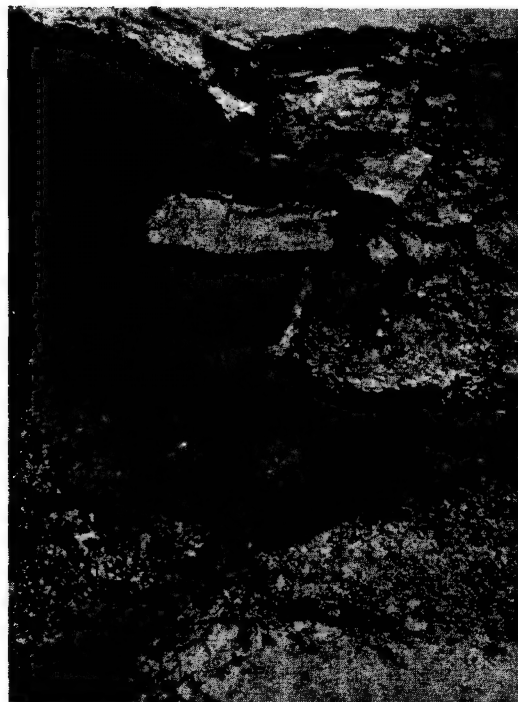
An oblique view of an area of frozen ground. The polygon pattern is formed by very slight depressions in which swamp grass is found. Arctic moss covers the surface on the interior of the polygon. Large masses of ground ice are coincident with the outlines.

FIG.9



A block diagram showing a section of frozen ground and the relationship between the polygonal surface pattern and the massive ground ice. See also Figures 11 and 12.

FIG.10



A "wedge" of ground ice melting after the surface insulation of moss had been removed. The distance from the ground surface to the top of the ice is about 12 inches.

FIG.11





The result of stripping this area was the formation of a polygon "trench" system. There has been no erosion or loss of soil. The runway in the background was similarly "dissected."

FIG.12

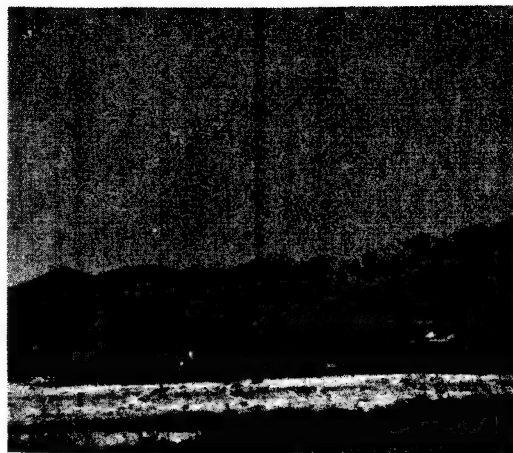
are associated with areas where the average annual temperature falls below the freezing point; under such circumstances the temperature of the ground is generally below freezing. Perennially frozen ground, or permafrost, exists under these conditions but the problem becomes critical only when water has been supplied to the soil and that water has been concentrated into ice lenses and masses of ground ice. The construction of buildings, roads, and runways or in fact any disturbance of the ground cover initiates melting and a resulting excessive settlement.

Photo-analysis of arctic areas is of value in that it permits (1) the location of ice-free deposits of sand and gravel, (2) the subdivision of frozen soil areas into several stages of permafrost development and (3) the identification of those types of bedrock that are free of permafrost and those seriously altered by accumulated ground ice.

Two general conditions are encountered. In areas where unconsolidated materials are present, the young deposits such as flood plain materials have ice present in minor lenses and veins. In older materials the ground ice has formed into massive wedges of ice that are often several feet wide at the surface and taper downward to depths of as much as forty feet. In plan these wedges form into the polygonal pattern shown in Figure 9. The block diagram in Figure 10 shows the relationship between the surface pattern and the sub-surface conditions. Figures 11 and 12 show the wedge form of the ground ice and the results of disturbing these areas.

#### ARID REGIONS.

In dry areas the excessive run-off occasioned by the lack of vegetation carries great masses of soil material and rock debris from the mountain slopes out into the low valley areas typical of these regions. Aerial photographs of these areas are of great value in selecting the best available location for engineering works. Railroads and highways, because of soil and water conditions are generally lo-



Alkali flats are found in the arid regions of all continents. In addition to identification of soil areas on the basis of texture, aerial photographs can be used to locate alkali soils, ground water seepage zones, and active channel areas. The white area in the foreground is crusted with salts of potassium, magnesium, sodium, calcium and other compounds. (Photo: H.E. Nelson)

FIG.13

cated on the transition slopes between the hills and valley floor. In this transition area the shifting channels and accumulating debris require detailed planning for the protection of the right-of-way. The photographs provide the precise record of details that are necessary for proper original location and subsequent protection.

Pipe lines, and airports as well as the other transportation lines also must transact the "Basin" areas such as that shown in Figure 13. Within these areas the various textural groups of soil materials must be identified largely on the basis of microrelief indicating the type of deposition and the gray values of the related soil areas. The gray tones alone have proved very accurate in typical areas. In these dry regions the presence of alkali, particularly in depressions, inverts the usual order of tones by producing light tones in the low areas. These alkali flats are relatively important since in these high concentrations of salts are to be found the same compounds used in the accelerated weathering or "soundness" tests of aggregates and concretes. Early disintegration of concrete and the rapid corrosion of pipe lines and metal culverts are associated with these alkali soils. For example, the United States National Bureau of Standards correlation shows that eight-inch steel pipes placed in such areas can be expected to corrode and leak within five years. Similarly, muck soils (also clearly delineated in photographs) will corrode pipe within seven years.

#### INDEPENDENT METHOD OF ANALYSIS.

As a means of cross-checking the described method of analysis of soil and ground conditions or when the identity of the land form is obscure, three elements of the soil pattern have



Areas marked "A" are volcanic vents representing high rock masses. Below them the sloping to level ground is composed of rock waste ranging from silt size to coarse gravel. These are assorted and transported by water into the valley. The two carving black lines are a railroad and highway. Washouts caused by the numerous channels and eventual burial by debris are the results of improper location in these regions.

FIG.14

been established as indicators of texture and/or other soil properties.

#### DRAINAGE AND EROSION.

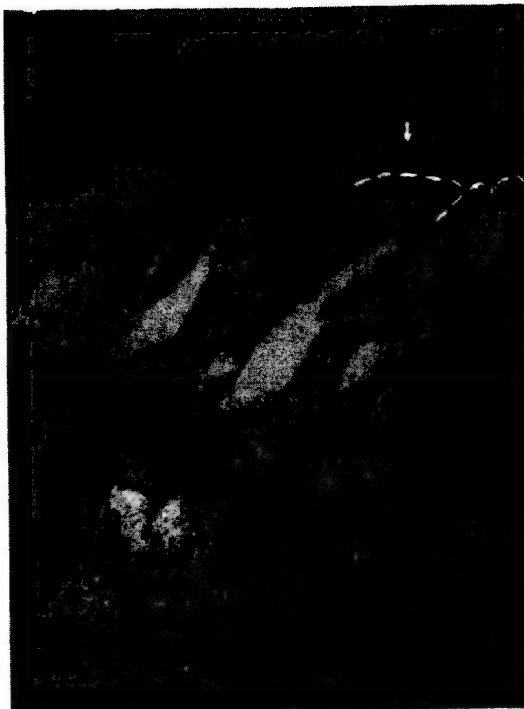
The amount and type of surface drainage on these land forms is related to slope and permeability of a land mass. Where there is a large amount of surface drainage on level to undulating relief, the soil material can be expected to be relatively impervious, while a lack of surface drainage indicates a porous land mass. Recent alluvium is an exception since it is periodically refreshed by overflow.

Not only does the presence of surface drainage indicate retarded internal drainage, but there is more to learn from the drainage pattern. Gullies and drainage ways, possess distinctive characteristics depending chiefly on the texture of the soil materials that are being eroded. Gully shapes both in cross section and profile are indicative of texture.

Earth materials, such as ice-laid drift and valley trains, that can be described as slightly cohesive are marked by short, sharpened, V-shaped gullies having a steep but rather uniform gradient from head to foot. In contrast, gullies in plastic, cohesive soil materials have long, low, uniform gradients. In cross section these gullies will have well-rounded, sloping sides. Where these characteristics change in the length of a gully, a change in the soil profile is indicated. Where gullies erode through a surface mantle and encounter a deep and contrasting sub-stratum, the cross-section shape will change.

Erosion features of sand-clays and silts have distinct and individual characteristics; their gullies, for instance, have a compound gradient and are generally U-shaped in cross section. See Figure 15.

Since these features are impartially recorded on an aerial photograph an interpreter



Gully erosion in silts. These are U-shaped gullies both in plan and cross-section. As opposed to gullies in clays or granular materials, these have a compound gradient. "Cat-steps" may be seen above the head of several of these gullies. Such erosion features are found in the loess areas of all continents.

(Photo: H.E. Nelson)

FIG.15

can make a deliberate and detailed study of this and other elements of the soil pattern.

#### COLOR

Like other elements in the soil pattern, color is only a relative indicator of texture. Each element by itself is ordinarily insufficient evidence on which to base a judgment of texture; therefore, it is desirable to examine and evaluate each of these elements present in an area. This is usually practical since a single photograph will record nearly 10 square miles of area. Light color tones (grays) are usually associated with well-drained soils, while clays, principally because of their water-retention capacity, appear dark. Well-drained silts, sands and sand-gravel mixtures appear as light tones on aerial photographs. Such color values are often ascribed to vegetation and cover crops. While surface cover obviously will tend to obliterate a soil color, there are few cultivated crops sufficiently extensive and dense to obscure entirely, the trend of the pattern. This condition is shown in Figures 5, 6, and 8.

Vegetation is a product, not only of soil and climate but of soil-climate - i.e., the same soil material occurring on different slopes will have different contents. This is particularly important in tropical regions where long seasons of high rainfall are common. While

the general impression gained from flying over a rain-forest area is one of monotonous uniformity, examination of airphotos of the same area will show definite vegetative patterns following corresponding trends in soil or drainage conditions. In spite of high rainfall, gravels and sands in well-drained positions will have a "dry" soil-climate in contrast to other textural combinations found in association with them. At the other extreme the dry climate of northern interior Alaska includes areas having a wet soil-climate regardless of texture. These

are coincident with the areas of perennially frozen ground, and here vegetation changes accordingly. Consequently, in areas where the ecologic balance is undisturbed, vegetation will reflect subtle changes in the soil-climate.

Combining these various elements of the soil pattern and interpreting them in the light of experience and principles that are universally applicable makes airphoto interpretation a medium of obtaining and presenting information regarding the physical properties and conditions of surface materials.

-O-O-O-O-O-O-

### III e 2 CORRELATION BETWEEN PERMAFROST AND SOILS AS INDICATED BY AERIAL PHOTOGRAPHS

K.B. WOODS  
JEAN E. HITTLE  
R.E. FROST

Purdue University

#### SUMMARY.

This paper reports, in part, the results of a study covering the relationship between soil textures, soil position, vegetation, and permafrost as indicated by airphoto patterns of materials from Arctic and Subarctic regions. The work was performed by the Engineering Experiment Station, Purdue University, for and in co-operation with the St. Paul District, Corps of Engineers, War Department. This phase of the permafrost program has been under way since 1945 and covers both the airphoto identification features as well as field observations in many sections of the Territory of Alaska.

On the basis of correlation surveys of many and varied areas it was found that the Territory could be divided into a series of regions, each of which had characteristics peculiar to that region. These areas, in effect, are climatic-vegetative bands consisting of (1) Tundra Zone Permafrost; (2) Timber Zone, Permafrost; and (3) Timber Zone, Unfrozen. These areas, generally speaking, are representative of physiographic regions.

In general each of these major areas produces a definite standard or typical airphoto pattern, the successful interpretation of which makes engineering soil evaluation possible. Even though the study is in the development stage, it has been found that airphotos can be used to evaluate and predict permafrost conditions.

The correlation between permafrost-soil conditions and their corresponding airphoto pattern was made first by obtaining high-grade aerial photographs for several and varied areas throughout the Territory. The areas for airphoto coverage were selected so as to include a range of climatic and physiographic conditions; also, the areas were selected so that rock textures from several geologic ages would be represented.

Experience has shown that trimetrogon aerial photographs having an approximate scale of 1 : 20,000 are best-suited to general airphoto-soil analysis. In addition it has been found desirable to obtain photo coverage of several square miles of a region so that all of the topographic variations can be associated with each other and thus assist in the interpretation of the physiographic land forms. The oblique photographs of the trimetrogon series are extremely useful in identifying local and surrounding physiographic land forms. In those cases where detailed analysis is required the conventional vertical aerial photographs having a scale of 1 : 10,000 are well adapted to the airphoto analysis of soils and permafrost conditions and should supplement the trimetrogon photo coverage.

After airphoto coverage was obtained for the several areas throughout Alaska, these airphotos were carefully studied. Detailed office

notes were made on the airphoto patterns for each of the areas being studied. This preliminary analysis consisted of identifying, where possible, the physiographic land forms; the erosional features; the prevailing types of vegetation and their association with topographic position. In those cases where the airphoto pattern could not be deciphered, the patterns were marked for field checking. Further, all available geological information covering the region being studied was reviewed and where this information dealt specifically with the prevailing soil and rock textures additional notes were taken.

Following the preliminary airphoto analysis, field parties were organized and were flown to the selected sites covered by photography. This feature of air transportation made it possible to cover remote areas; also the field parties were able to obtain general information of the topography and vegetation of sections not covered by aerial photographs.

The field work consisted of making detailed inspections of the local areas covered by photography. Borings were made to determine the characteristics of the soil profile. Field notations covered topographic position, the type of vegetative cover, the thickness of the organic surface horizon, the texture and character of the soil, and where possible the depth to permafrost. On the steep slope of bedrock areas



Airphoto pattern of a braided stream in a broad, silt-filled valley. In this instance permafrost prevails in the silt flood plains.

FIG.1

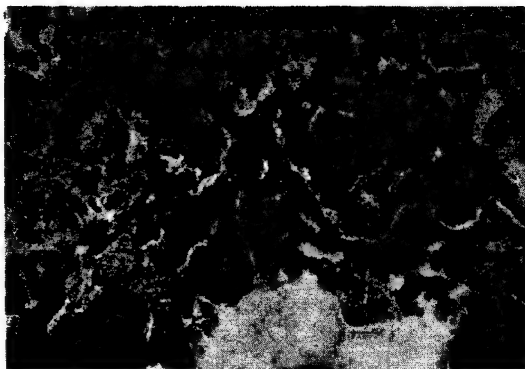
where the soil mantle was thin, practically all of these items were readily discerned by a visual inspection. However, in other sections, where the soil mantle was well-developed, a number of borings were necessary to determine the representative profile conditions. By selecting typical topographic positions for making the soil borings, it was possible to correlate the soil and permafrost conditions with the respective airphoto patterns in a relatively short period of time.

Ground photographs were taken of the local topography, vegetation, soil profile exposures, as well as any other features pertinent to the phenomena of permafrost. The "on-foot" inspections were supplemented by low-altitude reconnaissance flights over the survey areas. Photographs were taken of local features that would be of assistance in rendering an interpretation of the airphoto patterns.

After the airphoto patterns for several areas had been correlated with the permafrost-soil conditions it was found that the Territory of Alaska could be divided into a series of regions, each of which have characteristics peculiar to the region in question. The Tundra Zone for the most part is confined to the Coastal Plain and Arctic Piedmont regions. This includes the region north from the Brooks Range to the Arctic Ocean, most of the Seward Peninsula, and the Coastal regions adjacent to the lower reaches of the Yukon and Kuskokwim River valleys. The Timber Zone, Permafrost, in general, lies between the Alaska Range and the Brooks Range. This region may be considered a low, interior plateau which is traversed by many large rivers, including the Yukon, Tanana, Koyukuk, and the Kuskokwim. The Timber Zone, Unfrozen includes the Coastal region south of the Alaska Range. This section is rough topographically and is timbered along the immediate coast line and the major river valleys. The influence of the Japanese current gives this region a mild climate which is in contrast to the frigid climate of the interior regions.

#### Tundra Zone, Permafrost

The tundra zone includes the Arctic Coastal Plain, the Arctic Piedmont Region, and a major portion of the Seward Peninsula. The soils of the coastal plain sediments consist largely of fine sands, silts, fine gravels, and in some places, clays. The airphoto pattern



A typical airphoto pattern of a muskeg area in a broad, valley-fill region. The soils in this instance are frozen peat and silt.

FIG.2

of the coastal plain is characterized by polygons, extremely flat topography, numerous elongated lakes and elongated sand ridges. Two types of polygons prevail, including the depressed-channel and depressed-center types. In each instance the presence of these polygons indicates that detrimental permafrost exists. Throughout a great portion of the coastal plain there are frost mounds (often called pingos) some of which attain a height of 80 or 90 feet. The second important great soil area of the tundra zone is the Arctic Piedmont which lies between the Brooks Range and the Coastal plain. This is a broad, gently-tilted-shale-plateau-like region somewhat dissected by streams. The area contains clay and sandy shales, sandstones, broad alluvial flats of the river valleys, granular terraces, and in places a mantle of fluvial outwash which overlies the shale. These materials are also readily identifiable from airphotos despite the general permafrost condition and absence of vegetation other than the tundra type.

#### Timber Zone, Permafrost

The soils of the interior region between the Brooks Range and the Alaska Range consist primarily of vast expanses of fine-grained alluvial materials, bordered by low-lying hills of metamorphic, sedimentary, and igneous rocks. The transitions in topography between the low rock hills and the flat alluvial areas consist frequently of colluvial materials.

Generally speaking, the soil cover on the bedrock hills and the colluvial slopes is very thin; however, the soil mantle becomes thicker on the flatter portions of the colluvial slopes. Where the ground slope is favorable to good runoff there is but little permafrost development; in contrast, however, the flatter ground slopes frequently contain permafrost. This is especially true where fine-grained soil materials are encountered.

The airphoto pattern of the bedrock hills can be readily identified, in some instances, by the absence of vegetation; also the topographic expression of the hills can be seen in either oblique photographs or in stereoscopic vertical photographs. The colluvial slopes also have a distinctive airphoto pattern. The surface runoff produces an alignment of the surface vegetation which in turn gives a characteristic fan-like-flow markings to the airphoto pattern for these colluvial slopes.



Intense polygon development indicating detrimental permafrost.

FIG.3

Glaciation has played an important role in the distribution of soil materials in this region, particularly in those areas adjacent to the Brooks and Alaska Ranges. In the immediate vicinity of these mountains a wide range of glacial materials are to be found in the morainic deposits, granular outwash plains, and terraces. Also, streams emanating from the mountain glaciers have produced extensive granular outwash plains and gravel terraces which form the bench topography that continues from the foothills of the mountain ranges toward the major stream valleys.

Although there is some variation in the texture of the soil materials found in the outwash plains and terraces, they are all distinctly granular and are therefore well-drained when they occupy elevated positions. For this reason, permafrost in the detrimental stage occurs only rarely in these materials. Accordingly, these granular outwash plains and gravel terraces make exceptionally good sites for the location of structures, whether they be cities, highways, or airports. Moreover, the level topography of these granular deposits hold grading operations to a minimum.

The airphoto pattern for the granular outwash plains and gravel terraces can be identified principally on the basis of their level topography and the dense stands of poplar, birch, and aspen trees which seek, naturally, well-drained locations for growth. Areas supporting these types of timber growth produce an airphoto pattern that is in distinct contrast to the patterns for areas covered with black spruce, which grows readily in poorly-drained locations and is the predominate type of timber growth in the interior of Alaska.

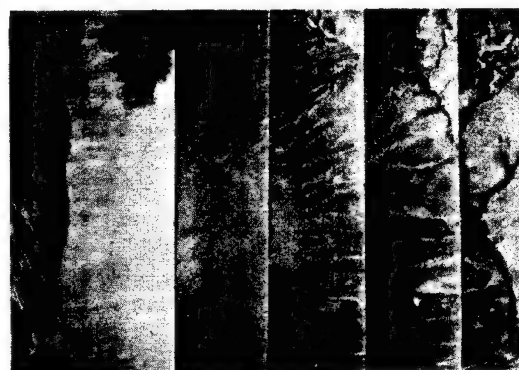
In addition to producing granular terraces and outwash plains, the glacial streams have also produced a marked effect upon the alluvial areas. Enormous quantities of fine sands and silts have been deposited in the river and stream valleys, thus producing vast expanses of alluvial sands and silts, studded with small lakes, muskeg bogs, and a lace work of stream meanders and meander scars. These features are readily seen in aerial photographs and serve to identify the airphoto patterns for alluvial areas.

In alluvial areas permafrost prevails under practically all conditions, since the low topographic position makes water readily available at all times. The surface vegetation con-



An airphoto pattern of a dissected basalt plateau. Permafrost prevails in the soil mantle developed on the basalt.

FIG.4



Contrasting airphoto patterns of contrasting soil types are illustrated in this photo. Two materials, upland residual soils and colluvial materials, are shown.

FIG.5

sists principally of sphagnum moss, which grows vigorously and overlies thick deposits of peat. This vegetative mantle acts as a natural thermal insulation for the permafrost and is a distinct factor in the growth and preservation of permafrost in these areas.

The combination of extremely low temperatures, available ground water, and to a certain extent fine-grained soil materials, produce ground surface features called polygons, which are shallow, trench-like depressions connected in the configuration of a polygon. Polygons in the interior of Alaska are associated with the severest form of permafrost since massive wedges of clear ice are found frequently in the substratum of the polygon trenches. The fine-textured sediments of the alluvial areas abound with polygons, which form a distinctive airphoto pattern despite the fact that in some areas polygons are difficult to see by ground inspections.

#### Timber Zone, Unfrozen

The predominate soil materials south of the Alaska Range consist of glacial outwash sediments. This area is still one of many act-



ive glaciers which continue to develop outwash-  
es and gravel terraces. In many areas these  
glacial sediments have been laid down over de-  
posits of soft clay-shale and lignite of Ter-  
tiary Age. Because of the highly plastic nature  
of this clay-like material it is an extremely  
undesirable engineering material and is to be  
avoided whenever possible. Permafrost in this  
region is not a problem since the climate is  
relatively mild. A mean annual temperature well  
above 32° F prevails.

The airphoto pattern for the sand and  
gravel terraces can be readily identified on  
the basis of the bench-like topography and the  
bench-like topography and the predominance of  
deciduous trees which seek well-drained loca-  
tions. The outwash areas which are extensive  
in this region contain "island" areas of sand  
and gravel terrace remnants which usually a  
growth of black spruce and are surrounded by  
shallow channels filled with moss and other

vegetal debris. These features form a distinct  
airphoto pattern for the outwash areas.

#### CONCLUSIONS

Even though the work on this project is  
not complete, it has been demonstrated that  
aerial photographs can be used to identify  
permafrost in Arctic and Subarctic regions. As  
a result, airphotos become an engineering tool  
in locating airports, highways, and railways,  
not only in developed areas but also in relat-  
ively undeveloped regions where maps and other  
sources of information on soils and materials  
of construction are meager. In Arctic and Sub-  
arctic regions the detrimental permafrost  
areas can be determined from the aerial photo-  
graphs and structures can be designed with at  
least some knowledge of subsurface ice condi-  
tions.

-O-O-O-O-O-O-

### III e 3

#### AERIAL PHOTOGRAPHS USED FOR AN ENGINEERING EVALUATION OF SOIL MATERIALS

R.E. FROST and K.B. WOODS

Purdue University

#### SYNOPSIS.

This paper reports, in part, the results of studies covering the use of aerial photographs  
in determining the distribution of soils, the boundaries between unlike soils, and the engineer-  
ing characteristics of soils and soil materials occurring on or near the earth's surface. The  
work was initiated originally by the Joint Highway Research Project— an organization sponsored  
jointly by Purdue University and the State Highway Commission of Indiana. During the last World  
War, the air photo method was extended to cover a study of United States soils. Currently, Pur-  
due University is co-operating with the Corps of Engineers, United States Army in a field and  
laboratory study to determine the engineering significance of the aerial photograph pattern of  
permanently frozen soils. The air photo studies have been under way for a period of more than  
six years and some statements of progress have been published in technical journals and bulle-  
tins. This paper consists essentially of a summary of the developments resulting from these  
studies.

The aerial photograph has become an important tool for all phases of Civil Engineering con-  
struction dealing with soils and rocks as surface materials—highways, airports, location of con-  
struction materials, and many others. In modern engineering the aerial photograph is almost in-  
dispensable, be the job one of the construction of a drainage map of a water-shed area, site  
selection for a highway, airport, or pipe line, or laying out the program for the sampling ope-  
rations necessary for completing a soil survey.

Aerial photographs have been used extensively and for many years as an aid in developing  
soil survey maps for agricultural use. Bushnell states (25 P. 41) that "Most of the areas pub-  
lished since 1912 are considered to be at least reasonably good, although all surveys made af-  
ter 1929 meet higher standards of accuracy because they have been made with the aid of aerial  
photographs."

#### PROCEDURES.

The procedures which were and are used in  
developing the air photo technique are logical  
and are easily followed. Essentially they con-  
sisted of detailed laboratory studies of aerial  
photographs covering the specific areas follow-  
ed by intensive field checks with the aerial  
photographs in hand. Step by step, the fine de-  
tails of the pattern of each aerial photograph  
were worked out in the field. By this method  
such items as soil-texture variations within  
the soil profile, ground-water conditions, and  
topographic position were gradually correlated  
with the pattern found on the aerial photograph.  
The next step consisted of checking widely se-  
parated areas which produced identical or near

identical airphoto patterns. Thus, it was es-  
tablished that a given soil material, includ-  
ing the entire developed soil profile, produc-  
ed a specific pattern on the airphoto, which  
pattern was similar for similar soil materials  
regardless of where or how far apart these si-  
milar materials occurred. The process, essen-  
tially, became one of "finger printing" the  
various materials within a region or regions.

It was found that aerial photographs could  
be used with speed and accuracy in establishing  
boundaries between areas of dissimilar textured  
soils. Furthermore, it was established early in  
the research that the resulting areas of simi-  
lar soils frequently coincided, either directly  
or indirectly, with areas mapped by pedological

or geological methods. These observations led to the conclusion that a thorough understanding of pedology and geology was essential in using aerial photographs to determine the processes of nature through which soils have been developed or transported. Finally, it was determined that the aerial photograph recorded fine variations in textures of soils and that minute details of a soil profile, generally, could be determined either by direct reading or by inference. Granular materials occurring in dunes, terraces, outwash plains, kames and eskers are among the most easily identifiable land forms and such rocks as limestones and trap can usually be mapped with relative ease. Since the aerial photograph can be used to determine characteristics of the soil profile, from the surface downward for several feet, it follows that one of the ultimate uses is that of developing engineering soil maps for large geographical units.

#### LIMITATIONS.

Many years of research have brought out limitations to the use of aerial photographs in determining soil conditions. One important factor is the scale of the photograph—the smaller the scale the less the amount of engineering information which can be obtained. The photographs must be used in stereo-pairs to develop a maximum of information. The time of year of flying is an important variable because of vegetation changes and because of variations in soil-moisture content. Vegetative cover has some influence on the ultimate value of airphotos in determining soil conditions, a dense forest cover being particularly serious. Certain field crops, such as soy beans, tend to obliterate the normal pattern. Finally, the ability, knowledge, and training of the interpreter, limits the ultimate use of the aerial photograph, regardless of the composition of the print.

#### ELEMENTS OF THE PATTERN.

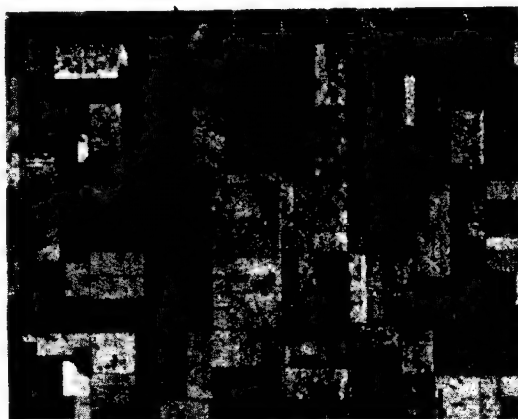
There are numerous elements of the airphoto pattern which must be studied and evaluated. Perhaps the most important of these is the position and topographic expression of the rock or soil material in relationship to the surrounding terrain. Of almost equal importance are the drainage characteristics. Variations in the drainage pattern are indicated by vegetation and vegetative bands, by slightly depressed channel-ways which accommodate local run-off and which are usually darker in color than are the surrounding soil-areas. The dark color is caused by increase in the organic content and by the fact that the soils in depressed areas contain a much higher moisture content than the adjacent soils in a higher topographic position. Erosion characteristics are also important in studying the airphoto pattern since they reflect rather accurately variations in the soil profile and they present a clue to the over-all soil texture. Finally, the agricultural usage, native vegetation, and man-made physical features are important factors which must be considered.

#### Topographic Expression.

Certain textures of soil and rock materials are usually to be found in certain standard topographic positions, the identification of which is relatively easy in matched aerial photographs when viewed stereoptically. For a great many of such soil and rock materials, the topographic features present the first clue in deciphering the airphoto pattern and in the de-

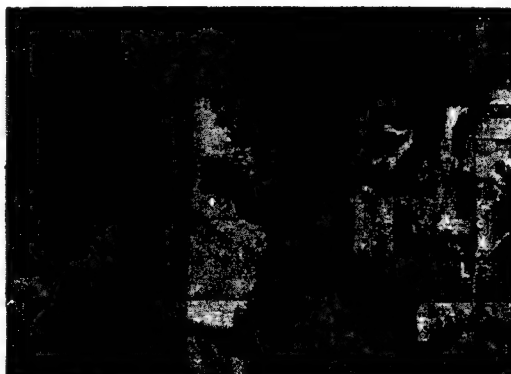
termination of the class of material being studied.

Because of the importance of granular materials for engineering construction, more than average emphasis has been placed on their airphoto identification. In glacial regions or in mountainous country, terraces, valleytrains, and fan-shaped deltas at the foot of mountains are usually indicative of granular materials. Gravel terraces form prominent features of glacial streams, important airphoto elements being flat-topped surfaces, steep faces adjacent to the stream proper, a slight tendency to develop a "mottled" pattern, and the general absence of streams crossing the terrace. (Fig. 1). The definition, topographic position, and use as a source of granular material of kames and eskers has been developed in detail and extensive treatment is not warranted here, (18), (19). Lake and coastal plain sands occur in level, subdued topographic positions which, added to information developed on the erosion, drainage, and particularly vegetation pattern, will usually be adequate to identify the material texturally. (Fig. 2).



The airphoto pattern produced by some granular soils is characterized by light color tones, current markings, flat topography, and a speckled mottling.

FIG.1



This is a typical airphoto pattern of a flat sand plain in a humid region.

FIG.2





This illustrates the photo pattern of one type of sand dune (arid climate).

FIG.3



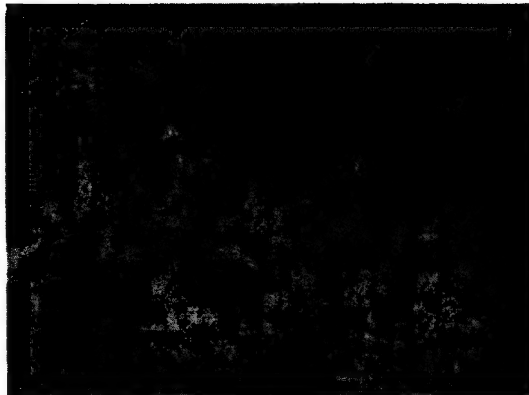
An illustration of sand dunes in a humid climate.

FIG.4



Wind blown silt (loess) is characterized by parallel ridging, a pinnate gully system, and light soft color tones.

FIG.5



Some limestones can be identified by the presence of sinkholes.

FIG.6



Flat-lying clay shales reflect in a pattern containing softly rounded slopes, light and dark color tones, a dendritic drainage pattern, and saucer shaped gullies.

FIG.7

Wind-deposited materials lend themselves to relatively easy airphoto identification chiefly because of their topographic peculiarities. Sands occur in well-defined and easily identified ridges, hills, and dunes. (Fig. 3 and 4). Silts occur in various topographic expressions, the most common of which is parallel ridges. (Fig. 5).

The airphoto identification of soils developed from the disintegration and decomposition of rock in place is approached, logically enough, by a study of the rock materials themselves. Here again a knowledge of the various topographic forms, typical of the material or materials in question, gives a clue to the type of rock being studied. For instance, limestones weather frequently to "karst" topography, the more soluble types forming innumerable sinkholes. The occurrence of "sinks" as illustrated in Figure 6 is almost certain proof of the rock material being limestone, and that the surface soils are a product of the weathering of limestone rocks. In contrast deep shales weather



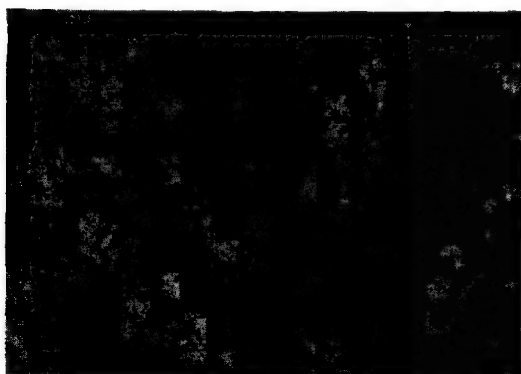
Thinly bedded sandstone and shale (flat lying) produces a pattern characterized by a dendritic drainage system, rugged topography, angularity in the topographic features, and V-shaped valleys.

FIG.8



This is the pattern of strata of massive sandstone and massive shale.

FIG.9



The Wisconsin glacial drift till plains are indicated by flat topography and an irregularly shaped light and dark mottling color tones.

FIG.10



The till plains of the Illinoian glacial drift regions are characterized by the white fringed gully system.

FIG.11

to soft slopes and they frequently occupy depressed situations, (Fig. 7). Massive sandstones frequently form cliffs and escarpments while interbedded shales with sandstones are usually dissected, (Fig. 8) which, in some instances, develops a banded pattern along the hill slopes, (Fig. 9.)

#### Drainage, Erosion and Color Tone Characteristics.

Till plains, being composed of deep deposits of unassorted sands, gravels, silt, and clays reflect variations in topography in the vegetation, drainage, and color-tone patterns. Slight depressions accumulate and hold, in the soil, more water than do the adjacent slight rises; more luxuriant vegetation results, more organic material accumulates and the resulting pattern is dark in tone in contrast to a light tone for the adjacent, better drained rises. (See Fig. 10). Older drift materials are characterized by a silty texture of the surface horizons, flat topography, and a "fringed" gully system. (Fig. 11).

Much research has been performed on the correlation of the airphoto drainage pattern with rock and soil textures 9), 23). Granular soils, being porous, are practically barren of a drainage pattern (Figs. 1 & 2), while clay-like materials develop an intensive dendritic pattern. Wind-blown silts, frequently develop parallel dendritic drainage patterns (Fig. 5) which is logical in considering the typical topographic expressions.

The erosion pattern frequently can be used to develop information of fine detail covering the soil layers making up the soil profile. An important feature is the gully-system-the arrangement or plan of the primary or secondary drainage pattern. The primary, or first order drainage, consists of the individual field gully developments; the secondary or second order drainage pattern consists of the channels, or gullies, which receive the runoff from the primary gullies. The arrangement of the primary and secondary gullies into a gully system is a clue to the soil type, method of deposition (in some instances), parent material, and soil texture. As an example, loessial soils are drained by a pinnate gully system. Illinoian drift soils are drained by a white fringed subdendritic gully system, and for gravel terraces, gully systems are rarely developed because of the porous nature of the soils. Soil textures are indicated from the

cross-section and the gradient of individual gullies. Detailed stereoscopic study of aerial photographs makes it possible actually to visualize gully cross-section and gradient. Briefly, a V-shaped gully accompanied by a short steep gradient, indicates granular or semi-granular well drained soils; U-shaped gullies (box-like section) indicate sand clays and loessial soils; broad saucer-shaped and well-rounded gullies accompanied by a long uniform gradient indicate poorly drained clays and silty clay (cohesive soils).

#### Soil Color.

The soil color, as indicated in airphotos, consists of tones of gray ranging from black to white (Fig. 8). The color tones reflected indicate the relationship between soil texture, topographic position, moisture content, and natural color tones. Proper evaluation of color tones is difficult and often misleading because of topographic position and climatic influence. For example, in a humid region it is possible for sand to photograph "black" adjacent to sand which will photograph "white". In certain glacial drift soils it is possible for organic silts and silty clays to photograph "black" adjacent to more granular soils which will photograph "white". Thus, the element photo soil-color tone is misleading unless other elements are evaluated such as topographic position, gully systems, or some other feature which will identify the materials. In arid regions color tones are often low in contrast because of the absence of soil moisture. If the interpreter properly evaluates the climatic influence, topographic position and other elements then the soil color tone as an element is of extreme importance. Erosional features, vegetative cover, and man-made physical features are important in suggesting or indicating the climatic influence and the local soil moisture variations. In areas of intense agricultural activity the natural vegetative cover has been destroyed and field patterns predominate. The physical features showing the influences and practices of man are governed by climatic conditions, soil type, and other surrounding natural features. Thus, the man-made features are indirect clues to soil types.

#### SOIL SURVEY, MAPPING, AND MATERIALS SURVEY.

Soil survey and mapping for highways and airports can be simplified by the use of airphotos after the pattern or patterns of the materials being mapped are understood.

From a study of airphoto index sheets of large areas, such as a county or a watershed area, it is often possible to map the general areal soil boundaries merely by inspection of the outstanding features of each soil type. It follows that soils mapping in many cases consists merely of separating parent-material areas or separating major airphoto patterns.

Within any general soil parent material area there may be many local variations in soil texture, and other engineering characteristics. These are due to topographic variations and differences in weathering. Detailed mapping, particularly along soil boundaries, is done by study of individual photographs made to a much larger scale than that of the index sheets (a scale of 1:20,000 is preferred). In many instances it is possible to map areal soil borders to within a few hundred feet of the exact border.

Soil surveying in the field can be simplified by considerable study of airphotos of an area prior to actual field sampling. The most efficient method consists of performing the

airphoto interpretation and field planning during winter months, followed by actual field inspections and sampling during the summer. After the major soil areas have been determined and delineated from the photographs representative locations can be selected for detailed study and sampling by the field party. Because soils and airphoto patterns are repetitive in nature it is not necessary to obtain profile samples at fixed intervals; rather samples are taken only where a change in soil areas is indicated on the airphotos. Thus, detailed profile sampling need be performed only in transition zones while a minimum of profile sampling is needed in any given parent-material region. Quite often one or two profile samples are typical of large areas such as broad gravel outwash plains, gravel terraces, and plains, loess and certain bedrock areas. The obtaining of additional samples other than these would be duplication of effort, and any variations that may occur in the physical characteristics would be within reasonable engineering design criteria.

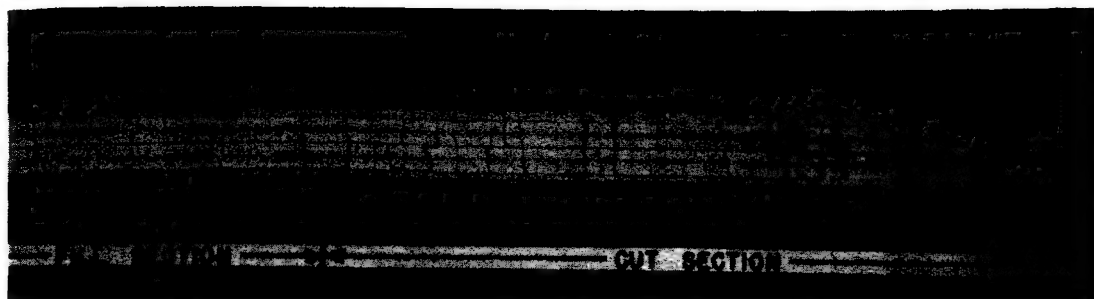
Perhaps one of the most important use of the airphotos for the engineer is in the study of materials and the prediction of soil characteristics and related engineering problems. By detailed study of the elements of the pattern it is possible to determine by indirect means the soil texture and natural drainage characteristics. Other properties, such as the classification tests limits and field densities, can not discerned directly by photo interpretation. However, it is possible to predict such values about a soil once the airphoto pattern of that soil type has been thoroughly studied and correlated with the engineering test data of similar soils which develop a similar airphoto pattern which have been field checked and analyzed in the laboratory. Thus, a silty-clay-drift material in one section of the country need not be actually sampled in the field to determine its characteristics. If the pattern is similar to that of a silty-clay-drift in another area which has been sampled and tested then the characteristics may be predicted within the required limits of design.

Within the past few years a new method has been developed for obtaining continuous strip photos at a low altitude. The process and the application of the method of making a performance survey has been described by Hittle 11). Figure 12 shows the type photograph and the fine detail which can be obtained with the continuous strip process.

#### SUMMARY OF RESULTS AND CONCLUSIONS.

In summary it is important to point out that large-scale research is being co-ordinated with routine work to develop further the airphoto techniques. Some currently active Indiana projects include 1) the development of an engineering soil map of the state with particular emphasis being placed on the location and distribution of construction materials, 2) the development of a drainage map of the entire state, constructed to a very fine detail, 3) low-altitude strip filming for use in making highway performance and location surveys and 4) co-operation with various governmental units in developing information for highway and airport site selection and in locating construction materials.

These project studies have already yielded important results: soil and location maps have been prepared from aerial photographs for several dozen major airfields in the United States; the aerial photographs have been used in establishing the location for seventeen county airfields in Indiana; detailed drainage maps for



The importance of subgrade soils in the performance of a portland cement concrete pavement is illustrated in this low altitude strip photograph of an Indiana pavement.

FIG.12

thirty Indiana counties have been completed; engineering soil maps for five Indiana counties are complete; performance surveys have been made on several dozen miles of highways by using low-altitude strip maps; and preliminary soil surveys have been made from aerial photographs for many Indiana highway projects.

On the basis of detailed study in the field and laboratory over a period of years the following conclusions have been reached:

- 1) Surveying via the media of airphotos makes it possible to locate and map engineering materials more accurately, more efficiently, more rapidly, and at a greater savings in cost than by other means.
- 2) Information required for the use of making surface drainage maps and engineering soils maps can be obtained more completely from airphotos than from any other means, especially in regions where the soils, drainage, and relief of the land are complex, full of detail, and often inaccessible. (9p.46.)
- 3) Only surface and near surface materials and patterns can be observed and determined; however, in some instances subsurface conditions can be inferred with a high degree of accuracy.
- 4) Low altitude continuous strip photos constitute an excellent tool for correlating highway and airport pavement performance with subgrade soils.

#### SPECIAL BIBLIOGRAPHY.

This is a partial list of Joint Highway Research Project Bulletins, Theses, and Papers covering Geology, Pedology, and Airphoto Interpretation for use in Engineering Soil Problems.

#### Bulletins and Theses.

- 1) "Distribution, Formation, and Engineering Characteristics of Soils," by D.J. Belcher, L.E. Gregg, and K.B. Woods; Engineering Bulletin of Purdue University, Research Series No. 87, Vol. 27, No. 1, January, 1943.
- 2) "The Origin, Distribution, and Airphoto Identification of United States Soils," by D.S. Jenkins, Civil Aeronautics Administration, and D.J. Belcher, L.E. Gregg, and K.B. Woods, Purdue University; Technical Development Report No. 52, Civil Aeronautics Administration, Washington, D.C., May, 1946.
- 3) "The Determination of Engineering Soil Characteristics by the Use of Aerial Photographs," by D. J. Belcher. A thesis submitted to the faculty of Purdue University in partial fulfillment of the requirements of the degree of Civil Engineer, March, 1943.
- 4) "Airphoto Patterns of Southern Indiana Soils," by Robert E. Frost. A thesis submitted to the faculty of Purdue University in partial fulfillment of the requirements for the degree of Civil Engineer, June, 1946.
- 5) "The Engineering Significance of Airphoto Patterns of Northern Indiana Soils," by Pacifico Montano. A thesis submitted to the faculty of Purdue University in partial fulfillment of the requirements for the degree of Master of Science in Civil Engineering, June, 1946.
- 6) "Airphoto Interpretation of Soils and Drainage of Parke County, Indiana," by Merle Parvis. A thesis submitted to the faculty of Purdue University in partial fulfillment of the requirements for the degree of Master of Science in Civil Engineering, June, 1946.
- 7) "Airphoto Interpretation of Drainage and Soils of Fountain County, Indiana," by S. T. Yang. A thesis submitted to the faculty of Purdue University in partial fulfillment of the requirements for the degree of Master of Science in Civil Engineering, February, 1947.
- 8) "Airphoto Interpretation of Soils and Drainage of Montgomery County, Indiana," by J.D. Mollard. A thesis submitted to the faculty of Purdue University in partial fulfillment of the requirements for the degree of Master of Science in Civil Engineering, February, 1947.
- 9) "Regional Drainage Patterns of Indiana," by Merle Parvis. A thesis submitted to the faculty of Purdue University in partial fulfillment of the requirements for the degree of Civil Engineer, June, 1947.
- 10) "Soils of Jamaica, B.W.I., Their Formation and Engineering Characteristics," by Frederick B. Hill. A thesis submitted to the faculty of Purdue University in partial fulfillment of the requirements for the degree of Master of Science in Civil Engineering, June, 1947.
- 11) "The Application of Aerial Strip-Photography to Highway Engineering," by Jean E. Hittle. A thesis submitted to the faculty of Purdue University in partial fulfillment of the requirements for the degree of Master of Science in Civil Engineering, June, 1947.
- 12) "The Use of Aerial Photographs in Identifying Granular Deposits and Other Soils," by Jean E. Hittle, Proceedings, Twenty-ninth Annual Purdue Road School, Engineering Bulletin of Purdue University, Extension Series No. 55, Vol. 27, No. 2, March, 1943.
- 13) "The Development of Engineering Soils Maps,"

- by D. J. Belcher, ibid.
- 14) "Engineering Significance of Soil Patterns," by D. J. Belcher; Proceedings, Highway Research Board, Vol. 23, 1945.
  - 15) "An Inventory of Granular Materials in Indiana," by J. E. Hittle; Proceedings, Thirtieth Annual Purdue Road School, Engineering Bulletin of Purdue University, Extension Series No. 56, Vol. 28, No. 2, March, 1944.
  - 16) "Identifying Land Forms and Soils by Aerial Photographs," by D. J. Belcher, ibid.
  - 17) "Identification of Granular Deposits by Aerial Photography," by E. E. Frost, Proceedings, Highway Research Board, Vol. 25, 1945.
  - 18) "The Use of Aerial Maps in Soil Studies and in the Location of Borrow Pits," by R. E. Frost; Proceedings, Kansas State Highway Engineering Conference, March, 1946.
  - 19) "Locating Granular Materials in Southern Indiana with Aerial Photography," by R. E. Frost; Proceedings, Thirty-second Annual Purdue Road School, Engineering Bulletin of Purdue University, Vol. 30, 1946.
  - 20) "Aerial Reconnaissance," by D. J. Belcher; Proceedings, Geological Society of America, Vol. 57, pp. 727-734, August, 1946.
  - 21) "New Glacial Features Identified by Airphotos in Mapping Program," by R. E. Frost and J. D. Mollard, Proceedings, Twenty-sixth Annual Meeting, Highway Research Board, Washington, D. C., December, 1946.
  - 22) "Application of Aerial Strip Photography to Highway and Airport Engineering," by J. E. Hittle, ibid.
  - 23) "Development of Drainage Maps from Aerial Photographs," by Merle Parvis, ibid.
  - 24) "Airphoto Mapping of Montgomery County Soils for Engineering Purposes," by J. D. Mollard, Proceedings, Thirty-third Annual Purdue Road School, February, 1947.
  - 25) "The Story of Indiana Soils," by T. M. Bushnell. Agricultural Experiment Station Purdue University, Special Circular 1, June, 1944.
  - 26) "The Correlation between Pavement Performance and Soil Textures," by K. B. Woods, Proceedings, Tennessee Road School, April, 1947.

-o-o-o-o-o-

## SUB-SECTION 9 1

### III 9 1

#### THE PERMAFROST INVESTIGATION IN ARCTIC AND SUBARCTIC REGIONS

WALTER K. WILSON, JR.

Colonel, Corps of Engineers District Engineer, St. Paul District

#### SUMMARY.

An intensive study of permafrost by the Corps of Engineers, St. Paul District, under the direction of the Chief of Engineers, was started in 1945 because of numerous construction failures at airfields in Alaska and a desire to determine the best designs and construction methods for arctic and subarctic regions. The field work has included studies of airfields constructed during the last war as well as an experimental plot developed at Fairbanks, Alaska for an intensive study of foundation conditions. Weather and ground temperature data are being correlated for various points in Alaska. Thermal properties of soils are being determined at the University of Minnesota, and field investigations are being made by Purdue University to develop methods of locating the best possible airfield sites from aerial photographs. From the studies in progress, it appears that it will require several years of observations to develop design criteria and methods for construction of airfields in arctic and subarctic regions.

Permafrost, or permanently frozen ground, is usually found in varying thicknesses below the surface of the earth in regions where the mean annual temperature is below 0° C. (See Figures 1 and 2). The permafrost phenomenon is quite extensive and covers about one-fifth of the world's land area. In the northern hemisphere, permafrost is found in about 80% of Alaska, 50% of Canada, and practically all of Siberia. Although its origin is not known, it is believed that permafrost was formed during the Ice Age. It exists both as a continuous layer and as discontinuous layers. Where it exists as continuous layers, its thickness has been found to range up to about 1500 feet. The permafrost is generally overlain by an active zone all, or the upper part, of which freezes each winter. (See Figure 8).

It has been known for a long time that permafrost exists in Alaska, northern Canada, and Siberia, however, its effect on construction had not been studied prior to World War II, except by the Russians who have made investigations in Siberia for many years as a result of failures of structures along the Trans-Siberian Railroad. Many of the Russian studies have been concerned with obtaining basic information relative to the factors which influence permafrost, as well as obtaining solutions to various engineering problems which have been caused by disturbing the natural regime of permafrost. Their investigations, as well as our own, indicate that important factors which influence permafrost are climate, ground water, vegetation and soil characteristics.





Horizontal ice ledges in the lower portion of a placer exposure. Frozen peat and silt separate the ice ledges.

FIG.1



3 July 1947 Ground ice and frozen silt in a foundation excavation.

FIG.2

American engineers were confronted with problems associated with permafrost during construction of the Alaska Highway in northern Canada and Alaska. Here the permafrost, in many places, was only a foot or so below the ground surface. (See Figure 3). Upon removal of the vegetation which is a natural insulator, the ground thawed rapidly and where fine-grained soil was present, serious difficulties were encountered in operating construction equipment. This problem was overcome, in some cases, by immediately backfilling the excavated area with sand and gravel to a sufficient depth to prevent further lowering of the permafrost surface and, in other cases, by constructing the road fill on the natural vegetative cover. As a by-product of permafrost, drainage ditches along the highway in cut sections frequently became filled with ice during the winter season and, in many instances, the icing would overflow the roadway to a considerable depth interfering with normal use of the highway. (See Figures 4 and 9). This condition was principally



3 July 1947 Concrete foundation in permafrost. Ground ice below topsoil layer is shown in background.

FIG.3

caused by the seasonal freezing downward from the surface of the ground under the ditch meeting the permafrost table which forced the ground water in the hillside to break out slightly upstream from the ditch. It has been possible to overcome this difficulty to some extent by clearing the natural insulating material from a strip of land uphill from the roadway and constructing a ditch and dike perpendicular to the direction of the ground water movement to permit intercepting, conveying or storage of surface and ground water away from the road. (See Figure 10).

The presence of permafrost also caused problems in the construction of many airfields which were built in Alaska during the recent war. Problems encountered in the construction of runways were essentially the same as those encountered in the construction of highways. Considerable damage was caused, in some instances, where sufficient insulating material was not substituted for the natural cover which was removed and where the fine-grained frost heaving material was not replaced by nonfrost heaving material. As a result, the runways of certain airfields had to be reconstructed. Problems also were encountered in connection with heated buildings in which conditions became progressively worse as the heat flowed into the ground over a period of time and caused the melting of the permafrost. (See Figure 11). Where the thawed soil was fine-grained, it lost most of the stability which it had while in a frozen condition and, as a result, the buildings placed on it settled and in some cases were severely damaged. It was as a result of these failures that the investigation of airfield construction in arctic and subarctic regions was initiated by the Chief of Engineers and assigned to the St. Paul District, Corps of Engineers, in January 1945. The investigation is still in progress under the general direction of the writer. It is expected that the investigation will continue for several years. The purpose of the investigation is primarily to develop design criteria and construction methods for airfield pavements, structures and utilities located in arctic and subarctic regions. Objectives of various phases of the investigation include:



12 April 1947 Encroachment of ice field on highway. Note artificial thawing of ditch and culvert.

FIG.4



13 October 1946 View of permafrost research areas near Fairbanks, Alaska,

FIG.5

- a). Study of the performance of existing airfield installations on permanently frozen ground.
  - b). The observation and correlation of the relationship between climatic conditions and soil conditions throughout Alaska.
  - c). The determination of the thermal properties of typical soils from Alaska by laboratory tests.
  - d). Study of heat transfer in soils and insulating materials and applications to design of runways, roads and buildings on permanently frozen ground.
  - e). Review of literature in English and foreign languages on permafrost and construction thereon.
  - f). Development of a method of identifying permafrost areas and soil types from terrain characteristics shown in aerial photographs.
  - g). Investigation of the applicability of geophysical methods to use in the location of permafrost in localized areas.
- Studies are now being made to attain



September 1946 Aerial view of ground polygons near Fairbanks, Alaska.

FIG.6

the above objectives by field forces in Alaska, by engineers at the University of Minnesota and Purdue University, and by District Office personnel. Field forces in Alaska under the jurisdiction of the St. Paul District Engineer are comprised of engineers, soils technicians, temperature observers, core and churn drill operators, and surveyors. Laboratory work is being done on thermal properties of soils and insulating materials by the University of Minnesota and on interpretation of aerial photographs by Purdue University under contract with the Government. The information collected is being analyzed by the Office of the St. Paul District Engineer. It is expected that the analysis will result in the development of the desired designs and construction procedures.

For the purpose of determining the performance of existing airfield installations on permanently frozen ground, observations are presently being made at Northway Airfield, Alaska (see Figure 7 for location) and, as new airfields are constructed in the permafrost region of Alaska, it is planned to make additional installations of equipment and make observations. The investigation at the airfields includes the making of core or churn borings, with a maximum diameter of eight inches, in the permanently frozen ground to depths of 50 to 75 feet and the installation of equipment for measuring temperatures in the boring holes at various depths below the surface. Observations of temperatures are made at regular intervals. The borings are logged and samples recovered are tested for their physical characteristics. Ground water wells are established throughout the area and vertical movement observation points are installed along the runways and in and adjacent to structures. From the observations made during the past two years at Northway, it is indicated that the permafrost under the runway has stabilized at a depth of about 10 feet below the surface as compared to a normal depth of about  $3\frac{1}{2}$  feet in the undisturbed ground. They also indicate that the permafrost surface under the hangar is receding progressively downward until it has now reached a depth of 24 feet below the floor level. Although vertical observations indicate a maximum settlement of one foot





Territory of Alaska general outline map

FIG.7

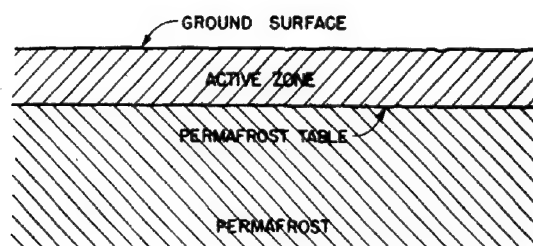
on the hangar floor and abutments, no apparent failure of the structure is eminent.

The investigation of the existing and proposed airfields did not provide certain basic information concerning various other types of construction that were considered desirable. In order to obtain this information, a research area was constructed near Fairbanks, Alaska in an area of fine-grained soil where the permafrost surface is from 3 to 4 feet below the ground surface. (See Figure 5). This research area has been divided into three subareas:

Area One, which has been subdivided into four parts, is being used principally to determine the effect of climate factors such as air temperatures, solar radiation, wind velocity, humidity, cloudiness, and precipitation. One part has been left in its natural state; the second has been cleared of trees and brush but has not been stripped; the third has been cleared of trees and brush and stripped to a depth of 12 inches. The fourth part is designed for solar radiation observations and is composed of three concrete slabs, 30 feet square and 6 inches thick. One slab has a natural concrete surface and the other two slabs are painted black and white, respectively, to determine the effect of color on the transfer of solar radiation into the ground. Temperature measuring instruments, vertical movement observation points, and ground water wells

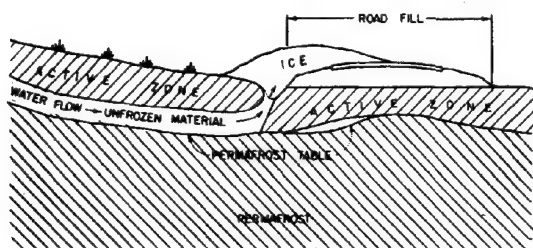
have been installed in or near each part of the section. Automatic temperature recording apparatus has been installed in the part designated for solar radiation observations.

Area Two is composed of 26 runway sections, each of which is 50 feet square, with a temperature well in the center of each section. The depth of the base course varies from two to twelve feet and the runway surfaces are concrete, asphalt and gravel. Insulating materials, including spruce boughs, moss, P.C. Foamglas, Zonolite concrete, and Cell concrete, have been included in the base course in several of the sections. Cell concrete is a product which is made in a special mixer using a Danish foam compound to produce a light weight, air entraining concrete. Zonolite concrete is made with Vermiculite, an expanded mica aggregate and P.C. Foamglas is a commercial slab-type insulation material. As the insulation materials have insufficient compressive strength for direct loading, they were placed in a layer 2 feet below the pavement surfaces. Prior to placing the base course for 23 of the test sections, the natural ground surface was stripped to a depth of one foot. The base course for the remaining three sections was placed on the natural ground. It is expected that, from a careful study of the transfer of heat through each of the runway sections, a guide for the design of an economical and stable runway can be developed.



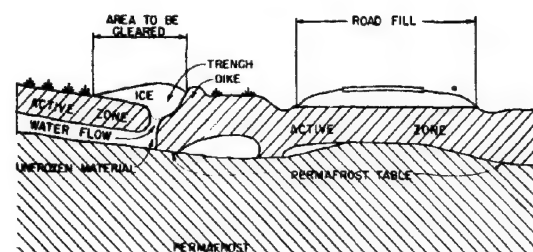
Natural permafrost conditions.

FIG. 8



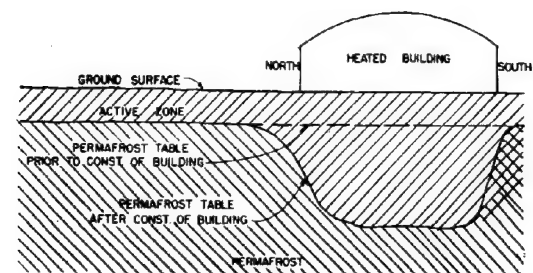
Induced field of surface ice uncontrolled.

FIG. 9



Induced fields of surface ice controlled.

FIG. 10



Effect of heated building on permafrost table.

FIG. 11

Area Three includes two types of experiments. The first is a study of different types of foundations under eleven heated buildings, eight of which are 16 feet square and three 32 feet square. Buildings are heat-

ed to a temperature of 15° C. and ground temperatures are measured weekly in several wells under each building. The base course under five of the small buildings is gravel ranging in thickness from two to six feet. One small building is placed on mud sills directly on the natural ground surface. The remaining two small buildings are supported on wooden posts extending 2½ feet above the natural ground surface to allow free air circulation under the building. One large building is placed on a foundation composed of a concrete slab with an intermediate insulating layer of hollow tile blocks through which air can be circulated. The second large building is supported on wooden piles set into permafrost with a 5 foot air space above the ground surface. The third large building has a raft type concrete foundation placed on a 5 foot gravel fill. Reinforced concrete posts support the building about 3 feet above the raft type foundation and permit air circulation under the building. The second type of experiment in Area Three is being made to determine the effect of depth to embedment of piling in permafrost on resistance to displacement by seasonal frost action in the ground zone above the permafrost.

As a supplement to the investigations at Northway Airfield and at the Research Area near Fairbanks, an investigation is being made to determine relations between climatic and ground conditions throughout the permafrost region of Alaska. For this study, ground temperature measuring equipment was installed in 20-foot deep boring holes at each of 15 weather stations. Observations of ground temperatures as well as climatic conditions are being made at these stations and the data collected are being studied.

Tests are being made by the Engineering Experiment Station of the University of Minnesota, under a contract with the Government, to determine the thermal conductivity and specific heat properties of certain soils, rock types, and insulating materials at various densities, moisture contents, and temperatures. Additional information concerning these tests may be found in the following papers by Miles S. Kersten who is in charge of this work for the University of Minnesota: "Thermal Conductivity of Soil", "Apparatus for Measuring Thermal Conductivity of Soil", and "Specific heat Tests on Soil". As the various reports on tests and observations from the University of Minnesota, field sources in Alaska, library and theoretical studies are collected, it is planned to correlate the data, evaluate the results and produce, if possible, guides for the design and construction of airfields in permafrost areas.

The feasibility of using aerial photographs in identifying permafrost areas on the ground is being investigated by Purdue University under a contract with the Government. From a field and office study of surface characteristics such as drainage, topography, vegetation and tree growth, as shown on aerial photographs, a technique has been developed whereby it is possible to select from the photographs, areas where construction can be successfully carried out as well as those areas which should be avoided. Figure 6 shows the pattern of ground polygons, an indication of fine-grained soil and ground ice which provide poor foundation conditions. The outlines of the polygons, as

shown on Figure 6, are formed by a series of ice wedges inclosing silt or fine-grained soil areas. It has been demonstrated in the United States that studies of aerial photographs can eliminate long and extensive ground explorations where an investigation is being made to determine the most suitable site in a large area and that brief ground explorations can then confirm the selected locations. Details concerning the techniques developed are contained in the paper entitled "Correlation Between Permafrost and Soils as Indicated by Aerial Photographs" by K.B. Woods and others of Purdue University.

Studies have been made to determine the feasibility of using geophysical methods for the location of permafrost. Both seismic and electrical resistivity methods have been tried and the latter method appears to have the better chance of successful application. However, the results obtained to date have not been entirely satisfactory, and it appears that further studies must be made to prove or disprove the practicability of using geophysical methods for the intended purpose.

#### CONCLUSIONS

It appears that it will require several years of observations in various locations and under a variety of conditions to determine thermal characteristics of permafrost areas and to develop design criteria and construction methods. Although definite con-

clusions cannot be made at this time, there are certain trends or tentative conclusions which engineers should consider in connection with new construction in arctic and sub-arctic regions. These trends are based on library research and on the results of this investigation.

Site selection is very important and, wherever possible, structures should be located on coarse-grained materials where the lowering of the permafrost surface will not cause deleterious settlement of the structures.

In areas where there is danger of settlement of structures due to melting of the permafrost, a space suitable for circulation of fresh air should be provided under heated buildings to prevent heat transfer into the ground.

In the construction of roads and runways, no fine-grained frost heaving soil should be permitted in the ground zone subject to seasonal frost.

Where there is danger of icing over roads, consideration should be given to cause induced icing some distance from the structure. Where possible, roads should be located to avoid side hills and incident icing problems.

Where complete information is available concerning soil characteristics and the extent of permafrost at a given site, it is possible through proper construction methods to avoid deleterious settlement of structures.

# TABLE OF CONTENTS

<u>SECTION I : THEORIES, HYPOTHESES, CONSIDERATIONS OF A GENERAL CHARACTER</u>		Page
Sub-section Ia : <u>GENERAL CONSIDERATIONS</u>		
Ia 1	Early history and bibliography of soil mechanics. J. Feld (U.S.A.)	1
Sub-section Ib : <u>GEOLOGY AND SOIL MECHANICS</u>		
Ib 1	Engineering uses and limitations of pedology for regional exploration of soils. H.F. Winterkorn (U.S.A.)	8
Sub-section Ic : <u>PHYSICAL AND PHYSICO-CHEMICAL PROPERTIES OF SOILS</u>		
Ic 1	Contribution to the theory of shrinking. R. Haefeli and G. Amberg (Switzerland)	13
Ic 2	Heat flow towards the floor of cold stores, situated in the ground level, and calculation of the insulation or the heating system to prevent frost penetration in the ground. R.F.X. Ruckli (Switzerland)	18
Ic 3	Physico-chemical properties of soils. H.F. Winterkorn (U.S.A.)	23
Sub-section Id : <u>STRESS - STRAIN RELATIONS : CONSOLIDATION</u>		
Id 1	Problems of soil settlement. T. Edelman (Netherlands)	30
Id 2	Precise determination of primary consolidation. A.H. Naylor and I.G.Doran (Ireland)	34
Id 3	The mathematical solution for early stages of consolidation. E.N.Fox (England)	41
Id 4	On the compressibility of preconsolidated soil-layers. R.Haefeli (Switzerland)	42
Sub-section Ie : <u>SHEARING STRENGTH AND EQUILIBRIUM OF SOILS</u>		
Ie 1	On the law of friction of sand. Takeo Mogami (Japan)	51
Ie 2	Determination of the bearing power of clay foundation. Takeo Mogami (Japan)	55
Ie 3	The stability of slopes acted upon by parallel seepage. R. Haefeli (Switzerland)	57
Ie 4	Limitation of the validity of application of the formulas from Prandtl - Buismann and from Andersen for the ultimate bearing capacity of the soil underneath footings. E. de Beer and M. Wallays (Belgium)	63
Ie 5	Improvement of the method of calculation of the equilibrium along sliding circles. H. Raedschelders (Belgium)	68
Ie 6	The $\phi = 0$ analysis of stability and its theoretical basis. A.W. Skempton (England)	72
Ie 7	A simplified method for computing the bearing capacity of the soil supporting footings or piers. L. Marivoet (Belgium)	78
Ie 8	Validity of Coulomb's law of stability. J. Jáky (Hungary)	87
Ie 9	State of stress in great depth. J. Jáky (Hungary)	
Ie 10	A fundamental theory of plastic deformation and breakage of soil. K.Hoshino (Japan)	93
Ie 11	On the bearing capacity of piles. J. Jáky (Hungary)	100
Sub-section If : <u>EARTH PRESSURE</u>		
If 1	Pressure in silos. J. Jáky (Hungary)	103
If 2	Calculations of sheet pile walls in cohesive soils. C.F.Kollbrunner (Switzerland)	108
Sub-section Ig : <u>STRESS DISTRIBUTION</u>		
Ig 1	Approximative calculations of the stress-distributions due to concentrated vertical loads. G.A. Oosterholt (Netherlands)	112
Ig 2	On the depth of foundation. F. Szélagowski (Poland)	115
Ig 3	Computation of beams resting on soil. E. de Beer (Belgium)	119
Ig 4	The influence of the heterogeneity of the soil mass on its deformation. K. Hruban (Czechoslovakia)	123
Ig 5	Sources of error in settlement estimate. K. Hruban (Czechoslovakia)	127
Ig 6	The mean elastic settlement of a uniformly loaded area at a depth below the ground surface. E.N. Fox (England)	129
Sub-section Ii : <u>MISCELLANEOUS</u>		
Ii 1	The concept of soil moisture deficit. R.K. Schofield and H.L. Penman (England)	132

<u>SECTION II : LABORATORY INVESTIGATIONS</u>		Page
Sub-section II a : <u>GENERAL</u>		
IIa 1	Effect of natural hardening of the unconfined compression strength of remolded clays. O. Moretto (Argentina)	137
IIa 2	The geotechnical properties of a deep stratum of post-glacial clay at Gosport. A.W. Skempton (England)	145
IIa 3	Laboratory studies relating to the clay fraction of cohesive soils. K.E. Clare (England)	151
Sub-section II b : <u>IDENTIFICATION TESTS</u>		
IIb 1	An experimental study of maximum and minimum porosities of sands. J.J. Kolbuszewski (England)	158
Sub-section II c : <u>CONSOLIDATION TESTS</u>		
IIc 1	Secondary time effect in the compression of unconsolidated sediments of volcanic origin. A. Croce (Italy)	166
IIc 2	Consolidation tests on soils containing stones. L.J. Murdock (England)	169
Sub-section II d : <u>TRIAXIAL TESTS</u>		
IIId 1	Correlation between the results of cell-tests and compression tests. E. de Beer (Belgium)	173
IIId 2	The angle of shearing resistance in cohesive soils for tests at constant water content. H.Q. Golder and A.W. Skempton (England)	185
IIId 3	A study of the immediate triaxial test on cohesive soils. A.W. Skempton (England)	192
IIId 4	A contribution to the study of the elastic properties of sand. G. Wilson and J.L.B. Sutton (England)	197
IIId 5	The determination of the shearing strength of varved clays and of their sensitivity to remolding. G.P. Tschebotarioff and J.R. Bayliss (U.S.A.)	203
Sub-section II e : <u>DIRECT SHEAR TESTS</u>		
IIe 1	A large shear box for testing sands and gravels. A.W. Bishop (England)	207
IIe 2	The shearing resistance of soils as determined by direct shear tests at a constant rate of strain. J. MacNeil Turnbull (Australia)	211
Sub-section II f : <u>ELECTRO-OSMOSIS</u>		
IIIf 1	Electro-osmosis. L. Casagrande (England)	218
Sub-section II g : <u>MISCELLANEOUS</u>		
IIIg 1	Laboratory compaction technique. A.L. Little (England)	224
IIIg 2	Some laboratory experiments in the waterproofing of soils. K.E. Clare (England)	230
IIIg 3	An investigation of the bearing capacity of shallow footings in dry sand. G.G. Meyerhof (England)	237
 <u>SECTION III : FIELD INVESTIGATIONS</u>		
Sub-section III a : <u>BORING AND SAMPLING</u>		
IIIa 1	Field tests with new combined loading test sampler for Harbour Extension Works. A. Mortensen (Denmark)	244
IIIa 2	Extractor for taking disturbed samples in hard ground. O. Wager (Sweden)	249
IIIa 3	Concerning the physical properties of clays. R.E. Fadum (England)	250
IIIa 4	A method of extracting long continuous cores of undisturbed soil. W.Kjellmann and T. Kallstenius (Sweden)	255
Sub-section III b : <u>MEASUREMENTS OF SPECIAL SOIL PROPERTIES</u>		
IIIB 1	Permeability of peat by water. J.L.A. Cuperus (Netherlands)	258
IIIB 2	Simple field tests for soils. A.H. Gawith (Australia)	264
IIIB 3	Determination in situ of the shear strength of undisturbed clay by means of a rotating auger. L. Carlson (Sweden)	265
IIIB 4	A practical method of rapid measurement of soil moisture and its applications. K. Hoshino (Japan)	270

	Page
IIIb 5 Testing of the elasticity and stress property of rock soil. F. Hörnlmann (Switzerland)	274
IIIb 6 Construction and method of operating of a new deepsounding apparatus. G. Plantema (Netherlands)	277
IIIb 7 Improved sounding apparatus, as developed in Holland since 1936. J. Vermeiden (Netherlands)	280
Sub-section III c : <u>MEASUREMENTS OF PRESSURES AND DEFORMATIONS</u>	
IIIc 1 Experience gained in the measurement of pore pressures in a dam and its foundation. M.G. Speedie (Australia)	287
IIIc 2 Some results of water pressure measurements in clay layers. E. de Beer and H. Raedschelders (Belgium)	294
IIIc 3 Loading tests on clay. S. Odenstad (Sweden)	299
IIIc 4 Measurement of pore water pressure. T.K. Huizinga (Netherlands)	303
IIIc 5 An electrically operating pore water pressure cell. R.G. Boiten and G. Plantema (Netherlands)	306
Sub-section III d : <u>VIBRATION RESEARCH</u>	
IIId 1 The resonance of machine foundations and the soil coefficients which affect it. G.P. Tschabotarioff and E.R. Ward (U.S.A.)	309
Sub-section III e : <u>AERIAL PHOTOGRAPHING</u>	
IIIe 1 The determination of soil conditions by aerial photographic analysis. D.J. Belcher (U.S.A.)	313
IIIe 2 Correlation between permafrost and soils as indicated by aerial photographs. K.B. Woods, J.E. Hittle and R.E. Frost (U.S.A.)	321
IIIe 3 Aerial photographs used for an engineering evaluation of soil materials. R.E. Frost and K.B. Woods (U.S.A.)	324
Sub-section III g : <u>MISCELLANEOUS</u>	
IIIg 1 The permafrost investigations in arctic and subarctic regions. W.K. Wilson (U.S.A.)	330

# AUTHOR INDEX

Amberg, G.	Ic 1	Haefeli, R.	Ic 1, Id 4 Ie 3	Pennan, H.L.	Ii 1
Bayliss, J.R.	IId 5	Hittle, J.E.	IIIe 2	Plantema, G.	IIIf 6, IIIf 5
Beer, E. de	Ie 4, Ig 3 IIId 1, IIIf 2	Hörnlimann, F.	IIIf 5	Raedschelders, H.	Ie 5 IIIf 2
Belcher, D.J.	IIIf 1	Hoshino, K.	Ie 10, IIIf 4	Rückli, R.F.X.	Ic 2
Bishop, A.W.	IIe 1	Hruban, K.	Ig 4, Ig 5	Schofield, R.K.	Ii 1
Boiten, R.G.	IIIf 5	Huizinga, T.K.	IIIf 4	Skempton, A.W.	Ie 6, IIa 2 IIId 2, IIId 3
Carlson, L.	IIIf 3	Jáky, J.	Ie 8, Ie 9 Ie 11, If 1	Speedie, M.G.	IIIf 1
Cassagrande, L.	IIIf 1	Kallstenius, T.	IIIf 4	Sutton, J.L.E.	IIId 4
Clare, K.E.	IIa 3, IIg 2	Kjellmann, W.	IIIf 4	Szelagowski, F.	Ig 2
Croce, A.	IIc 1	Kolbuszewski, J.J.	IIIf 1	Tschebotarioff, G.P.	IIId 5 IIId 1
Cuperus, J.L.A.	IIIf 1	Kollbrunner, C.F.	If 2	Turnbull, J. MacNeil	IIe 2
Doran, I.G.	Id 2	Little, A.L.	IIg 1	Vermeiden, J.	IIIf 7
Edelman, T.	Id 1	MacNeil Turnbull, J.	IIe 2	Wager, O.	IIIf 2
Padum, R.E.	IIIf 3	Marivoet, L.	Ie 7	Wallays, M.	Ie 4
Feld, J.	Ia 1	Mayerhoff, G.C.	IIg 3	Ward, E.R.	IIId 1
Fox, E.W.	Id 3, Ig 6	Mogami, T.	Ie 1, Ie 2	Wilson, G.	IIId 4
Frost, R.E.	IIIf 2, IIIf 3	Moretto, O.	IIa 1	Wilson, W.K.	IIIf 1
Gawith, A.H.	IIIf 2	Mortensen, A.	IIIf 1	Winterkorn, H.F.	Ib 1, Ic 3
Golder, H.Q.	IIId 2	Murdock, L.J.	IIc 2	Woods, K.B.	IIIf 2, IIIf 3
		Naylor, A.H.	Id 2		
		Odenstad, S.	IIIf 3		
		Oosterholt, G.A.	Ig 1		

PRINTED BY GEER. KRESMAAT  
Special printers for export  
HAARLEM - THE NETHERLANDS









